PNNL-28107

High-Resolution Regional Wave Hindcast for the U.S. West Coast

September 2018

Z Yang
WC Wu
T Wang
L Castrucci

Prepared for the U.S. Department of Energy
under Contract DE-AC05-76RL01830

DISCLAIMER

This report was prepared as an account of work sponsored by an agency of the United States Government. Neither the United States Government nor any agency thereof, nor Battelle Memorial Institute, nor any of their employees, makes **any warranty, express or implied, or assumes any legal liability or responsibility for the accuracy, completeness, or usefulness of any information, apparatus, product, or process disclosed, or represents that its use would not infringe privately owned rights**. Reference herein to any specific commercial product, process, or service by trade name, trademark, manufacturer, or otherwise does not necessarily constitute or imply its endorsement, recommendation, or favoring by the United States Government or any agency thereof, or Battelle Memorial Institute. The views and opinions of authors expressed herein do not necessarily state or reflect those of the United States Government or any agency thereof.

PACIFIC NORTHWEST NATIONAL LABORATORY
operated by
BATTELLE
for the
UNITED STATES DEPARTMENT OF ENERGY
under Contract DE-AC05-76RL01830

Printed in the United States of America

Available to DOE and DOE contractors from the
Office of Scientific and Technical Information,
P.O. Box 62, Oak Ridge, TN 37831-0062;
ph: (865) 576-8401
fax: (865) 576-5728
email: reports@adonis.osti.gov

Available to the public from the National Technical Information Service
5301 Shawnee Rd., Alexandria, VA 22312
ph: (800) 553-NTIS (6847)
email: orders@ntis.gov <http://www.ntis.gov/about/form.aspx>
Online ordering: http://www.ntis.gov

PNNL-28107

High-Resolution Regional Wave Hindcast for the U.S. West Coast

September 2018

Z Yang
WC Wu
T Wang
L Castrucci

Prepared for
the U.S. Department of Energy
under Contract DE-AC05-76RL01830

Pacific Northwest National Laboratory
Richland, Washington 99352

Summary

This report summarizes modeling efforts for the simulation of wave climate along the U.S. West Coast using an unstructured, nested-grid modeling approach that incorporates a global-regional nested grid using WAVEWATCH III® and the high-resolution UnSWAN (Unstructured-grid Simulating Waves Nearshore) model. Wave resource and long-term wave bulk parameters were simulated and subsequently validated with wave buoy data within the model domain.

Overall, model results match observations at buoys well. The model hindcast was able to reproduce the seasonal variation of the sea state with large waves that occur in the winter and early spring months when wind forcing is strong and the calm sea state during the summer when wind forcing is weak.

The nested-grid modeling framework employed in this study provides a powerful and efficient modeling approach to accurately simulate wave climate at regional and long-term temporal scales with sufficiently fine resolutions in the nearshore region. Results can be used to inform the deployment of wave energy converters and other nearshore instrumentation/devices in nearshore regions, assist in prioritizing hotspots for near-term market opportunities and development, and provide wave resource assessment data and information to inform resource estimates for marine and hydrokinetic energy technologies.

Acknowledgments

This study was funded by the U.S. Department of Energy, Office of Energy Efficiency & Renewable Energy, Water Power Technologies Office under Contract DE-AC05-76RL01830 to Pacific Northwest National Laboratory.

A steering committee, chaired by Bryson Robertson, program manager at the West Coast Wave Initiative, Institute of Energy Systems, at the University of Victoria, was organized to provide external oversight for, input to and review of this model study. Steering committee members included Prof. Tuba Özkan-Haller, a wave modeling expert at Oregon State University; Dr. Arun Chawla, team lead of the WAVEWATCH III® (WWIII) model suite at the National Oceanic and Atmospheric Administration's (NOAA's) National Center for Environmental Prediction; Dr. Brian Polagye, a marine hydrokinetic energy expert at the Northwest National Renewable Energy Center at the University of Washington; Dr. Julie Thomas, program manager and principal investigator for the Coastal Data Information Program from University of California San Diego; Dr. Pukha Lenee-Bluhm, a wave energy expert from Columbia Power; and Mr. Sean Anderton, a manager for technical support from Ocean Renewable Power Company.

Acronyms and Abbreviations

CDIP	Coastal Data Information Program
CFL	Courant–Friedrichs–Lewis
CFSR	Climate Forecast System Reanalysis
EPRI	Electric Power Research Institute, Inc.
Hz	hertz
IEC	International Electrotechnical Commission
km	kilometer(s)
kW/m	kilowatt(s) per meter
m	meter(s)
MHK	marine and hydrokinetic
NDBC	National Data Buoy Center
NCEP	National Centers for Environmental Prediction
NOAA	National Oceanic and Atmospheric Administration
NREL	National Renewable Energy Laboratory
PE	percentage error
R	correlation coefficient
RMSE	root-mean-square-error
s	second(s)
SI	scatter index
ST	source term
SWAN	Simulating WAves Nearshore
TS	Technical Specification
UnSWAN	Unstructured-grid Simulating Waves Nearshore
WEC	Wave Energy Converter
WWIII	WAVEWATCH III
yr	year(s)

Contents

Summary iii
Acknowledgments v
Acronyms and Abbreviations vii
1.0 Introduction 1
2.0 Methods 2
2.1 WWIII Model Configuration 2
2.2 UnSWAN Model Configuration 5
2.3 Model Forcing 7
2.4 Measured Data for Model Validation 8
3.0 Model Hindcast and Validation 11
3.1 Simulation of IEC Resource Parameters 12
3.2 Model Validation 18
4.0 Conclusion 30
5.0 References 31
Appendix A – Monthly Distributions of IEC Wave Resource Parameters from 1979–2010 along the West Coast A.1
Appendix B – Comparisons of Model-Simulated Six IEC Parameters with Observed Data at NDBC and CDIP Buoys B.1
Appendix C – Performance Metrics for Simulated IEC Resource Parameters C.1
Appendix D – Temporal Averages of Performance Metrics for Simulated IEC Resource Parameters D.1

Figures

Figure 1.1. Annual wave power density distribution in U.S. coastal regions, based on NOAA's 4 arc-minute resolution WWIII hindacsts 1
Figure 2.1. Model domains of U.S. West Coast 4
Figure 2.2. Bathymetry distribution for the WWIII models on U.S. West Coast 5
Figure 2.3. Bathymetry distribution of the UnSWAN model for the U.S. West Coast 6
Figure 2.4. The global distribution of CFSR wind field on December 3, 2007 7
Figure 2.5. Simulated monthly average significant wave height withWWIII for July and November 8
Figure 2.6. Wave buoy stations for model validation 11
Figure 3.1. Simulated 32-year annual distribution of six IEC wave resource parameters 15
Figure 3.2. Simulated monthly distribution of six IEC wave resource parameters in July 16
Figure 3.3. Simulated monthly distribution of six IEC wave resource parameters in December 17
Figure 3.4. Time series and scatter plots of the six modeled and observed IEC wave resource parameters for 2008 at Buoy 46211 in Washington. 20
Figure 3.5. Time series and scatter plots of the six modeled and observed IEC wave resource parameters for 2008 at Buoy 46229 in Oregon. 21
Figure 3.6. Time series and scatter plots of the six modeled and observed IEC wave resource parameters for 2008 at Buoy 46026 in Northern California. 22
Figure 3.7. Time series and scatter plots of the six modeled and observed IEC wave resource parameters for 2008 at Buoy 46215 in Southern California. 23
Figure 3.8. Time series and scatter plots of the six modeled and observed IEC wave resource parameters from April 2017 to March 2018 at Buoy 46260 in Oregon. 24
Figure 3.9. Time series and scatter plots of the six modeled and observed IEC wave resource parameters from April 2017 to March 2018 at Buoy 46261 in Oregon. 25
Figure 3.10. Time series and scatter plots of the six modeled and observed IEC wave resource parameters from April 2017 to March 2018 at Buoy 46263 in California. 26

Tables

Table 2.1. Summary of nested WWIII model grids 3
Table 2.2. Model run time steps for the WWIII model 3
Table 2.3. Summary of wave buoys with directional spectral data and long-term bulk parameter for model validation 9
Table 3.1. Performance metrics of the six simulated IEC resource parameters for 2008 at Buoy 46211 27
Table 3.2. Performance metrics of the six simulated IEC resource parameters for 2008 at Buoy 46229 27
Table 3.3. Performance metrics of the six simulated IEC resource parameters for 2008 at Buoy 46026 27
Table 3.4. Performance metrics of the six simulated IEC resource parameters for 2008 at Buoy 46215 28
Table 3.5. Performance metrics of the six simulated IEC resource parameters for the 4/2017–3/2018 period at Buoy 46260 28
Table 3.6. Performance metrics of the six simulated IEC resource parameters for the 4/2017–3/2018 period at Buoy 46261 28
Table 3.7. Performance metrics of the six simulated IEC resource parameters for the 4/2017–3/2018 period at Buoy 46263 28
Table 3.8. Summary of temporal averages of the root-mean-square-error and linear correlation coefficient for the six IEC wave resource parameters at buoys with spectral data 29
Table 3.9. Comparison of percentage mean errors of power density at selected buoys between the current PNNL study and the EPRI study 29

1.0 Introduction

Ocean wave has the highest energy resource among the U.S. marine and hydrokinetic (MHK) energy resources, including wave, tidal and ocean currents, ocean thermal technology, and river stream. The first U.S. nationwide wave resource assessment was conducted based on the 4 arc-minute resolution, 51-month wave hindcasts generated by the National Oceanic and Atmospheric Administration (NOAA) using nested-grid WAVEWATCHIII® model (WWIII) (EPRI, 2011; Tolman and WAVEWATCH III Development Group, 2014). The Electric Power Research Institute, Inc.'s (EPRI's) study showed that the U.S. West Coast has the second largest wave resource among all U.S. major coastal regions (Figure 1.1). The nationwide wave resource assessment provides a valuable first-order estimate of wave resources at a regional scale, which helps identify and prioritize hotspots for near-term market development. However, there are concerns that the shallow-water processes in the nearshore regions were not well reproduced due to the coarse-grid resolution; therefore, there is high uncertainty in resource estimates, especially in the nearshore region (Council, 2013). Most wave energy converters (WECs) are designed for deployment in nearshore areas because of low deployment and maintenance costs, as well as low risk under extreme sea states. Therefore, it is important to conduct a long-term, high-resolution wave hindcast in nearshore, shallow-water areas to improve the accuracy of hindcasts and reduce the uncertainties of previous resource assessment.

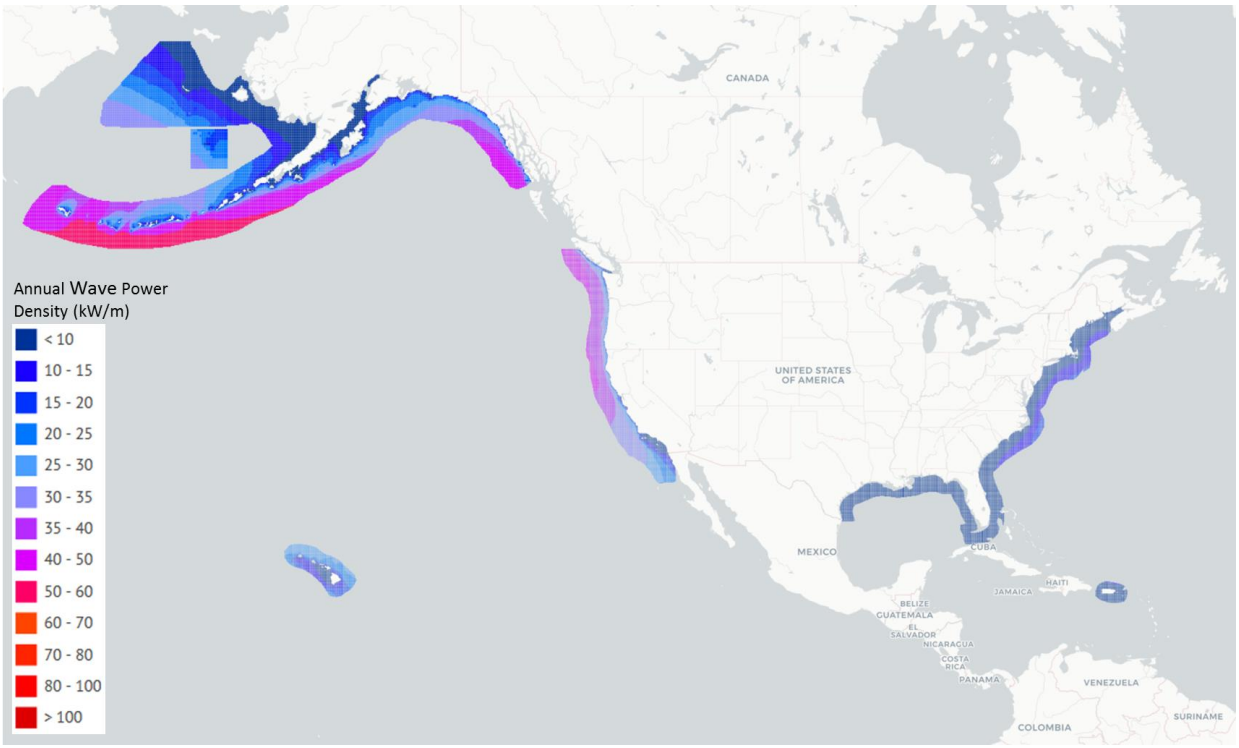

Figure 1.1. Annual wave power density distribution in U.S. coastal regions, based on NOAA's 4 arc-minute resolution WWIII hindcasts.[1]

Simulation of wave climate with fine-grid resolution at a regional scale requires extensive computational resources. The unstructured-grid modeling approach not only provides flexibility in accurately fitting the mesh boundary to the shoreline and refining the grid resolution in the area of interest, but also maintains great computational efficiency for a large model domain. In recent years, there has been significant

[1] This image was obtained from https://maps.nrel.gov/mhk-atlas.

development in unstructured-grid third-generation wave models. For example, Unstructured-grid Simulating WAve Nearshore (UnSWAN; (SWAN, 2015) has been widely used to simulate wave climates in many regions around the world (Cobell et al., 2013; Gallagher et al., 2014; Mao et al., 2016; Mediavilla and Sepulveda, 2016; Roland and Ardhuin, 2014; Wu et al., 2018; Yuk et al., 2016; Zijlema, 2010).

In this study, the WWIII and UnSWAN models were applied to simulate high-resolution wave climates along the U.S. West Coast. International Electrotechnical Commission (IEC) wave resource parameters, as well as long-term wave bulk parameters, were simulated and validated against measurements at wave buoys maintained by NOAA's National Data Buoy Center (NDBC) and the Coastal Data Information Program (CDIP). Wave partition outputs along the nearshore region of the West Coast were generated to support wave classification development. Spatial and temporal variabilities of wave climate on the West Coast were analyzed based on the long-term model hindcast. This study demonstrates that the nested-grid modeling framework using the WWIII and UnSWAN models provides a powerful modeling approach to characterizing wave resource accurately over greater temporal and regional scales with high resolutions in the nearshore region.

2.0 Methods

A nested-grid modeling approach using structured WWIII and UnSWAN models was used in this study. Three levels of nested grids using the WWIII model were set up to simulate wave climates from global to region scales and provide open boundary conditions to the high-resolution nearshore UnSWAN model for the West Coast. The WWIII model grid configurations are listed in Table 2.1. The Level 1 grid (L1) is the global model with a resolution of 0.5 degree, about 39 km in the zonal direction at 45ºN and 55.6 km in the meridional direction. Level 2 (L2) and Level 3 (L3) have grid resolutions of 6 arc-minutes and 1 arc-minute, respectively. The WWIII L3 and UnSWAN model domains are shown in Figure 2.1. Based on a wave model test bed study (Yang et al., 2017), the source term ST4 physics package (Ardhuin et al., 2010) in WWIII improved model prediction of wave power density. Therefore, the ST4 physics package was used in all WWIII model runs conducted in this study.

2.1 WWIII Model Configuration

To drive the high-resolution UnSWAN model for the West Coast, a nested-grid modeling approach was employed for this study. Three levels of structured-grid WWIII models were used, similar to other previous studies conducted in the Pacific Northwest (García-Medina et al., 2014; García-Medina et al., 2013; Wu et al., 2018; Yang et al., 2017). The L1 model is based on the NOAA National Centers for Environmental Prediction's (NCEP's) global WWIII model with 0.5-degree grid resolution. The L2 regional grid with a resolution of six arc-minutes was nested into the global model, and the L3 grid with a resolution of 1 arc-minute was nested into the regional L2 grid. The model domain coverage, spatial resolution, and grid size (number of grid points) for the global and the two intermediate nested grids are summarized in Table 2.1. Model output from the L3 grid provides open wave boundary conditions for the UnSWAN model (Figure 2.1).

Table 2.1. Summary of nested WWIII model grids.

Grid Name	Coverage	Resolution (long x lat)	Grid Size
Global Grid L1	77.5°S – 77.5°N; 0 – 360°W	0.5° × 0.5°	223,920
Nested Grid L2	28.5° – 50.5°N; 132° – 113.5°W	0.1° × 0.1° (6' × 6')	12,231
Nested Grid L3	30.5° – 49.5°N; 128° – 115.5°W	1' × 1'	124,046

Model time steps used in WWIII are summarized in Table 2.2. For WWIII, each model grid requires four time steps: (1) the global time step Δt_g, (2) the spatial propagation time step Δt_{xy}, (3) the intra-spectral propagation time step Δt_k, and (4) the source term time step Δt_s (Tolman et al. 2014). The spatial propagation time step Δt_{xy} must conform with the Courant–Friedrichs–Lewis (CFL) limit to ensure model stability.

Table 2.2. Model run time steps for the WWIII model (L1–L3 grids).

WWIII Nested Grid	Δt_g (s)	Δt_{xy} (s)	Δt_k (s)	Δt_s (s)
L1 (global)	3,600	480	1,800	30
L2	600	240	300	15
L3	100	45	50	15

All WWIII simulations used 29 frequency bins, 24 direction bins, a logarithmic increment factor of 1.1, a minimum frequency of 0.035 Hz, and a maximum frequency of 0.505 Hz. This spectral resolution meets the minimum requirements specified by the IEC technical specification (TS; (IEC, 2015)), i.e., a minimum of 25 frequency components and 24 to 48 directional components and a frequency range covering at least 0.04 to 0.5 Hz.

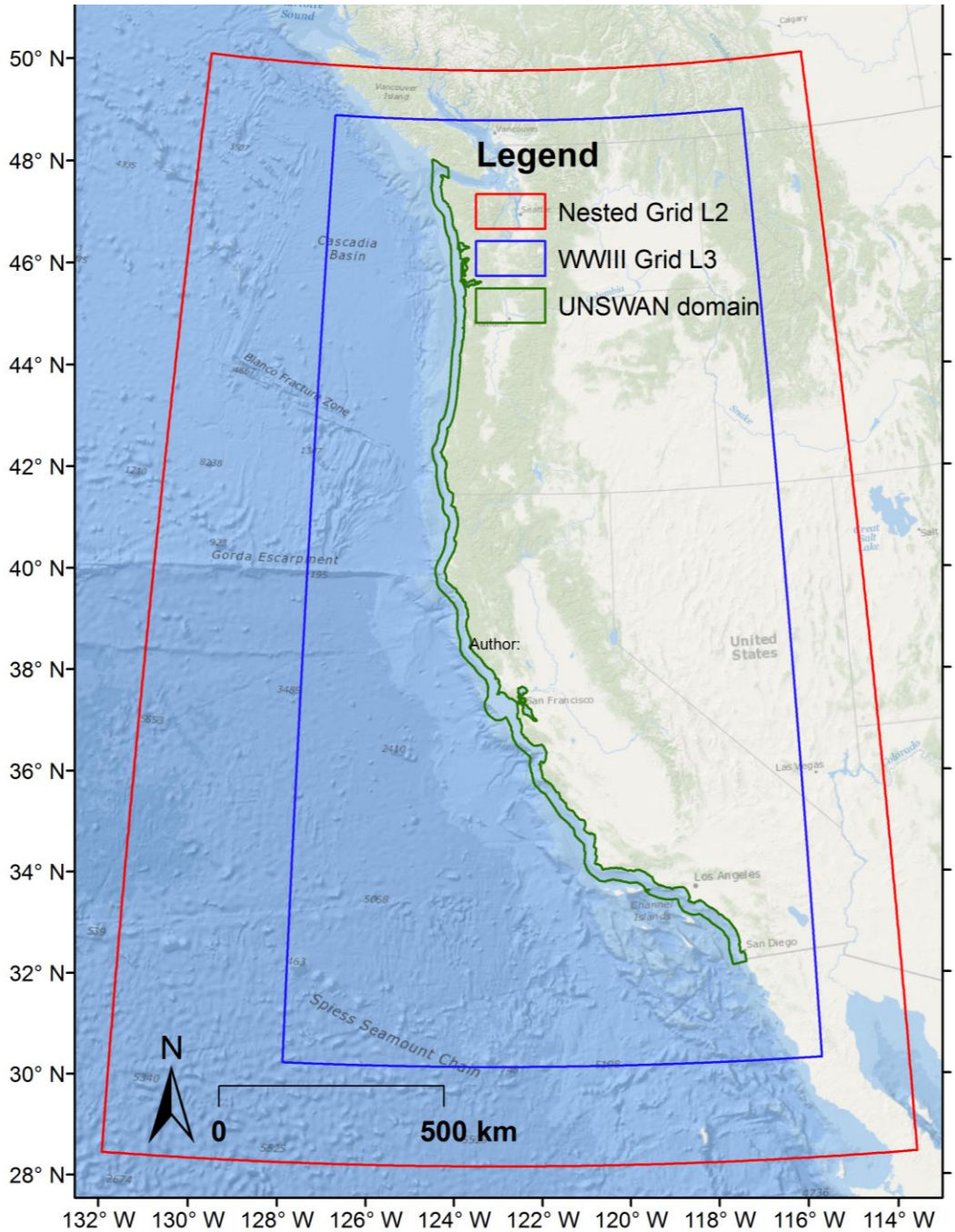

Figure 2.1. Model domains of U.S. West Coast. Red and blue lines represents the L2 and L3 WWIII model domains, respectively. The green line represents the high-resolution UnSWAN West Coast model domain.

Model bathymetry for all grid levels was interpolated from three NOAA bathymetry data sets: (1) the 1 arc-minute ETOPO1 Global Relief Model, (2) the 3 arc-second Coastal Relief Model, and (3) the high-resolution 1/3 arc-second tsunami bathymetry data. The 1 arc-minute ETOPO1 Global Relief Model was

used for the outer-shelf region and the deep ocean basins. The 3 arc-second Coastal Relief Model and tsunami bathymetry data for the inner-shelf region were used for the L2 and L3 model grids (Figure 2.2).

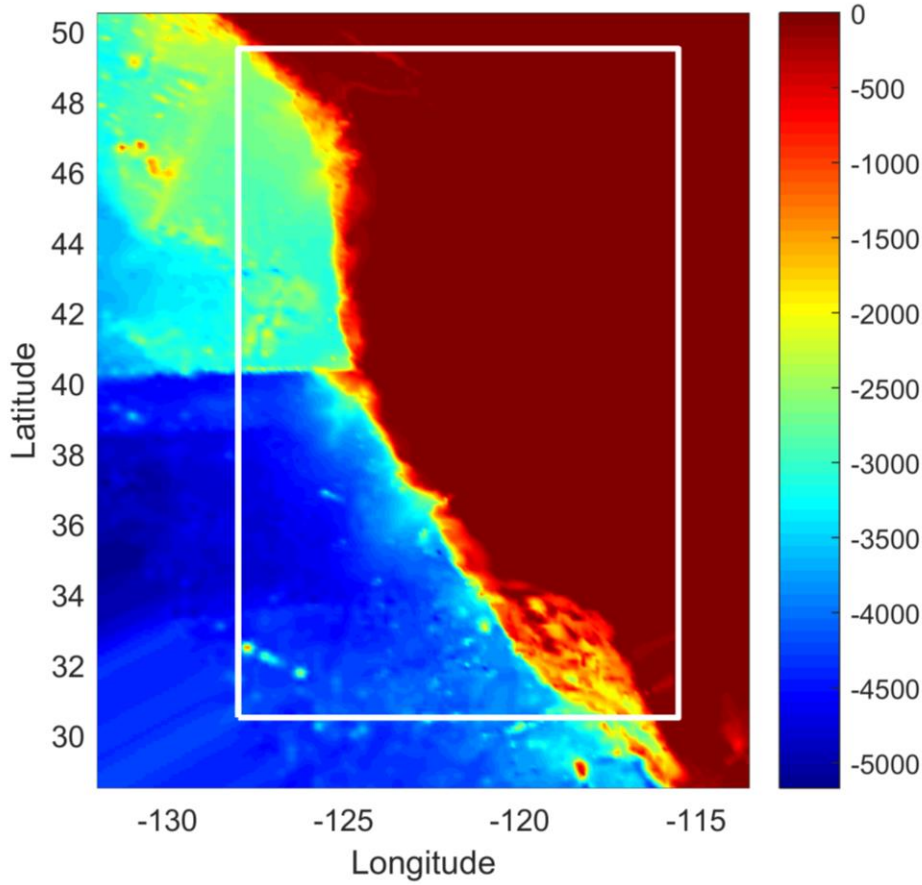

Figure 2.2. Bathymetry distribution for the WWIII models on U.S. West Coast. The white box indicates the regional L3 domain with 1 arc-minute resolution.

2.2 UnSWAN Model Configuration

As a fourth level, the UnSWAN model is used for the high-resolution nearshore simulation. In this study, a time step of 60 seconds was used for the UnSWAN simulations. This time step is sufficient to resolve the time variations of the computed wave field, given that the wind forcing and open boundary conditions are at hourly intervals. Sensitivity tests with smaller time steps, such as 10 and 5 seconds, showed no improvement in the predicted wave parameters. Another important parameter that affects the accuracy of model results is the maximum number of iterations of solution solver. In this study, a maximum value of 20-iteration (default value) was used in all simulations, although 95% of the solutions converged within 5-iteration. All UnSWAN model parameters in frequency and direction spaces are specified to be the same as the WWIII model parameters.

The UnSWAN model domain for the West Coast was defined by the nearshore region approximately 30 km offshore from the north end at the entrance of the Strait of Juan de Fuca to the south end between the U.S. and Mexico border (Figure 2.1). The unstructured grid consists of 435,369 nodes and 857,394 elements. The grid resolution varies from approximately 200 m along the shoreline to 350 m at the open boundary, approximately 30 km offshore. Model bathymetry was interpolated from the same bathymetric

data sets used in the WWIII model. Figure 2.3 shows the model bathymetry of the entire West Coast domain and the two map inserts show the grid distributions for the Columbia River Estuary and San Francisco Bay. While the inner continental shelf on the West Coast is generally narrow compared to the U.S. East Coast, the inner shelf on the Washington, Oregon, and northern California coasts is generally wider than that in the southern California, i.e., south of Monterey Bay. The bathymetry off the shore of the southern California coast is also much more complex; it features steep slopes, submarine canyons, and channel islands, which results in very complex wave sea states in comparison to the Pacific Northwest and northern California coasts.

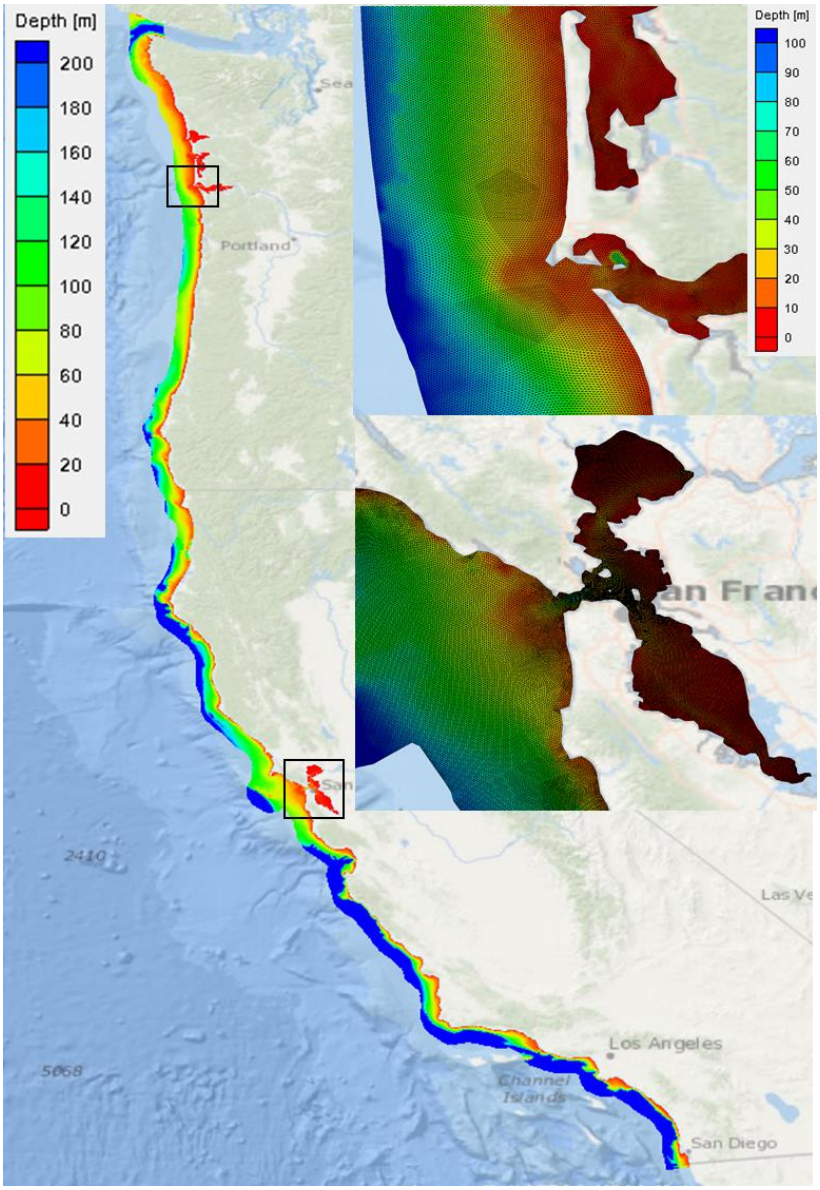

Figure 2.3. Bathymetry distribution of the UnSWAN model for the U.S. West Coast. The two map inserts show the close-up model grid and bathymetry for the Columbia River Estuary and San Francisco Bay areas.

2.3 Model Forcing

In this study, the model hindcast covered the long-term period of 32 years from 1979 to 2010, which corresponds to the data availability period of the Climate Forecast System Reanalysis (CFSR), produced by NCEP. The wind forcing data (wind speeds and directions) for the wave hindcast were obtained from CFSR and interpolated onto the model grid points at hourly intervals. Comparison of CFSR wind speed with observed data at a number of NDBC buoy stations indicated that the CFSR wind speed is generally in good agreement with the observed speed and reasonably captures the diurnal and seasonal variabilities. The CFSR data meet the minimum one-hour temporal resolution requirements specified by the IEC TS (IEC, 2015) for design assessments. Figure 2.4 shows an example of global CFSR wind speed distribution on December 3, 2007.

The sea ice coverage data were downloaded from the same NCEP CFSR data set as the wind data, except that the original sea ice data were defined in the NCEP T382 Gaussian Grid that has a spatial resolution of 38 km. The sea ice data were subsequently re-projected onto the same 0.5 × 0.5 degree regular grid as the wind forcing data and implemented as daily temporal resolution. As indicated in previous studies (García-Medina et al., 2014; Yang et al., 2017), the effect of tides and currents on wave climate on the West Coast at regional scales is not important. Therefore, currents induced by tides and ocean circulations were not considered in this study.

In addition to the long-term 32-year model hindcast, a year-long simulation was conducted for the period of March 2017 to April 2018 for validation purposes, corresponding to the new shallow-water buoy measurements conducted by National Renewable Energy Laboratory (NREL). The model configuration for the year-long simulation was kept the same as those in the long-term model hindcast. Wind forcing was obtained from the second version of CFSR (CFSv2), which covers the period from 2011 to the present.

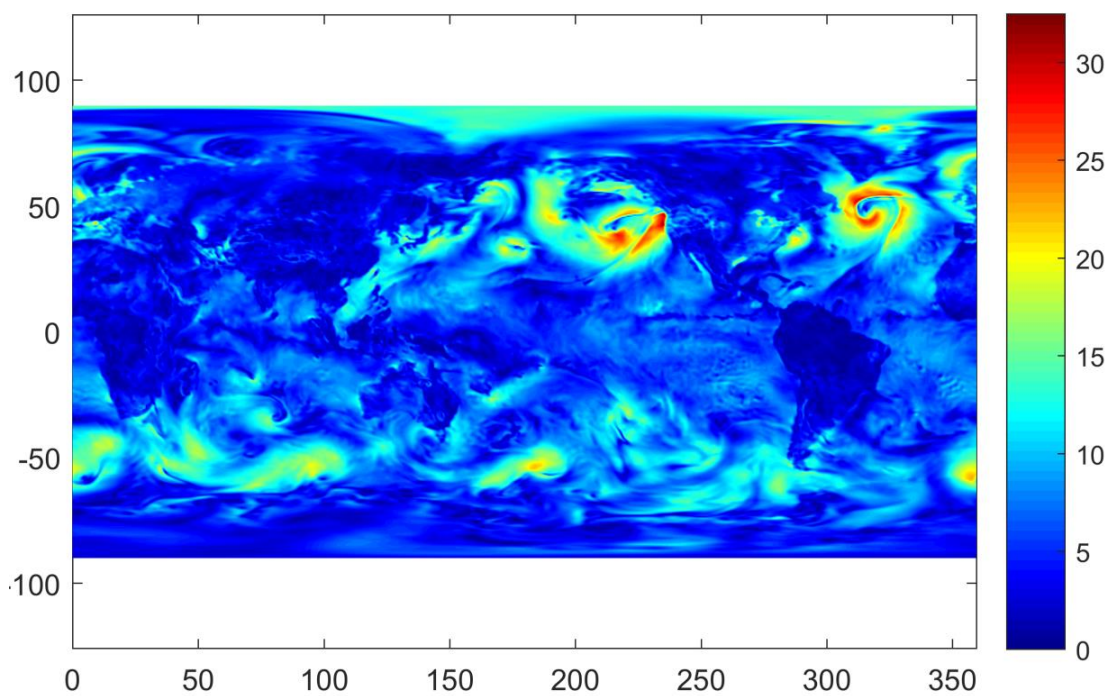

Figure 2.4. The global distribution of CFSR wind field on December 3, 2007. The extra-tropical wind storm "Great Coastal Gale" is well presented in the northeastern Pacific Ocean.

The UnSWAN model was driven by the WWIII model outputs along the UnSWAN model open boundary. Full 2D spectral boundary conditions were used at the open boundary to allow for the propagation of multimodal sea states.

Figure 2.5 shows monthly averaged significant wave height distribution around U.S. continental coastal waters and Caribbean Islands simulated using the nested-grid WWIII for July and November, respectively. Improvement in spatial resolution along the U.S. West Coast is shown clearly. In Section 3.0, **Figure 3.1** also shows that significant wave height in November (winter) is much higher than that in July (summer).

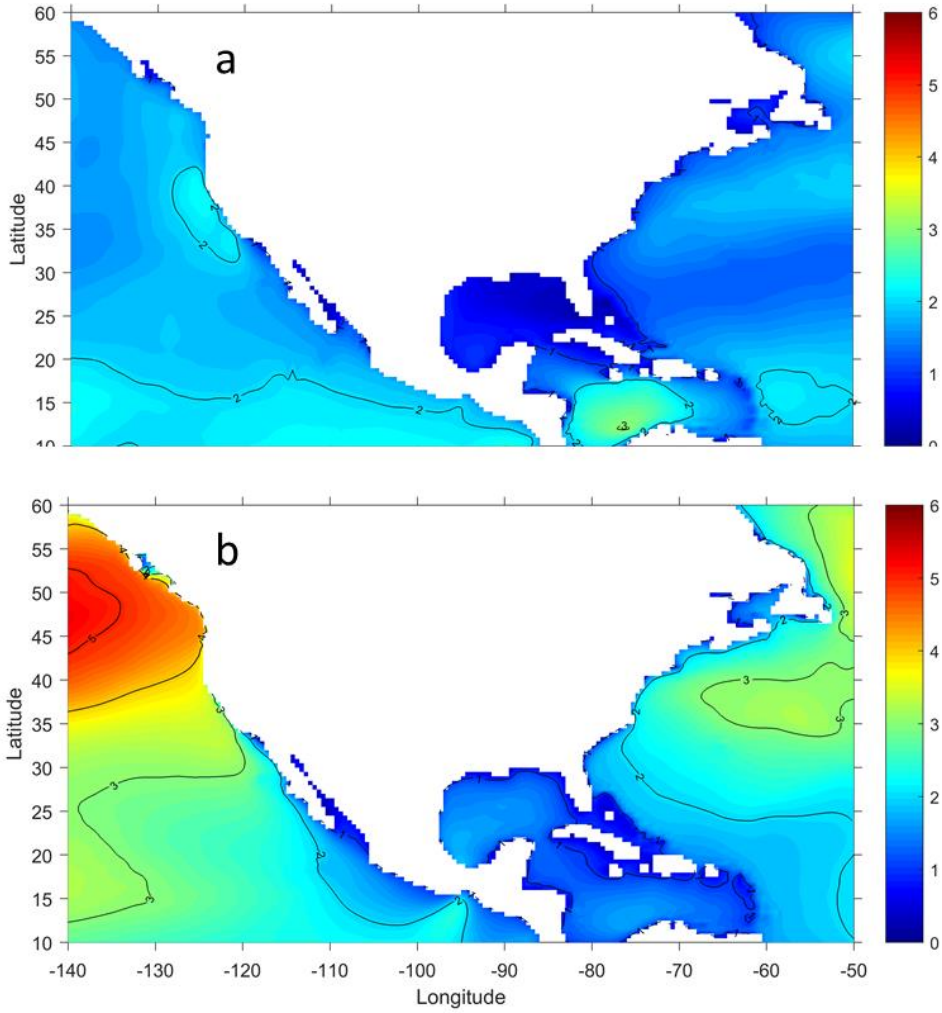

Figure 2.5. Simulated monthly average significant wave height (m) with (a) WWIII for July and (b) November.

2.4 Measured Data for Model Validation

Model validation was conducted using measured data from wave buoys maintained by NDBC and CDIP. Two types of measured data are available from these wave buoys—directional spectral data and bulk wave parameters. In this study, buoys with either wave spectral data or bulk parameters having at least 20 years of record from 1979 to 2010 were used for model validation. A total of 28 wave buoys on the West

Coast meet these criteria (Table 2.3). A total of 23 buoys with spectral data can be used to calculate the six IEC resource parameters for model validation. Five bulk parameter buoys with long-term records (> 20 years) can be used to validate the model by comparing bulk parameters, such as significant wave height, peak period and peak direction. Note that some of the spectral buoy stations also contain long-term (>20 years) measurements of bulk parameters.

Table 2.3. Summary of wave buoys with directional spectral[(a)] data and long-term (>20 years) bulk parameter for model validation.

Agency	Buoy	Longitude	Latitude	Depth (m)	Period		Years	
					Param	Spec	Param	Spec
NDBC	46087	-124.728	48.494	257	2004 - 2009	2004 - 2009	6	6
NDBC	46041	-124.731	47.353	114	1987 - 2010	1998 - 2010	24	13
CDIP	46211	-124.244	46.858	40	1981 - 1983 1985 - 2010	1993 - 2010	29	18
NDBC	46029	-124.514	46.159	145	1984 - 1987 1991 - 2010	1997 - 2010	24	14
NDBC	46005	-131.001	46.1	2853	1979 - 2004 2006 - 2008 2010		30	0
NDBC	46050	-124.526	44.656	137	1991 - 2010	2008 - 2010	20	3
CDIP	46229	-124.551	43.766	183	2005 - 2010	2006 - 2010	6	5
NDBC	46015	-124.832	42.764	420	2002 - 2010	2007 - 2010	9	4
NDBC	46002	-130.474	42.589	3368	1979 - 1998 2000 - 2009		30	0
NDBC	46027	-124.382	41.852	46	1983 - 2010	2005 - 2010	28	6
NDBC	46022	-124.531	40.72	391	1982 - 2010	2007 - 2010	29	4
CDIP	46213	-124.719	40.288	367	2004 - 2010	2004 - 2010	7	7
NDBC	46014	-123.974	39.235	256	1981 - 2010		30	0
NDBC	46013	-123.307	38.238	123	1981 - 2010	2007 - 2010	30	4
NDBC	46026	-122.839	37.755	53	1982 - 2010	2007 - 2010	29	4
NDBC	46012	-122.881	37.363	209	1980 - 2010	2010	31	1
NDBC	46042	-122.452	36.791	2098	1987 - 2010	1998 - 2010	24	13
CDIP	46236	-121.949	36.76	168	2007 - 2010	2007 - 2010	4	4
NDBC	46028	-121.858	35.712	1036	1983 - 2010	2002 - 2010	28	9
CDIP	46215	-120.859	35.204	23	1983 - 2010	1996 - 2010	28	15
NDBC	46011	-121.019	34.956	465	1980 - 1992 1994 - 2010	2005 - 2010	30	6
NDBC	46023	-120.967	34.714	384	1982 - 2010		29	0
CDIP	46216	-119.803	34.333	183	2002 - 2010	2002 - 2010	9	9
NDBC	46063	-120.699	34.273	632	1998 - 2009	2006 - 2009	12	4
CDIP	46221	-118.633	33.854	363	2000 - 2010	2000 - 2010	11	11
NDBC	46025	-119.053	33.749	905	1982 - 2010	2008 - 2010	29	3

Agency	Buoy	Longitude	Latitude	Depth (m)	Period		Years	
					Param	Spec	Param	Spec
CDIP	46224	-117.471	33.179	220	1997 - 2010	1997 - 2010	14	14
NDBC	46047	-119.498	32.398	1442	1991 - 1993 1999 - 2010	2007 - 2010	15	4
NREL	46260	-124.29	43.586	87	2017 - 2018	2017 - 2018	1	1
NREL	46261	-124.225	43.76	44.2	2017 - 2018	2017 - 2018	1	1
NREL	46263	-123.912	39.37	130	2017 - 2018	2017 - 2018	1	1

In addition to the wave data for the 1979–2010 period, measurements from three new Waverider® buoys from April 2017 to March 2018 were also used for model validation. The new buoys were deployed by NREL along the Oregon and California coasts to fill the data gaps at shallow to intermediate water depths. Locations of wave buoys for model validation are shown in Figure 2.6. The distribution of these wave buoys covers the entire West Coast, providing sufficient data sets for a thorough model validation.

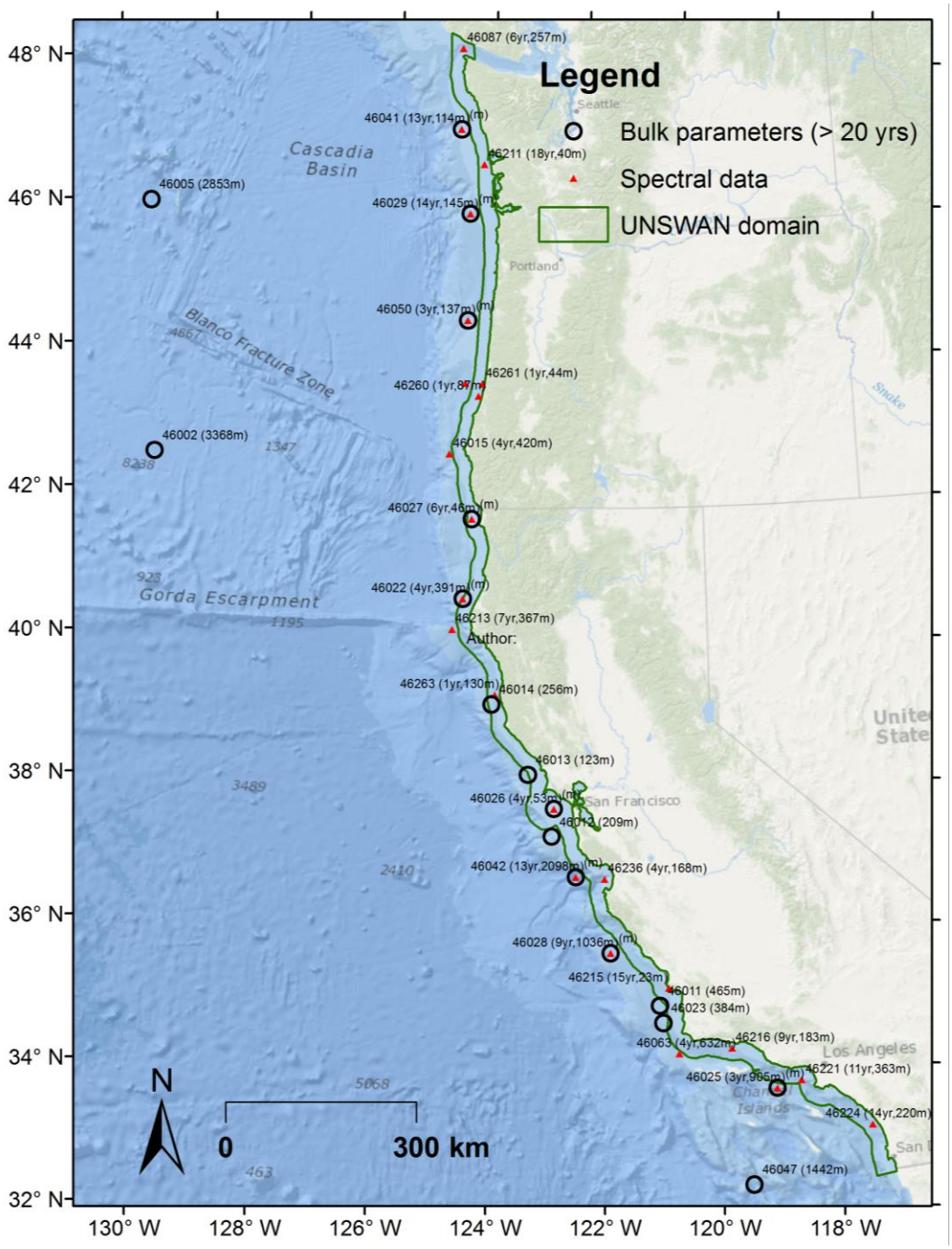

Figure 2.6. Wave buoy stations for model validation. Red triangle represents wave buoys with 2D spectral data and black circle represents wave buoys with at least 20 years of records for wave bulk parameters.

3.0 Model Hindcast and Validation

The regional wave hindcast for the West Coast was conducted using the WWIII and UnSWAN models for the period of 1979–2010, as well as the period of 4/2017–3/2018. Model hindcast and validation for

the six IEC-recommended wave resource parameters derived from the model hindcast and measured spectral data are described in this section.

3.1 Simulation of IEC Resource Parameters

The six wave resource parameters recommended by IEC TS (2015) were calculated based on model results of directional wave spectra and measured wave spectral data. The six IEC parameters include omnidirectional wave power, significant wave height, energy period, spectral width, direction of maximum directionally resolved wave power, and directionality coefficient, which are defined below.

The omnidirectional wave power, J, is the sum of the contributions to energy flux from each of the components of the wave spectrum,

$$J = \rho g \sum_{i,j} c_{g,i} S_{ij} \Delta f_i \, \Delta\theta_j \tag{1}$$

where
ρ = the density of sea water,
g = the acceleration due to gravity,
$c_{g,i}$ = the group velocity,
Δf_i = the frequency bin width at each discrete frequency index i, and
$\Delta\theta_i$ = the direction bin width at each discrete direction index j.

Directionally integrated parameters are calculated from one-dimensional (unresolved) frequency variance density using the equation

$$S_i = \sum_j S_{ij} \Delta\theta_j. \tag{2}$$

For the purpose of the present study the significant wave height is defined as the zeroth frequency of the spectral moment as

$$H_s \sim H_{m0} = 4\sqrt{m_0}\,, \tag{3}$$

where the moments of a variance spectrum are generally defined as

$$m_n = \sum_i f_i^n S_i \Delta f_i. \tag{4}$$

H_s is typically paired with the energy period, T_e, calculated as

$$T_e = \frac{m_{-1}}{m_0}, \tag{5}$$

to define a wave climate's sea state. The energy period is the variance-weighted mean period of the directionally unresolved variance density spectrum. It is preferred over the peak period, because it is not sensitive to the spectral shape.

The spectral width, ϵ_0

$$\epsilon_0 = \sqrt{\frac{m_0 m_{-2}}{(m_{-1})^2} - 1}, \tag{6}$$

is a measure of the spreading of energy along the wave spectrum. The directionally resolved wave power is the sum of the wave power at each direction, θ:

$$J_\theta = \rho g \sum_{i,j} c_{g,i} S_{ij} \Delta f_i \, \Delta\theta_j cos(\theta - \theta_j)\delta \tag{7}$$

$$\begin{cases} \delta = 1, \ cos(\theta - \theta_j) \geq 0 \\ \delta = 0, \ cos(\theta - \theta_j) < 0 \end{cases}$$

where J_θ is the directionally resolved wave power in direction θ. The maximum time-averaged wave power propagating in a single direction, J_{θ_J}, is the maximum value of J_θ. The corresponding direction, θ_J, is the direction of maximum directionally resolved wave power and describes the characteristic direction of the sea state.

The directionality coefficient, d, is the ratio of maximum directionally resolved wave power to the omnidirectional wave power,

$$d_\theta = \frac{J_{\theta_{jmax}}}{J}, \tag{8}$$

which is a characteristic measure of directional spreading of wave power.

Out of the six IEC parameters, only two parameters—significant wave height (H_s) and energy period (T_e)—are calculated in UnSWAN and WWIII models as default bulk parameters. Therefore, the UnSWAN and WWIII source codes were modified to calculate the other four IEC parameters (J, ϵ_0, θ_J, d_θ) internally. The model source codes were also modified to include all six IEC parameters in the bulk parameter output option.

Figure 3.1 shows the two-dimensional (2D) distributions of the 32-year annual averages of six IEC parameters simulated by UnSWAN. In general, high wave power density occurs along the Washington, Oregon, and northern California coasts. Mean significant wave height and mean energy period are generally greater than 2 m and 10 s, respectively, on the Washington, Oregon, and northern California coasts. Wave power drops rapidly on the southern California coast, especially south of Santa Maria. Spatial distribution of mean spectral width varies in a small range, from 0.3 to 0.4 on the Washington, Oregon, and northern California coasts, and up to 0.5 on the southern California coast. The mean direction of maximum directionally resolved wave power typically falls in the range of 270º to 330º (from the northwest direction) along most of the West Coast, except in southern California, where wave action primarily propagates from the southwest direction (210º – 270º). The directionality coefficient on the West Coast is generally above 0.8, indicating a narrow spread of wave power. The spatial variation of the IEC parameters across-shore is clearly seen in the high-resolution model results (e.g., H_s, T_e, and d_θ), which is important for wave resource characterization related to WEC project siting.

Monthly averaged 2D distributions of the six IEC parameters based on 32 years of model results were also calculated. Horizontal 2D plots of the monthly results from January to December are provided in Appendix A. Examples of 2D distributions of the monthly averages of six IEC parameters in July and

December are shown in Figure 3.2 and Figure 3.3, respectively, in which strong seasonal variations are shown. J, H_s, T_e, and d_θ are much greater in winter (December) than those in the summer (July). Although not as strong as other four IEC parameters, weak seasonal variations are observed in ϵ_0 and θ_J, with both being slightly greater in the summer.

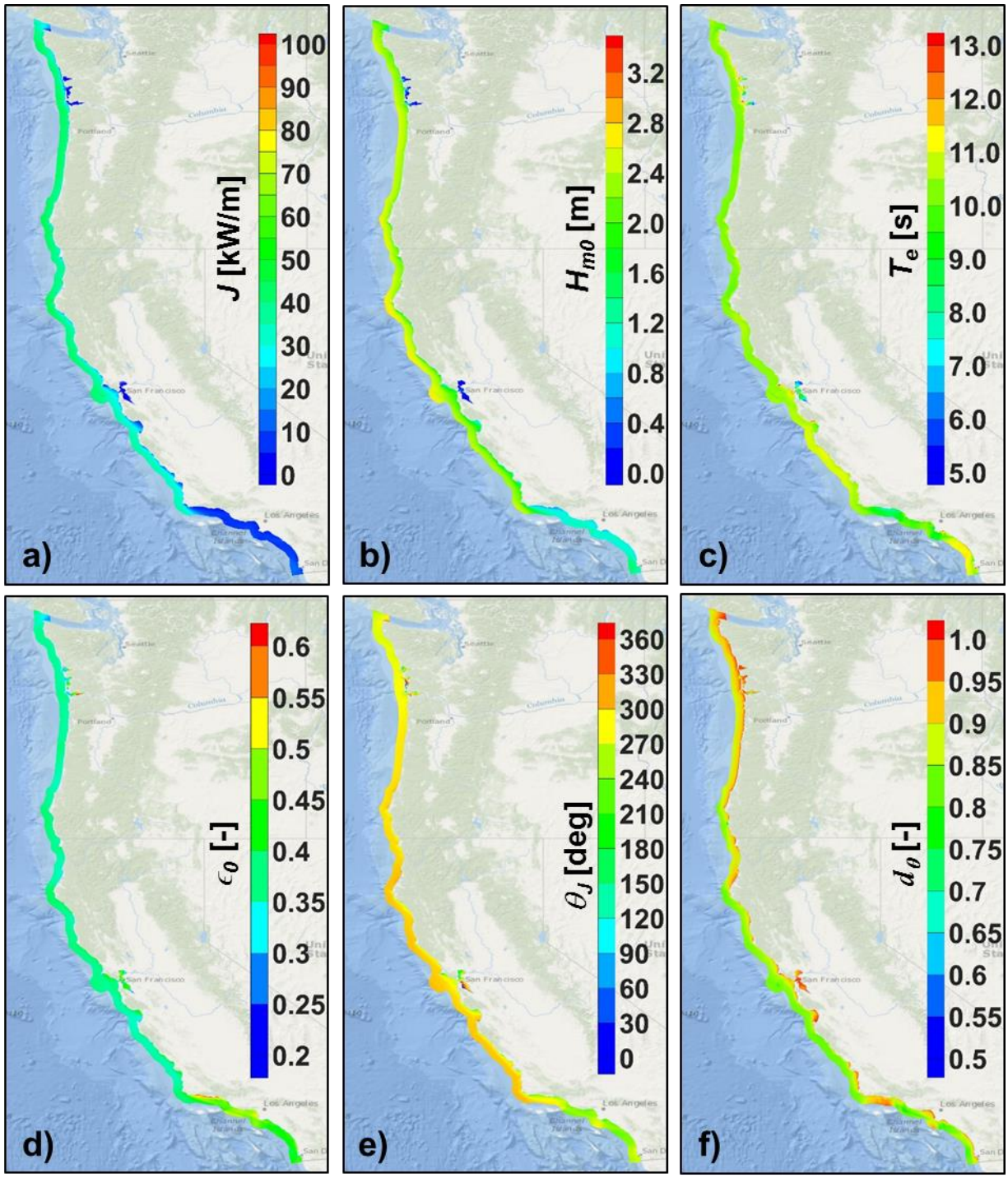

Figure 3.1. Simulated 32-year annual distribution of six IEC wave resource parameters: (a) omnidirectional wave power, (b) significant wave height, (c) energy period, (d) spectral width, (e) direction of maximum directionally resolved wave power, and (f) directionality coefficient.

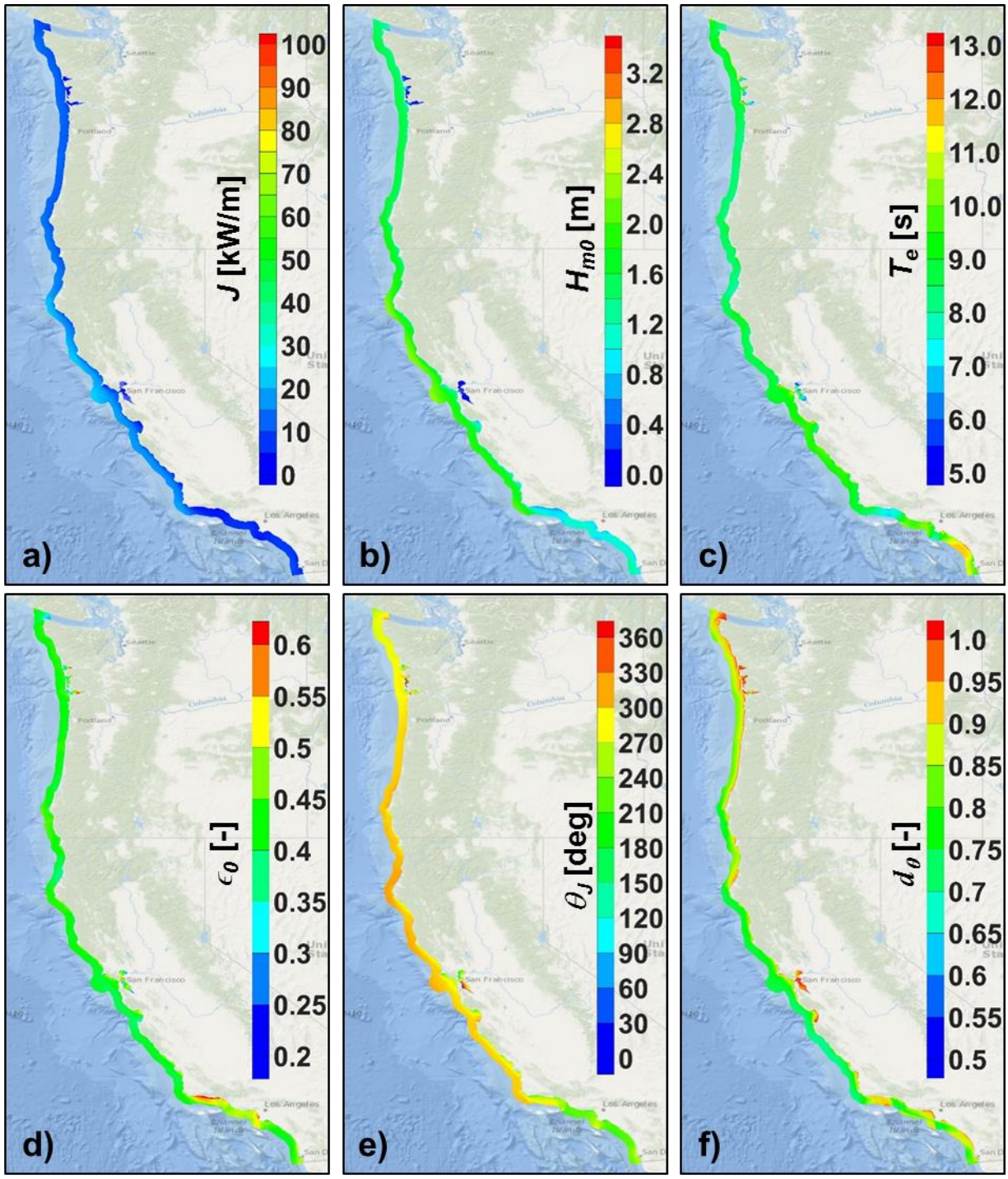

Figure 3.2. Simulated monthly distribution of six IEC wave resource parameters in July: (a) omnidirectional wave power, (b) significant wave height, (c) energy period, (d) spectral width, (e) direction of maximum directionally resolved wave power, and (f) directionality coefficient.

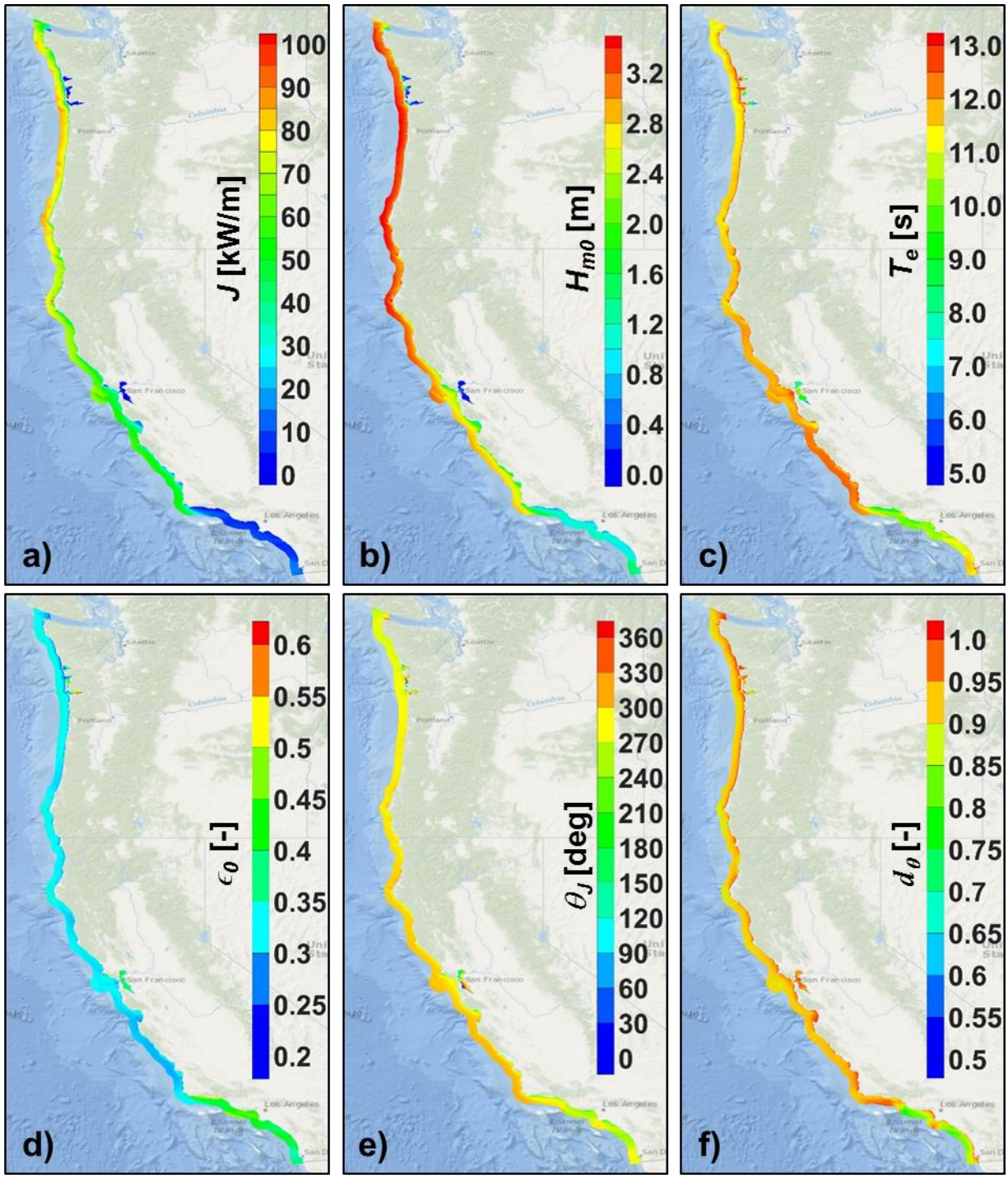

Figure 3.3. Simulated monthly distribution of six IEC wave resource parameters in December: (a) omnidirectional wave power, (b) significant wave height, (c) energy period, (d) spectral width, (e) direction of maximum directionally resolved wave power, and (f) directionality coefficient.

3.2 Model Validation

In this study, model validation was conducted by comparing six simulated and measured IEC parameters at buoy stations. Specifically, comparisons of time history and scatter plots of the simulated and measured six IEC parameters were generated and model performance metrics were calculated to evaluate the model skills for reproducing the six IEC parameters. The following common model performance metrics used in previous studies (García-Medina et al., 2014; García-Medina et al., 2013; Wu et al., 2018; Yang et al., 2017) were adopted in this study for model validation.

The root-mean-square-error (*RMSE*), *aka* root-mean-square-deviation, is defined as

$$RMSE = \sqrt{\frac{\sum_{i=1}^{N}(P_i - M_i)^2}{N}} \tag{9}$$

where N is the number of observations, M_i is the measured value, and P_i is the predicted value.

RMSE represents the sample standard deviation of the differences between predicted values and measured values.

The percentage error (*PE*) is defined as

$$PE(\%) = \frac{100}{N}\sum_{i=1}^{N}\left(\frac{P_i - M_i}{M_i}\right) \tag{10}$$

and is the average *PE* over the period of comparison.

The scatter index (*SI*) is the *RMSE* normalized by the average of all measured values over the value of comparison, where

$$SI = \frac{RMSE}{\bar{M}}, \tag{11}$$

where the overbar indicates the mean of the measured values.

Model bias, which represents the average difference between the predicted and measured value, is defined as

$$Bias = \frac{1}{N}\sum_{i=1}^{N}(P_i - M_i). \tag{12}$$

Percentage bias, which is defined as

$$Bias(\%) = \frac{\sum_{i=1}^{N} P_i - \sum_{i=1}^{N} M_i}{\sum_{i=1}^{N} M_i} \cdot 100 \tag{13}$$

is also commonly used to normalize bias.

The linear correlation coefficient, R, is defined as

$$R = \frac{\sum_{i=1}^{N}(M_i - \bar{M})(P_i - \bar{P})}{\sqrt{\left(\sum_{i=1}^{N}(M_i - \bar{M})^2\right)\left(\sum_{i=1}^{N}(P_i - \bar{P})^2\right)}} \tag{14}$$

and is a measure of the strength of the linear relationship between the predicted and measured values.

Comparisons of time series and scatter plots of the six IEC parameters between model results and observed data for every year at each station were generated. There are a total of 166 year-station time series and scatter plots, which are presented in Appendix B. Here only few examples at selected stations and for selected years are presented. Figure 3.4 to Figure 3.7 show time series and scatter plots of modeled results and observed data at Station 46211 in Washington, Station 46229 in Oregon, Station 46026 in northern California, and Station 46215 in southern California for the year of 2008, respectively. Overall, model results match observed data well. Both model results and observations showed similar trends in the seasonality of the six IEC parameters on the Washington, Oregon, and California coasts. Similar to the 2D distributions of the six IEC parameters (Figure 3.1), significant wave height and wave power density on the Washington and Oregon coasts (Stations 46211 and 46229) are generally greater than those on the California coast. Time series plots also show strong seasonal variability in J, H_s, and T_e, as indicated by the 2D plots (Figure 3.2 and Figure 3.3).

Comparisons of model-simulated and data-derived IEC parameters at the three shallow-water buoy stations (46260, 46261, and 46263) for the 4/2017–3/2018 period are shown in Figure 3.8 through Figure 3.10. Similarly, the model performed very well in reproducing the time histories of the IEC parameters at these shallow-water buoy stations, especially in capturing the extreme wave events that occurred in January 2018.

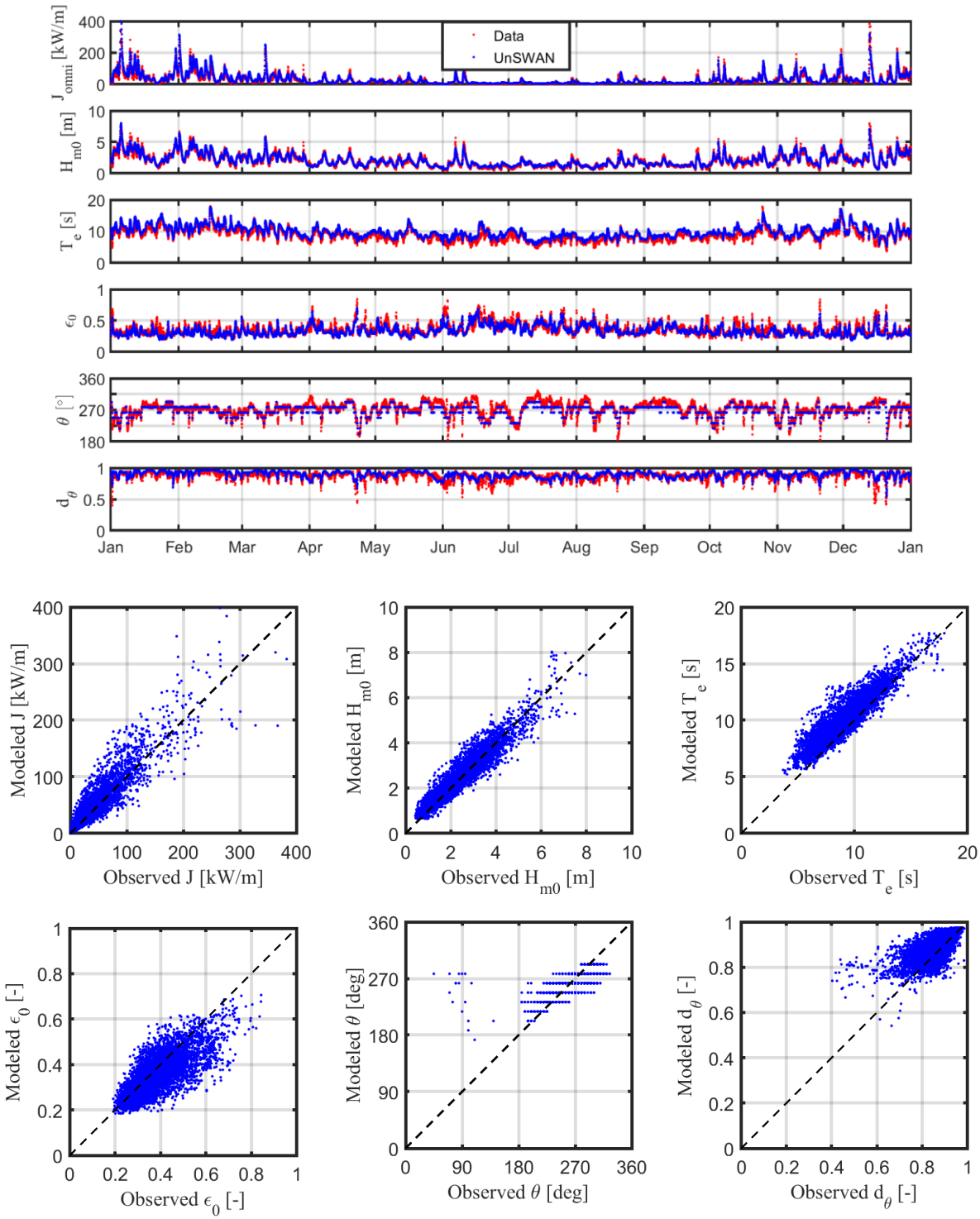

Figure 3.4. Time series (top) and scatter plots (bottom) of the six modeled and observed IEC wave resource parameters for 2008 at Buoy 46211 in Washington.

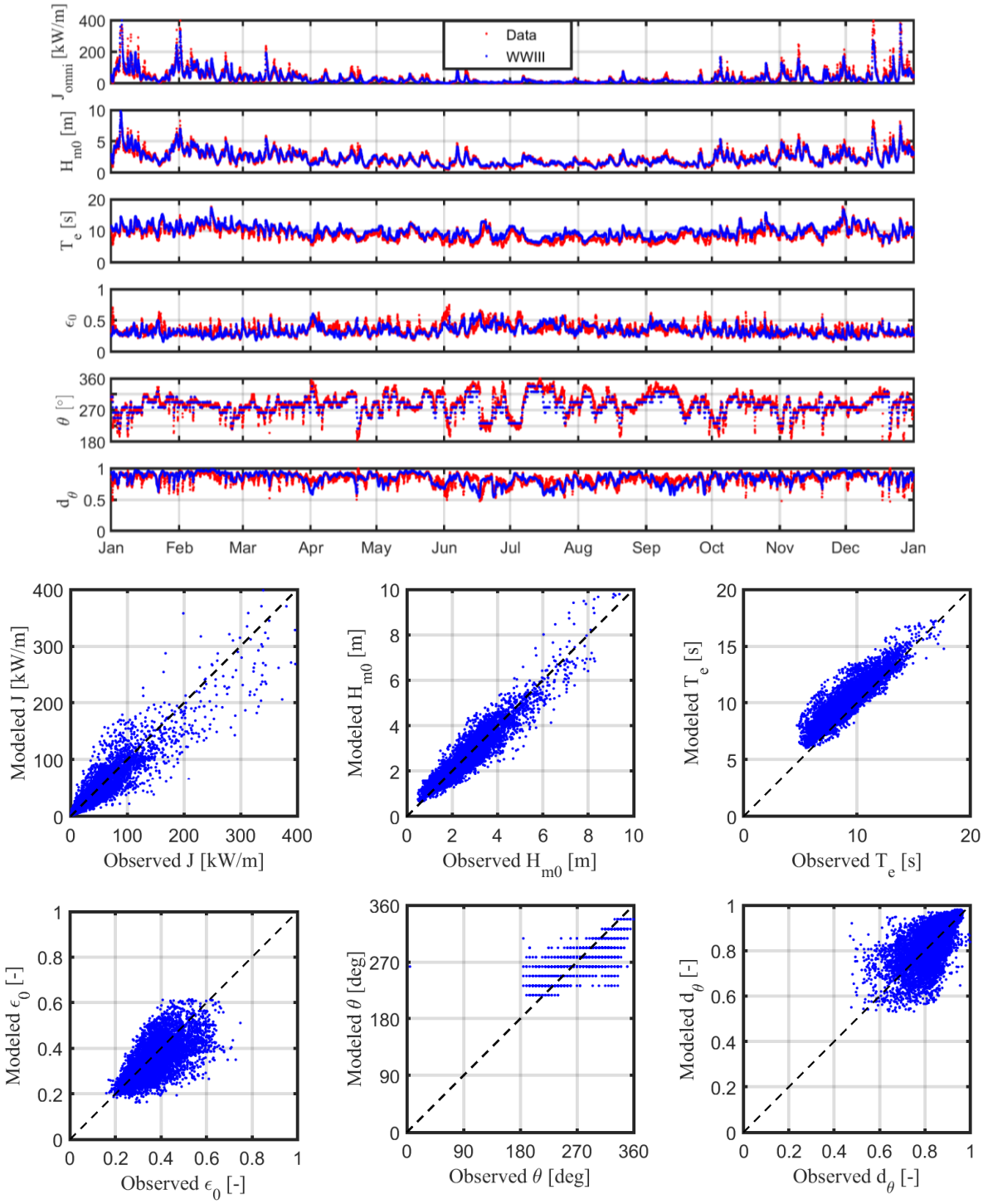

Figure 3.5. Time series (top) and scatter plots (bottom) of the six modeled and observed IEC wave resource parameters for 2008 at Buoy 46229 in Oregon.

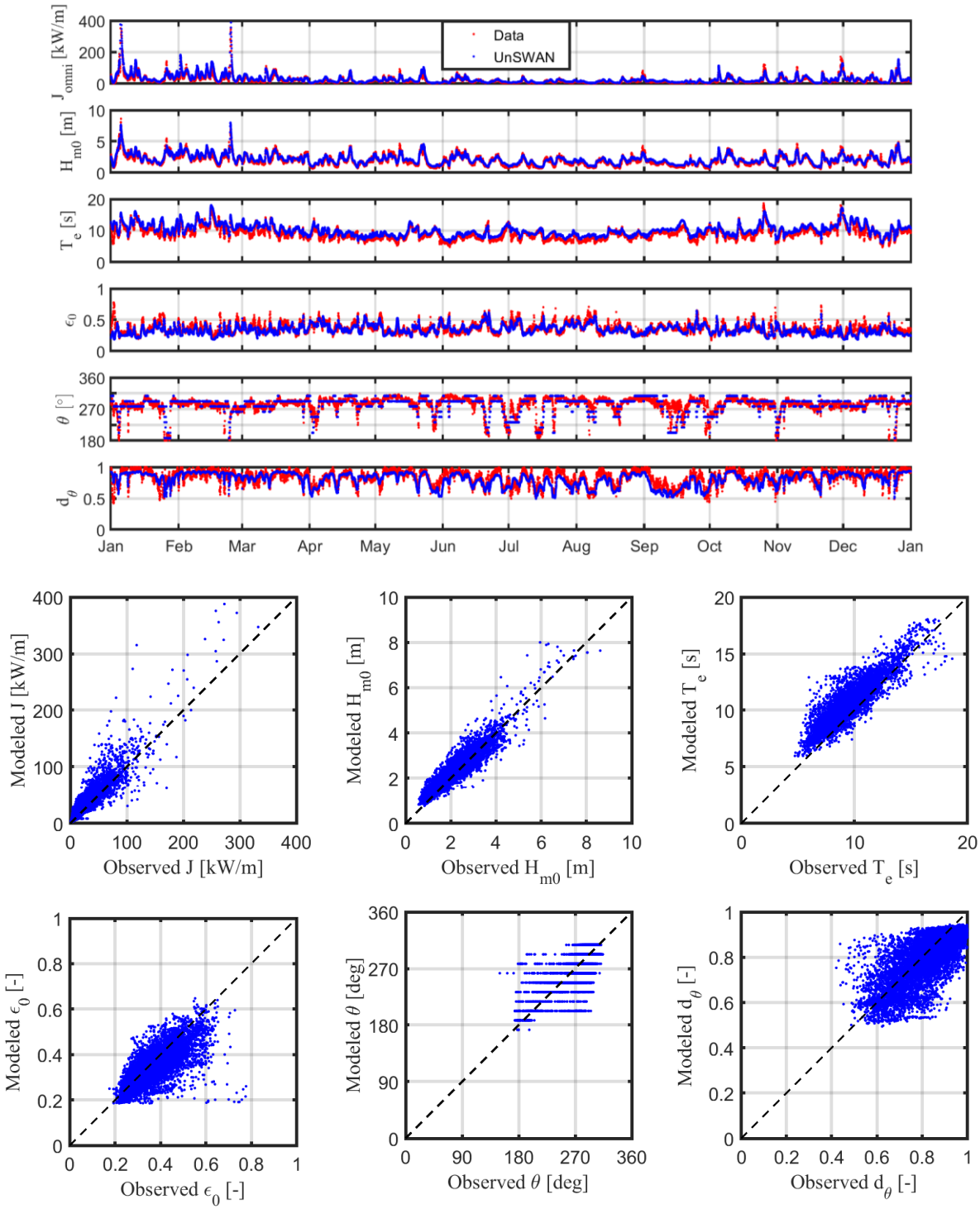

Figure 3.6. Time series (top) and scatter plots (bottom) of the six modeled and observed IEC wave resource parameters for 2008 at Buoy 46026 in Northern California.

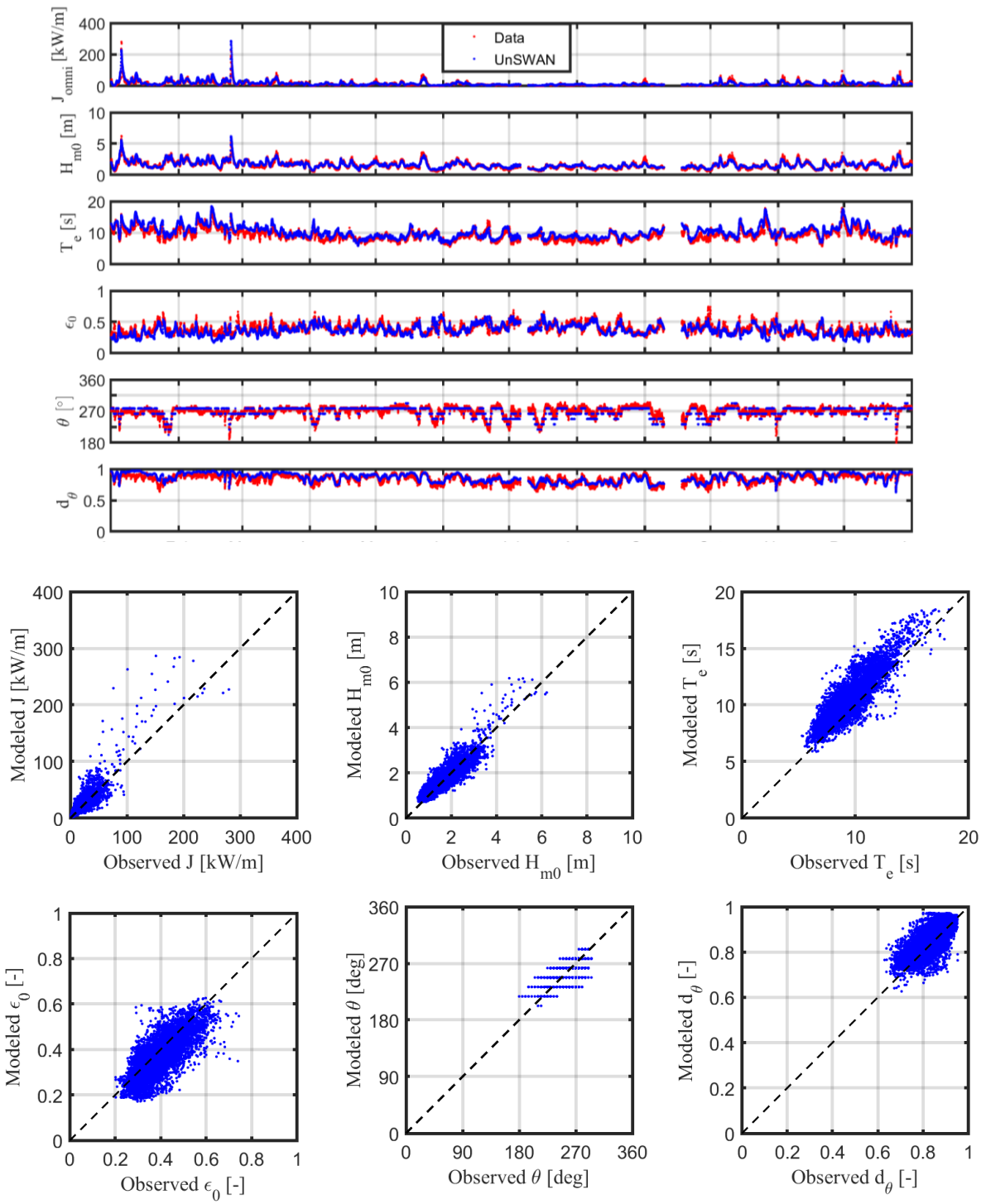

Figure 3.7. Time series (top) and scatter plots (bottom) of the six modeled and observed IEC wave resource parameters for 2008 at Buoy 46215 in Southern California.

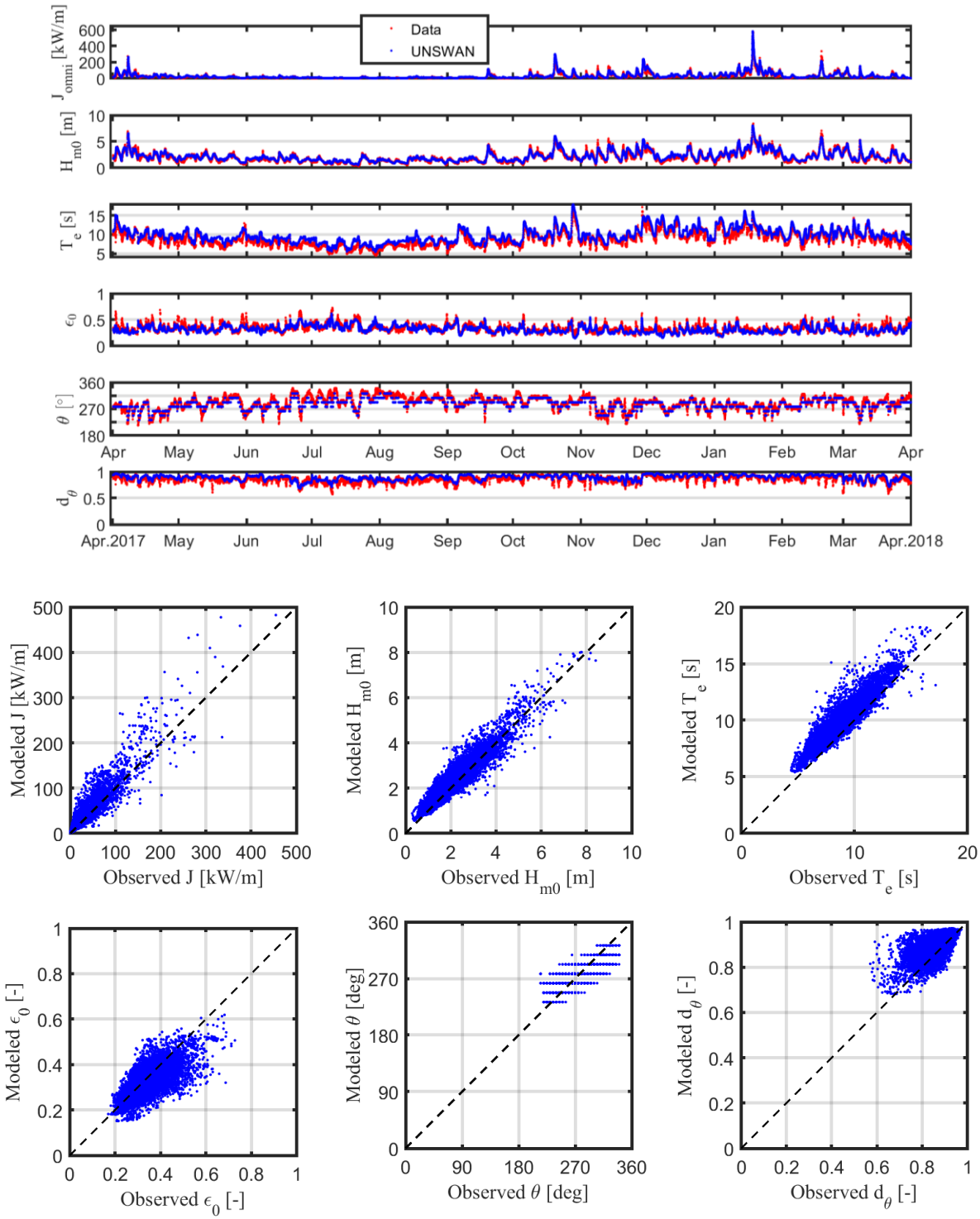

Figure 3.8. Time series (top) and scatter plots (bottom) of the six modeled and observed IEC wave resource parameters from April 2017 to March 2018 at Buoy 46260 in Oregon.

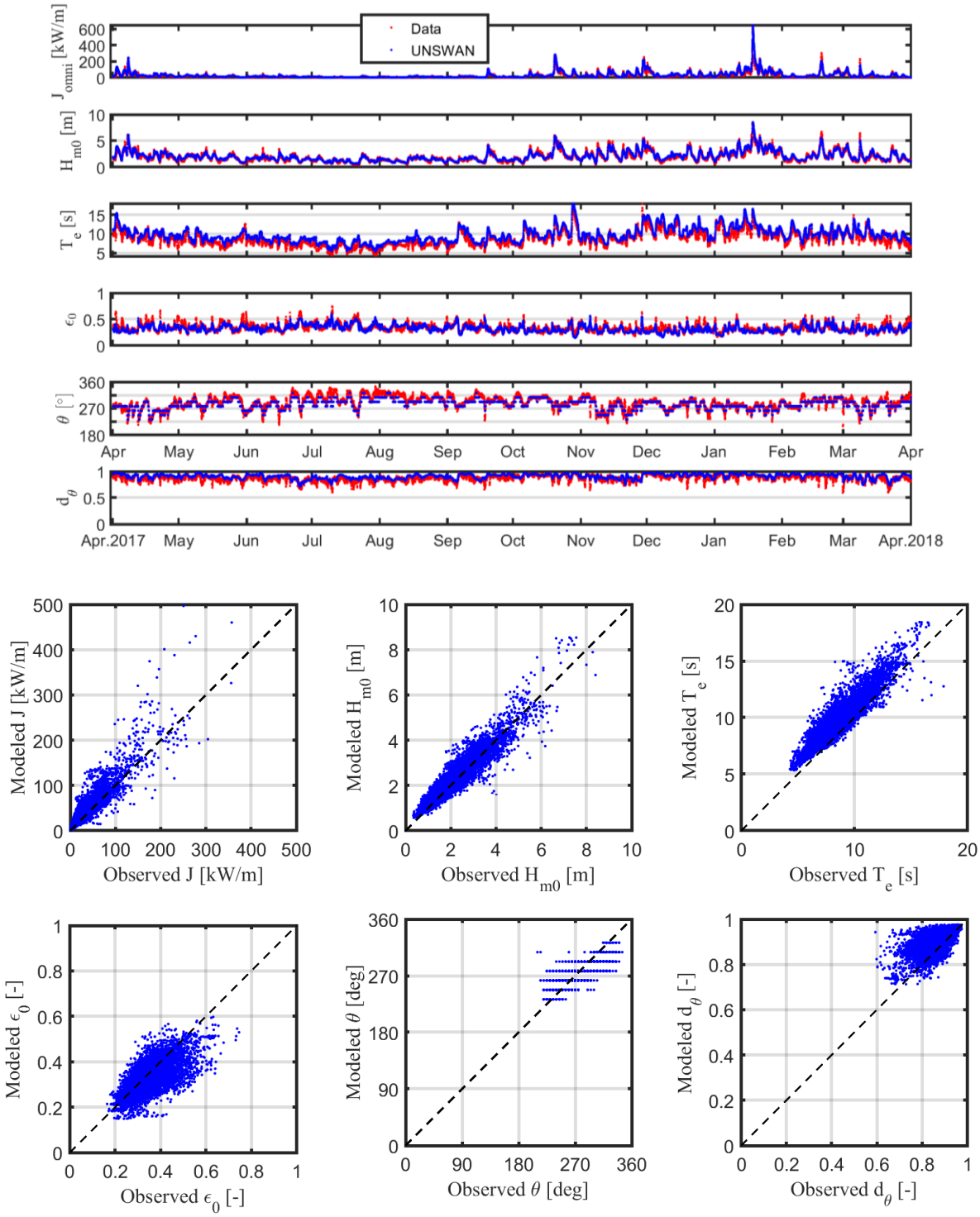

Figure 3.9. Time series (top) and scatter plots (bottom) of the six modeled and observed IEC wave resource parameters from April 2017 to March 2018 at Buoy 46261 in Oregon.

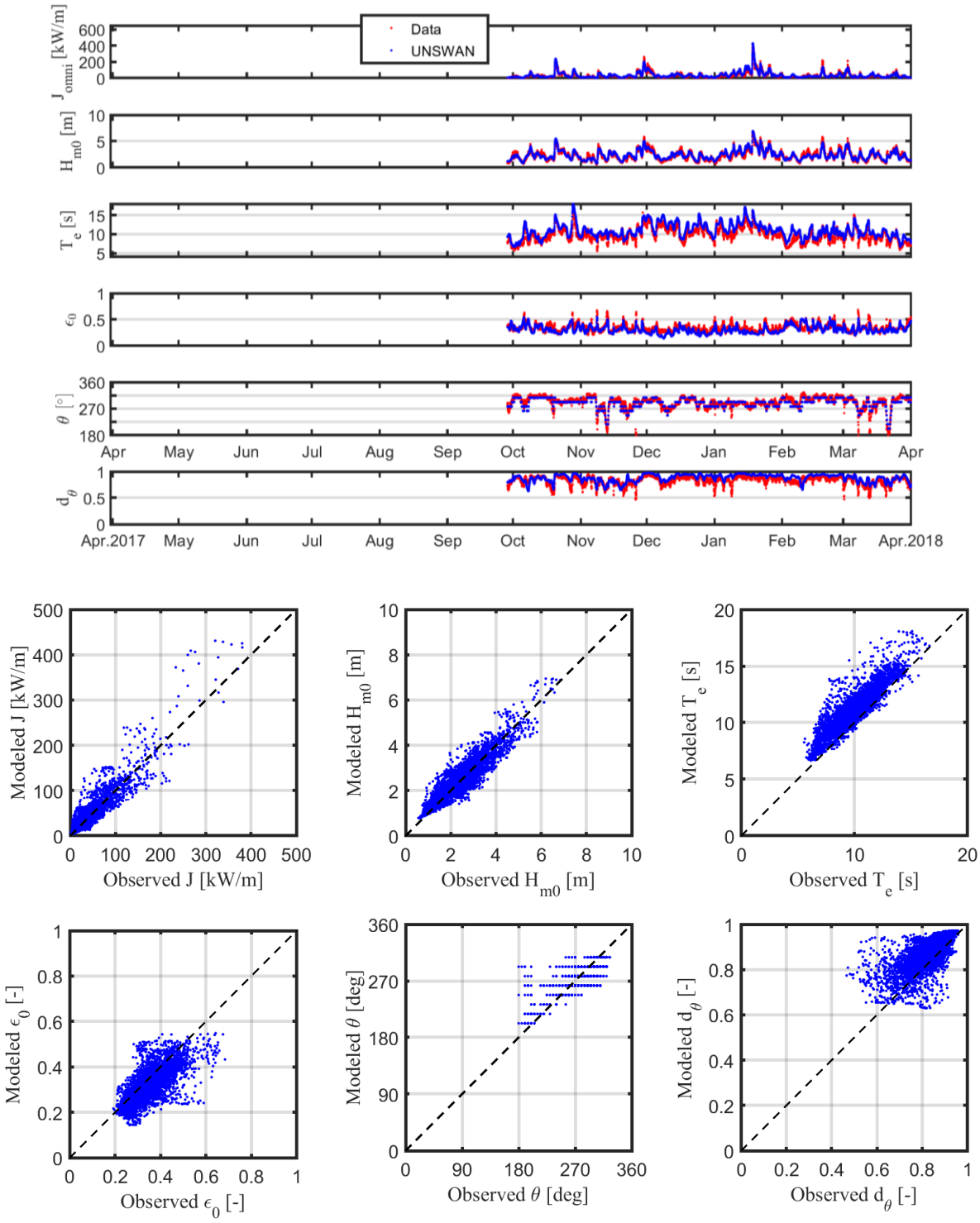

Figure 3.10. Time series (top) and scatter plots (bottom) of the six modeled and observed IEC wave resource parameters from October 2017 to March 2018 at Buoy 46263 in California.

The results of the yearly averages of performance metrics (error statistics) for the six IEC resource parameters were calculated at every spectral buoy station and are provided in Appendix C. Examples of performance metrics for the six simulated IEC resource parameters at Buoys 46211, 46229, 46026, and

46215 for the year 2008 are shown in Table 3.1 through Table 3.4, respectively. The error statistics between model results and observed data at the new buoy stations at Buoys 46260, 46261, and 46263 are shown in Table 3.5 through Table 3.7.

The 32-year averages of all model performance error statistics for the six IEC resource parameters at every buoy station were calculated and are provided in Appendix D. As an example, root-mean-square-error (RMSE) and linear correlation coefficient (R), as listed in Table 3.8, are the most-commonly used model performance metrics.

Overall, error statistics between model results and observed data show good model performance in simulating the six IEC parameters. For example, the R values are above 0.9 for J, H_s, and T_e at most stations and above 0.6 for ϵ_0, θ_J, and d_θ, which are also considered well correlated considering the challenge of simulating wave direction and spectral spreading at a model spectral resolution of 15° as well as high uncertainties in the direction measurements.

Table 3.1. Performance metrics of the six simulated IEC resource parameters for 2008 at Buoy 46211.

Parameter	RMSE	PE (%)	SI	Bias	Bias (%)	R
J (kW/m)	16	34.2	0.55	4	15.2	0.93
H_s (m)	0.32	7.4	0.16	0.07	3.6	0.95
T_e (s)	1.2	11.3	0.13	0.9	10.2	0.92
ϵ_0 (-)	0.06	-5.8	0.17	-0.03	-7.1	0.78
θ (degrees)	13.5	-1.2	0.05	-4	-1.6	0.80
d_θ (-)	0.05	2.9	0.06	0.02	2.6	0.72

Table 3.2. Performance metrics of the six simulated IEC resource parameters for 2008 at Buoy 46229.

Parameter	RMSE	PE (%)	SI	Bias	Bias (%)	R
J (kW/m)	19	11.8	0.50	-2	-4.1	0.93
H_s (m)	0.37	3.1	0.16	0.00	0.0	0.95
T_e (s)	1.2	11.6	0.14	0.9	10.3	0.91
ϵ_0 (-)	0.07	-3.8	0.19	-0.02	-5.3	0.69
θ (degrees)	16.5	-0.9	0.06	-5	-1.6	0.85
d_θ (-)	0.07	1.1	0.08	0.01	0.8	0.68

Table 3.3. Performance metrics of the six simulated IEC resource parameters for 2008 at Buoy 46026.

Parameter	RMSE	PE (%)	SI	Bias	Bias (%)	R
J (kW/m)	14	46.8	0.60	6	26.5	0.93
H_s (m)	0.34	12.4	0.17	0.16	8.1	0.94
T_e (s)	1.3	12.0	0.14	1.0	11.0	0.91
ϵ_0 (-)	0.06	-5.1	0.17	-0.02	-6.3	0.73
θ (degrees)	16.0	0.2	0.06	0	0.0	0.77
d_θ (-)	0.08	-2.2	0.10	-0.02	-2.9	0.74

Table 3.4. Performance metrics of the six simulated IEC resource parameters for 2008 at Buoy 46215.

Parameter	RMSE	PE (%)	SI	Bias	Bias (%)	R
J (kW/m)	9	27.9	0.57	2	14.0	0.89
H_s (m)	0.27	6.5	0.17	0.05	3.4	0.90
T_e (s)	1.3	10.0	0.14	0.9	9.6	0.88
ϵ_0 (-)	0.06	-5.4	0.16	-0.02	-6.0	0.76
θ (degrees)	10.6	-0.5	0.04	-2	-0.6	0.73
d_θ (-)	0.05	2.3	0.06	0.02	2.2	0.77

Table 3.5. Performance metrics of the six simulated IEC resource parameters for the 4/2017–3/2018 period at Buoy 46260.

Parameter	RMSE	PE (%)	SI	Bias	Bias (%)	R
J (kW/m)	16	44.2	0.62	6	24.0	0.94
H_s (m)	0.36	10.3	0.18	0.14	6.7	0.94
T_e (s)	1.3	12.4	0.14	1.0	11.5	0.92
ϵ_0 (-)	0.06	-5.1	0.17	-0.02	-6.5	0.72
θ (degrees)	12.1	-1.2	0.04	-4	-1.4	0.86
d_θ (-)	0.06	4.0	0.06	0.03	3.8	0.67

Table 3.6. Performance metrics of the six simulated IEC resource parameters for the 4/2017–3/2018 period at Buoy 46261.

Parameter	RMSE	PE (%)	SI	Bias	Bias (%)	R
J (kW/m)	18	46.5	0.71	7	26.5	0.93
H_s (m)	0.35	8.4	0.17	0.10	4.9	0.94
T_e (s)	1.3	12.5	0.15	1.0	11.6	0.92
ϵ_0 (-)	0.06	-4.6	0.17	-0.02	-6.0	0.71
θ (degrees)	12.3	-1.6	0.04	-5	-1.8	0.86
d_θ (-)	0.06	4.2	0.06	0.03	4.0	0.66

Table 3.7. Performance metrics of the six simulated IEC resource parameters for the 10/2017–3/2018 period at Buoy 46263.

Parameter	RMSE	PE (%)	SI	Bias	Bias (%)	R
J (kW/m)	16	27.6	0.47	4	11.8	0.92
H_s (m)	0.38	6.0	0.17	0.06	2.7	0.92
T_e (s)	1.4	12.0	0.14	1.1	11.2	0.89
ϵ_0 (-)	0.06	-8.6	0.19	-0.03	-9.5	0.71
θ (degrees)	11.9	-0.6	0.04	-2	-0.8	0.82
d_θ (-)	0.08	6.0	0.09	0.05	5.5	0.69

Table 3.8. Summary of temporal averages of the root-mean-square-error and linear correlation coefficient for the six IEC wave resource parameters at buoys with spectral data.

	J (kW/m)		*H_s (m)*		*T_e (s)*		*ε_o (-)*		*θ (degrees)*		*$d\theta$ (-)*	
Buoy #	*RMSE*	*R*	*RMSE*	*R*	*RMSE*	*R*	*RMSE*	*R*	*RMSE*	*R*	*RMSE*	*R*
46041	20	0.94	0.37	0.96	1.2	0.89	0.06	0.71	20.3	0.68	0.10	0.50
46087	18	0.88	0.45	0.90	1.1	0.85	0.07	0.54	21.4	0.56	0.11	0.41
46063	14	0.90	0.37	0.92	1.3	0.88	0.06	0.72	20.8	0.55	0.09	0.68
46042	15	0.92	0.35	0.94	1.1	0.90	0.06	0.78	25.3	0.60	0.10	0.72
46025	3	0.86	0.21	0.88	1.7	0.76	0.09	0.55	32.7	0.47	0.16	0.19
46028	16	0.91	0.40	0.92	1.3	0.89	0.07	0.71	32.2	0.42	0.12	0.59
46015	20	0.93	0.40	0.95	1.4	0.88	0.08	0.61	31.5	0.64	0.12	0.37
46026	14	0.91	0.36	0.93	1.3	0.90	0.06	0.75	17.8	0.68	0.09	0.67
46022	24	0.91	0.48	0.92	1.1	0.89	0.06	0.62	28.8	0.75	0.10	0.54
46027	19	0.90	0.45	0.91	1.2	0.91	0.07	0.63	14.9	0.84	0.08	0.51
46050	17	0.93	0.37	0.95	1.3	0.88	0.07	0.58	25.2	0.70	0.11	0.36
46029	21	0.93	0.40	0.96	1.2	0.88	0.06	0.72	22.8	0.66	0.10	0.55
46216	5	0.87	0.34	0.85	1.4	0.80	0.10	0.60	11.6	0.43	0.06	0.67
46229	19	0.93	0.37	0.95	1.3	0.90	0.07	0.70	18.1	0.82	0.07	0.68
46213	17	0.91	0.40	0.93	1.0	0.91	0.06	0.79	22.3	0.79	0.07	0.79
46224	3	0.76	0.19	0.82	1.7	0.75	0.10	0.57	16.6	0.81	0.07	0.43
46221	4	0.73	0.26	0.77	1. 9	0.69	0.11	0.49	21.3	0.68	0.09	0.30
46211	18	0.92	0.35	0.95	1.2	0.91	0.06	0.77	12.2	0.82	0.05	0.75
46236	10	0.91	0.32	0.92	1.4	0.88	0.08	0.77	9.7	0.71	0.04	0.80
46215	9	0.90	0.27	0.91	1.2	0.89	0.06	0.80	10.2	0.73	0.05	0.80

Finally, the percentage mean error of wave power density ($(J_m/J_o - 1)\times100$ (%), as defined by EPRI (2012), was calculated based on current study results and compared to the results obtained by EPRI's study at the validation stations selected by EPRI on the West Coast (Table 3.9). It can be seen that the percentage mean error of power density at all the selected validation stations were improved greatly compared to EPRI's study's results, which was based on NOAA's 4 arc-minute resolution, 51-month hindcast. The percentage mean errors were reduced by a range from 9% to 82%, based on the high-resolution model handcast.

Table 3.9. Comparison of percentage mean errors of power density at selected buoys between the current PNNL study and the EPRI study.

Percentage mean error = $(J_m/J_o - 1)\times100$ (%)			
Station	PNNL	EPRI (2012)	Percentage Reduction
46041	3	17	82
46211	14	19	26
46050	10	11	9
46025	-9	-20	55
46022	12	17	29
46027	4	19	79

4.0 Conclusion

The use of coarse-grid-resolution models generate concerns about the accurate reproducibility of shallow-water processes in nearshore regions. Therefore, high-resolution wave hindcasts are critical to improving the accuracy of and reducing the uncertainties of wave resource assessments. This study applies an unstructured-, nested-grid modeling approach, incorporating a global-regional nested grid, using the WWIII and high-resolution UnSWAN models, to simulate wave climates along the U.S. West Coast for long-term period of 32 years. The IEC wave resource parameters were simulated and subsequently validated with wave buoy data within the model domain.

Model performance metrics, such as root-mean-square-error, percentage error, scatter index, model bias, percentage bias, and correlation coefficient, were used to evaluate the model skill for reproducing wave resource parameters, including the omnidirectional wave power (J), significant wave height (H_s), energy period (T_e), spectral width (ϵ_0), direction (θ), and directionality coefficient (d_θ). Overall, the model results for the six IEC wave resource parameters match well with the measured data. UnSWAN was able to reproduce the seasonal variation of the sea state with large waves that occur in the winter and early spring months (November–March) when wind forcing is strong and the calmed sea state during the summer (June–August) when wind forcing is weak. The percentage mean error of power density at selected buoys was also compared to results presented by EPRI (EPRI 2011). Results show the percentage mean error of power density at all selected buoys was significantly improved based on high-resolution hindcast results generated in this study.

Monthly 2D distributions of IEC parameters were calculated and are provided in Appendix A. Detailed model and data comparisons of time series and scatter plots for the six IEC parameters were generated at 28 buoys for the 1979–2011 period and are presented in Appendix B. The yearly error statistics for the simulated six IEC parameters at each station are provided in Appendix C and the the 32-year averages at each station are provided in Appendix D. The high-resolution model results generated from this study can be used to inform the design and deployment of WECs in nearshore regions, assist in prioritizing hotspots for near-term market opportunities and development, and update wave resource assessment data for the U.S. Department of Energy Marine and Hydrokinetic Energy Atlas.[2]

[2] https://maps.nrel.gov/mhk-atlas

5.0 References

Ardhuin, F., Rogers, E., Babanin, A. V., Filipot, J.-F., Magne, R., Roland, A., van der Westhuysen, A., Queffeulou, P., Lefevre, J.-M., Aouf, L., and Collard, F., 2010, Semiempirical Dissipation Source Functions for Ocean Waves. Part I: Definition, Calibration, and Validation: Journal of Physical Oceanography, v. 40, no. 9, p. 1917-1941.

Cobell, Z., Zhao, H. H., Roberts, H. J., Clark, F. R., and Zou, S., 2013, Surge and Wave Modeling for the Louisiana 2012 Coastal Master Plan: Journal of Coastal Research, p. 88-108.

Council, N. R., 2013, An Evaluation of the U.S. Department of Energy's Marine and Hydrokinetic Resource Assessments.

EPRI, 2011, Mapping and Assessment of the United States Ocean Wave Energy Resource: Electric Power Research Institute.

Gallagher, S., Tiron, R., and Dias, F., 2014, A long-term nearshore wave hindcast for Ireland: Atlantic and Irish Sea coasts (1979-2012): Ocean Dynamics, v. 64, no. 8, p. 1163-1180.

García-Medina, G., Özkan-Haller, H. T., and Ruggiero, P., 2014, Wave resource assessment in Oregon and southwest Washington, USA: Renewable Energy, v. 64, p. 203-214.

García-Medina, G., Özkan-Haller, H. T., Ruggiero, P., and Oskamp, J., 2013, An Inner-Shelf Wave Forecasting System for the U.S. Pacific Northwest: Weather and Forecasting, v. 28, no. 3, p. 681-703.

IEC, 2015, Marine energy – wave, tidal and other water current converters – Part 101: Wave energy resource assessment and characterization: International Electrotechnical Commission, IEC TS 62600-101.

Mao, M., van der Westhuysen, A. J., Xia, M., Schwab, D. J., and Chawla, A., 2016, Modeling wind waves from deep to shallow waters in Lake Michigan using unstructured SWAN: Journal of Geophysical Research-Oceans, v. 121, no. 6, p. 3836-3865.

Mediavilla, D. G., and Sepulveda, H. H., 2016, Nearshore assessment of wave energy resources in central Chile (2009-2010): Renewable Energy, v. 90, p. 136-144.

Roland, A., and Ardhuin, F., 2014, On the developments of spectral wave models: numerics and parameterizations for the coastal ocean: Ocean Dynamics, v. 64, no. 6, p. 833-846.

SWAN, 2015, SWAN: User Manual, Cycle III version 41.01A: Delft University of Technology.

Tolman, H. L., and WAVEWATCH III Development Group, 2014, User manual and system documentation of WAVEWATCH III® version 4.18: National Oceanic and Atmospheric Administration, National Weather Service, National Centers for Environmental Prediction, MMAB Contribution No. 316.

Wu, W.-C., Yang, Z., and Wang, T., 2018, Wave Resource Characterization Using an Unstructured Grid Modeling Approach: Energies, v. 11, no. 3, p. 15.

Yang, Z., Neary, V. S., Wang, T., Gunawan, B., Dallman, A. R., and Wu, W., 2017, A wave model test bed study for wave energy resource characterization: Renewable Energy.

Yuk, J. H., Kim, K. O., Jung, K. T., and Choi, B. H., 2016, Swell Prediction for the Korean Coast: Journal of Coastal Research, v. 32, no. 1, p. 131-141.

Zijlema, M., 2010, Computation of wind-wave spectra in coastal waters with SWAN on unstructured grids: Coastal Engineering, v. 57, no. 3, p. 267-277.

Appendix A – Monthly Distributions of IEC Wave Resource Parameters from 1979–2010 along the West Coast

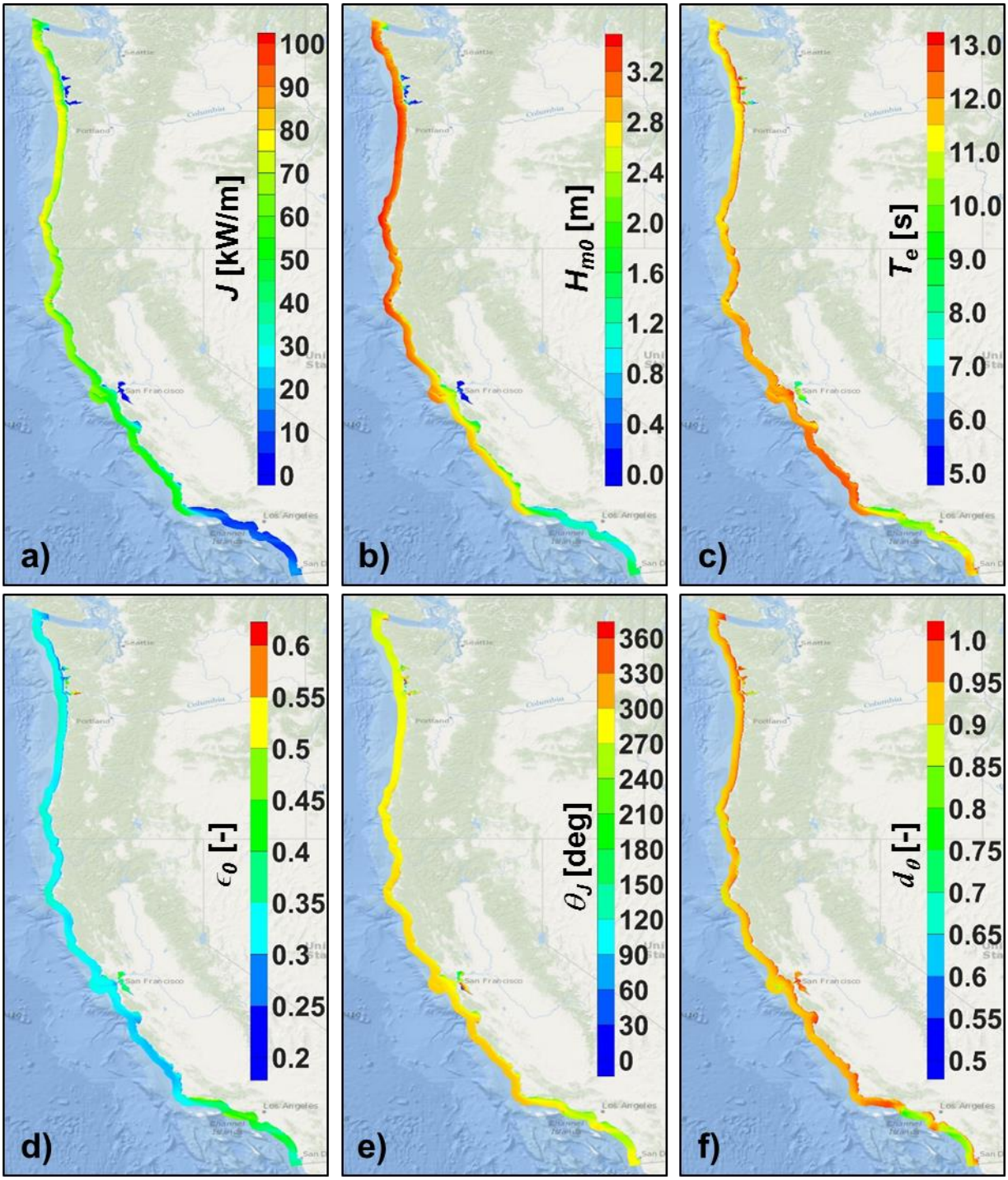

Figure A.1. Monthly distributions of six IEC parameters in January: (a) omnidirectional wave power, (b) significant wave height, (c) energy period, (d) spectral width, (e) direction of maximum directionally resolved wave power, and (f) directionality coefficient along the West Coast.

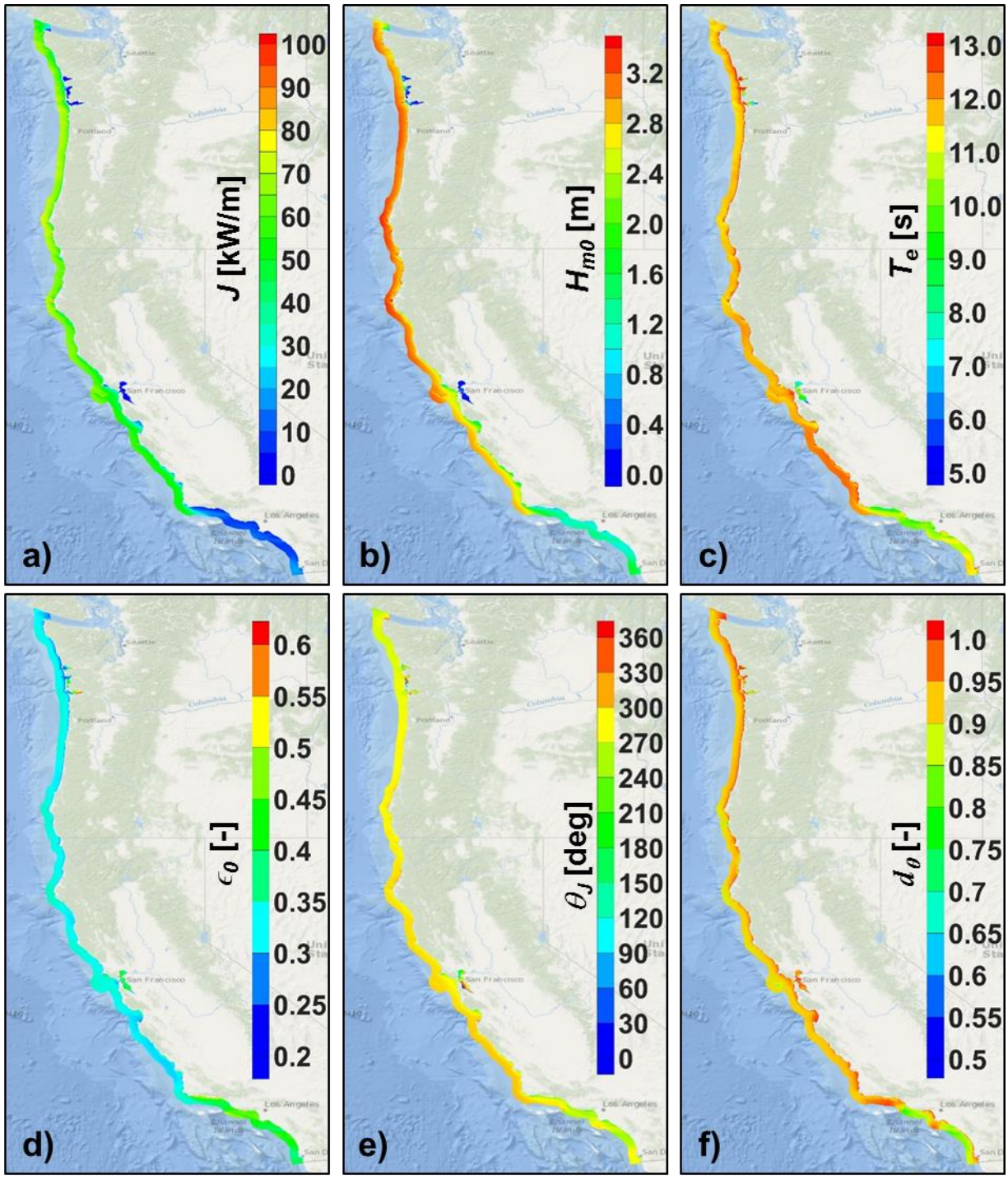

Figure A.2. Monthly distributions of six IEC parameters in February: (a) omnidirectional wave power, (b) significant wave height, (c) energy period, (d) spectral width, (e) direction of maximum directionally resolved wave power, and (f) directionality coefficient along the West Coast.

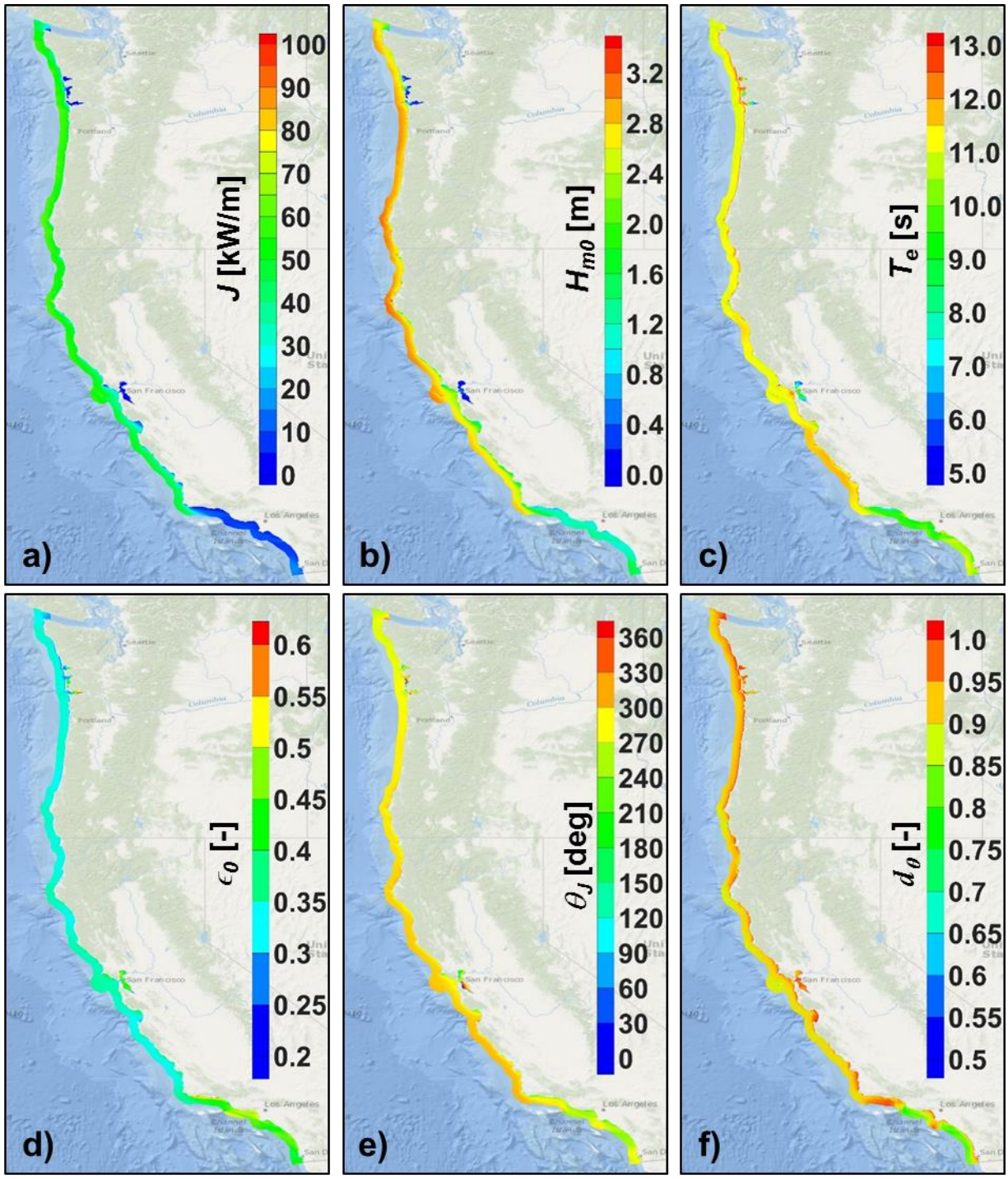

Figure A.3. Monthly distributions of six IEC parameters in March: (a) omnidirectional wave power, (b) significant wave height, (c) energy period, (d) spectral width, (e) direction of maximum directionally resolved wave power, and (f) directionality coefficient along the West Coast.

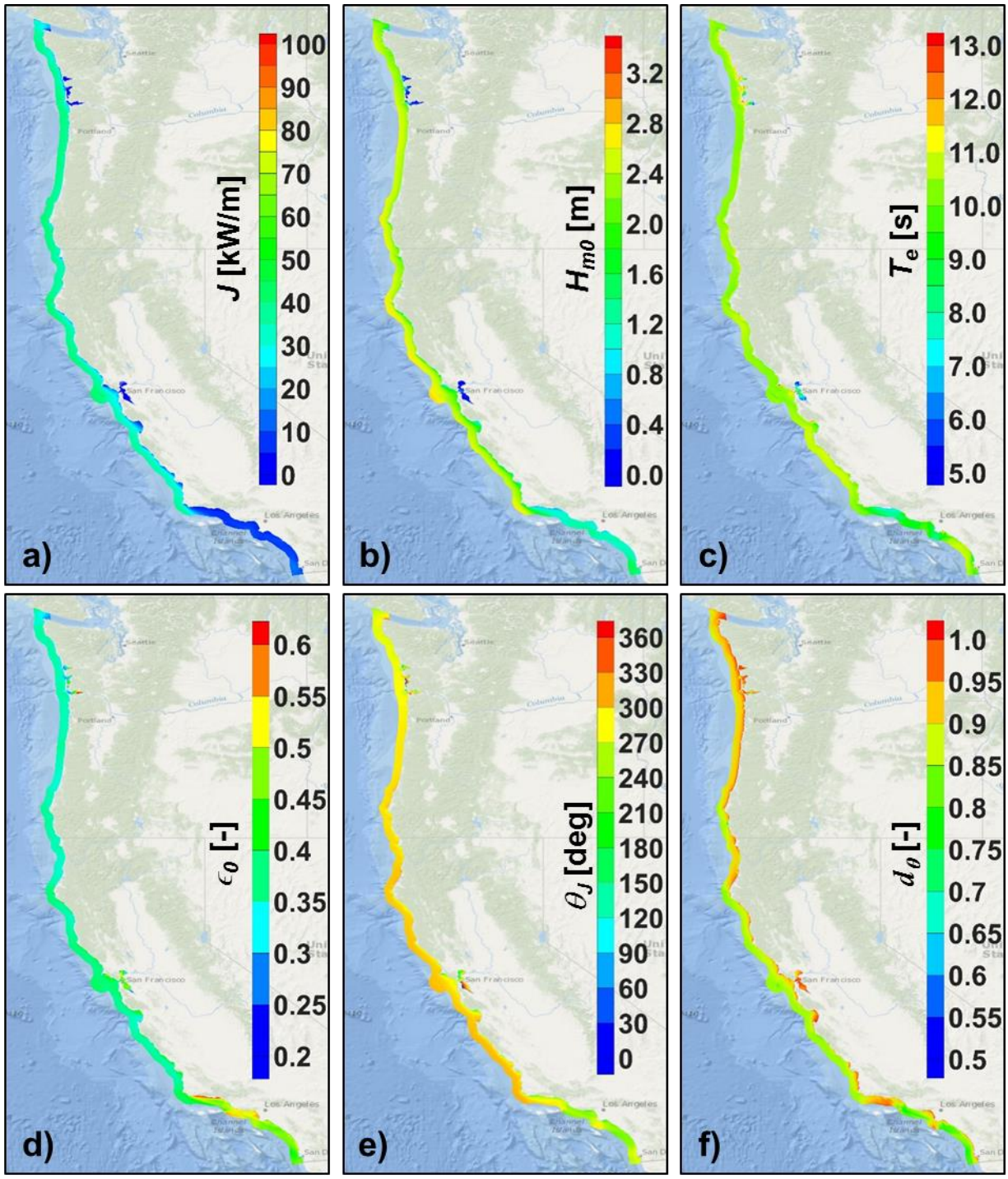

Figure A.4. Monthly distributions of six IEC parameters in April: (a) omnidirectional wave power, (b) significant wave height, (c) energy period, (d) spectral width, (e) direction of maximum directionally resolved wave power, and (f) directionality coefficient along the West Coast.

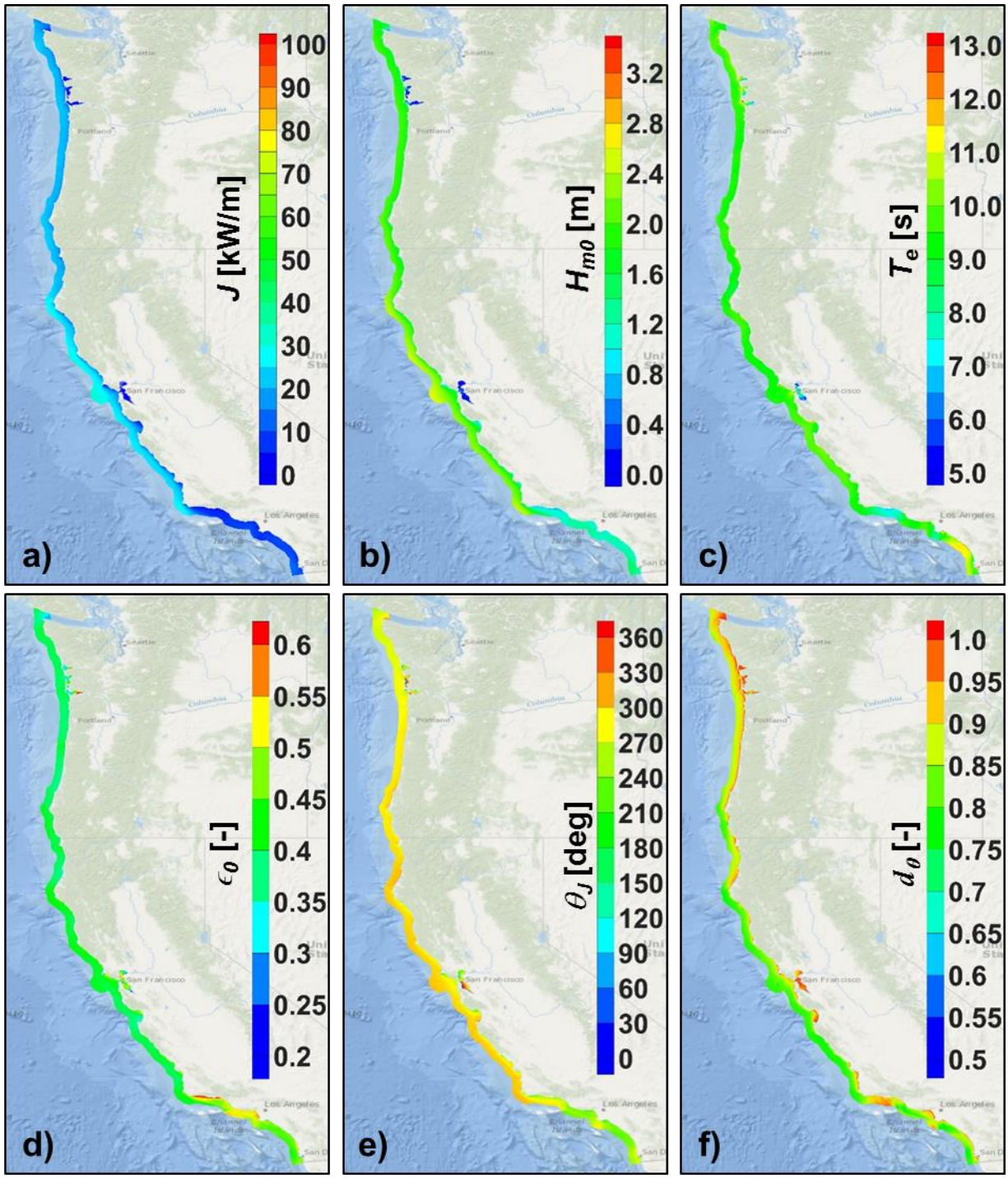

Figure A.5. Monthly distributions of six IEC parameters in May: (a) omnidirectional wave power, (b) significant wave height, (c) energy period, (d) spectral width, (e) direction of maximum directionally resolved wave power, and (f) directionality coefficient along the West Coast.

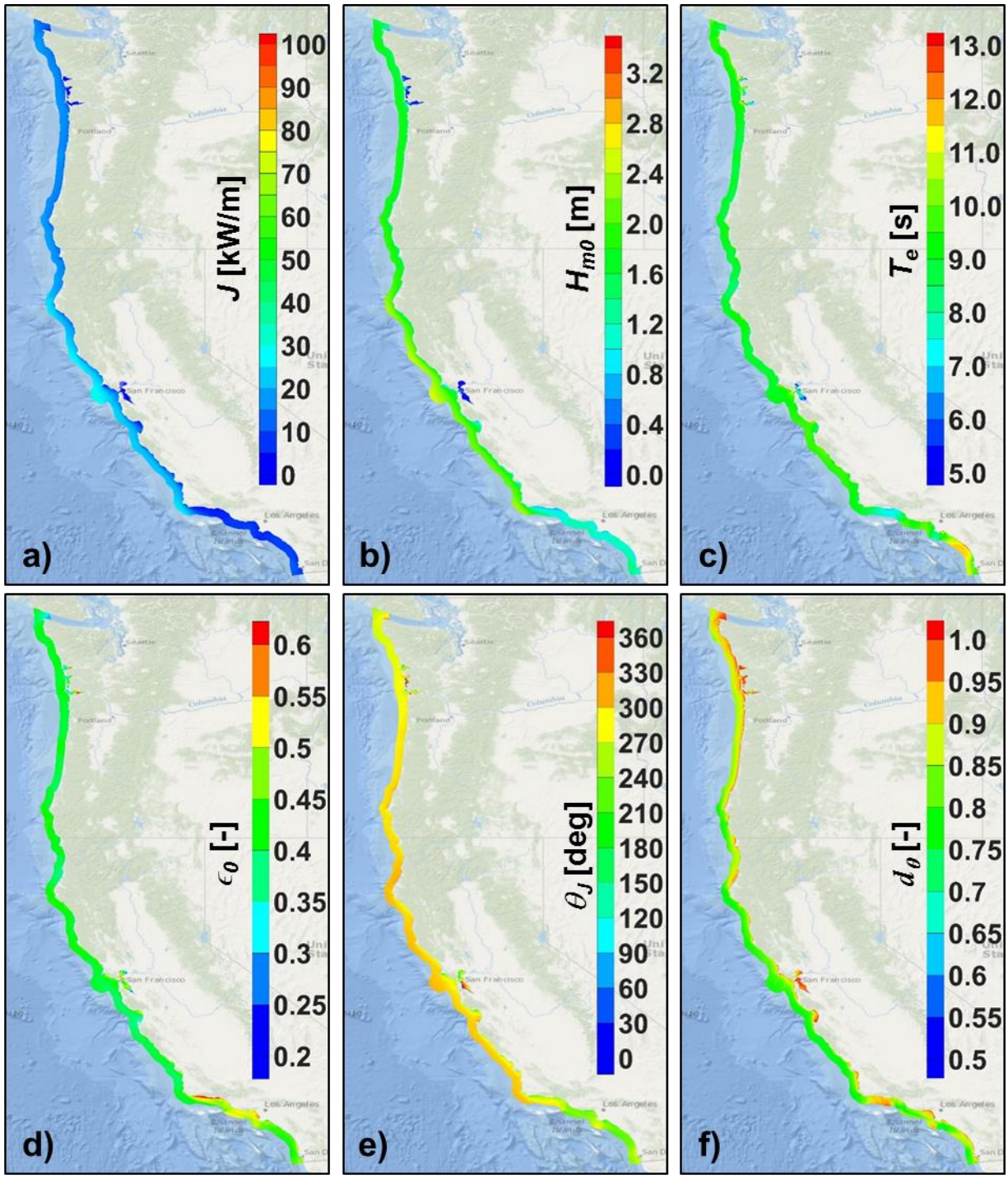

Figure A.6. Monthly distributions of six IEC parameters in June: (a) omnidirectional wave power, (b) significant wave height, (c) energy period, (d) spectral width, (e) direction of maximum directionally resolved wave power, and (f) directionality coefficient along the West Coast.

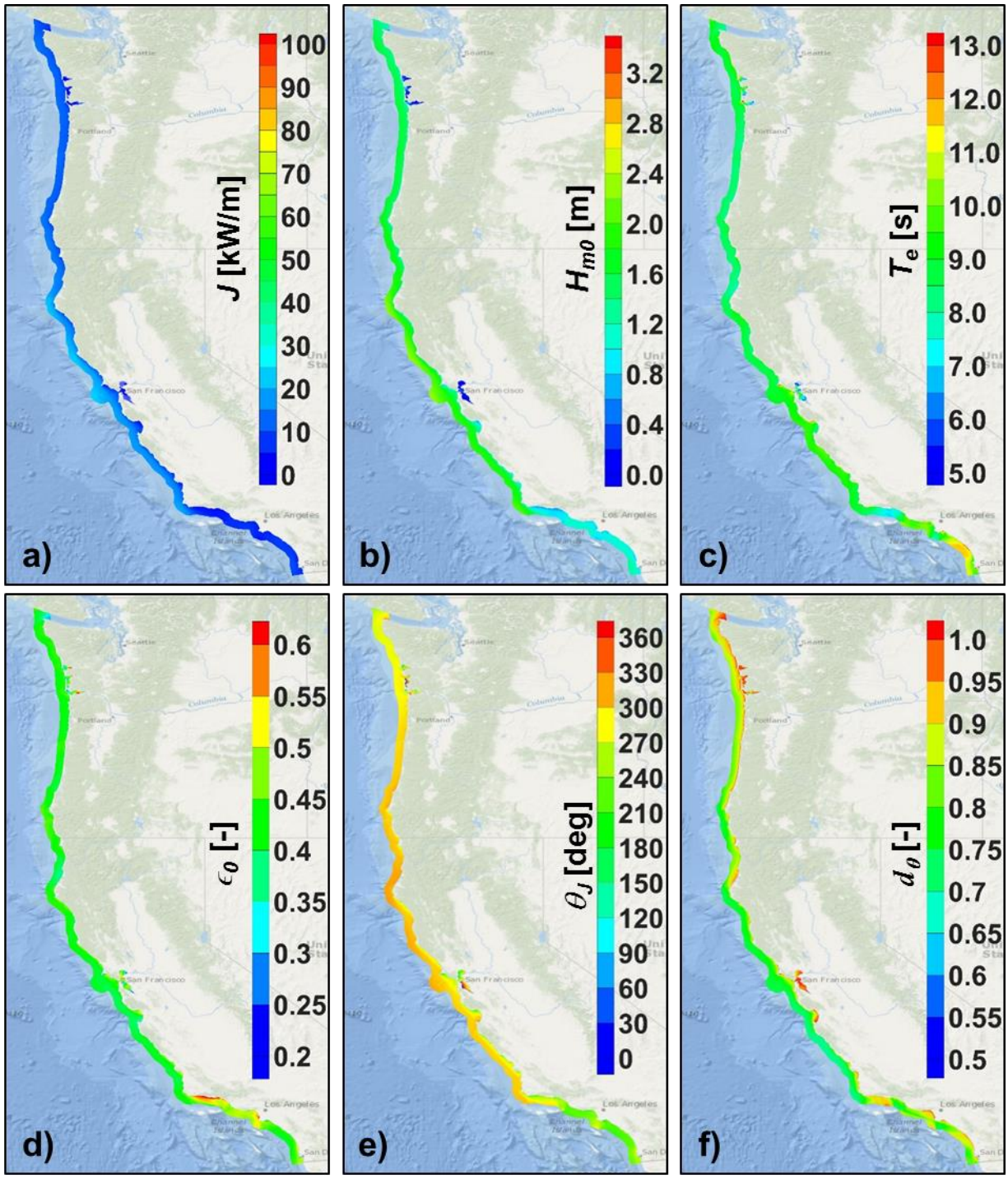

Figure A.7. Monthly distributions of six IEC parameters in July: (a) omnidirectional wave power, (b) significant wave height, (c) energy period, (d) spectral width, (e) direction of maximum directionally resolved wave power, and (f) directionality coefficient along the West Coast.

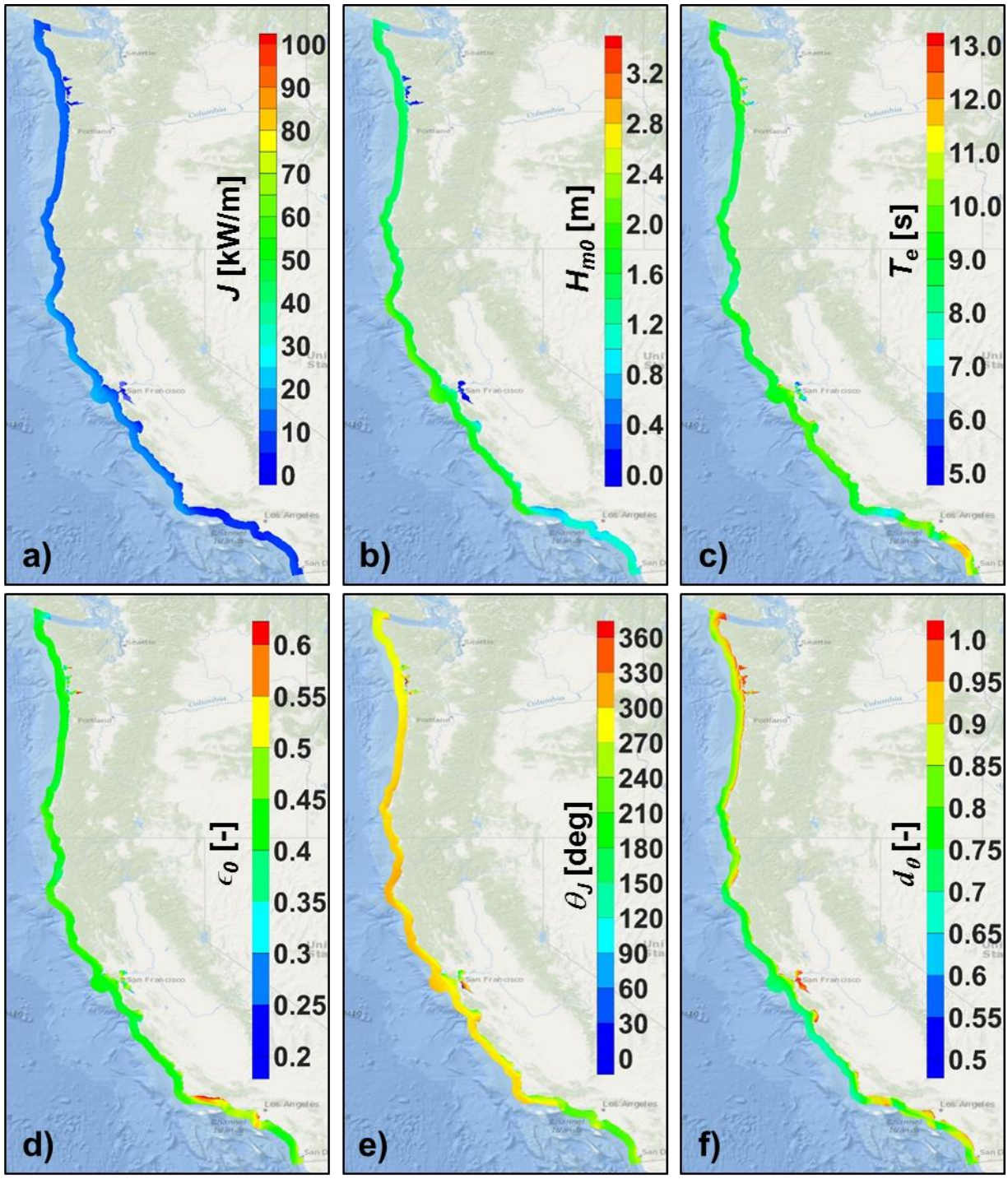

Figure A.8. Monthly distributions of six IEC parameters in August: (a) omnidirectional wave power, (b) significant wave height, (c) energy period, (d) spectral width, (e) direction of maximum directionally resolved wave power, and (f) directionality coefficient along the West Coast.

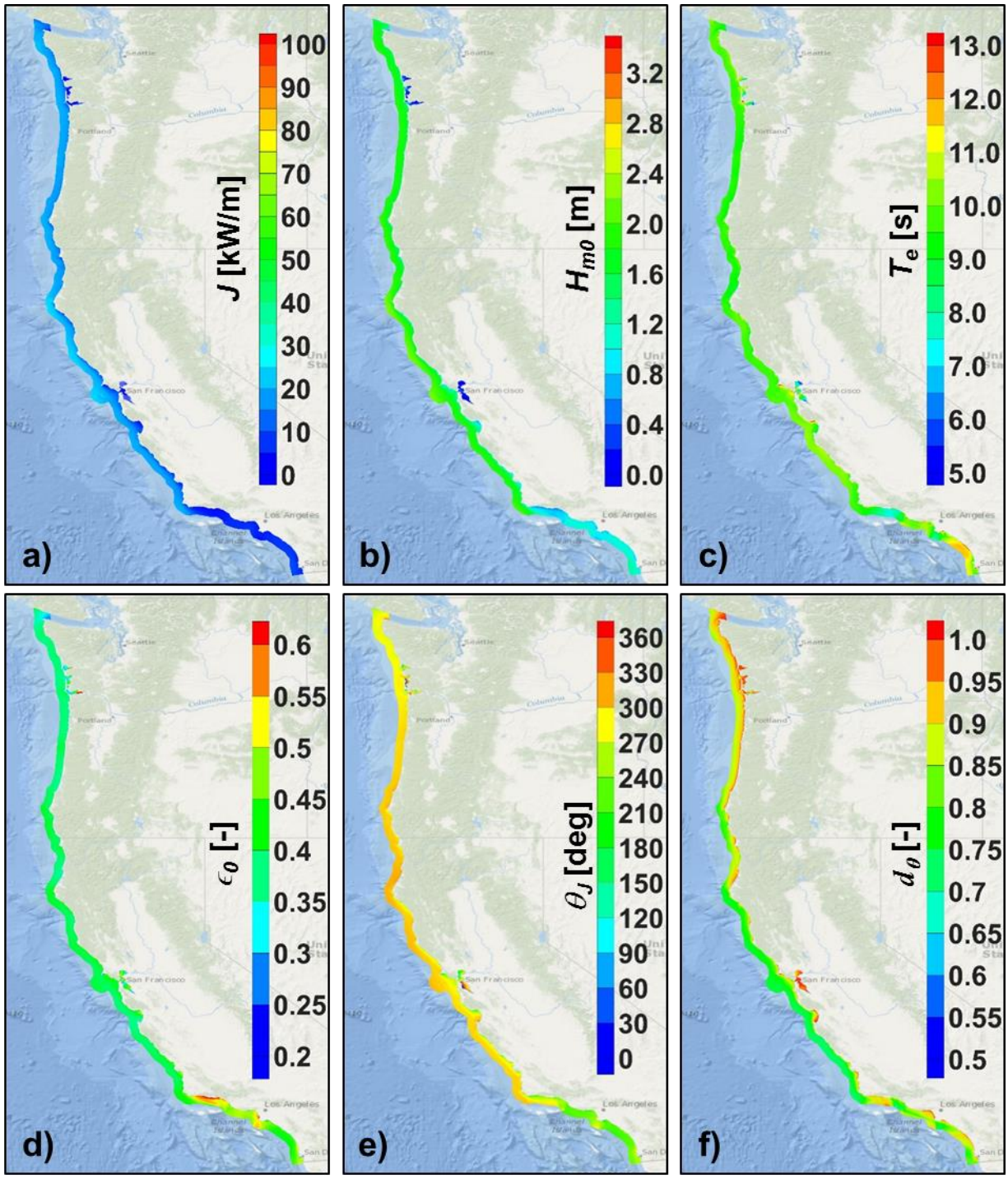

Figure A.9. Monthly distributions of six IEC parameters in September: (a) omnidirectional wave power, (b) significant wave height, (c) energy period, (d) spectral width, (e) direction of maximum directionally resolved wave power, and (f) directionality coefficient along the West Coast.

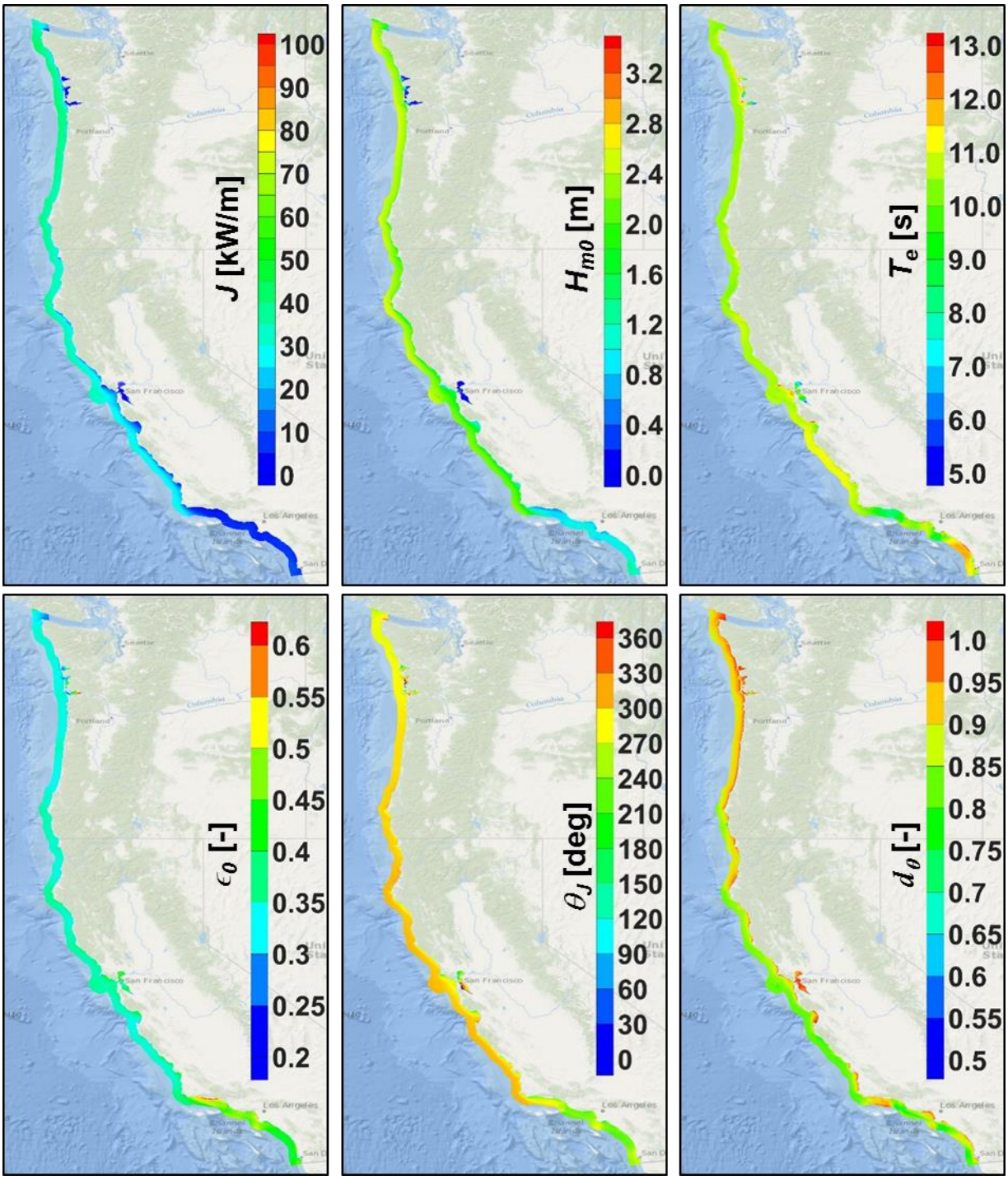

Figure A.10. Monthly distributions of six IEC parameters in October: (a) omnidirectional wave power, (b) significant wave height, (c) energy period, (d) spectral width, (e) direction of maximum directionally resolved wave power, and (f) directionality coefficient along the West Coast.

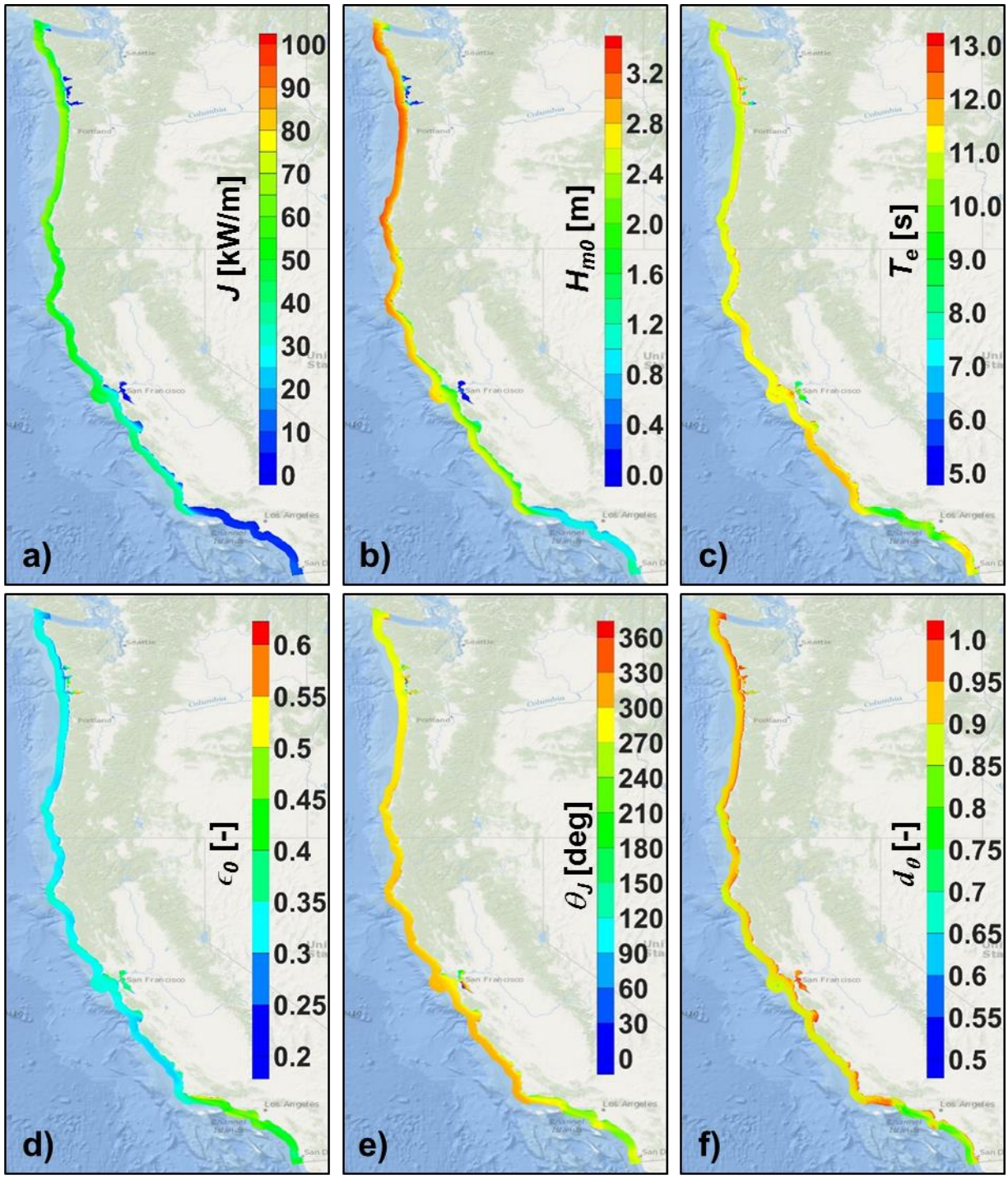

Figure A.11. Monthly distributions of six IEC parameters in November: (a) omnidirectional wave power, (b) significant wave height, (c) energy period, (d) spectral width, (e) direction of maximum directionally resolved wave power, and (f) directionality coefficient along the West Coast.

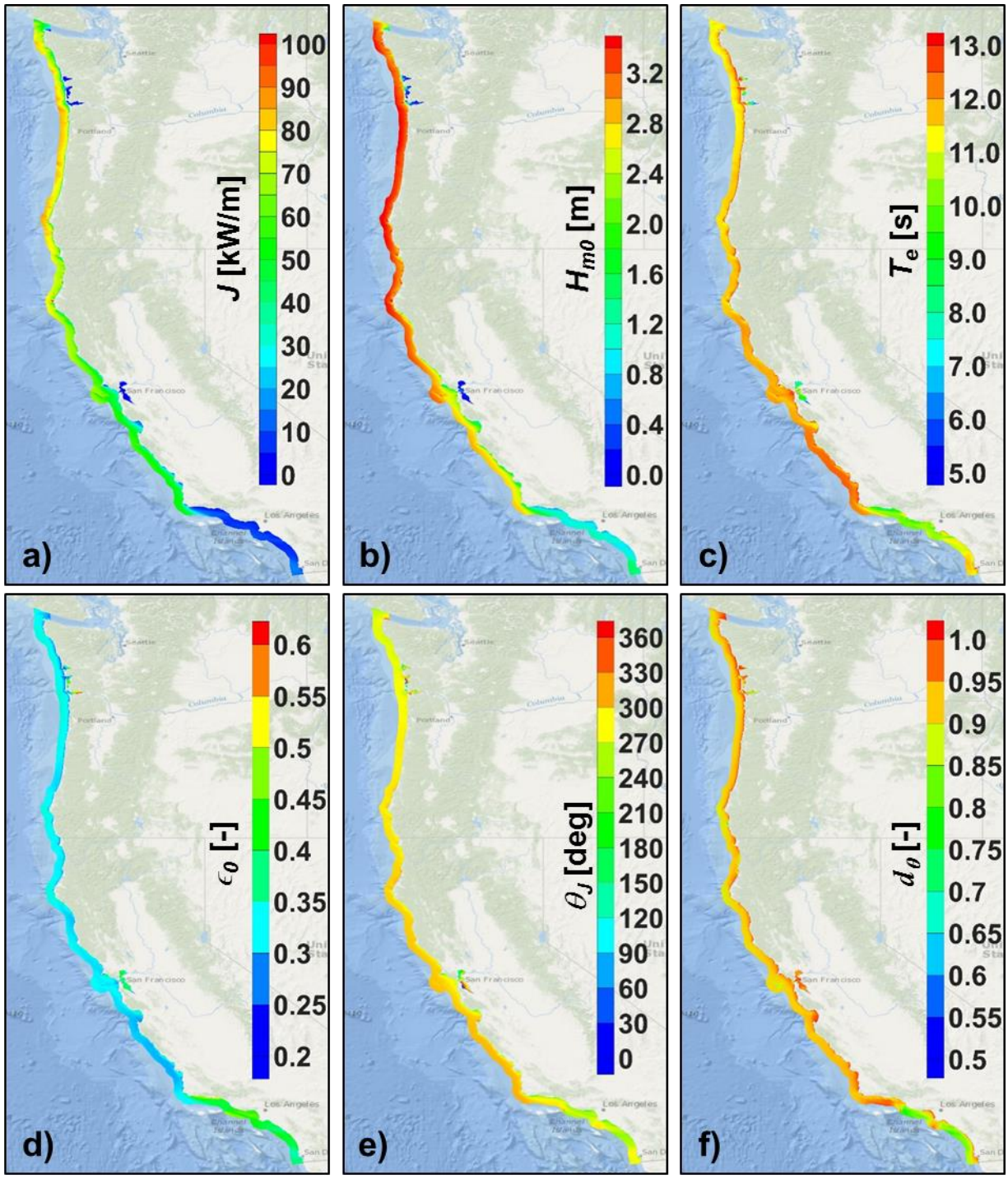

Figure A.12. Monthly distributions of six IEC parameters in December: (a) omnidirectional wave power, (b) significant wave height, (c) energy period, (d) spectral width, (e) direction of maximum directionally resolved wave power, and (f) directionality coefficient along the West Coast.

Appendix B – Comparisons of Model-Simulated Six IEC Parameters with Observed Data at NDBC and CDIP Buoys

Figure B.1 through Figure B.83 are National Data Buoy Center-related plots; Figure B.84 through Figure B.166 are Coastal Data Information Program-related plots.

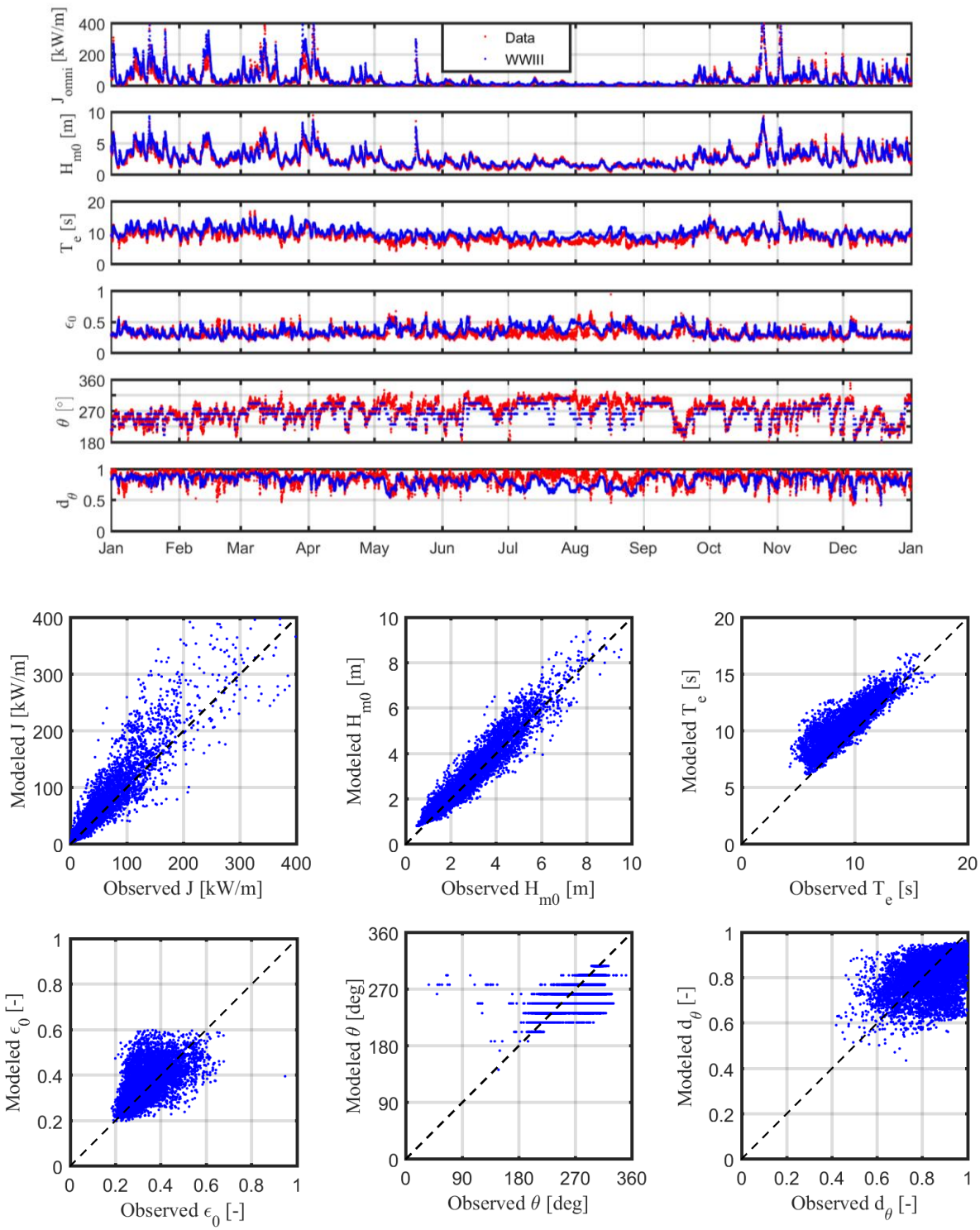

Figure B.1. Comparisons of time series (top) and scatter plots (bottom) of the six WWIII model-simulated IEC parameters with observed data at NDBC Buoy 46029 for 2010.

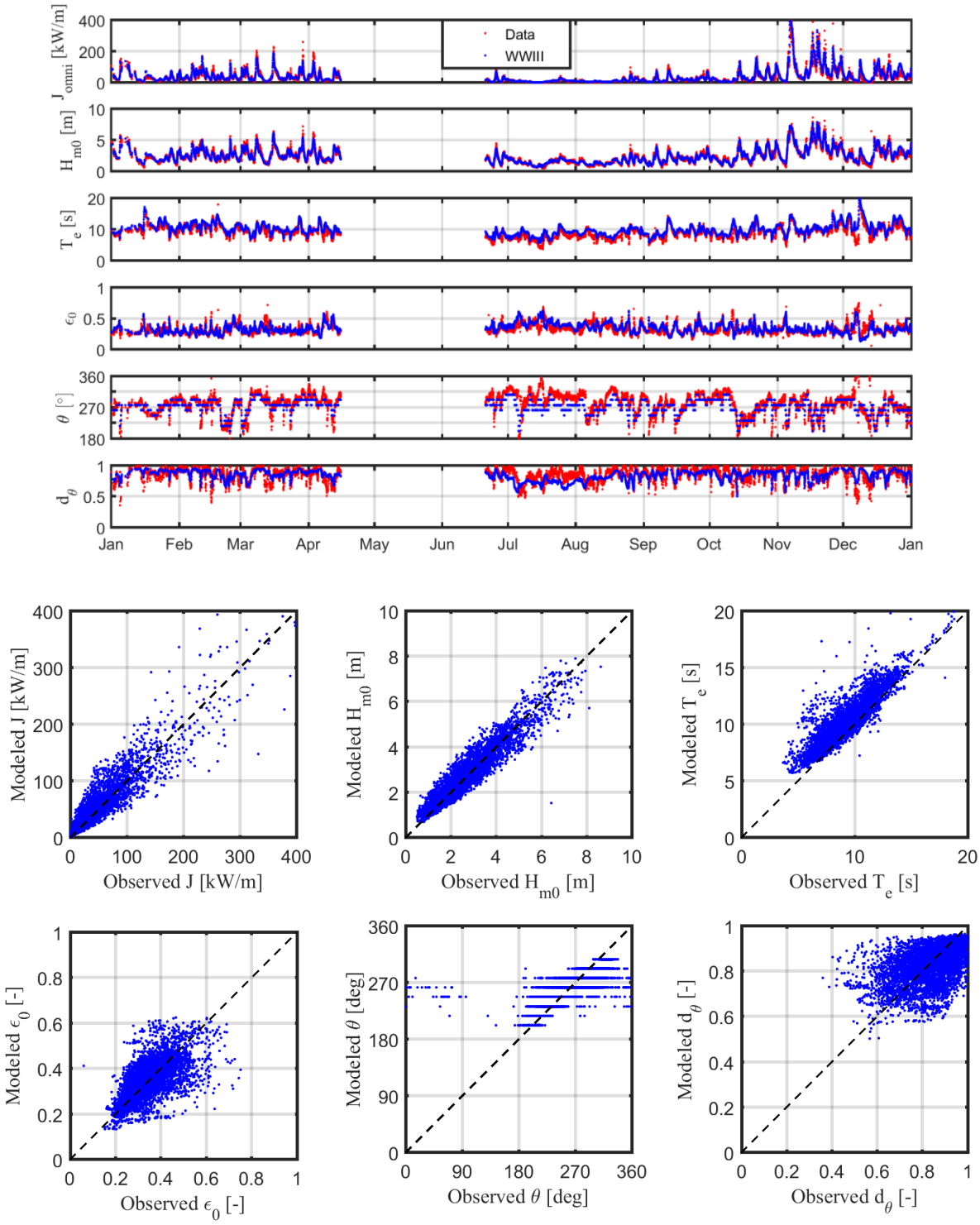

Figure B.2. Comparisons of time series (top) and scatter plots (bottom) of the six WWIII model-simulated IEC parameters with observed data at NDBC Buoy 46029 for 2009.

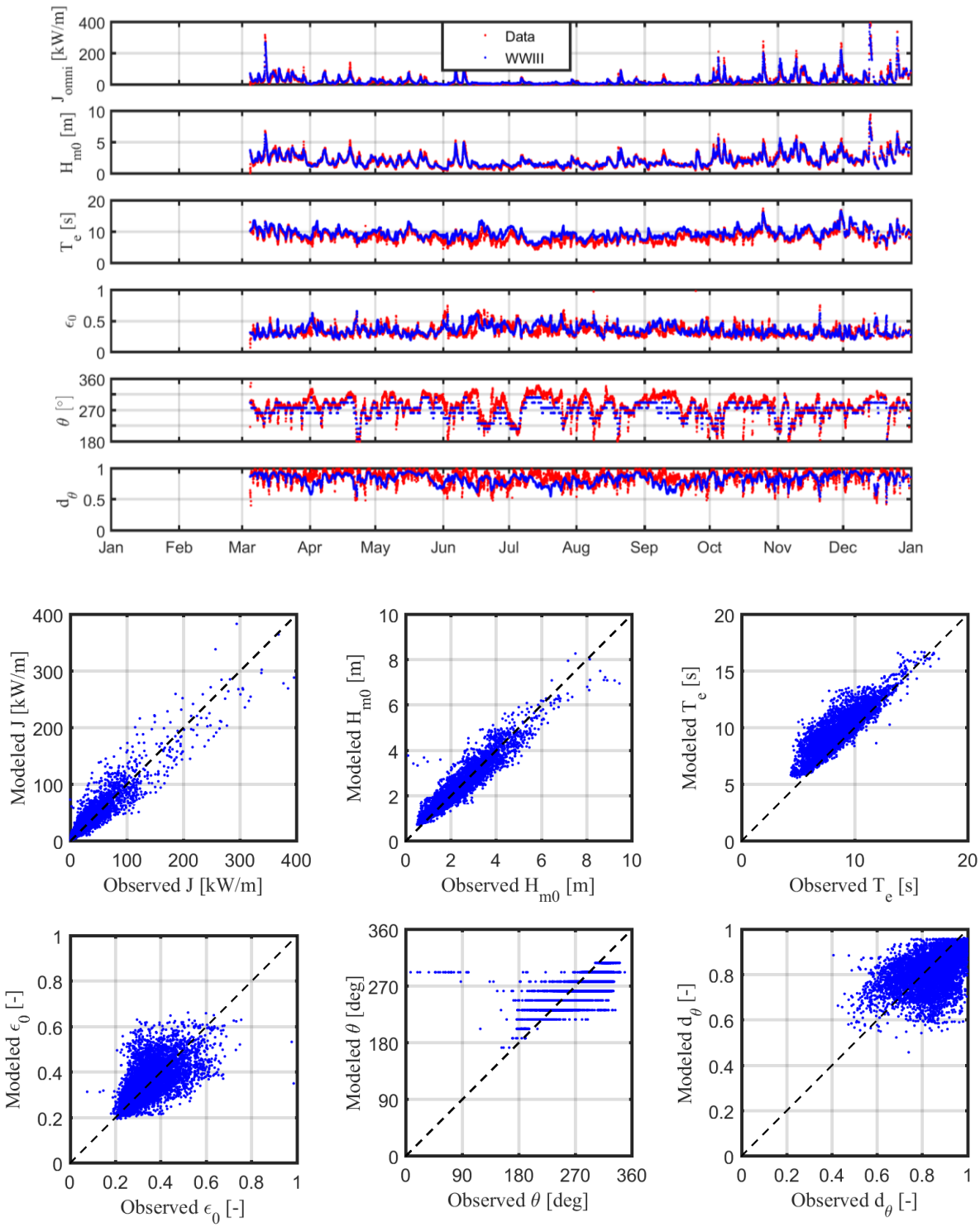

Figure B.3. Comparisons of time series (top) and scatter plots (bottom) of the six WWIII model-simulated IEC parameters with observed data at NDBC Buoy 46029 for 2008.

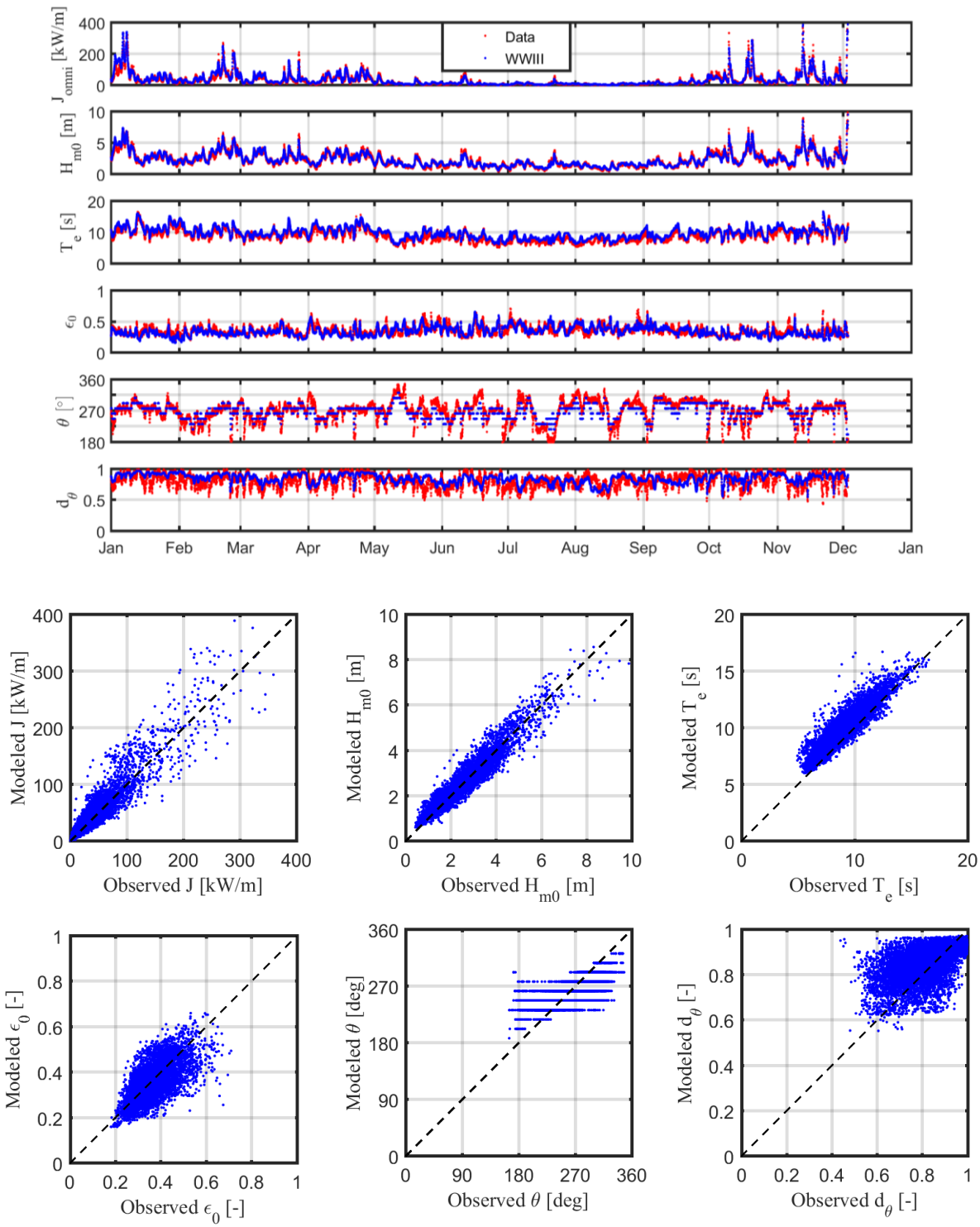

Figure B.4. Comparisons of time series (top) and scatter plots (bottom) of the six WWIII model-simulated IEC parameters with observed data at NDBC Buoy 46029 for 2007.

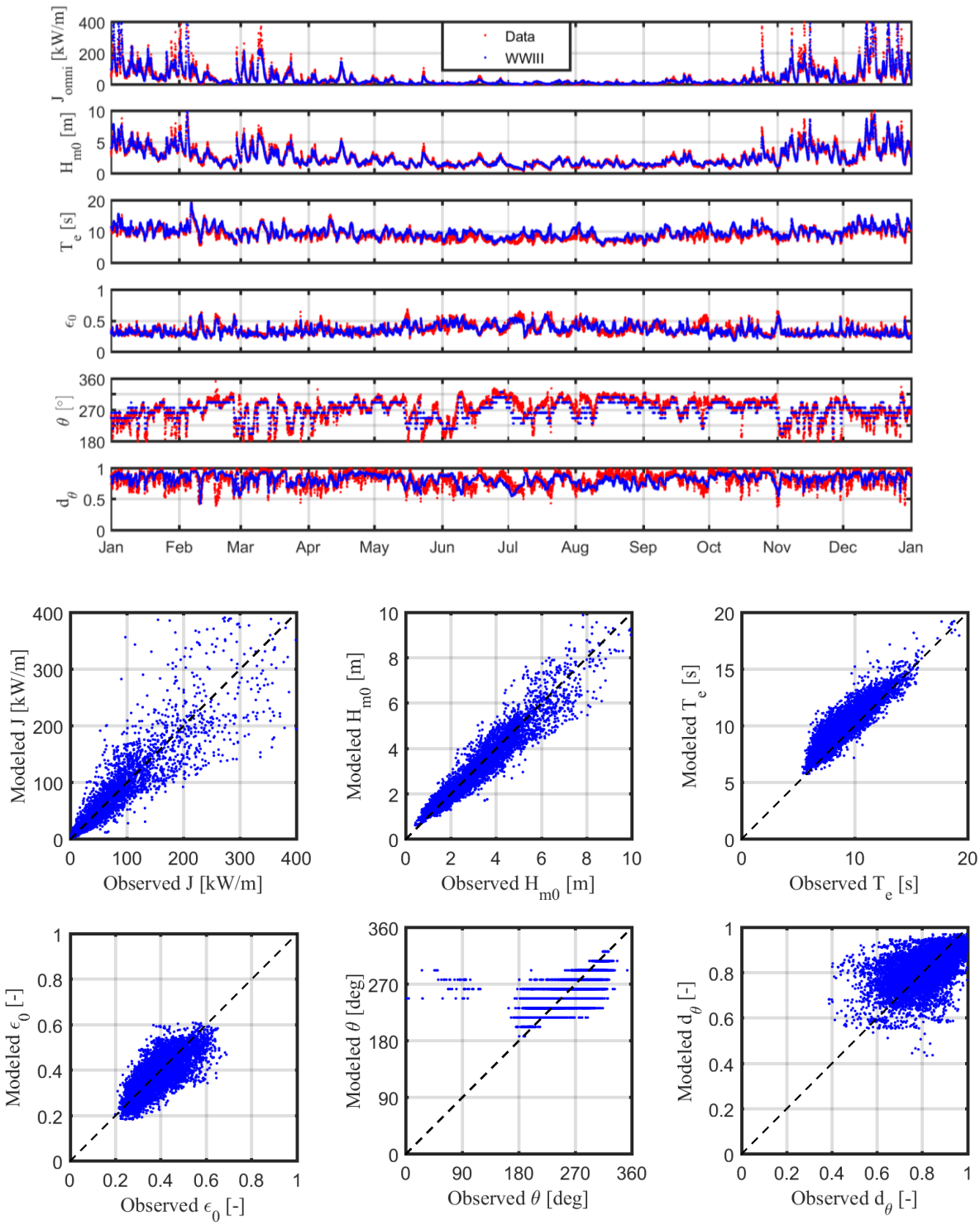

Figure B.5. Comparisons of time series (top) and scatter plots (bottom) of the six WWIII model-simulated IEC parameters with observed data at NDBC Buoy 46029 for 2006.

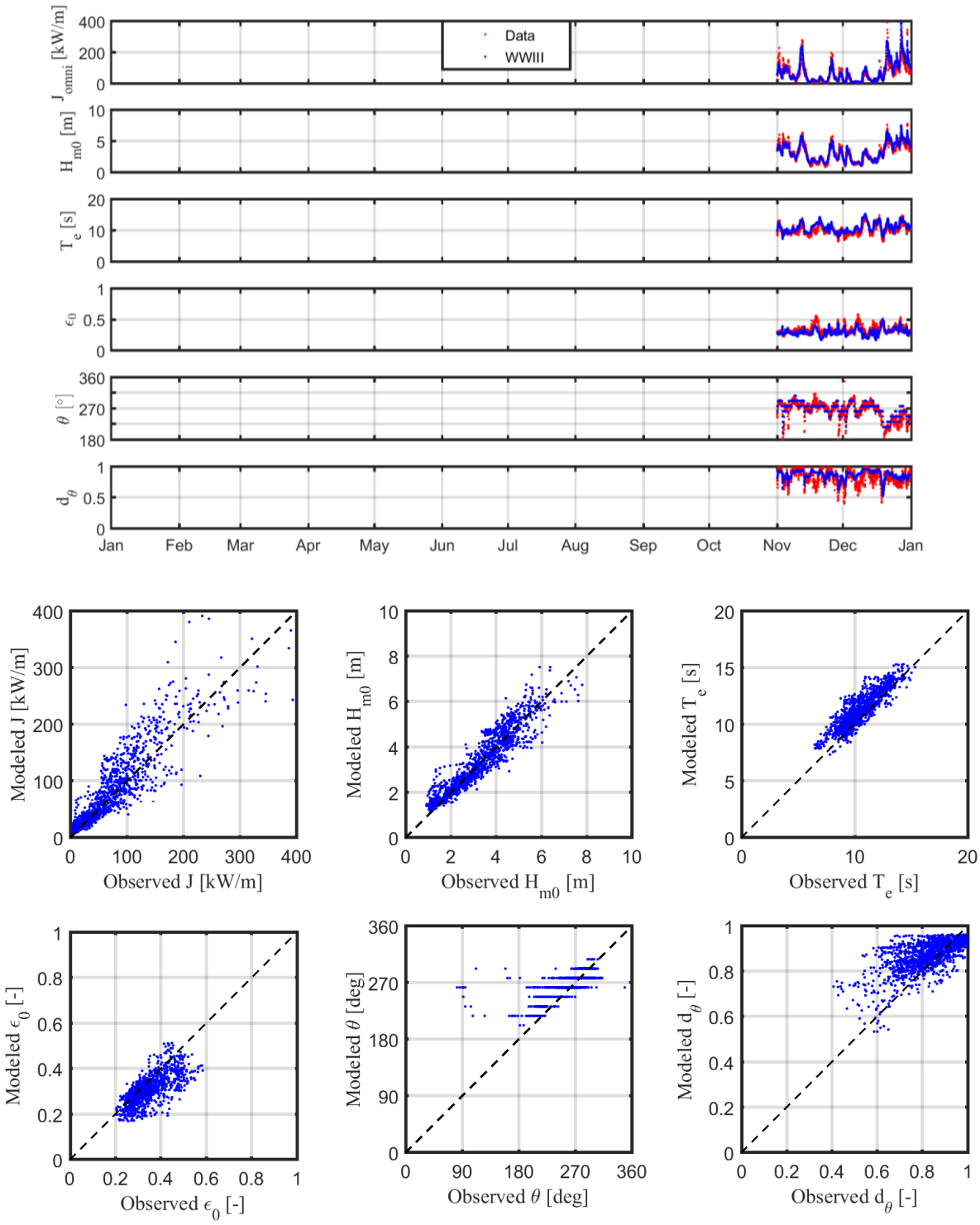

Figure B.6. Comparisons of time series (top) and scatter plots (bottom) of the six WWIII model-simulated IEC parameters with observed data at NDBC Buoy 46029 for 2005.

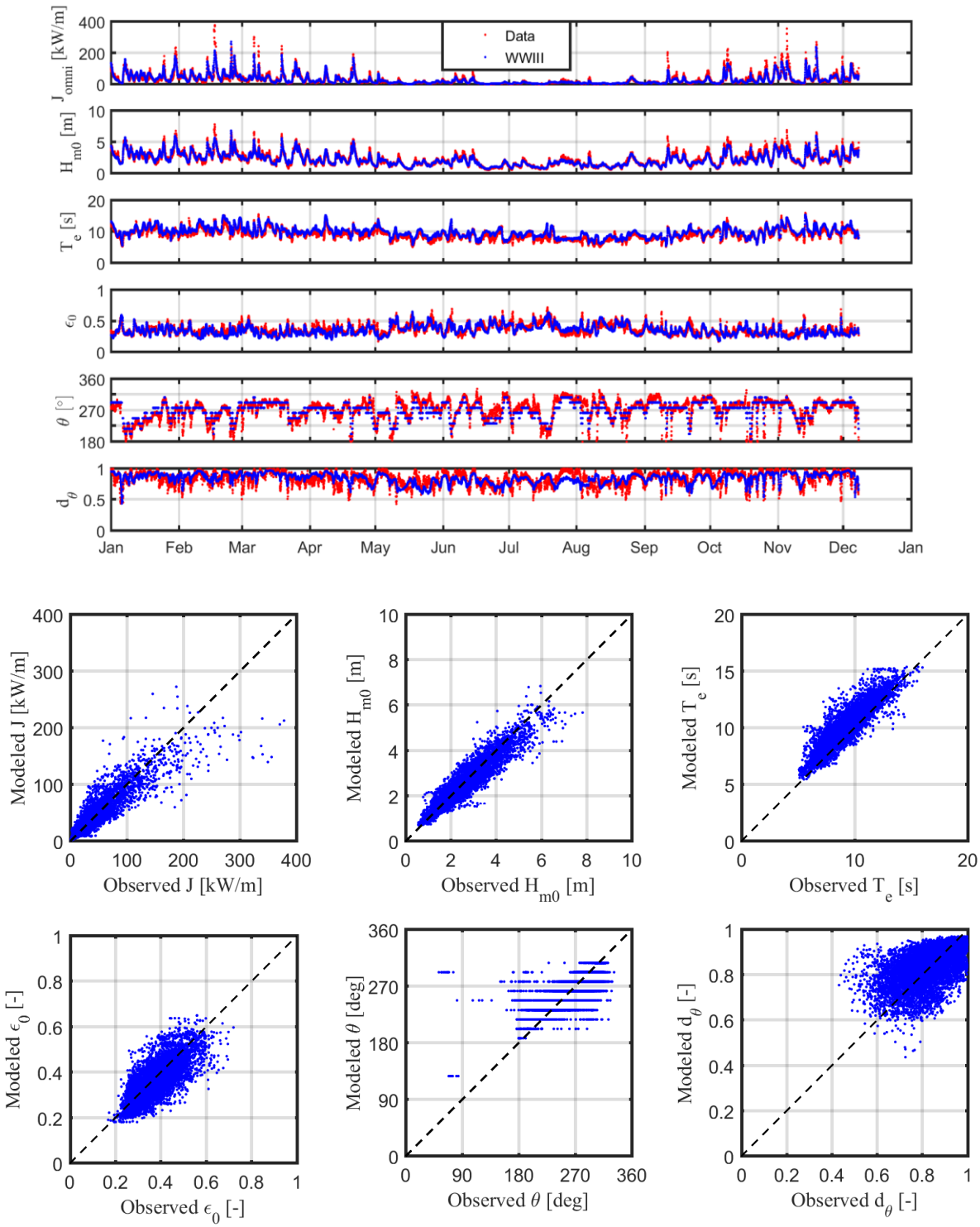

Figure B.7. Comparisons of time series (top) and scatter plots (bottom) of the six WWIII model-simulated IEC parameters with observed data at NDBC Buoy 46029 for 2004.

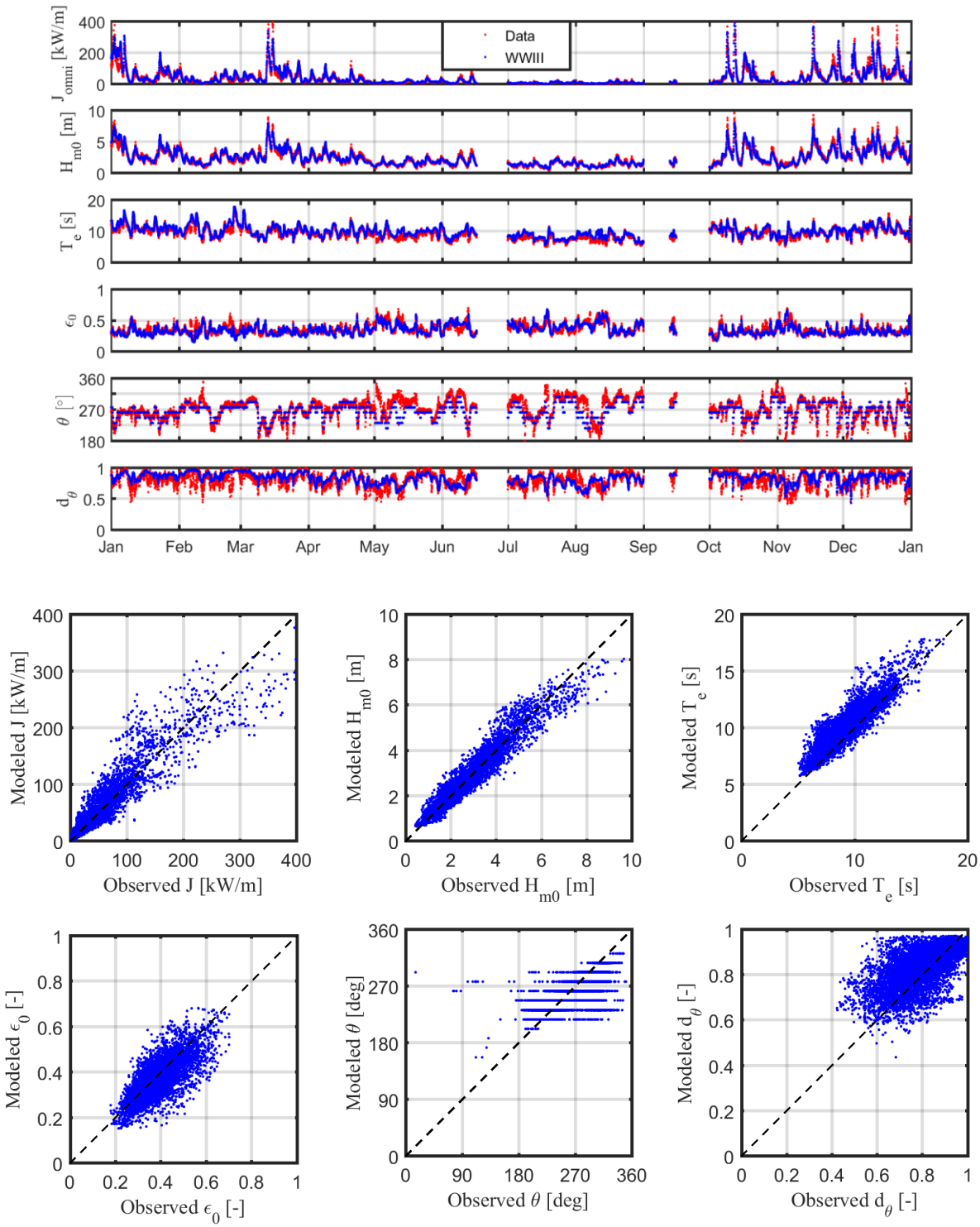

Figure B.8. Comparisons of time series (top) and scatter plots (bottom) of the six WWIII model-simulated IEC parameters with observed data at NDBC Buoy 46029 for 2003.

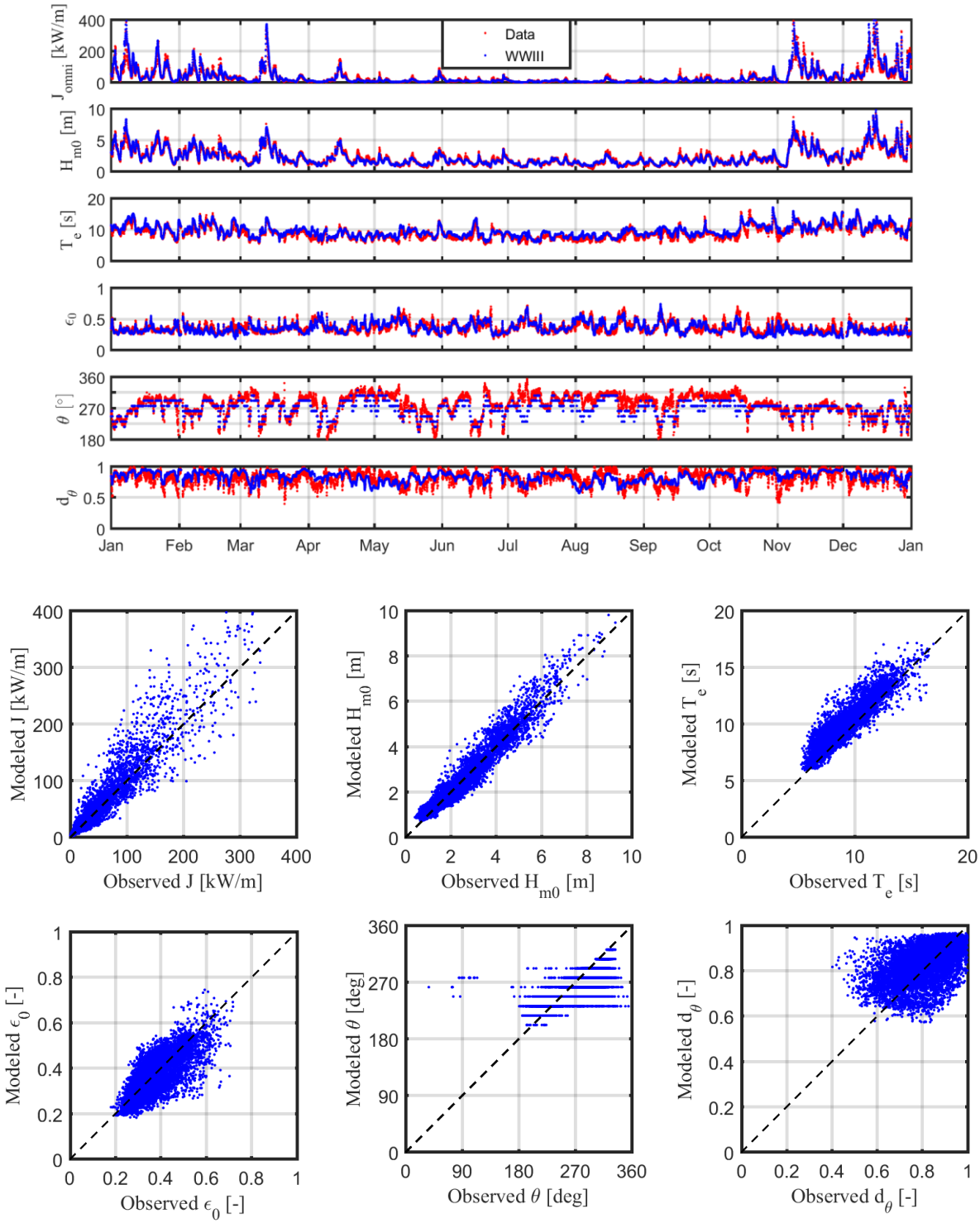

Figure B.9. Comparisons of time series (top) and scatter plots (bottom) of the six WWIII model-simulated IEC parameters with observed data at NDBC Buoy 46029 for 2002.

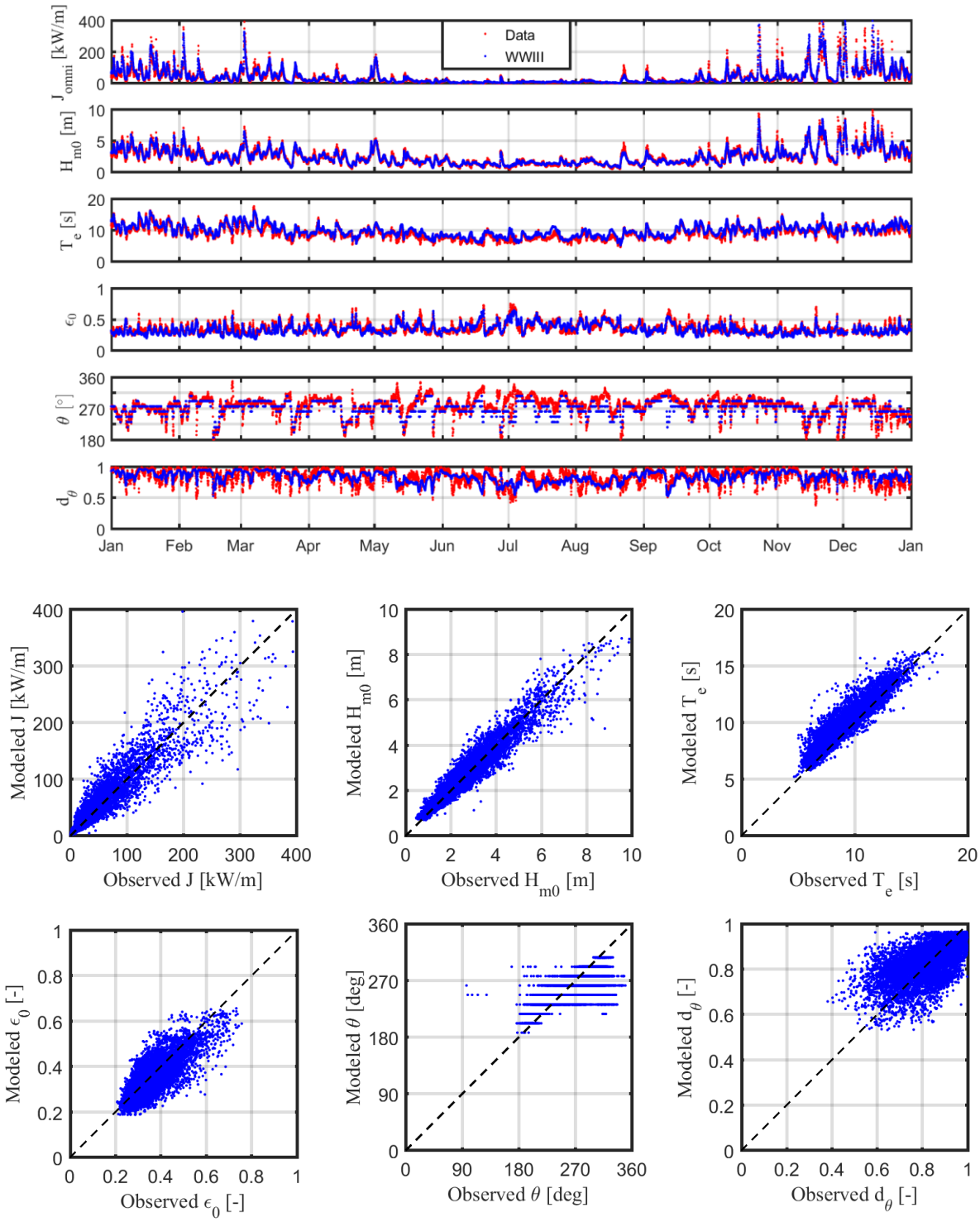

Figure B.10. Comparisons of time series (top) and scatter plots (bottom) of the six WWIII model-simulated IEC parameters with observed data at NDBC Buoy 46029 for 2001.

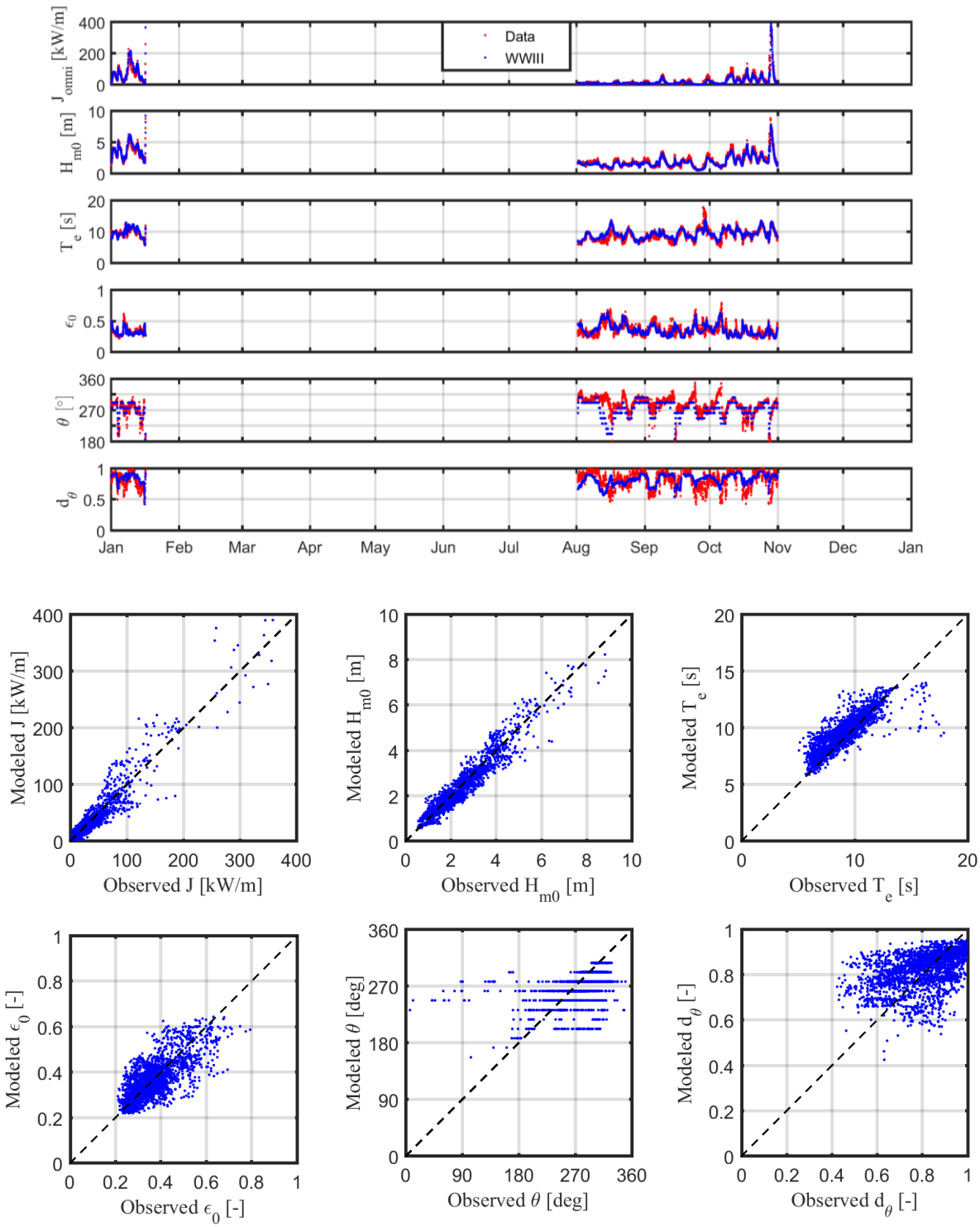

Figure B.11. Comparisons of time series (top) and scatter plots (bottom) of the six WWIII model-simulated IEC parameters with observed data at NDBC Buoy 46029 for 2000.

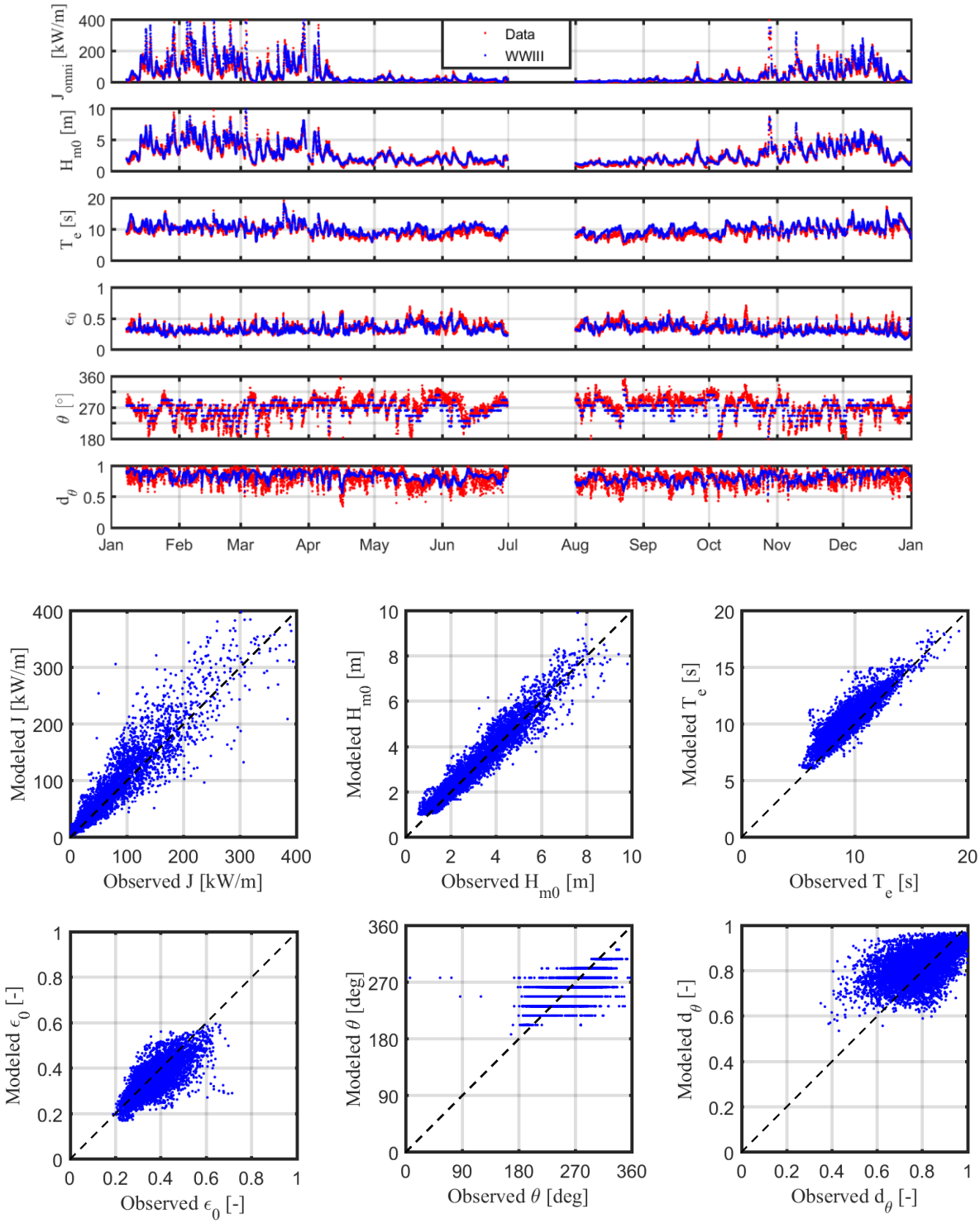

Figure B.12. Comparisons of time series (top) and scatter plots (bottom) of the six WWIII model-simulated IEC parameters with observed data at NDBC Buoy 46029 for 1999.

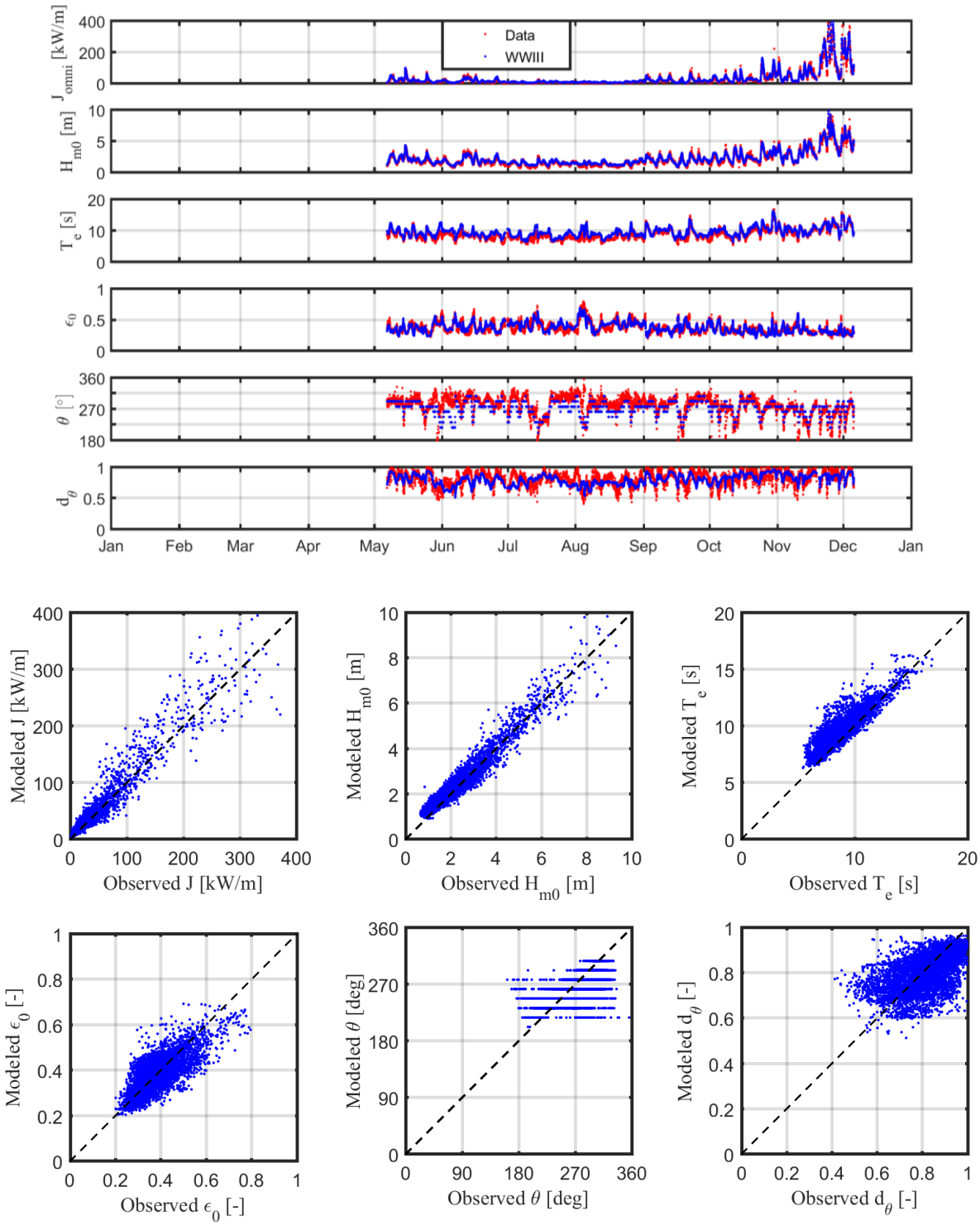

Figure B.13. Comparisons of time series (top) and scatter plots (bottom) of the six WWIII model-simulated IEC parameters with observed data at NDBC Buoy 46029 for 1998.

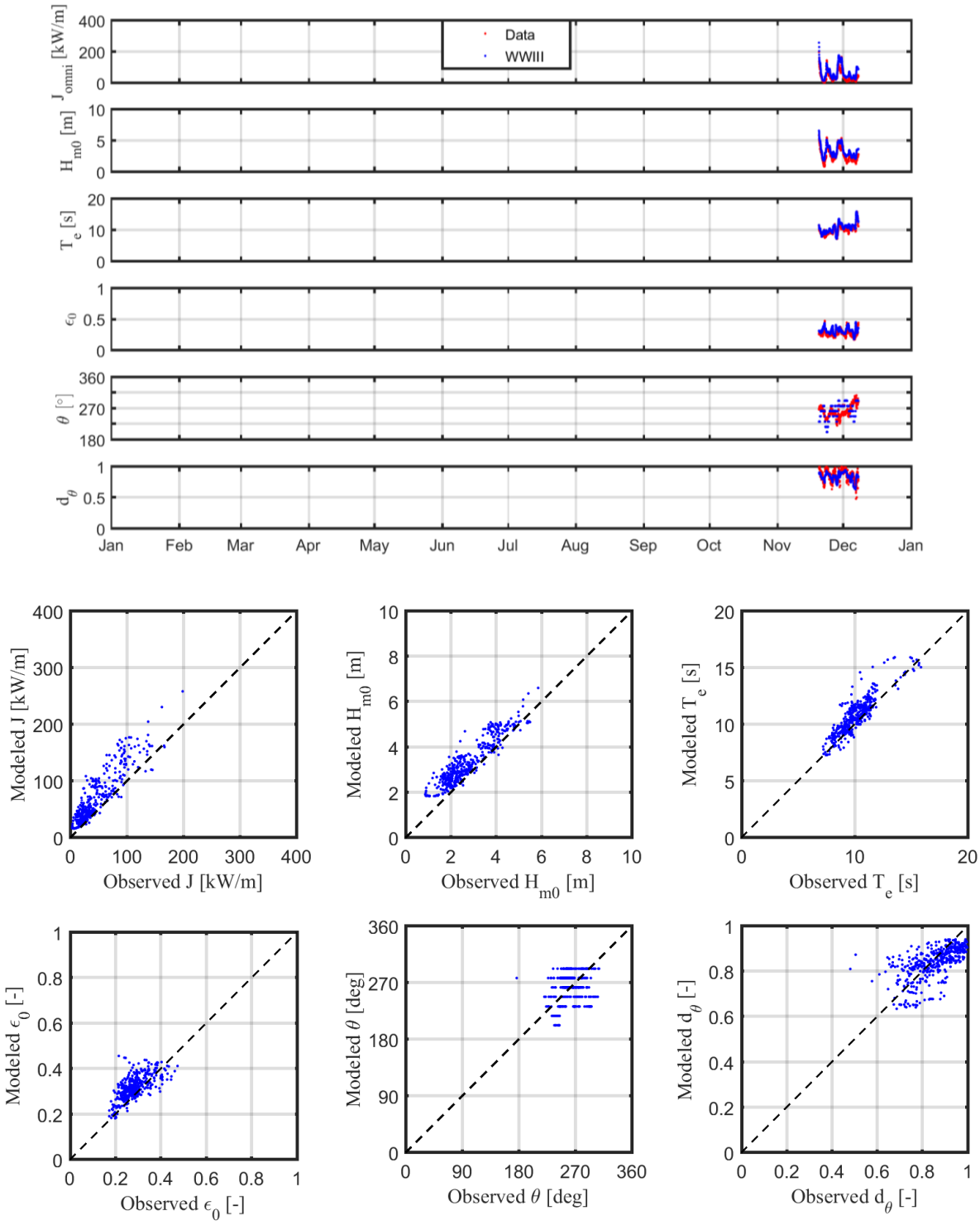

Figure B.14. Comparisons of time series (top) and scatter plots (bottom) of the six WWIII model-simulated IEC parameters with observed data at NDBC Buoy 46029 for 1997.

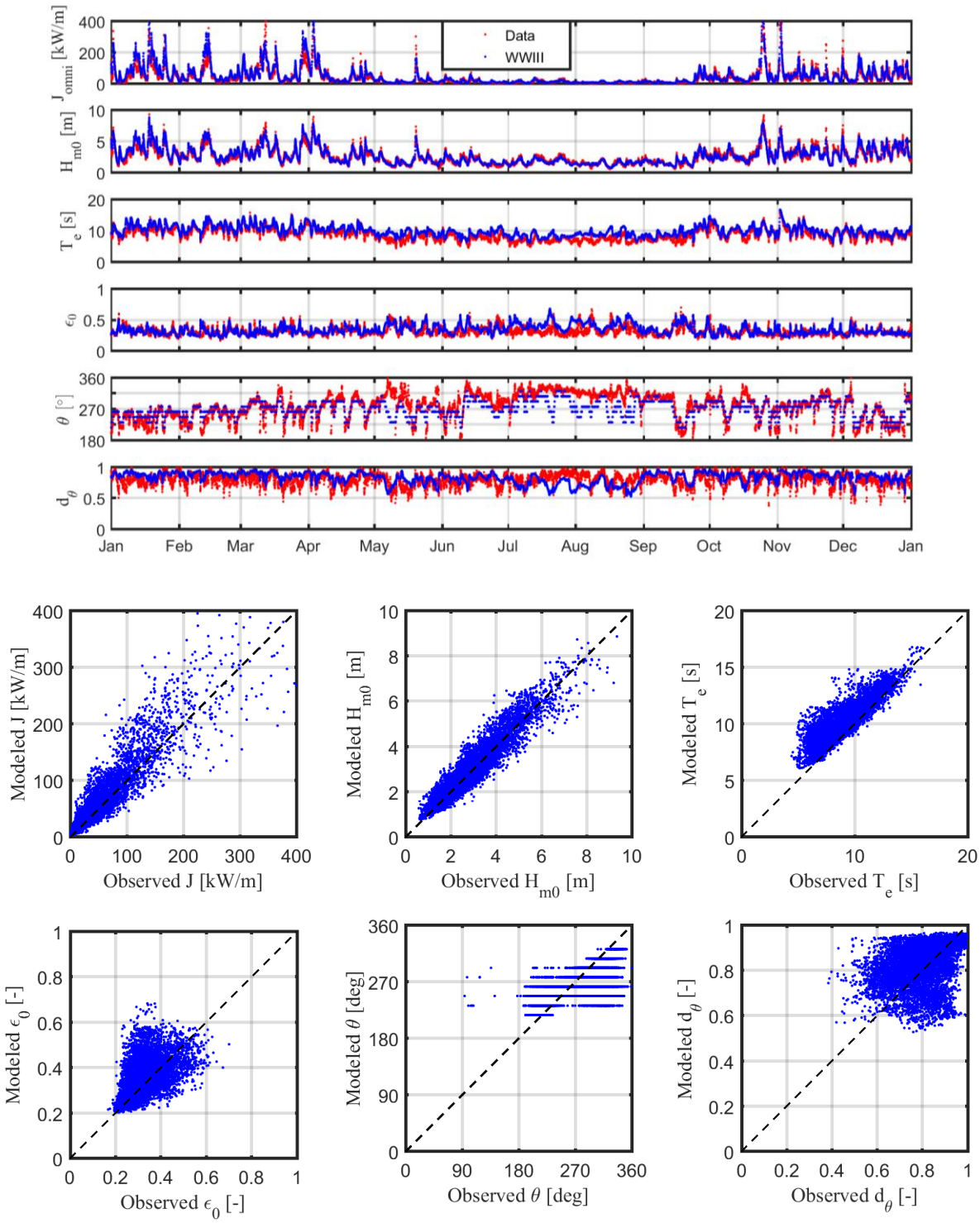

Figure B.15. Comparisons of time series (top) and scatter plots (bottom) of the six WWIII model-simulated IEC parameters with observed data at NDBC Buoy 46050 for 2010.

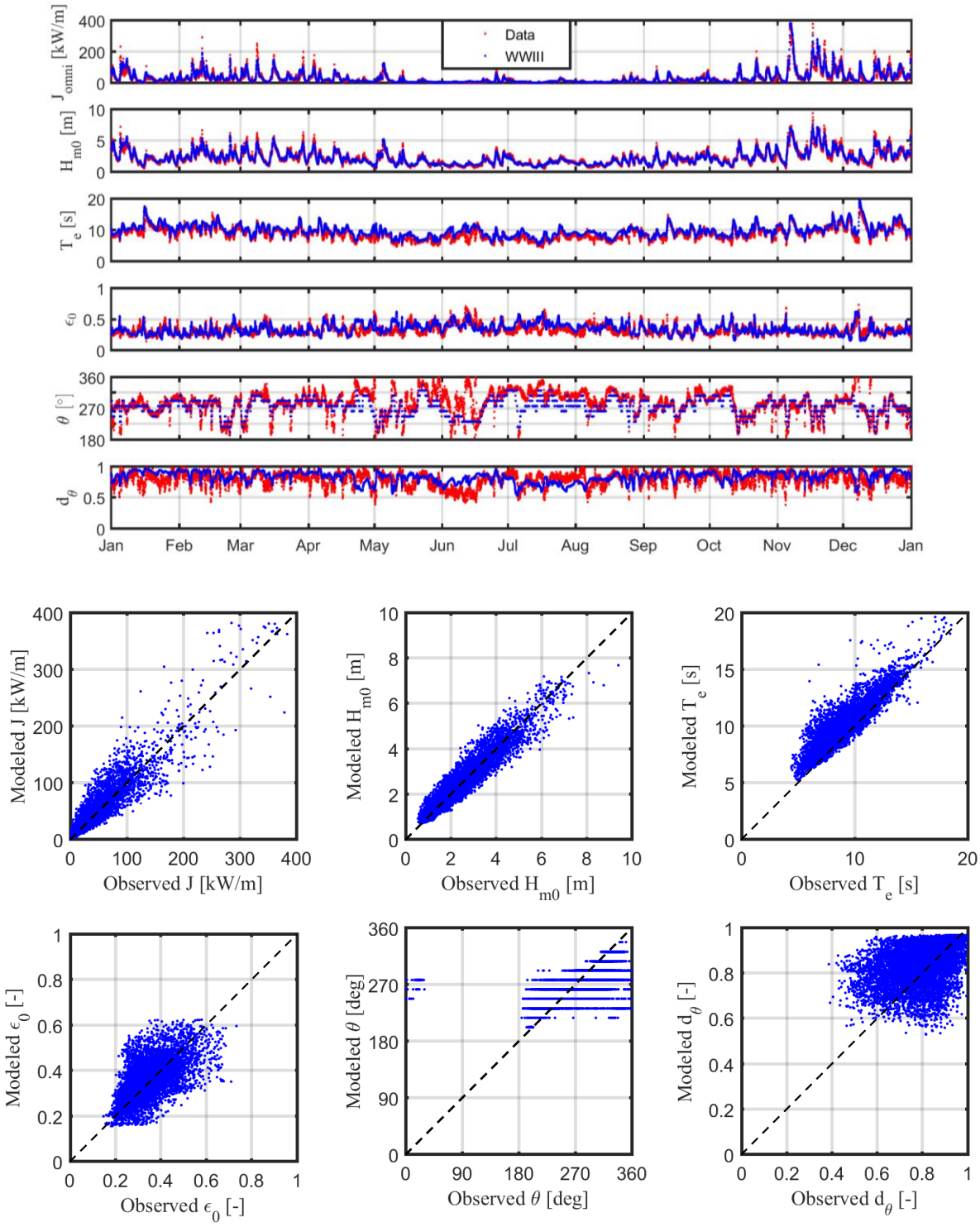

Figure B.16. Comparisons of time series (top) and scatter plots (bottom) of the six WWIII model-simulated IEC parameters with observed data at NDBC Buoy 46050 for 2009.

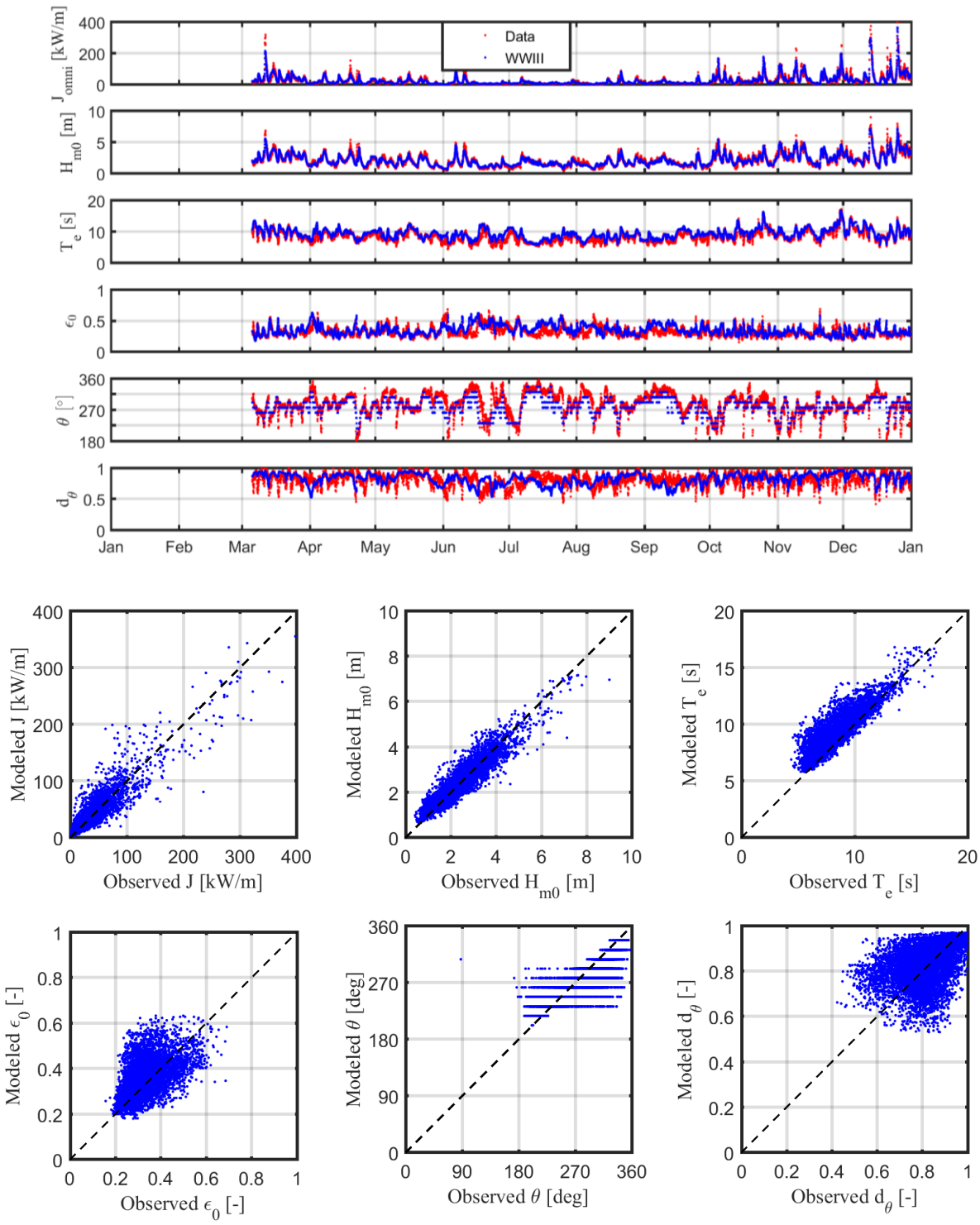

Figure B.17. Comparisons of time series (top) and scatter plots (bottom) of the six WWIII model-simulated IEC parameters with observed data at NDBC Buoy 46050 for 2008.

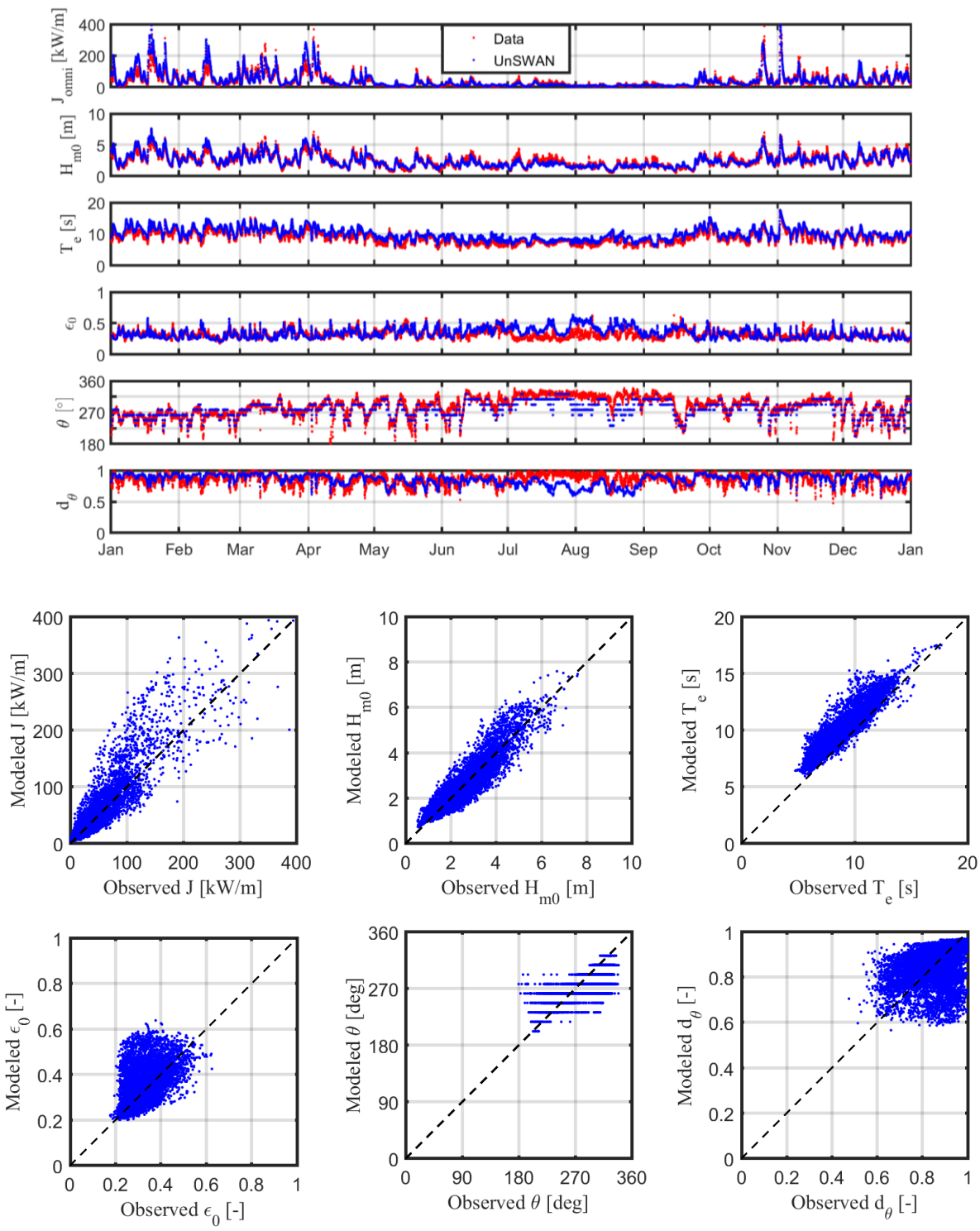

Figure B.18. Comparisons of time series (top) and scatter plots (bottom) of UnSWAN simulated six IEC parameters with observed data at NDBC Buoy 46027 for 2010.

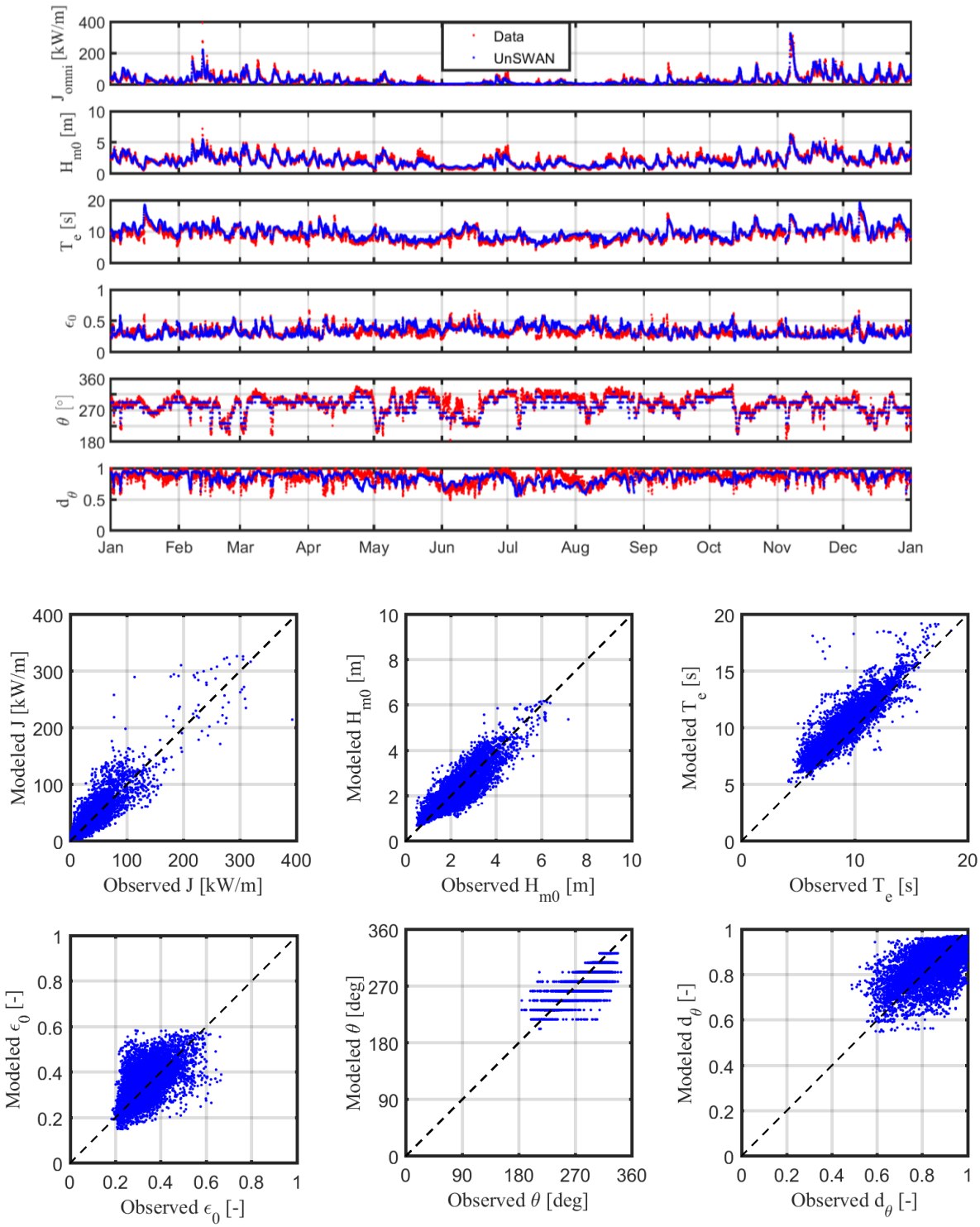

Figure B.19. Comparisons of time series (top) and scatter plots (bottom) of UnSWAN simulated six IEC parameters with observed data at NDBC Buoy 46027 for 2009.

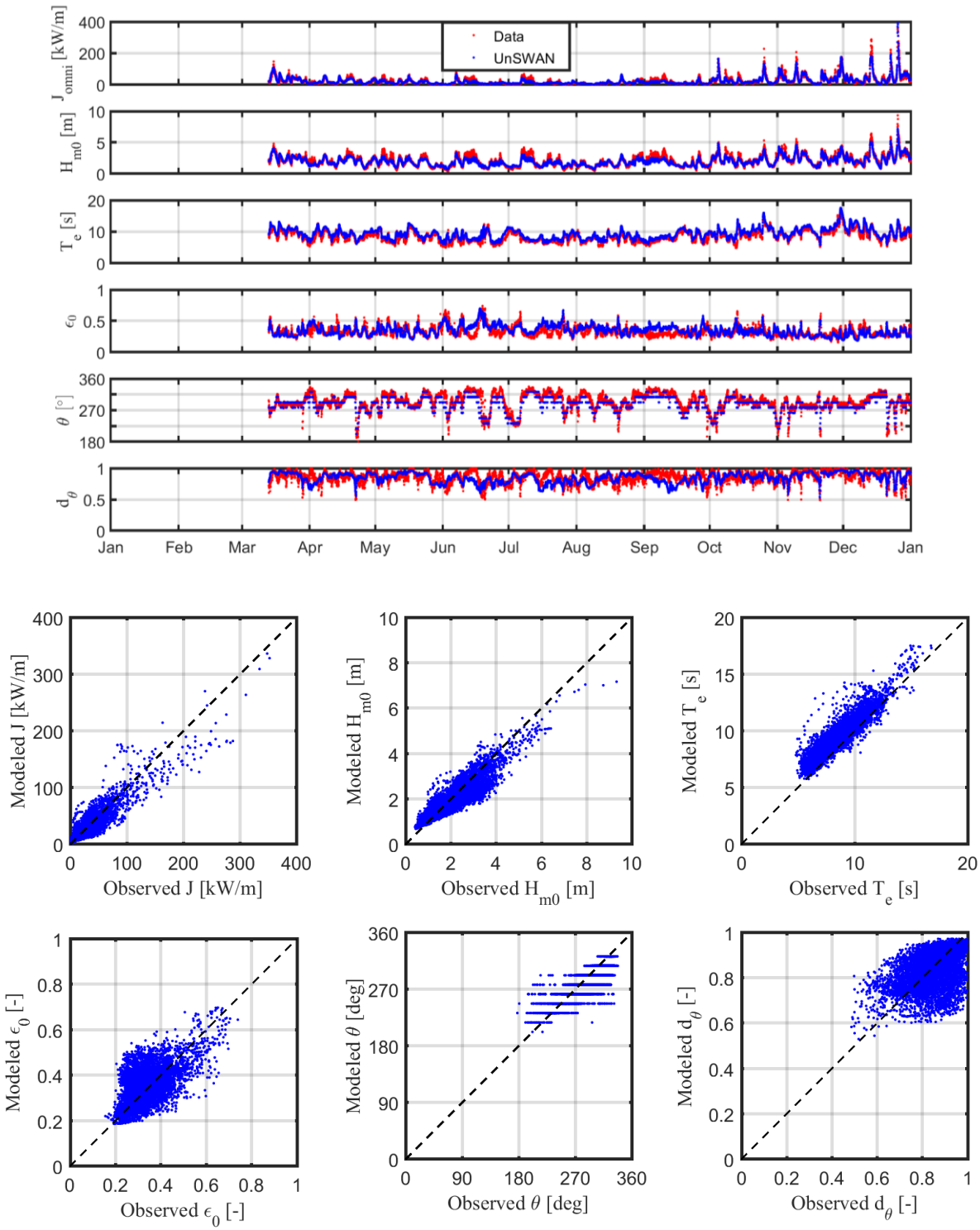

Figure B.20. Comparisons of time series (top) and scatter plots (bottom) of UnSWAN simulated six IEC parameters with observed data at NDBC Buoy 46027 for 2008.

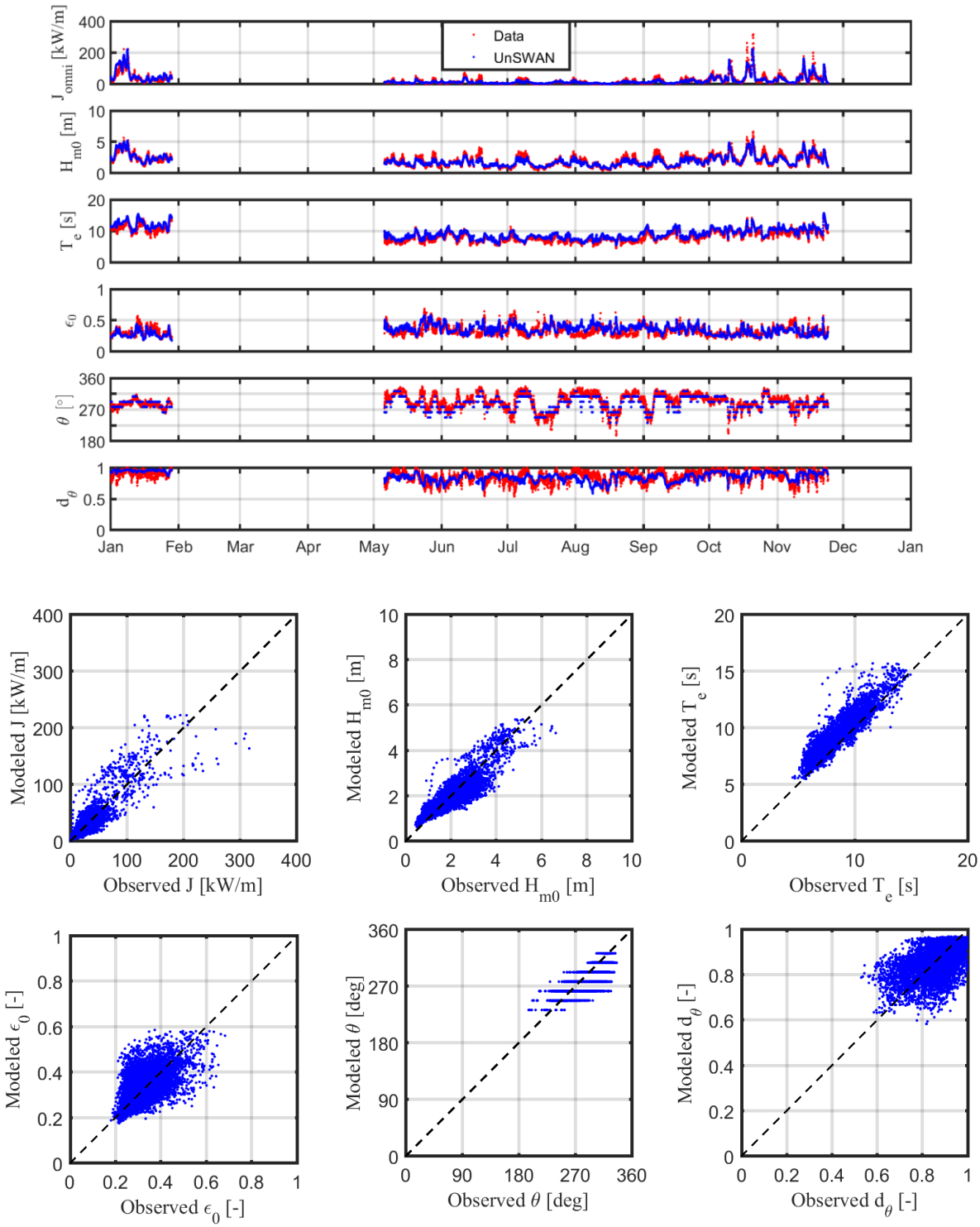

Figure B.21. Comparisons of time series (top) and scatter plots (bottom) of UnSWAN simulated six IEC parameters with observed data at NDBC Buoy 46027 for 2007.

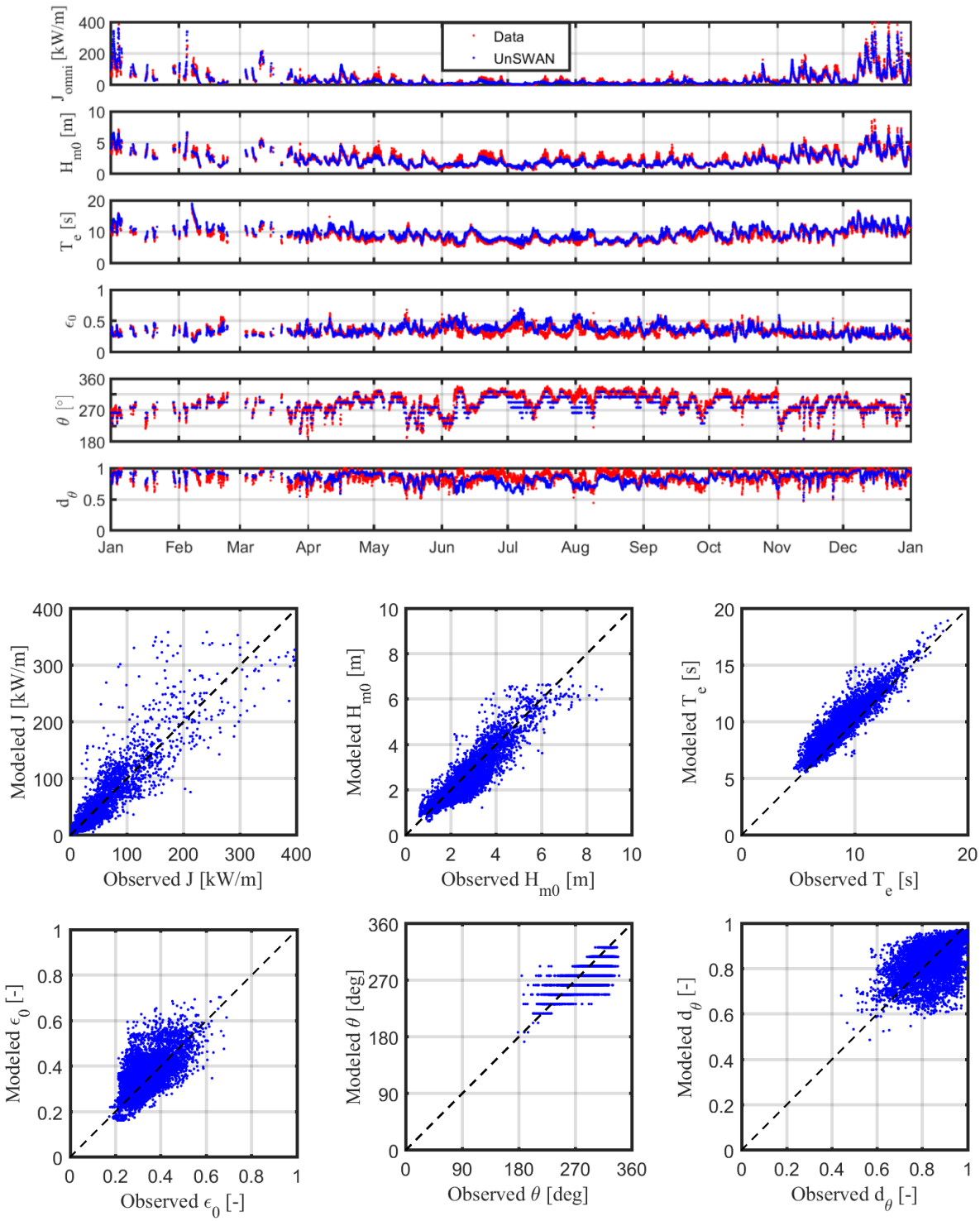

Figure B.22. Comparisons of time series (top) and scatter plots (bottom) of UnSWAN simulated six IEC parameters with observed data at NDBC Buoy 46027 for 2006.

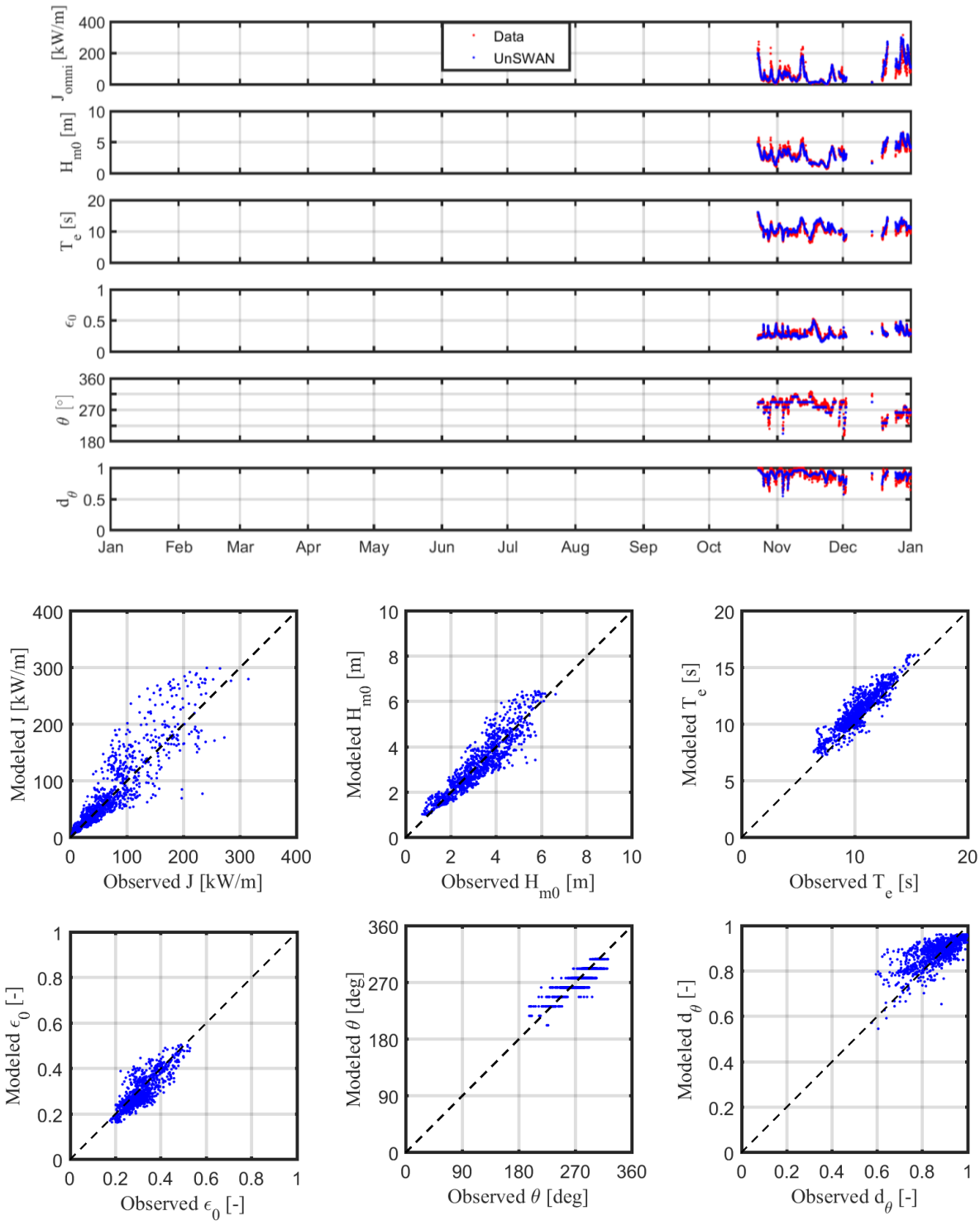

Figure B.23. Comparisons of time series (top) and scatter plots (bottom) of UnSWAN simulated six IEC parameters with observed data at NDBC Buoy 46027 for 2005.

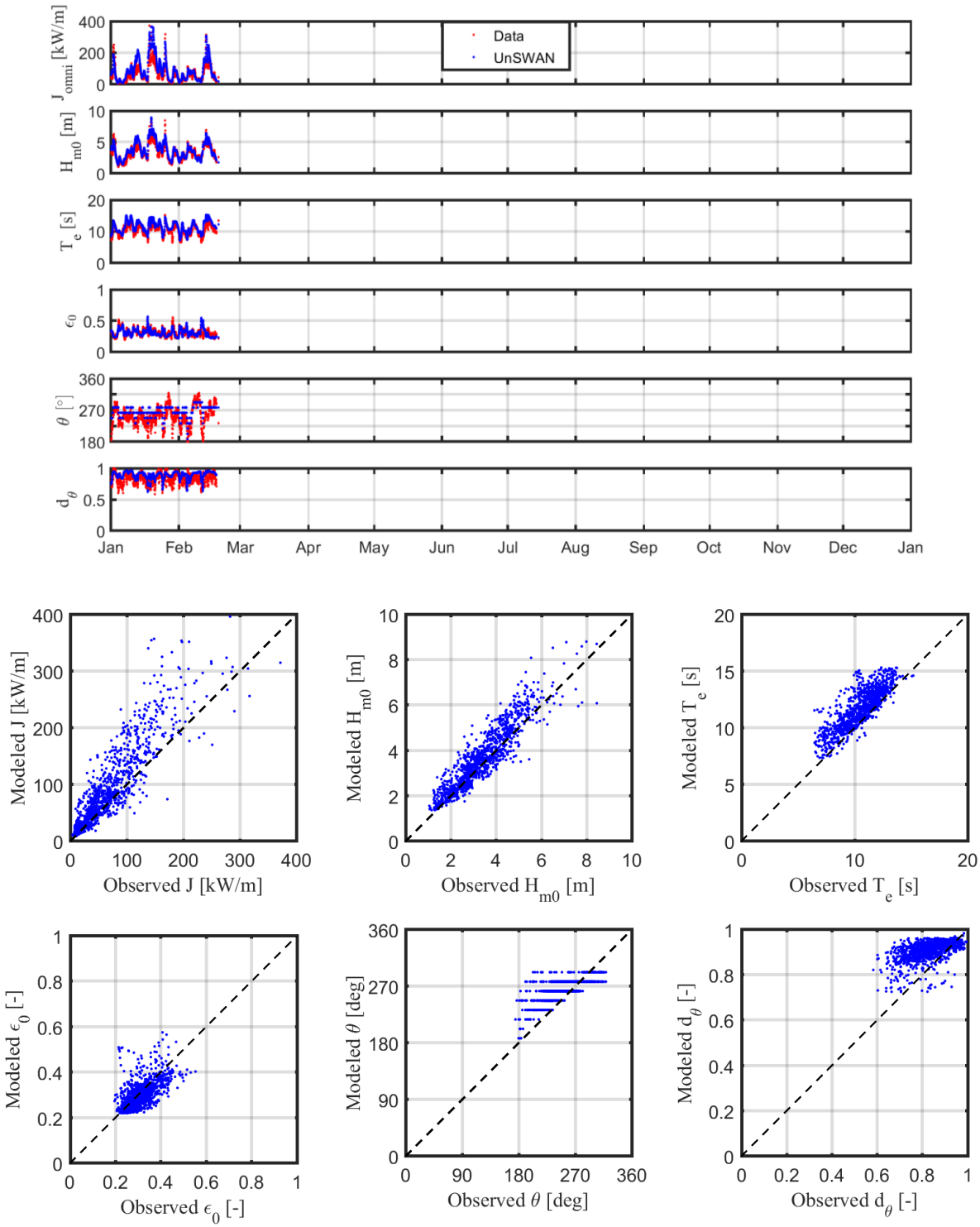

Figure B.24. Comparisons of time series (top) and scatter plots (bottom) of UnSWAN simulated six IEC parameters with observed data at NDBC Buoy 46022 for 2010.

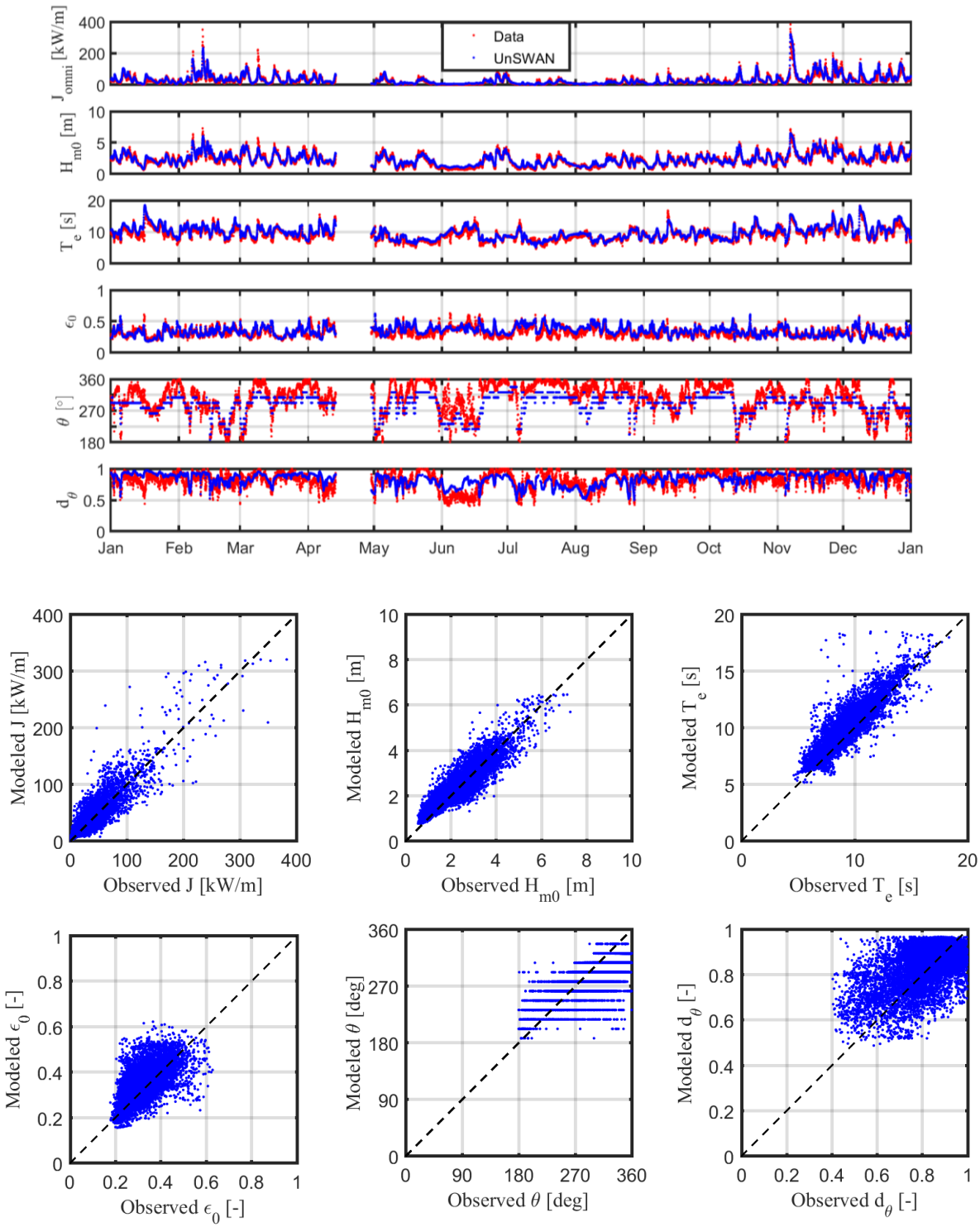

Figure B.25. Comparisons of time series (top) and scatter plots (bottom) of UnSWAN simulated six IEC parameters with observed data at NDBC Buoy 46022 for 2009.

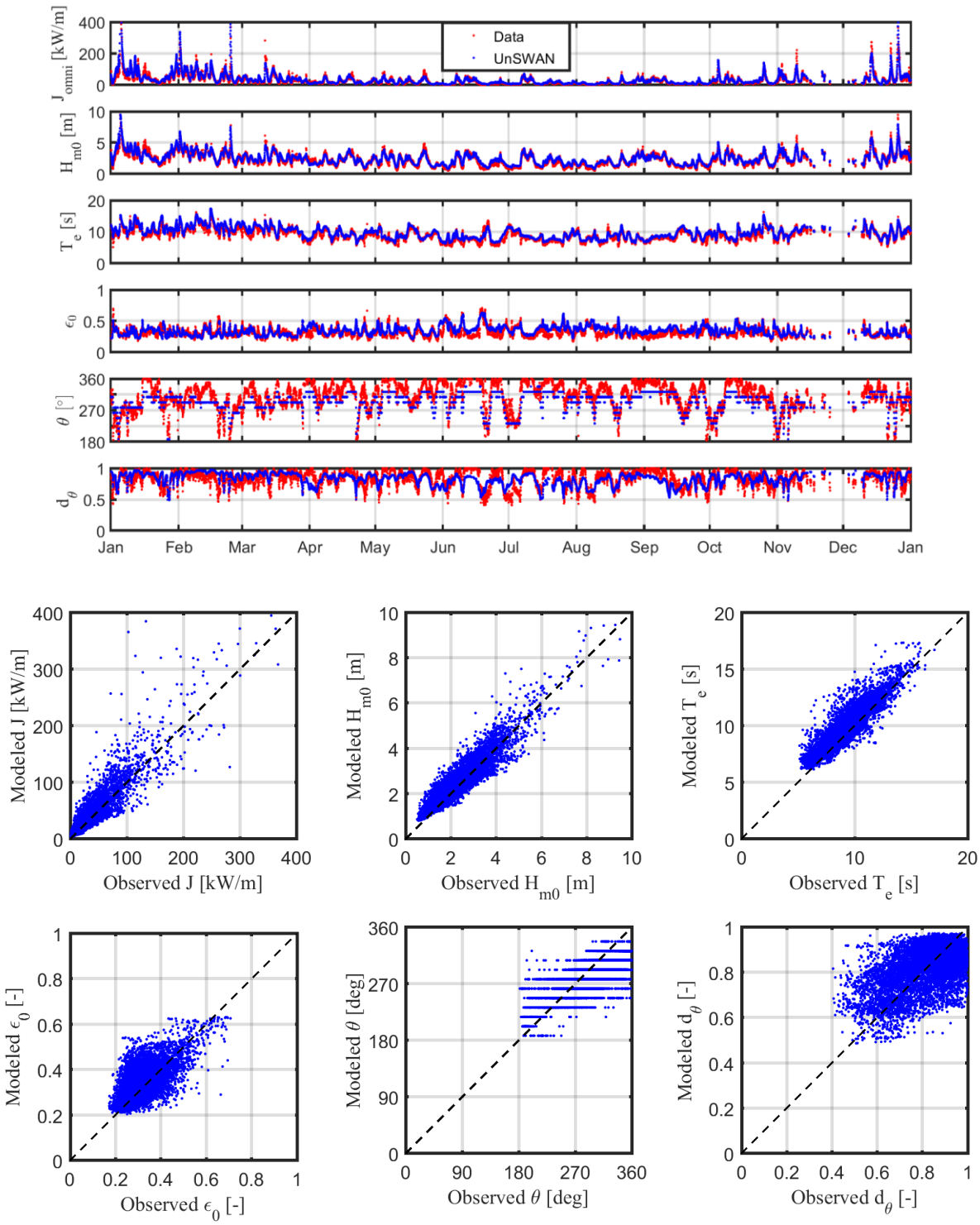

Figure B.26. Comparisons of time series (top) and scatter plots (bottom) of UnSWAN simulated six IEC parameters with observed data at NDBC Buoy 46022 for 2008.

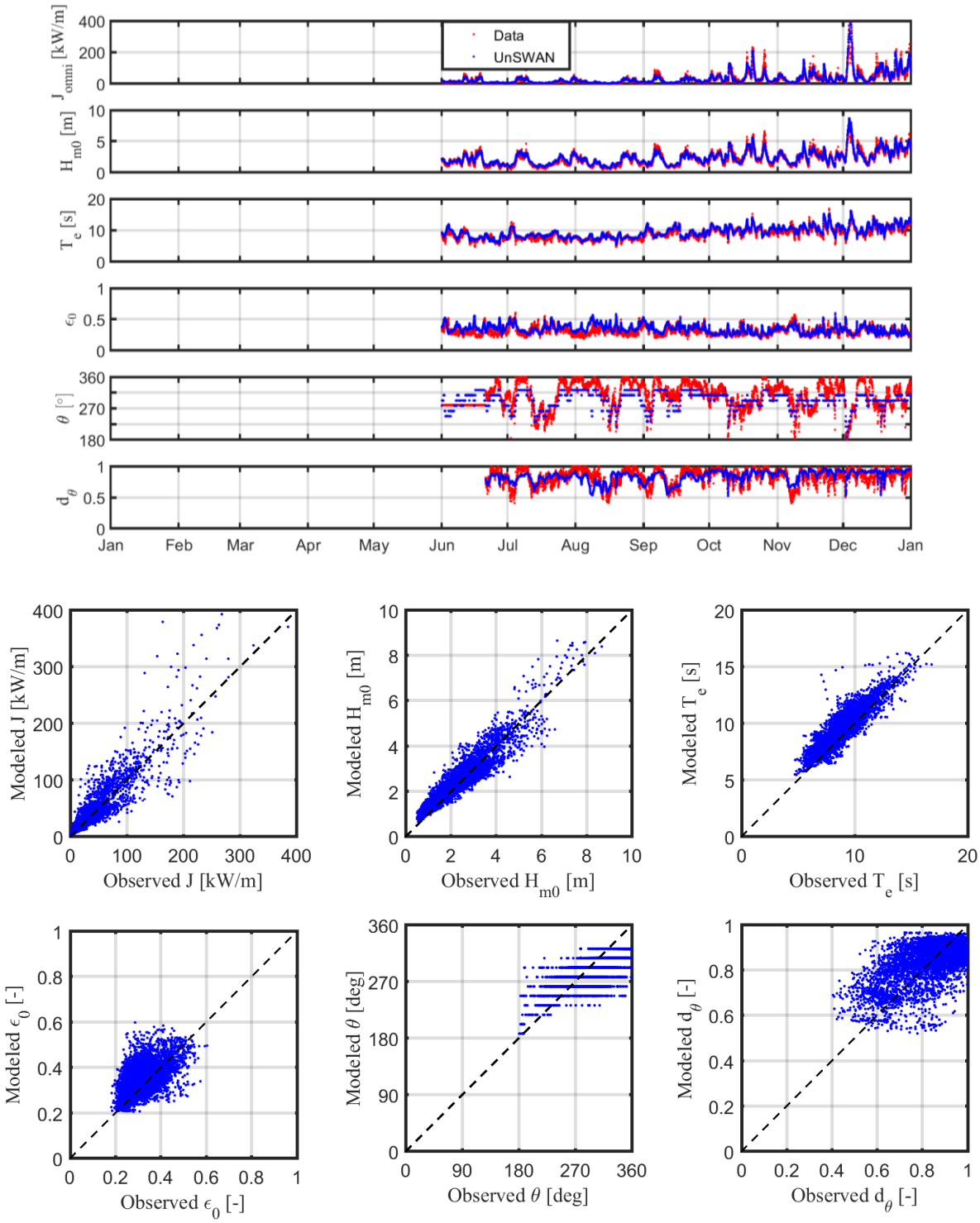

Figure B.27. Comparisons of time series (top) and scatter plots (bottom) of UnSWAN simulated six IEC parameters with observed data at NDBC Buoy 46022 for 2007.

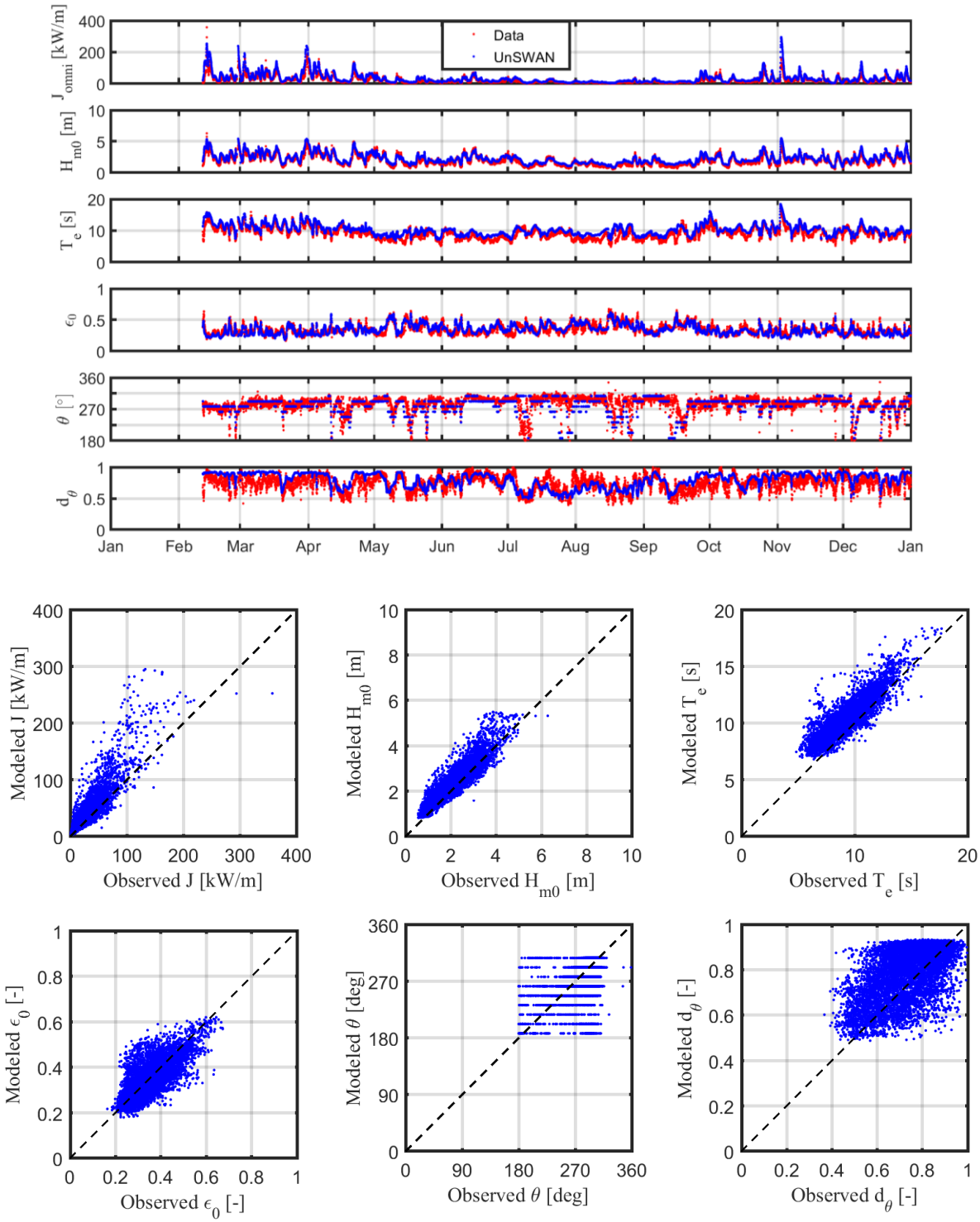

Figure B.28. Comparisons of time series (top) and scatter plots (bottom) of UnSWAN simulated six IEC parameters with observed data at NDBC Buoy 46026 for 2010.

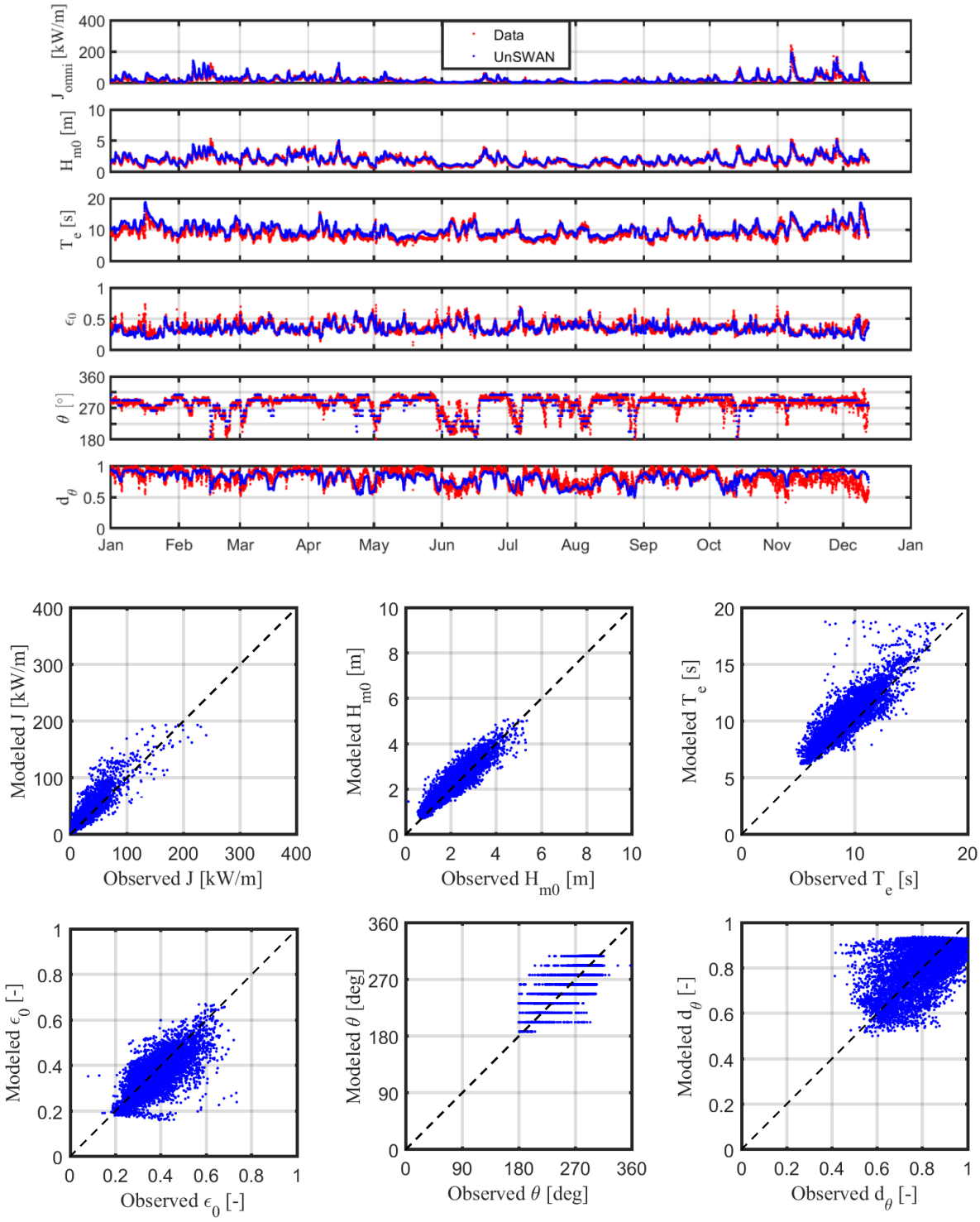

Figure B.29. Comparisons of time series (top) and scatter plots (bottom) of UnSWAN simulated six IEC parameters with observed data at NDBC Buoy 46026 for 2009.

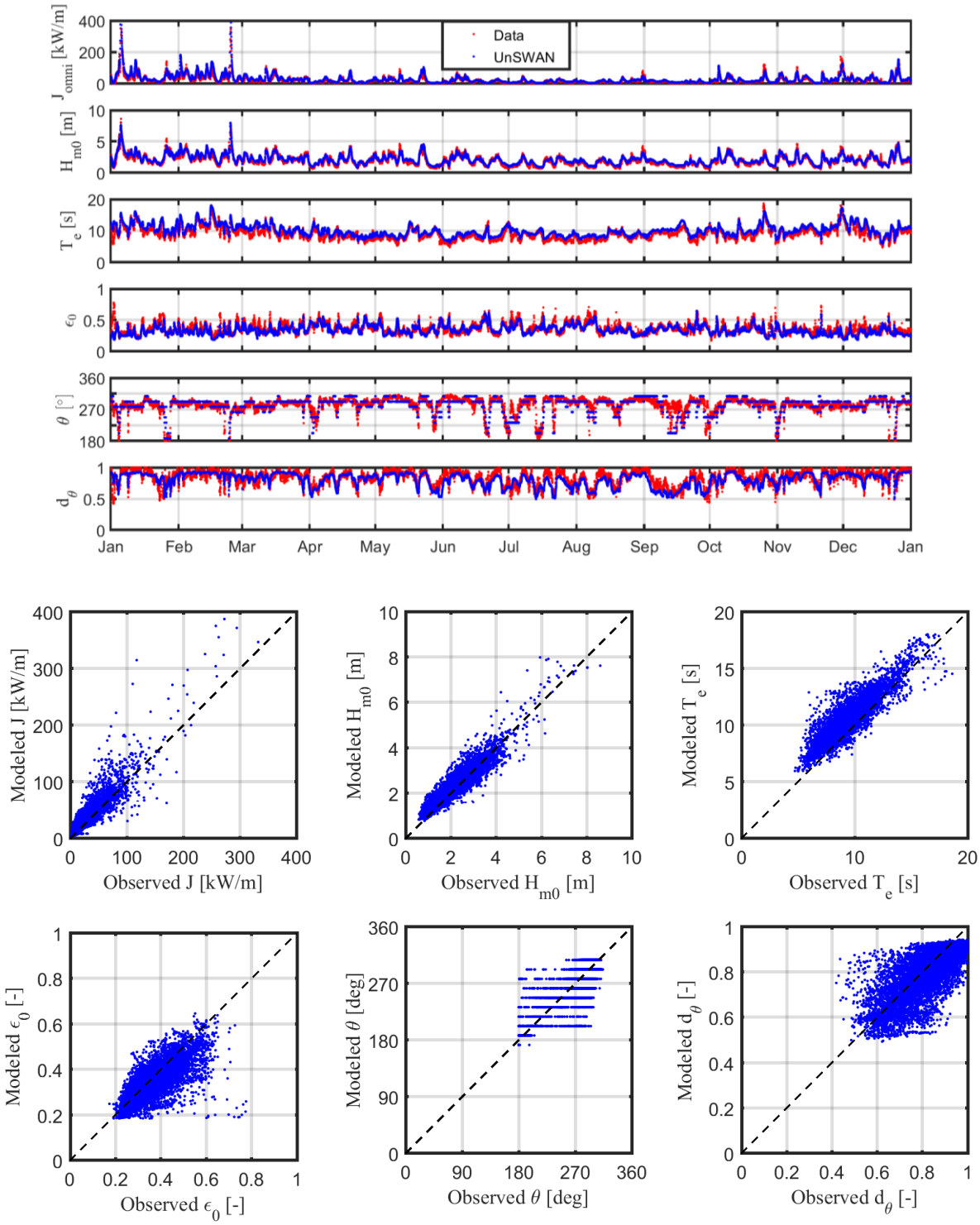

Figure B.30. Comparisons of time series (top) and scatter plots (bottom) of UnSWAN simulated six IEC parameters with observed data at NDBC Buoy 46026 for 2008.

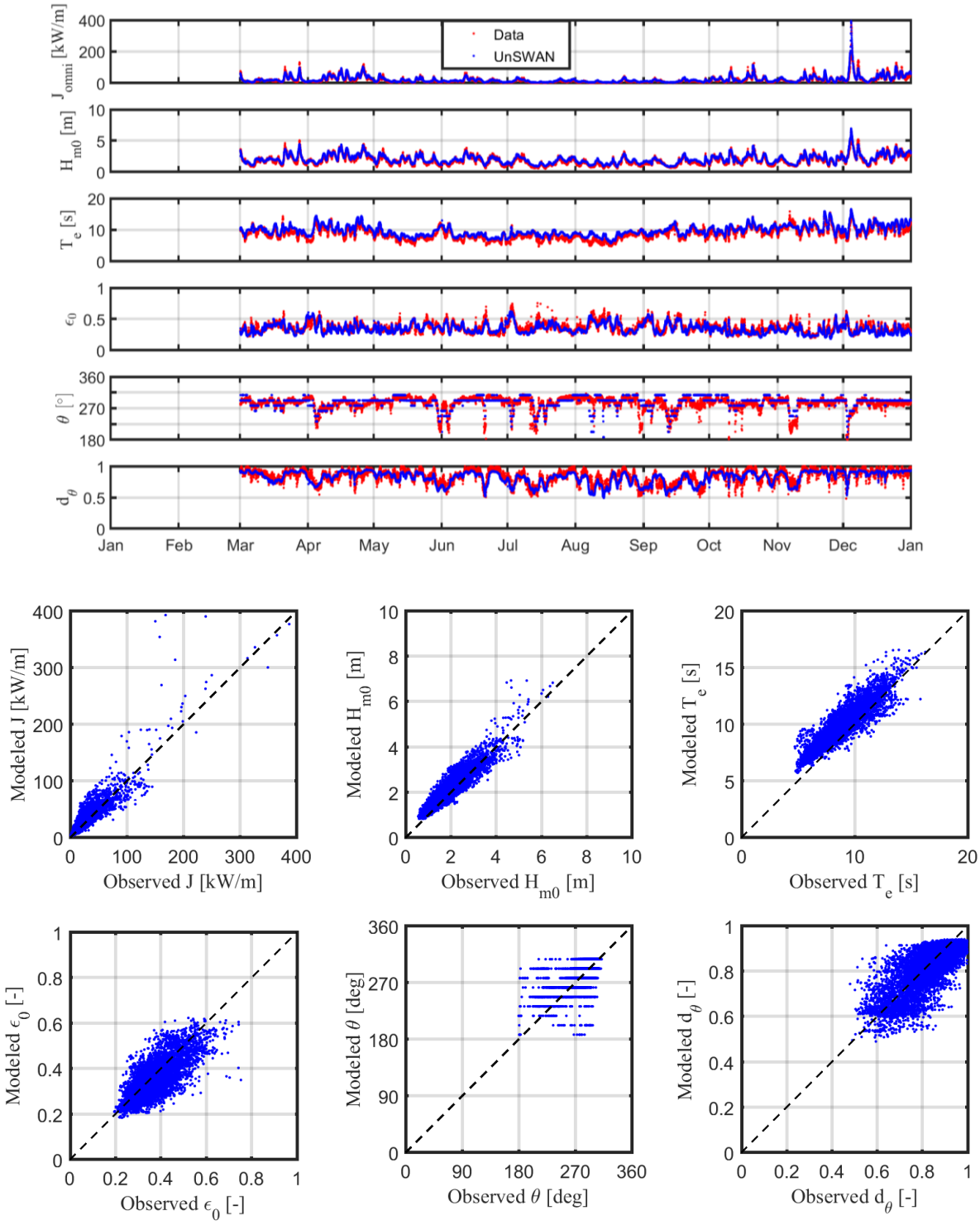

Figure B.31. Comparisons of time series (top) and scatter plots (bottom) of UnSWAN simulated six IEC parameters with observed data at NDBC Buoy 46026 for 2007.

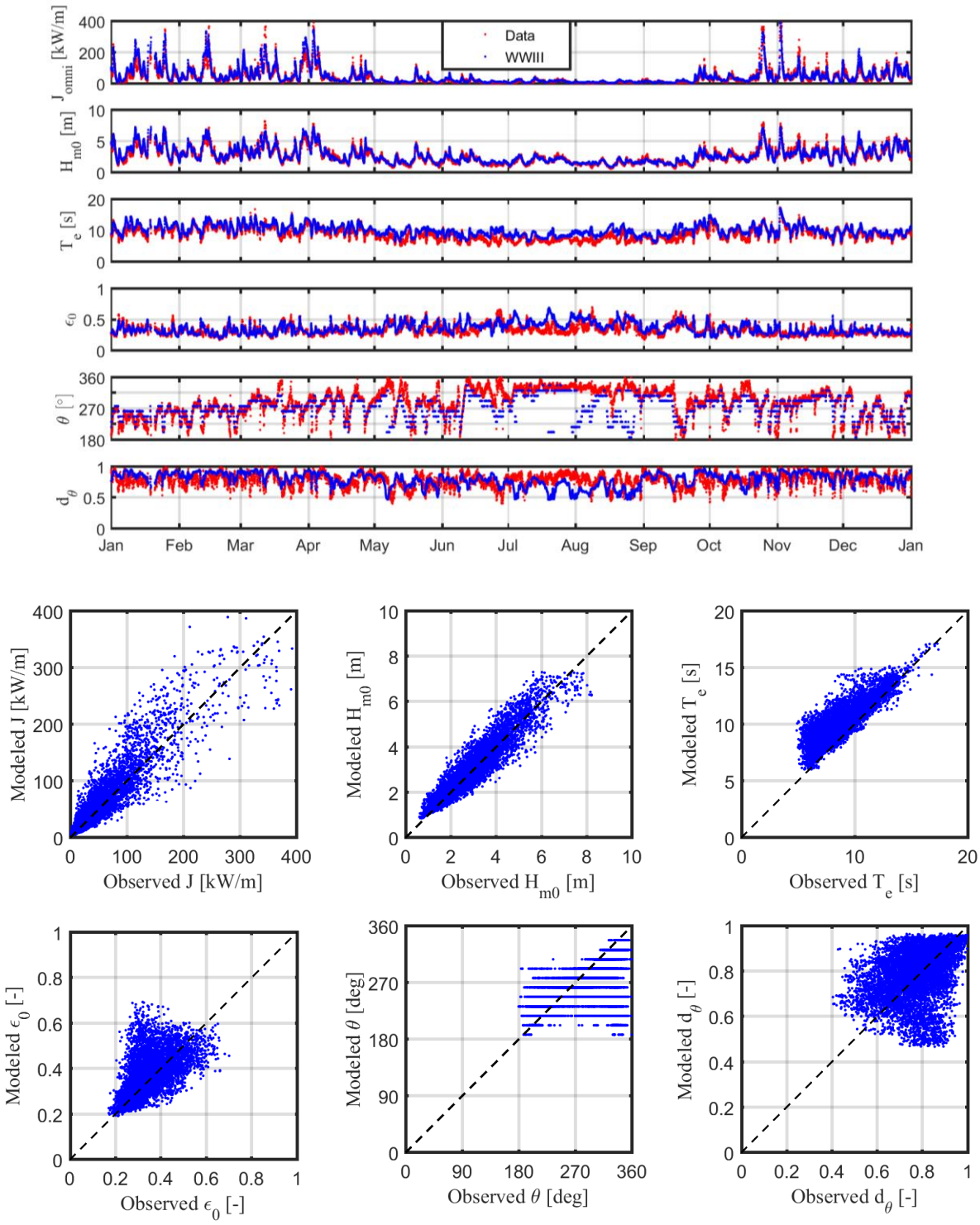

Figure B.32. Comparisons of time series (top) and scatter plots (bottom) of the six WWIII model-simulated IEC parameters with observed data at NDBC Buoy 46015 for 2010.

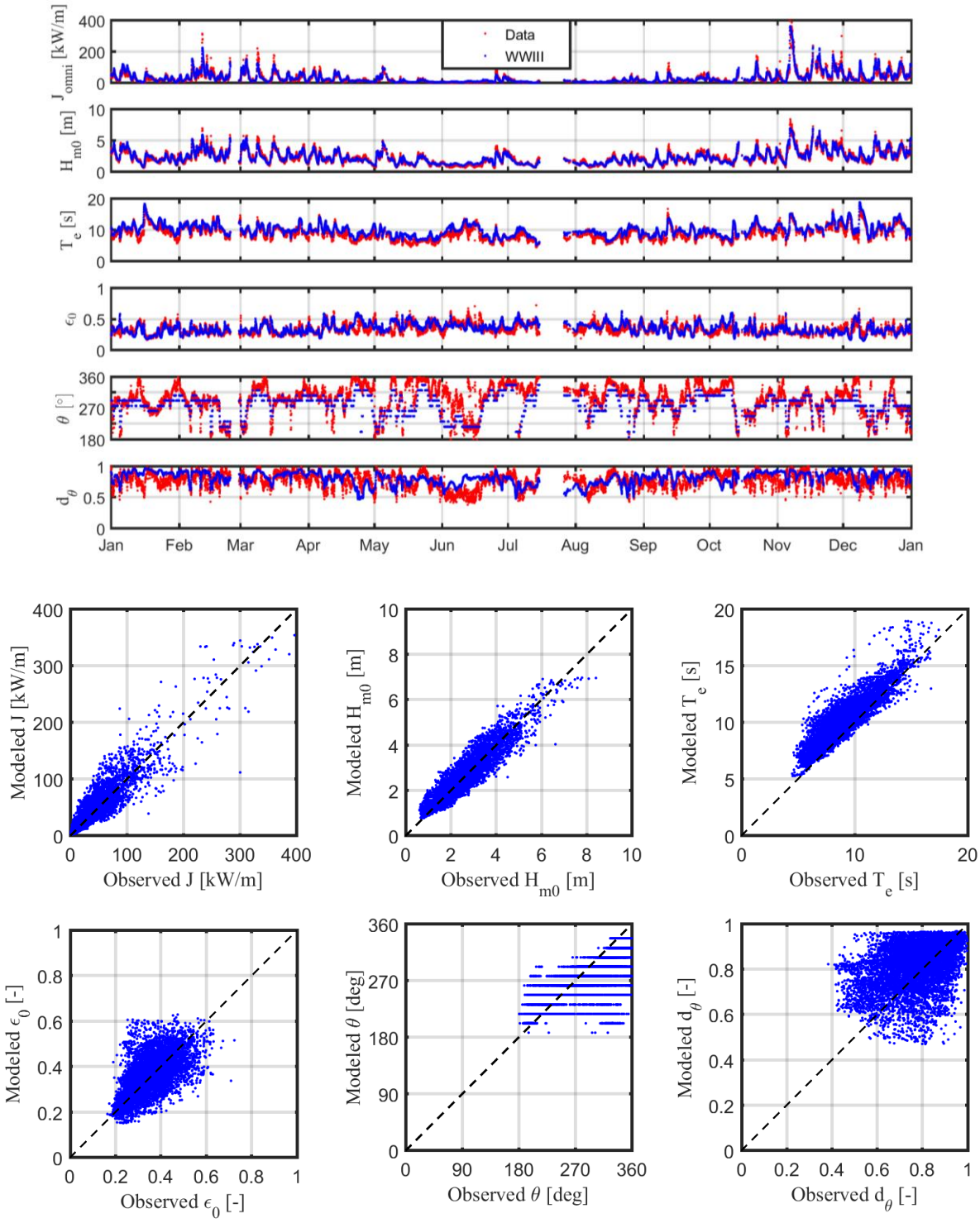

Figure B.33. Comparisons of time series (top) and scatter plots (bottom) of the six WWIII model-simulated IEC parameters with observed data at NDBC Buoy 46015 for 2009.

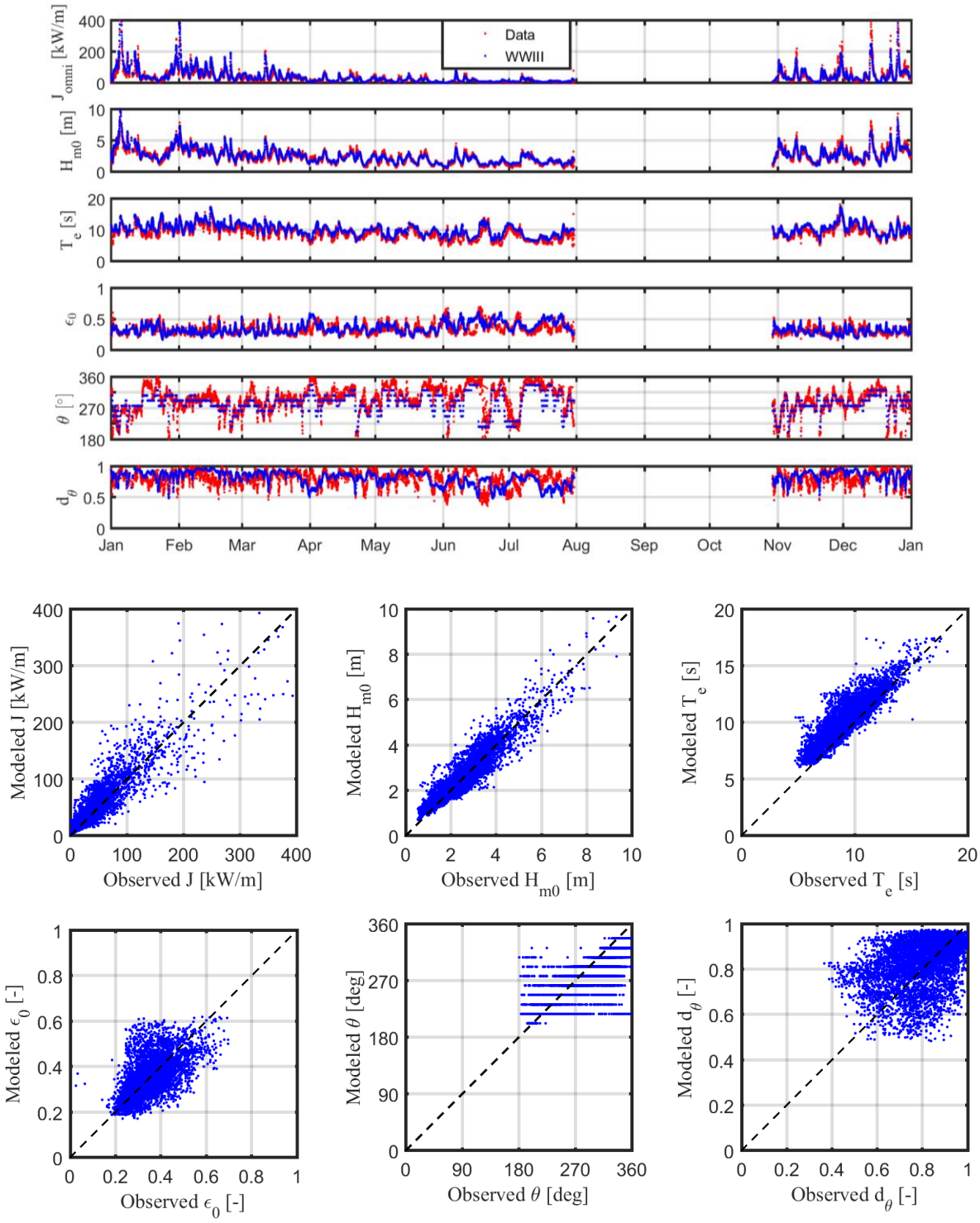

Figure B.34. Comparisons of time series (top) and scatter plots (bottom) of the six WWIII model-simulated IEC parameters with observed data at NDBC Buoy 46015 for 2008.

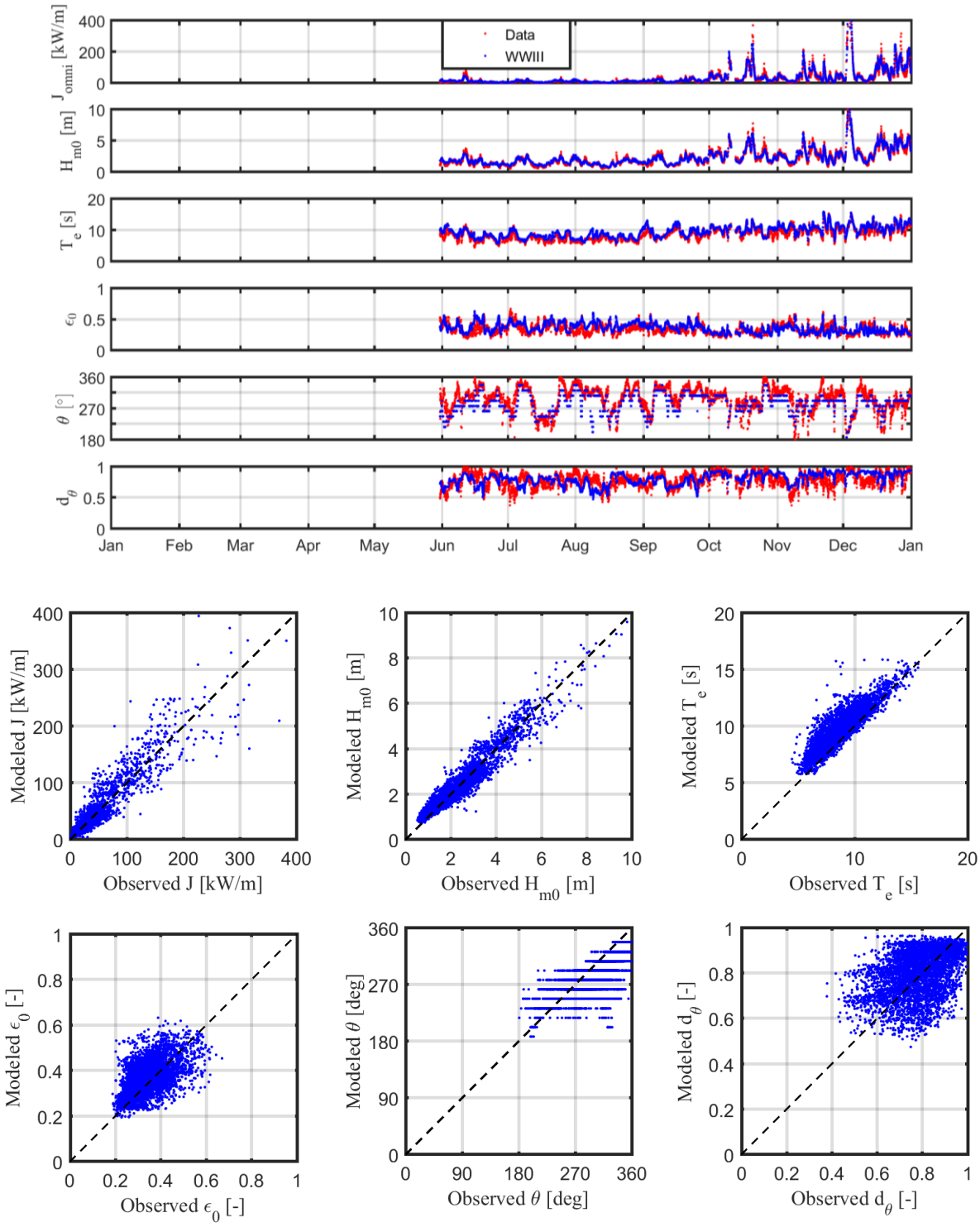

Figure B.35. Comparisons of time series (top) and scatter plots (bottom) of the six WWIII model-simulated IEC parameters with observed data at NDBC Buoy 46015 for 2007.

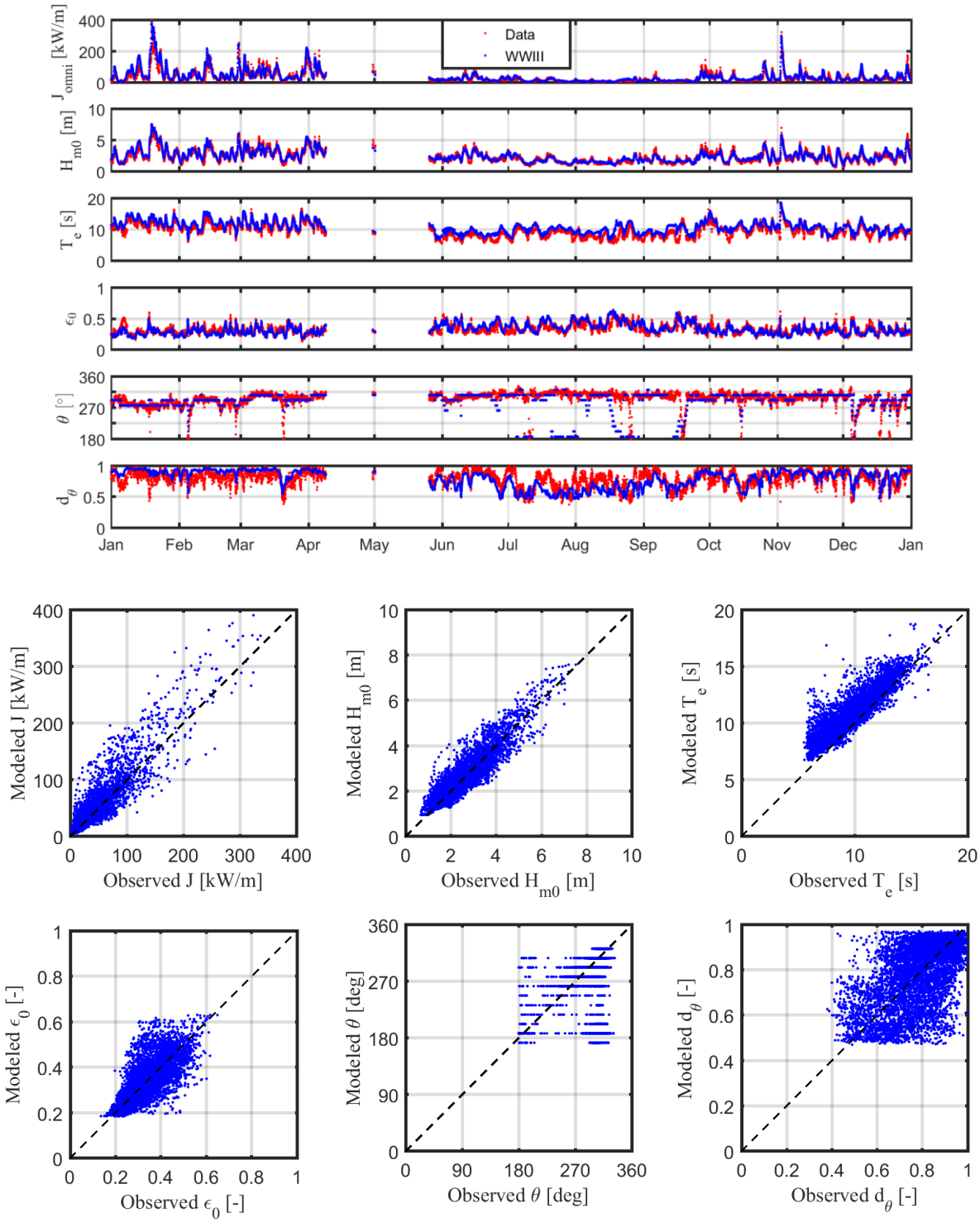

Figure B.36. Comparisons of time series (top) and scatter plots (bottom) of the six WWIII model-simulated IEC parameters with observed data at NDBC Buoy 46028 for 2010.

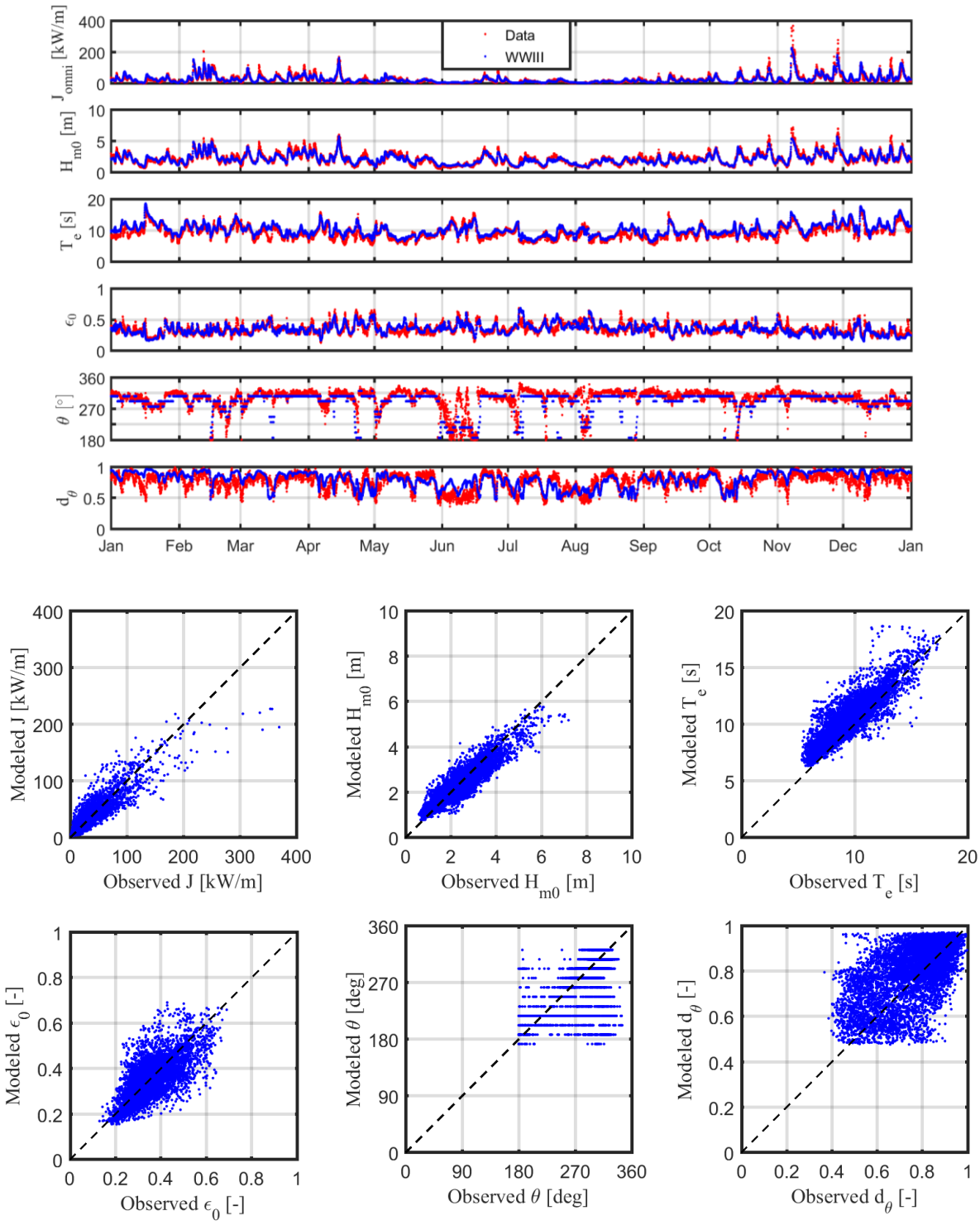

Figure B.37. Comparisons of time series (top) and scatter plots (bottom) of the six WWIII model-simulated IEC parameters with observed data at NDBC Buoy 46028 for 2009.

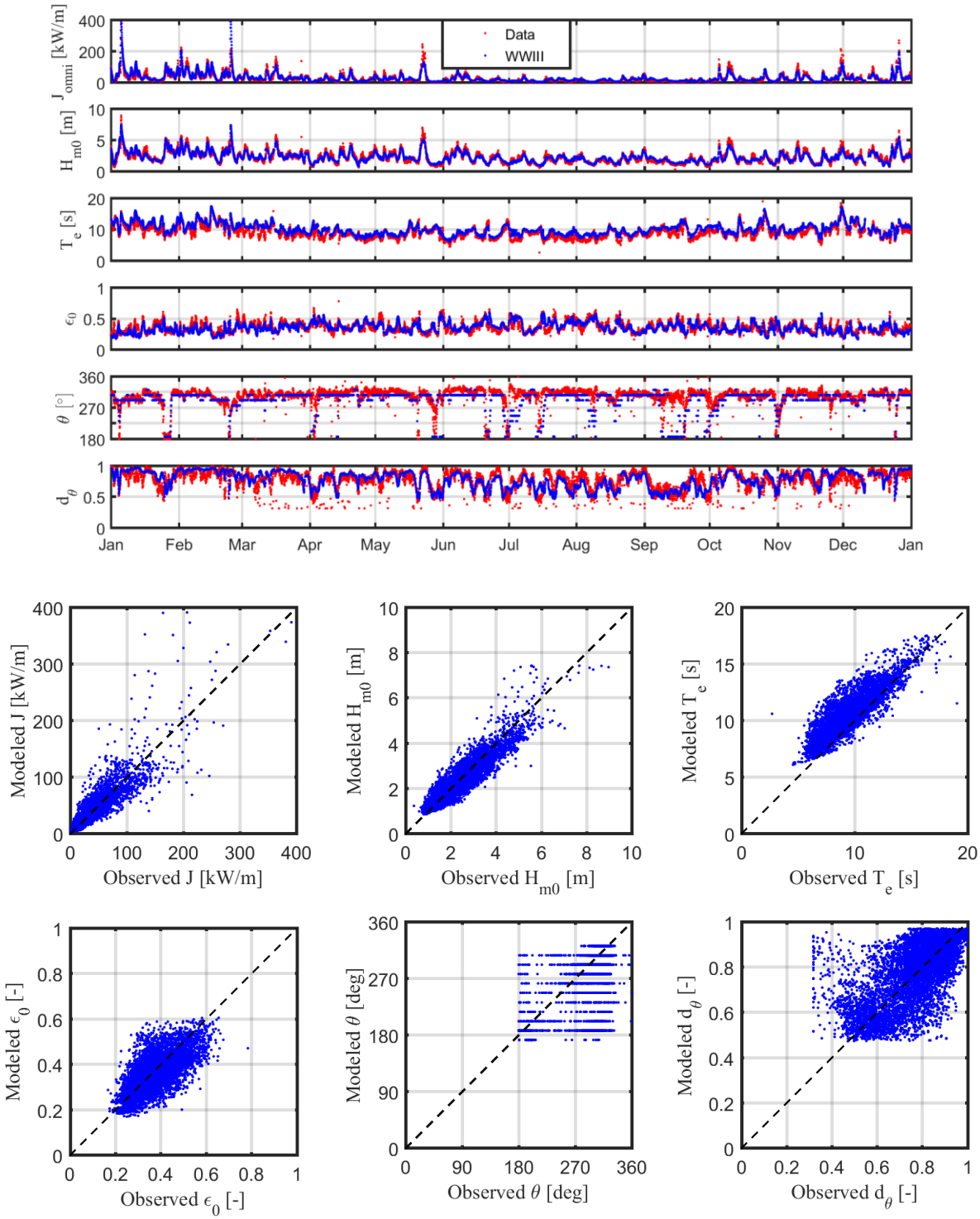

Figure B.38. Comparisons of time series (top) and scatter plots (bottom) of the six WWIII model-simulated IEC parameters with observed data at NDBC Buoy 46028 for 2008.

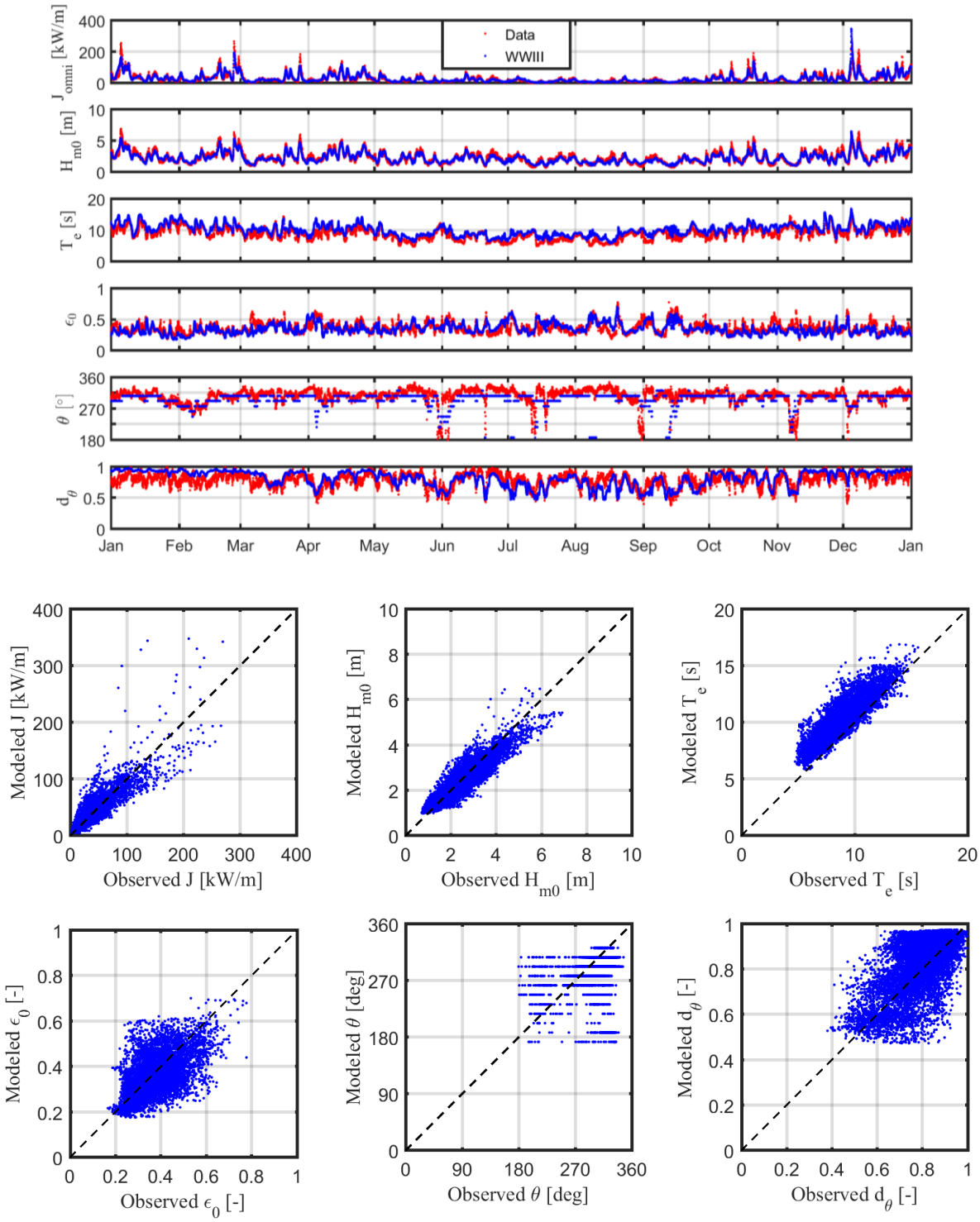

Figure B.39. Comparisons of time series (top) and scatter plots (bottom) of the six WWIII model-simulated IEC parameters with observed data at NDBC Buoy 46028 for 2007.

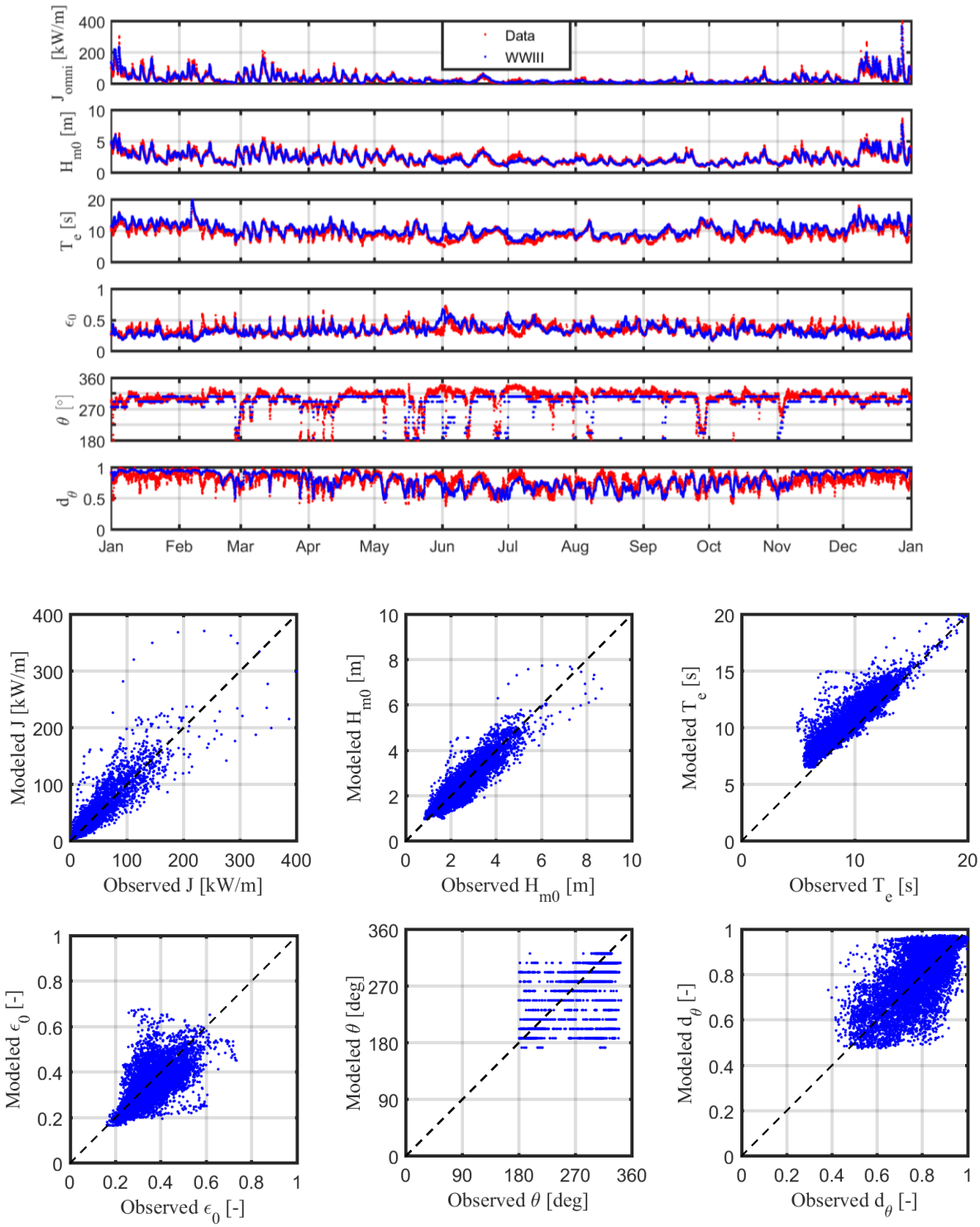

Figure B.40. Comparisons of time series (top) and scatter plots (bottom) of the six WWIII model-simulated IEC parameters with observed data at NDBC Buoy 46028 for 2006.

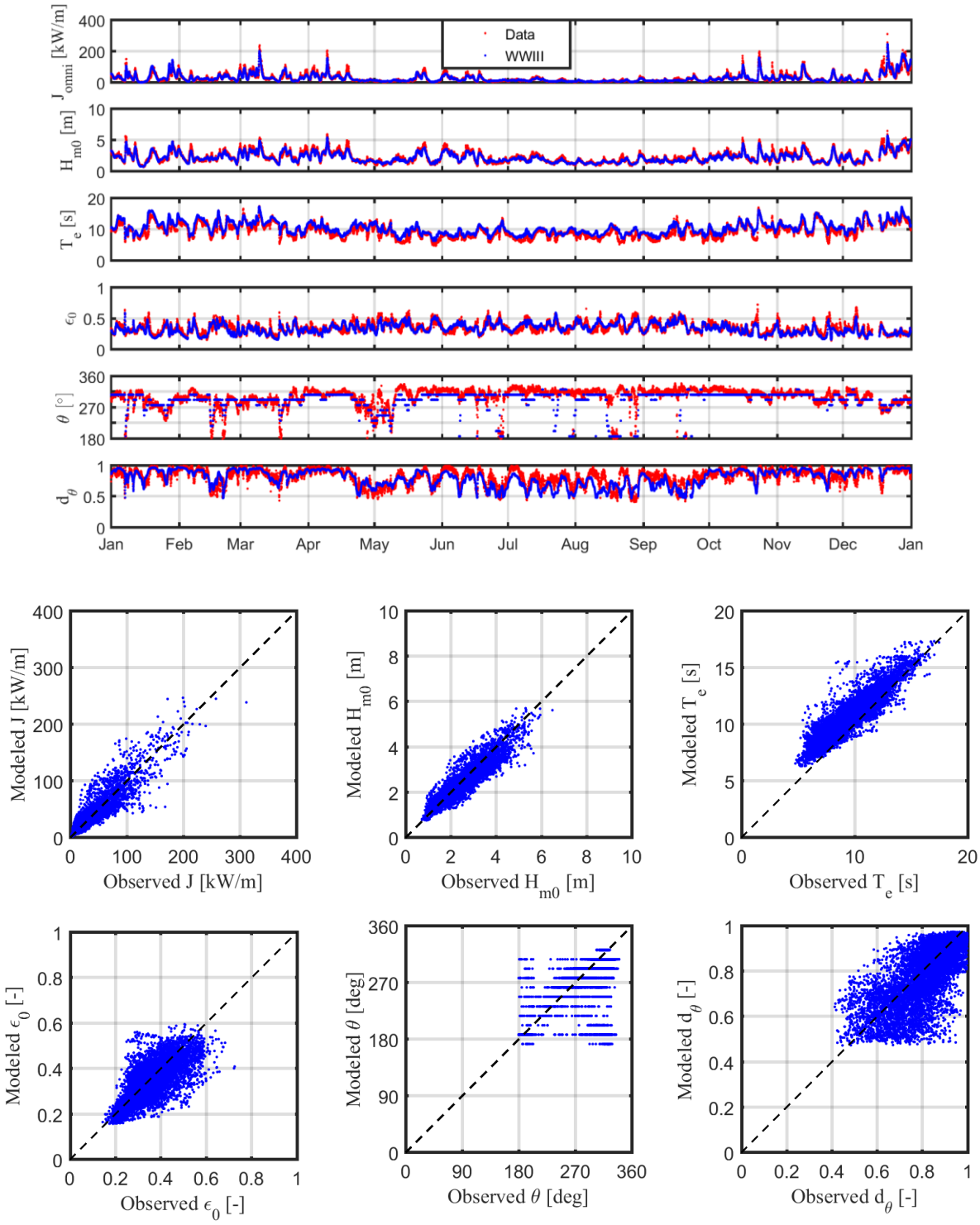

Figure B.41. Comparisons of time series (top) and scatter plots (bottom) of the six WWIII model-simulated IEC parameters with observed data at NDBC Buoy 46028 for 2005.

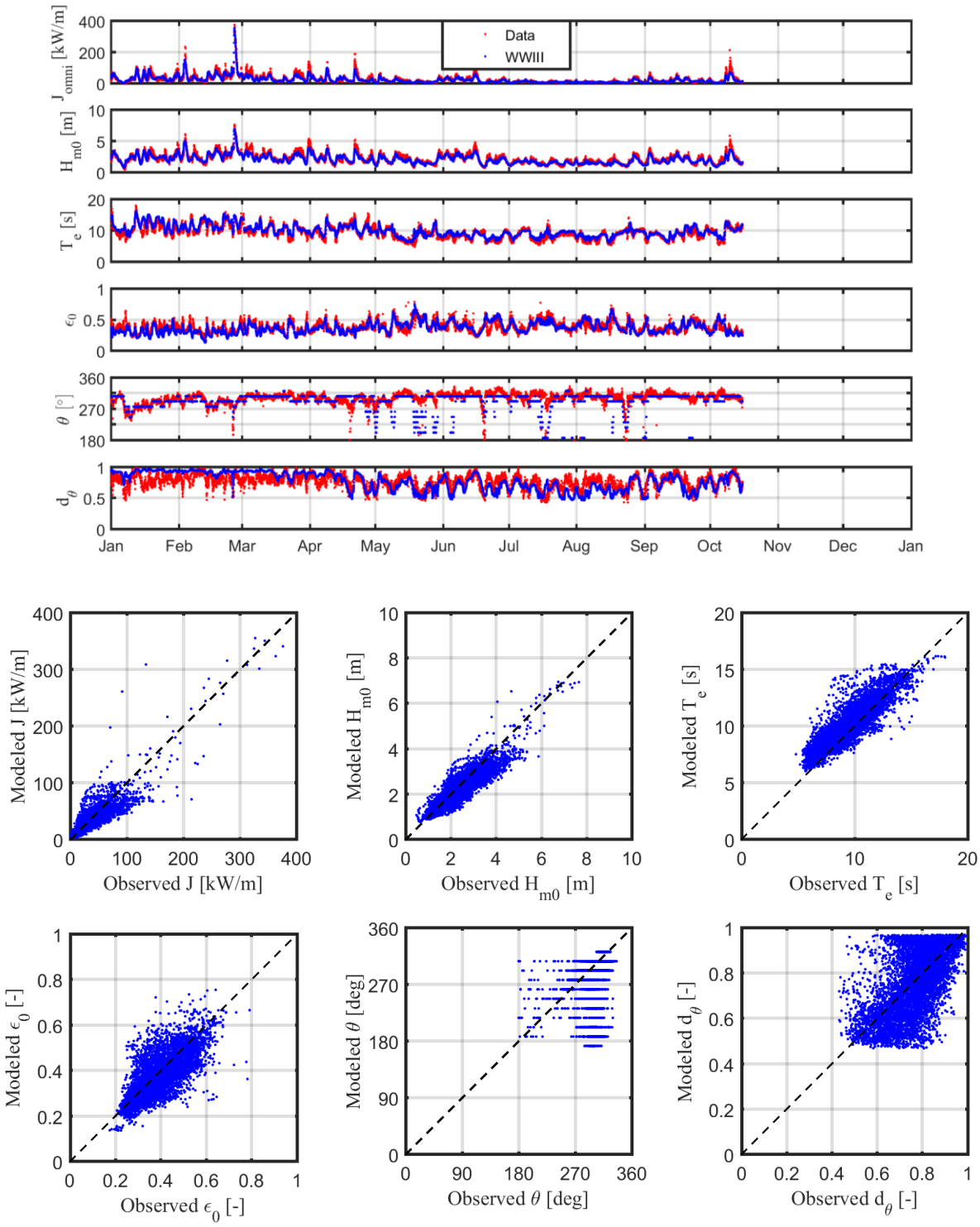

Figure B.42. Comparisons of time series (top) and scatter plots (bottom) of the six WWIII model-simulated IEC parameters with observed data at NDBC Buoy 46028 for 2004.

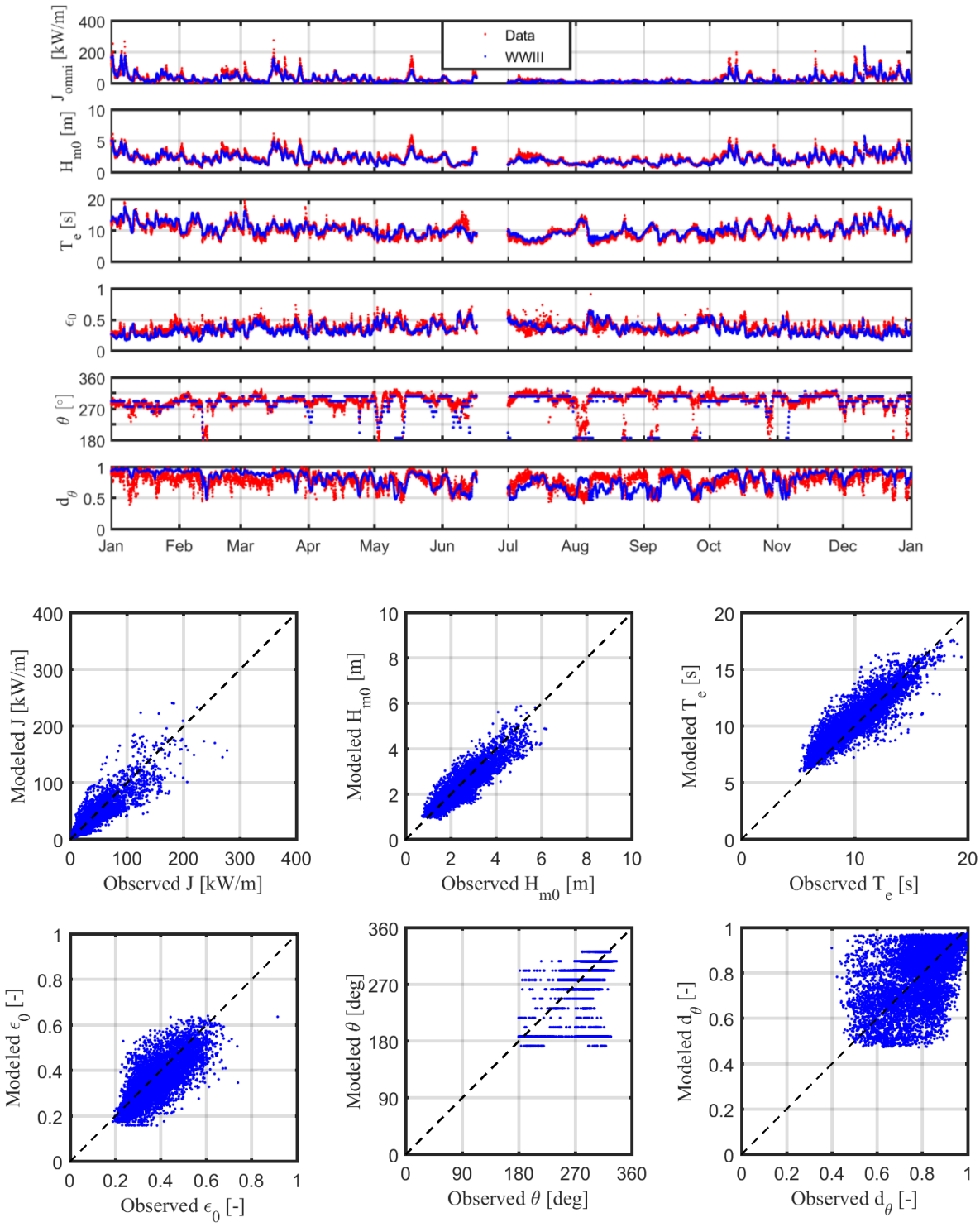

Figure B.43. Comparisons of time series (top) and scatter plots (bottom) of the six WWIII model-simulated IEC parameters with observed data at NDBC Buoy 46028 for 2003.

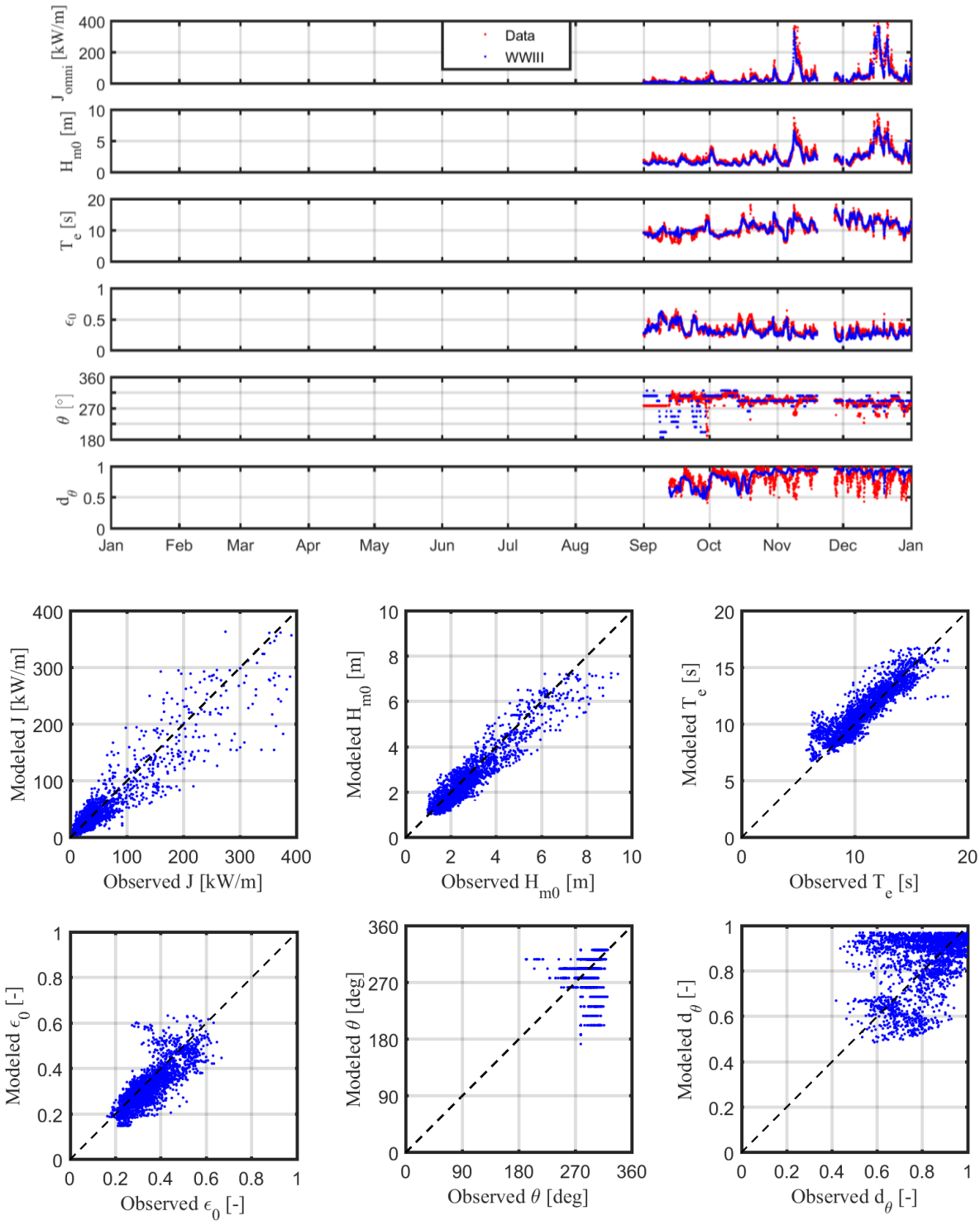

Figure B.44. Comparisons of time series (top) and scatter plots (bottom) of the six WWIII model-simulated IEC parameters with observed data at NDBC Buoy 46028 for 2002.

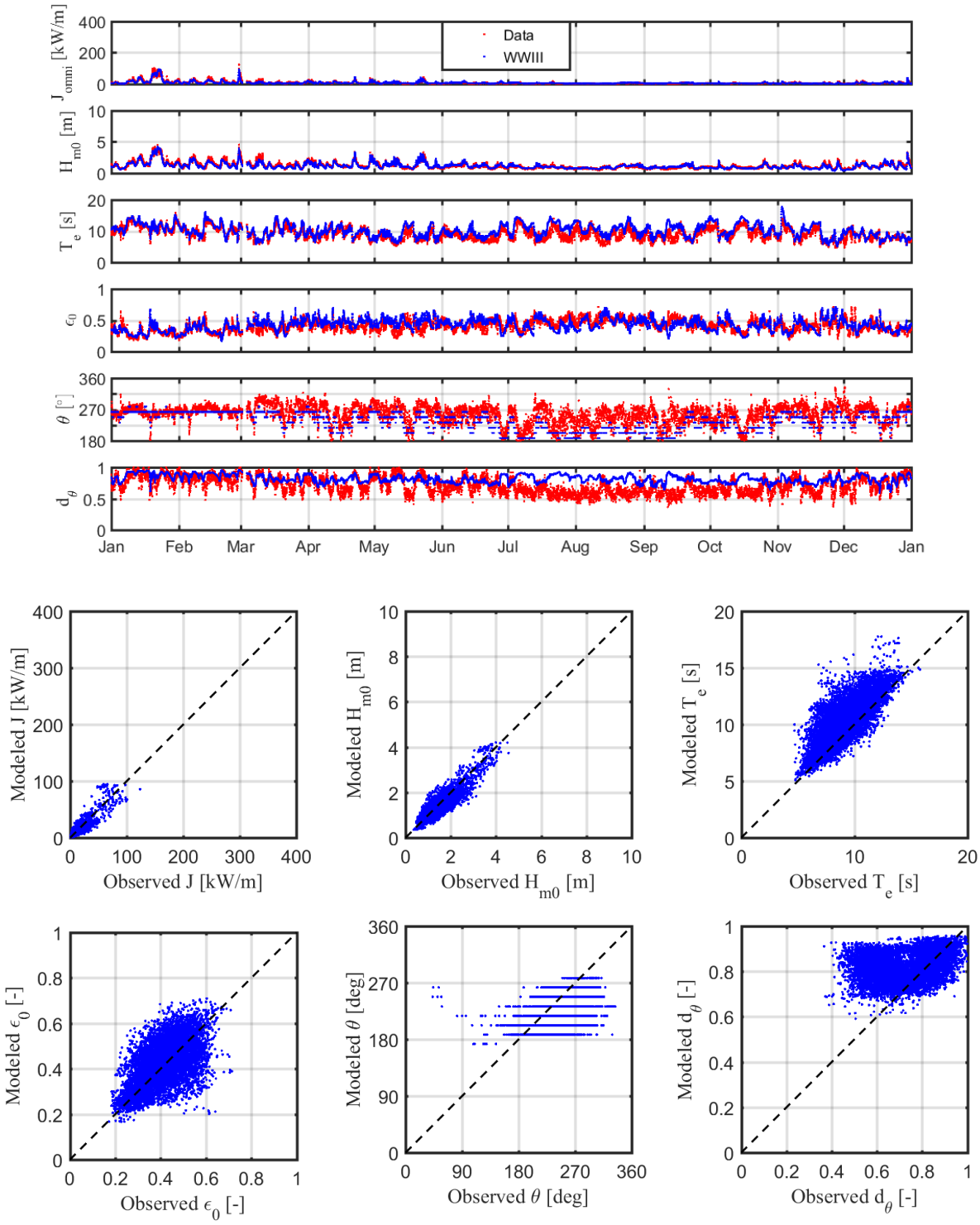

Figure B.45. Comparisons of time series (top) and scatter plots (bottom) of the six WWIII model-simulated IEC parameters with observed data at NDBC Buoy 46025 for 2010.

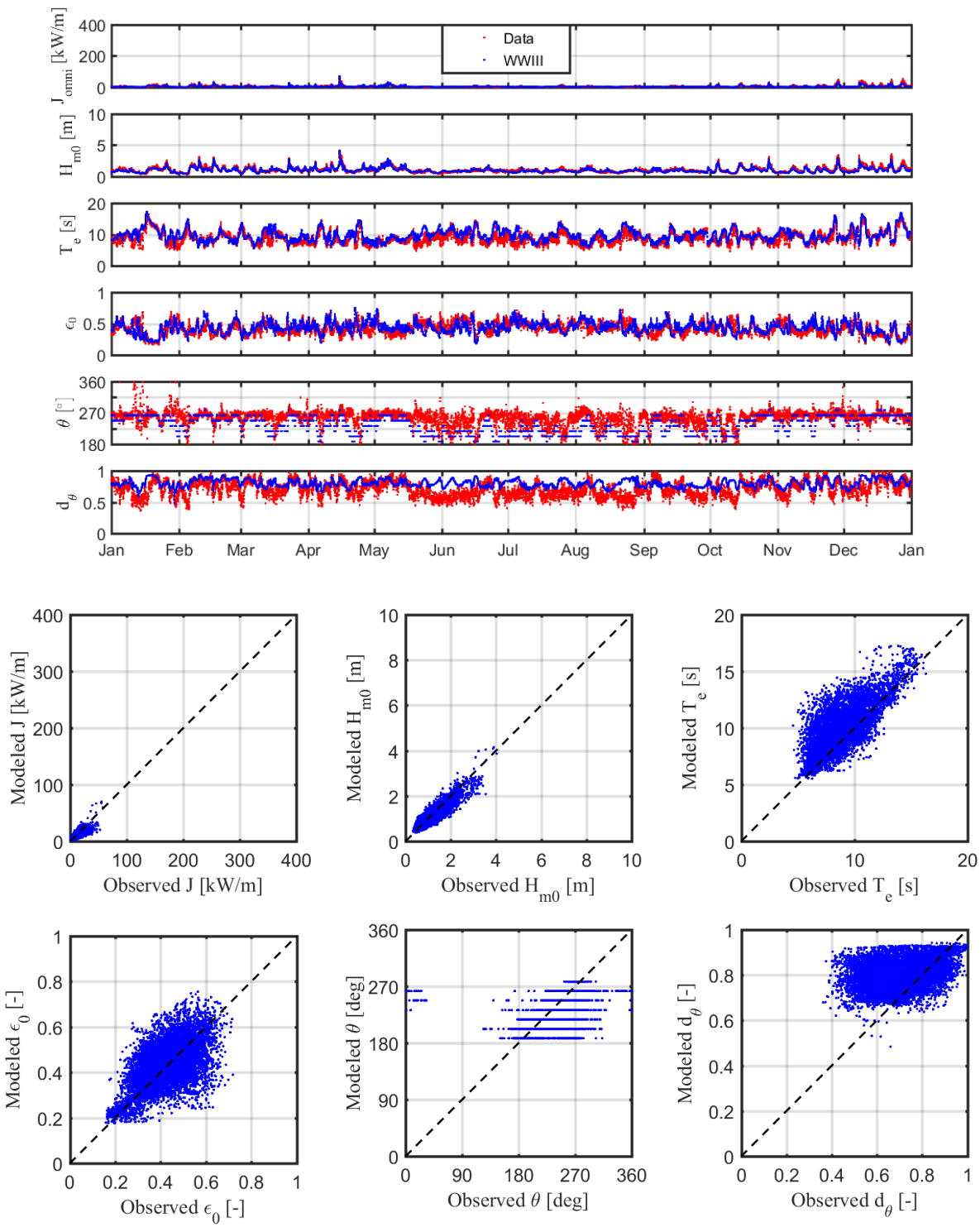

Figure B.46. Comparisons of time series (top) and scatter plots (bottom) of the six WWIII model-simulated IEC parameters with observed data at NDBC Buoy 46025 for 2009.

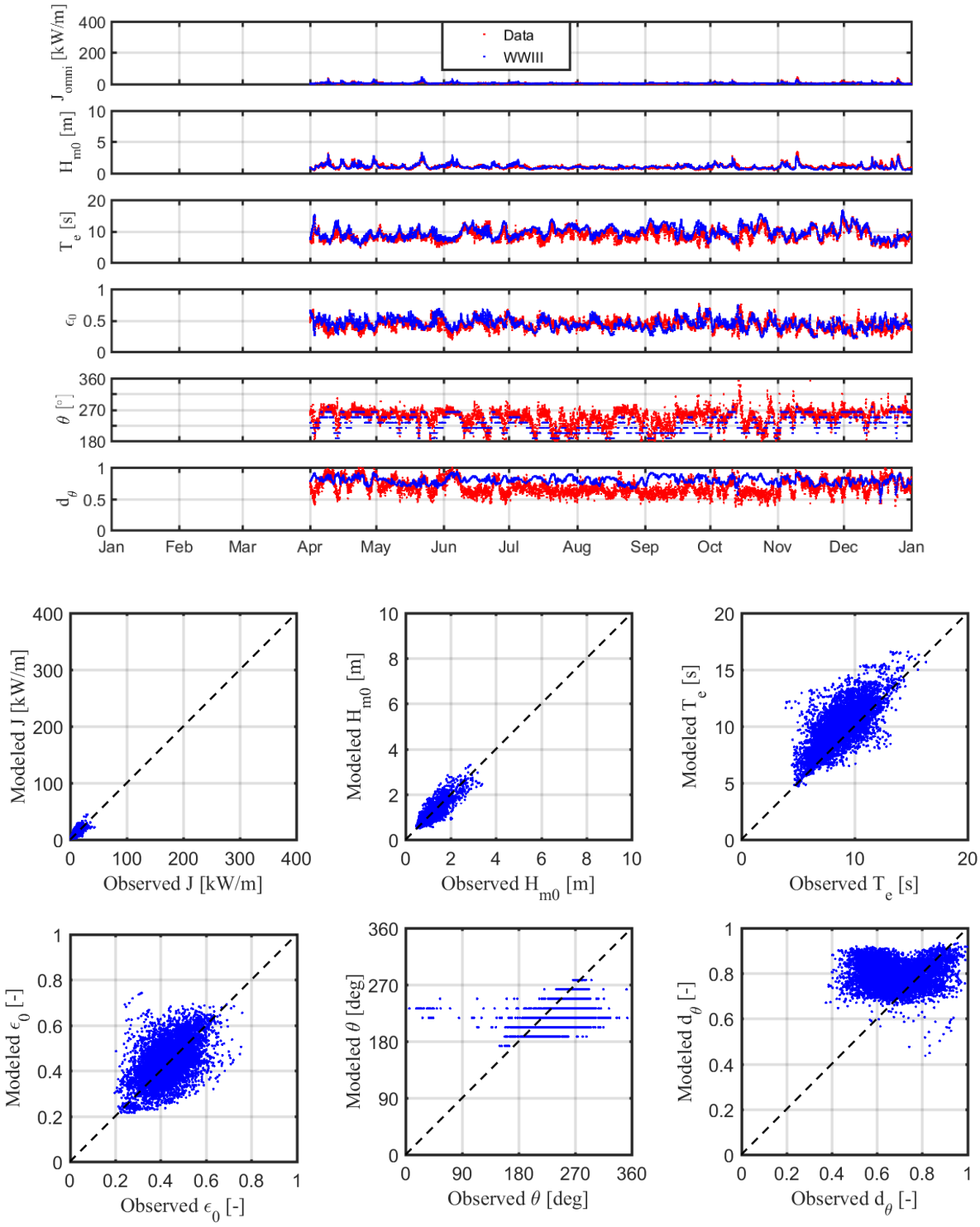

Figure B.47. Comparisons of time series (top) and scatter plots (bottom) of the six WWIII model-simulated IEC parameters with observed data at NDBC Buoy 46025 for 2008.

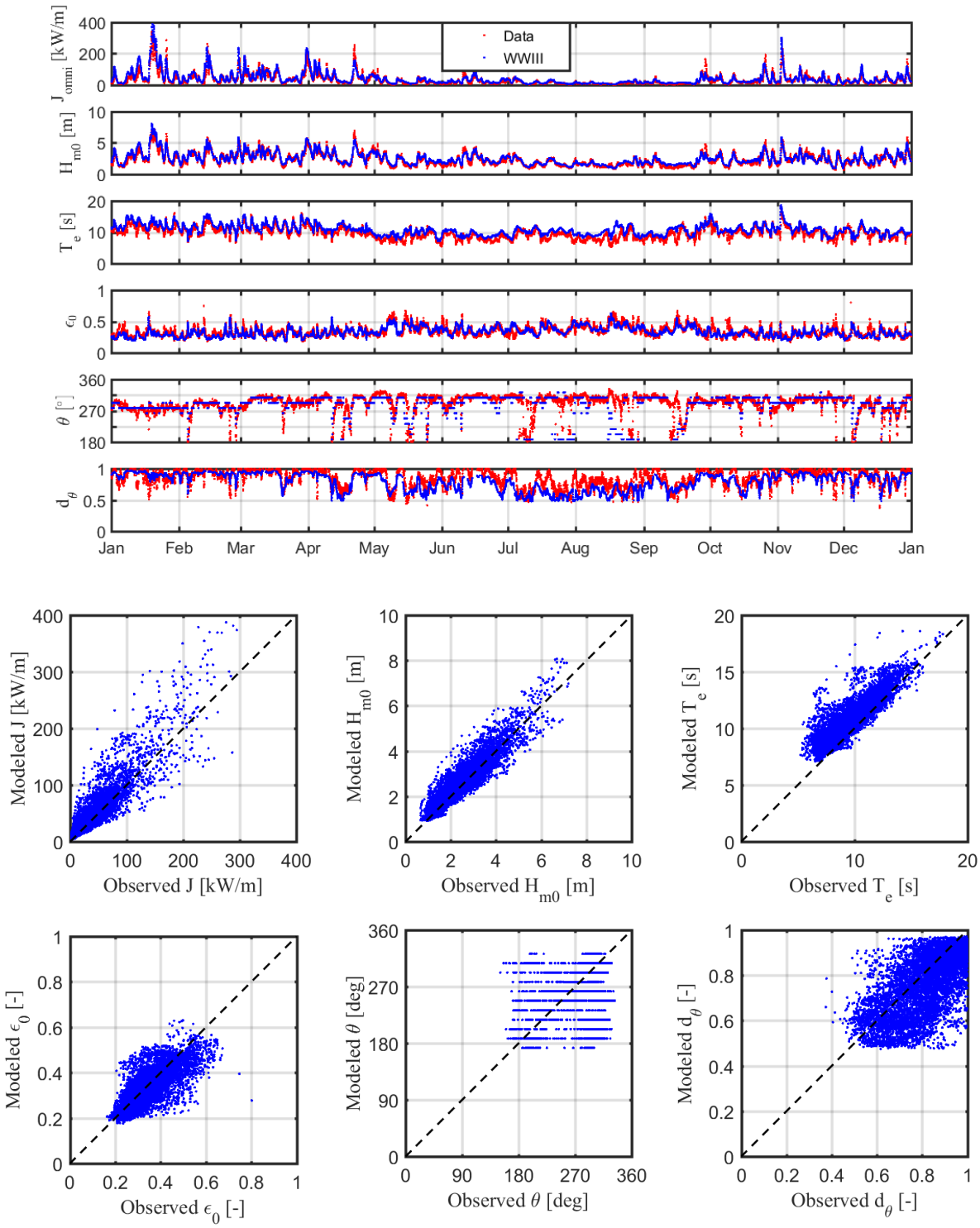

Figure B.48. Comparisons of time series (top) and scatter plots (bottom) of the six WWIII model-simulated IEC parameters with observed data at NDBC Buoy 46042 for 2010.

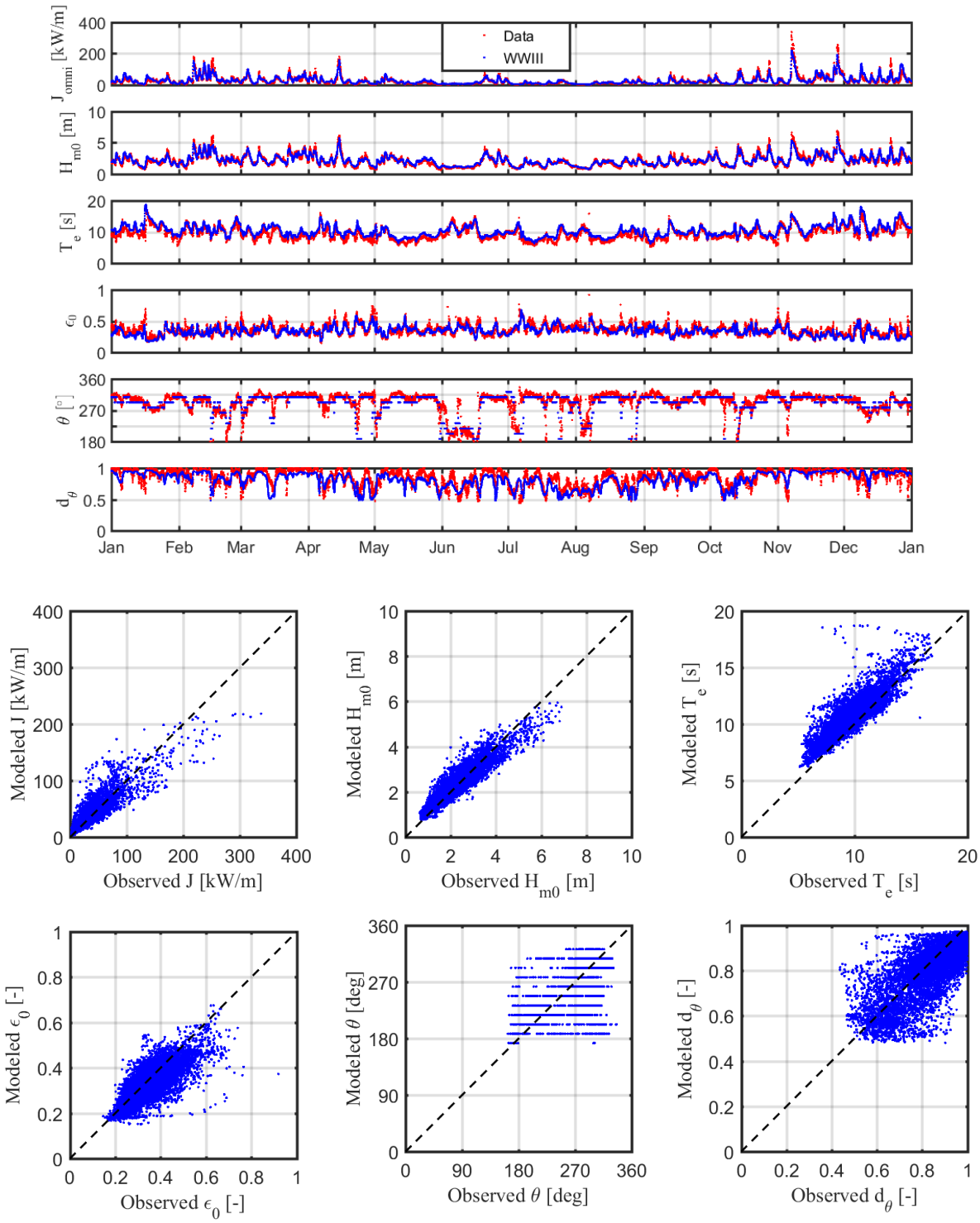

Figure B.49. Comparisons of time series (top) and scatter plots (bottom) of the six WWIII model-simulated IEC parameters with observed data at NDBC Buoy 46042 for 2009.

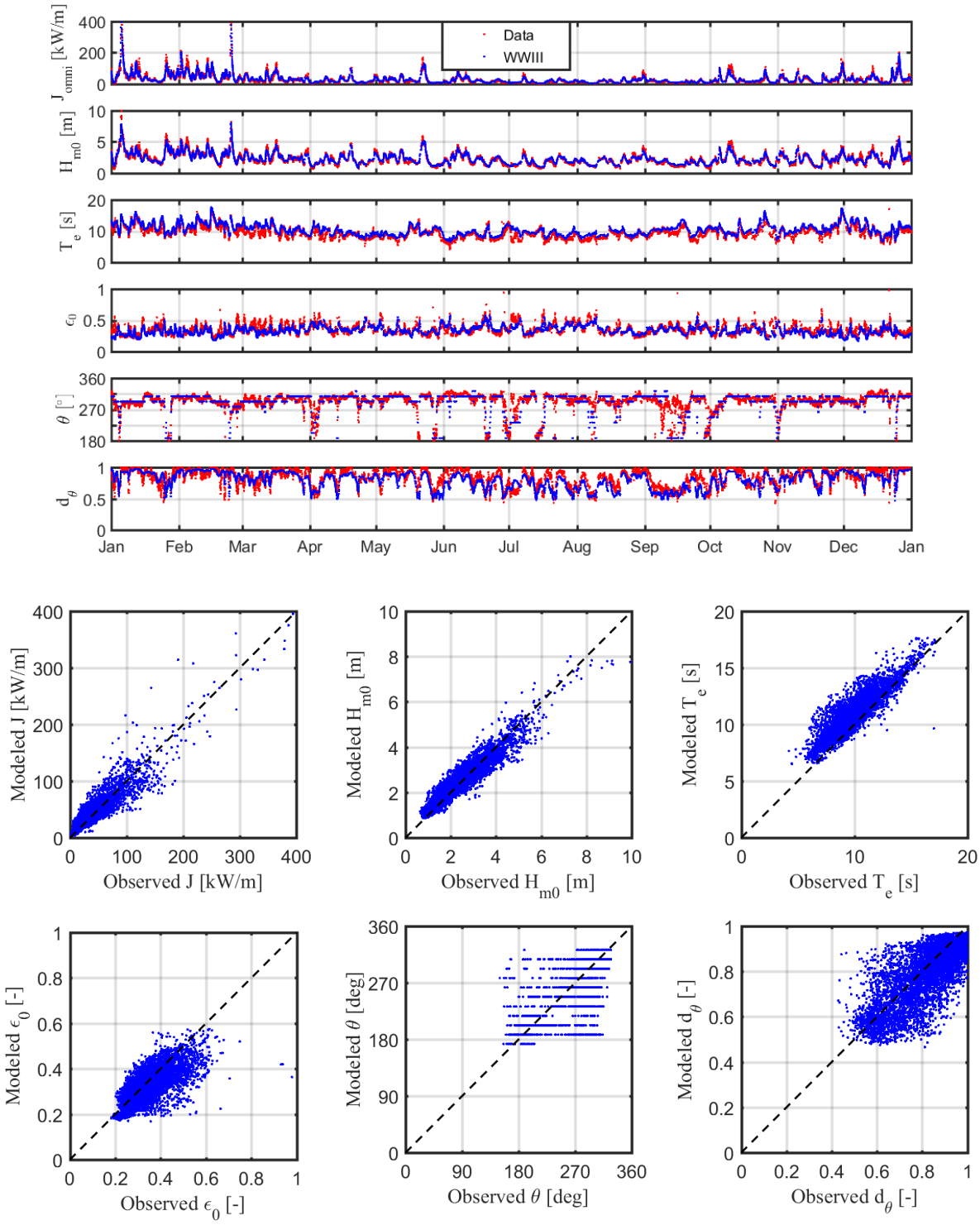

Figure B.50. Comparisons of time series (top) and scatter plots (bottom) of the six WWIII model-simulated IEC parameters with observed data at NDBC Buoy 46042 for 2008.

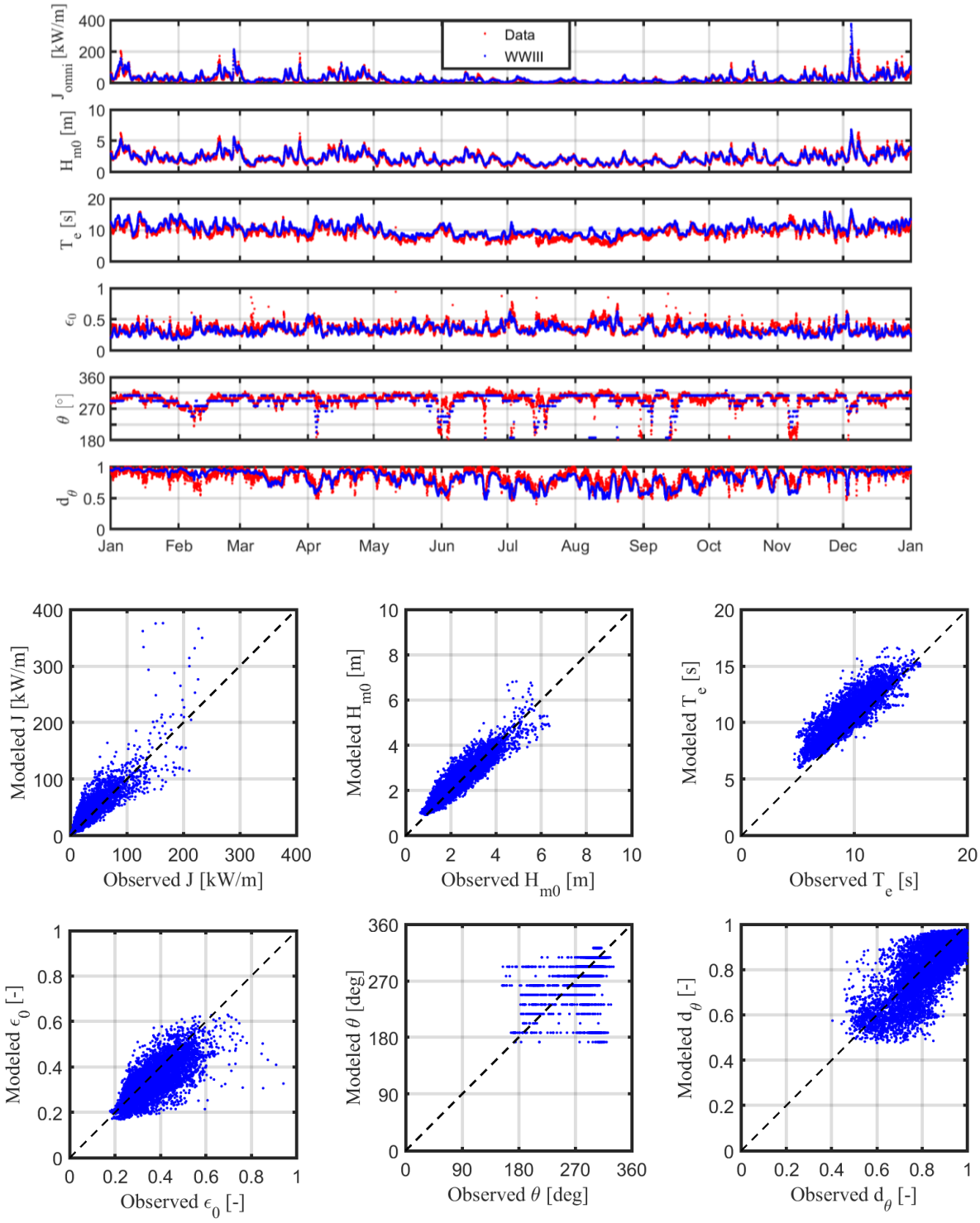

Figure B.51. Comparisons of time series (top) and scatter plots (bottom) of the six WWIII model-simulated IEC parameters with observed data at NDBC Buoy 46042 for 2007.

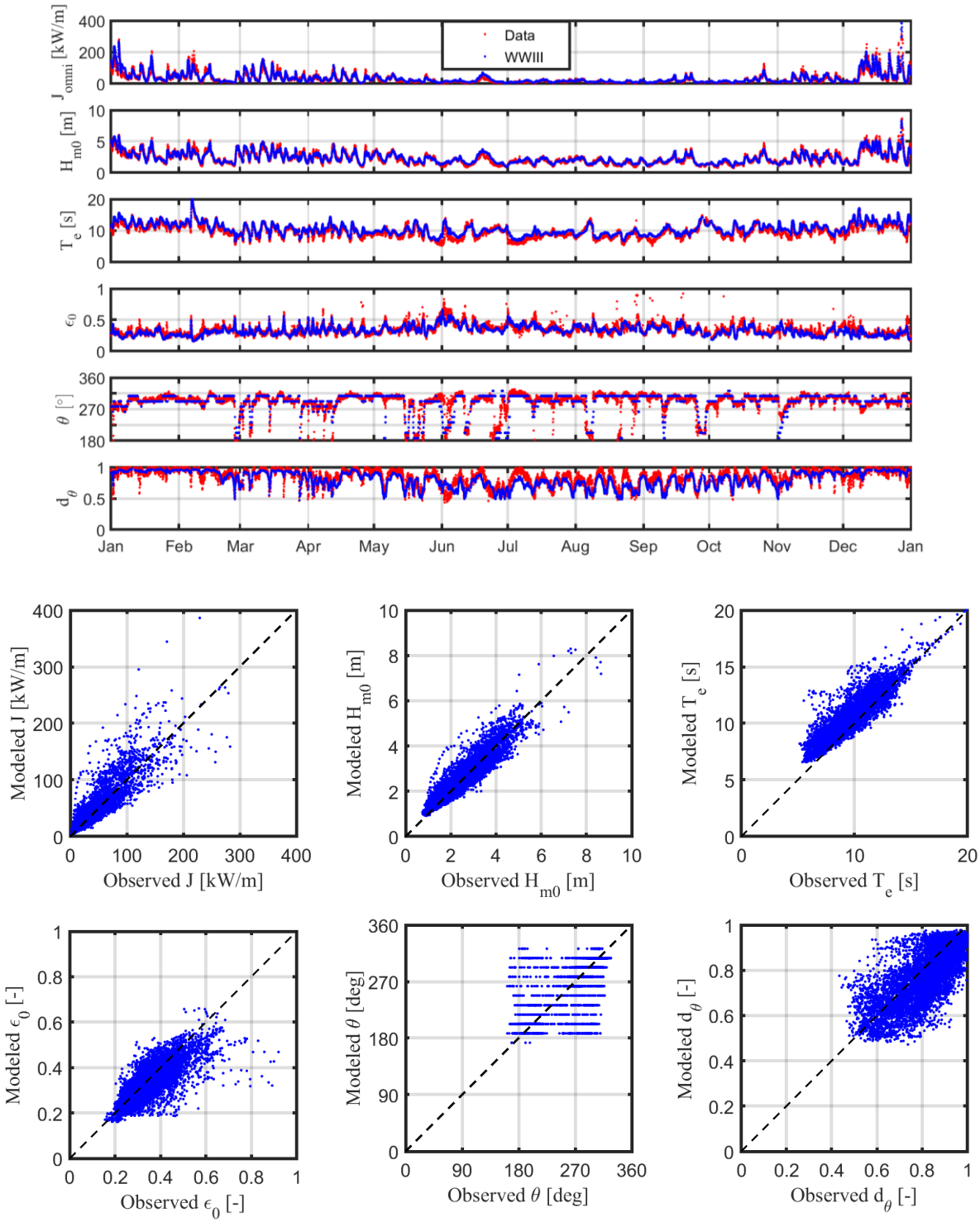

Figure B.52. Comparisons of time series (top) and scatter plots (bottom) of the six WWIII model-simulated IEC parameters with observed data at NDBC Buoy 46042 for 2006.

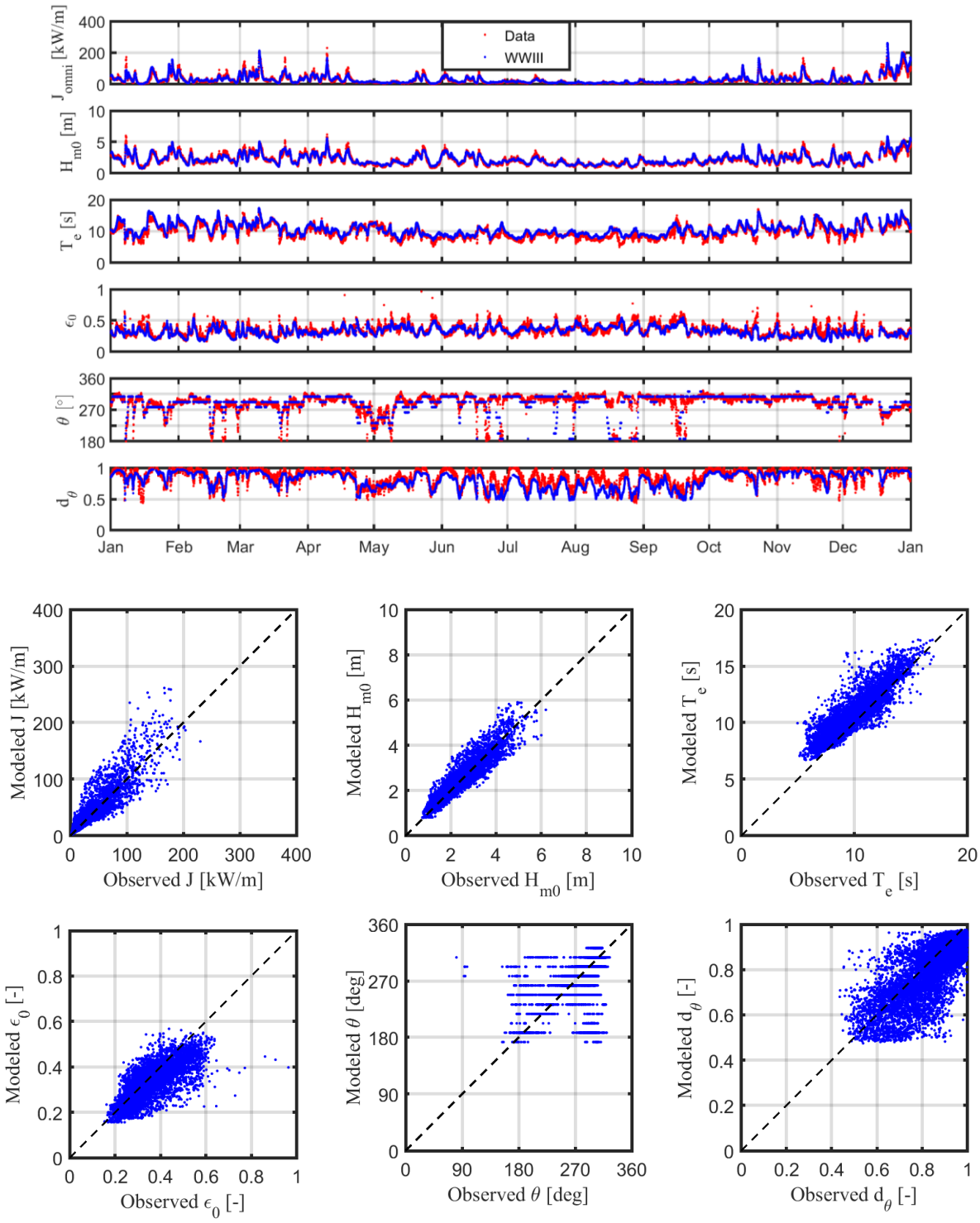

Figure B.53. Comparisons of time series (top) and scatter plots (bottom) of the six WWIII model-simulated IEC parameters with observed data at NDBC Buoy 46042 for 2005.

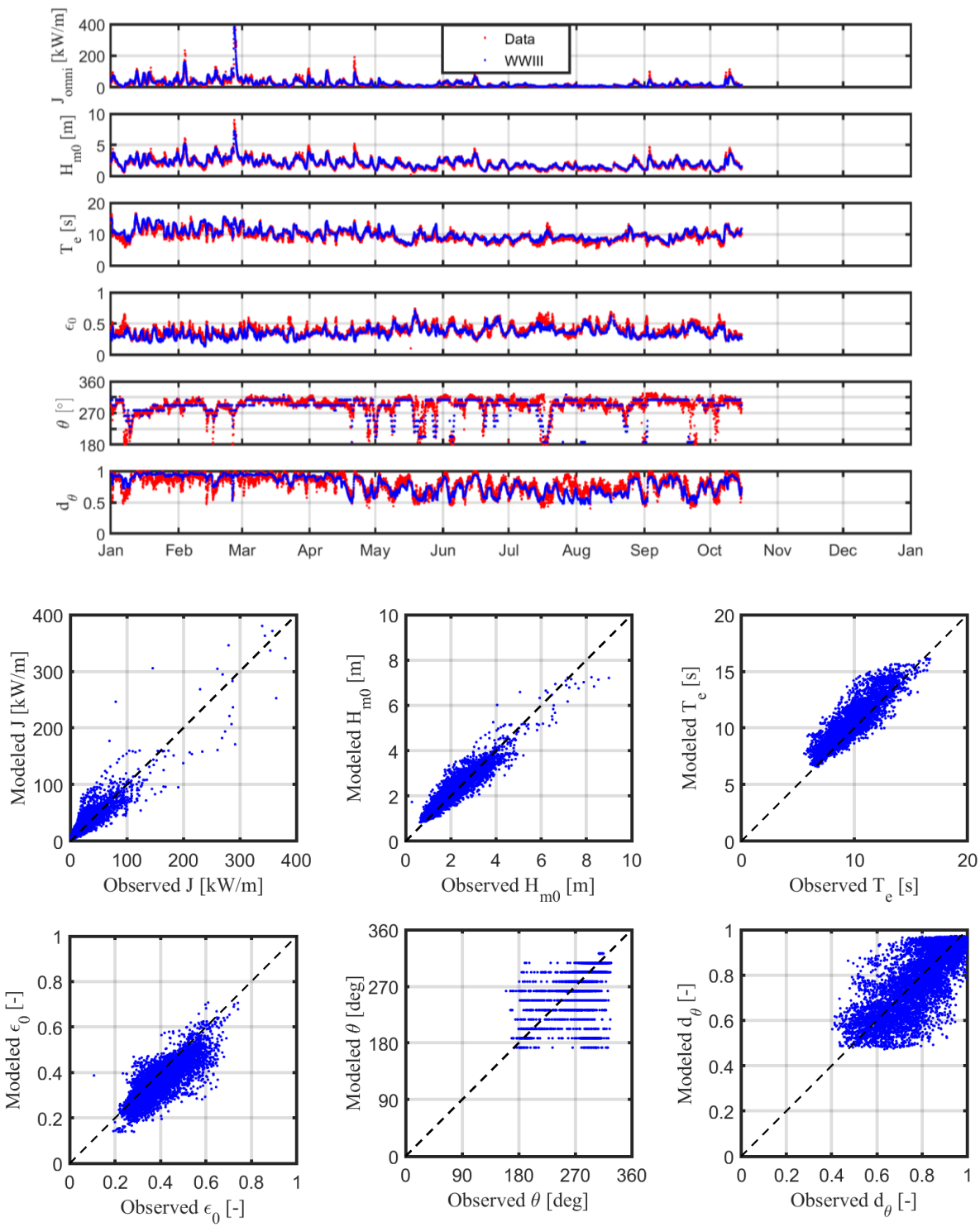

Figure B.54. Comparisons of time series (top) and scatter plots (bottom) of the six WWIII model-simulated IEC parameters with observed data at NDBC Buoy 46042 for 2004.

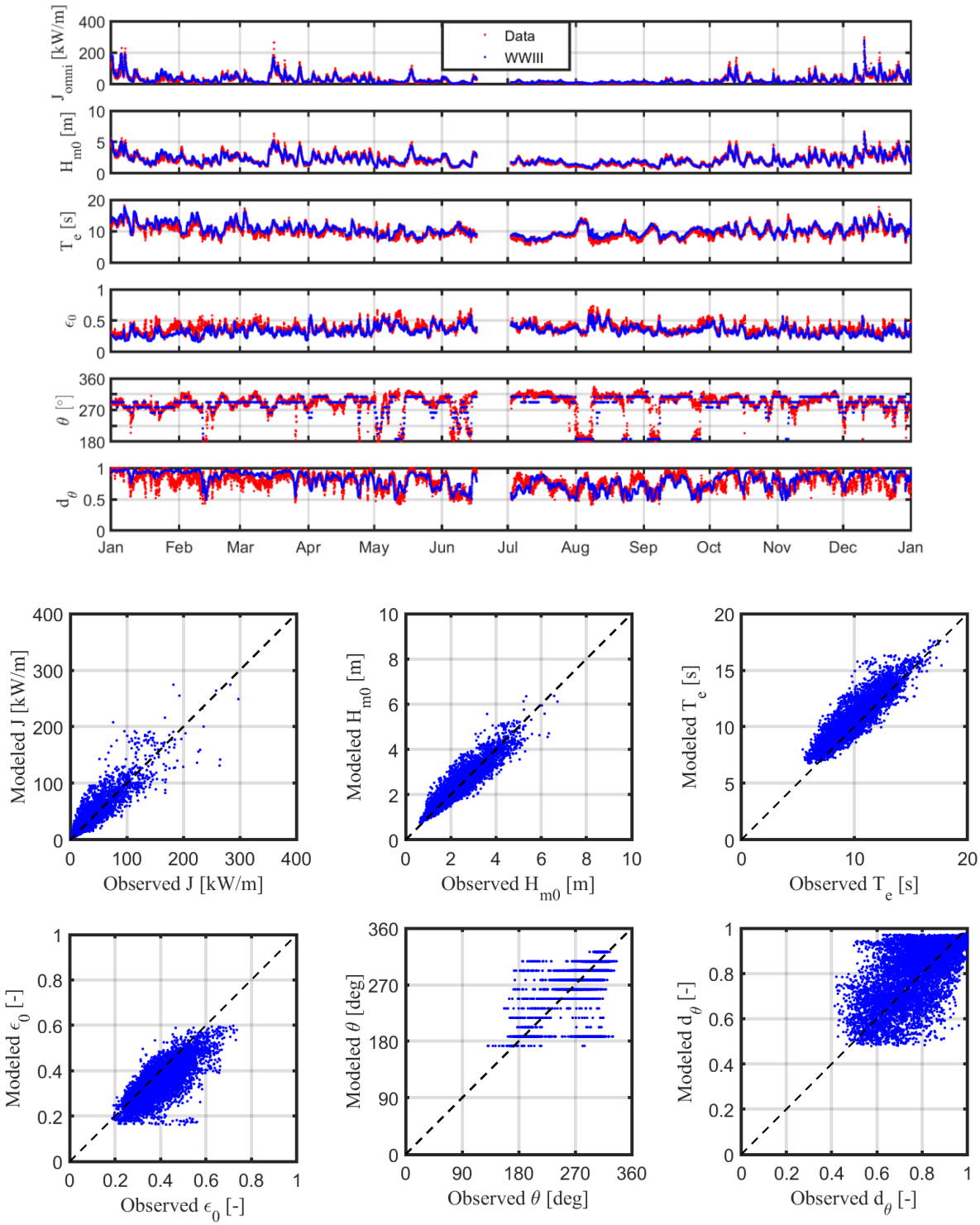

Figure B.55. Comparisons of time series (top) and scatter plots (bottom) of the six WWIII model-simulated IEC parameters with observed data at NDBC Buoy 46042 for 2003.

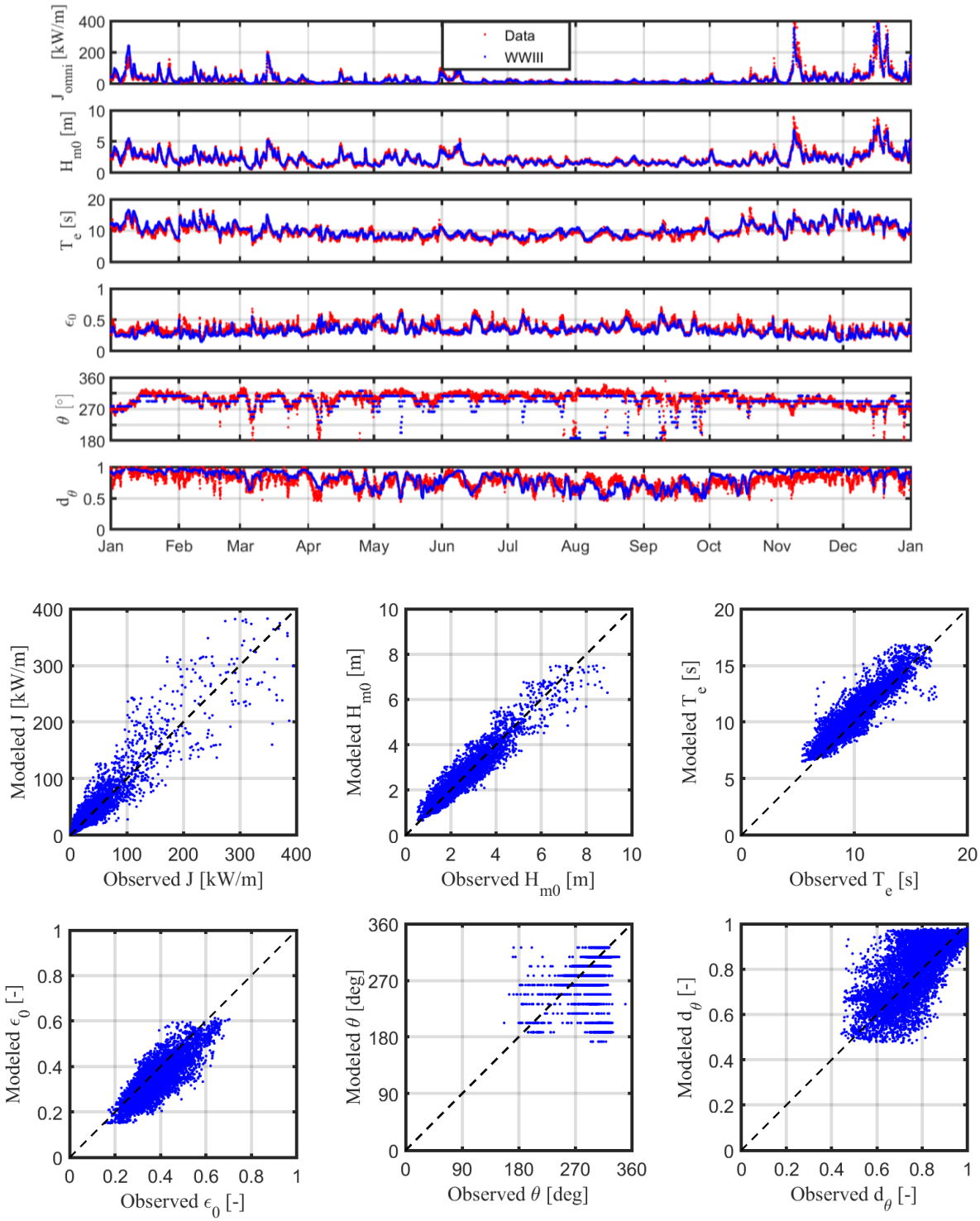

Figure B.56. Comparisons of time series (top) and scatter plots (bottom) of the six WWIII model-simulated IEC parameters with observed data at NDBC Buoy 46042 for 2002.

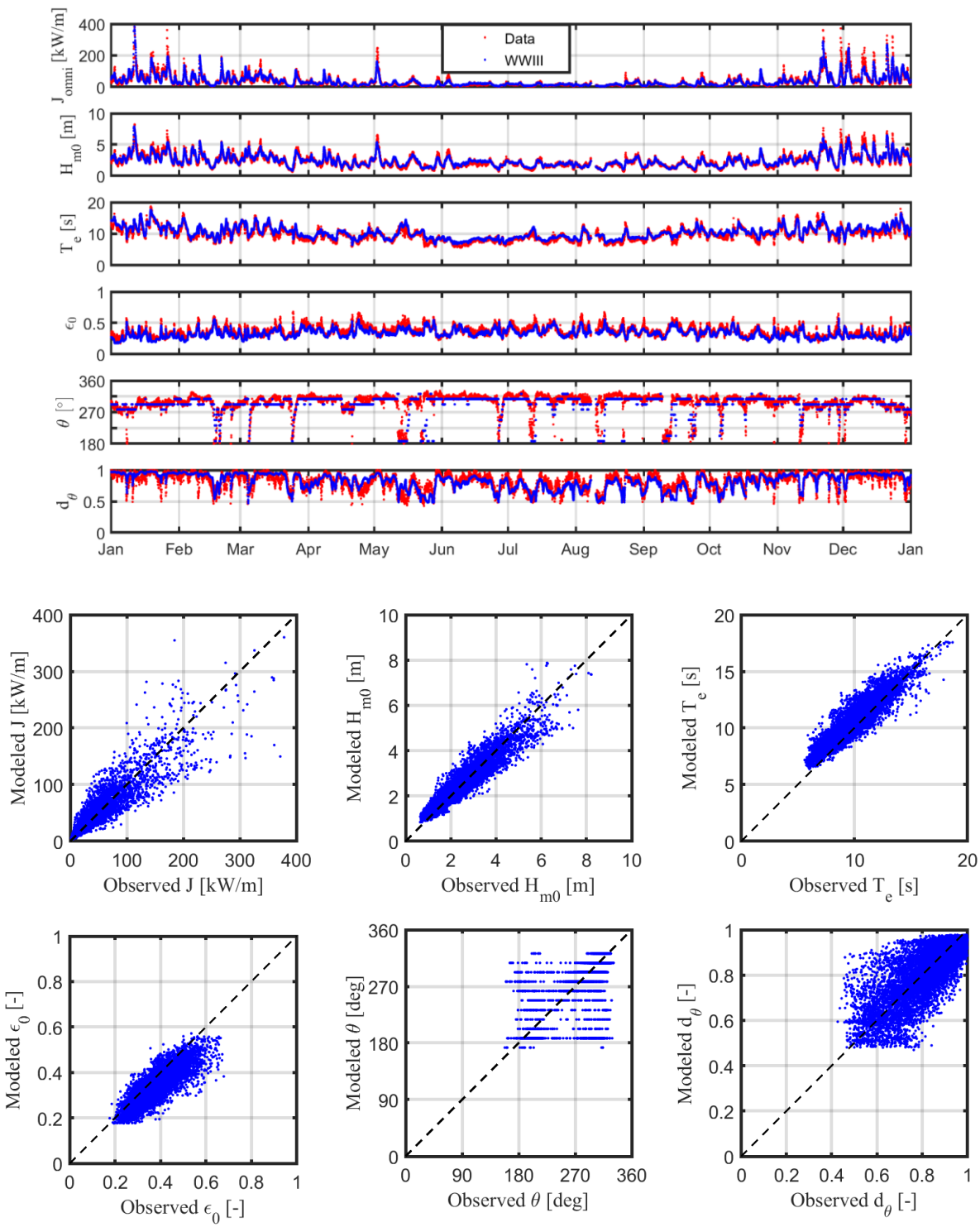

Figure B.57. Comparisons of time series (top) and scatter plots (bottom) of the six WWIII model-simulated IEC parameters with observed data at NDBC Buoy 46042 for 2001.

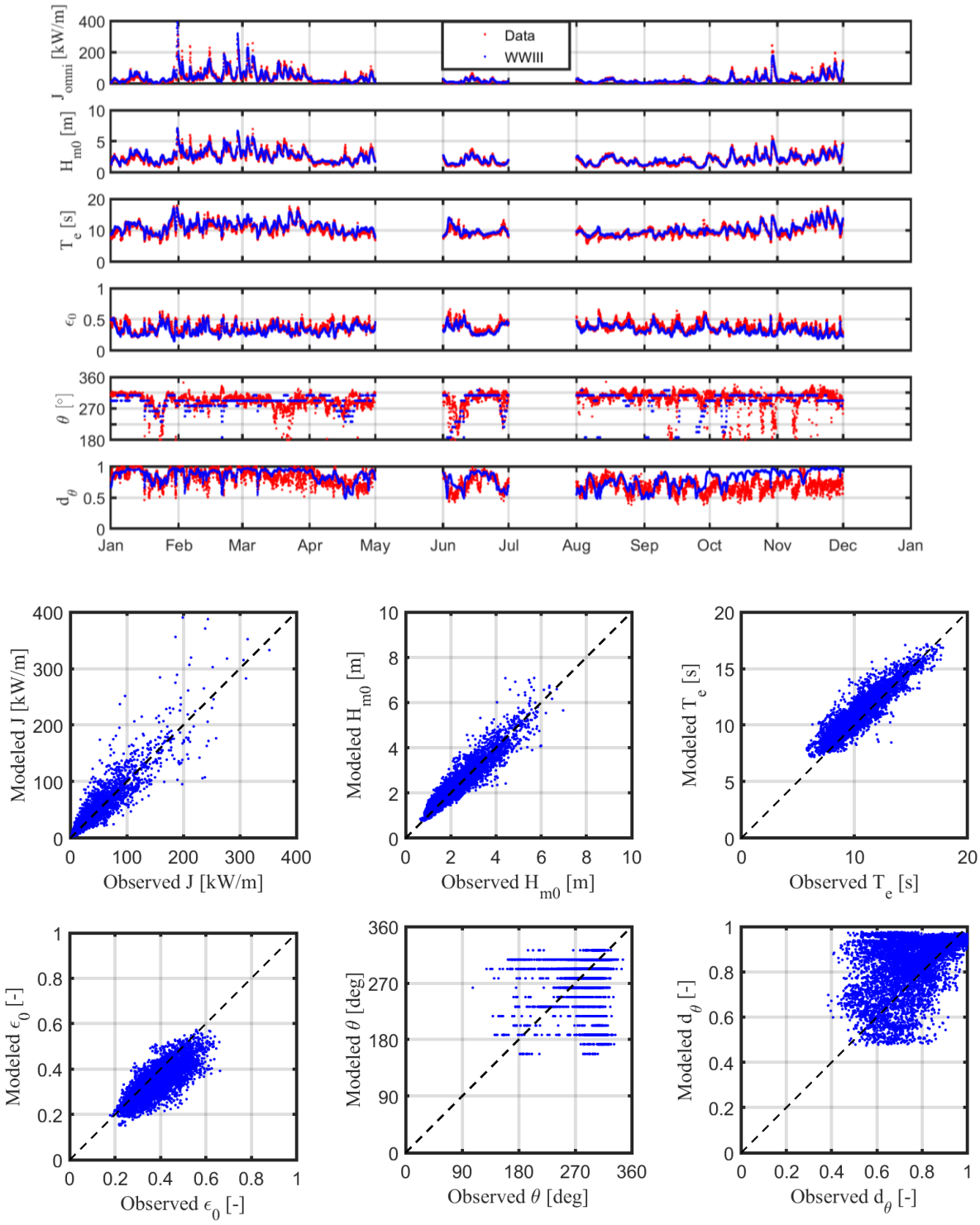

Figure B.58. Comparisons of time series (top) and scatter plots (bottom) of the six WWIII model-simulated IEC parameters with observed data at NDBC Buoy 46042 for 2000.

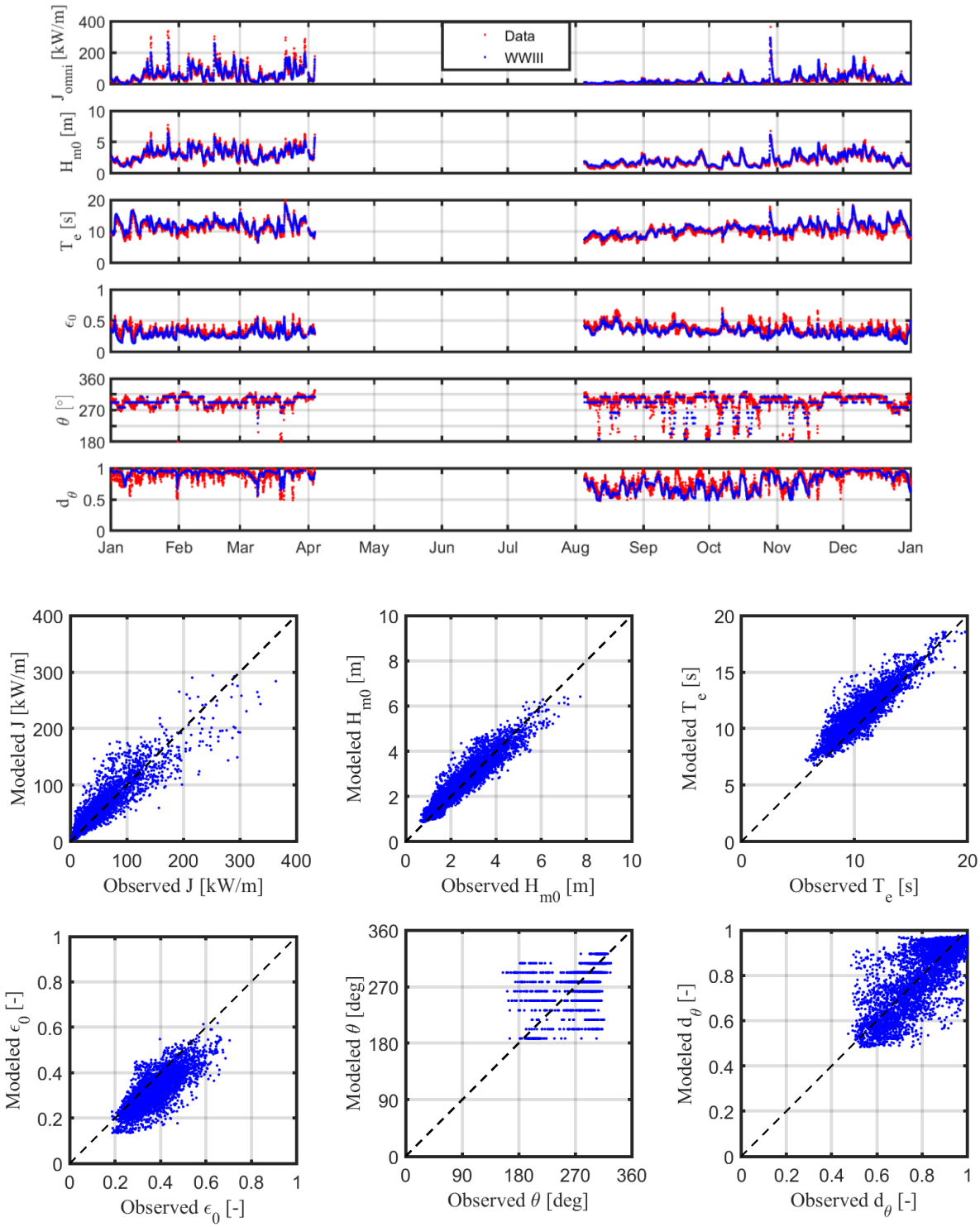

Figure B.59. Comparisons of time series (top) and scatter plots (bottom) of the six WWIII model-simulated IEC parameters with observed data at NDBC Buoy 46042 for 1999.

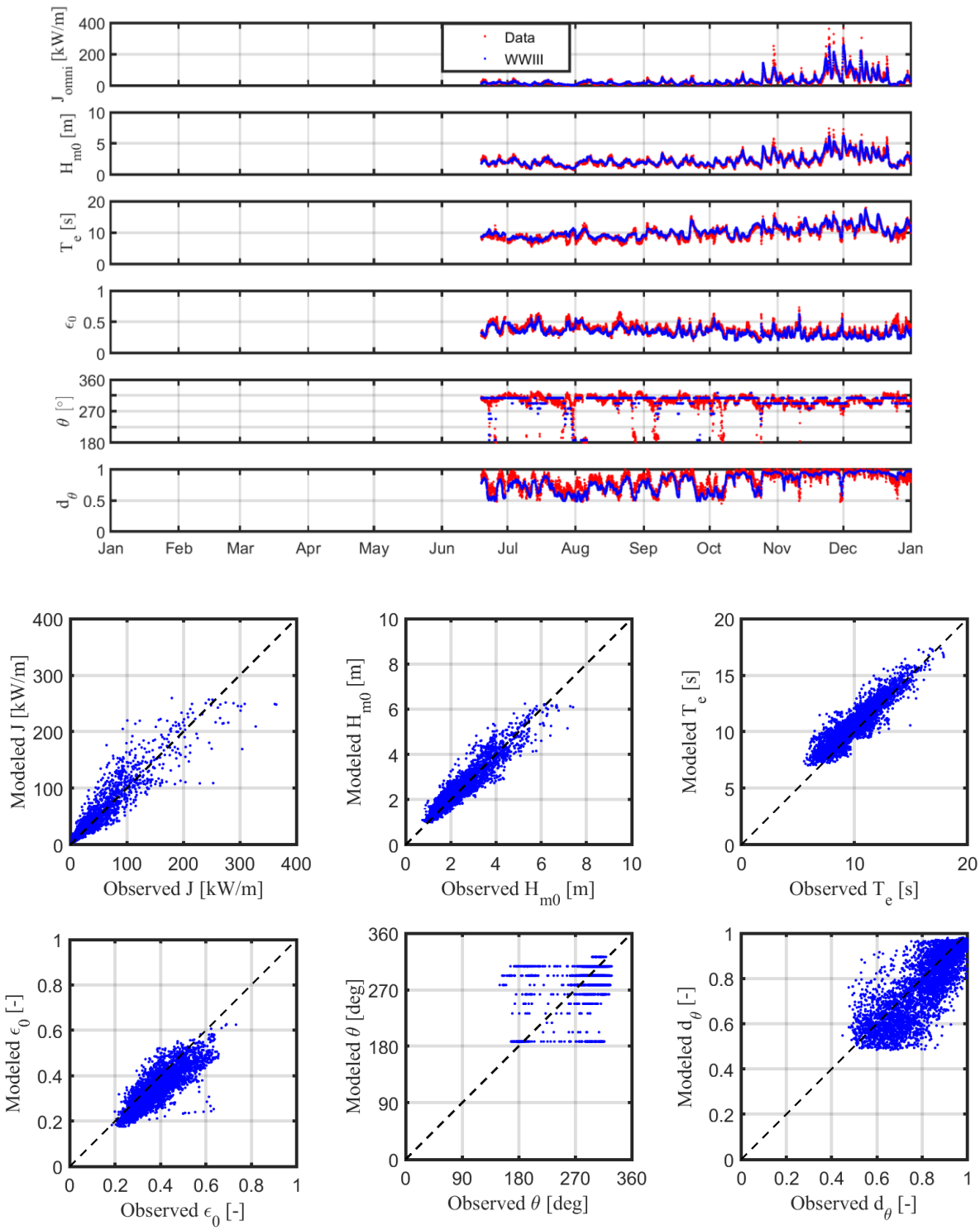

Figure B.60. Comparisons of time series (top) and scatter plots (bottom) of the six WWIII model-simulated IEC parameters with observed data at NDBC Buoy 46042 for 1998.

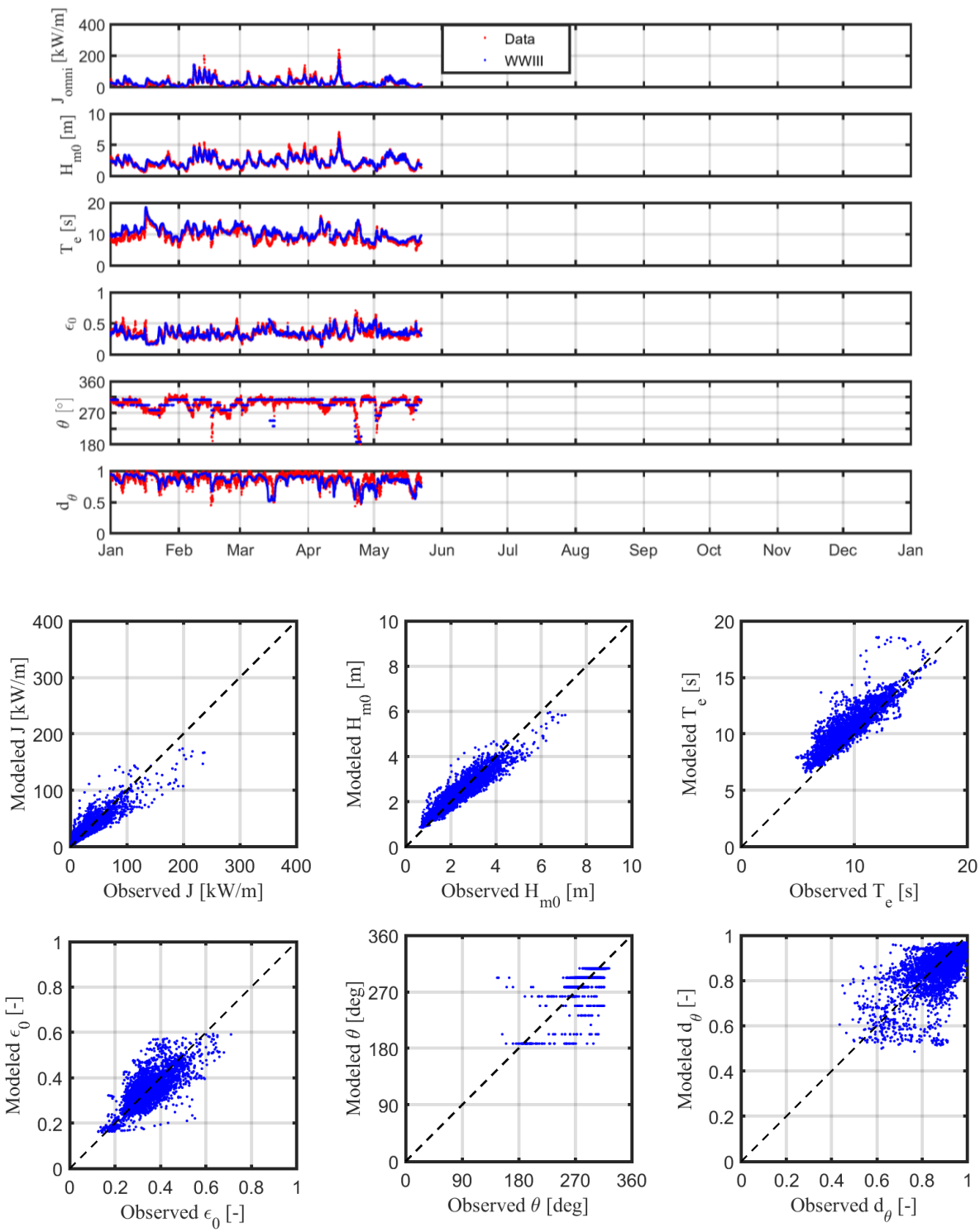

Figure B.61. Comparisons of time series (top) and scatter plots (bottom) of the six WWIII model-simulated IEC parameters with observed data at NDBC Buoy 46063 for 2009.

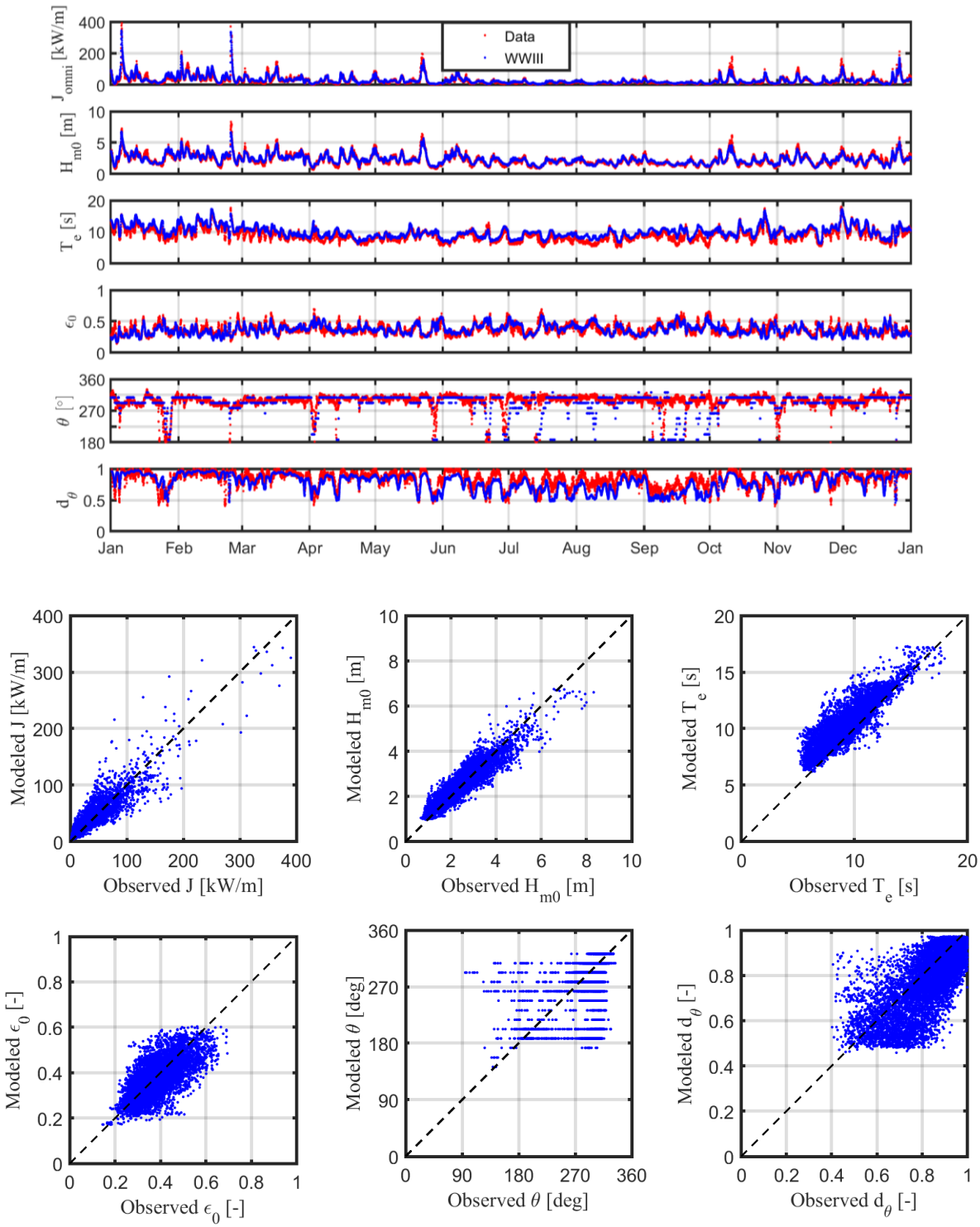

Figure B.62. Comparisons of time series (top) and scatter plots (bottom) of the six WWIII model-simulated IEC parameters with observed data at NDBC Buoy 46063 for 2008.

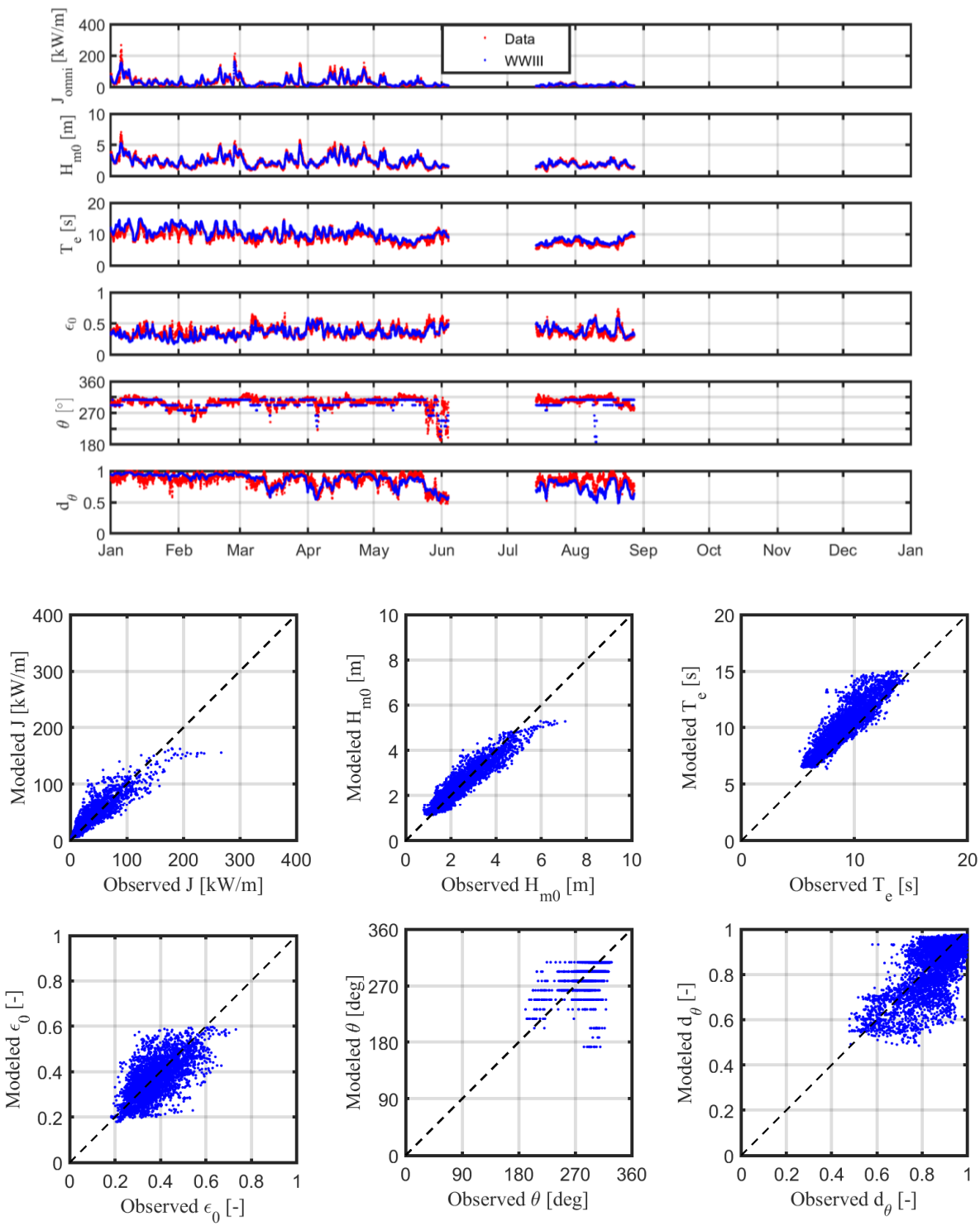

Figure B.63. Comparisons of time series (top) and scatter plots (bottom) of the six WWIII model-simulated IEC parameters with observed data at NDBC Buoy 46063 for 2007.

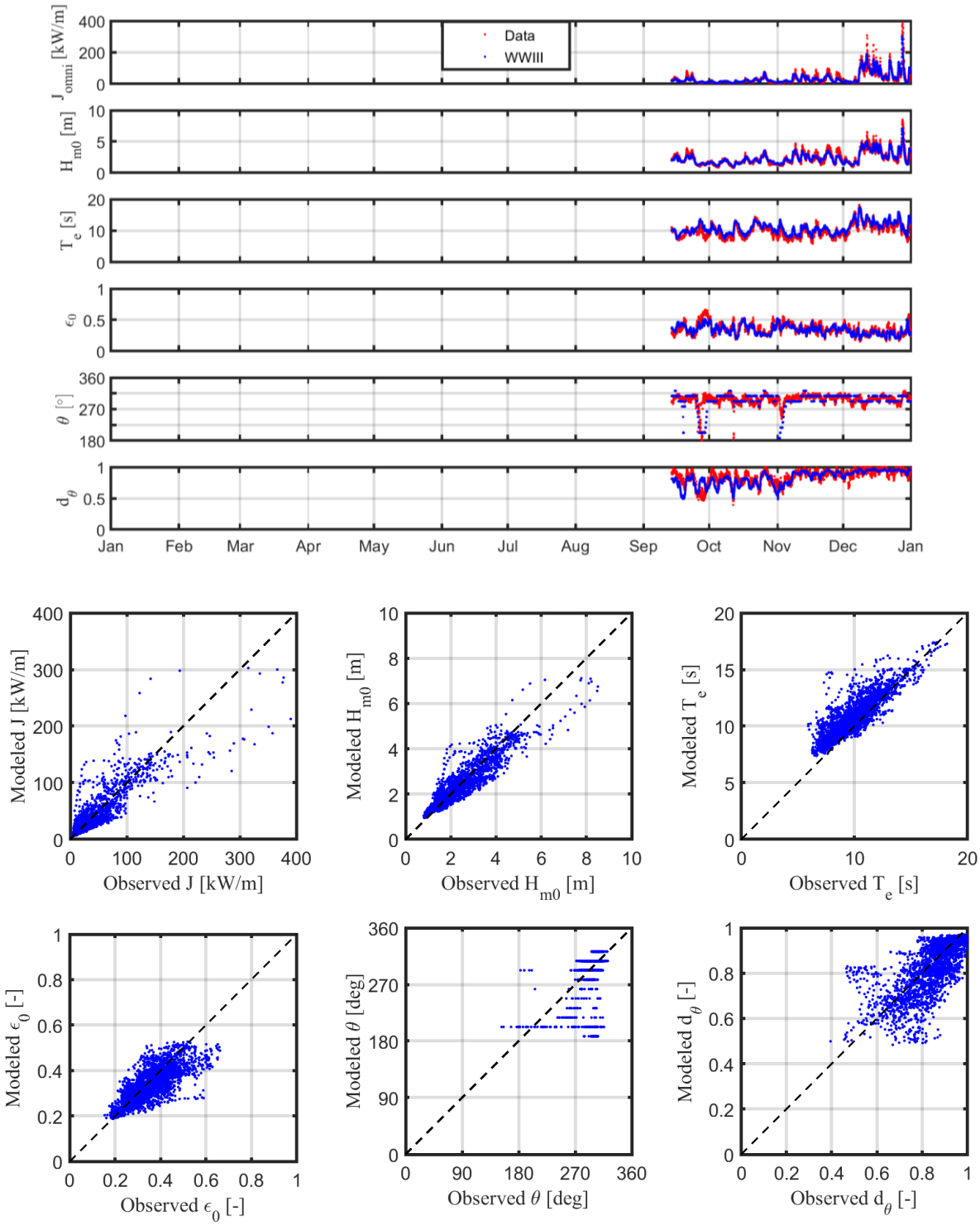

Figure B.64. Comparisons of time series (top) and scatter plots (bottom) of the six WWIII model-simulated IEC parameters with observed data at NDBC Buoy 46063 for 2006.

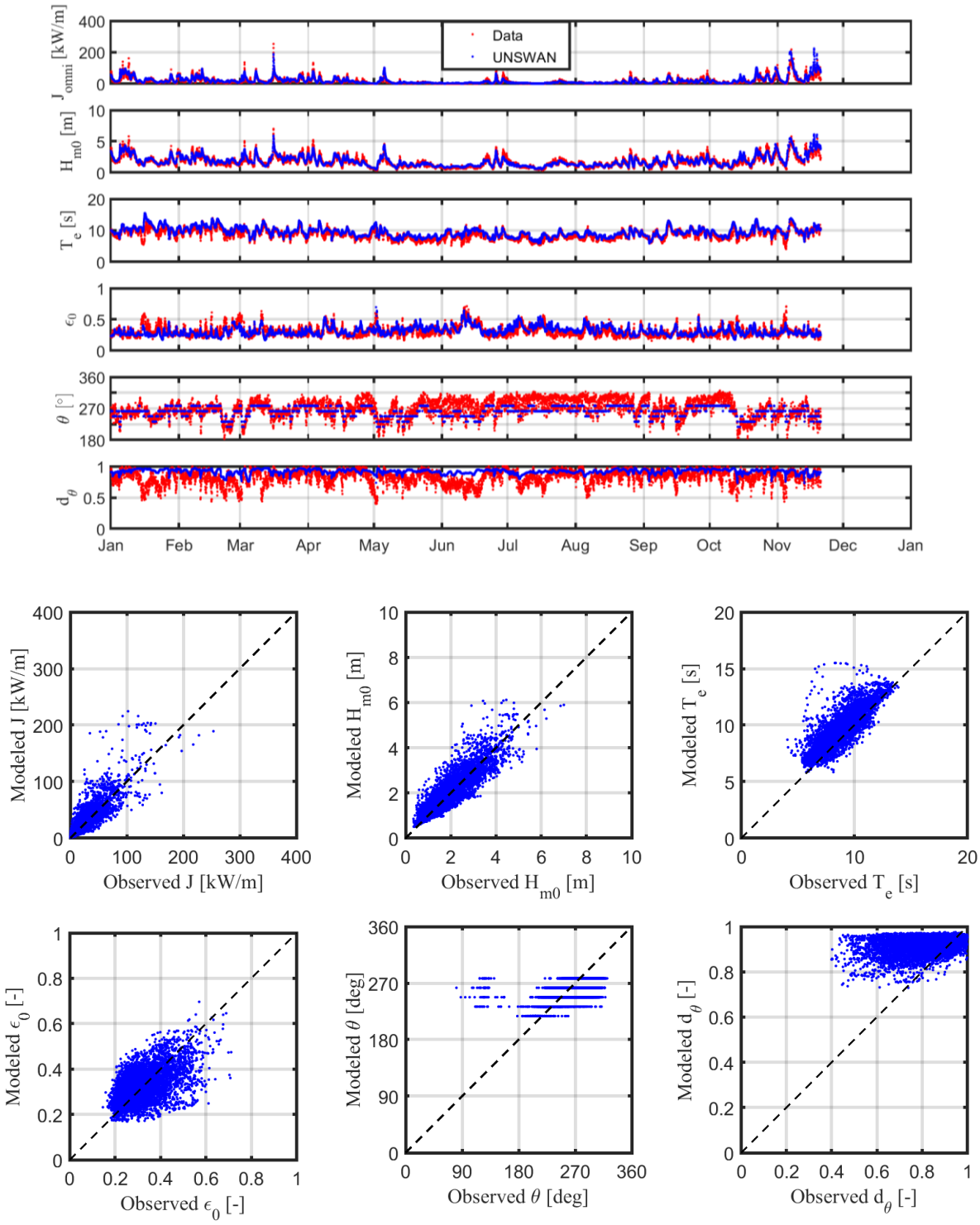

Figure B.65. Comparisons of time series (top) and scatter plots (bottom) of UnSWAN simulated six IEC parameters with observed data at NDBC Buoy 46087 for 2009.

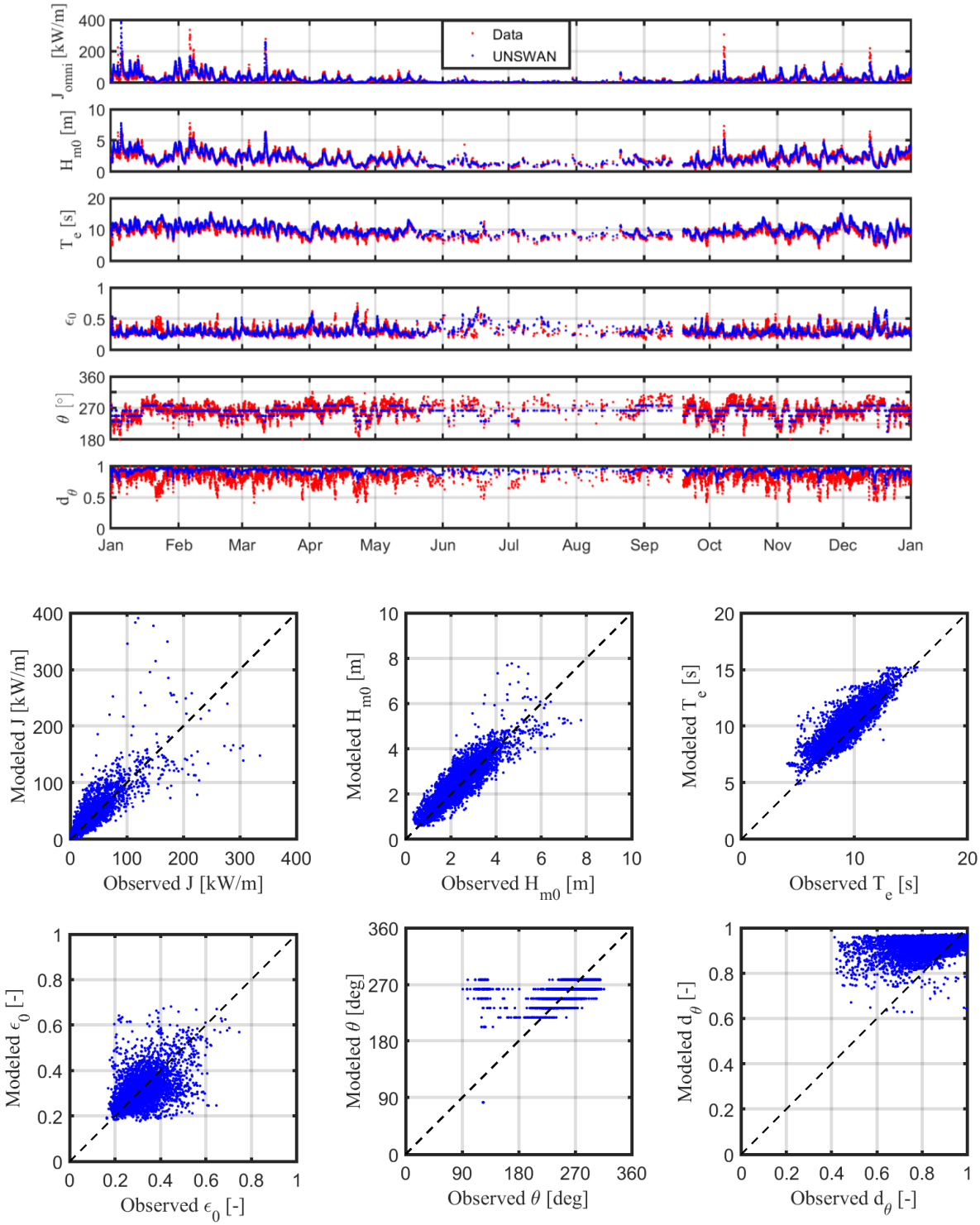

Figure B.66. Comparisons of time series (top) and scatter plots (bottom) of UnSWAN simulated six IEC parameters with observed data at NDBC Buoy 46087 for 2008.

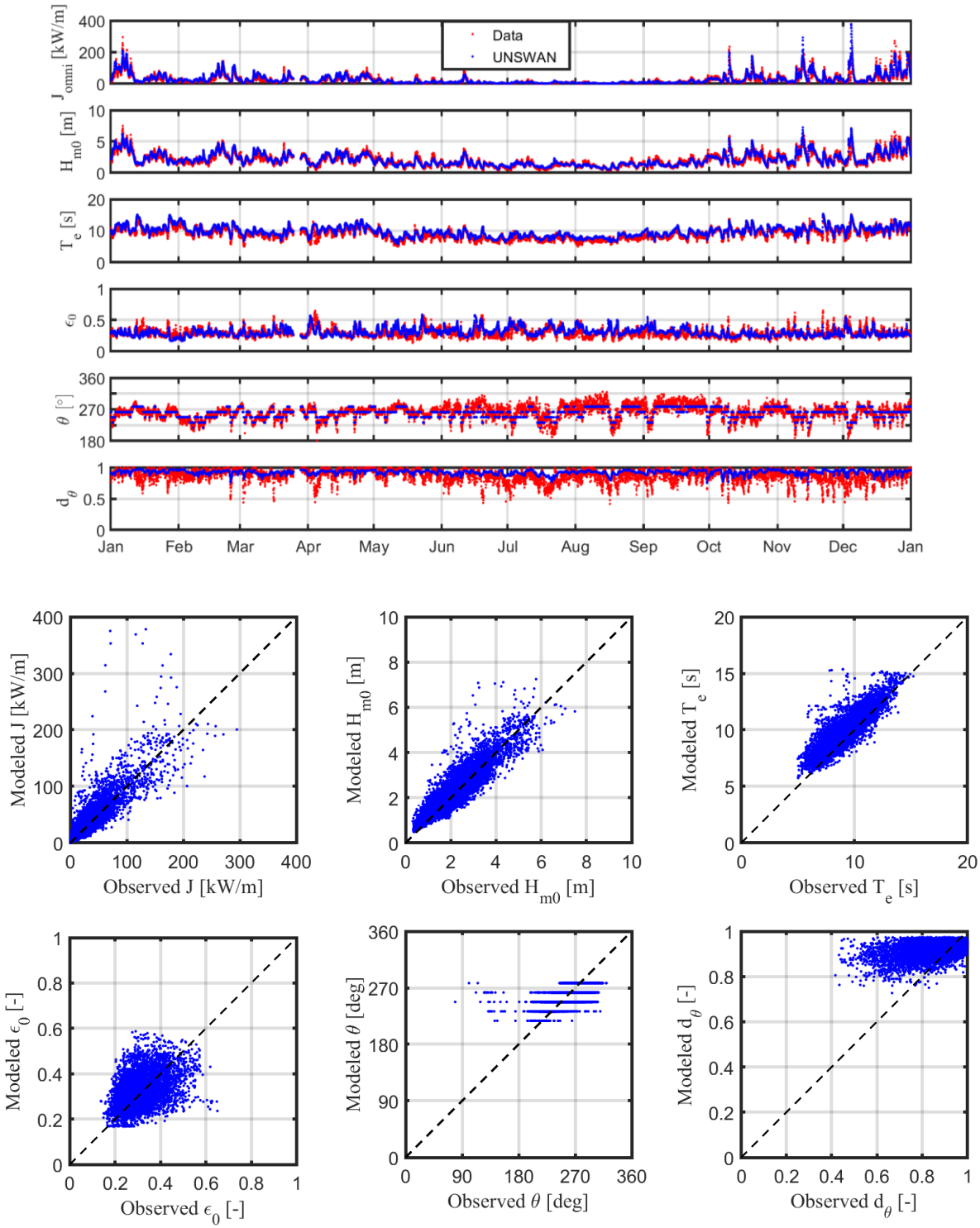

Figure B.67. Comparisons of time series (top) and scatter plots (bottom) of UnSWAN simulated six IEC parameters with observed data at NDBC Buoy 46087 for 2007.

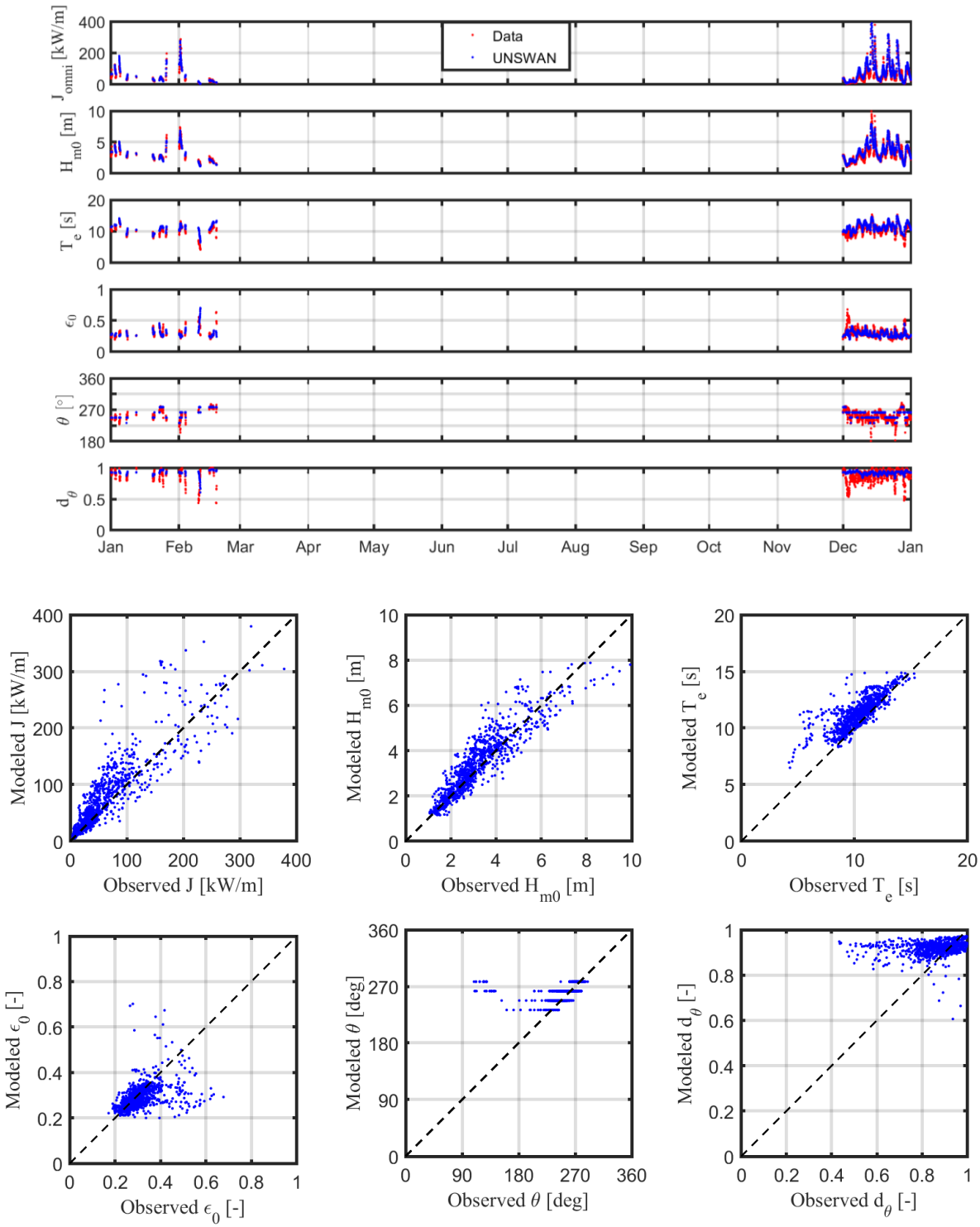

Figure B.68. Comparisons of time series (top) and scatter plots (bottom) of UnSWAN simulated six IEC parameters with observed data at NDBC Buoy 46087 for 2006.

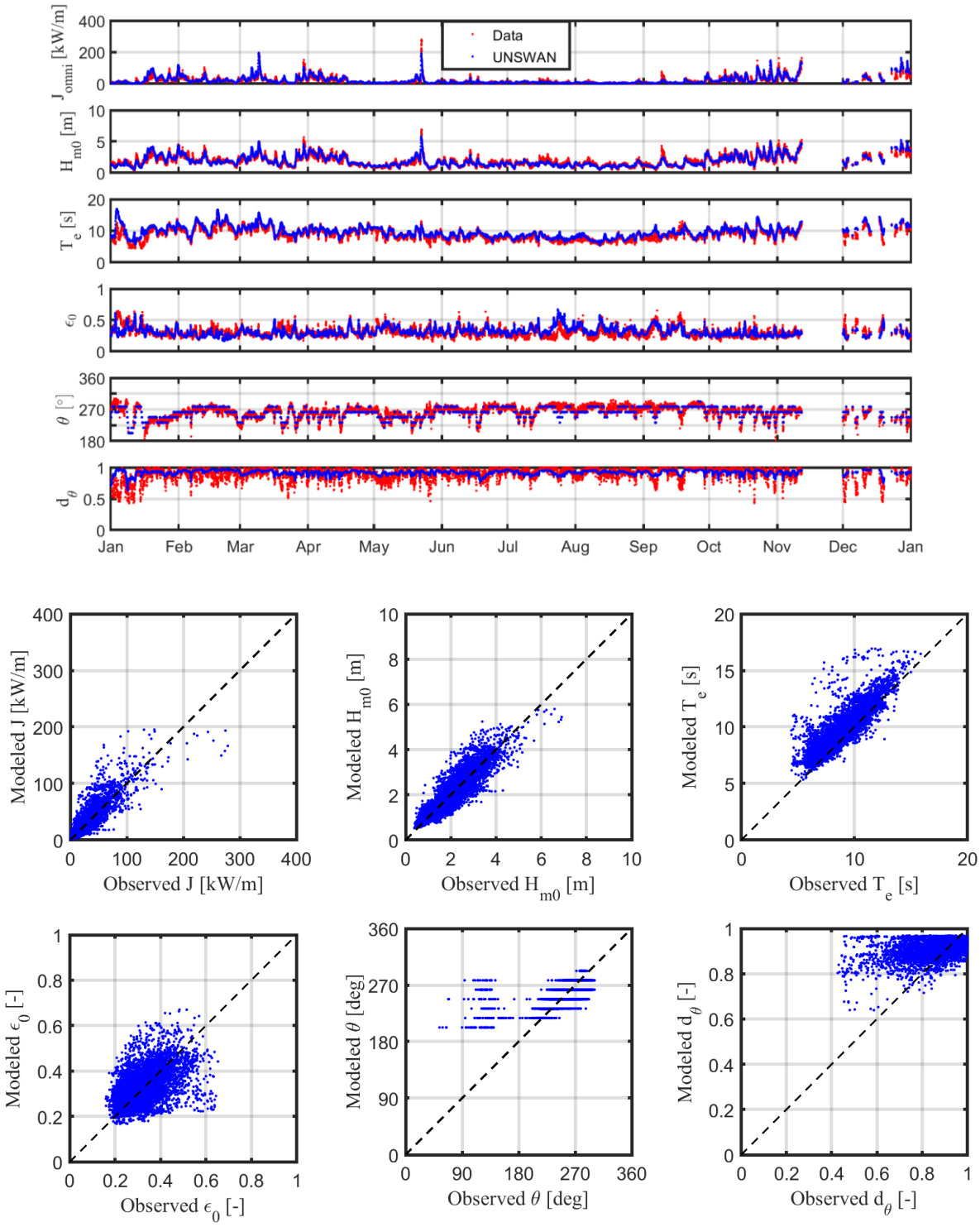

Figure B.69. Comparisons of time series (top) and scatter plots (bottom) of UnSWAN simulated six IEC parameters with observed data at NDBC Buoy 46087 for 2005.

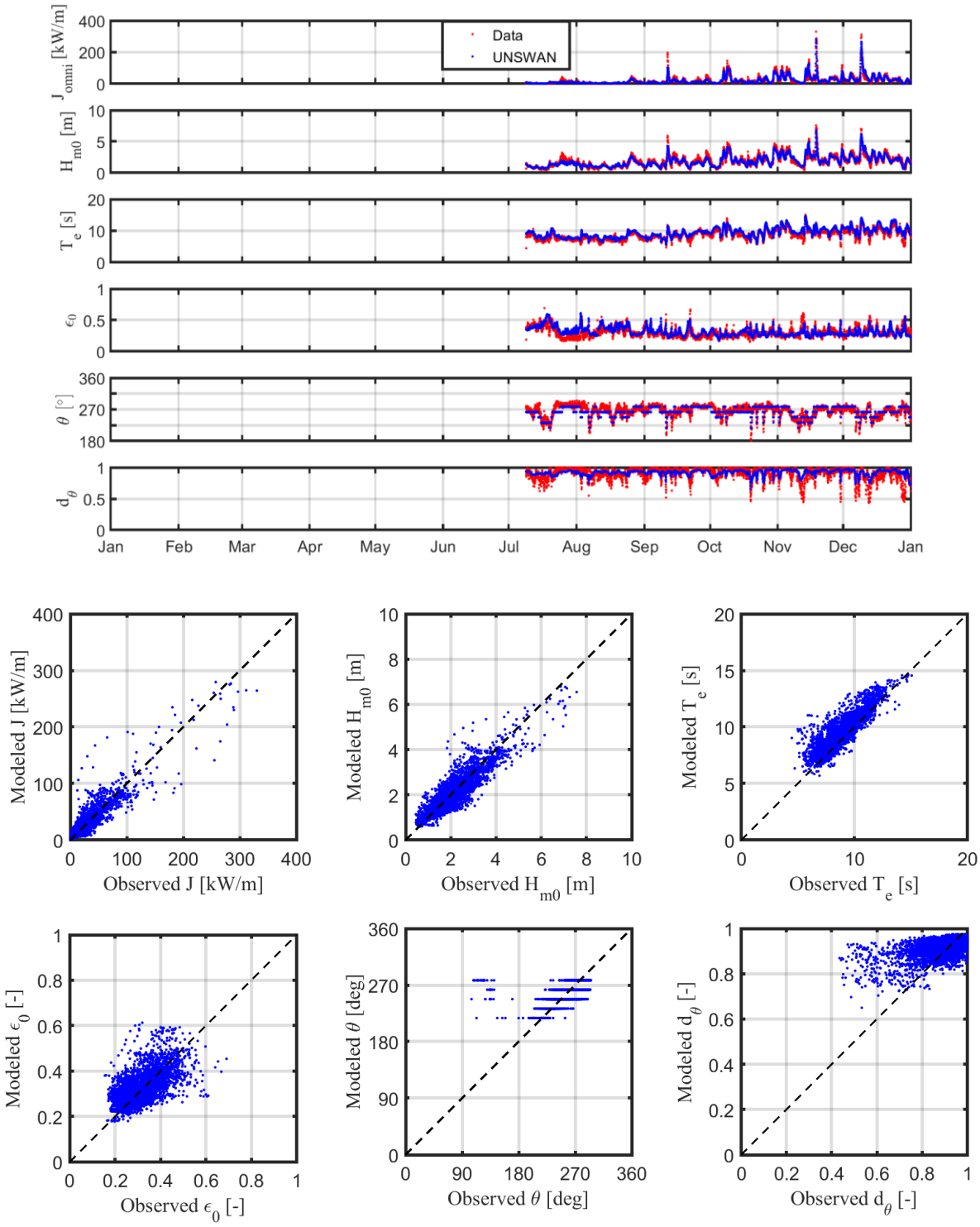

Figure B.70. Comparisons of time series (top) and scatter plots (bottom) of UnSWAN simulated six IEC parameters with observed data at NDBC Buoy 46087 for 2004.

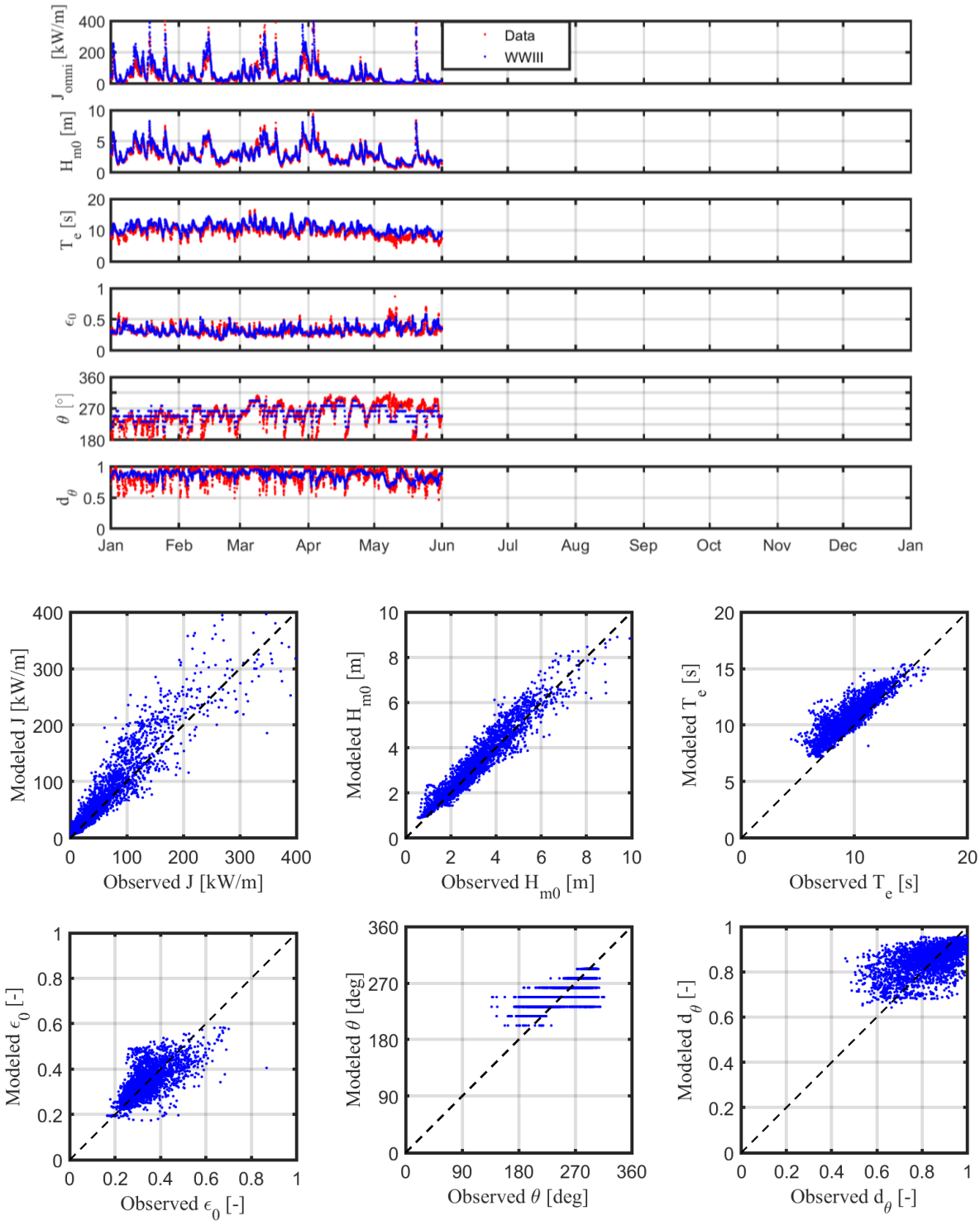

Figure B.71. Comparisons of time series (top) and scatter plots (bottom) of the six WWIII model-simulated IEC parameters with observed data at NDBC Buoy 46041 for 2010.

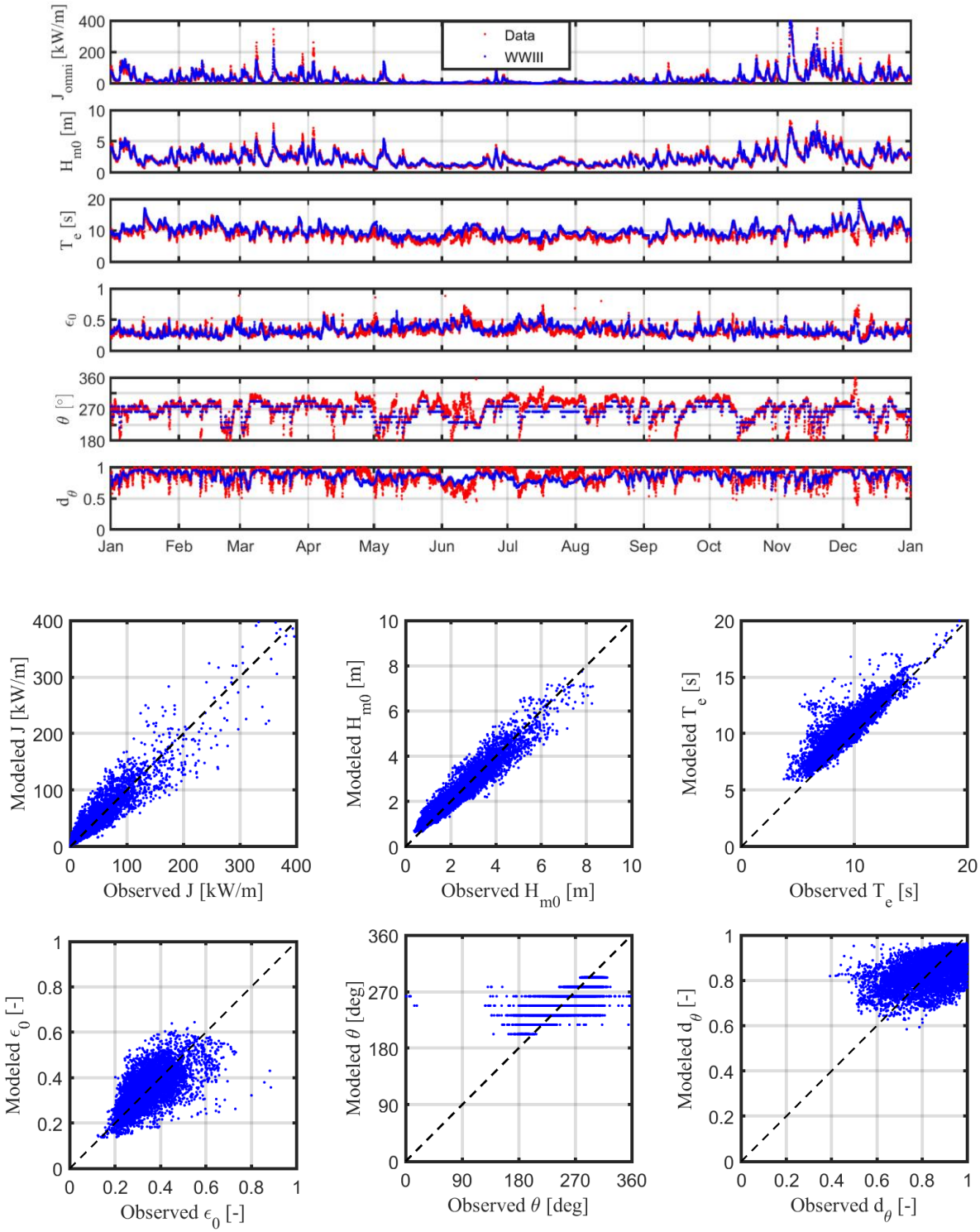

Figure B.72. Comparisons of time series (top) and scatter plots (bottom) of the six WWIII model-simulated IEC parameters with observed data at NDBC Buoy 46041 for 2009.

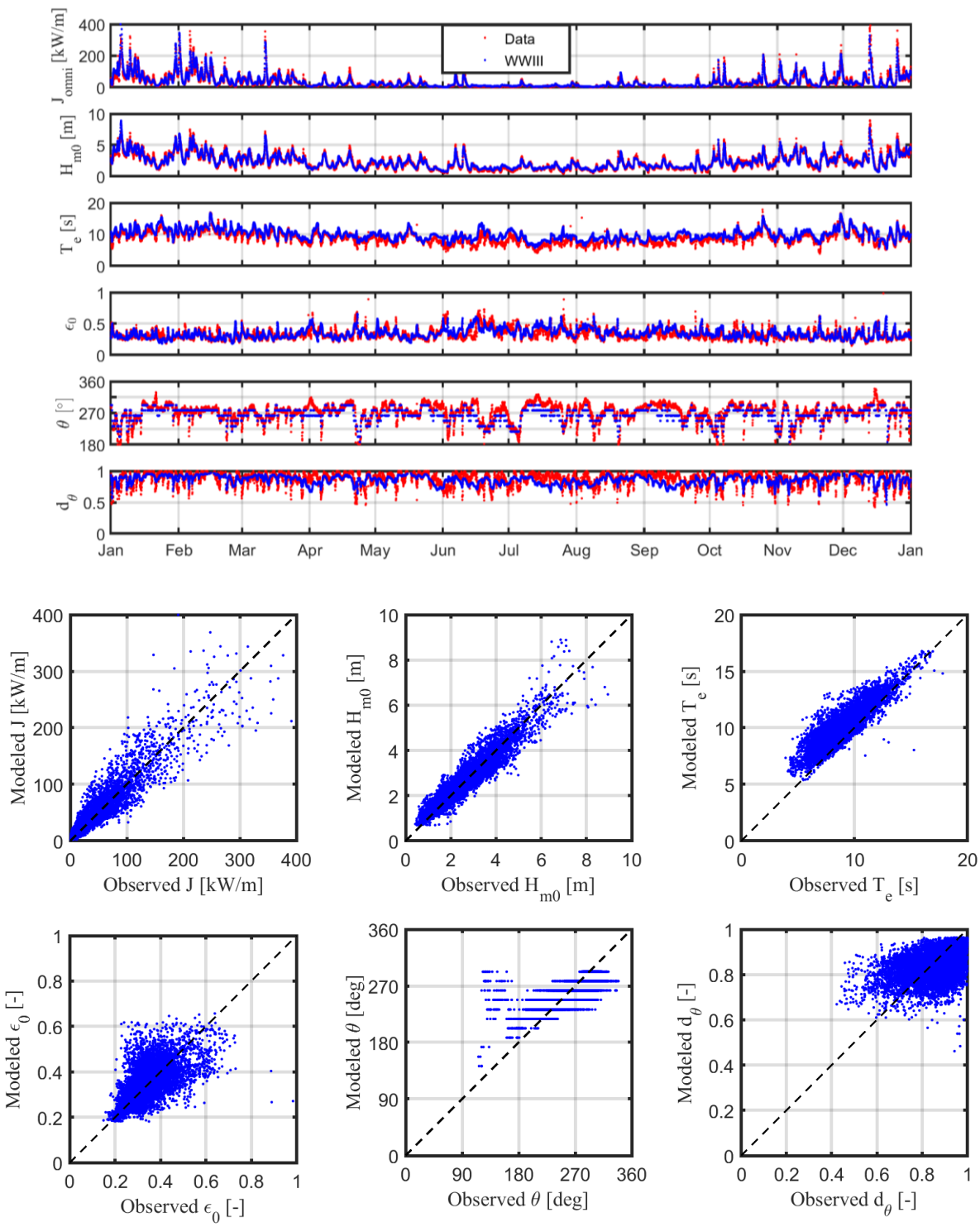

Figure B.73. Comparisons of time series (top) and scatter plots (bottom) of the six WWIII model-simulated IEC parameters with observed data at NDBC Buoy 46041 for 2008.

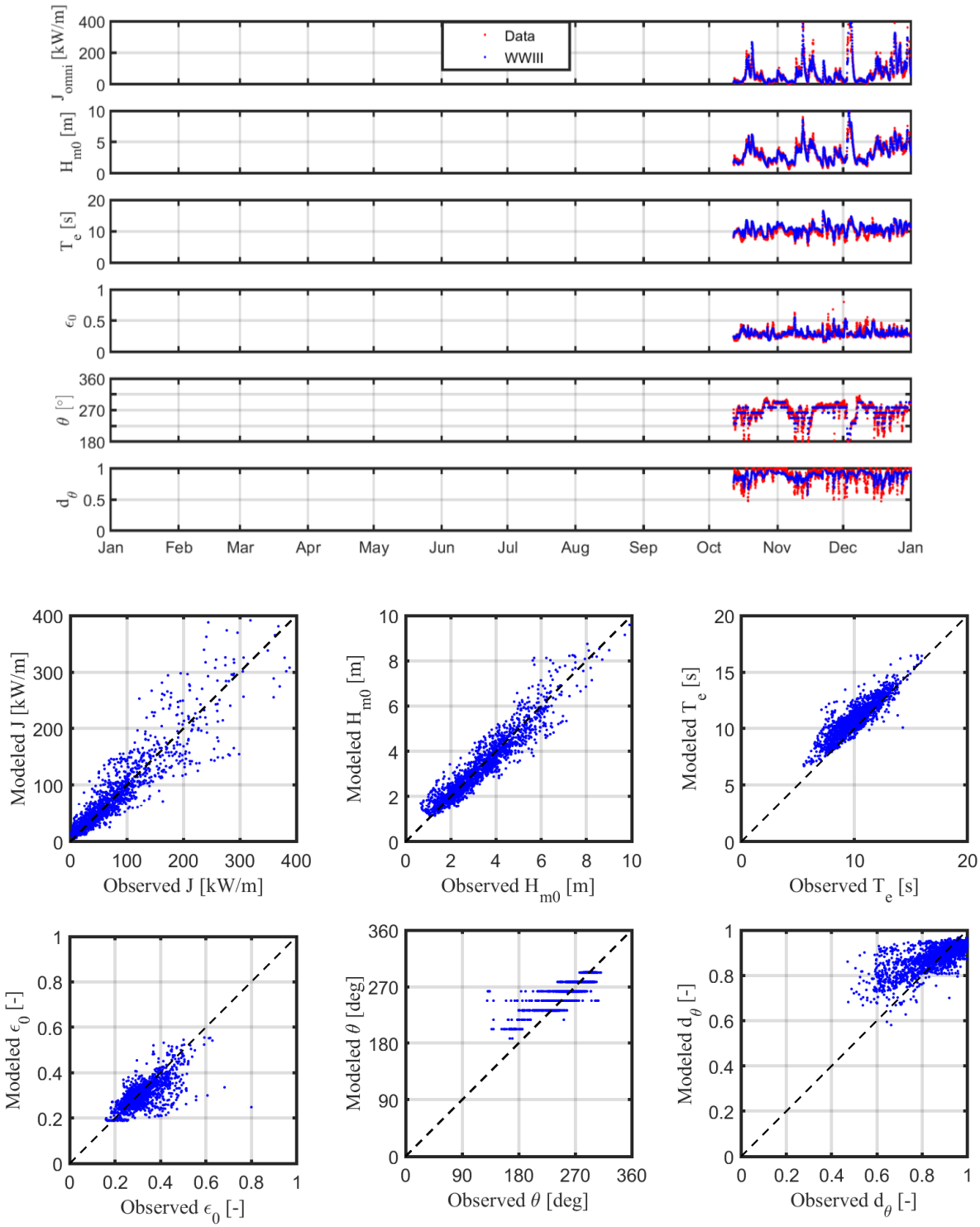

Figure B.74. Comparisons of time series (top) and scatter plots (bottom) of the six WWIII model-simulated IEC parameters with observed data at NDBC Buoy 46041 for 2007.

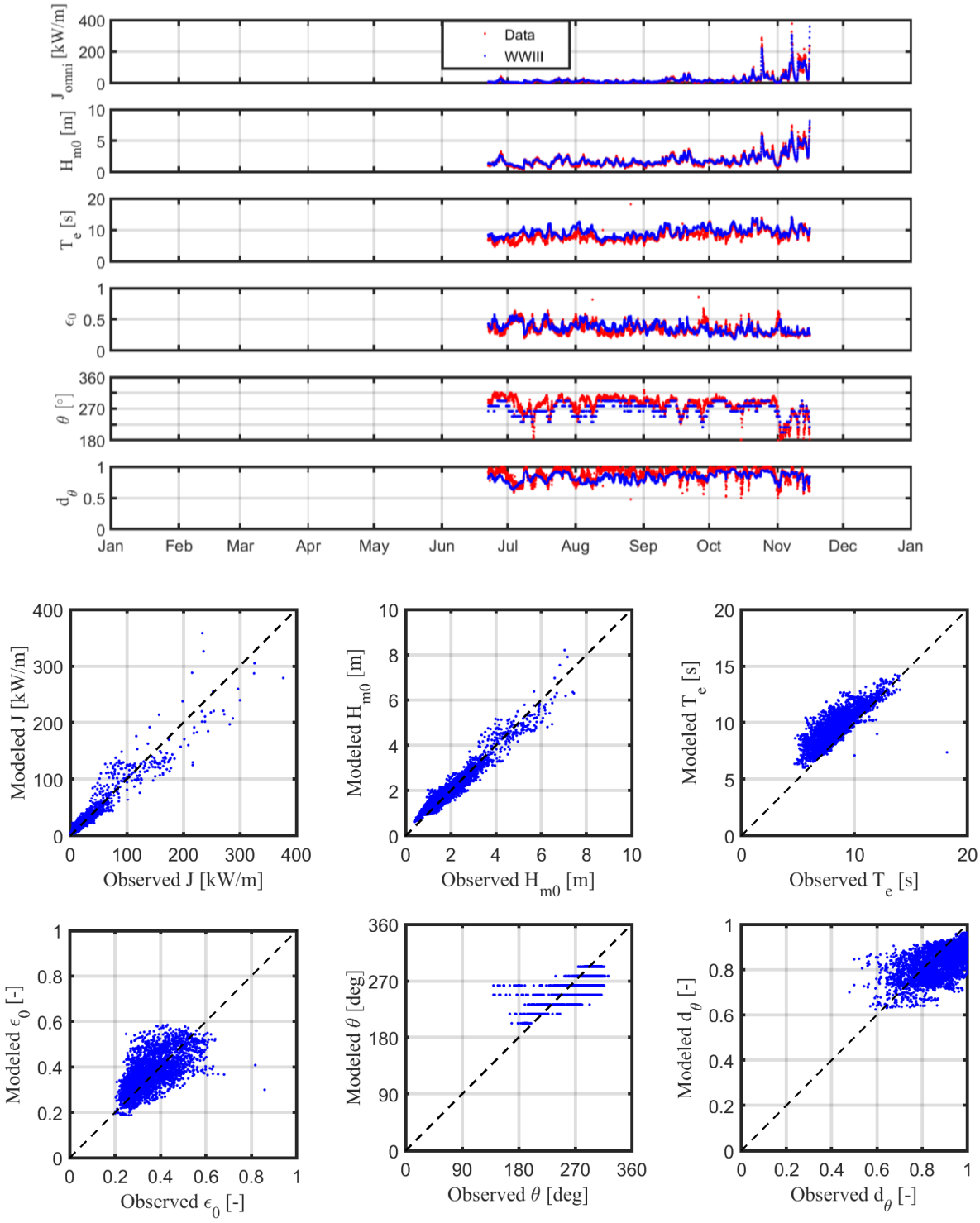

Figure B.75. Comparisons of time series (top) and scatter plots (bottom) of the six WWIII model-simulated IEC parameters with observed data at NDBC Buoy 46041 for 2006.

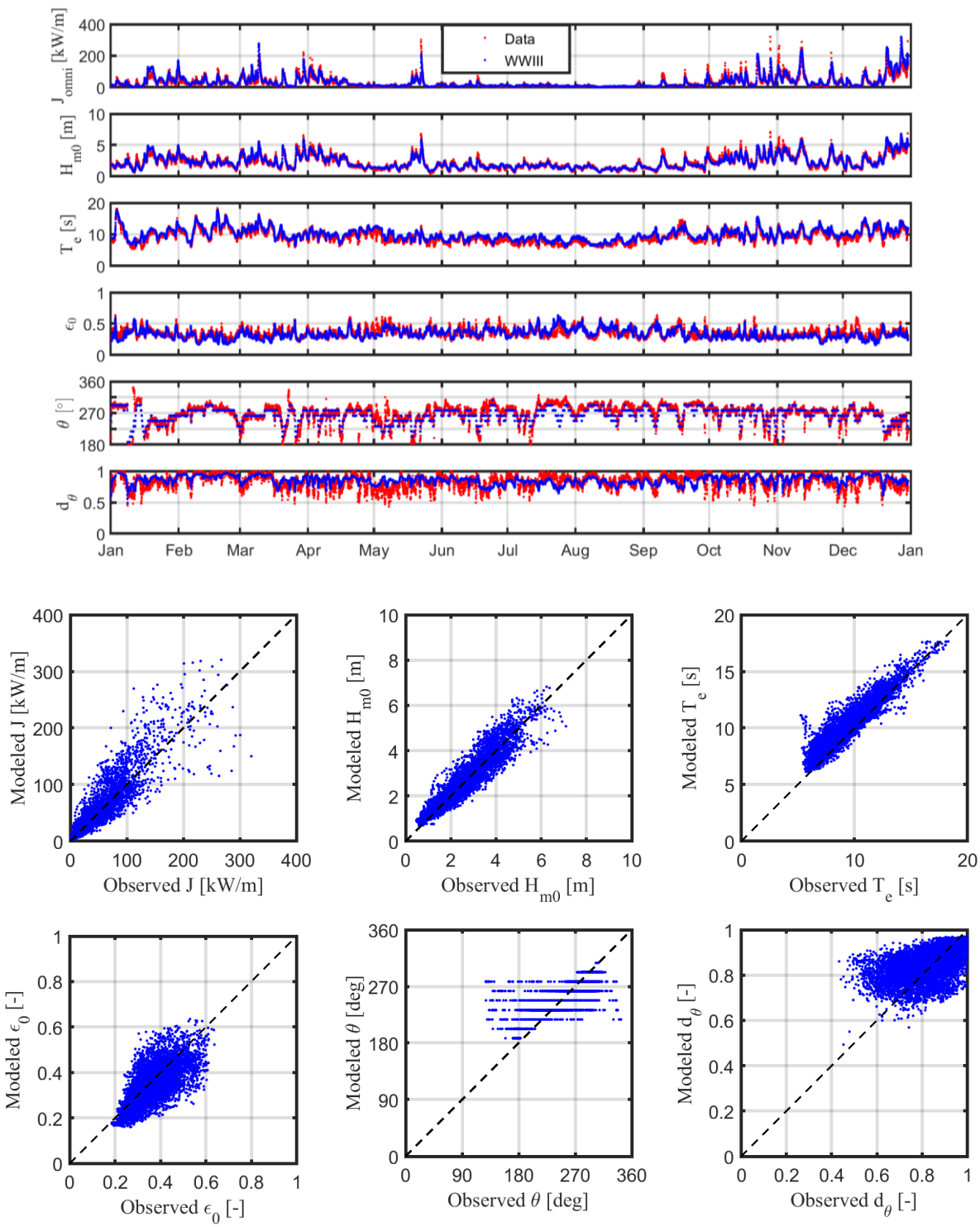

Figure B.76. Comparisons of time series (top) and scatter plots (bottom) of the six WWIII model-simulated IEC parameters with observed data at NDBC Buoy 46041 for 2005.

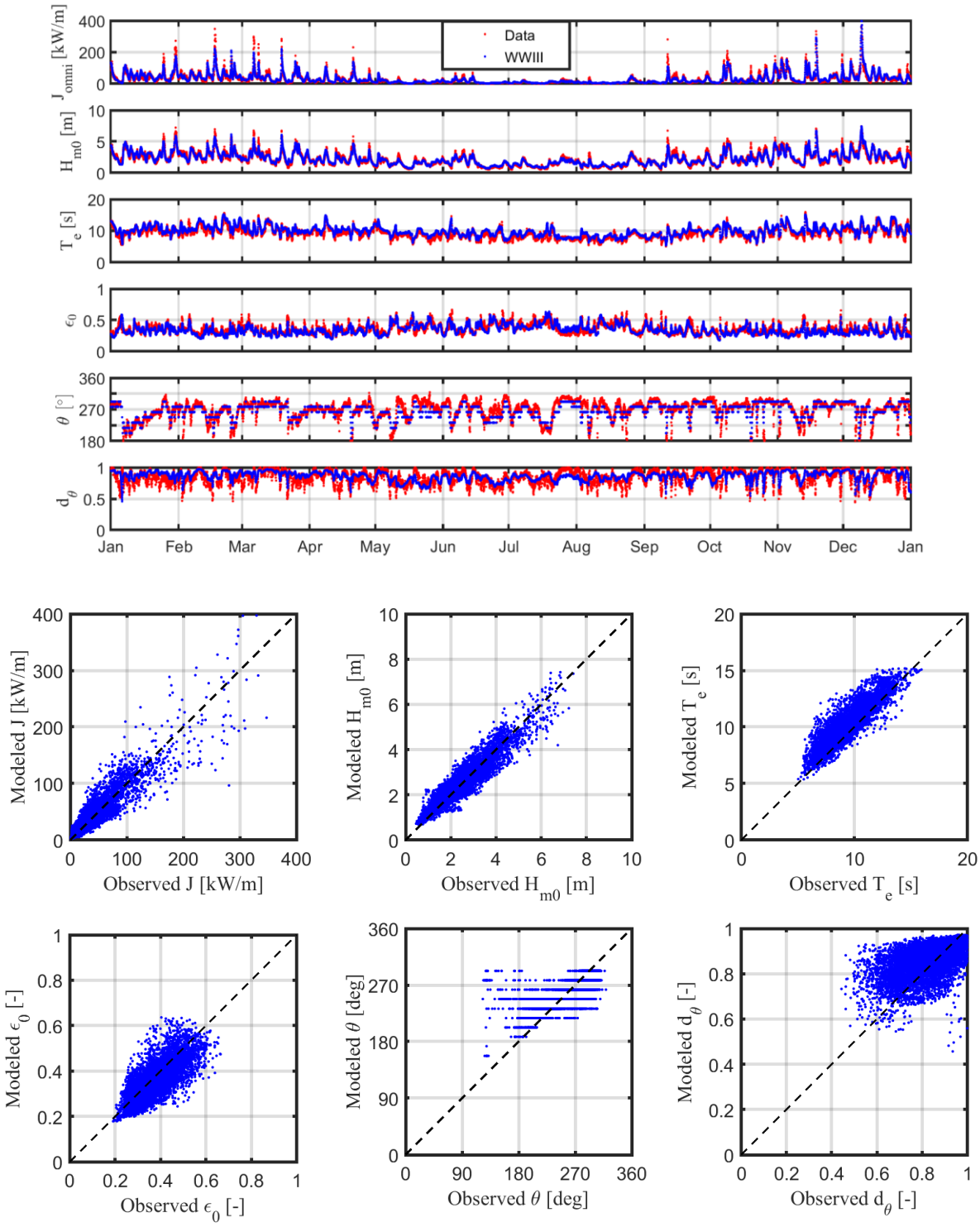

Figure B.77. Comparisons of time series (top) and scatter plots (bottom) of the six WWIII model-simulated IEC parameters with observed data at NDBC Buoy 46041 for 2004.

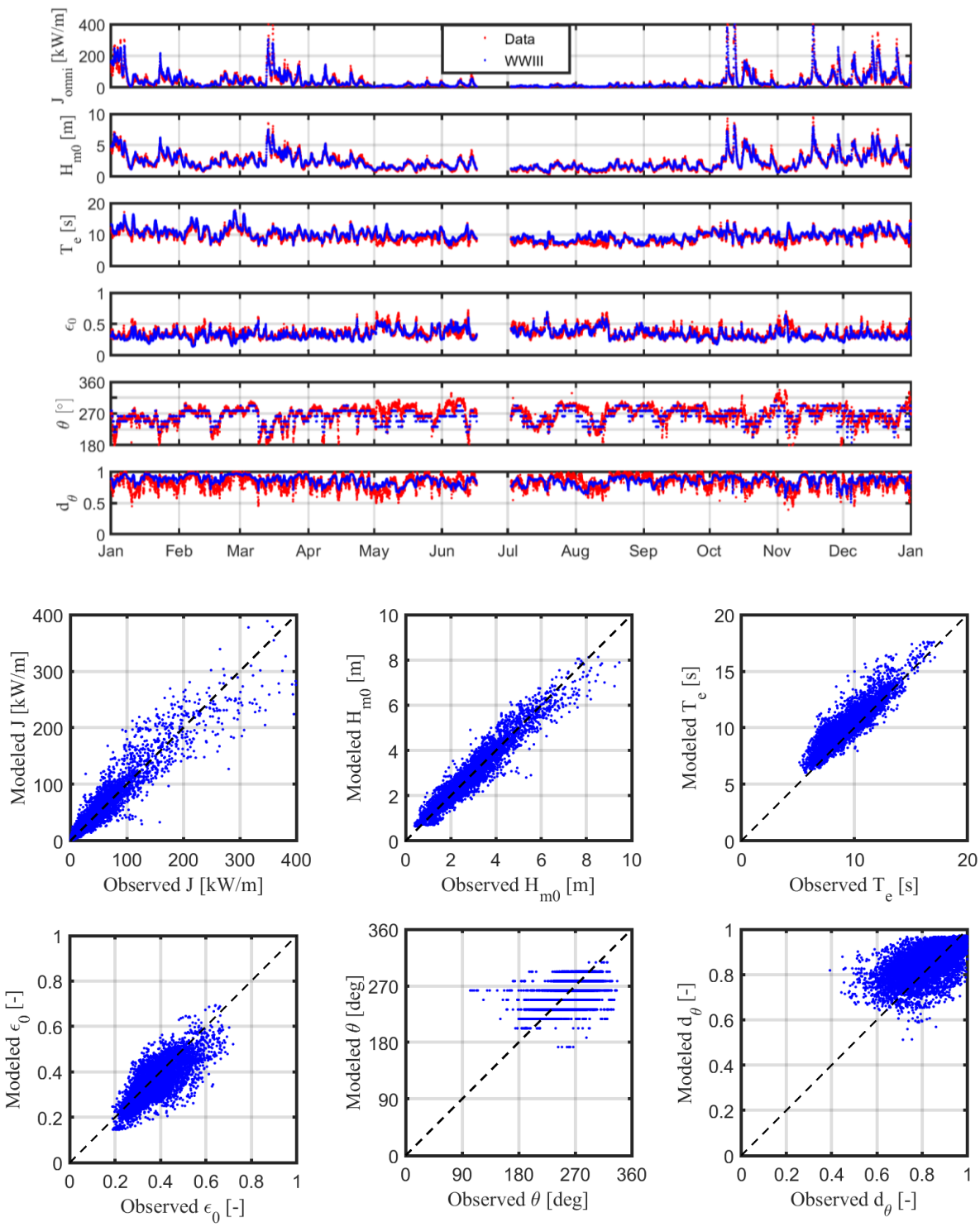

Figure B.78. Comparisons of time series (top) and scatter plots (bottom) of the six WWIII model-simulated IEC parameters with observed data at NDBC Buoy 46041 for 2003.

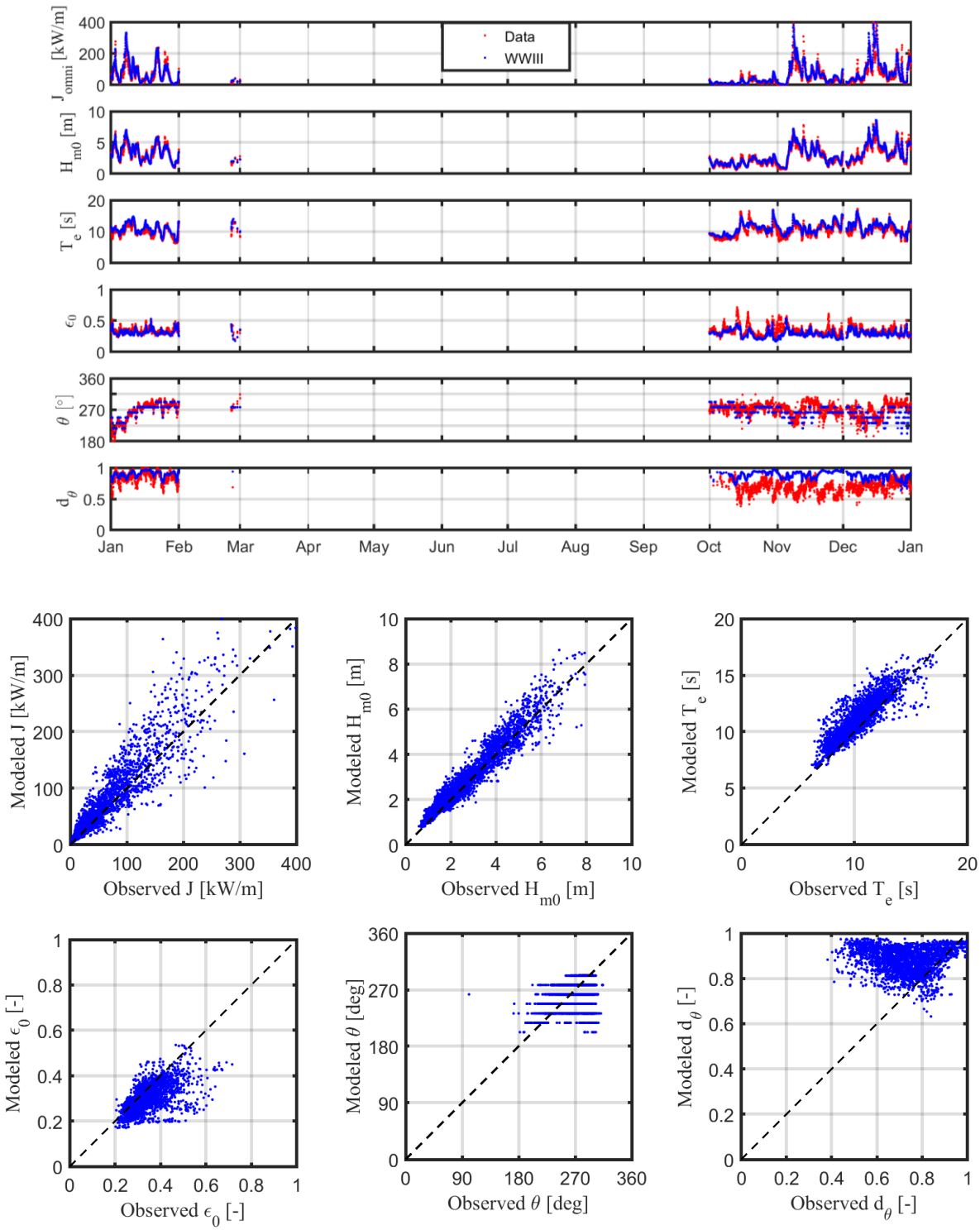

Figure B.79. Comparisons of time series (top) and scatter plots (bottom) of the six WWIII model-simulated IEC parameters with observed data at NDBC Buoy 46041 for 2002.

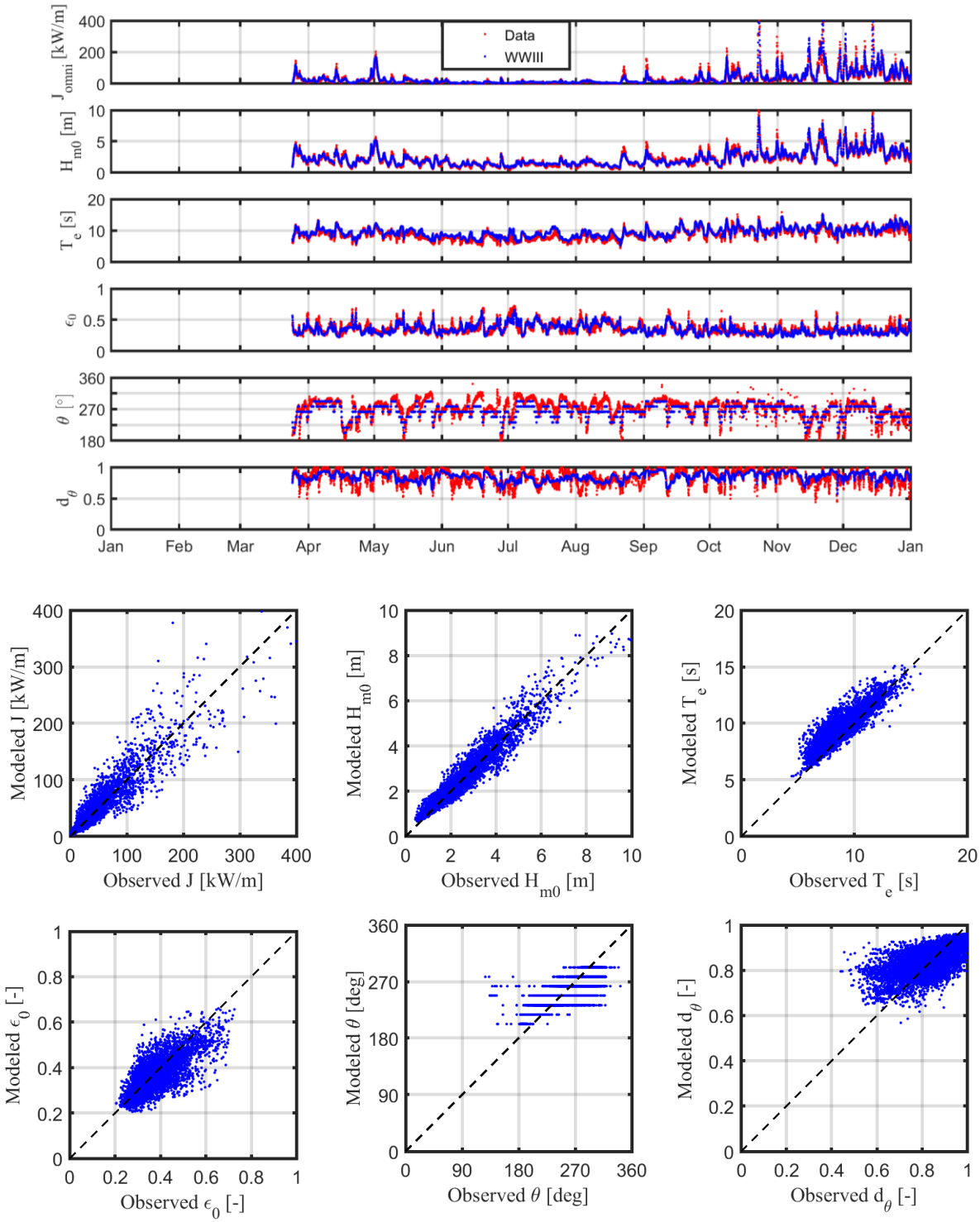

Figure B.80. Comparisons of time series (top) and scatter plots (bottom) of the six WWIII model-simulated IEC parameters with observed data at NDBC Buoy 46041 for 2001.

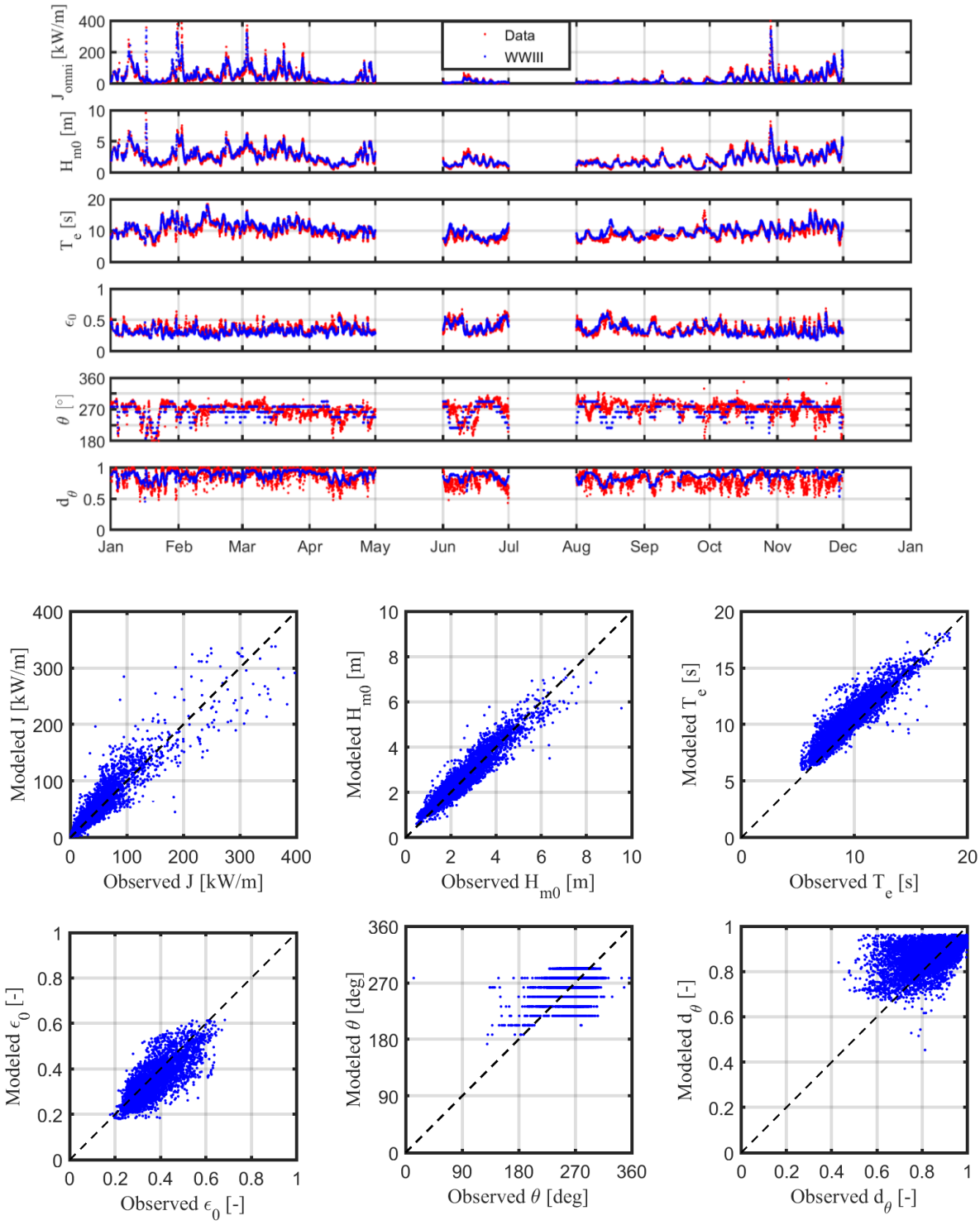

Figure B.81. Comparisons of time series (top) and scatter plots (bottom) of the six WWIII model-simulated IEC parameters with observed data at NDBC Buoy 46041 for 2000.

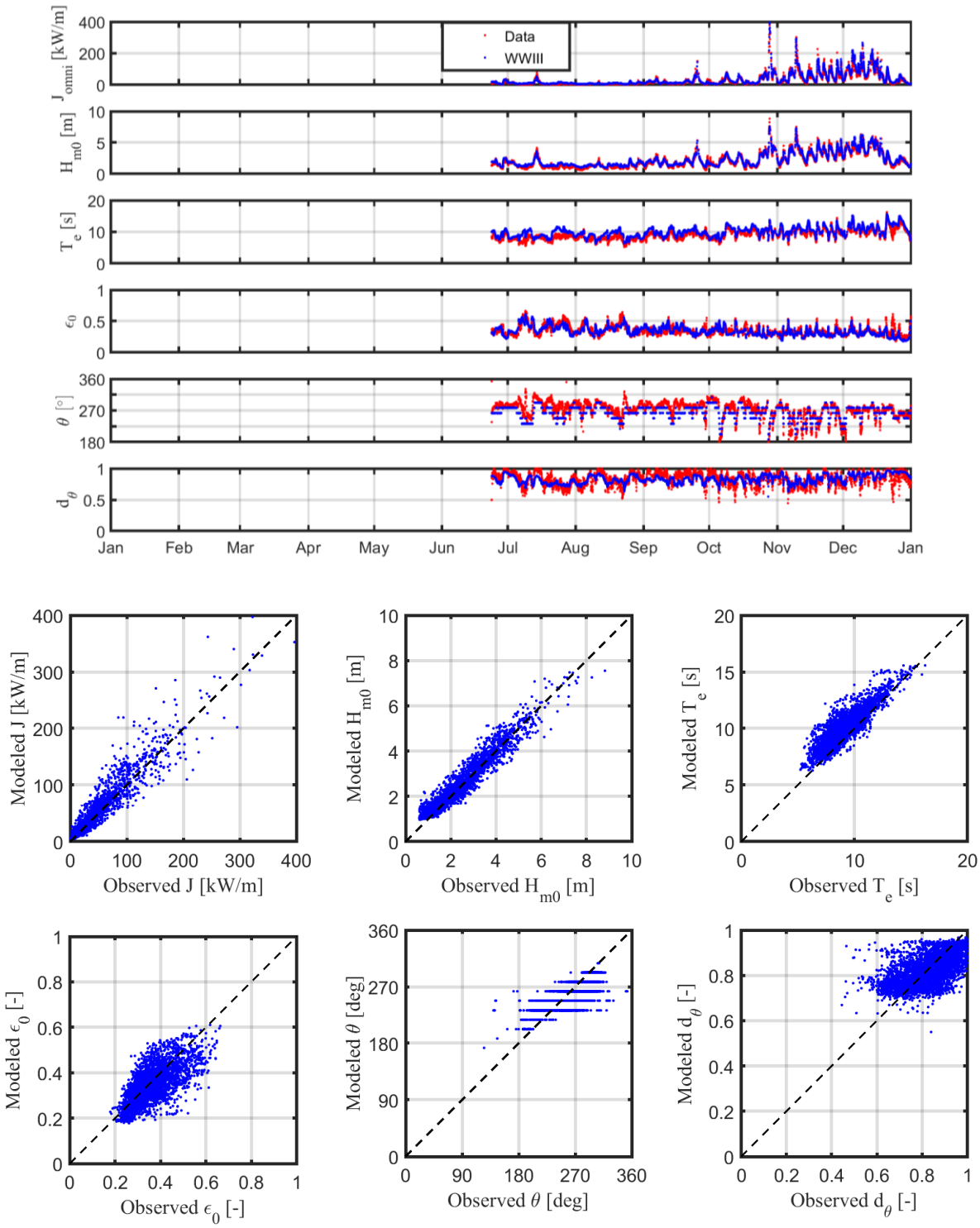

Figure B.82. Comparisons of time series (top) and scatter plots (bottom) of the six WWIII model-simulated IEC parameters with observed data at NDBC Buoy 46041 for 1999.

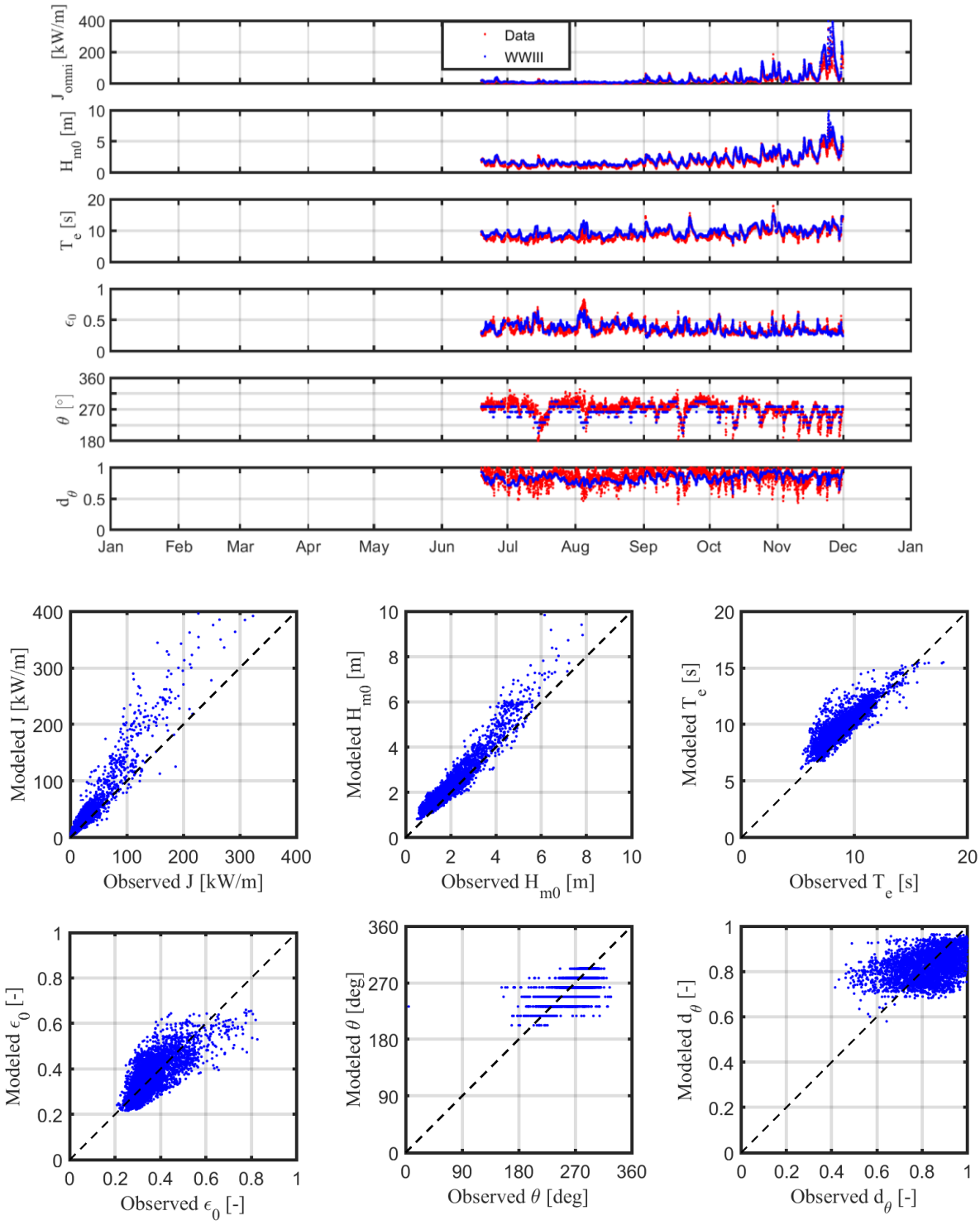

Figure B.83. Comparisons of time series (top) and scatter plots (bottom) of the six WWIII model-simulated IEC parameters with observed data at NDBC Buoy 46041 for 1998.

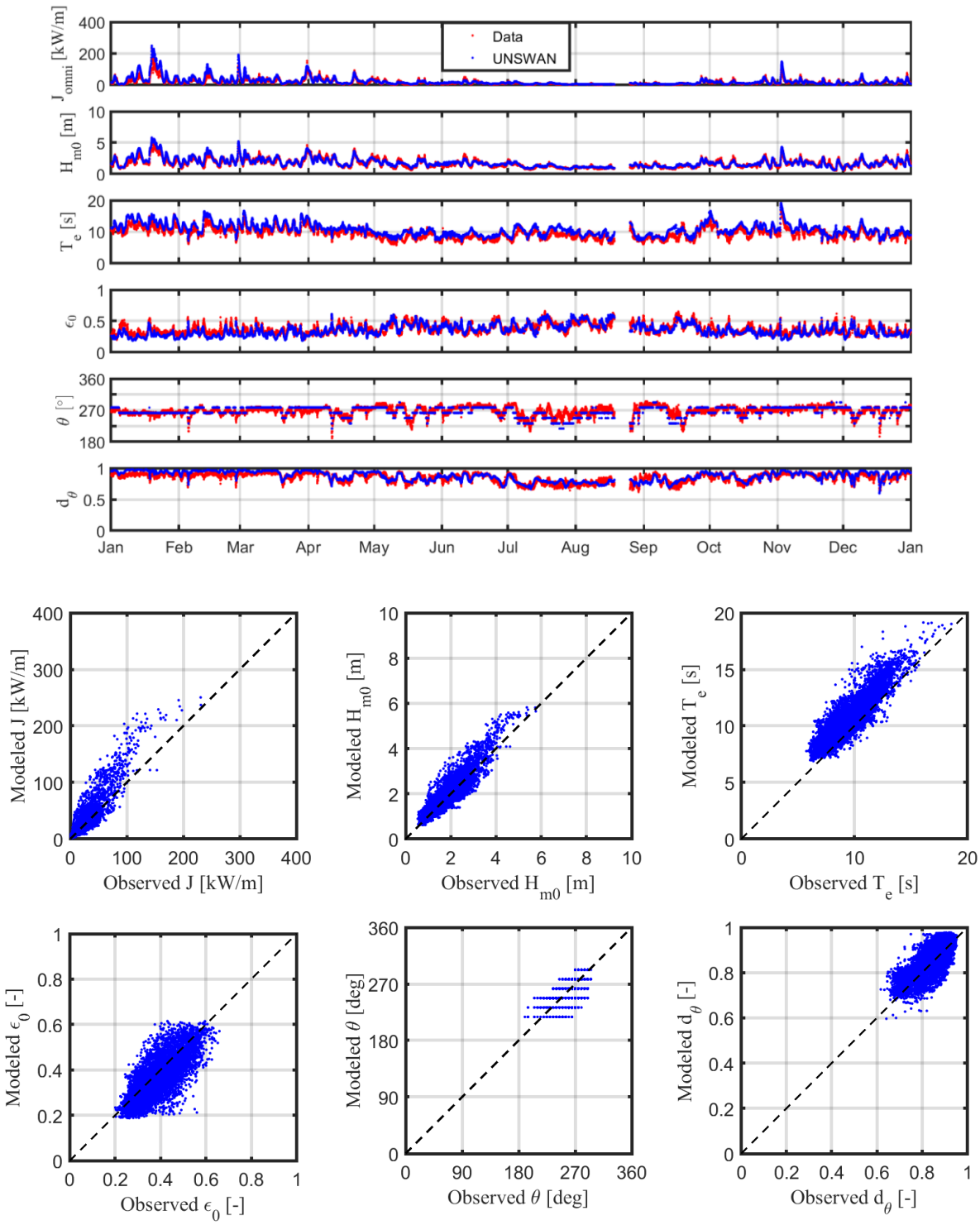

Figure B.84. Comparisons of time series (top) and scatter plots (bottom) of UnSWAN simulated six IEC parameters with observed data at CDIP Buoy 46215 for 2010.

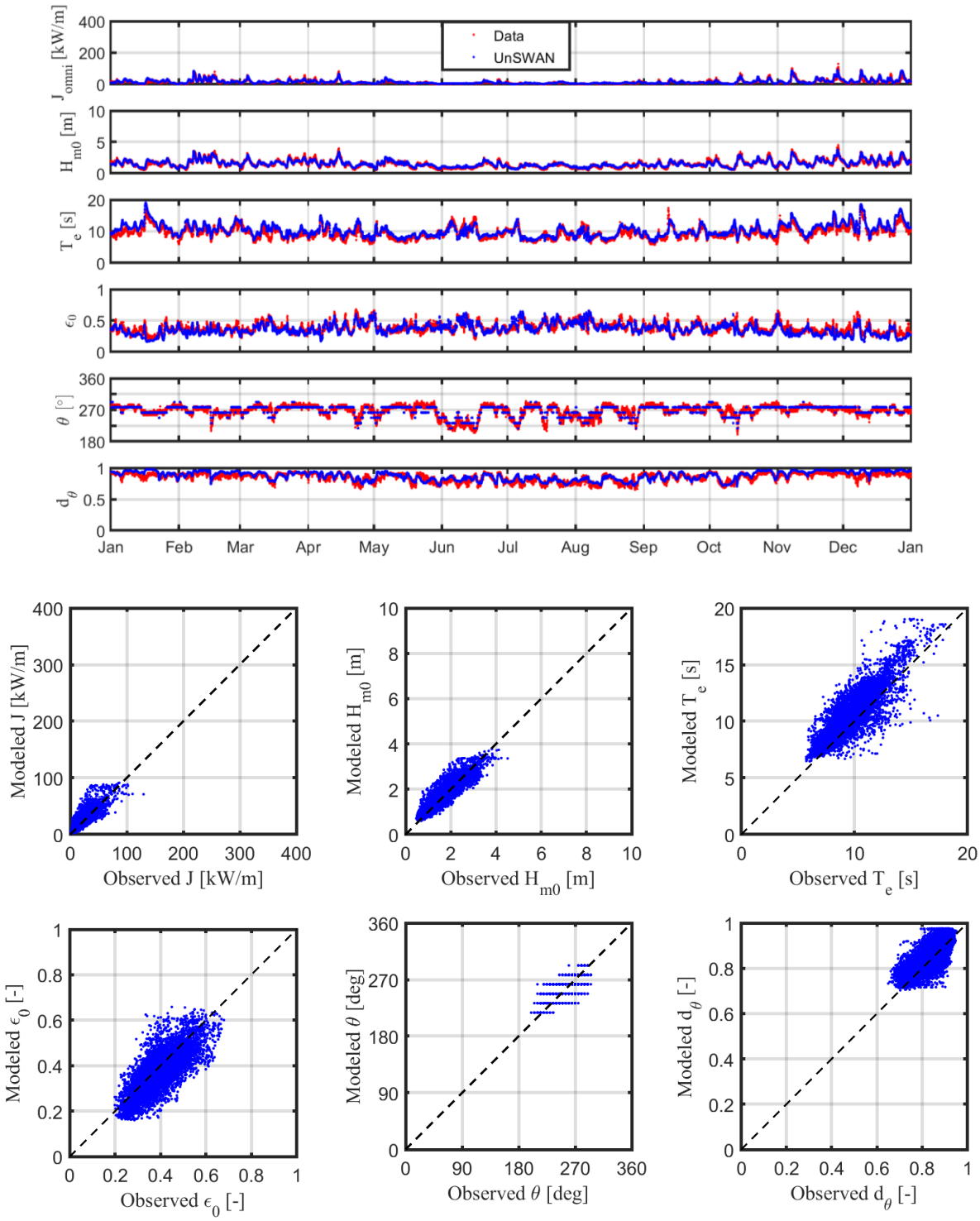

Figure B.85. Comparisons of time series (top) and scatter plots (bottom) of UnSWAN simulated six IEC parameters with observed data at CDIP Buoy 46215 for 2009.

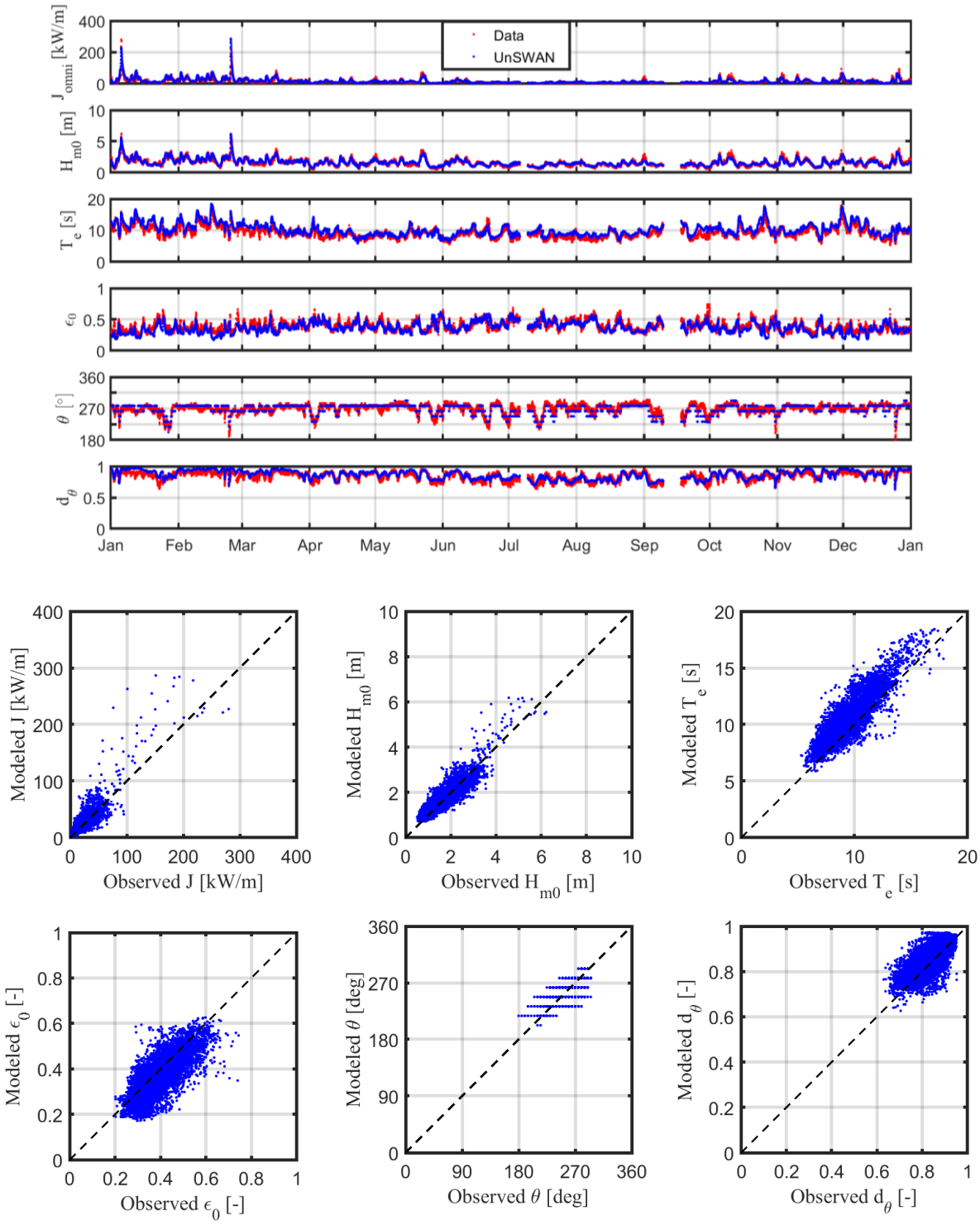

Figure B.86. Comparisons of time series (top) and scatter plots (bottom) of UnSWAN simulated six IEC parameters with observed data at CDIP Buoy 46215 for 2008.

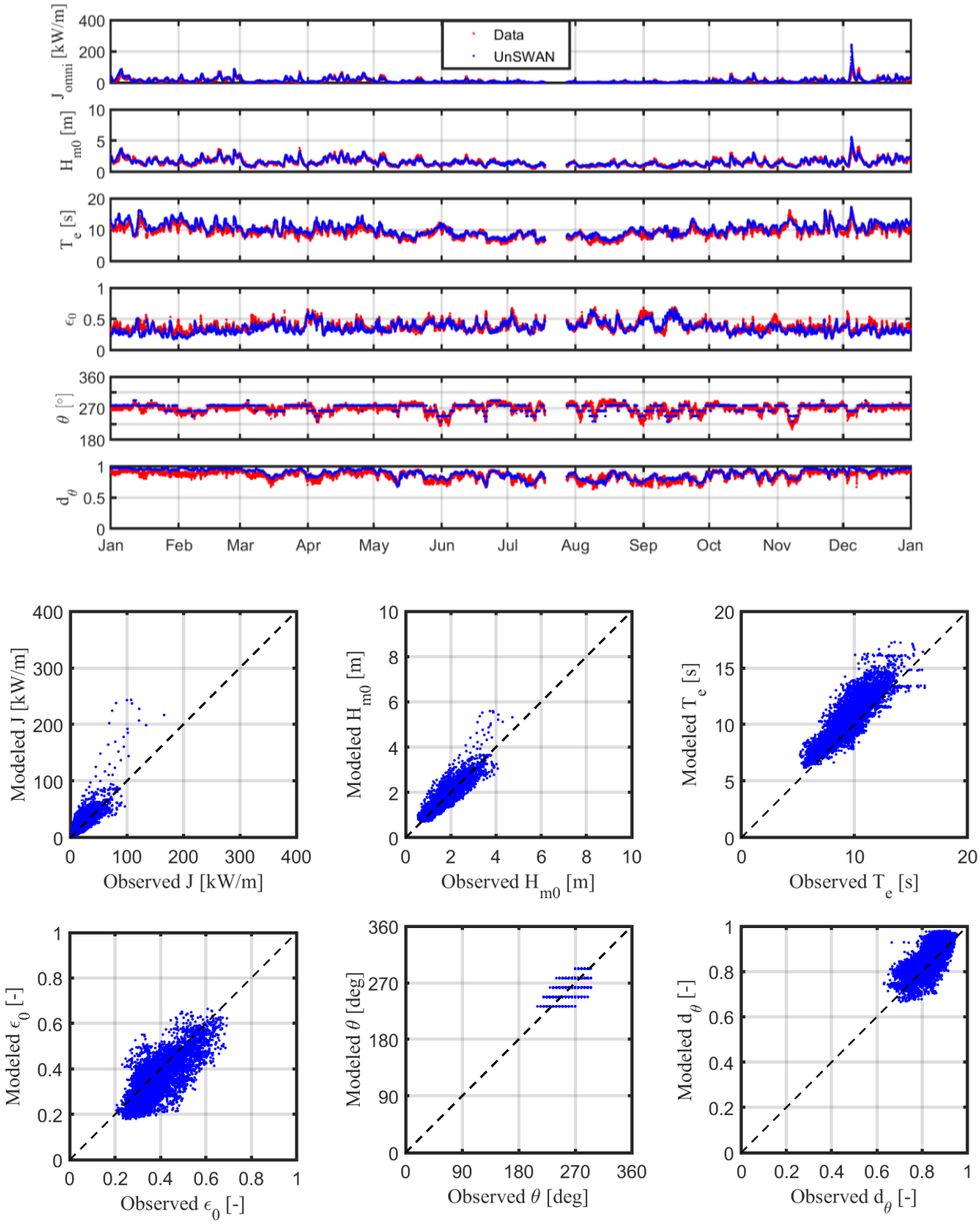

Figure B.87. Comparisons of time series (top) and scatter plots (bottom) of UnSWAN simulated six IEC parameters with observed data at CDIP Buoy 46215 for 2007.

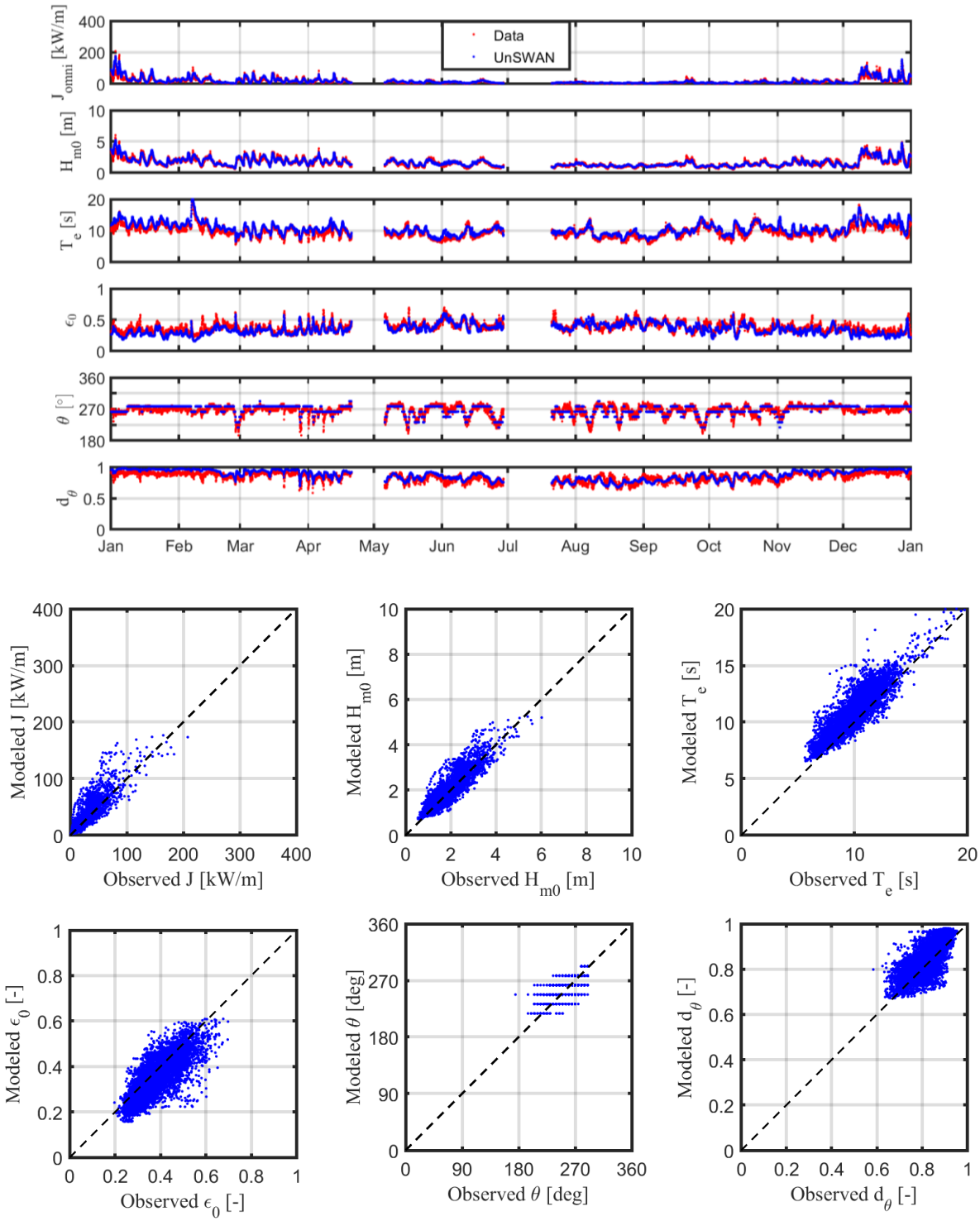

Figure B.88. Comparisons of time series (top) and scatter plots (bottom) of UnSWAN simulated six IEC parameters with observed data at CDIP Buoy 46215 for 2006.

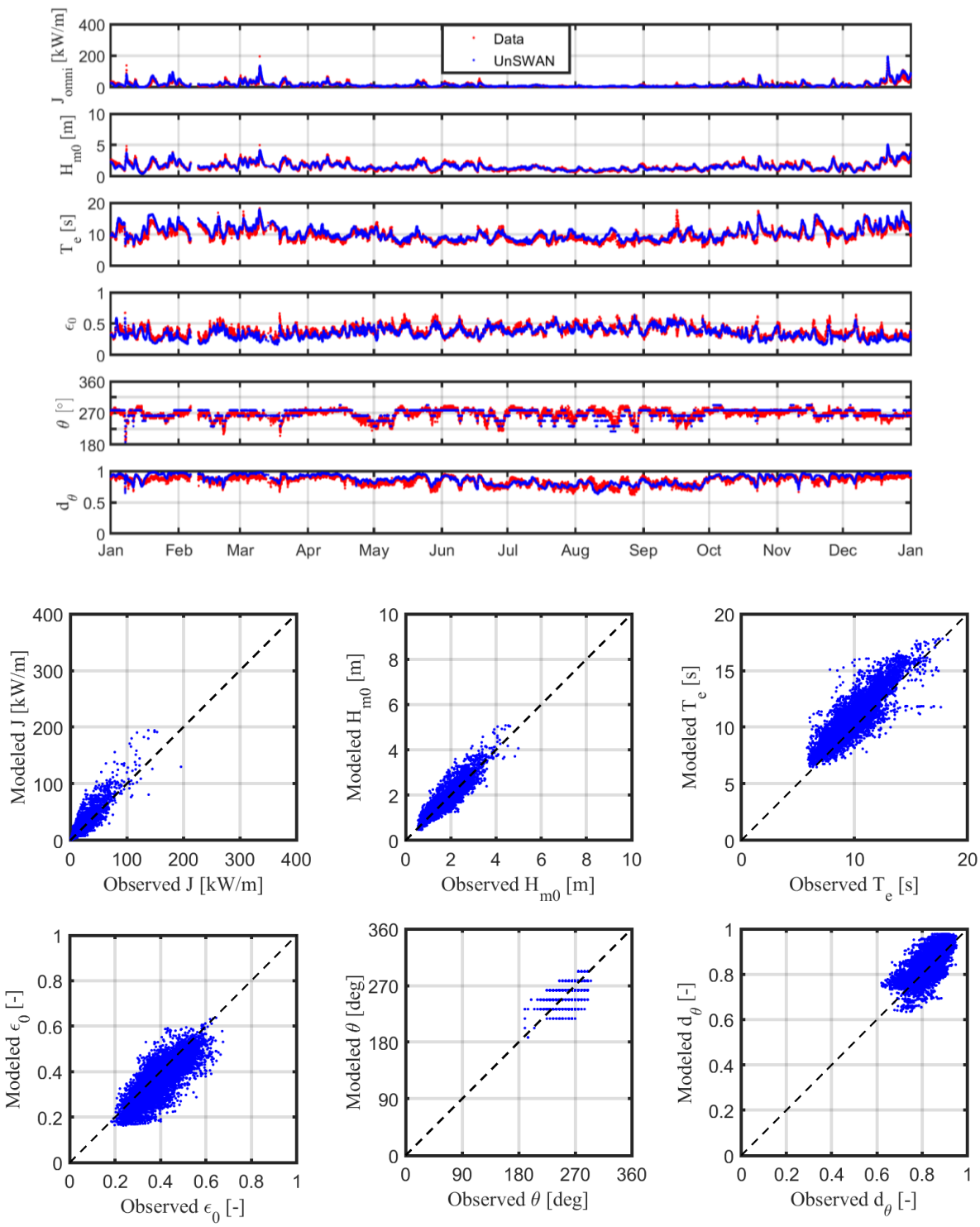

Figure B.89. Comparisons of time series (top) and scatter plots (bottom) of UnSWAN simulated six IEC parameters with observed data at CDIP Buoy 46215 for 2005.

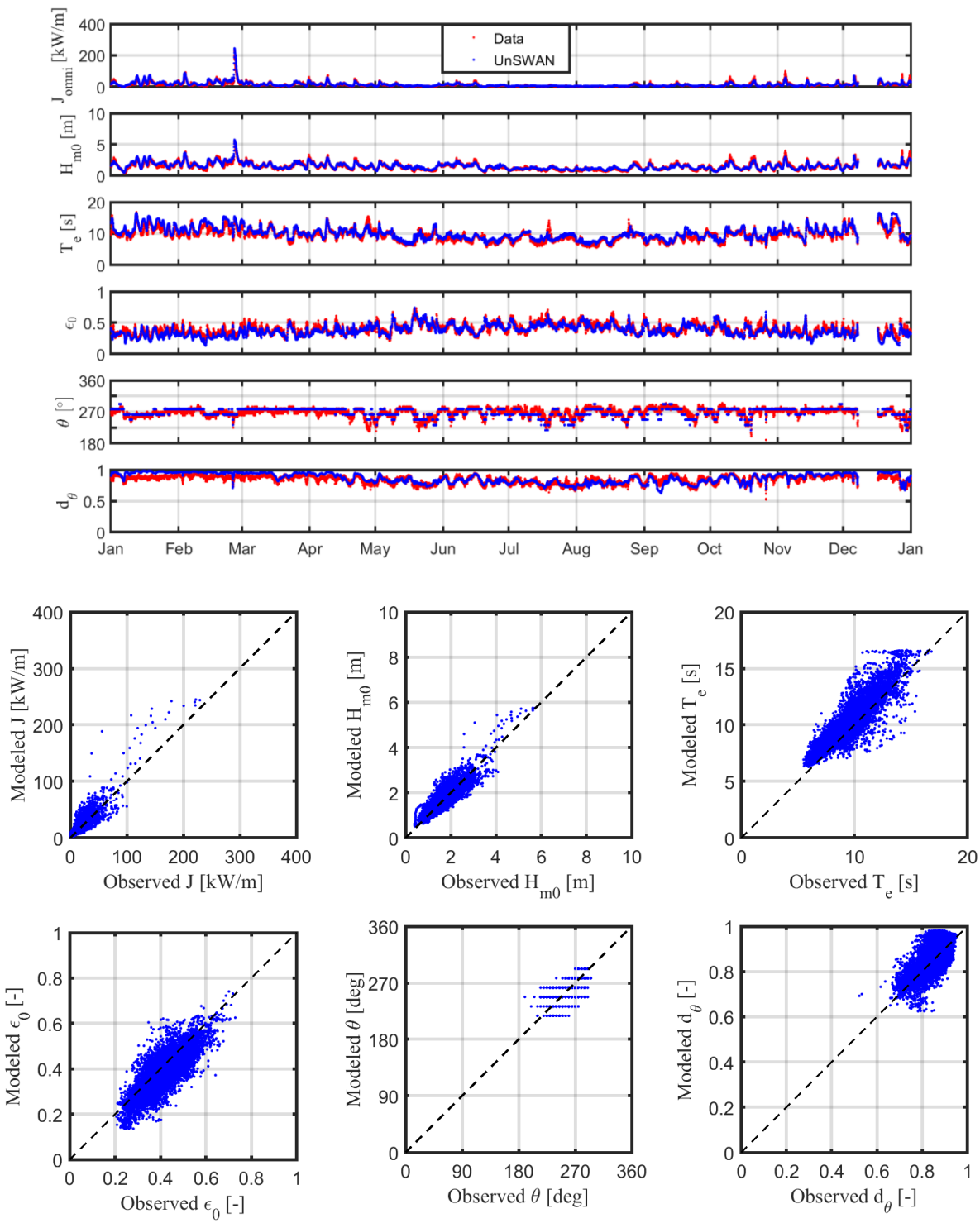

Figure B.90. Comparisons of time series (top) and scatter plots (bottom) of UnSWAN simulated six IEC parameters with observed data at CDIP Buoy 46215 for 2004.

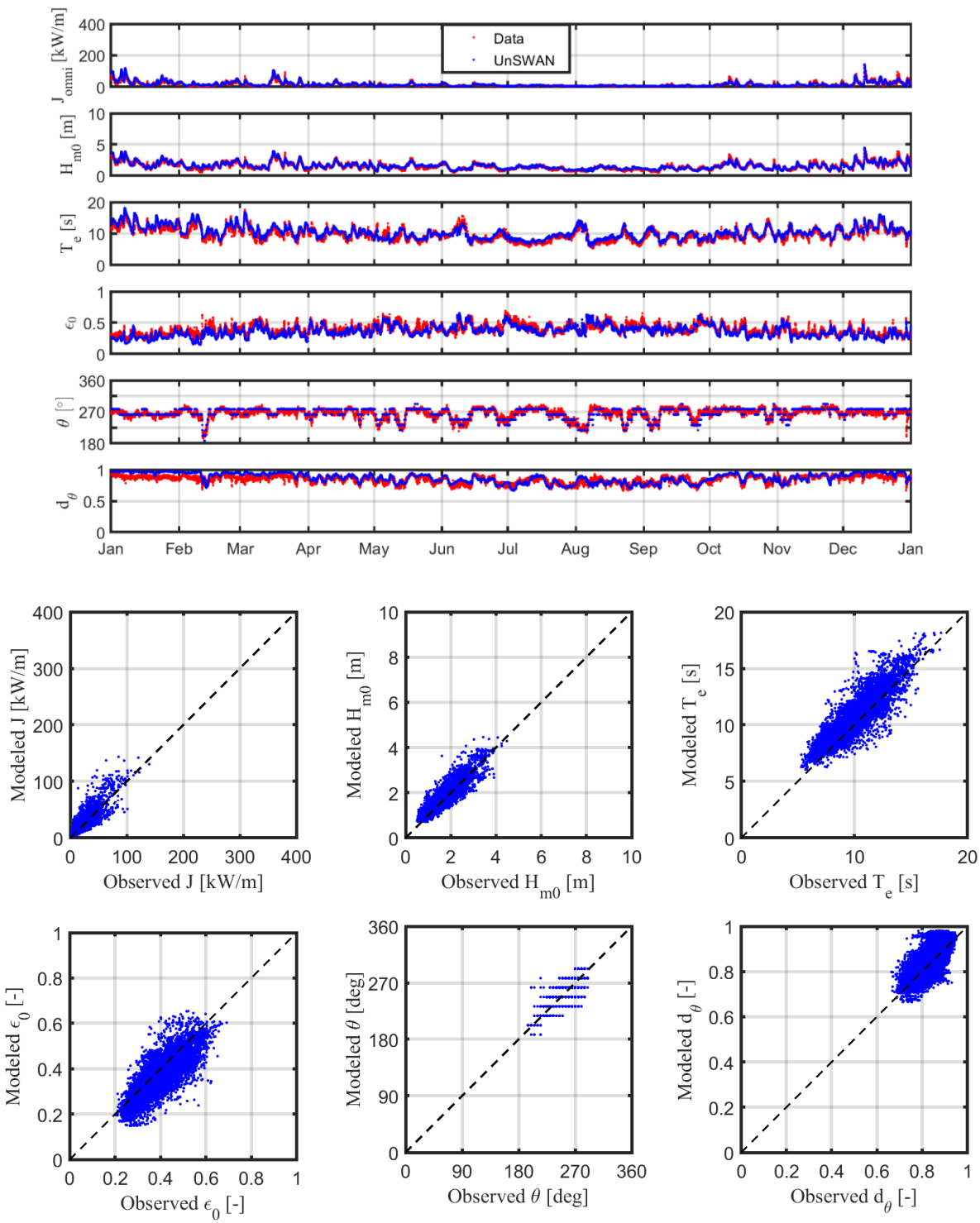

Figure B.91. Comparisons of time series (top) and scatter plots (bottom) of UnSWAN simulated six IEC parameters with observed data at CDIP Buoy 46215 for 2003.

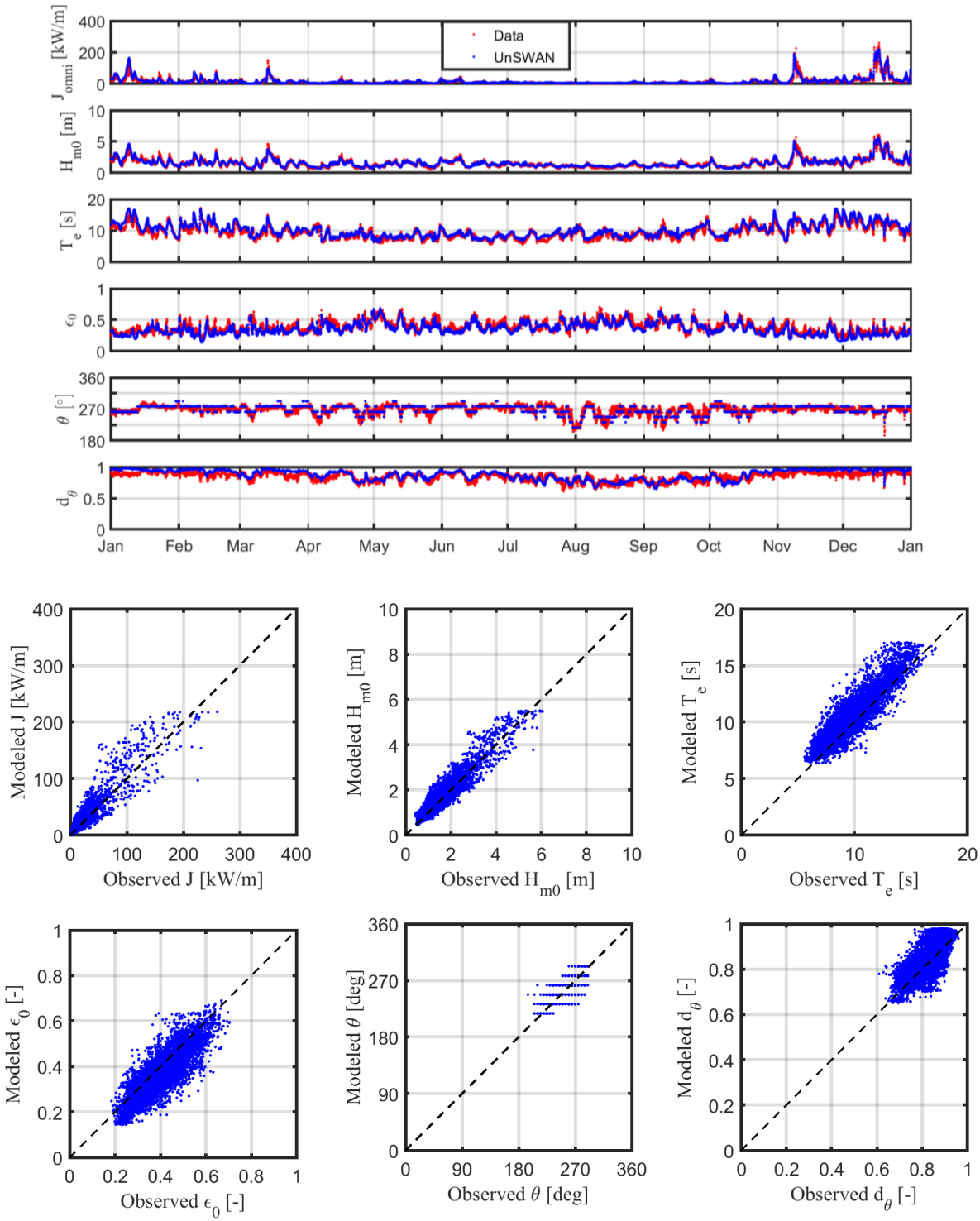

Figure B.92. Comparisons of time series (top) and scatter plots (bottom) of UnSWAN simulated six IEC parameters with observed data at CDIP Buoy 46215 for 2002.

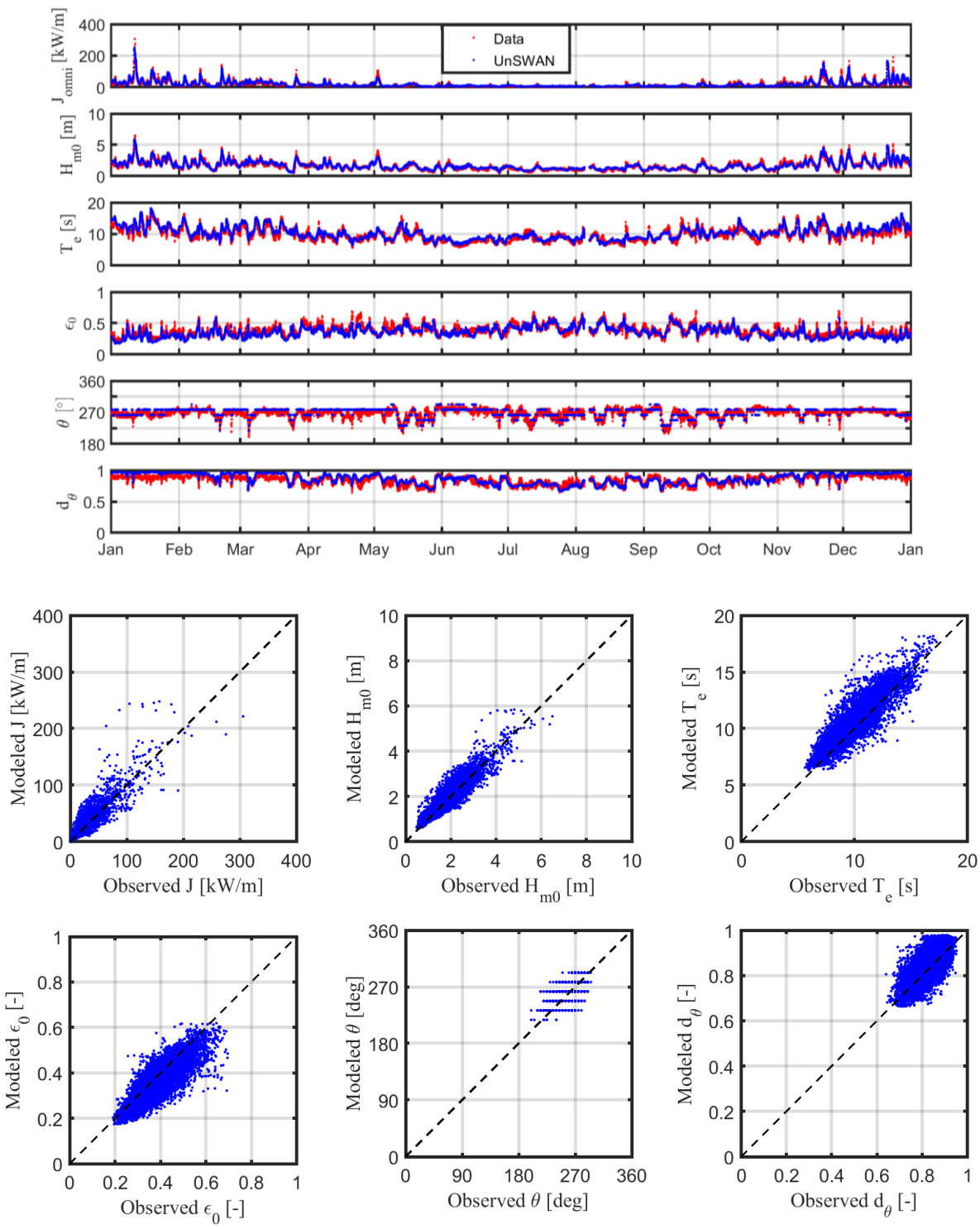

Figure B.93. Comparisons of time series (top) and scatter plots (bottom) of UnSWAN simulated six IEC parameters with observed data at CDIP Buoy 46215 for 2001.

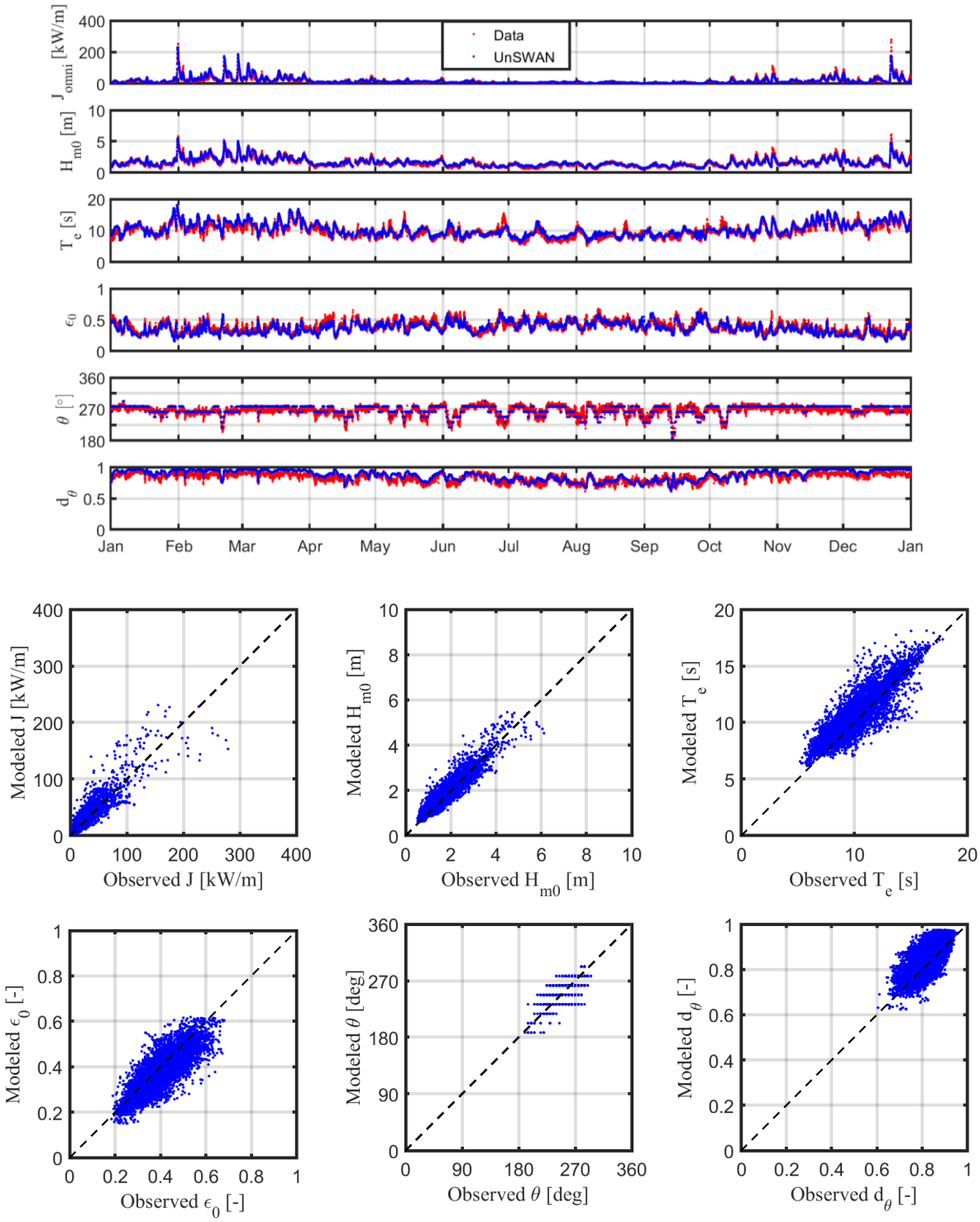

Figure B.94. Comparisons of time series (top) and scatter plots (bottom) of UnSWAN simulated six IEC parameters with observed data at CDIP Buoy 46215 for 2000.

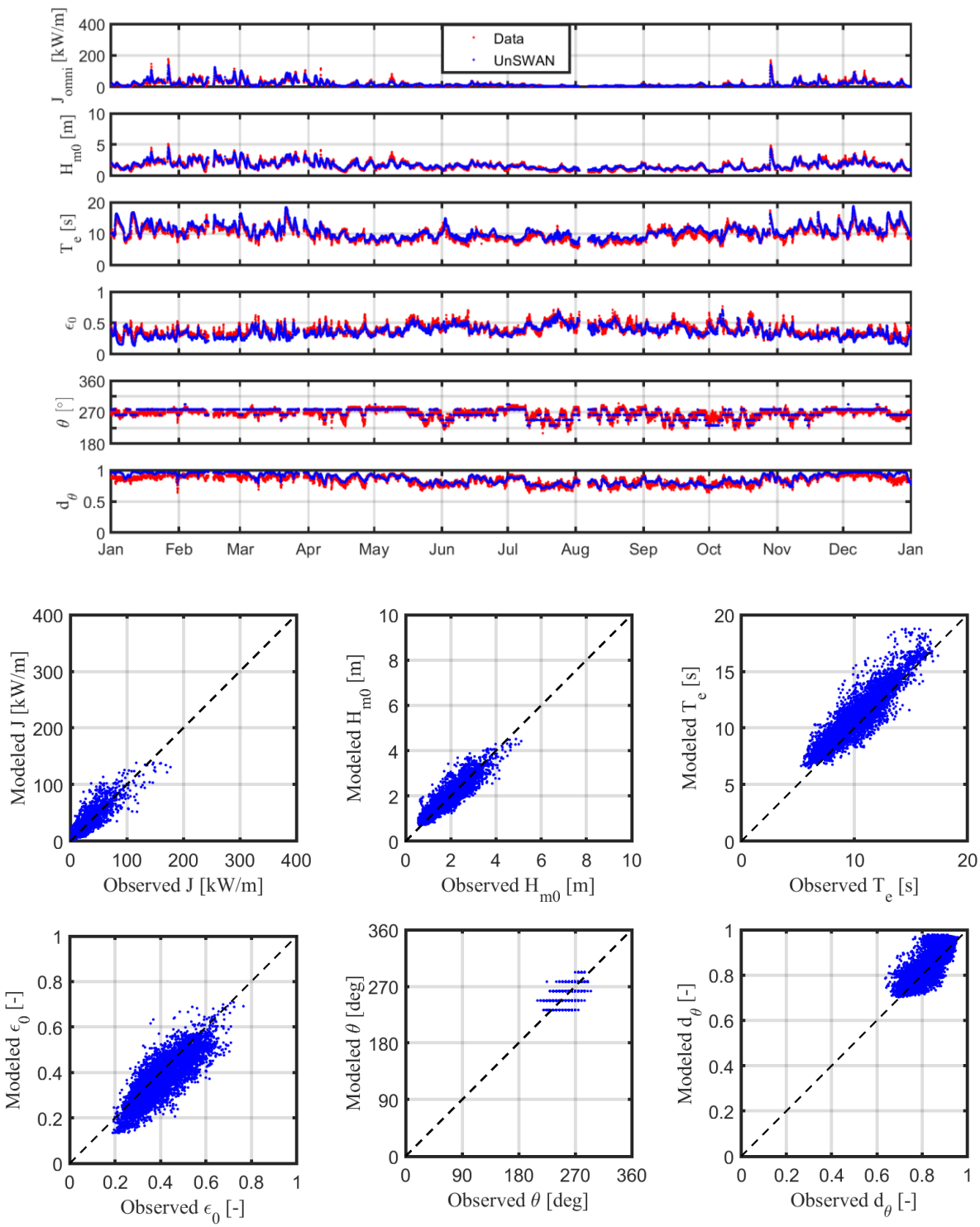

Figure B.95. Comparisons of time series (top) and scatter plots (bottom) of UnSWAN simulated six IEC parameters with observed data at CDIP Buoy 46215 for 1999.

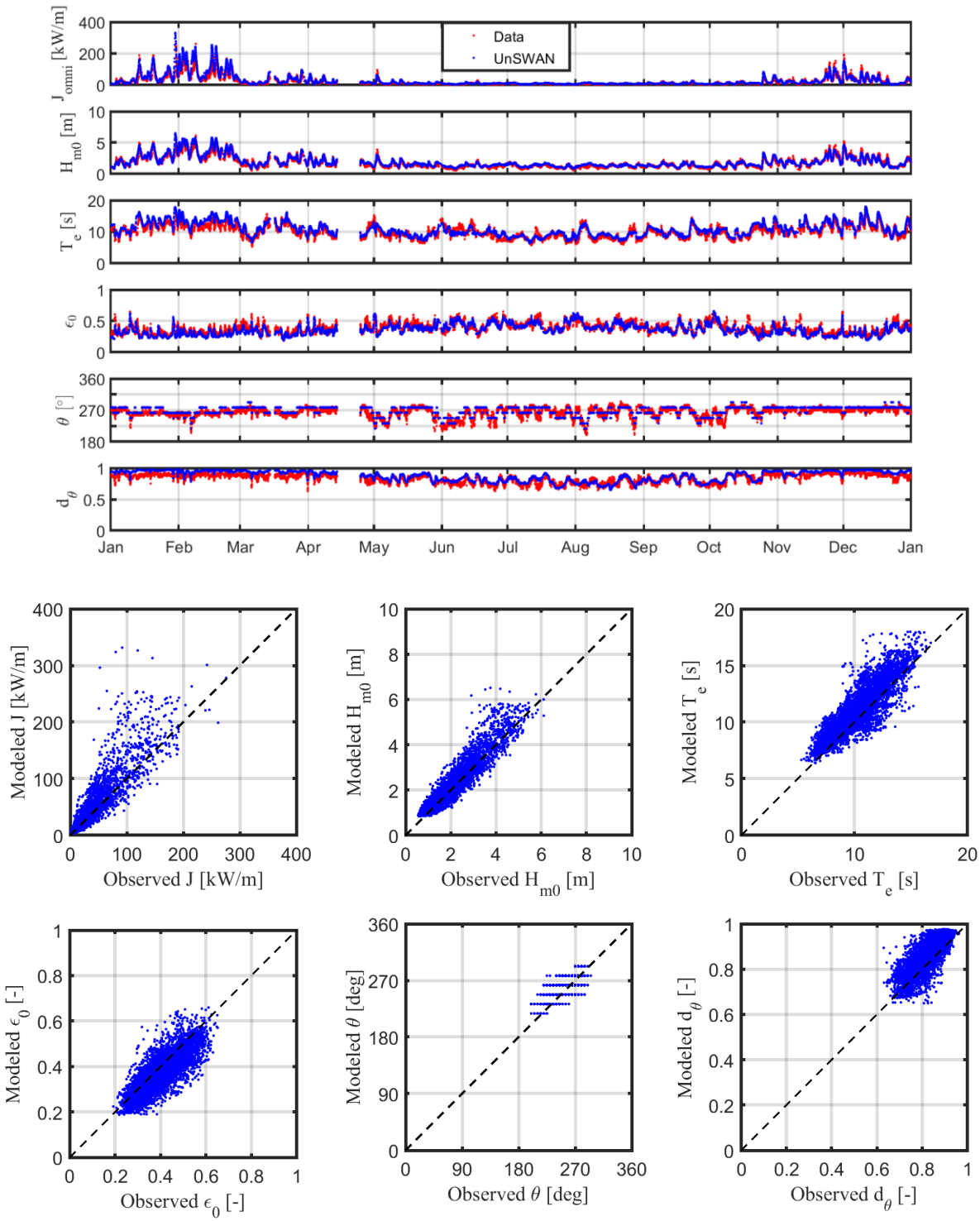

Figure B.96. Comparisons of time series (top) and scatter plots (bottom) of UnSWAN simulated six IEC parameters with observed data at CDIP Buoy 46215 for 1998.

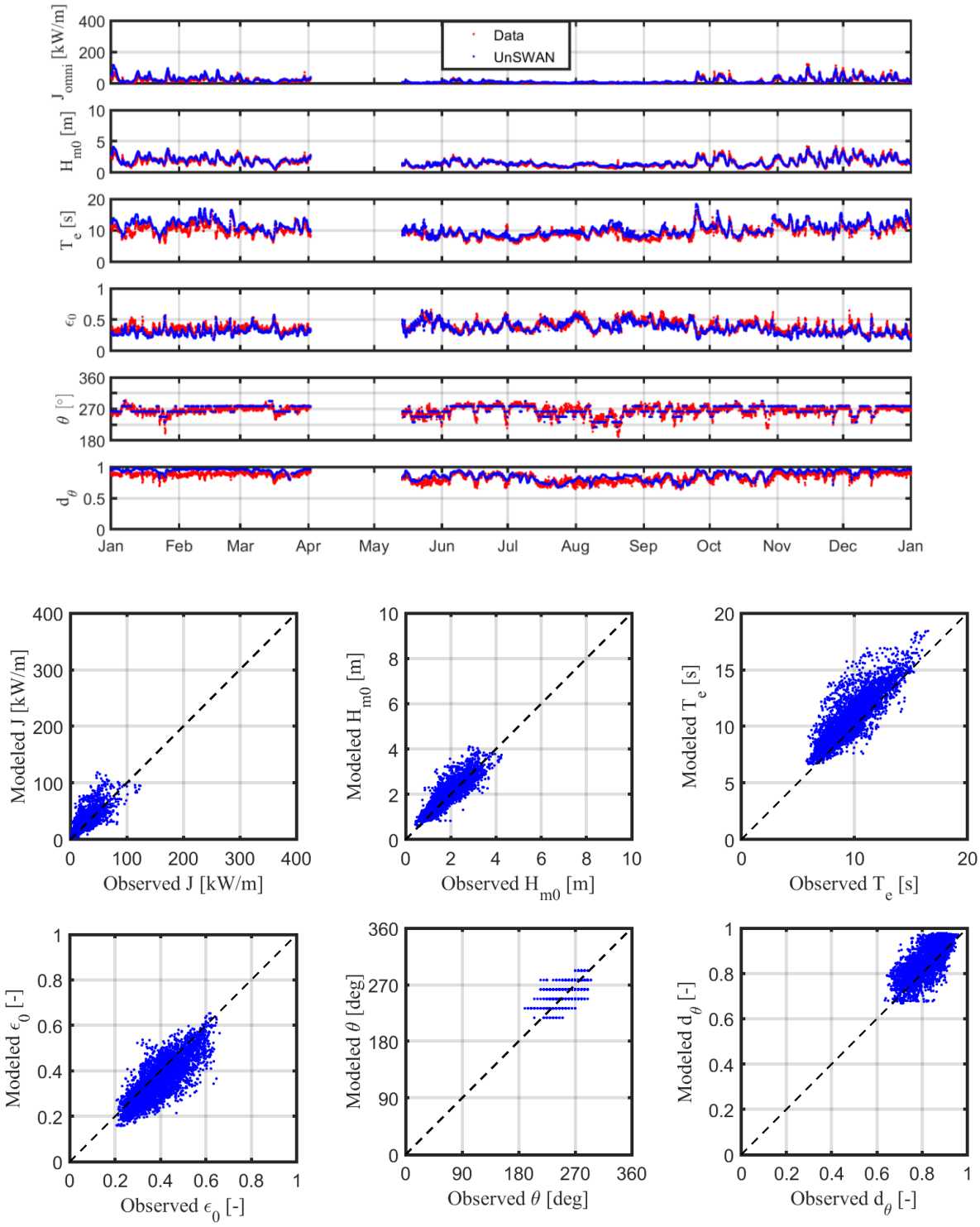

Figure B.97. Comparisons of time series (top) and scatter plots (bottom) of UnSWAN simulated six IEC parameters with observed data at CDIP Buoy 46215 for 1997.

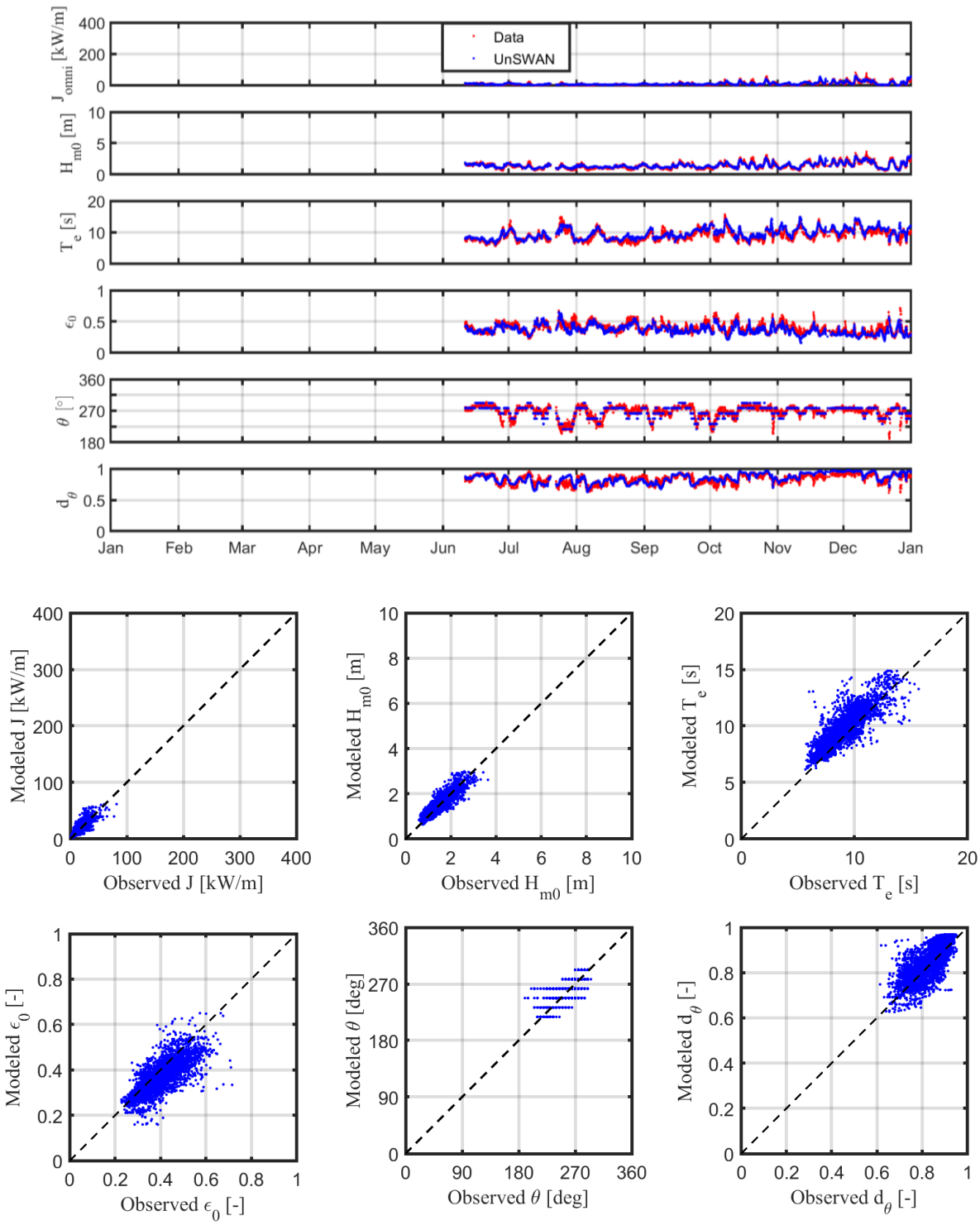

Figure B.98. Comparisons of time series (top) and scatter plots (bottom) of UnSWAN simulated six IEC parameters with observed data at CDIP Buoy 46215 for 1996.

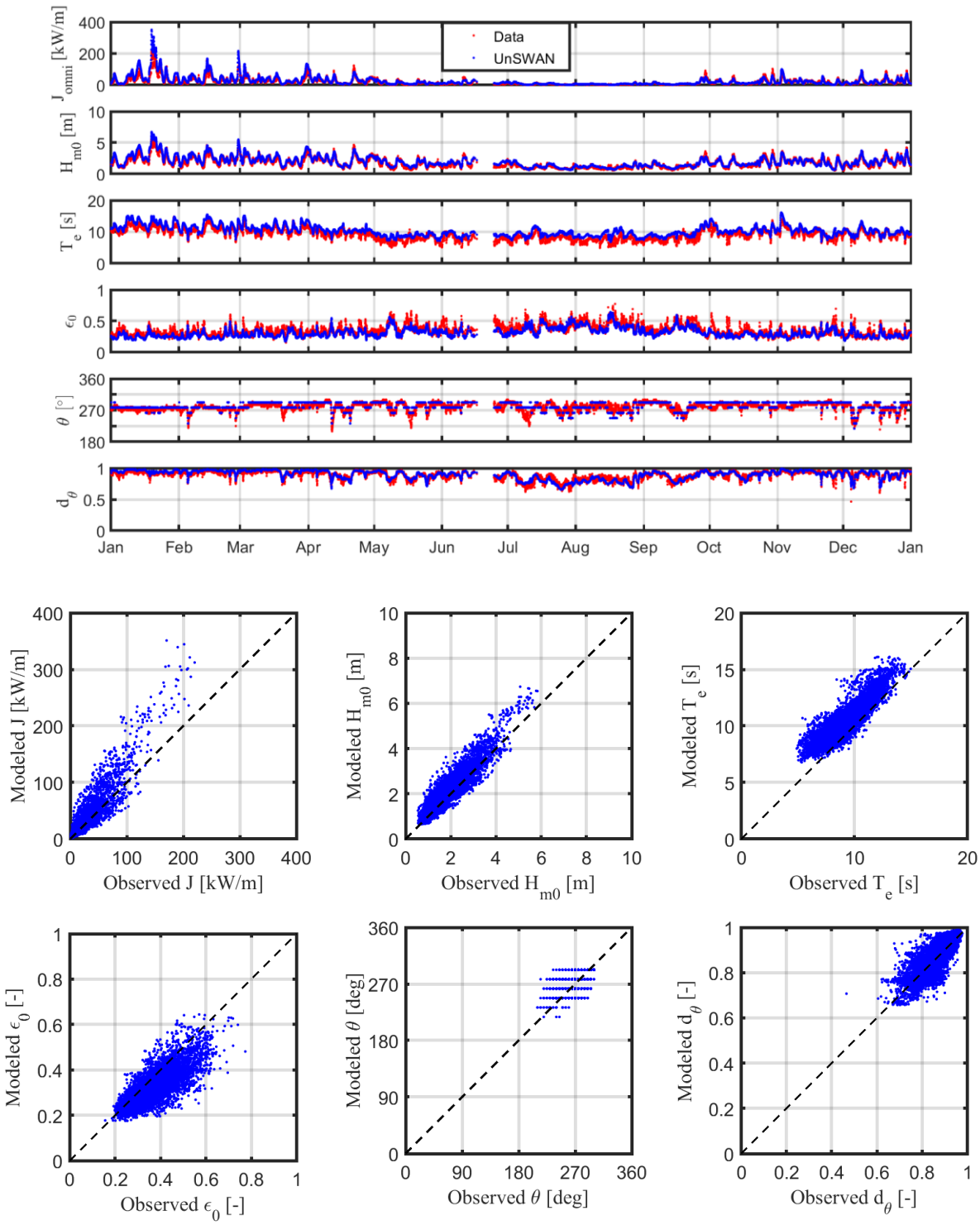

Figure B.99. Comparisons of time series (top) and scatter plots (bottom) of UnSWAN simulated six IEC parameters with observed data at CDIP Buoy 46236 for 2010.

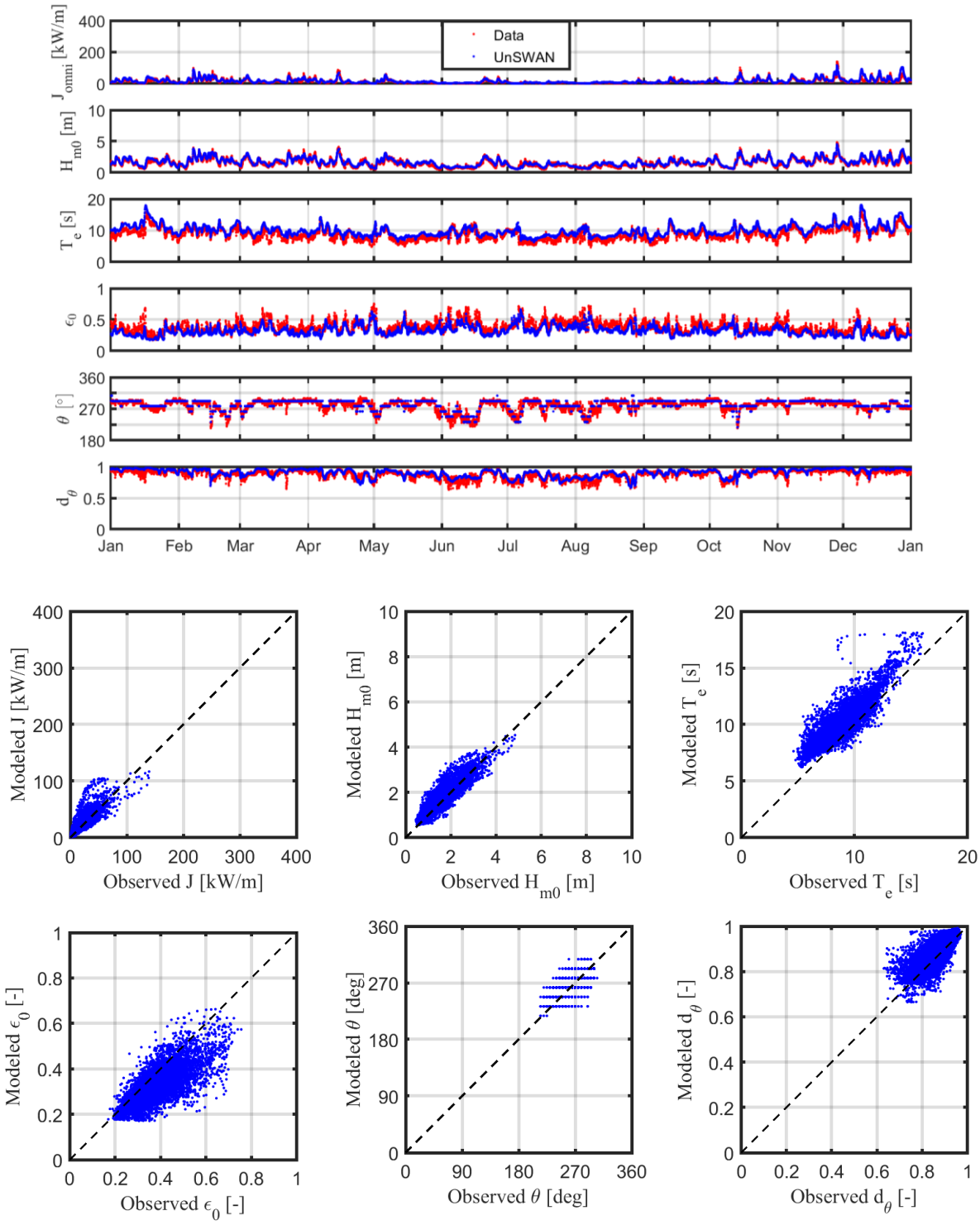

Figure B.100. Comparisons of time series (top) and scatter plots (bottom) of UnSWAN simulated six IEC parameters with observed data at CDIP Buoy 46236 for 2009.

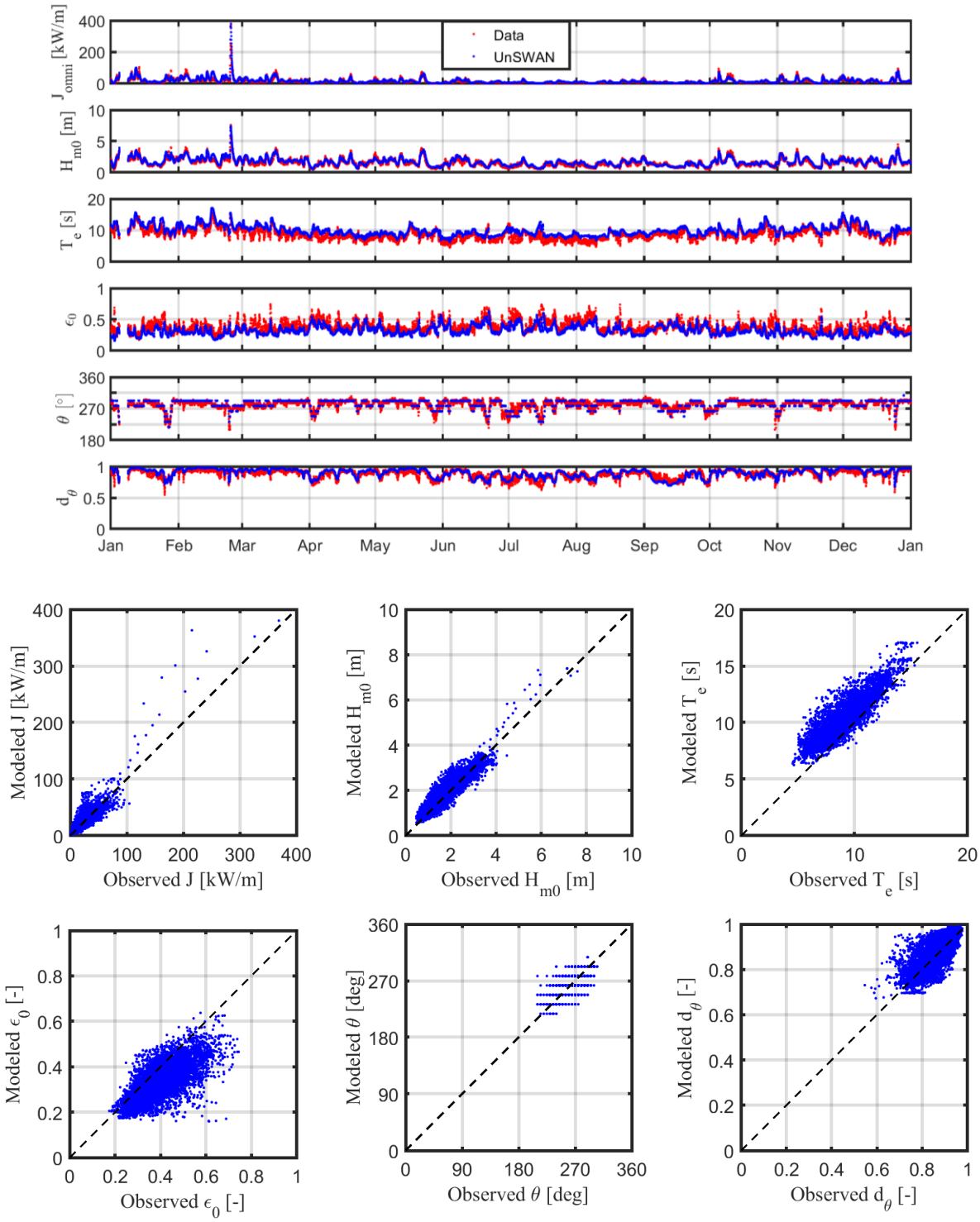

Figure B.101. Comparisons of time series (top) and scatter plots (bottom) of UnSWAN simulated six IEC parameters with observed data at CDIP Buoy 46236 for 2008.

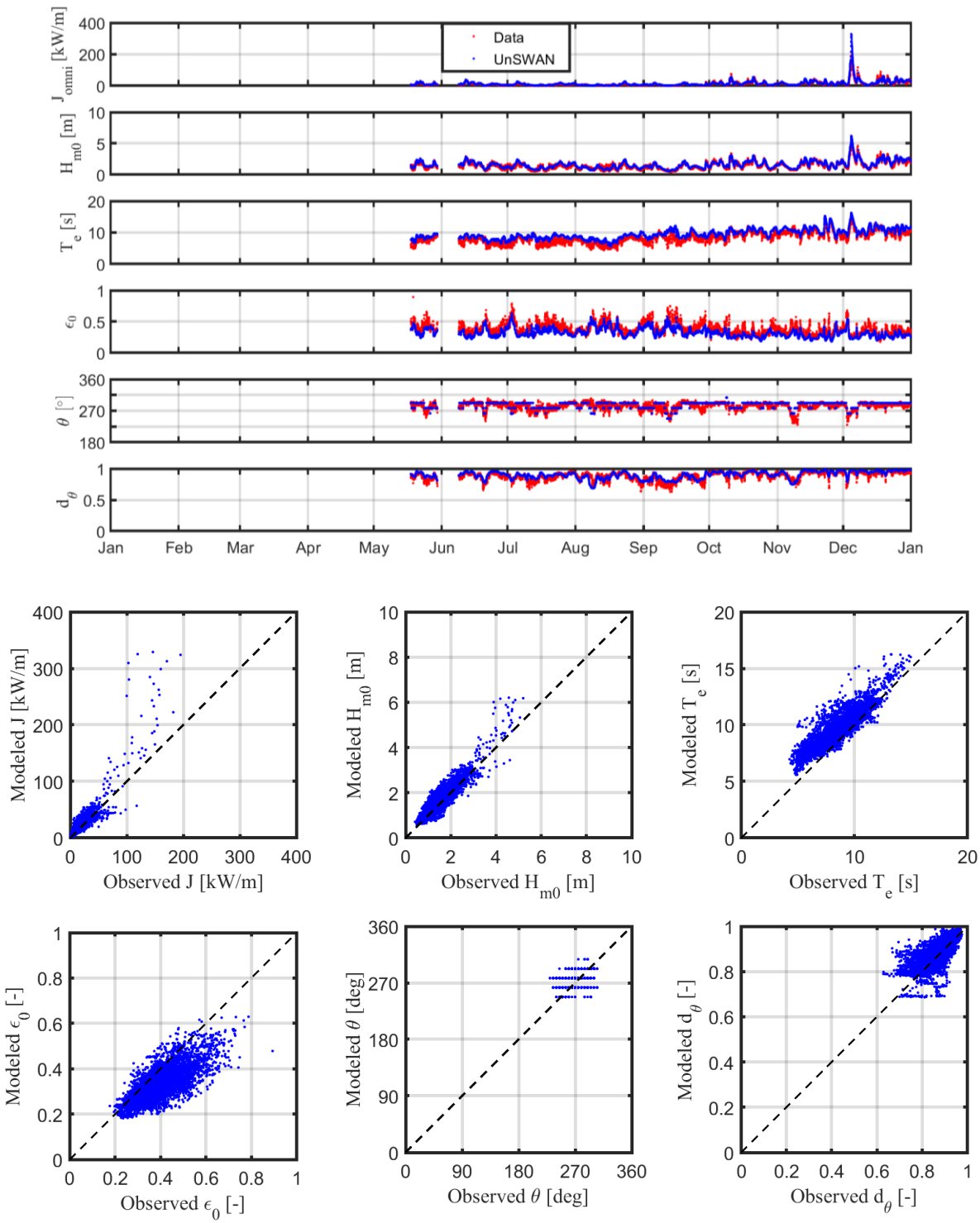

Figure B.102. Comparisons of time series (top) and scatter plots (bottom) of UnSWAN simulated six IEC parameters with observed data at CDIP Buoy 46236 for 2007.

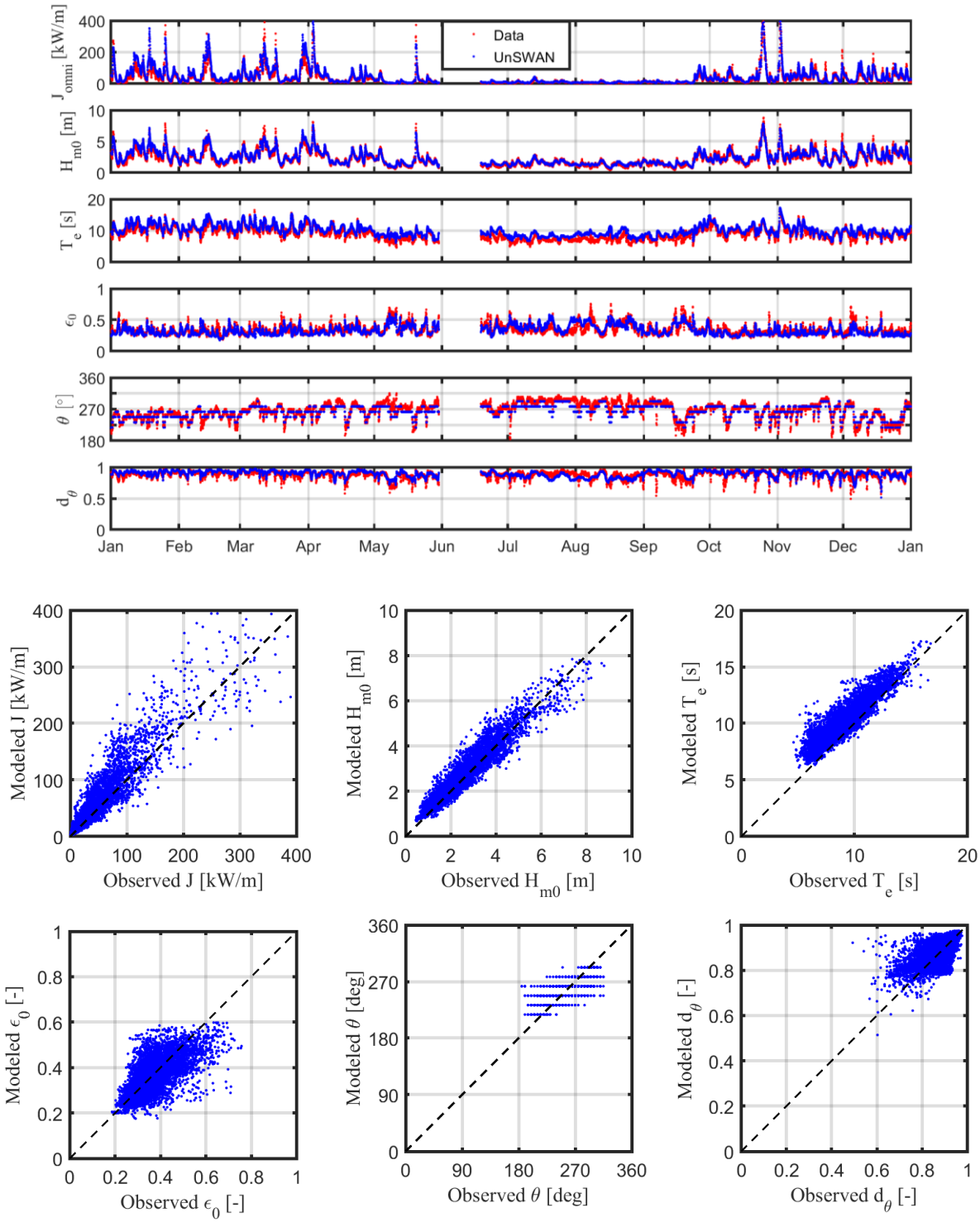

Figure B.103. Comparisons of time series (top) and scatter plots (bottom) of UnSWAN simulated six IEC parameters with observed data at CDIP Buoy 46211 for 2010.

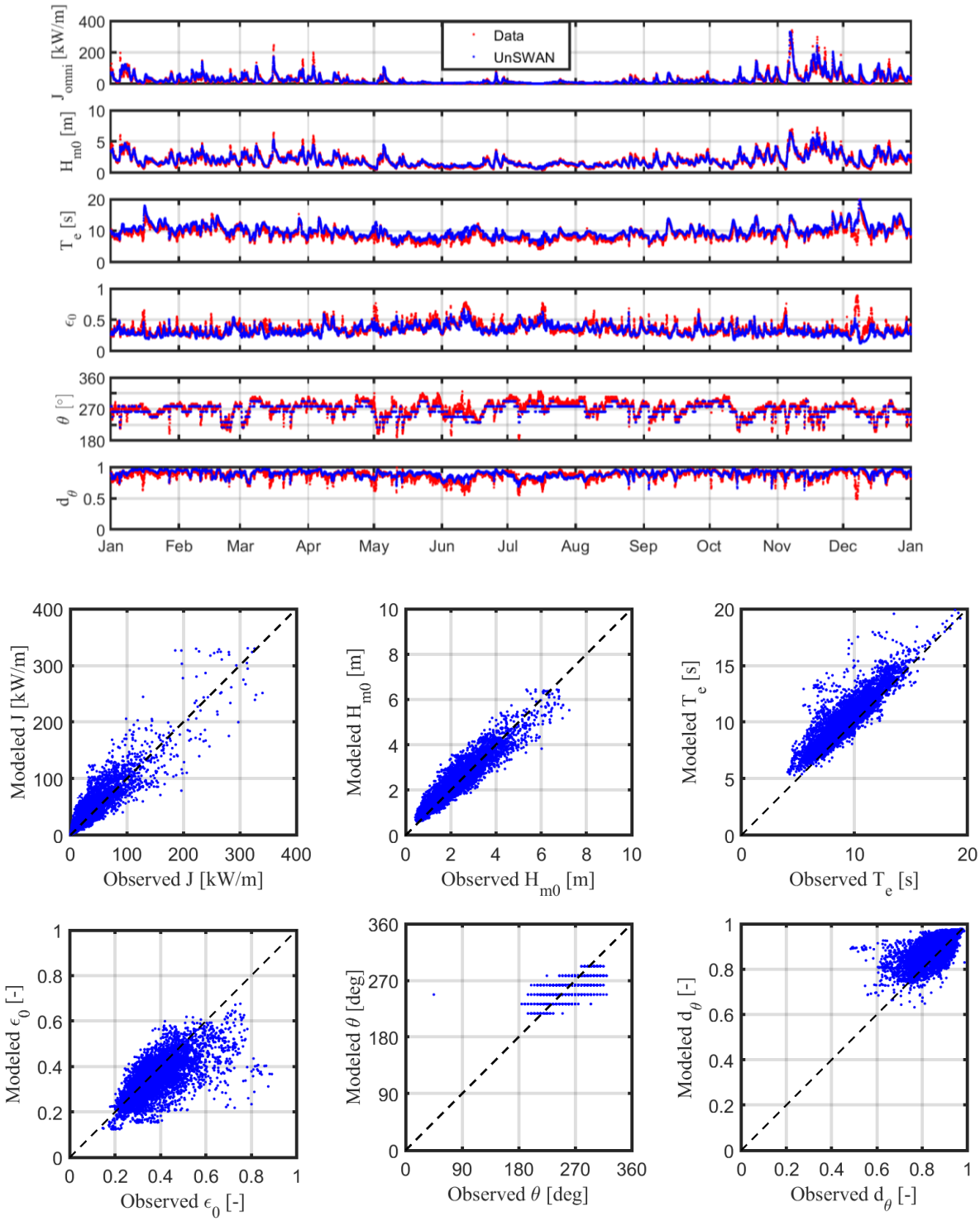

Figure B.104. Comparisons of time series (top) and scatter plots (bottom) of UnSWAN simulated six IEC parameters with observed data at CDIP Buoy 46211 for 2009.

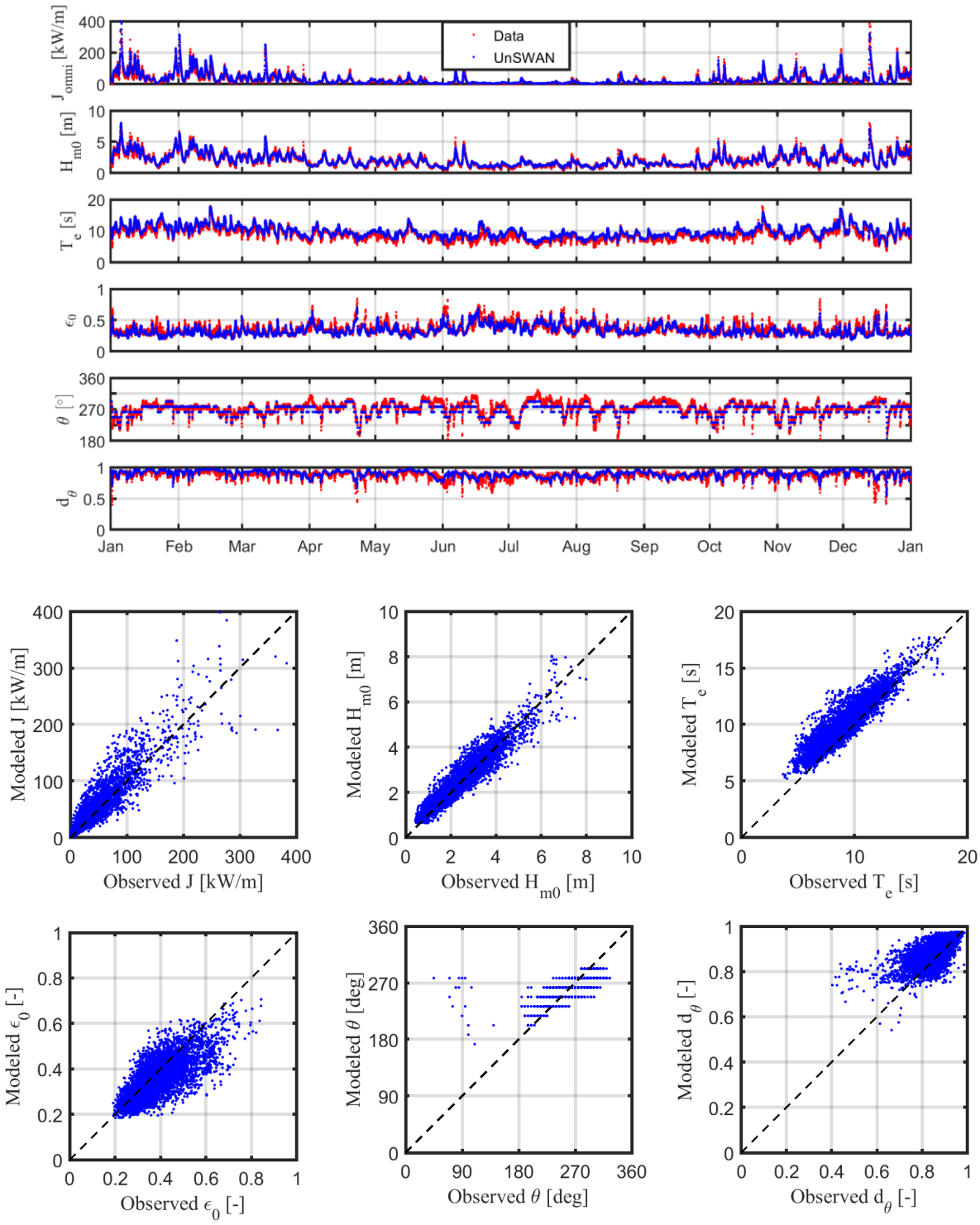

Figure B.105. Comparisons of time series (top) and scatter plots (bottom) of UnSWAN simulated six IEC parameters with observed data at CDIP Buoy 46211 for 2008.

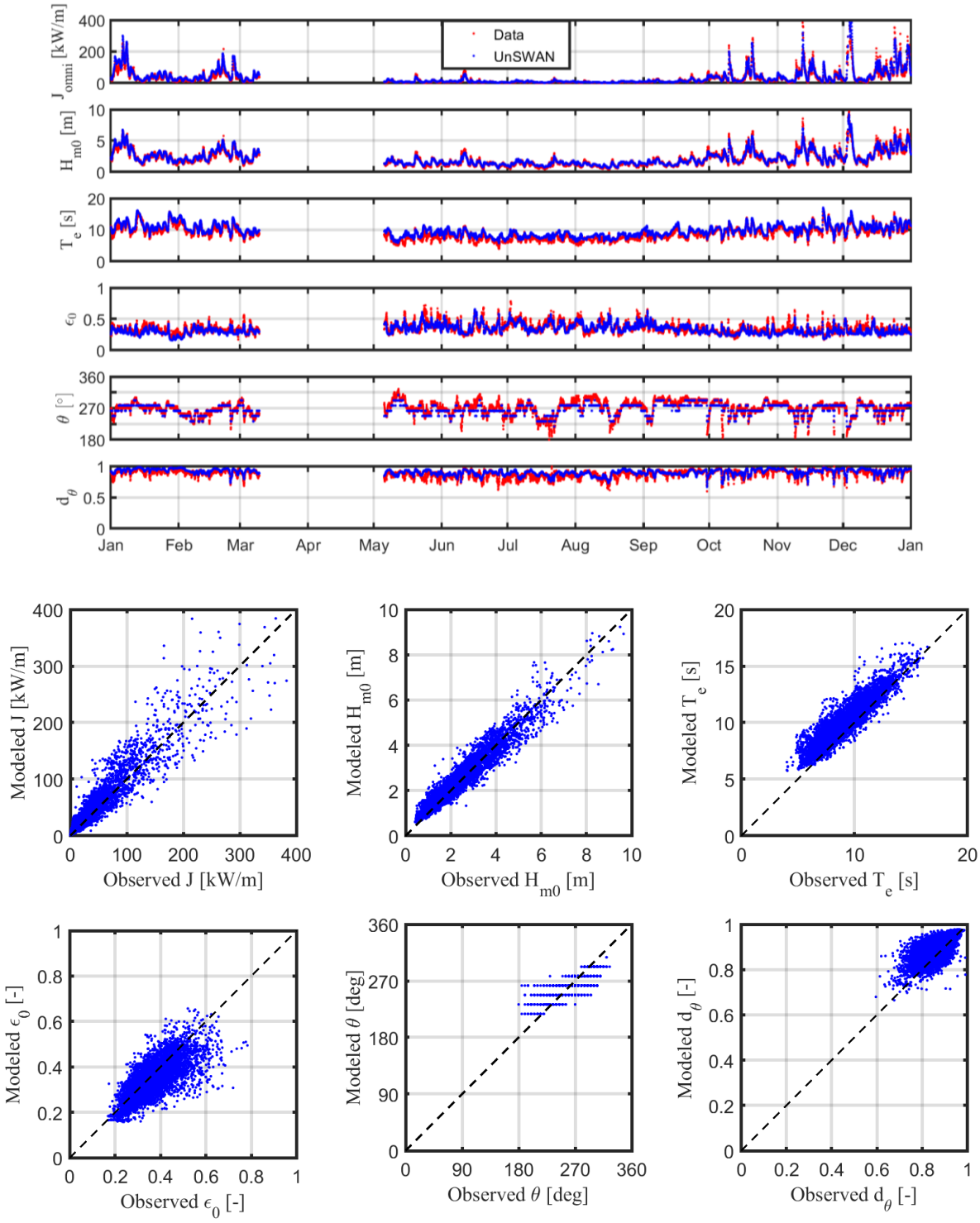

Figure B.106. Comparisons of time series (top) and scatter plots (bottom) of UnSWAN simulated six IEC parameters with observed data at CDIP Buoy 46211 for 2007.

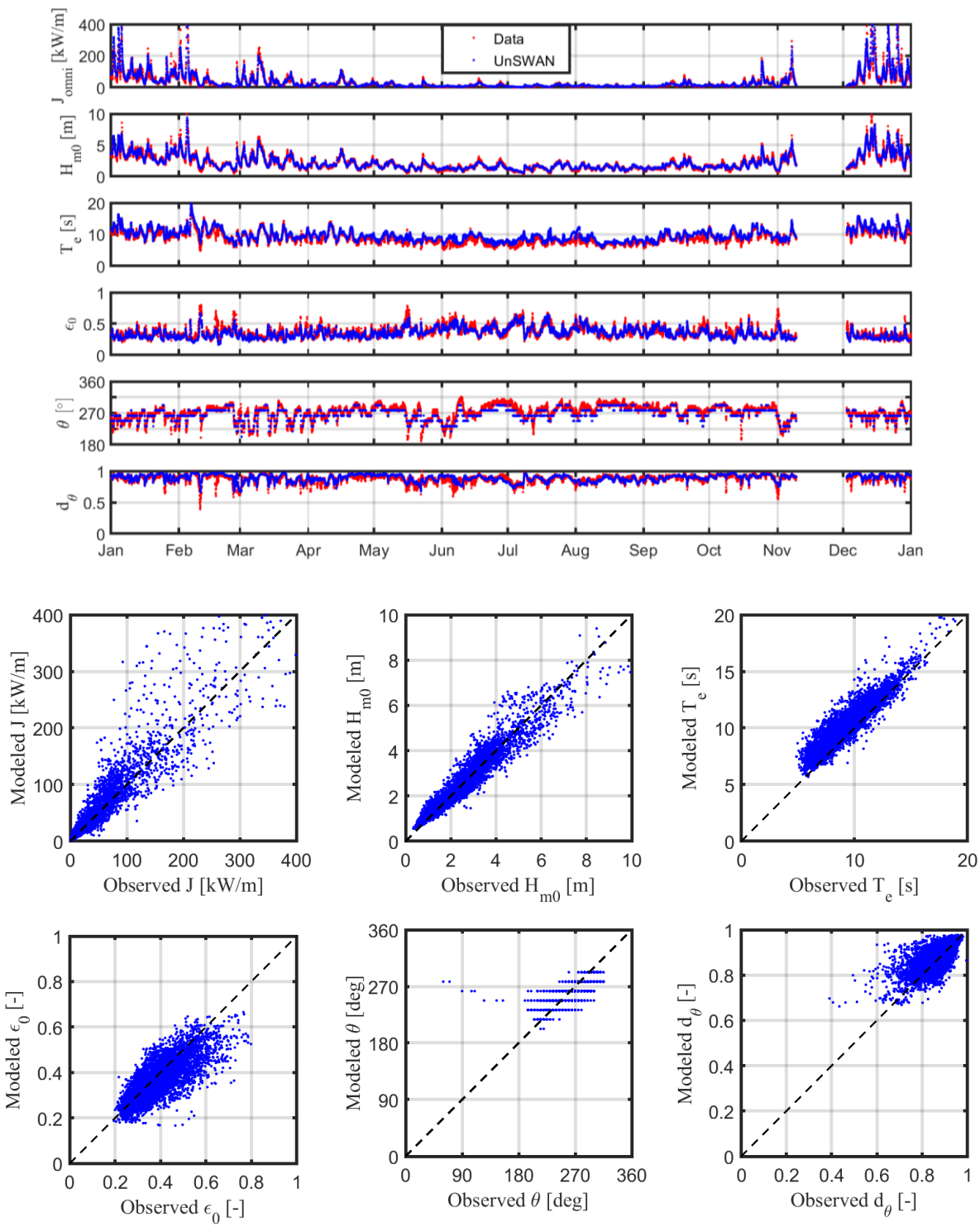

Figure B.107. Comparisons of time series (top) and scatter plots (bottom) of UnSWAN simulated six IEC parameters with observed data at CDIP Buoy 46211 for 2006.

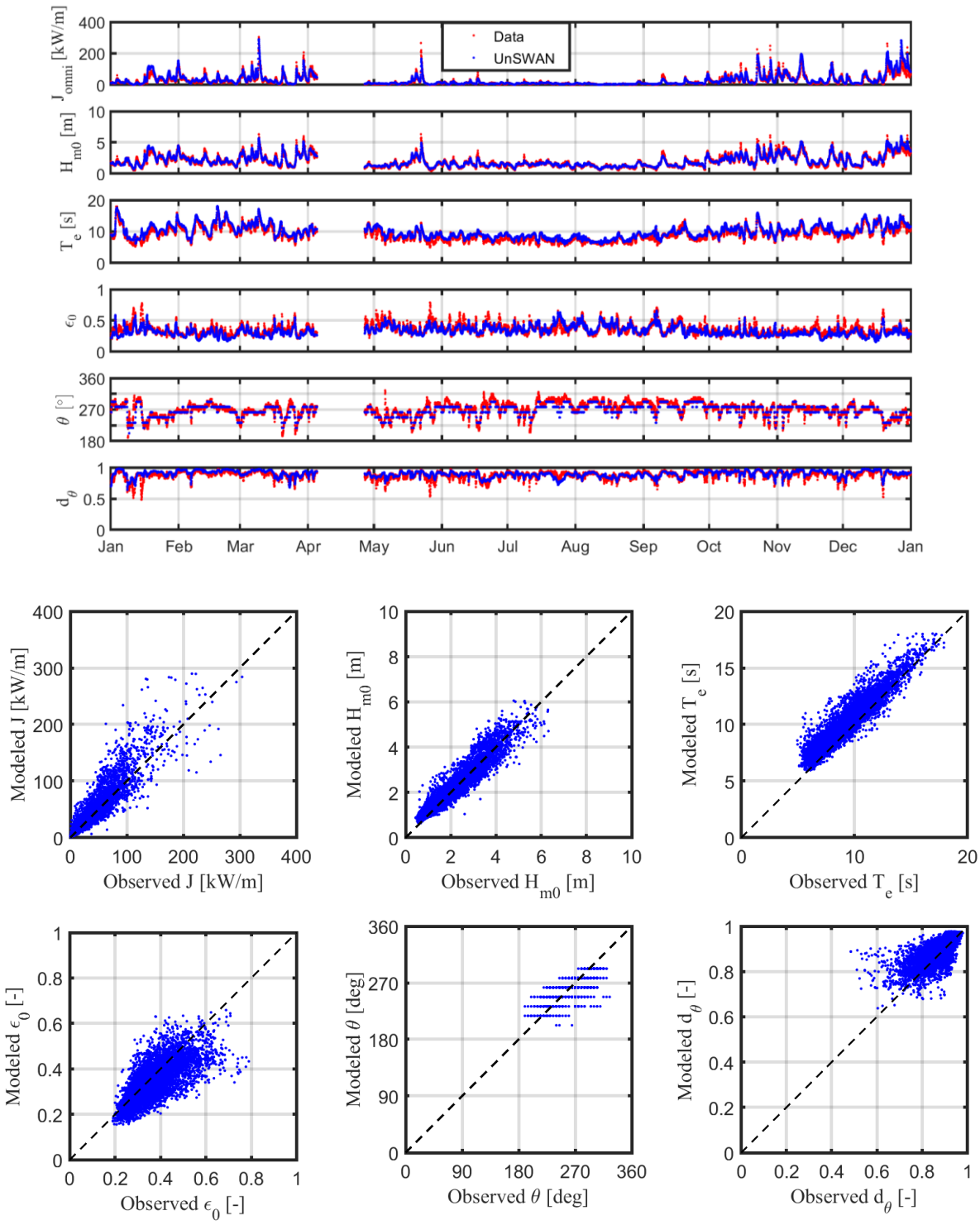

Figure B.108. Comparisons of time series (top) and scatter plots (bottom) of UnSWAN simulated six IEC parameters with observed data at CDIP Buoy 46211 for 2005.

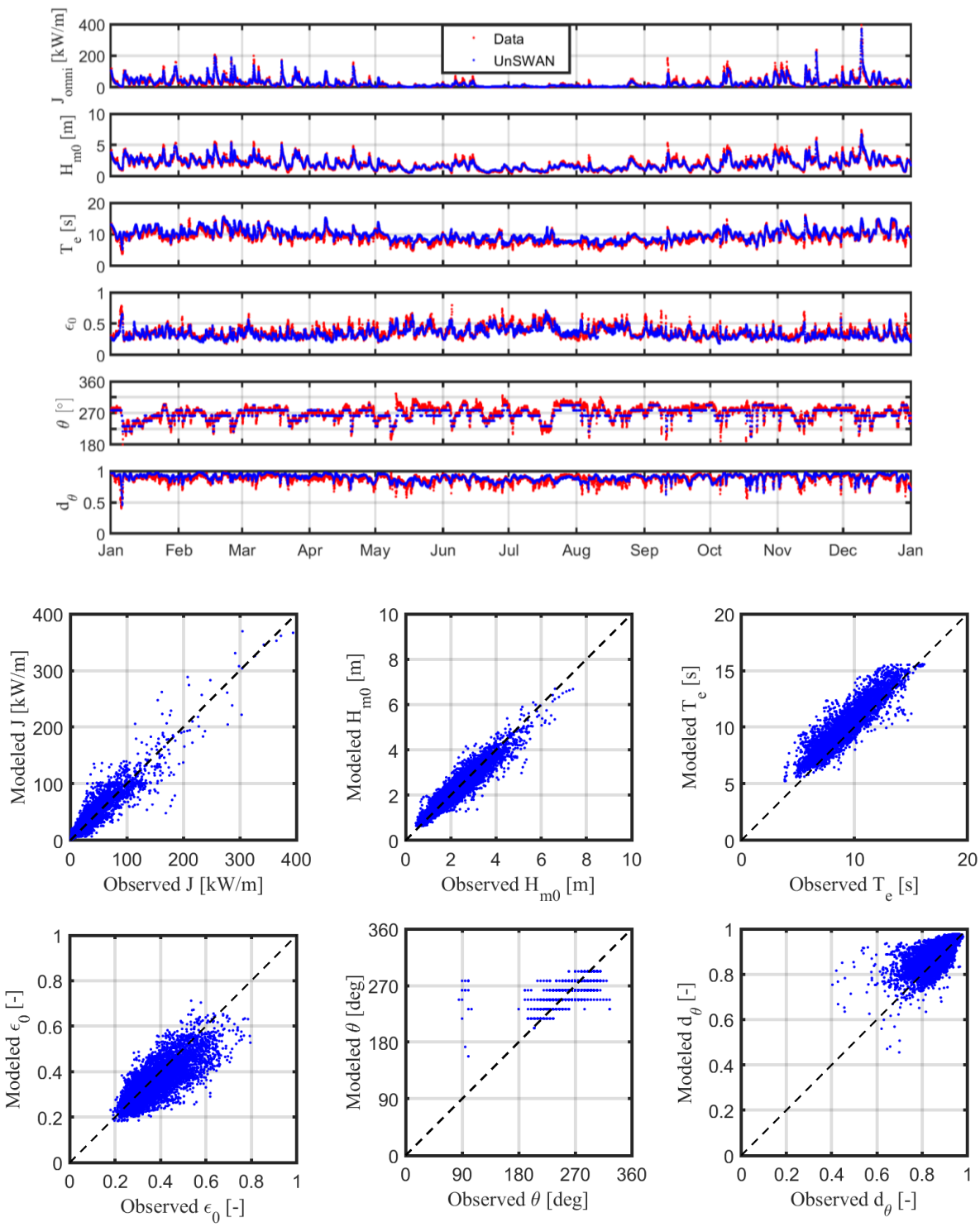

Figure B.109. Comparisons of time series (top) and scatter plots (bottom) of UnSWAN simulated six IEC parameters with observed data at CDIP Buoy 46211 for 2004.

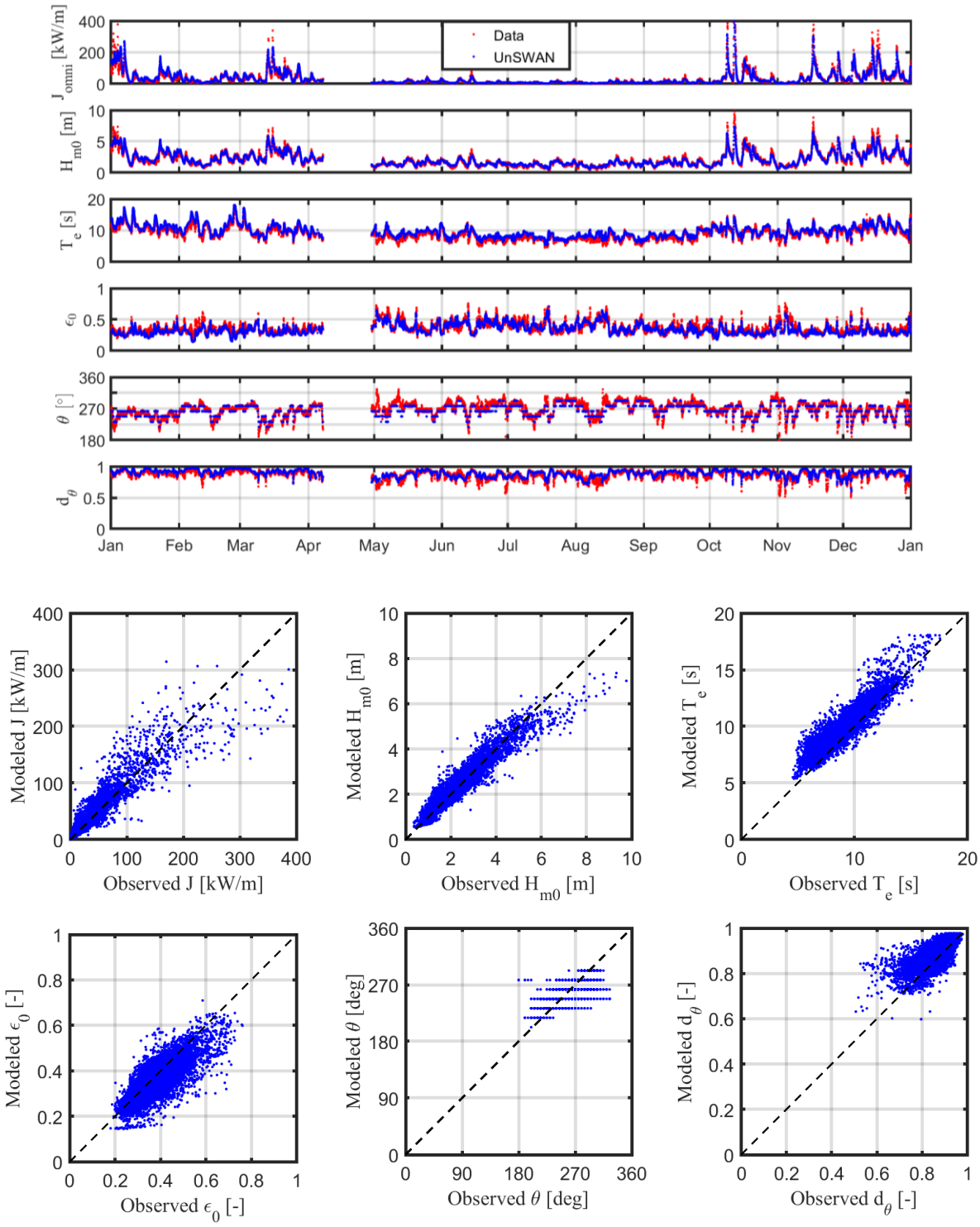

Figure B.110. Comparisons of time series (top) and scatter plots (bottom) of UnSWAN simulated six IEC parameters with observed data at CDIP Buoy 46211 for 2003.

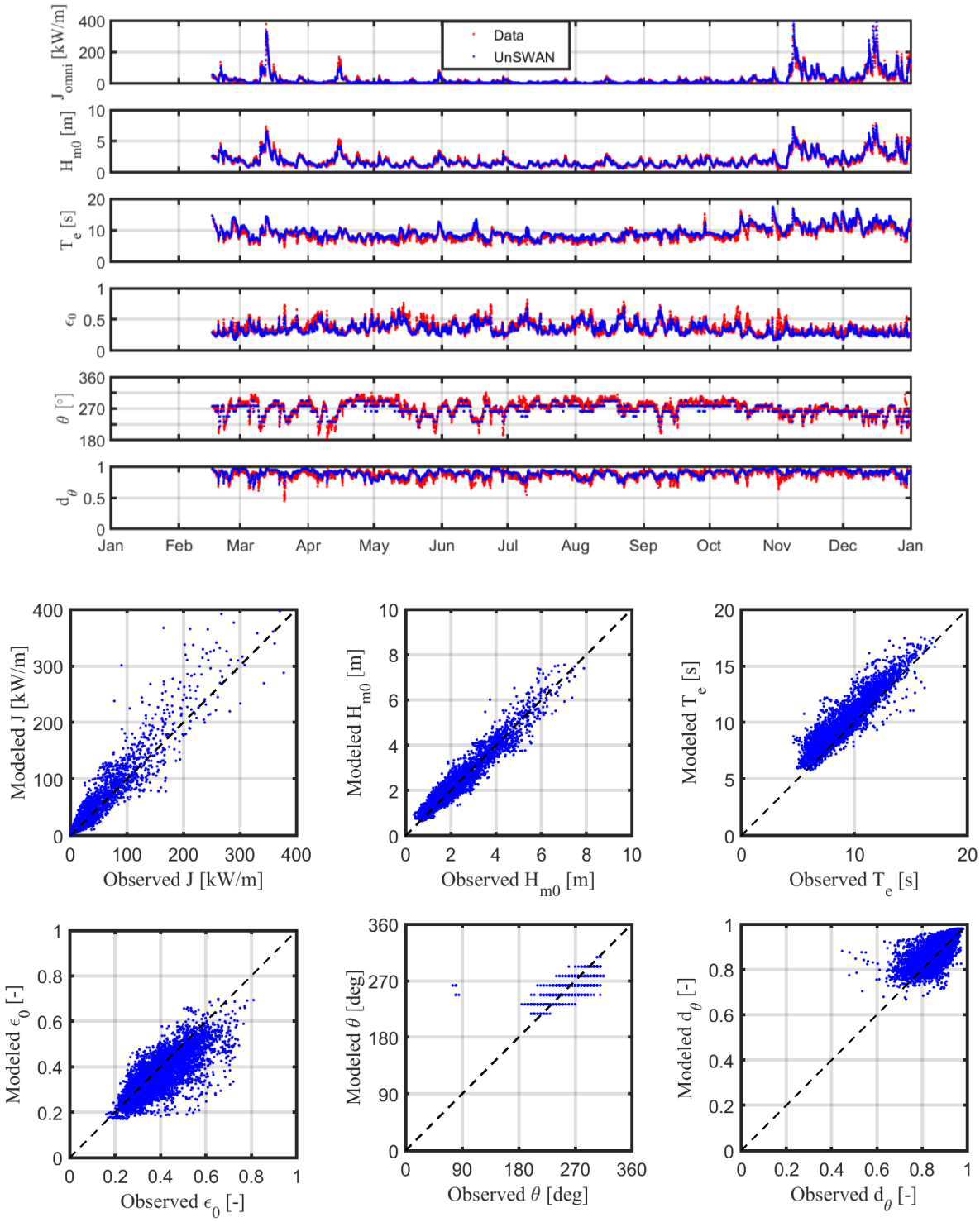

Figure B.111. Comparisons of time series (top) and scatter plots (bottom) of UnSWAN simulated six IEC parameters with observed data at CDIP Buoy 46211 for 2002.

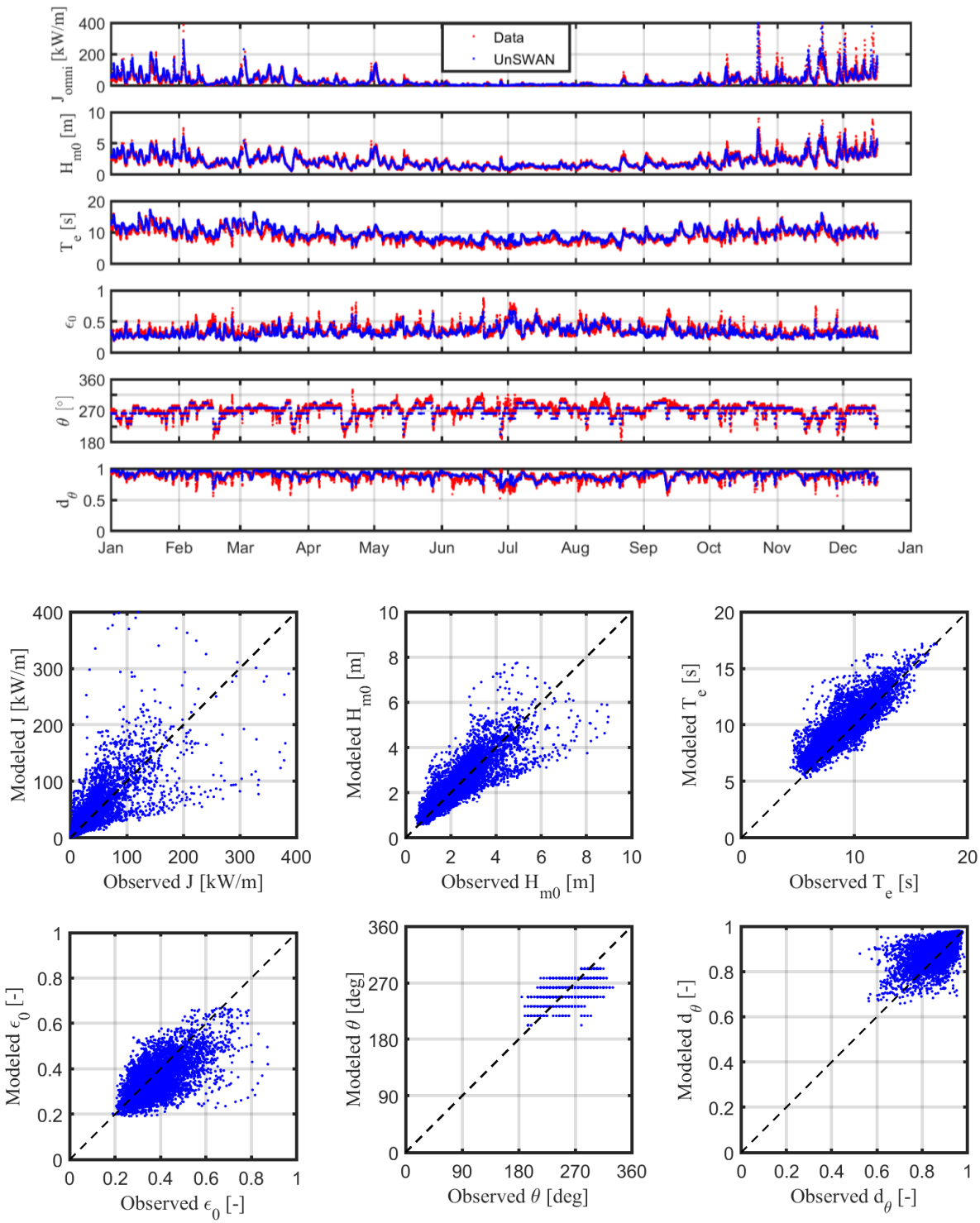

Figure B.112. Comparisons of time series (top) and scatter plots (bottom) of UnSWAN simulated six IEC parameters with observed data at CDIP Buoy 46211 for 2001.

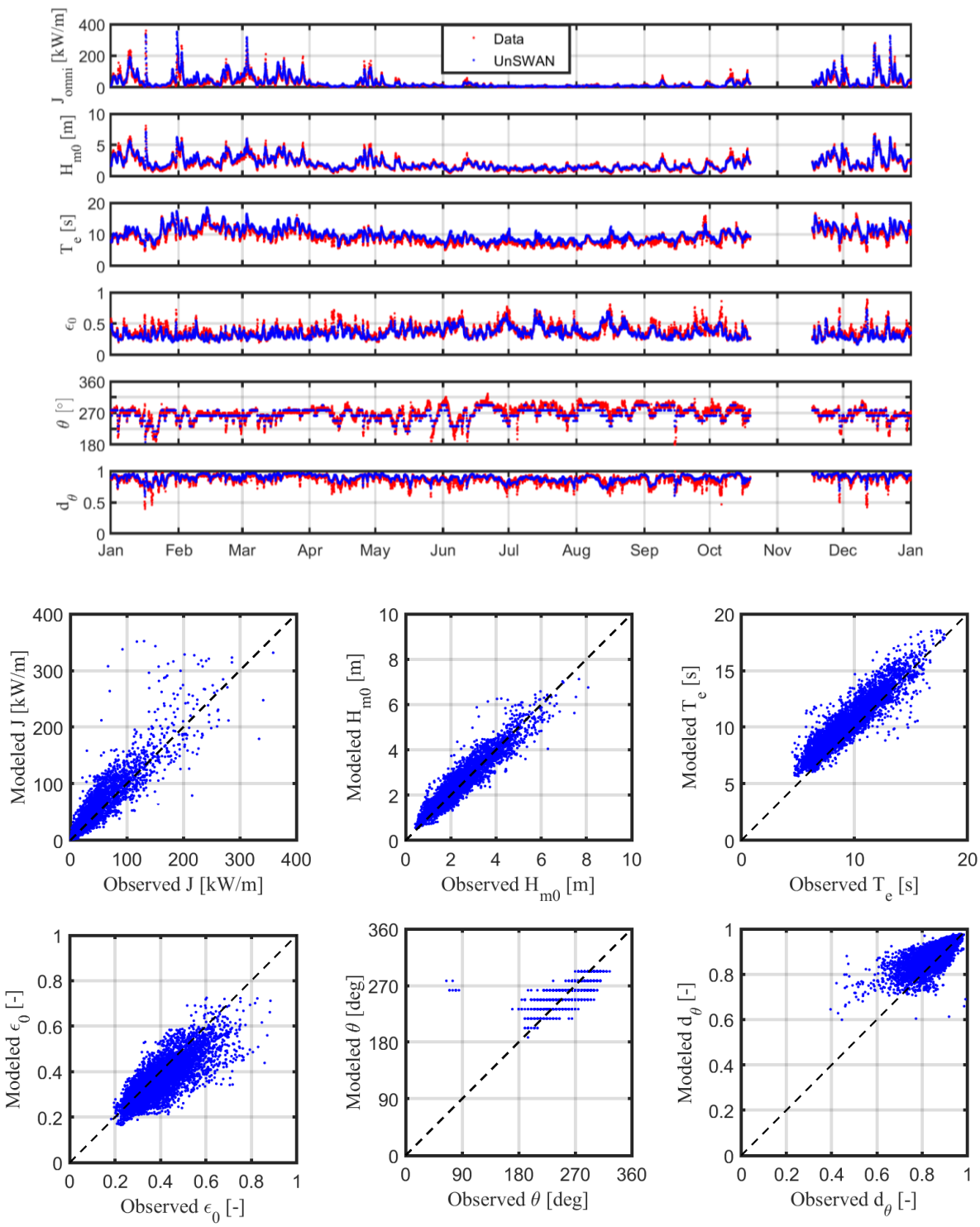

Figure B.113. Comparisons of time series (top) and scatter plots (bottom) of UnSWAN simulated six IEC parameters with observed data at CDIP Buoy 46211 for 2000.

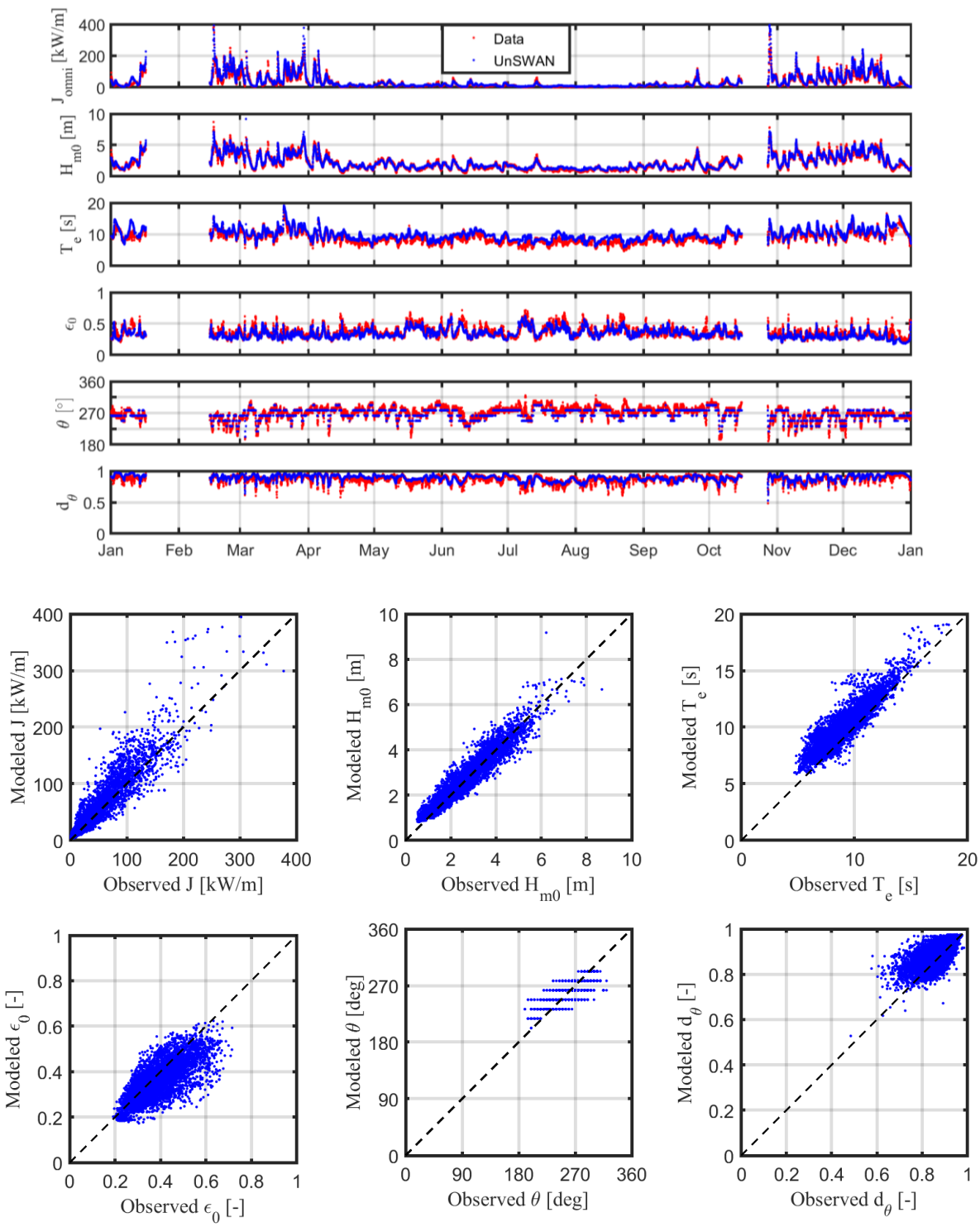

Figure B.114. Comparisons of time series (top) and scatter plots (bottom) of UnSWAN simulated six IEC parameters with observed data at CDIP Buoy 46211 for 1999.

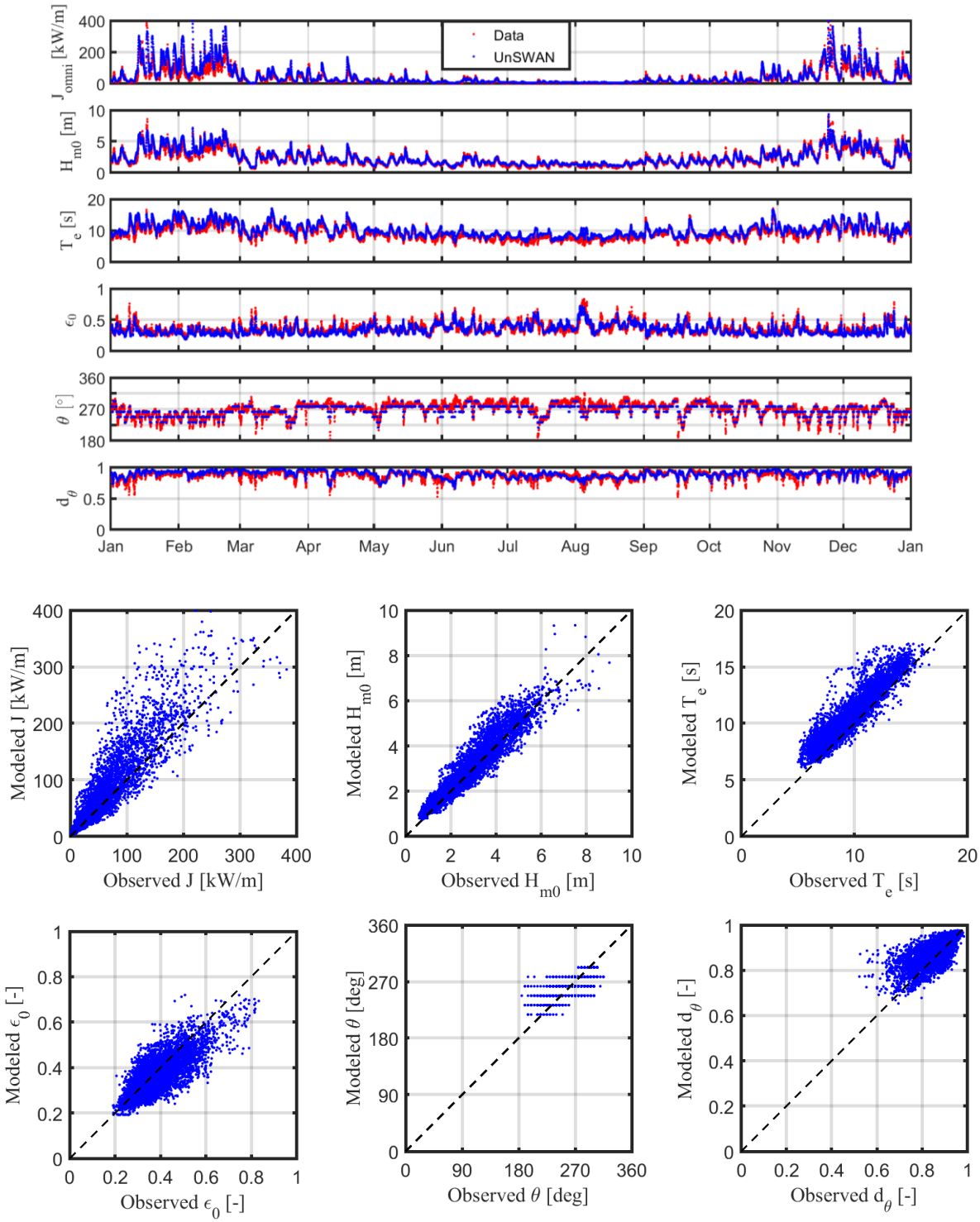

Figure B.115. Comparisons of time series (top) and scatter plots (bottom) of UnSWAN simulated six IEC parameters with observed data at CDIP Buoy 46211 for 1998.

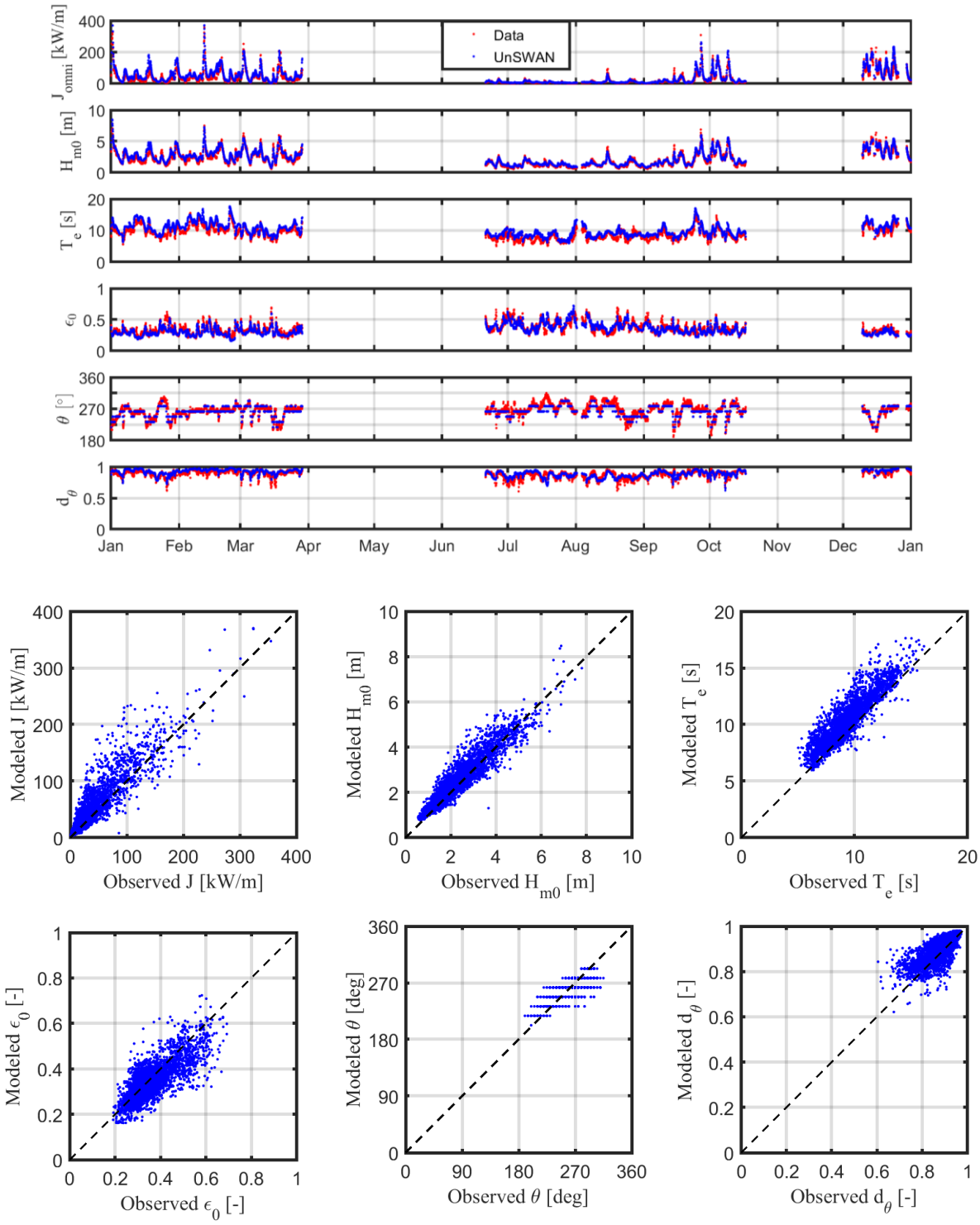

Figure B.116. Comparisons of time series (top) and scatter plots (bottom) of UnSWAN simulated six IEC parameters with observed data at CDIP Buoy 46211 for 1997.

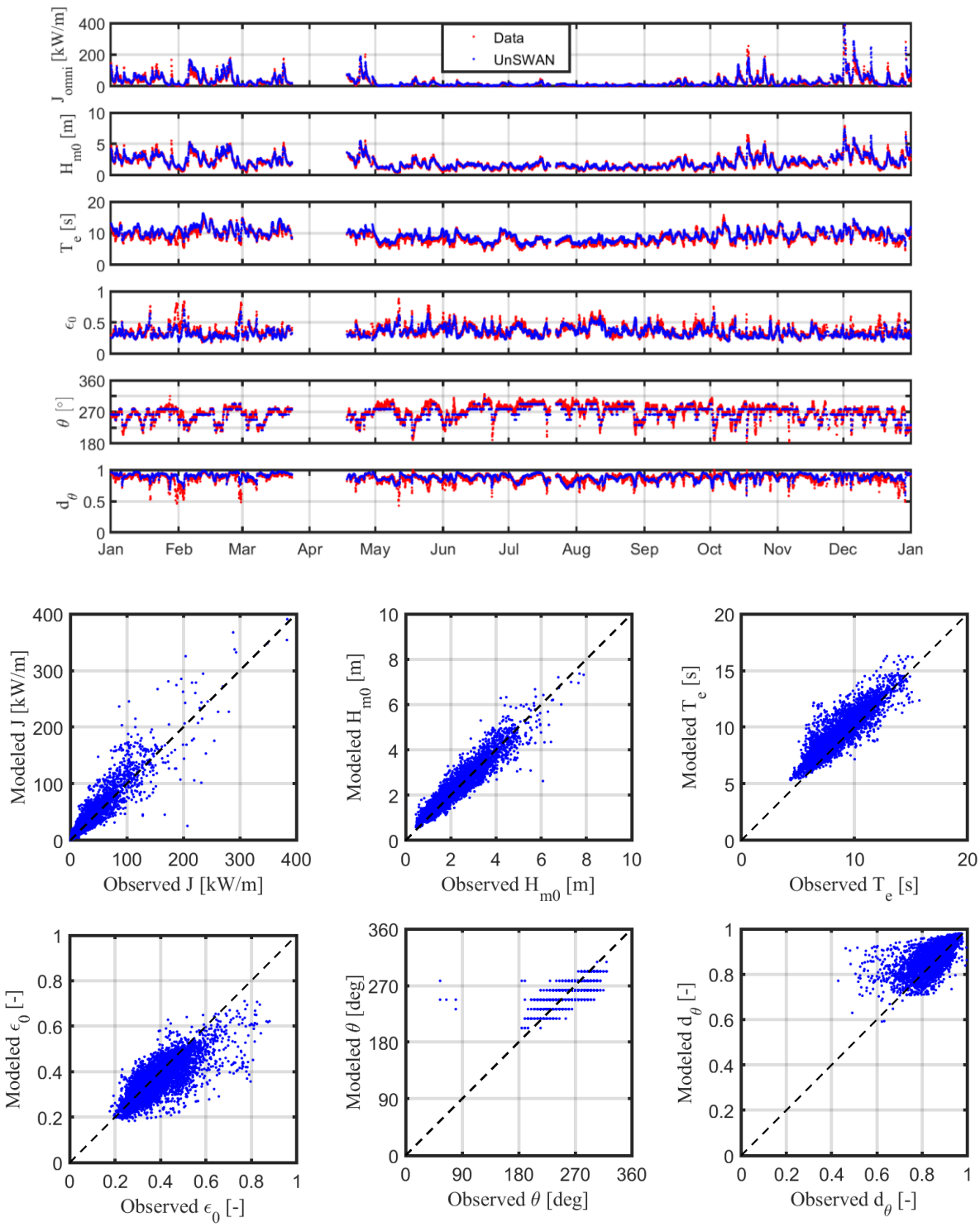

Figure B.117. Comparisons of time series (top) and scatter plots (bottom) of UnSWAN simulated six IEC parameters with observed data at CDIP Buoy 46211 for 1996.

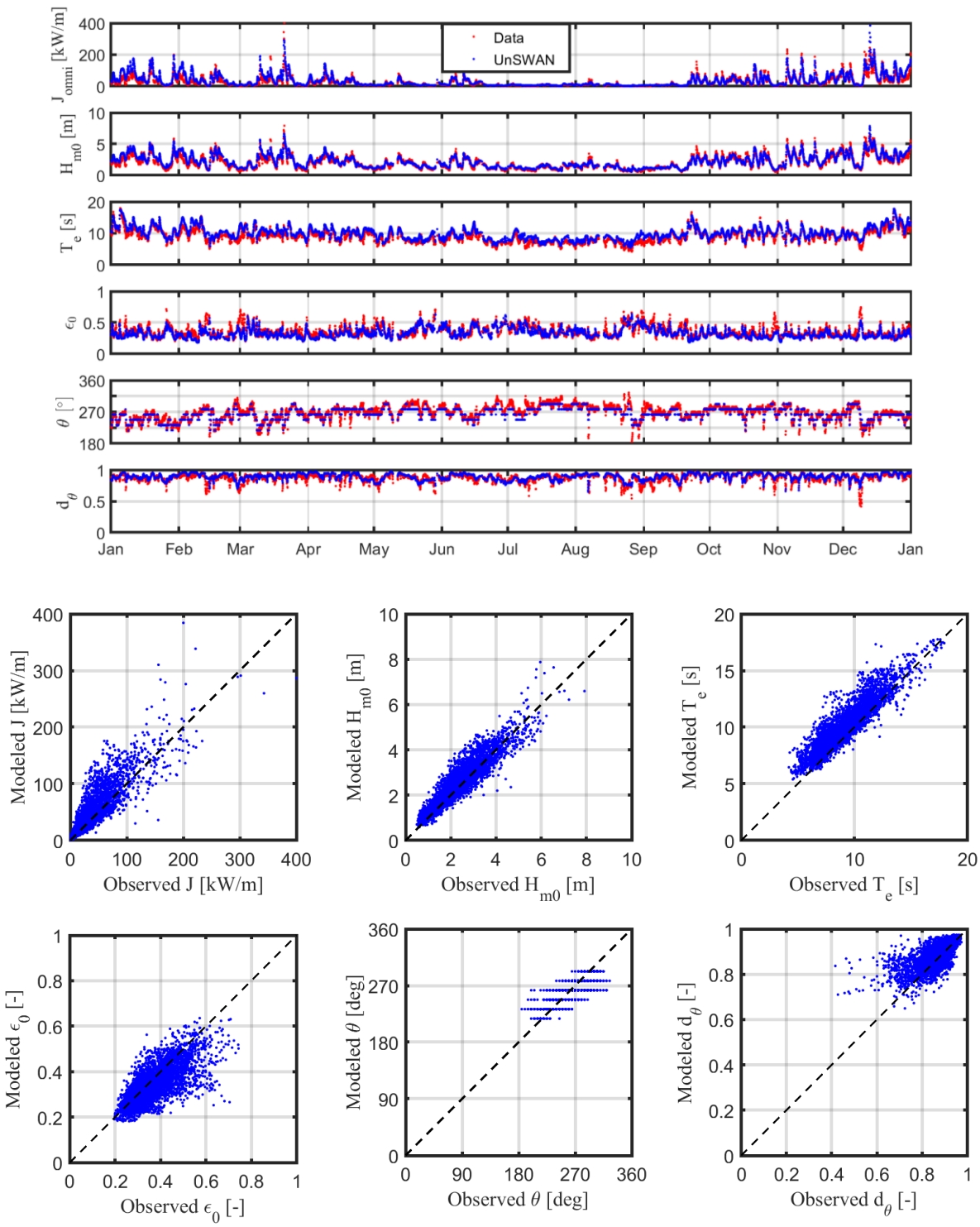

Figure B.118. Comparisons of time series (top) and scatter plots (bottom) of UnSWAN simulated six IEC parameters with observed data at CDIP Buoy 46211 for 1995.

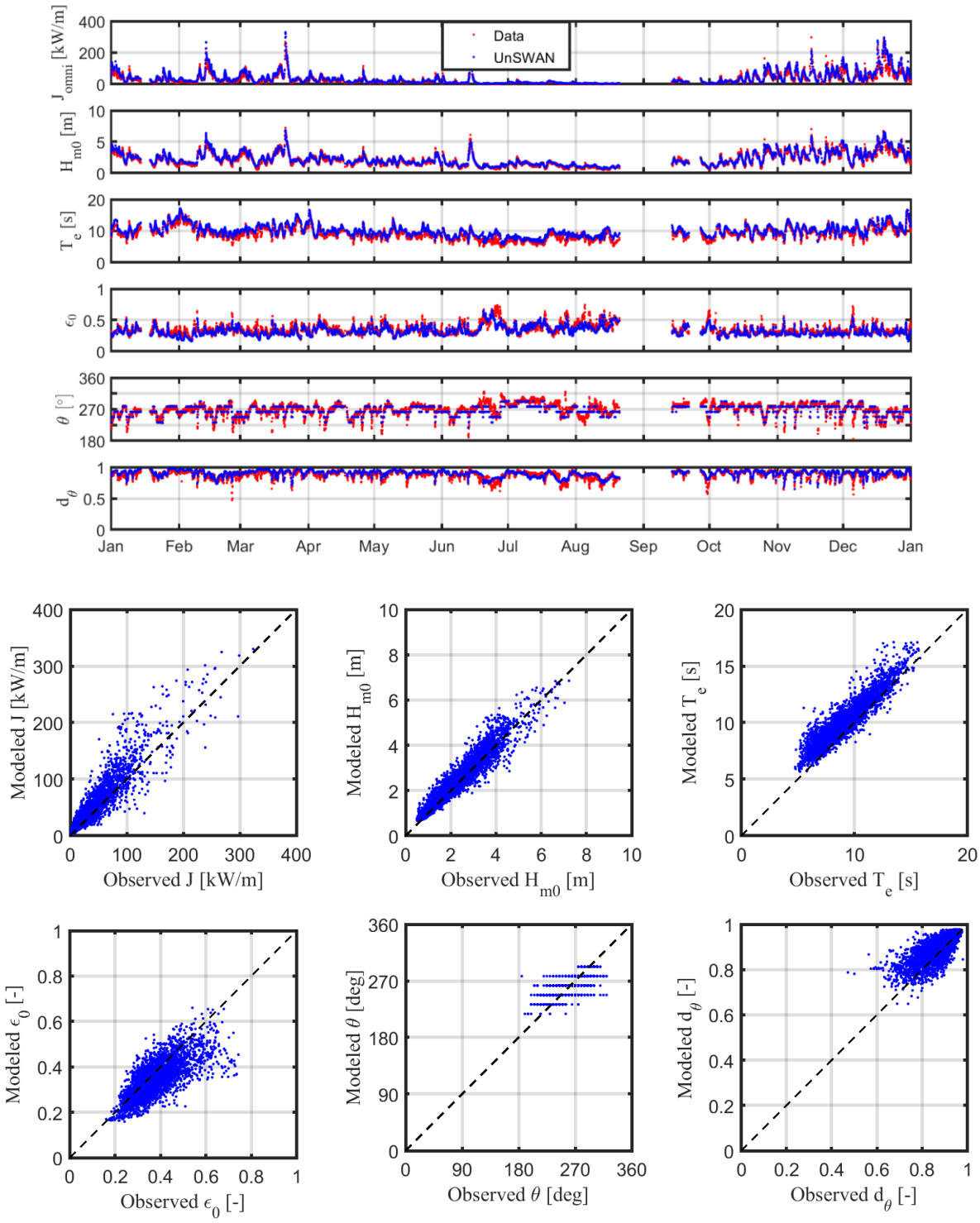

Figure B.119. Comparisons of time series (top) and scatter plots (bottom) of UnSWAN simulated six IEC parameters with observed data at CDIP Buoy 46211 for 1994.

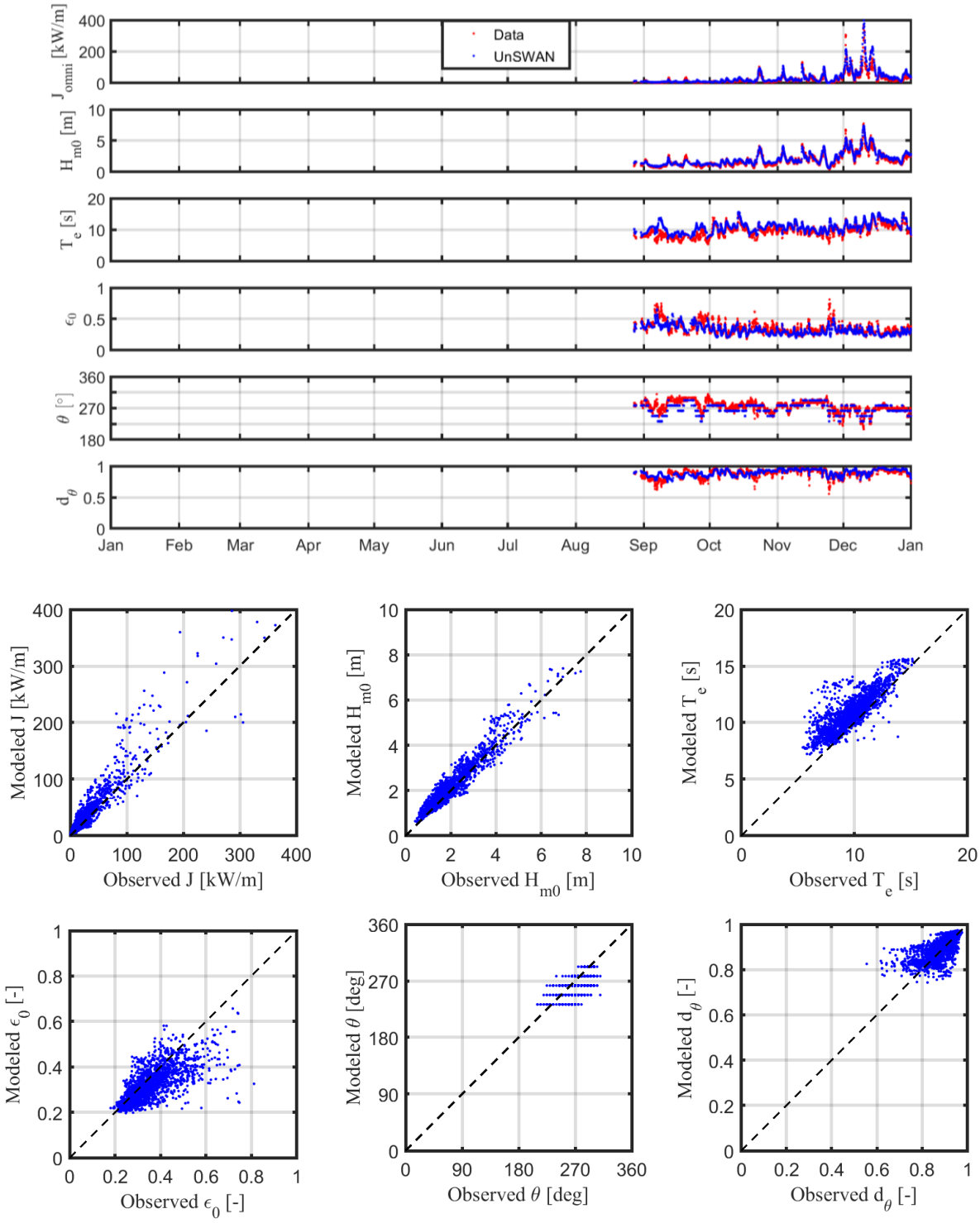

Figure B.120. Comparisons of time series (top) and scatter plots (bottom) of UnSWAN simulated six IEC parameters with observed data at CDIP Buoy 46211 for 1993.

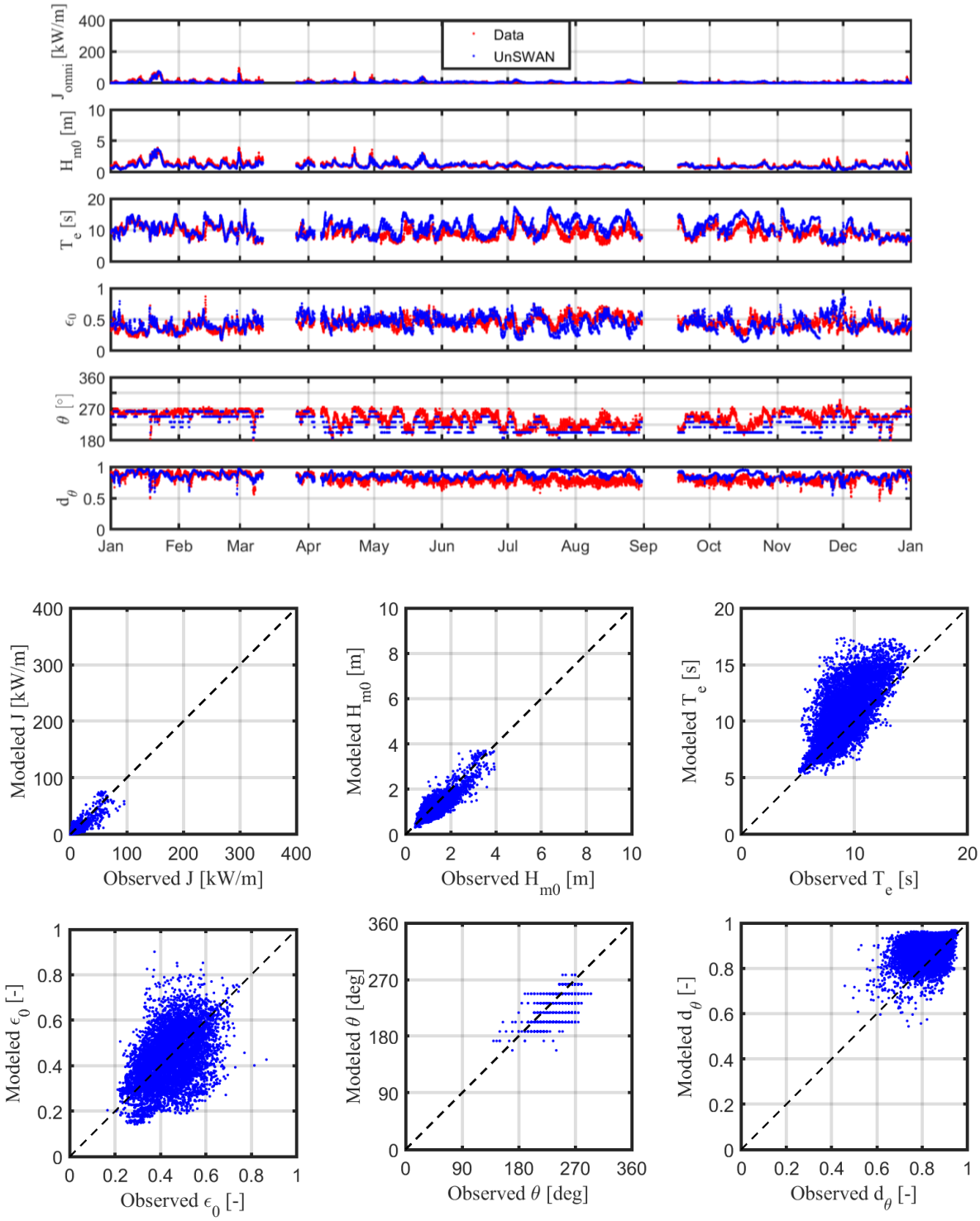

Figure B.121. Comparisons of time series (top) and scatter plots (bottom) of UnSWAN simulated six IEC parameters with observed data at CDIP Buoy 46221 for 2010.

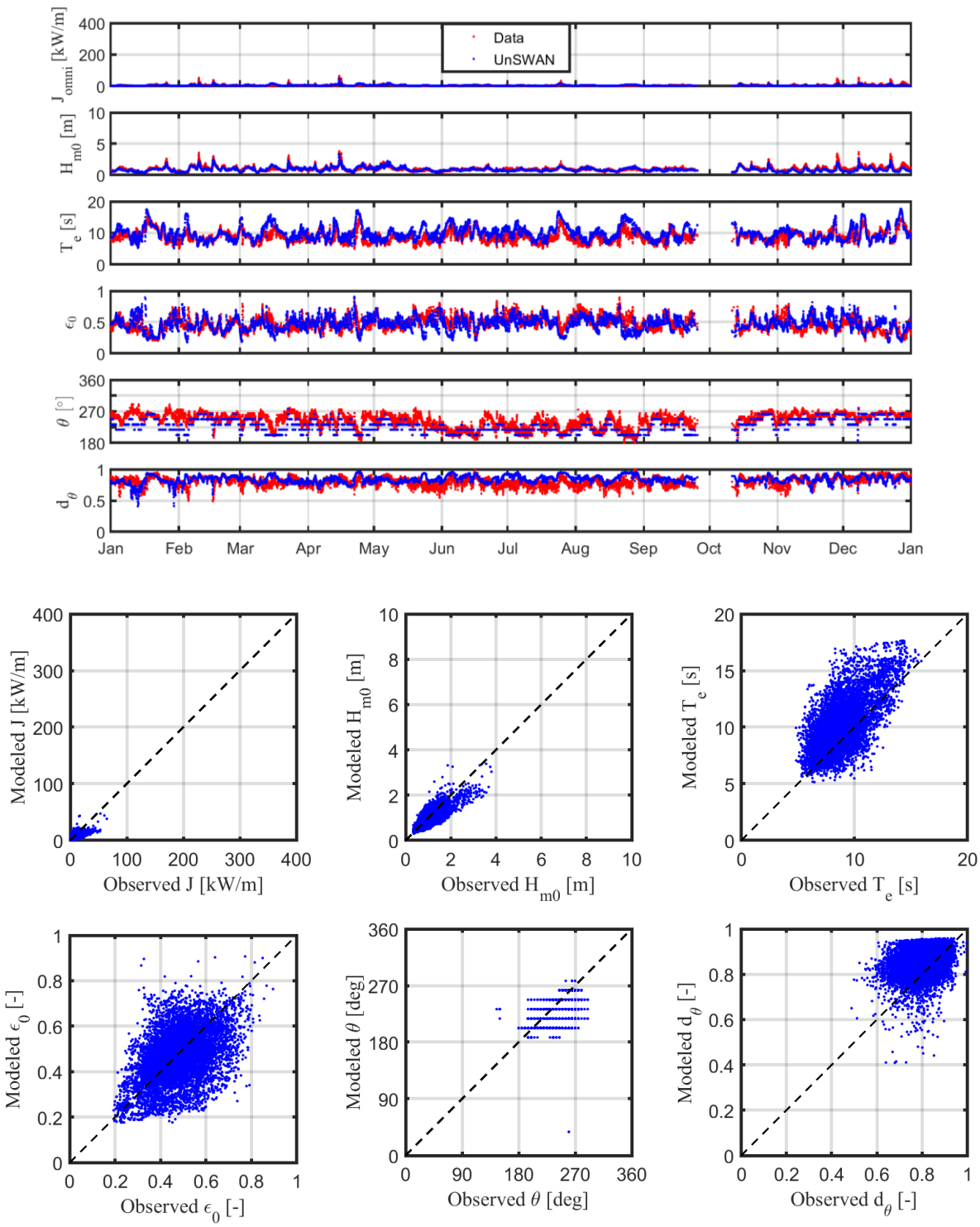

Figure B.122. Comparisons of time series (top) and scatter plots (bottom) of UnSWAN simulated six IEC parameters with observed data at CDIP Buoy 46221 for 2009.

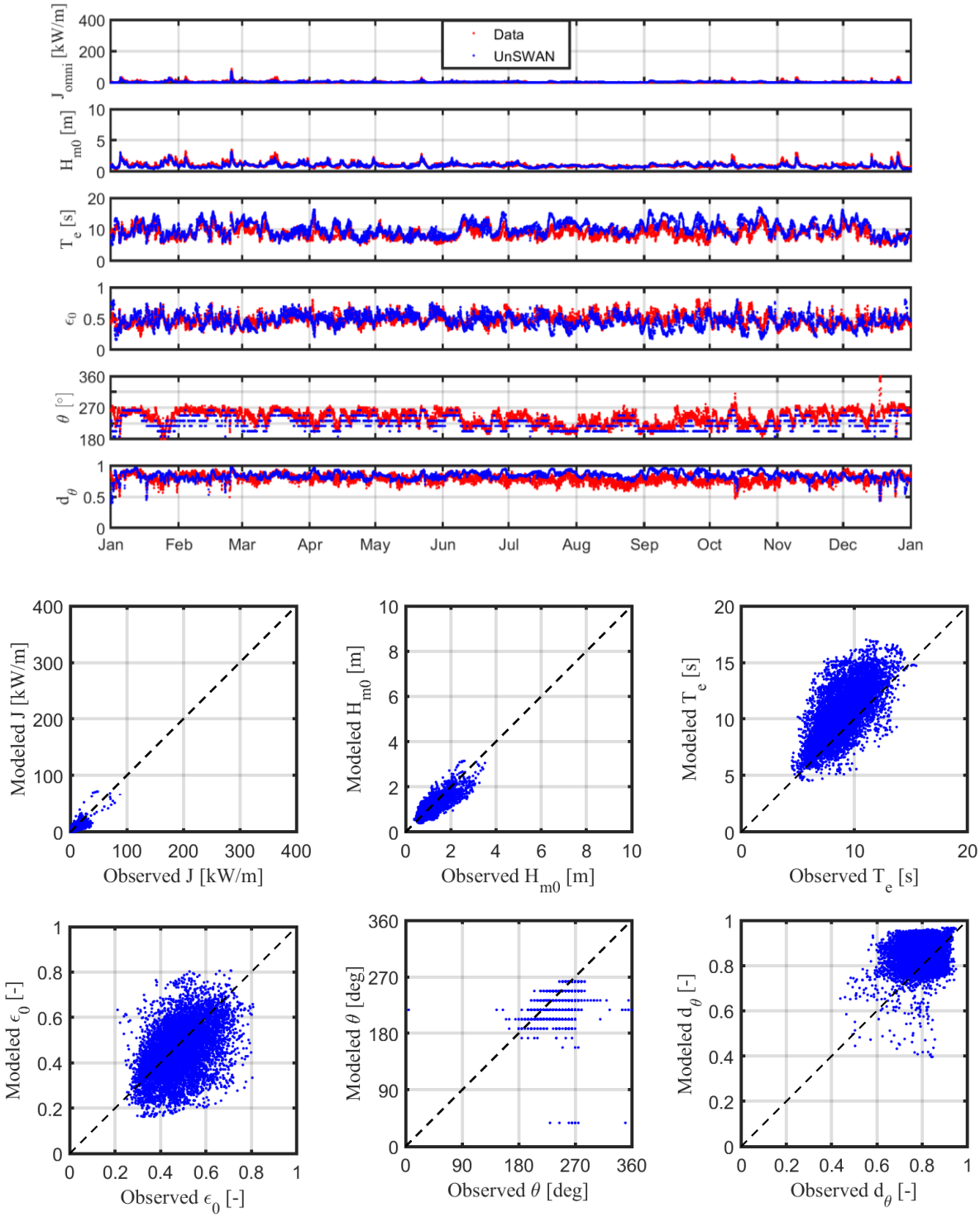

Figure B.123. Comparisons of time series (top) and scatter plots (bottom) of UnSWAN simulated six IEC parameters with observed data at CDIP Buoy 46221 for 2008.

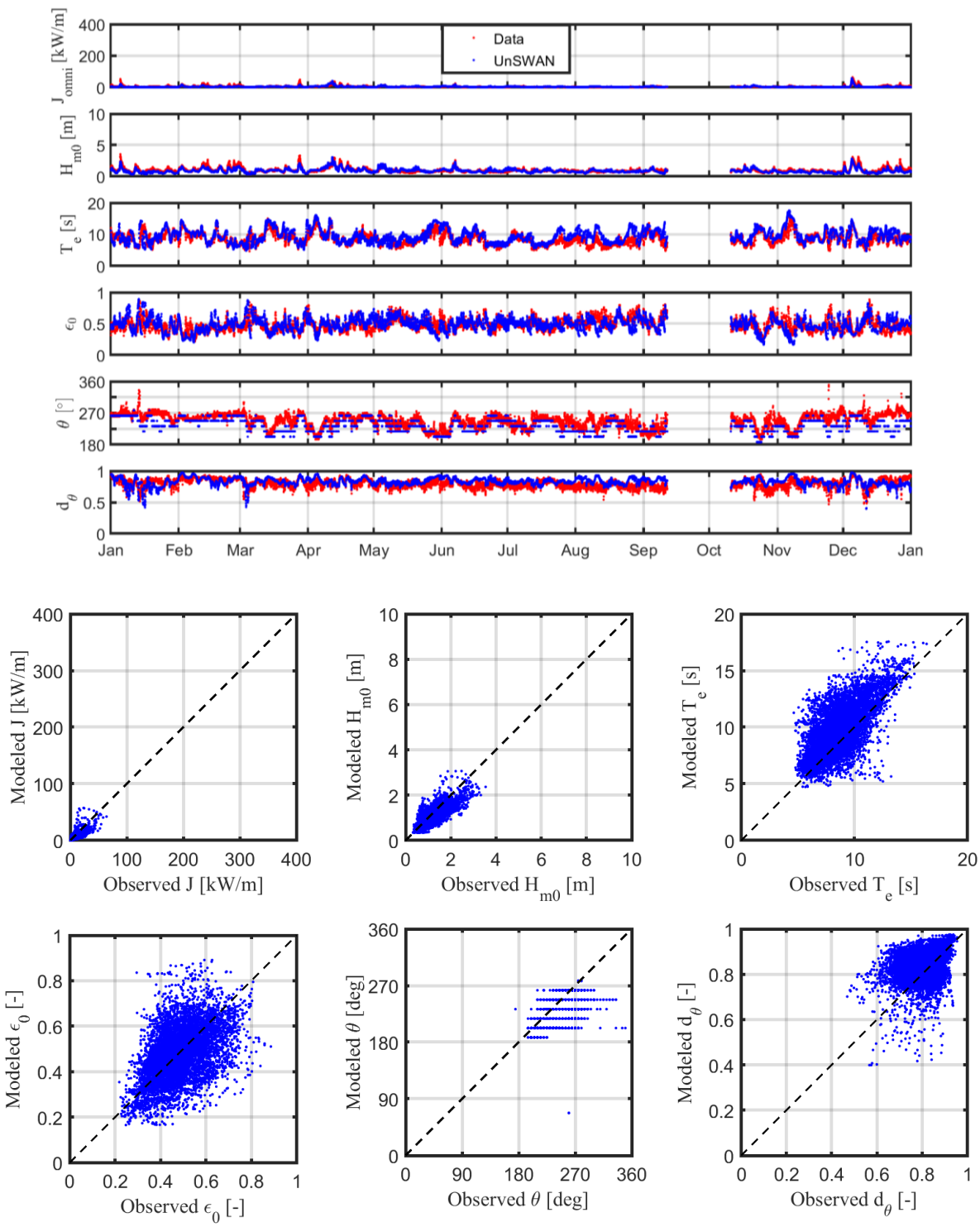

Figure B.124. Comparisons of time series (top) and scatter plots (bottom) of UnSWAN simulated six IEC parameters with observed data at CDIP Buoy 46221 for 2007.

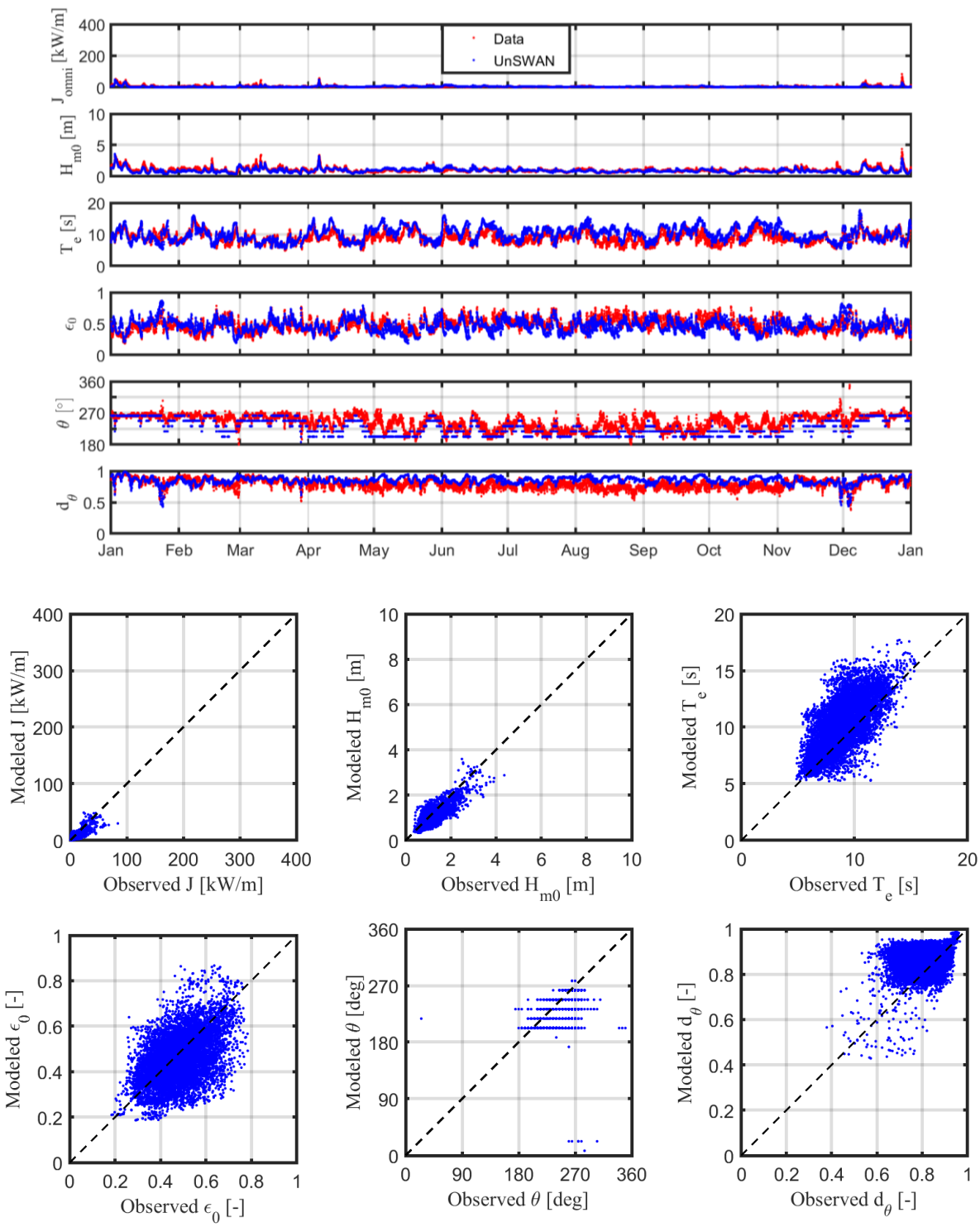

Figure B.125. Comparisons of time series (top) and scatter plots (bottom) of UnSWAN simulated six IEC parameters with observed data at CDIP Buoy 46221 for 2006.

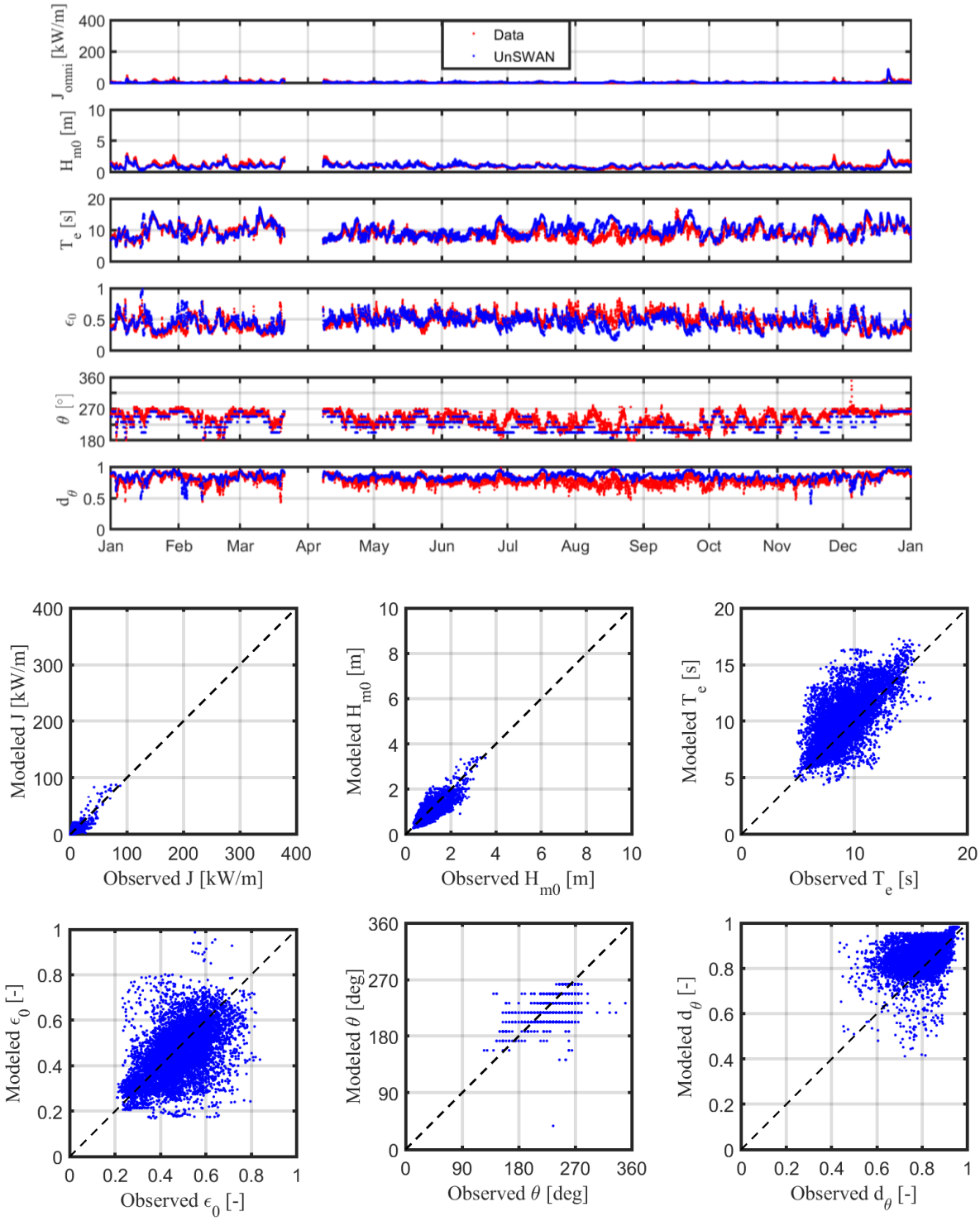

Figure B.126. Comparisons of time series (top) and scatter plots (bottom) of UnSWAN simulated six IEC parameters with observed data at CDIP Buoy 46221 for 2005.

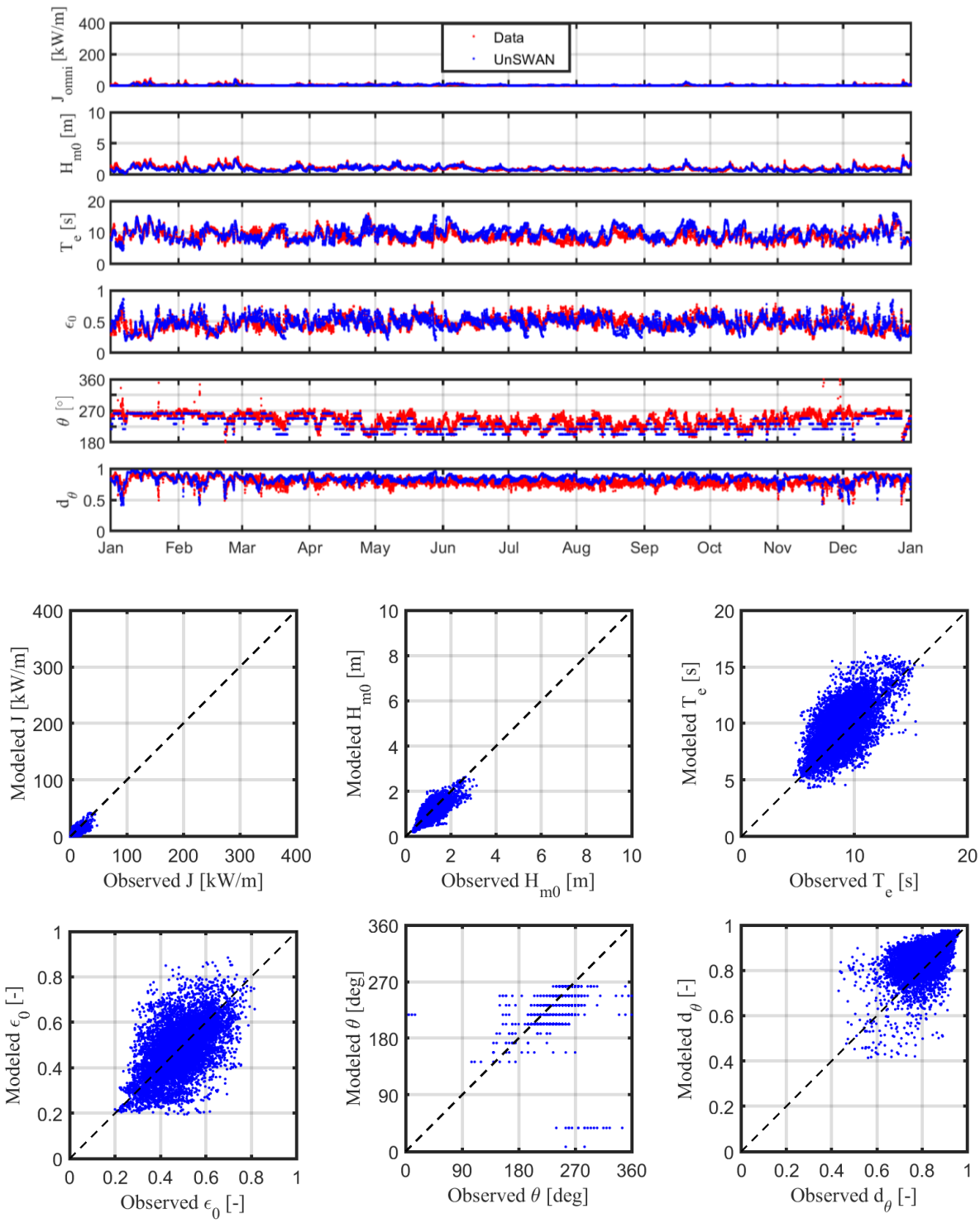

Figure B.127. Comparisons of time series (top) and scatter plots (bottom) of UnSWAN simulated six IEC parameters with observed data at CDIP Buoy 46221 for 2004.

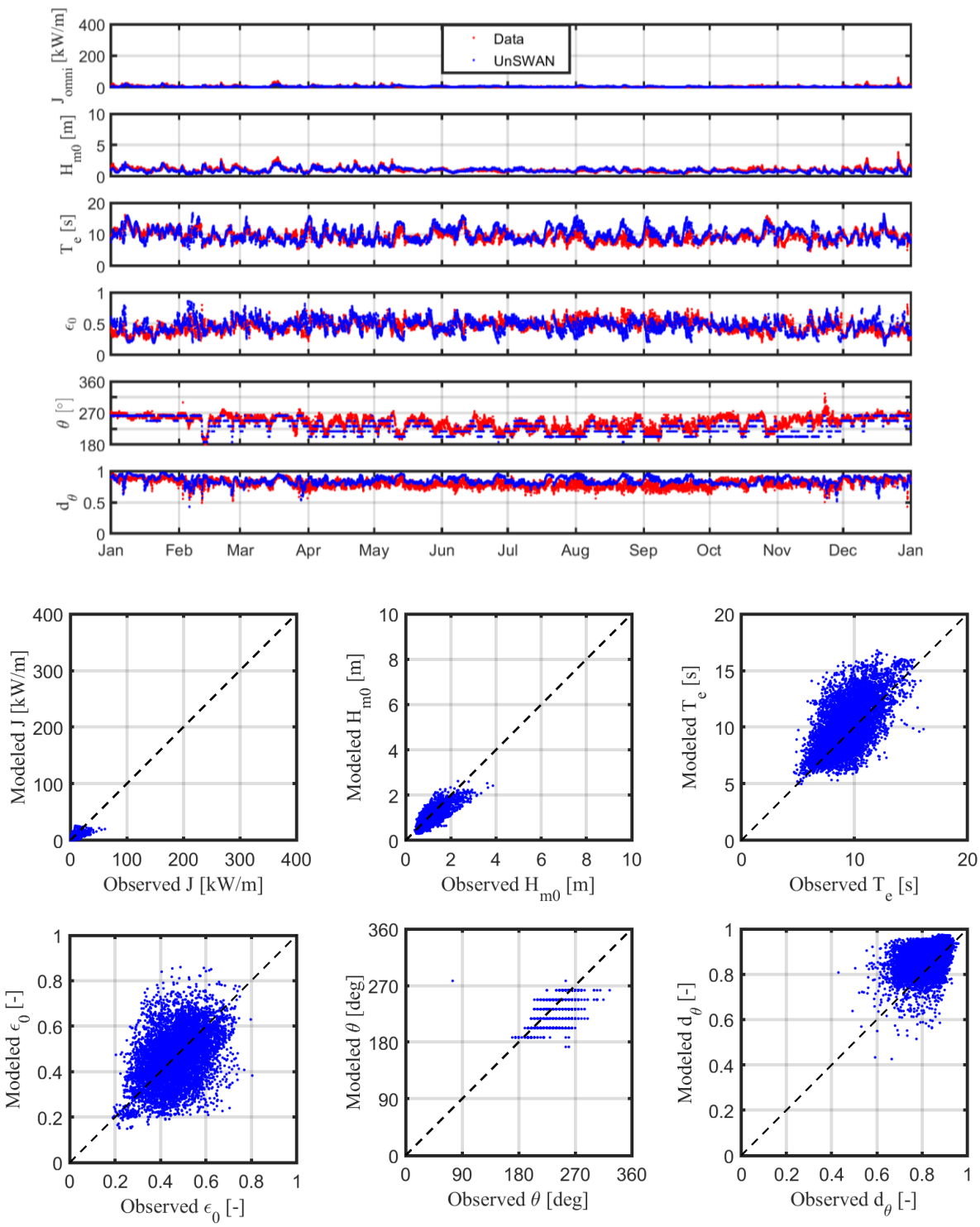

Figure B.128. Comparisons of time series (top) and scatter plots (bottom) of UnSWAN simulated six IEC parameters with observed data at CDIP Buoy 46221 for 2003.

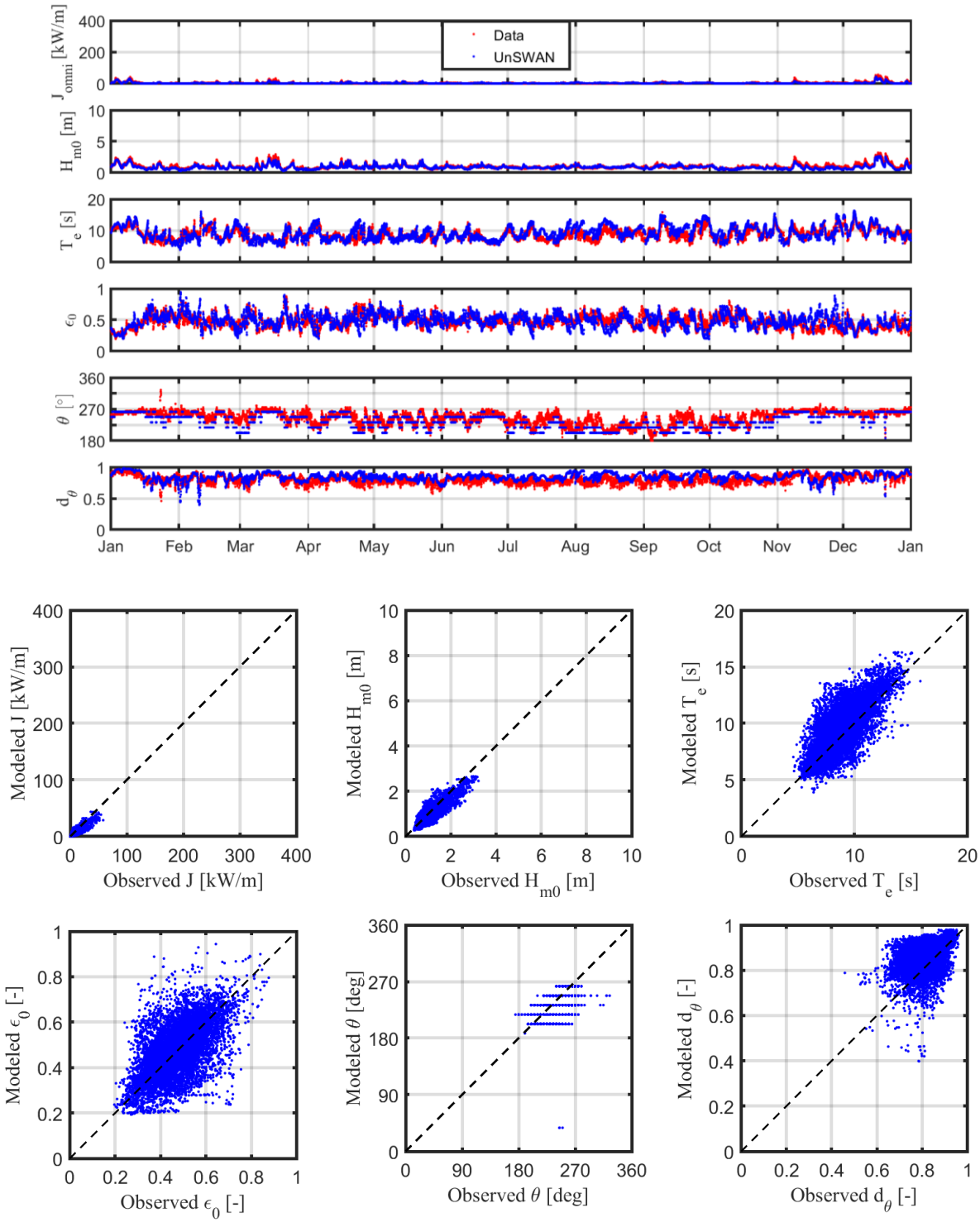

Figure B.129. Comparisons of time series (top) and scatter plots (bottom) of UnSWAN simulated six IEC parameters with observed data at CDIP Buoy 46221 for 2002.

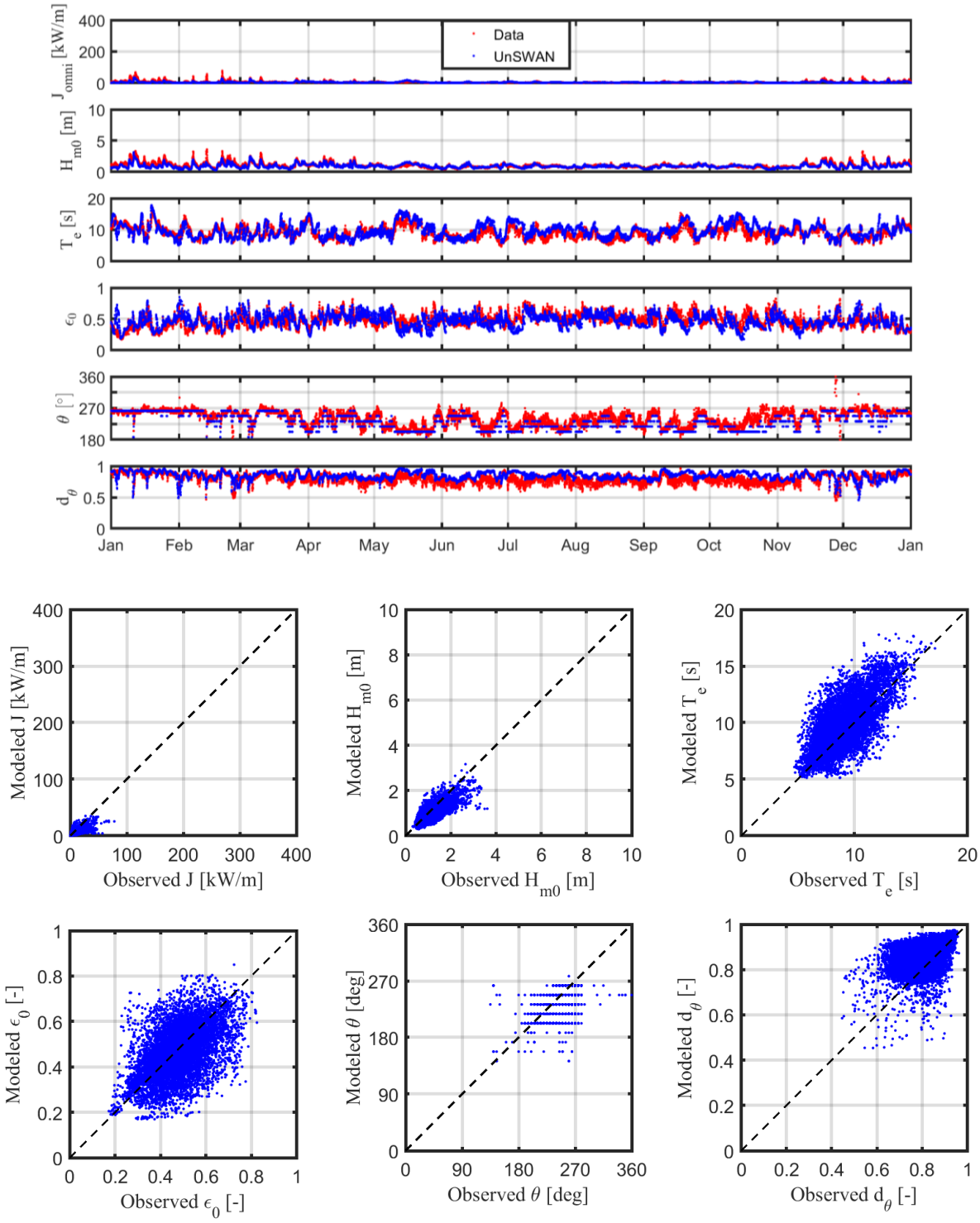

Figure B.130. Comparisons of time series (top) and scatter plots (bottom) of UnSWAN simulated six IEC parameters with observed data at CDIP Buoy 46221 for 2001.

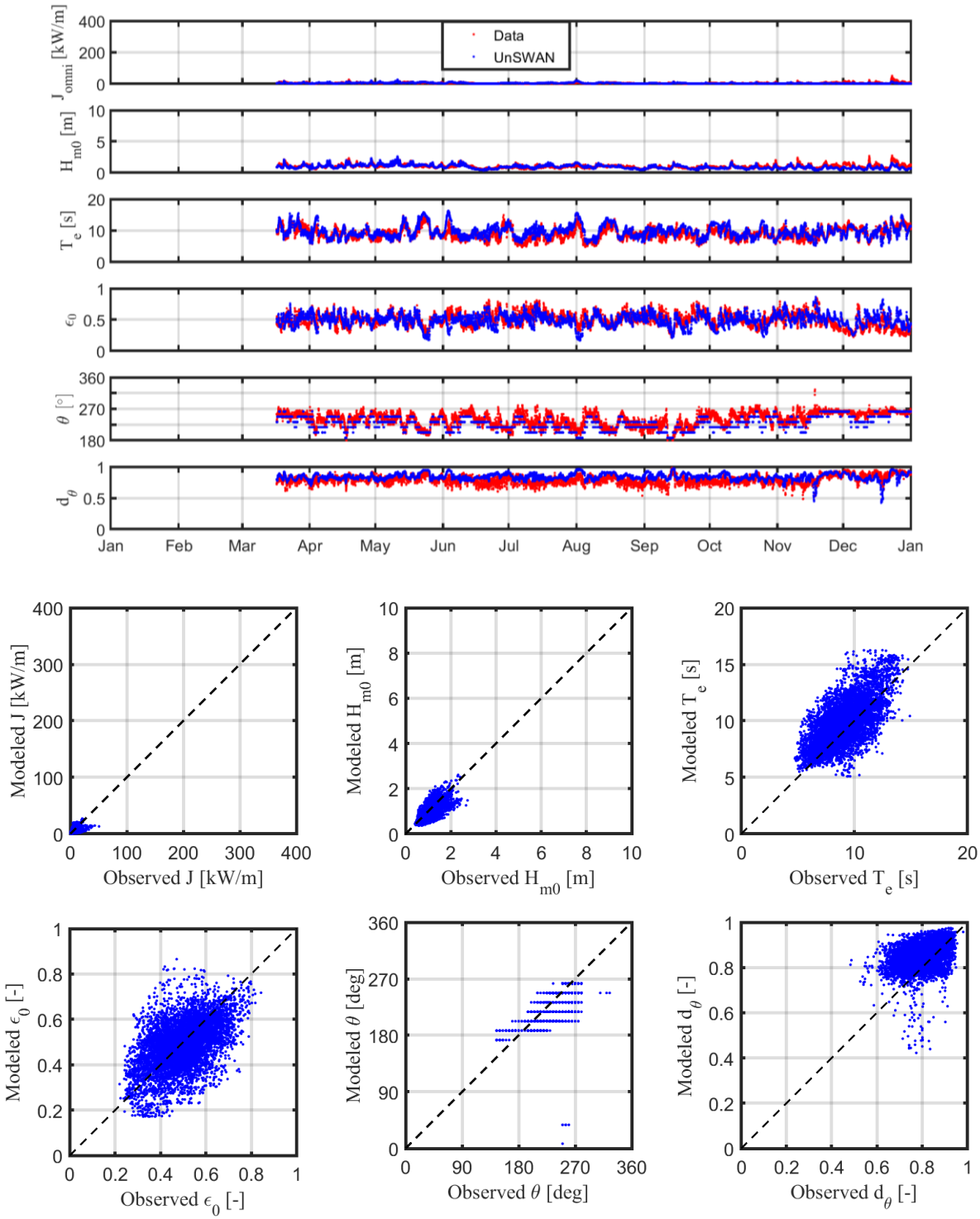

Figure B.131. Comparisons of time series (top) and scatter plots (bottom) of UnSWAN simulated six IEC parameters with observed data at CDIP Buoy 46221 for 2000.

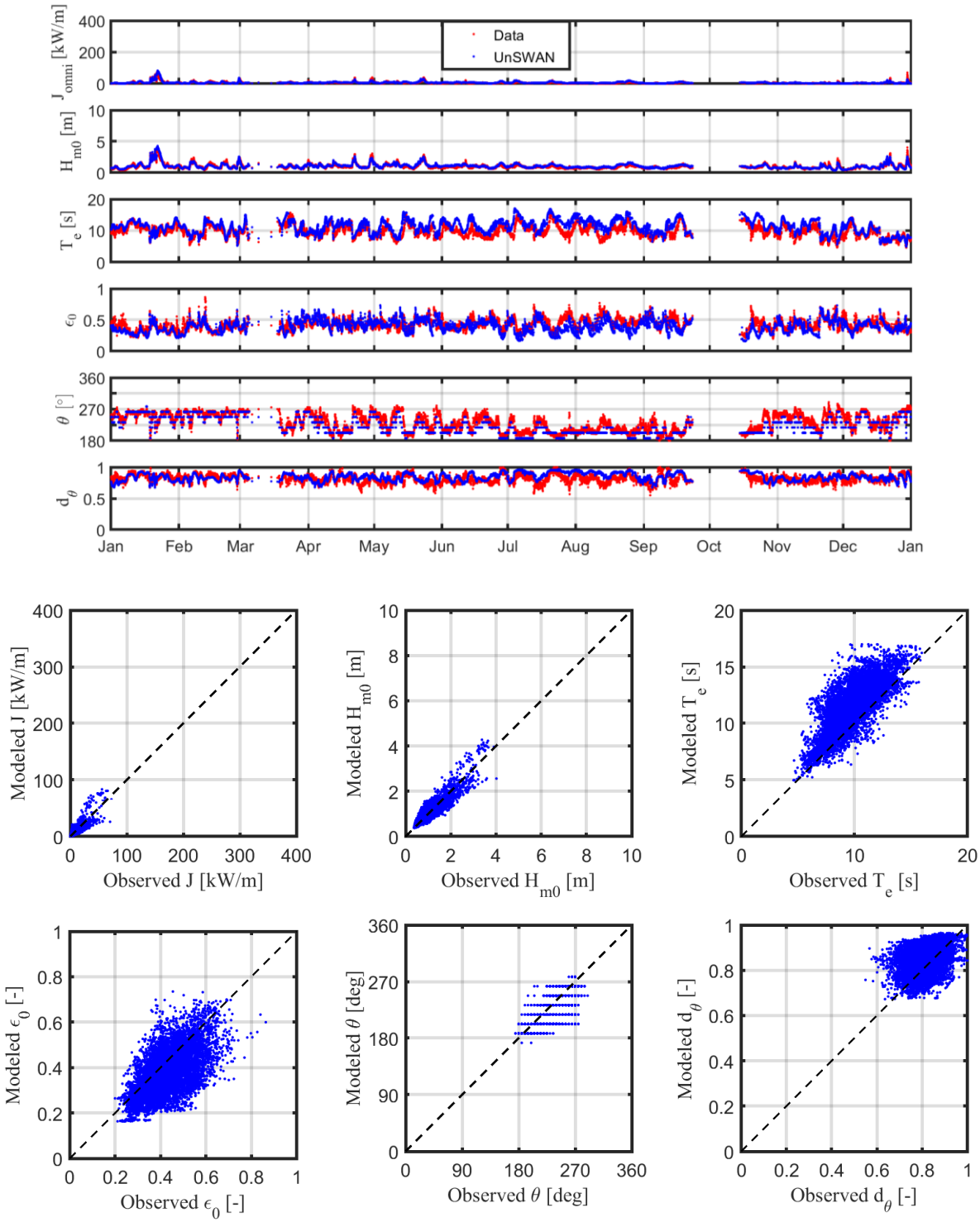

Figure B.132. Comparisons of time series (top) and scatter plots (bottom) of UnSWAN simulated six IEC parameters with observed data at CDIP Buoy 46224 for 2010.

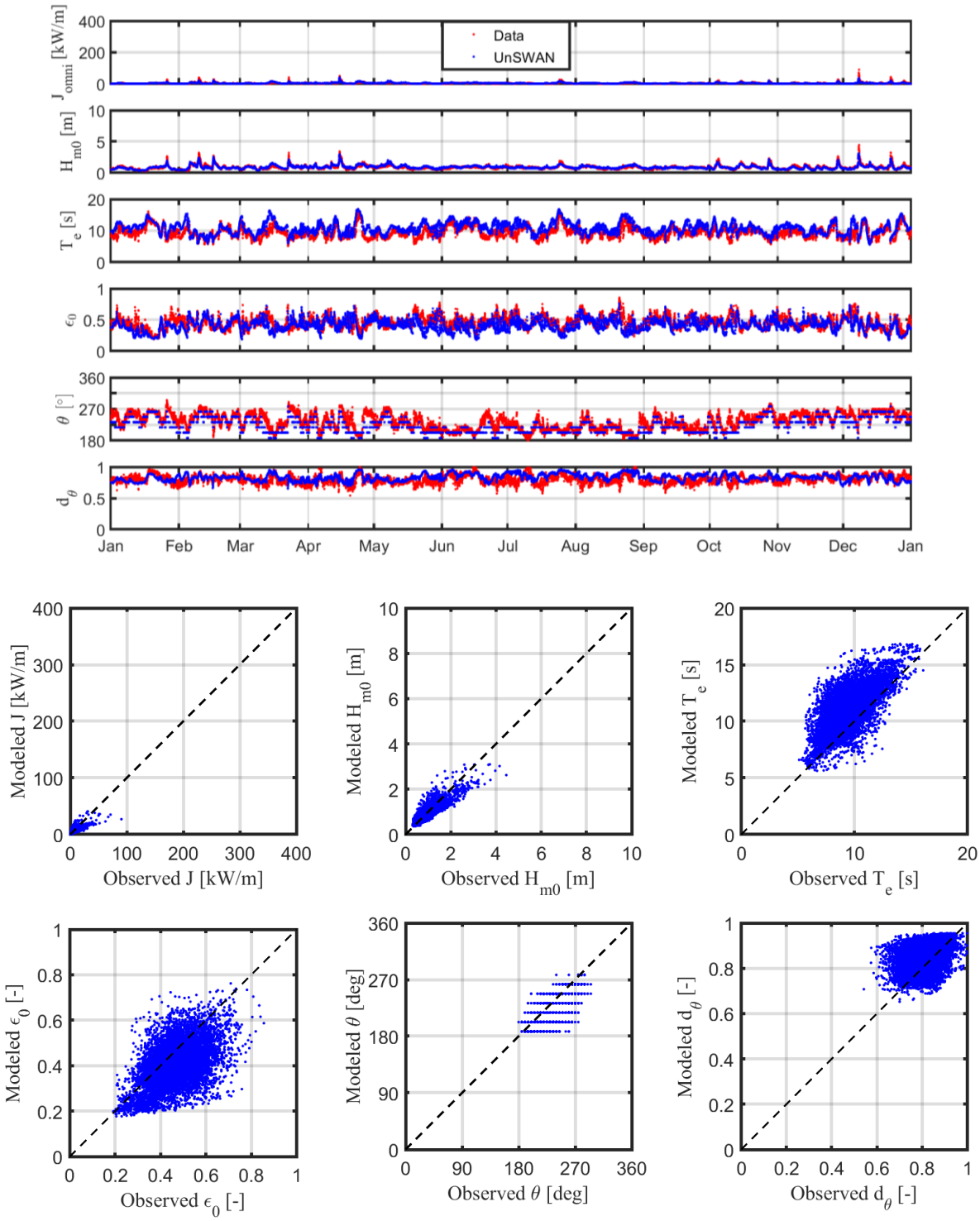

Figure B.133. Comparisons of time series (top) and scatter plots (bottom) of UnSWAN simulated six IEC parameters with observed data at CDIP Buoy 46224 for 2009.

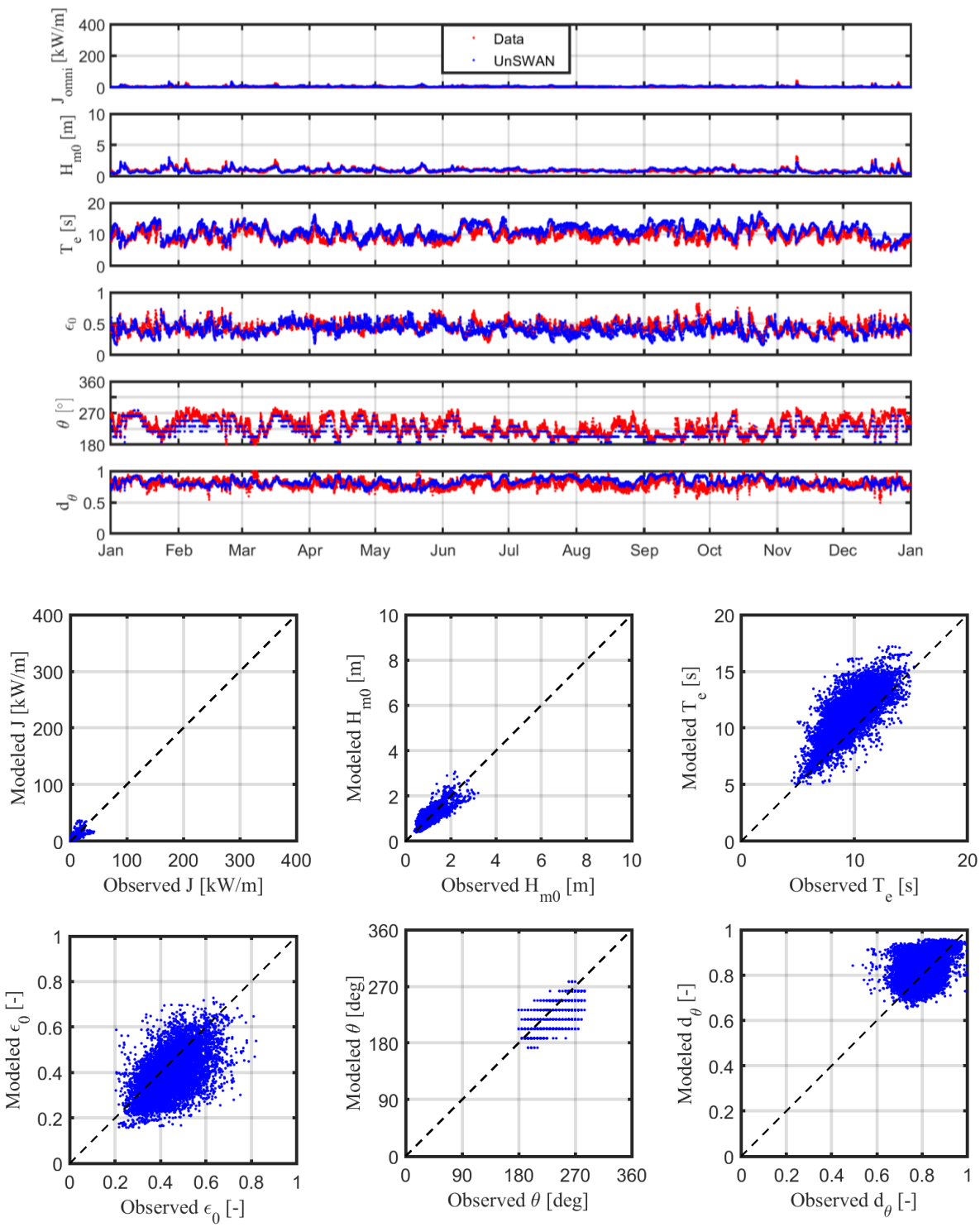

Figure B.134. Comparisons of time series (top) and scatter plots (bottom) of UnSWAN simulated six IEC parameters with observed data at CDIP Buoy 46224 for 2008.

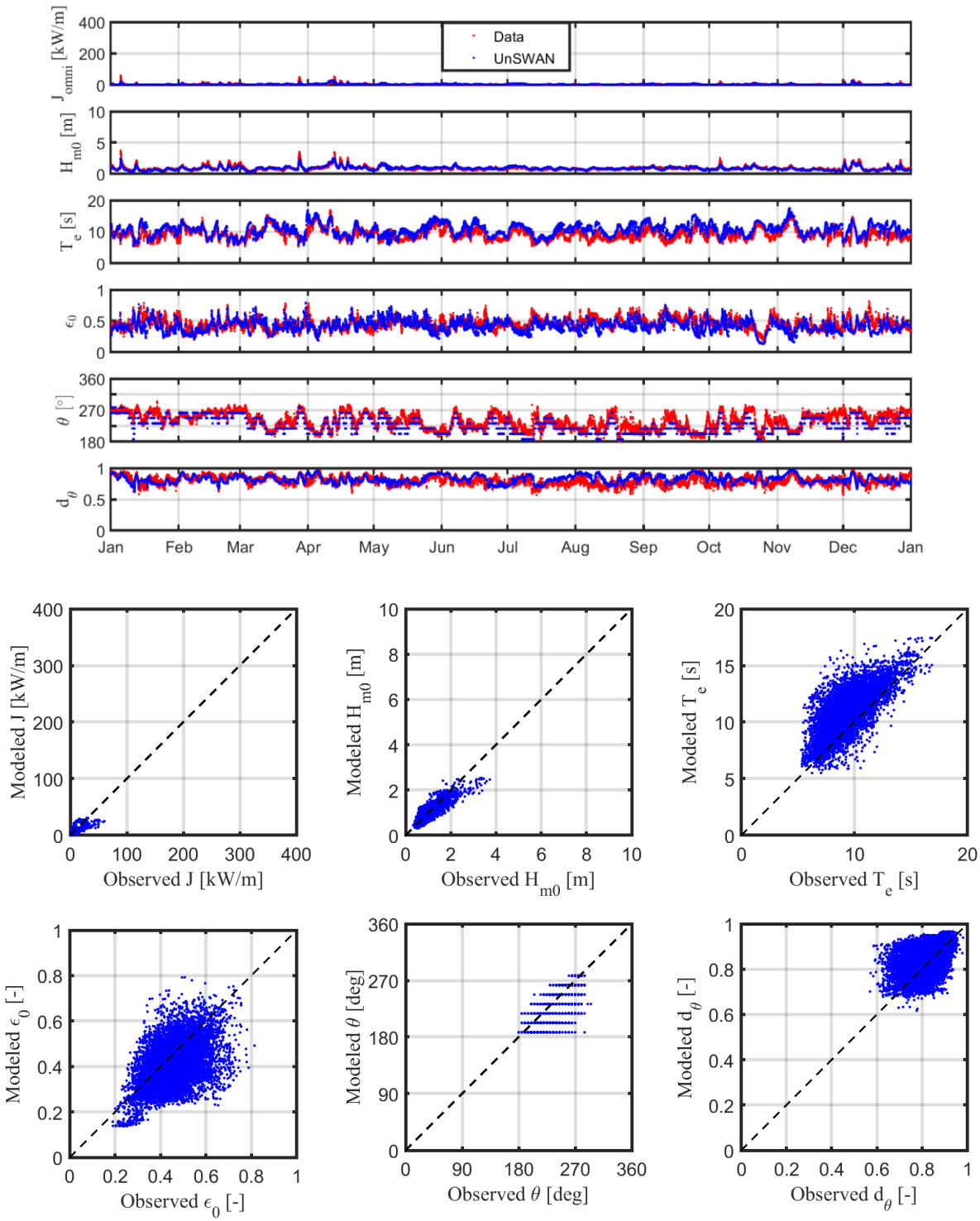

Figure B.135. Comparisons of time series (top) and scatter plots (bottom) of UnSWAN simulated six IEC parameters with observed data at CDIP Buoy 46224 for 2007.

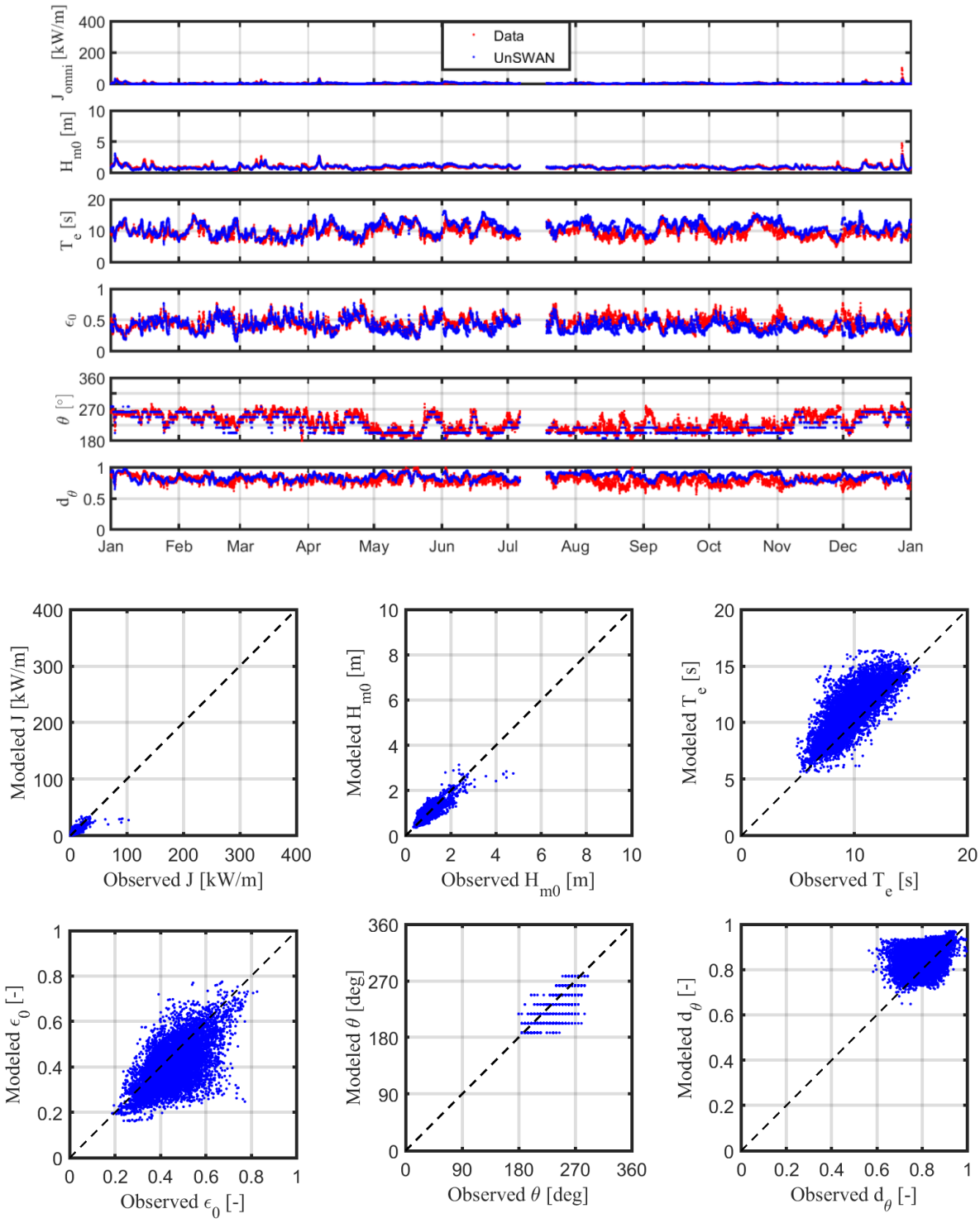

Figure B.136. Comparisons of time series (top) and scatter plots (bottom) of UnSWAN simulated six IEC parameters with observed data at CDIP Buoy 46224 for 2006.

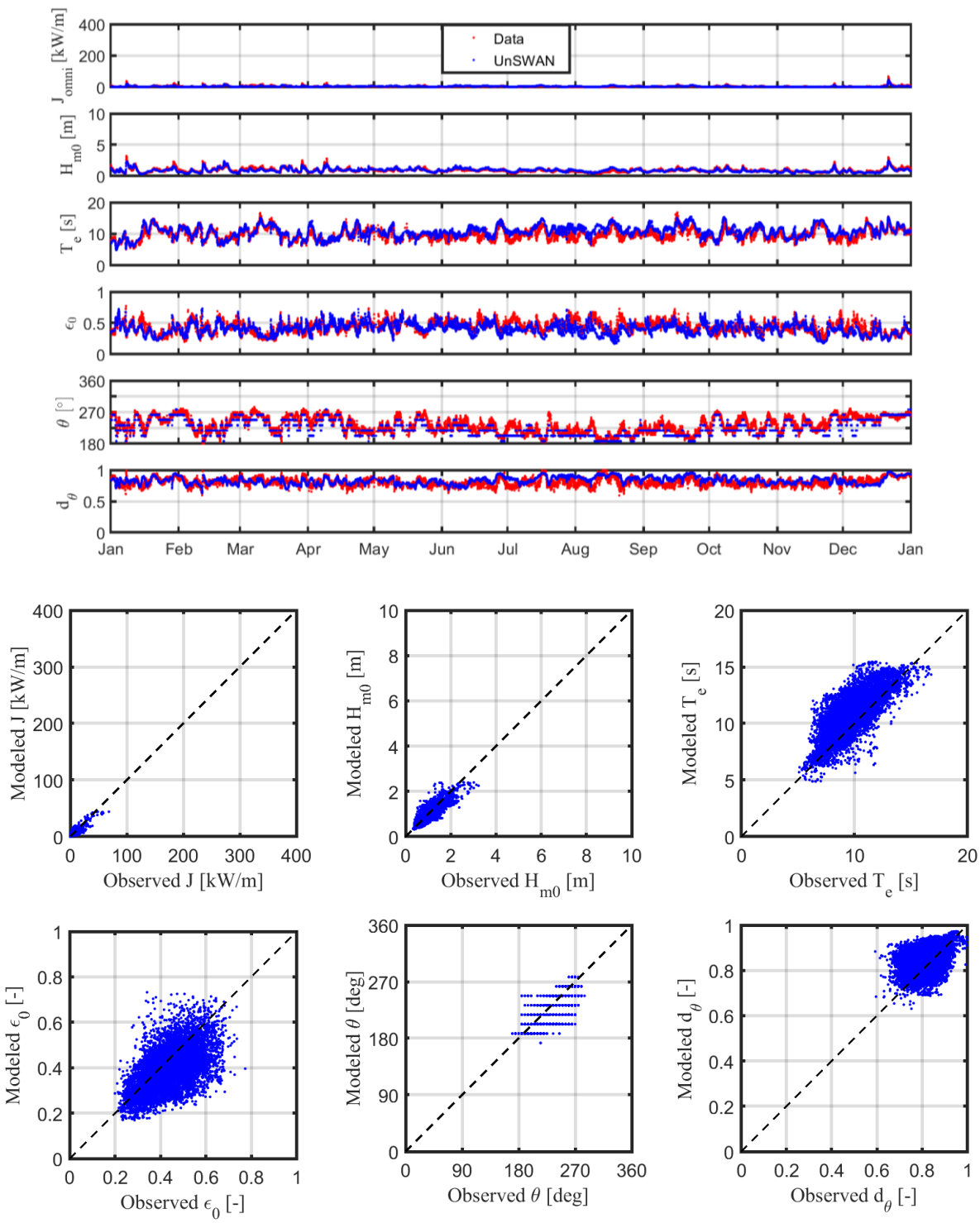

Figure B.137. Comparisons of time series (top) and scatter plots (bottom) of UnSWAN simulated six IEC parameters with observed data at CDIP Buoy 46224 for 2005.

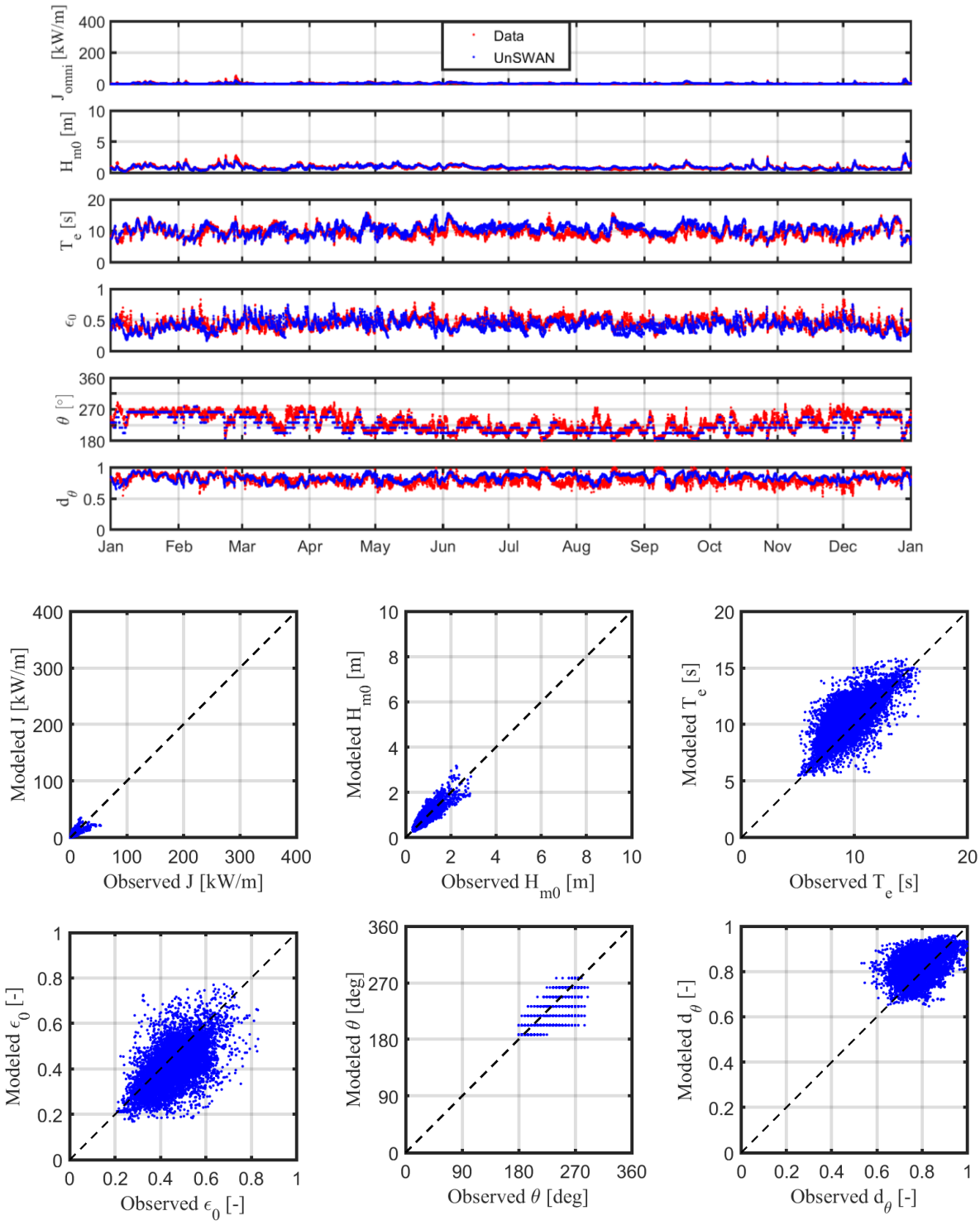

Figure B.138. Comparisons of time series (top) and scatter plots (bottom) of UnSWAN simulated six IEC parameters with observed data at CDIP Buoy 46224 for 2004.

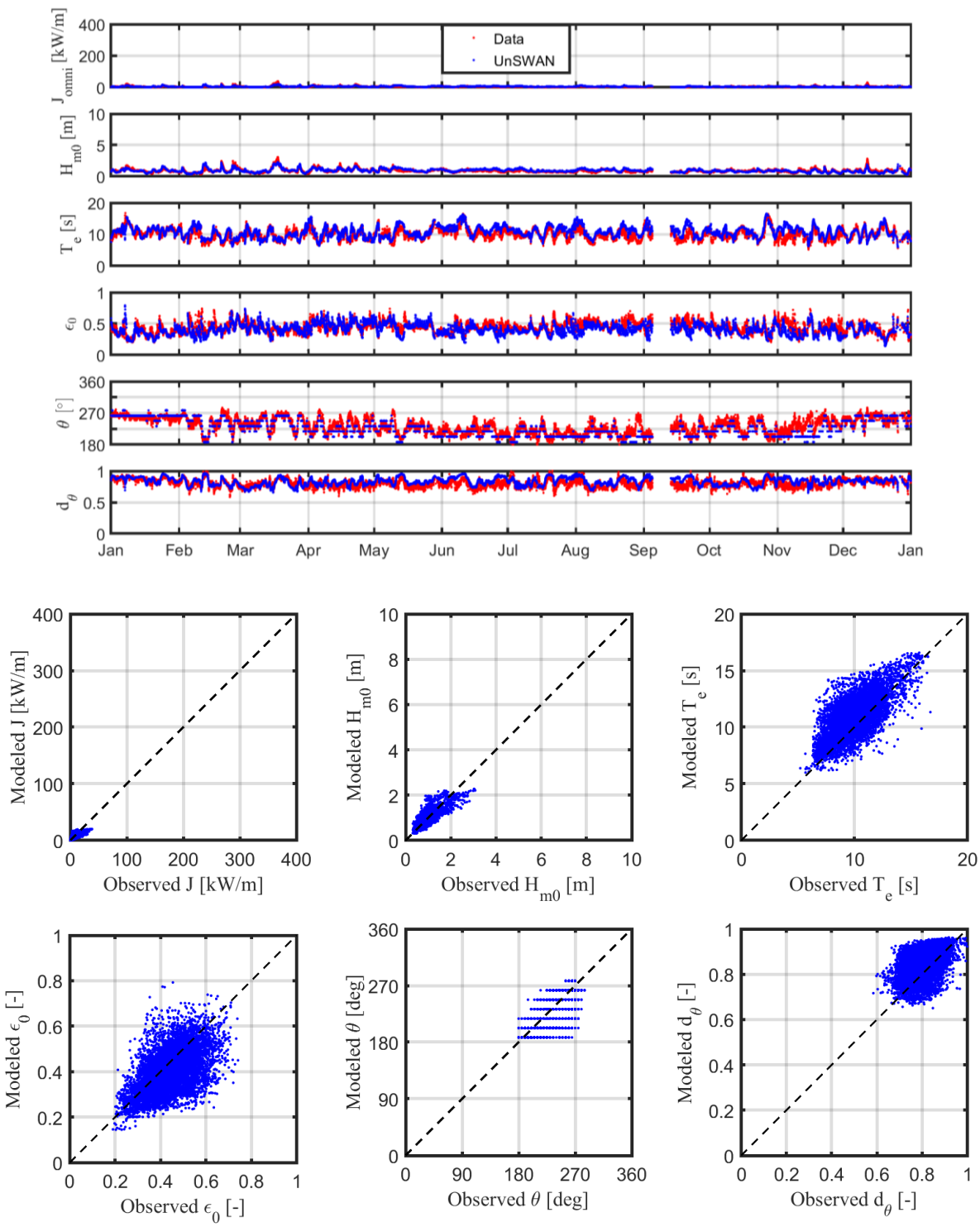

Figure B.139. Comparisons of time series (top) and scatter plots (bottom) of UnSWAN simulated six IEC parameters with observed data at CDIP Buoy 46224 for 2003.

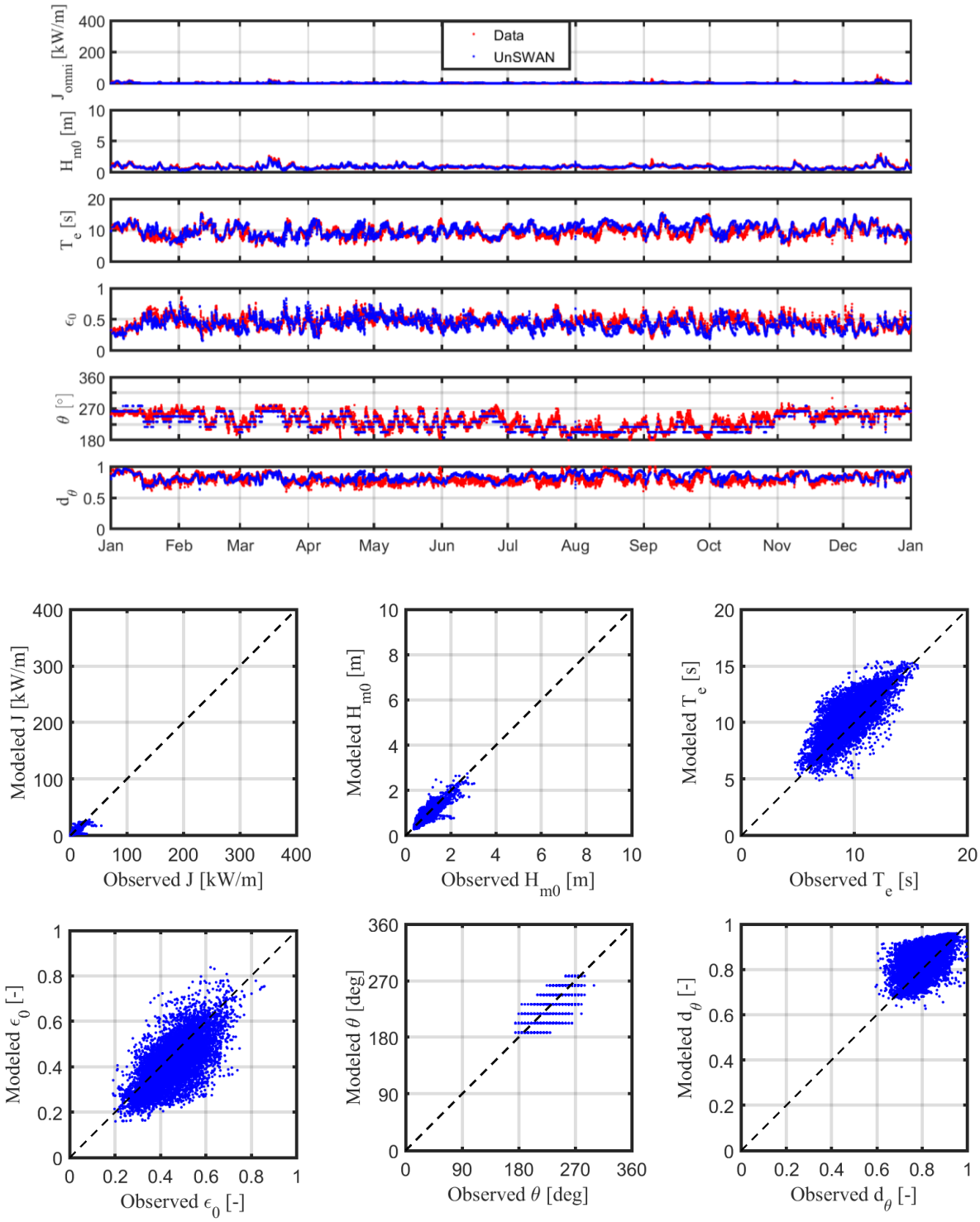

Figure B.140. Comparisons of time series (top) and scatter plots (bottom) of UnSWAN simulated six IEC parameters with observed data at CDIP Buoy 46224 for 2002.

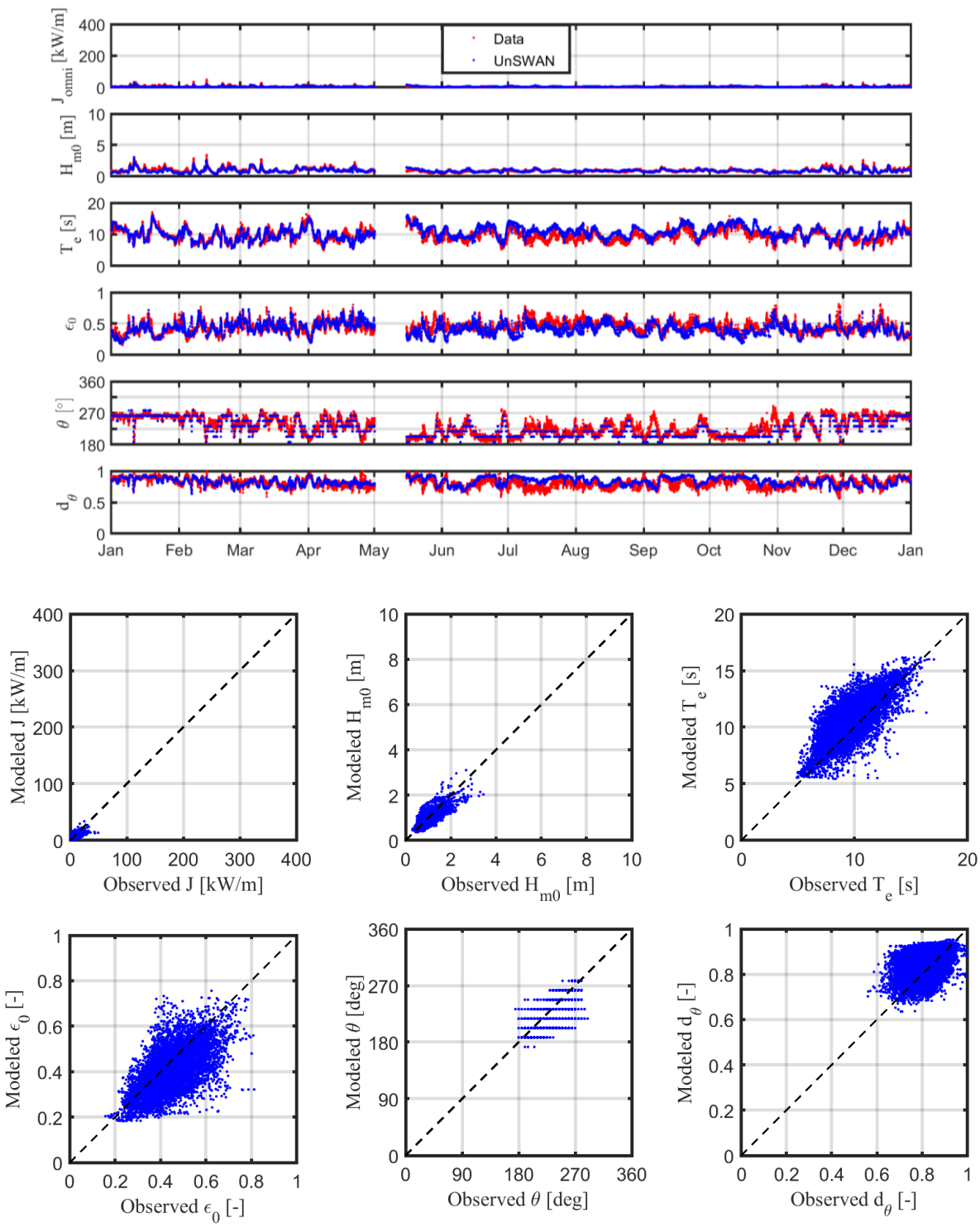

Figure B.141. Comparisons of time series (top) and scatter plots (bottom) of UnSWAN simulated six IEC parameters with observed data at CDIP Buoy 46224 for 2001.

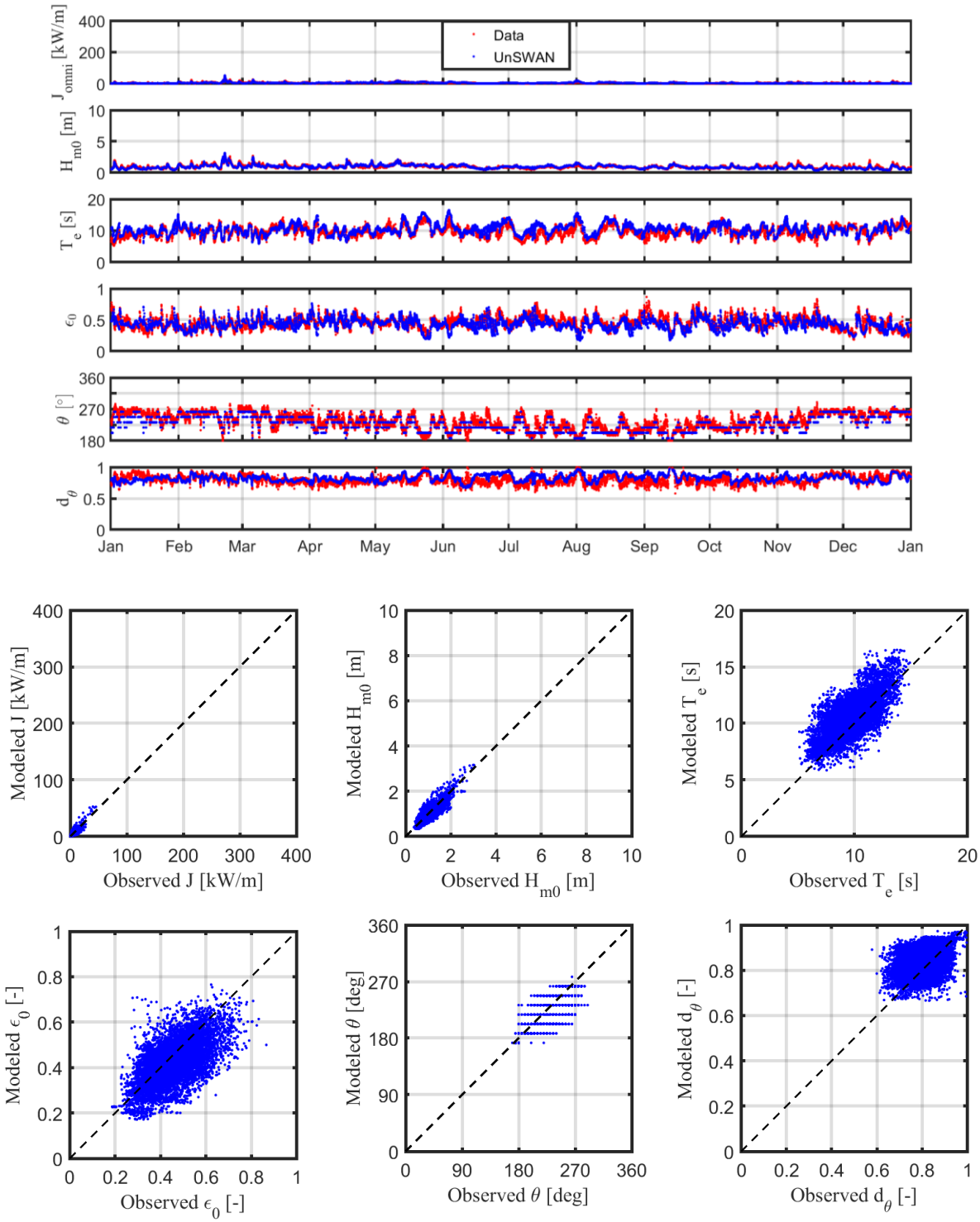

Figure B.142. Comparisons of time series (top) and scatter plots (bottom) of UnSWAN simulated six IEC parameters with observed data at CDIP Buoy 46224 for 2000.

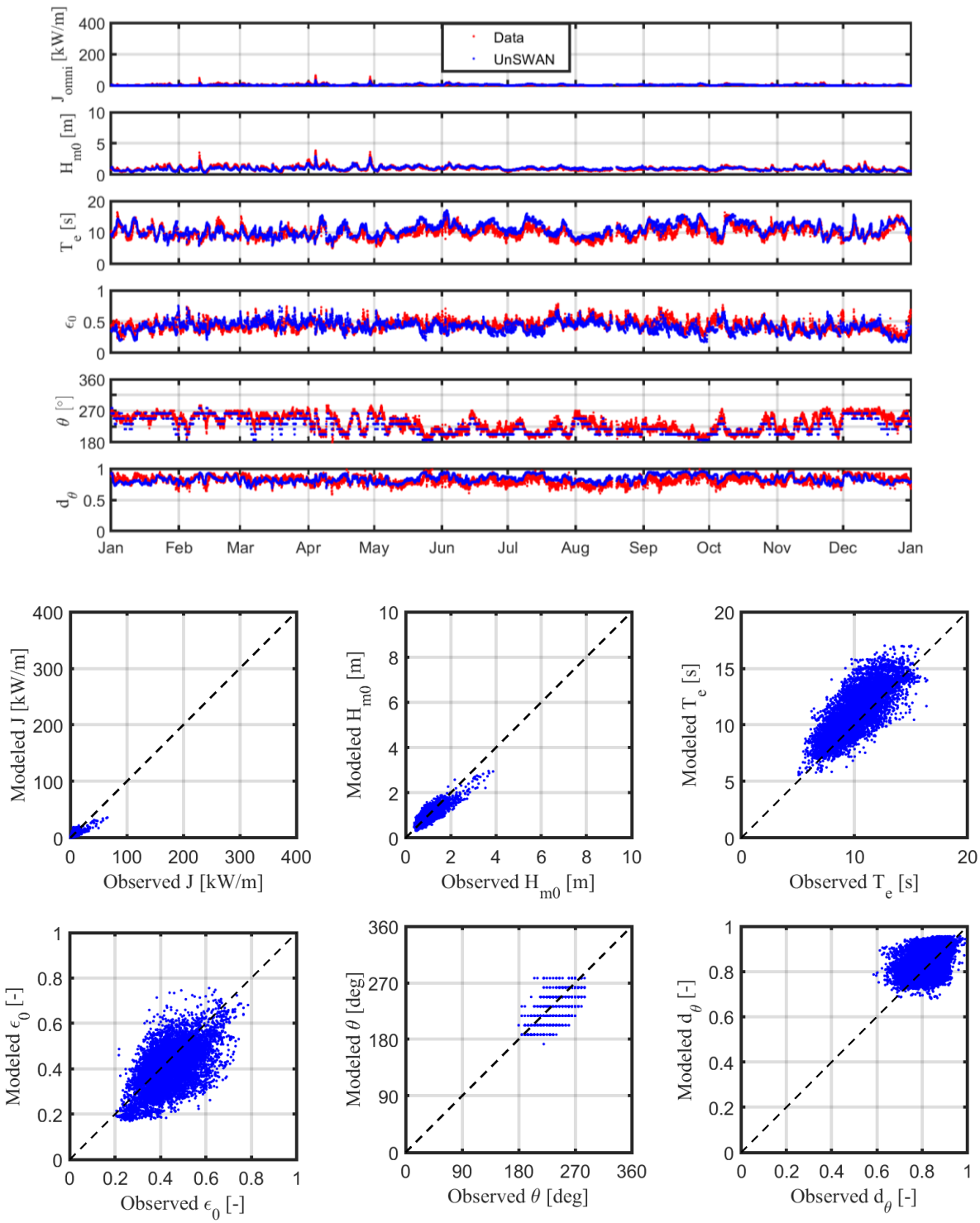

Figure B.143. Comparisons of time series (top) and scatter plots (bottom) of UnSWAN simulated six IEC parameters with observed data at CDIP Buoy 46224 for 1999.

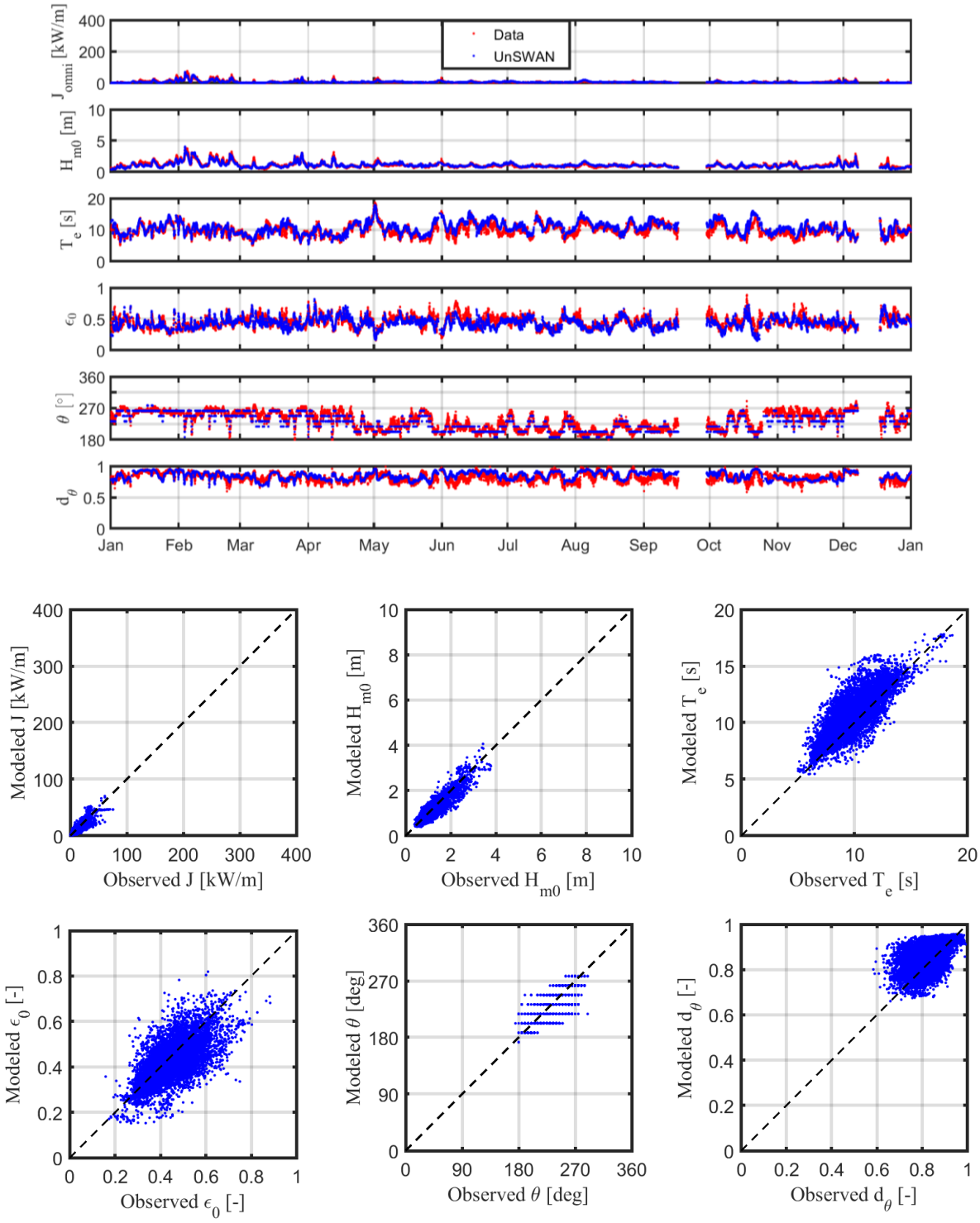

Figure B.144. Comparisons of time series (top) and scatter plots (bottom) of UnSWAN simulated six IEC parameters with observed data at CDIP Buoy 46224 for 1998.

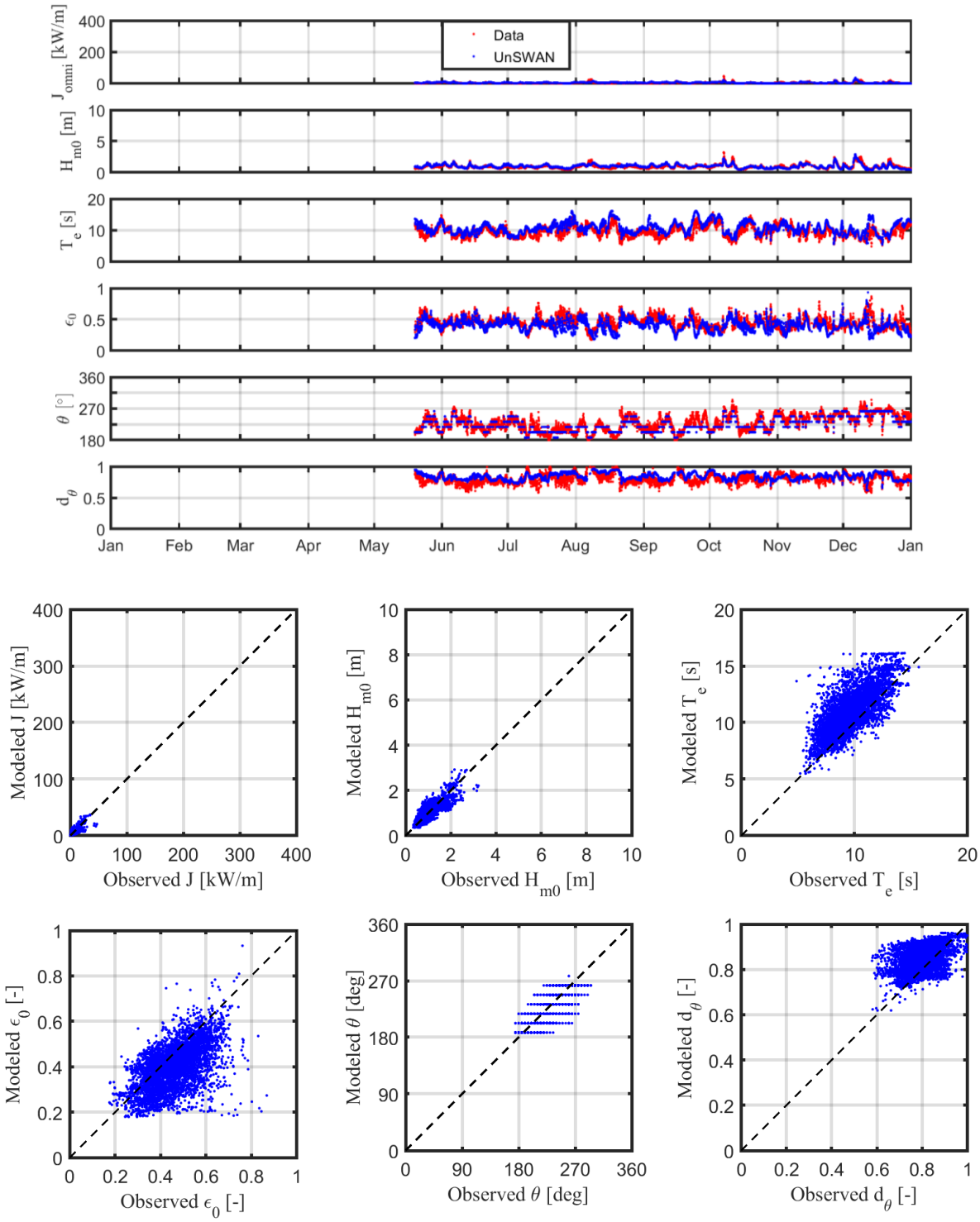

Figure B.145. Comparisons of time series (top) and scatter plots (bottom) of UnSWAN simulated six IEC parameters with observed data at CDIP Buoy 46224 for 1997.

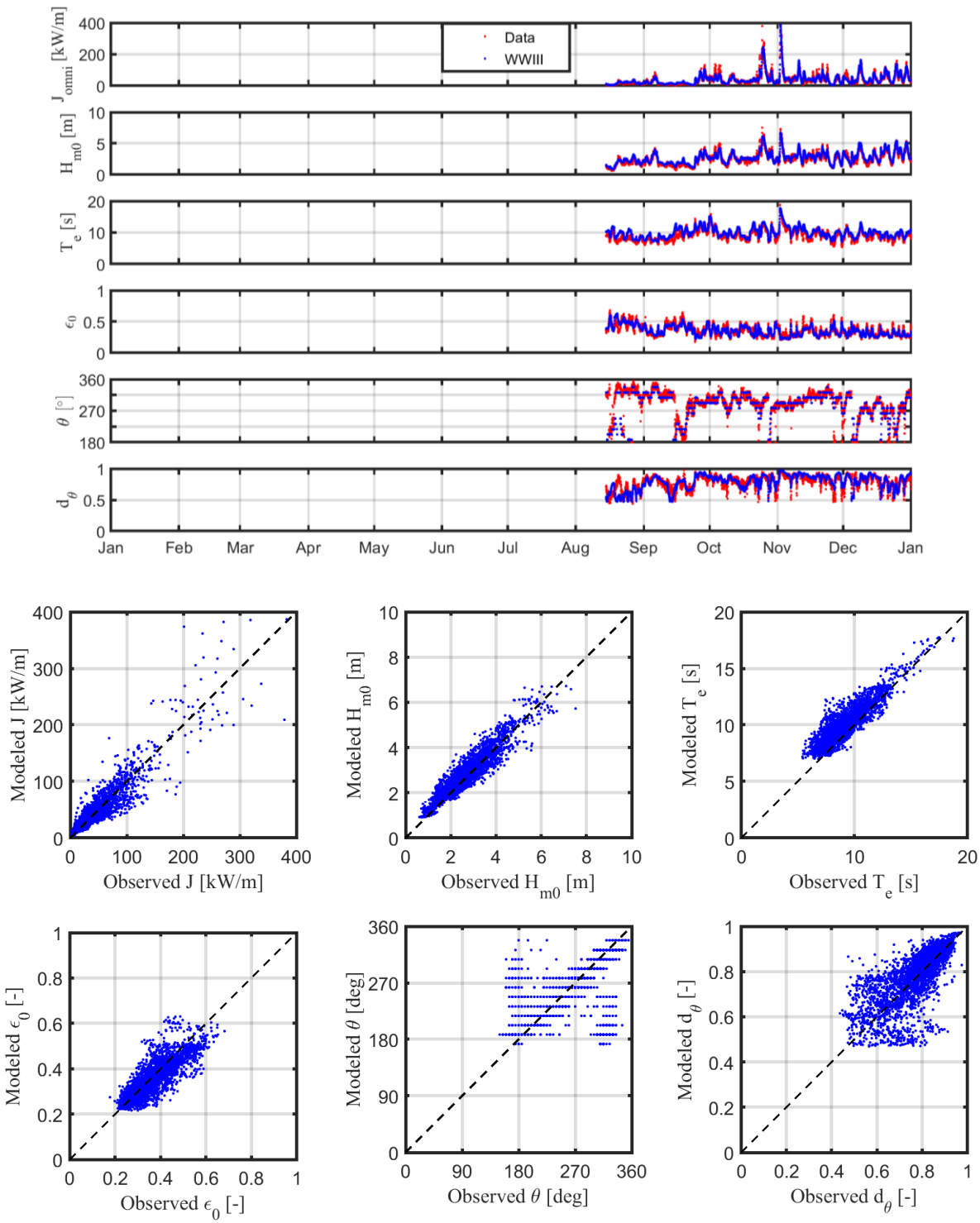

Figure B.146. Comparisons of time series (top) and scatter plots (bottom) of the six WWIII model-simulated IEC parameters with observed data at CDIP Buoy 46213 for 2010.

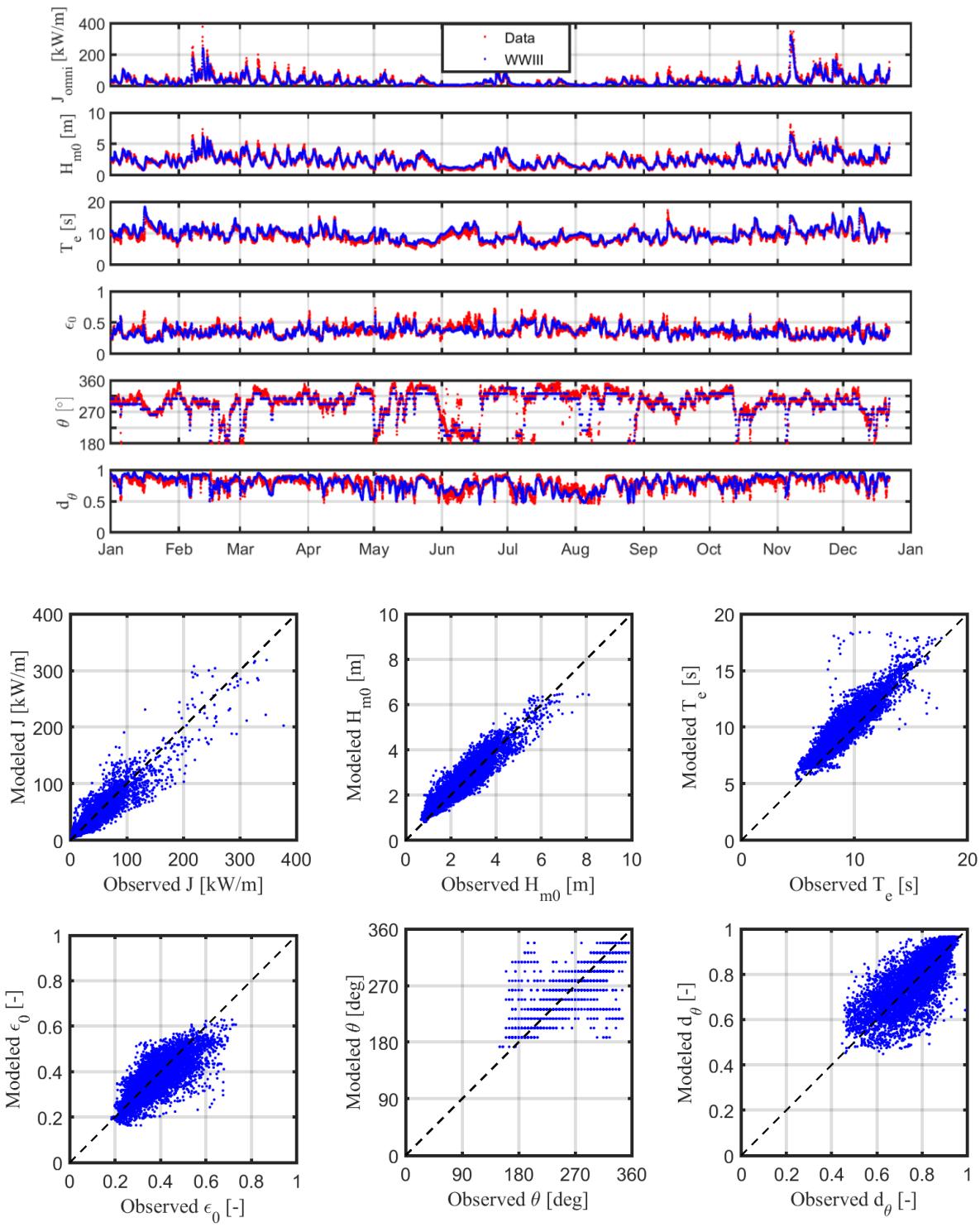

Figure B.147. Comparisons of time series (top) and scatter plots (bottom) of the six WWIII model-simulated IEC parameters with observed data at CDIP Buoy 46213 for 2009.

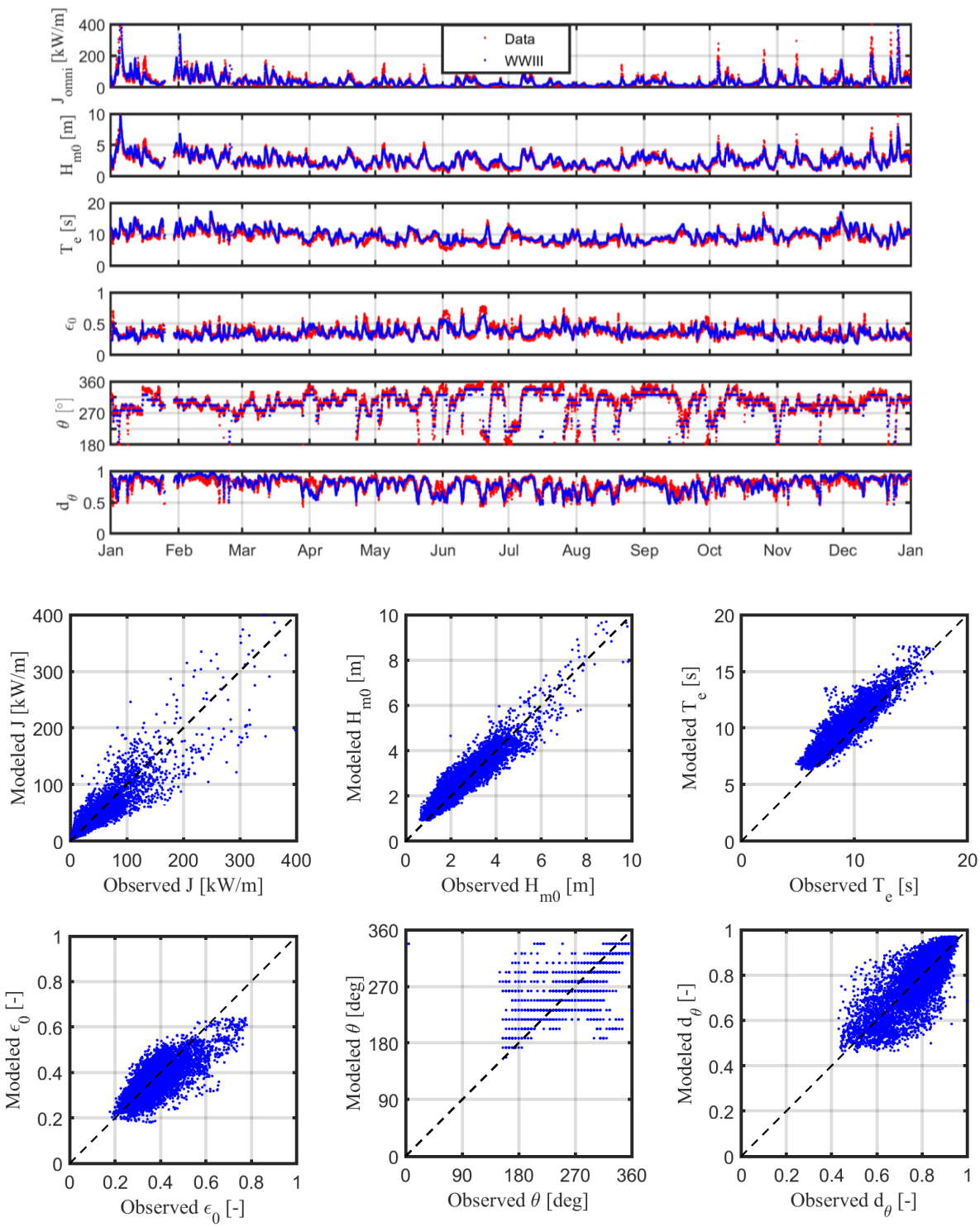

Figure B.148. Comparisons of time series (top) and scatter plots (bottom) of the six WWIII model-simulated IEC parameters with observed data at CDIP Buoy 46213 for 2008.

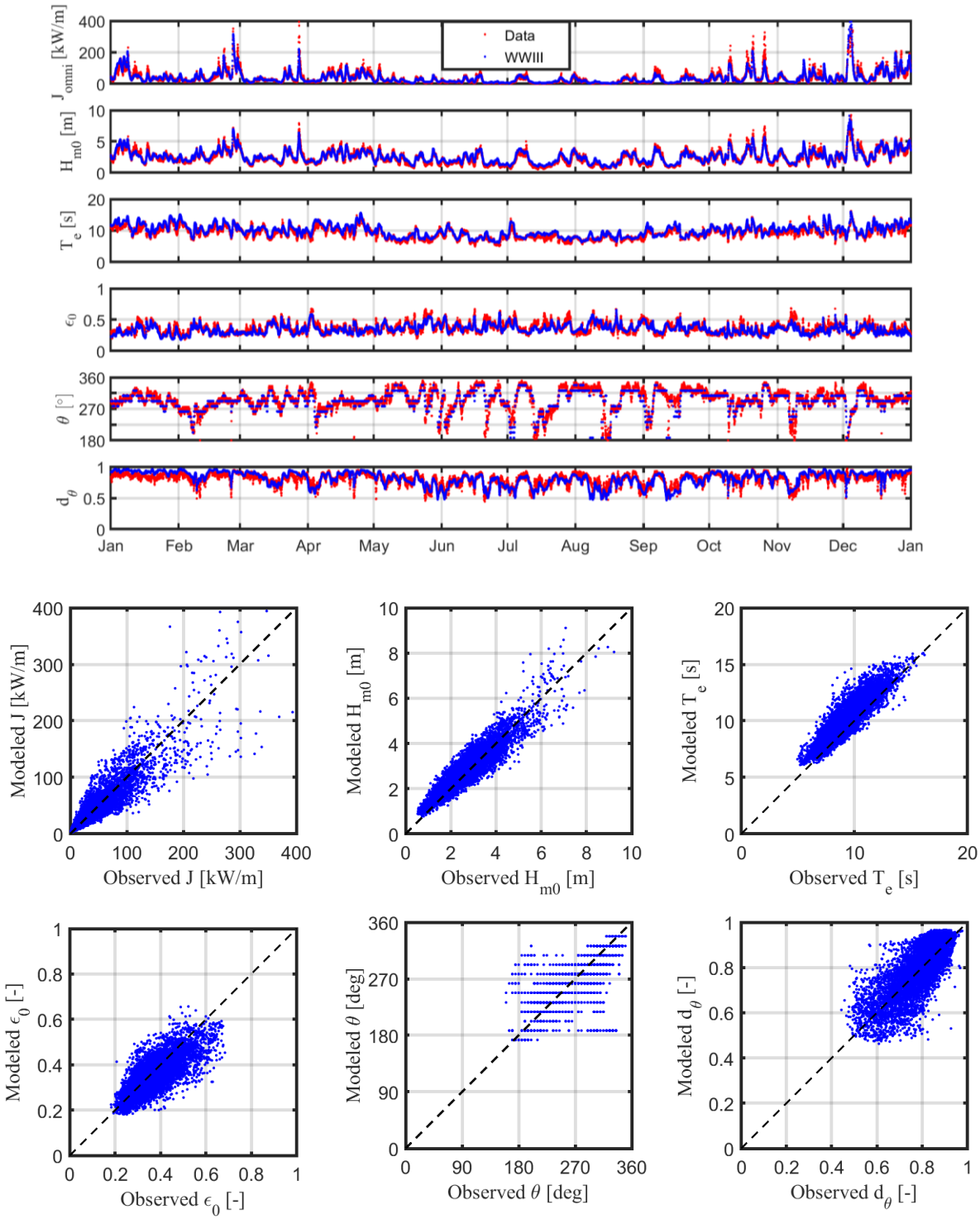

Figure B.149. Comparisons of time series (top) and scatter plots (bottom) of the six WWIII model-simulated IEC parameters with observed data at CDIP Buoy 46213 for 2007.

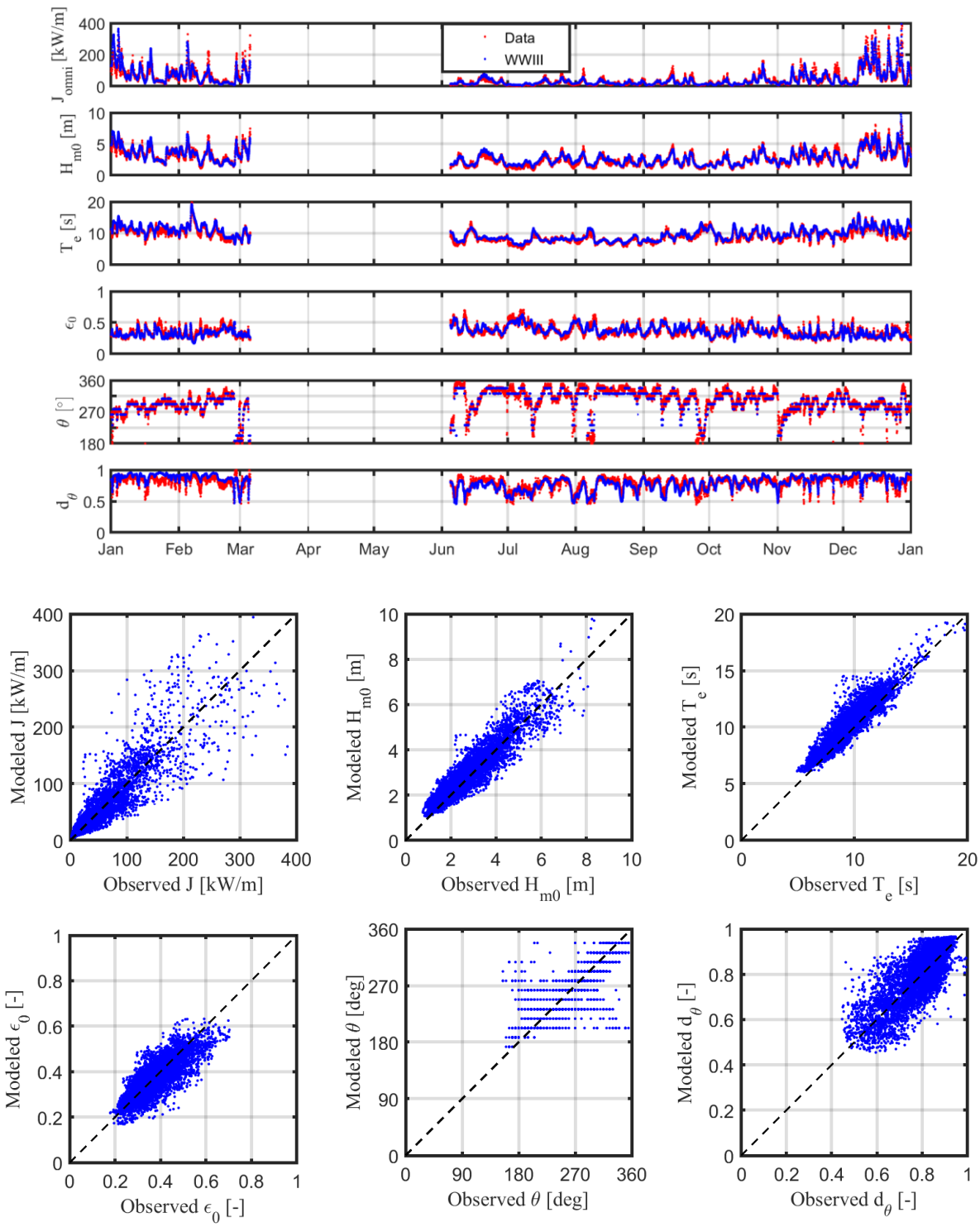

Figure B.150. Comparisons of time series (top) and scatter plots (bottom) of the six WWIII model-simulated IEC parameters with observed data at CDIP Buoy 46213 for 2006.

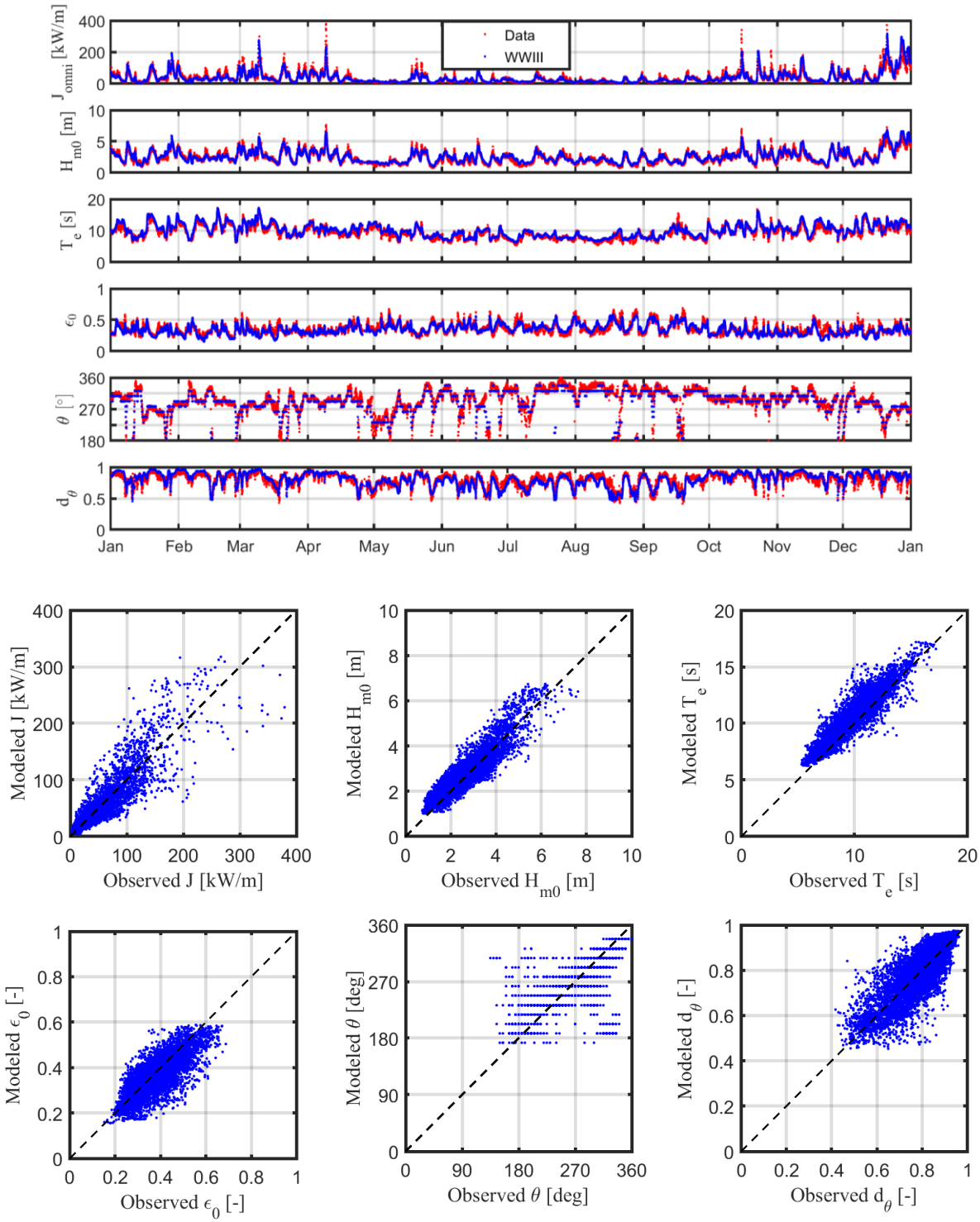

Figure B.151. Comparisons of time series (top) and scatter plots (bottom) of the six WWIII model-simulated IEC parameters with observed data at CDIP Buoy 46213 for 2005.

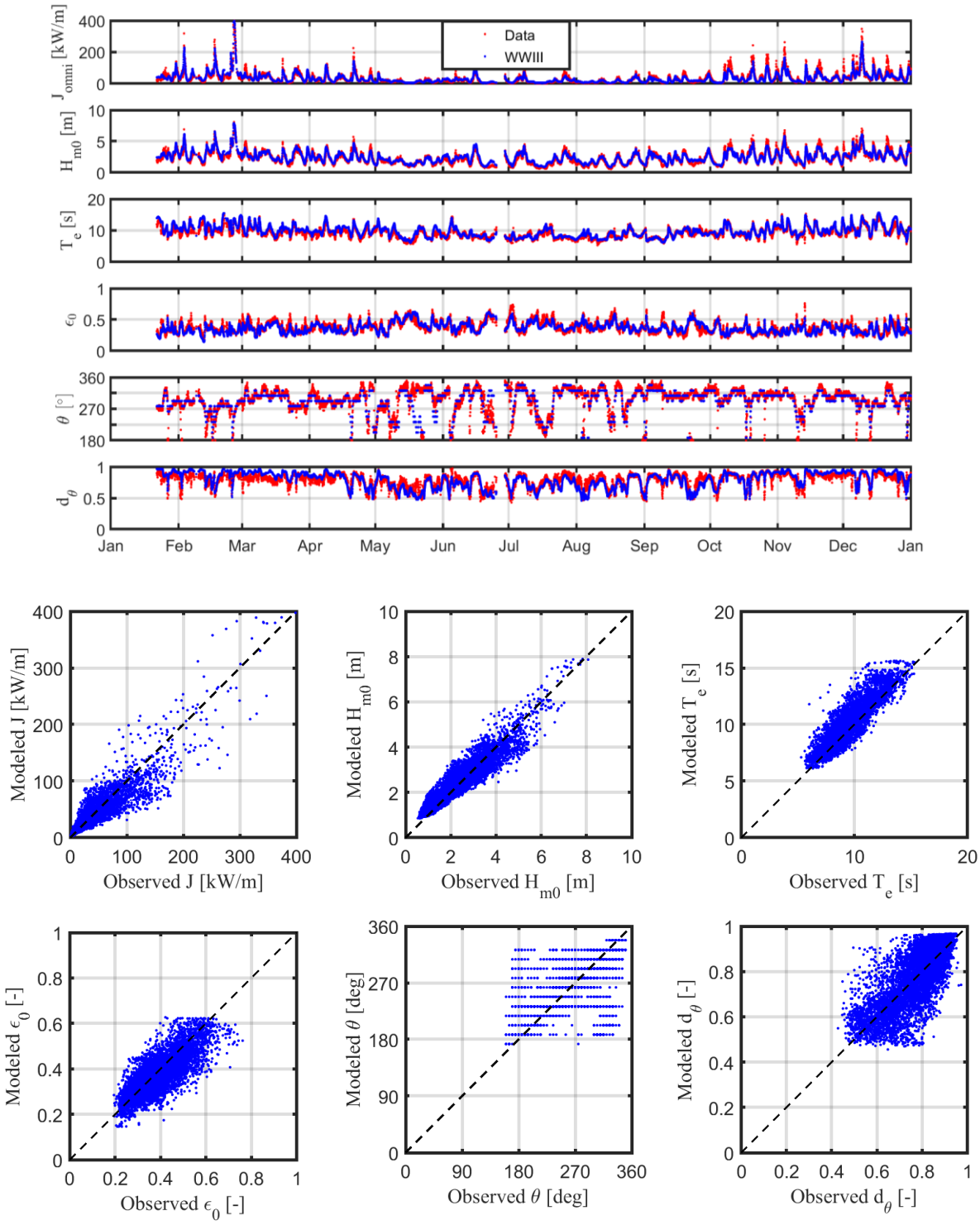

Figure B.152. Comparisons of time series (top) and scatter plots (bottom) of the six WWIII model-simulated IEC parameters with observed data at CDIP Buoy 46213 for 2004.

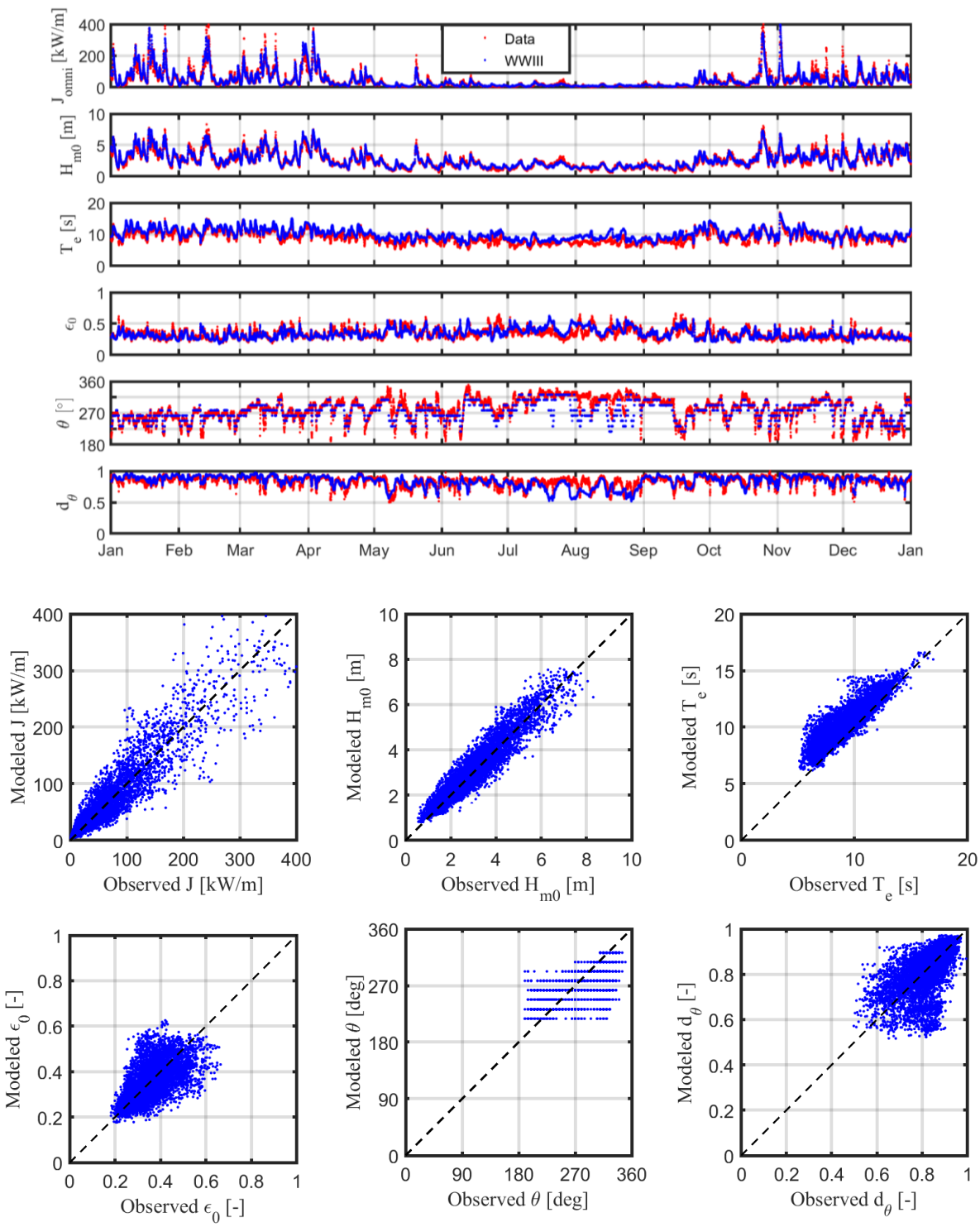

Figure B.153. Comparisons of time series (top) and scatter plots (bottom) of the six WWIII model-simulated IEC parameters with observed data at CDIP Buoy 46229 for 2010.

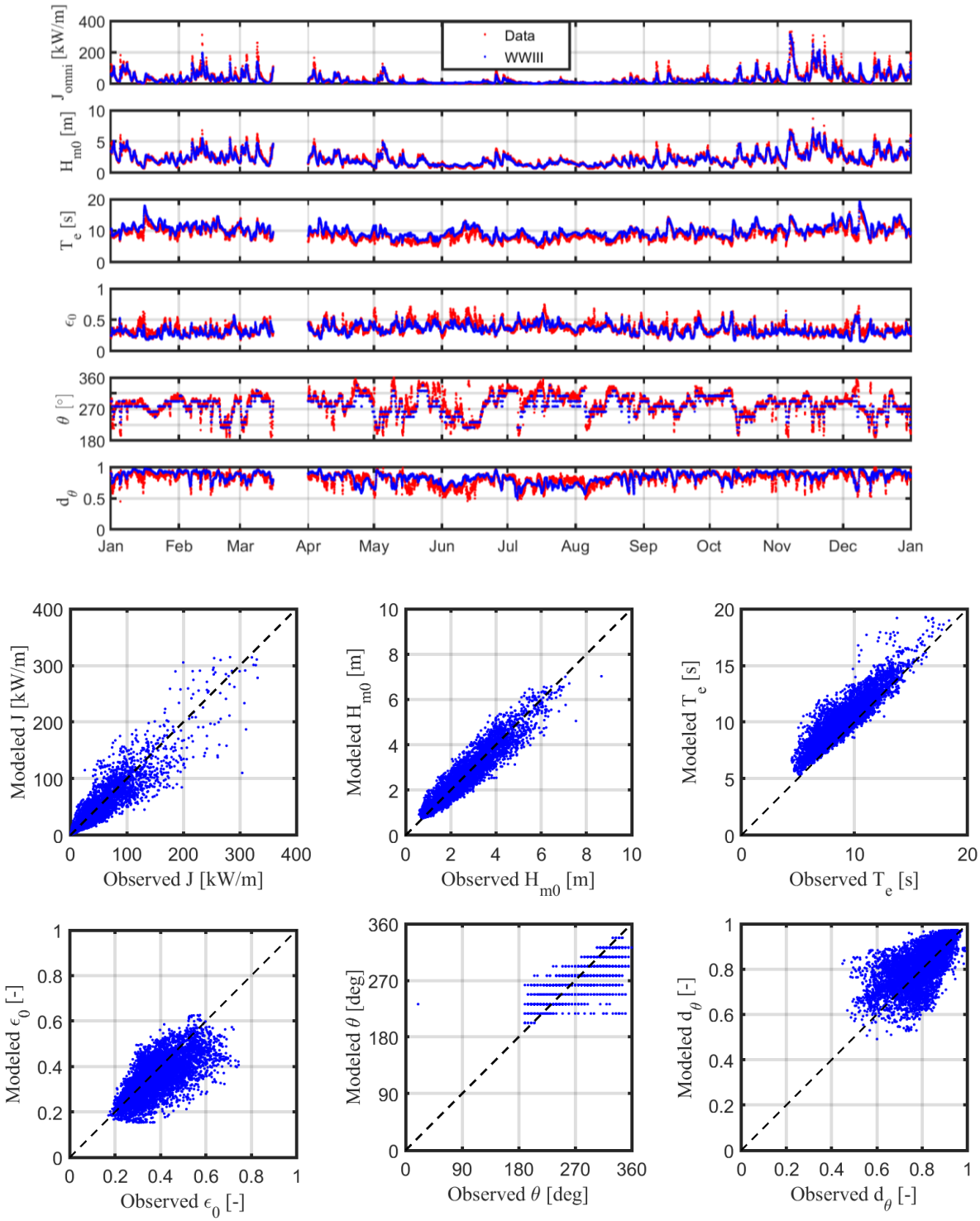

Figure B.154. Comparisons of time series (top) and scatter plots (bottom) of the six WWIII model-simulated IEC parameters with observed data at CDIP Buoy 46229 for 2009.

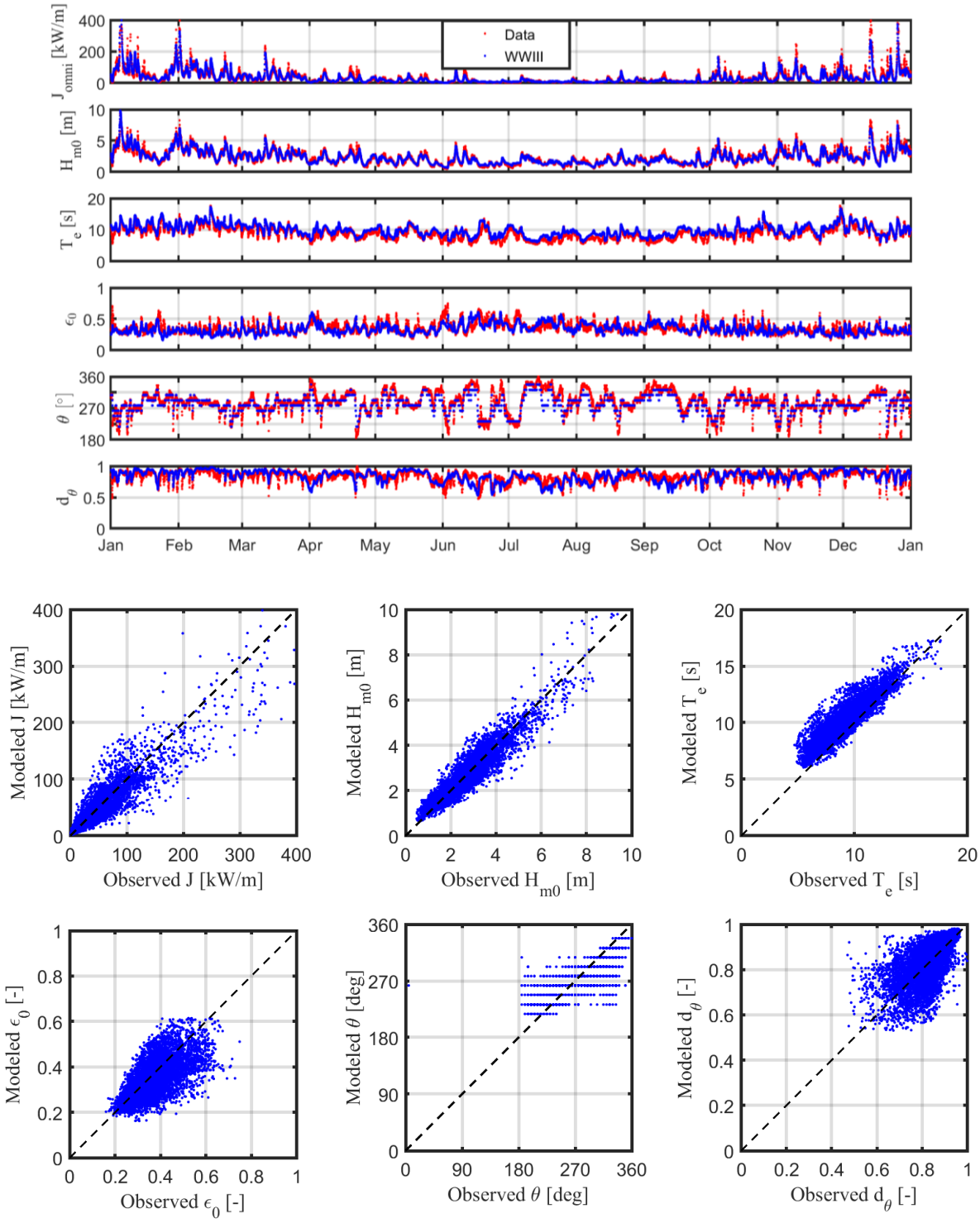

Figure B.155. Comparisons of time series (top) and scatter plots (bottom) of the six WWIII model-simulated IEC parameters with observed data at CDIP Buoy 46229 for 2008.

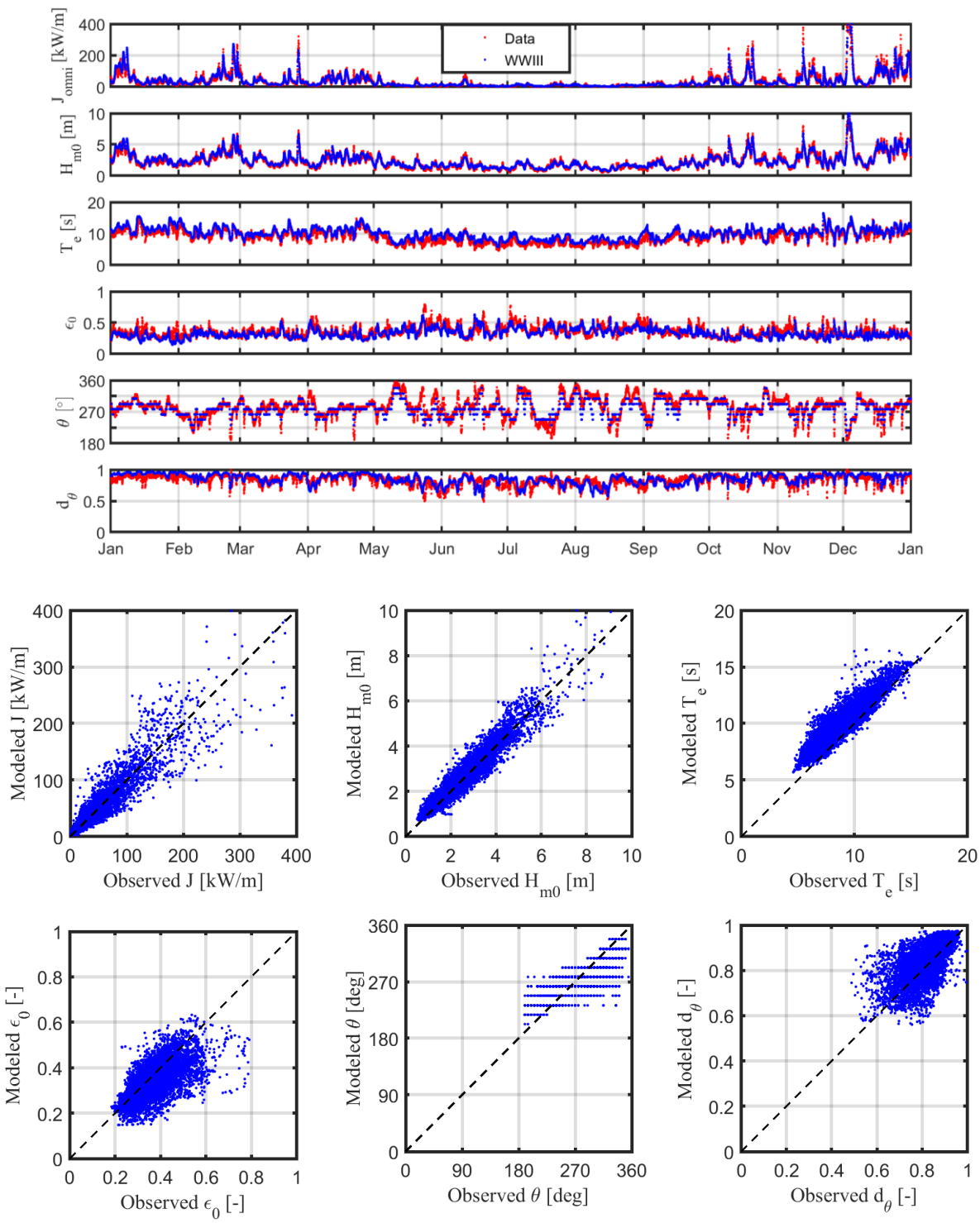

Figure B.156. Comparisons of time series (top) and scatter plots (bottom) of the six WWIII model-simulated IEC parameters with observed data at CDIP Buoy 46229 for 2007.

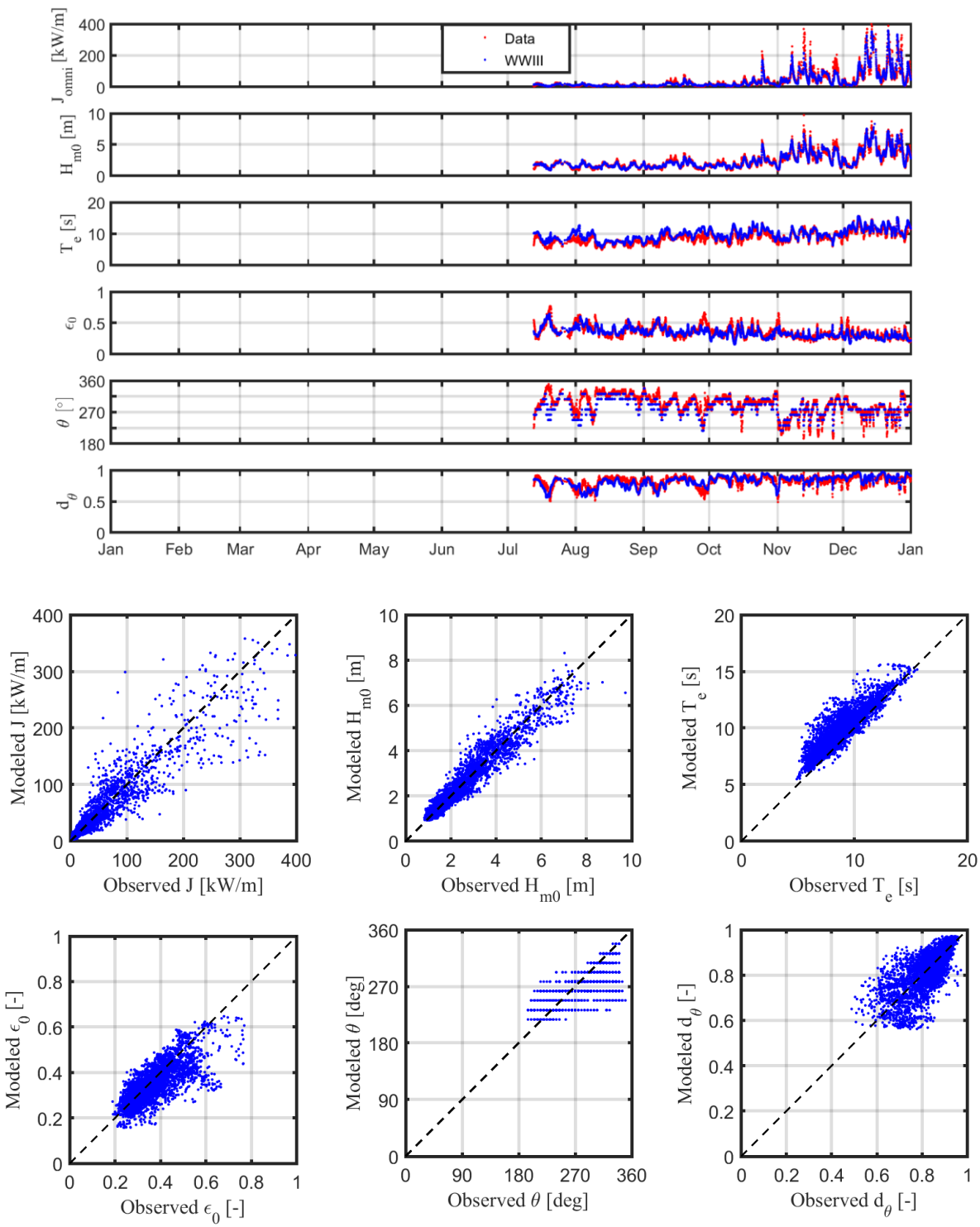

Figure B.157. Comparisons of time series (top) and scatter plots (bottom) of the six WWIII model-simulated IEC parameters with observed data at CDIP Buoy 46229 for 2006.

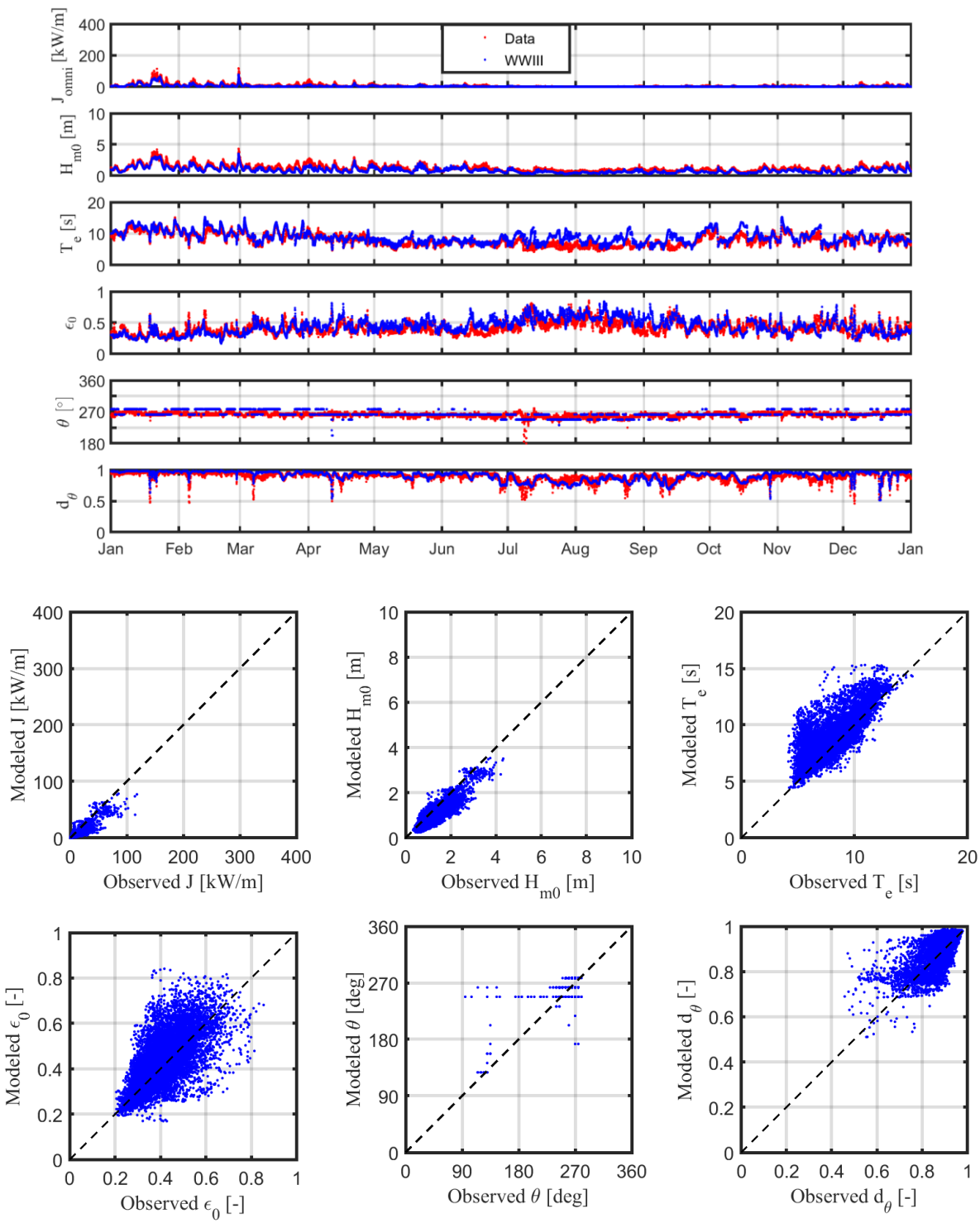

Figure B.158. Comparisons of time series (top) and scatter plots (bottom) of the six WWIII model-simulated IEC parameters with observed data at CDIP Buoy 46216 for 2010.

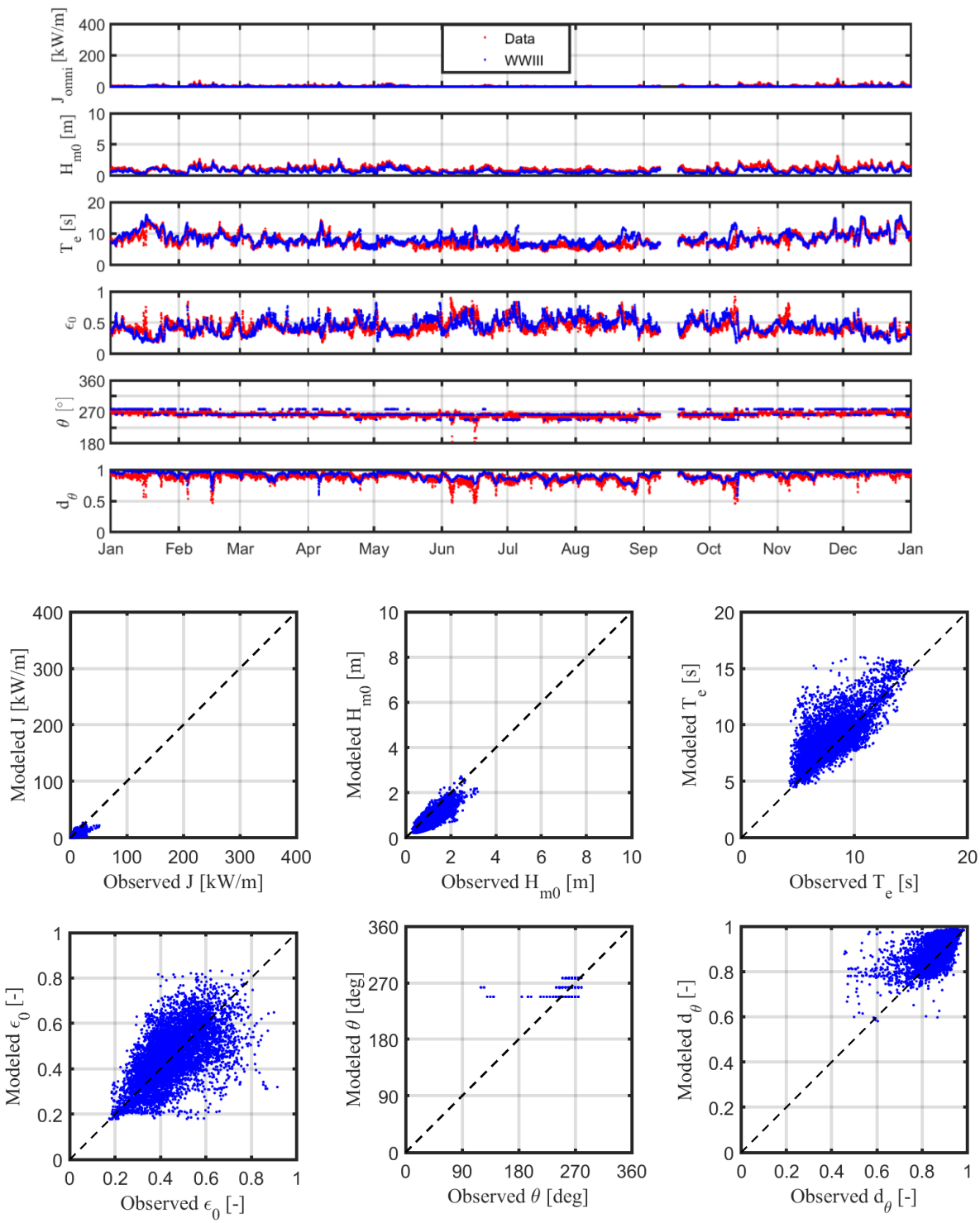

Figure B.159. Comparisons of time series (top) and scatter plots (bottom) of the six WWIII model-simulated IEC parameters with observed data at CDIP Buoy 46216 for 2009.

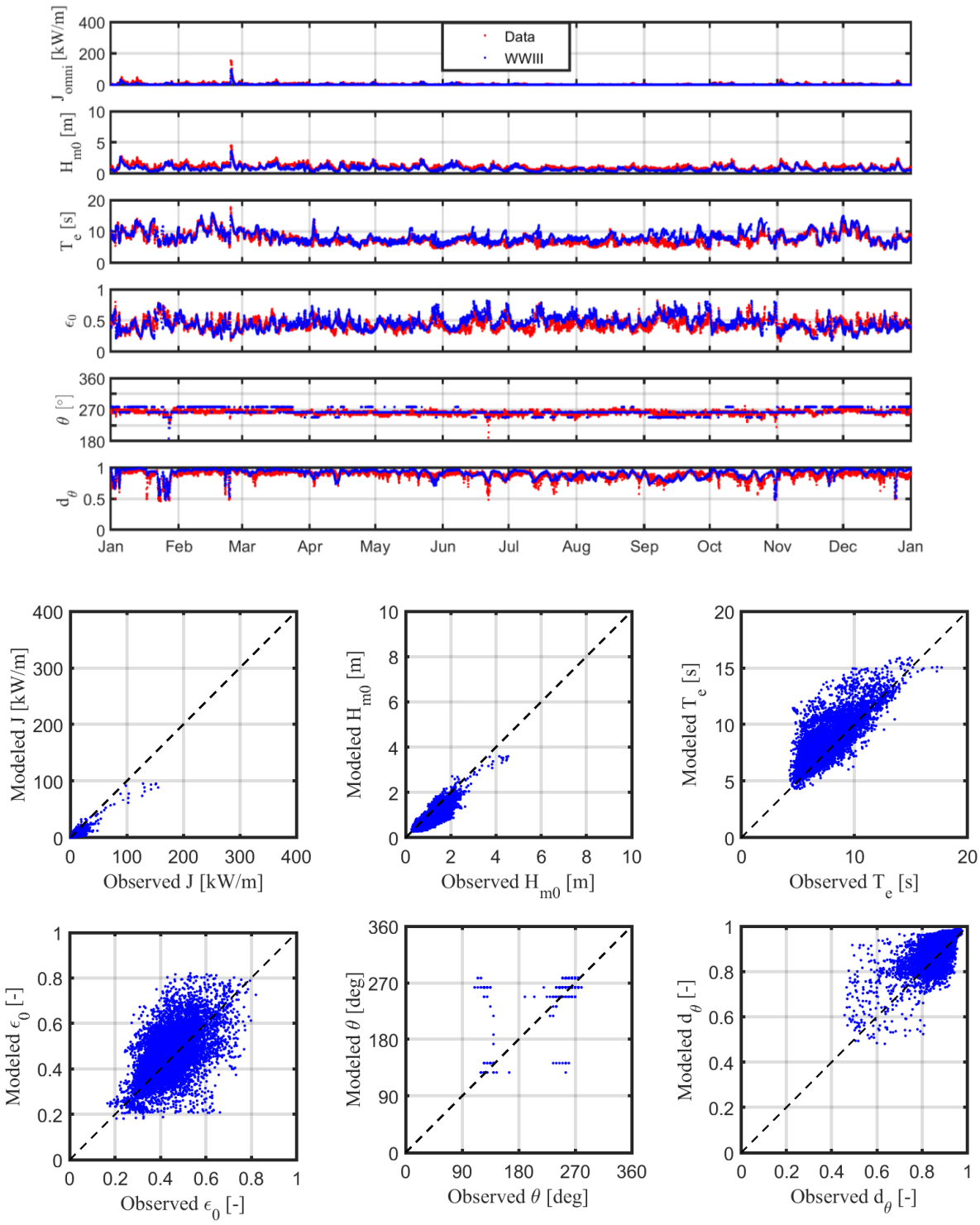

Figure B.160. Comparisons of time series (top) and scatter plots (bottom) of the six WWIII model-simulated IEC parameters with observed data at CDIP Buoy 46216 for 2008.

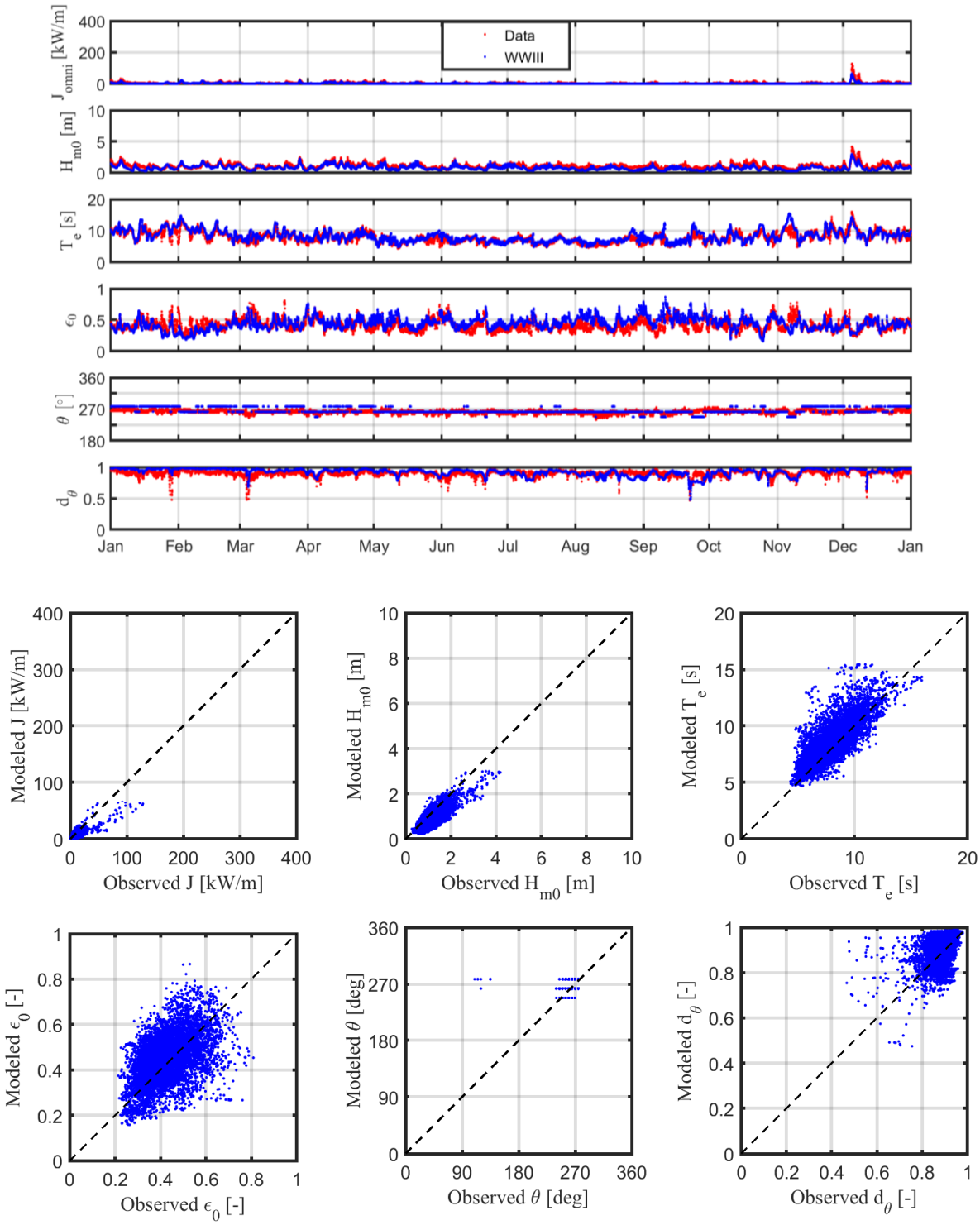

Figure B.161. Comparisons of time series (top) and scatter plots (bottom) of the six WWIII model-simulated IEC parameters with observed data at CDIP Buoy 46216 for 2007.

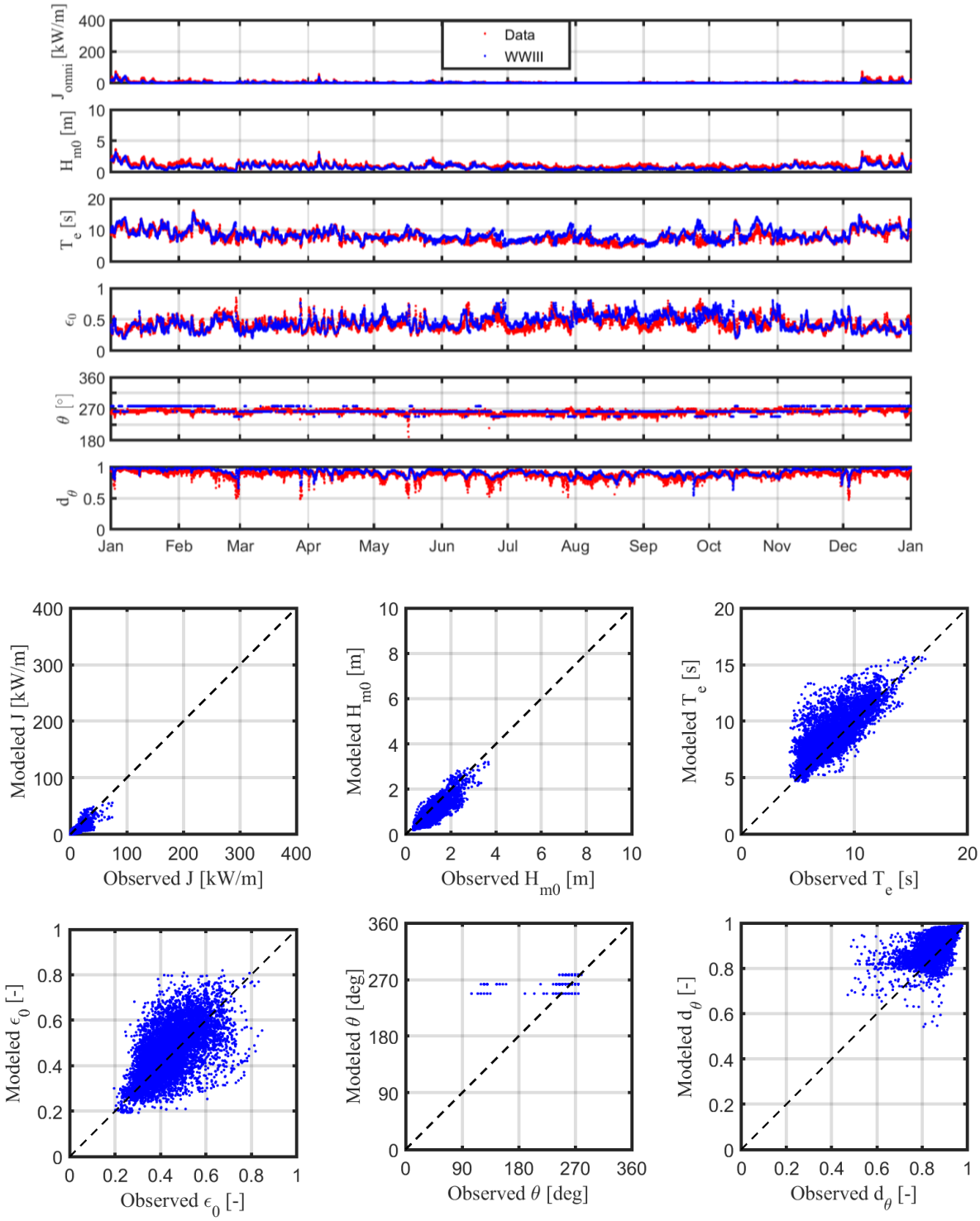

Figure B.162. Comparisons of time series (top) and scatter plots (bottom) of the six WWIII model-simulated IEC parameters with observed data at CDIP Buoy 46216 for 2006.

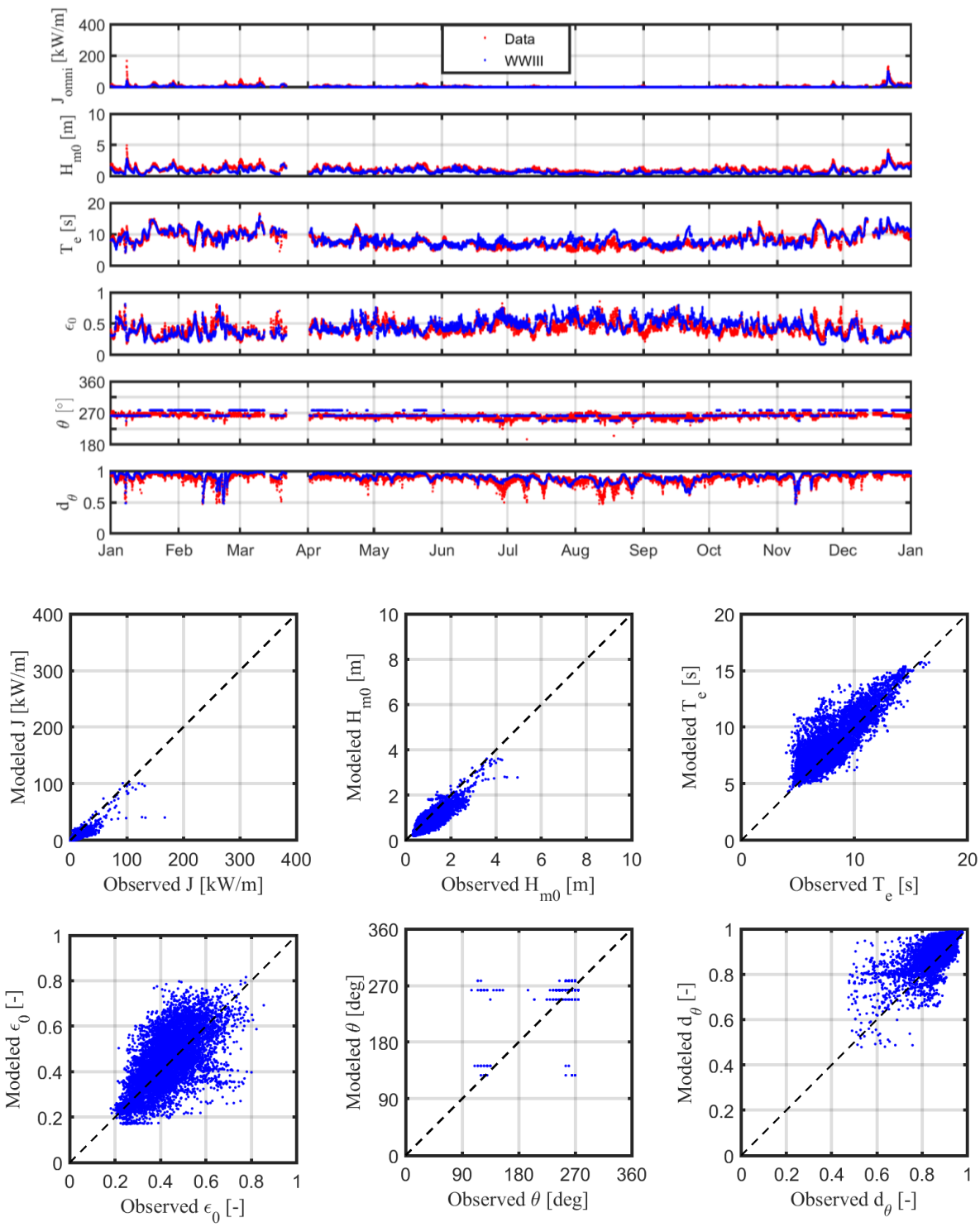

Figure B.163. Comparisons of time series (top) and scatter plots (bottom) of the six WWIII model-simulated IEC parameters with observed data at CDIP Buoy 46216 for 2005.

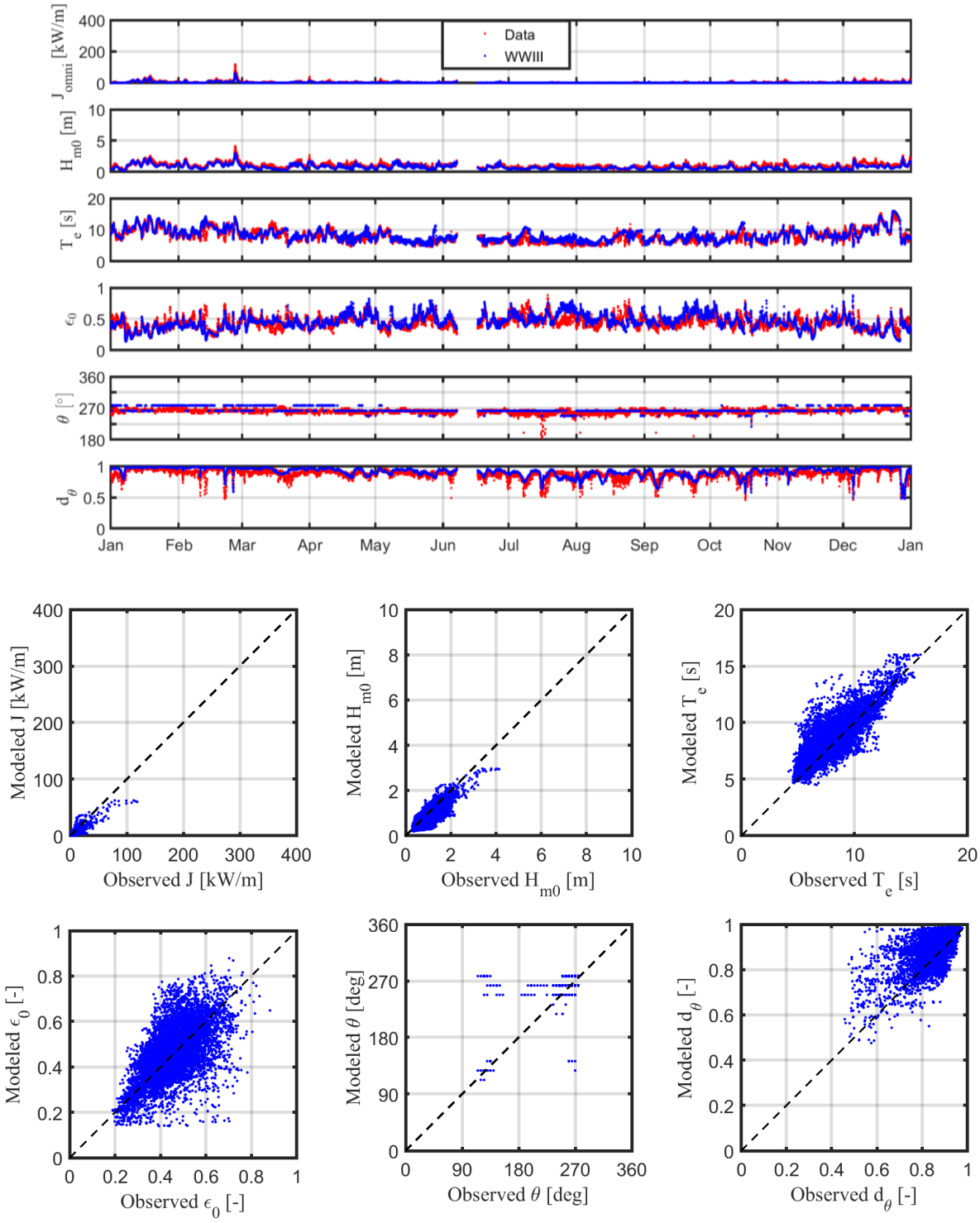

Figure B.164. Comparisons of time series (top) and scatter plots (bottom) of the six WWIII model-simulated IEC parameters with observed data at CDIP Buoy 46216 for 2004.

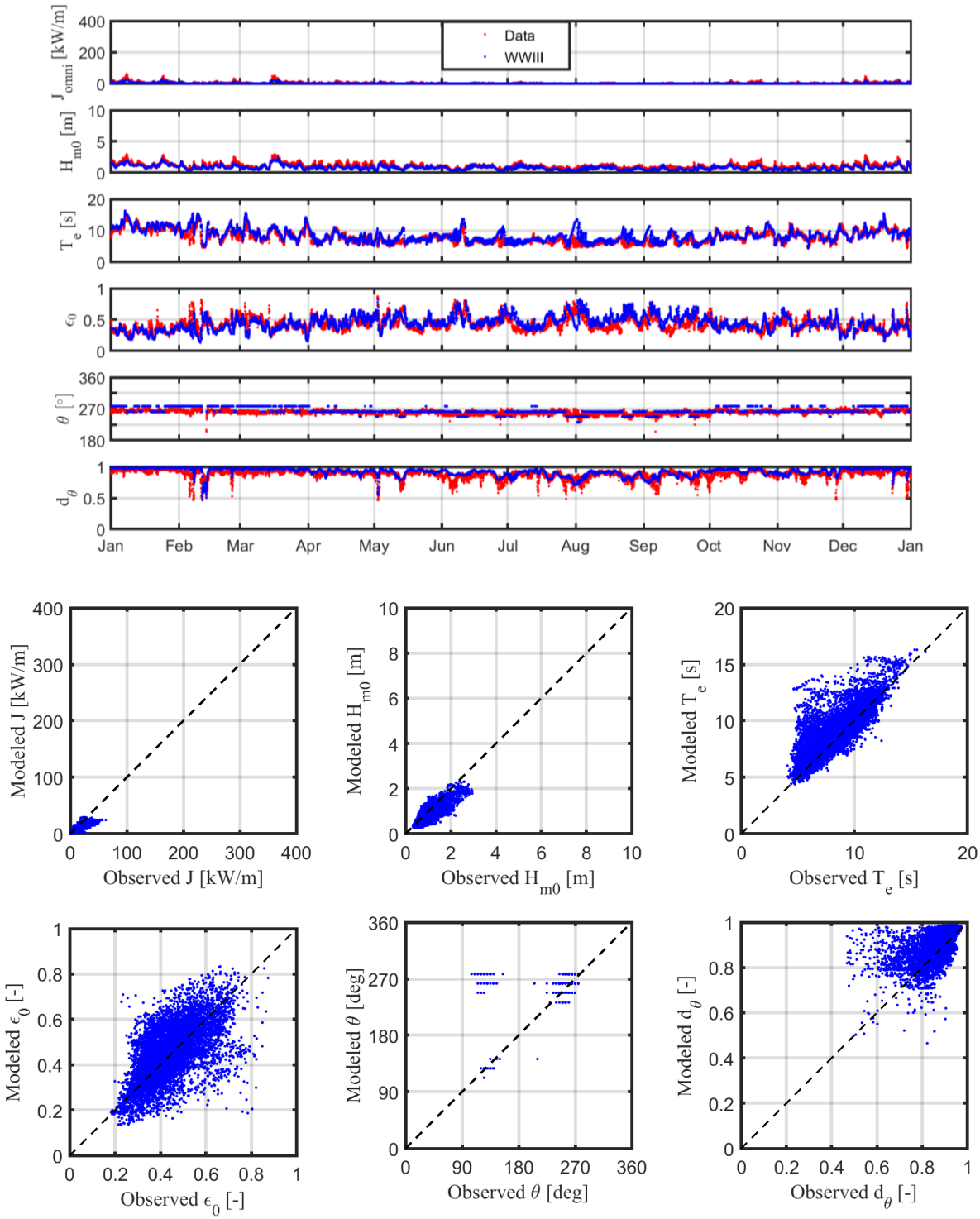

Figure B.165. Comparisons of time series (top) and scatter plots (bottom) of the six WWIII model-simulated IEC parameters with observed data at CDIP Buoy 46216 for 2003.

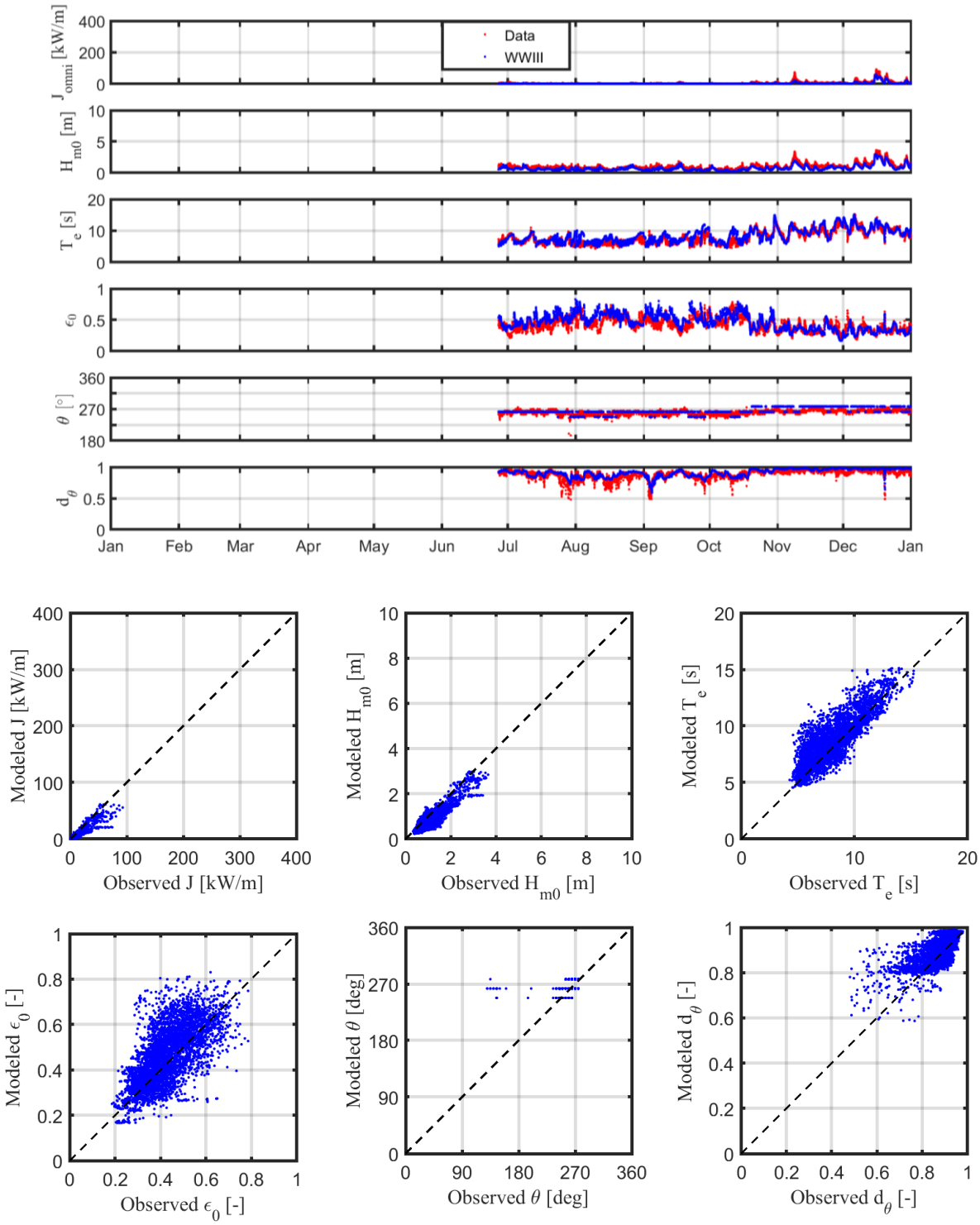

Figure B.166. Comparisons of time series (top) and scatter plots (bottom) of the six WWIII model-simulated IEC parameters with observed data at CDIP Buoy 46216 for 2002.

Appendix C – Performance Metrics for Simulated IEC Resource Parameters

Table C.1 through Table C.84 are National Data Buoy Center-related tables; Table C.85 through Table C.166 are Coastal Data Information Program-related tables.

C.1 NDBC Tables

C.1.1 Station 46029

Table C.1. WWIII performance metrics for NDBC Station 46029 for 2010.

Parameter	RMSE	PE (%)	SI	Bias	Bias (%)	R
J (kW/m)	25	42.1	0.60	9	22.1	0.94
H_s (m)	0.42	8.3	0.16	0.15	5.8	0.96
T_e (s)	1.5	14.2	0.16	1.1	12.6	0.85
ϵ_0 (-)	0.07	8.0	0.22	0.02	6.1	0.60
θ (degrees)	22.1	-1.8	0.08	-7	-2.6	0.71
d_θ (-)	0.10	-2.1	0.12	-0.03	-3.1	0.47

Table C.2. WWIII performance metrics for NDBC Station 46029 for 2009.

Parameter	RMSE	PE (%)	SI	Bias	Bias (%)	R
J (kW/m)	20	29.3	0.55	4	9.7	0.91
H_s (m)	0.38	4.9	0.16	0.05	1.9	0.95
T_e (s)	1.3	11.0	0.15	0.9	9.8	0.86
ϵ_0 (-)	0.07	3.2	0.20	0.00	1.4	0.66
θ (degrees)	22.3	2.9	0.08	-7	-2.4	0.73
d_θ (-)	0.10	0.6	0.11	-0.01	-0.7	0.52

Table C.3. WWIII performance metrics for NDBC Station 46029 for 2008.

Parameter	RMSE	PE (%)	SI	Bias	Bias (%)	R
J (kW/m)	13	50.3	0.53	3	9.9	0.93
H_s (m)	0.34	7.5	0.16	0.06	2.9	0.95
T_e (s)	1.7	13.6	0.20	1.0	11.9	0.76
ϵ_0 (-)	0.07	5.3	0.21	0.01	3.2	0.62
θ (degrees)	23.6	-2.5	0.08	-11	-3.8	0.70
d_θ (-)	0.10	-1.6	0.12	-0.02	-2.6	0.47

Table C.4. WWIII performance metrics for NDBC Station 46029 for 2007.

Parameter	RMSE	PE (%)	SI	Bias	Bias (%)	R
J (kW/m)	16	27.9	0.50	3	10.1	0.93
H_s (m)	0.34	5.6	0.15	0.06	2.4	0.96
T_e (s)	1.1	10.0	0.12	0.8	9.3	0.92
ϵ_0 (-)	0.06	-2.0	0.17	-0.01	-2.9	0.70
θ (degrees)	20.0	0.0	0.07	-2	-0.7	0.76
d_θ (-)	0.10	6.2	0.12	0.04	5.0	0.54

Table C.5. WWIII performance metrics for NDBC Station 46029 for 2006.

Parameter	RMSE	PE (%)	SI	Bias	Bias (%)	R
J (kW/m)	28	18.7	0.60	1	2.3	0.92
H_s (m)	0.41	2.3	0.16	-0.02	-0.7	0.96
T_e (s)	1.1	8.8	0.12	0.7	8.1	0.90
ϵ_0 (-)	0.05	-1.4	0.15	-0.01	-2.4	0.79
θ (degrees)	23.4	3.0	0.09	-2	-0.8	0.71
d_θ (-)	0.09	2.7	0.11	0.01	1.4	0.56

Table C.6. WWIII performance metrics for NDBC Station 46029 for 2005.

Parameter	RMSE	PE (%)	SI	Bias	Bias (%)	R
J (kW/m)	28	24.9	0.44	7	11.5	0.91
H_s (m)	0.48	5.2	0.15	0.08	2.4	0.94
T_e (s)	1.0	7.4	0.10	0.7	6.9	0.89
ϵ_0 (-)	0.06	-8.2	0.17	-0.03	-9.3	0.71
θ (degrees)	23.0	4.3	0.09	7	2.7	0.73
d_θ (-)	0.10	7.2	0.12	0.05	5.8	0.65

Table C.7. WWIII performance metrics for NDBC Station 46029 for 2004.

Parameter	RMSE	PE (%)	SI	Bias	Bias (%)	R
J (kW/m)	15	14.6	0.48	0	-0.3	0.91
H_s (m)	0.35	0.9	0.15	-0.04	-1.8	0.95
T_e (s)	1.0	8.4	0.11	0.7	7.8	0.89
ϵ_0 (-)	0.06	-2.9	0.15	-0.01	-3.6	0.77
θ (degrees)	19.7	0.4	0.07	-1	-0.5	0.74
d_θ (-)	0.09	2.2	0.11	0.01	1.2	0.57

Table C.8. WWIII performance metrics for NDBC Station 46029 for 2003.

Parameter	RMSE	PE (%)	SI	Bias	Bias (%)	R
J (kW/m)	20	19.9	0.49	2	5.3	0.94
H_s (m)	0.36	3.6	0.14	0.03	1.2	0.96
T_e (s)	1.0	8.0	0.11	0.7	7.4	0.91
ϵ_0 (-)	0.06	-3.7	0.16	-0.02	-4.4	0.78
θ (degrees)	22.3	-1.5	0.08	-6	-2.3	0.71
d_θ (-)	0.09	5.2	0.11	0.03	4.0	0.63

Table C.9. WWIII performance metrics for NDBC Station 46029 for 2002.

Parameter	RMSE	PE (%)	SI	Bias	Bias (%)	R
J (kW/m)	20	20.2	0.56	4	11.4	0.95
H_s (m)	0.34	3.4	0.15	0.04	1.5	0.97
T_e (s)	1.0	8.3	0.12	0.7	7.6	0.92
ϵ_0 (-)	0.06	-2.1	0.16	-0.01	-3.0	0.78
θ (degrees)	22.9	-2.5	0.08	-9	-3.3	0.74
d_θ (-)	0.10	3.8	0.12	0.02	2.5	0.52

Table C.10. WWIII performance metrics for NDBC Station 46029 for 2001.

Parameter	RMSE	PE (%)	SI	Bias	Bias (%)	R
J (kW/m)	20	20.6	0.49	2	5.2	0.94
H_s (m)	0.37	3.7	0.15	0.03	1.2	0.96
T_e (s)	1.0	8.1	0.11	0.7	7.2	0.92
ϵ_0 (-)	0.05	-3.2	0.15	-0.01	-4.0	0.80
θ (degrees)	19.5	-1.8	0.07	-6	-2.3	0.73
d_θ (-)	0.09	2.1	0.10	0.01	1.0	0.62

Table C.11. WWIII performance metrics for NDBC Station 46029 for 2000.

Parameter	RMSE	PE (%)	SI	Bias	Bias (%)	R
J (kW/m)	14	8.7	0.47	-1	-2.5	0.95
H_s (m)	0.33	-0.7	0.15	-0.06	-2.8	0.96
T_e (s)	1.1	5.6	0.12	0.4	4.4	0.84
ϵ_0 (-)	0.06	0.5	0.18	0.00	-1.2	0.76
θ (degrees)	29.8	-0.1	0.11	-9	-3.1	0.49
d_θ (-)	0.12	3.7	0.14	0.01	1.6	0.46

Table C.12. WWIII performance metrics for NDBC Station 46029 for 1999.

Parameter	RMSE	PE (%)	SI	Bias	Bias (%)	R
J (kW/m)	26	34.6	0.50	7	13.4	0.94
H_s (m)	0.40	8.7	0.15	0.13	4.8	0.97
T_e (s)	1.1	8.8	0.11	0.8	8.2	0.90
ϵ_0 (-)	0.05	-4.0	0.15	-0.02	-5.1	0.76
θ (degrees)	21.2	-0.4	0.08	-3	-1.3	0.68
d_θ (-)	0.10	5.4	0.12	0.03	4.0	0.54

Table C.13. WWIII performance metrics for NDBC Station 46029 for 1998.

Parameter	RMSE	PE (%)	SI	Bias	Bias (%)	R
J (kW/m)	18	40.5	0.55	4	13.1	0.95
H_s (m)	0.34	10.8	0.16	0.14	6.4	0.97
T_e (s)	1.1	9.8	0.12	0.8	8.9	0.89
ϵ_0 (-)	0.06	1.0	0.16	0.00	-0.4	0.77
θ (degrees)	24.4	-2.4	0.09	-8	-3.0	0.59
d_θ (-)	0.10	0.2	0.12	-0.01	-1.1	0.53

Table C.14. WWIII performance metrics for NDBC Station 46029 for 1997.

Parameter	RMSE	PE (%)	SI	Bias	Bias (%)	R
J (kW/m)	30	83.7	0.69	23	53.0	0.90
H_s (m)	0.72	27.6	0.26	0.59	21.6	0.92
T_e (s)	1.0	6.3	0.10	0.6	6.2	0.88
ϵ_0 (-)	0.06	14.1	0.20	0.04	12.5	0.66
θ (degrees)	25.3	0.9	0.10	1	0.6	0.22
d_θ (-)	0.08	-1.1	0.09	-0.02	-1.8	0.60

C.1.2 Station 46050

Table C.15. WWIII performance metrics for NDBC Station 46050 for 2010.

Parameter	RMSE	PE (%)	SI	Bias	Bias (%)	R
J (kW/m)	23	32.8	0.54	7	15.9	0.93
H_s (m)	0.41	4.7	0.16	0.07	2.8	0.95
T_e (s)	1.5	14.3	0.16	1.1	12.5	0.87
ϵ_0 (-)	0.08	8.4	0.23	0.02	6.7	0.54
θ (degrees)	27.5	-1.5	0.10	-7	-2.5	0.69
d_θ (-)	0.11	5.3	0.14	0.03	4.0	0.33

Table C.16. WWIII performance metrics for NDBC Station 46050 for 2009.

Parameter	RMSE	PE (%)	SI	Bias	Bias (%)	R
J (kW/m)	15	29.6	0.49	3	10.4	0.93
H_s (m)	0.36	4.8	0.16	0.04	1.8	0.95
T_e (s)	1.3	11.4	0.14	0.9	10.3	0.90
ϵ_0 (-)	0.07	5.3	0.21	0.01	3.2	0.63
θ (degrees)	26.0	3.8	0.09	-8	-2.9	0.63
d_θ (-)	0.12	7.4	0.15	0.04	5.6	0.37

Table C.17. WWIII performance metrics for NDBC Station 46050 for 2008.

Parameter	RMSE	PE (%)	SI	Bias	Bias (%)	R
J (kW/m)	13	29.8	0.52	2	7.3	0.92
H_s (m)	0.35	4.9	0.17	0.03	1.2	0.94
T_e (s)	1.2	11.5	0.14	0.9	10.2	0.88
ϵ_0 (-)	0.08	8.6	0.23	0.02	6.6	0.56
θ (degrees)	22.0	-2.2	0.08	-8	-2.8	0.77
d_θ (-)	0.11	3.4	0.13	0.02	2.2	0.37

C.1.3 Station 46027

Table C.18. UnSWAN performance metrics for NDBC Station 46027 for 2010.

Parameter	RMSE	PE (%)	SI	Bias	Bias (%)	R
J (kW/m)	23	27.0	0.59	6	15.4	0.91
H_s (m)	0.43	2.6	0.17	0.01	0.3	0.92
T_e (s)	1.3	13.3	0.15	1.1	12.3	0.91
ϵ_0 (-)	0.08	7.8	0.23	0.02	6.4	0.54
θ (degrees)	18.2	-1.7	0.06	-6	-2.2	0.81
d_θ (-)	0.10	0.4	0.12	0.00	-0.4	0.35

Table C.19. UnSWAN performance metrics for NDBC Station 46027 for 2009.

Parameter	RMSE	PE (%)	SI	Bias	Bias (%)	R
J (kW/m)	15	26.4	0.53	2	7.8	0.90
H_s (m)	0.43	3.2	0.20	-0.03	-1.4	0.89
T_e (s)	1.3	10.9	0.14	0.9	9.9	0.90
ϵ_0 (-)	0.07	4.0	0.21	0.01	2.4	0.59
θ (degrees)	15.6	-2.1	0.05	-7	-2.4	0.84
d_θ (-)	0.08	1.2	0.09	0.00	0.5	0.58

Table C.20. UnSWAN performance metrics for NDBC Station 46027 for 2008.

Parameter	RMSE	PE (%)	SI	Bias	Bias (%)	R
J (kW/m)	12	17.7	0.48	-1	-3.5	0.92
H_s (m)	0.42	0.1	0.20	-0.10	-5.0	0.90
T_e (s)	1.1	10.5	0.13	0.8	9.6	0.92
ϵ_0 (-)	0.07	5.3	0.21	0.01	3.2	0.61
θ (degrees)	15.1	-2.1	0.05	-7	-2.4	0.84
d_θ (-)	0.09	-0.3	0.10	-0.01	-1.0	0.46

Table C.21. UnSWAN performance metrics for NDBC Station 46027 for 2007.

Parameter	RMSE	PE (%)	SI	Bias	Bias (%)	R
J (kW/m)	14	25.0	0.58	1	3.2	0.89
H_s (m)	0.42	2.8	0.21	-0.06	-2.8	0.89
T_e (s)	1.1	10.5	0.13	0.8	9.8	0.92
ϵ_0 (-)	0.07	5.9	0.22	0.01	3.6	0.54
θ (degrees)	14.2	-1.8	0.05	-6	-2.0	0.81
d_θ (-)	0.08	0.8	0.09	0.00	0.1	0.51

Table C.22. UnSWAN performance metrics for NDBC Station 46027 for 2006.

Parameter	RMSE	PE (%)	SI	Bias	Bias (%)	R
J (kW/m)	22	9.5	0.58	0	-0.5	0.91
H_s (m)	0.49	-3.0	0.20	-0.14	-5.9	0.91
T_e (s)	1.1	9.7	0.13	0.8	9.0	0.92
ϵ_0 (-)	0.07	7.0	0.21	0.02	5.5	0.64
θ (degrees)	15.8	-2.2	0.05	-7	-2.4	0.83
d_θ (-)	0.09	0.2	0.10	0.00	-0.5	0.45

Table C.23. UnSWAN performance metrics for NDBC Station 46027 for 2005.

Parameter	RMSE	PE (%)	SI	Bias	Bias (%)	R
J (kW/m)	29	15.4	0.44	6	9.0	0.89
H_s (m)	0.49	1.6	0.16	0.01	0.2	0.92
T_e (s)	1.0	7.7	0.10	0.8	7.4	0.91
ϵ_0 (-)	0.04	-4.9	0.13	-0.02	-5.2	0.84
θ (degrees)	10.5	-0.4	0.04	-2	-0.6	0.89
d_θ (-)	0.06	2.5	0.07	0.02	2.0	0.72

C.1.4 Station 46022

Table C.24. UnSWAN performance metrics for NDBC Station 46022 for 2010.

Parameter	RMSE	PE (%)	SI	Bias	Bias (%)	R
J (kW/m)	47	43.0	0.67	24	34.7	0.88
H_s (m)	0.66	11.3	0.20	0.34	10.1	0.91
T_e (s)	1.4	10.8	0.14	1.1	10.2	0.84
ϵ_0 (-)	0.05	-0.2	0.17	0.00	-1.4	0.61
θ (degrees)	25.2	7.0	0.10	15	6.1	0.72
d_θ (-)	0.10	8.0	0.12	0.06	7.2	0.46

Table C.25. UnSWAN performance metrics for NDBC Station 46022 for 2009.

Parameter	RMSE	PE (%)	SI	Bias	Bias (%)	R
J (kW/m)	15	36.2	0.51	4	11.9	0.90
H_s (m)	0.43	10.0	0.19	0.10	4.5	0.91
T_e (s)	1.1	7.3	0.12	0.6	6.7	0.89
ϵ_0 (-)	0.07	8.5	0.21	0.02	6.7	0.64
θ (degrees)	31.5	-4.1	0.10	-15	-4.9	0.78
d_θ (-)	0.11	5.1	0.14	0.03	3.4	0.55

Table C.26. UnSWAN performance metrics for NDBC Station 46022 for 2008.

Parameter	RMSE	PE (%)	SI	Bias	Bias (%)	R
J (kW/m)	17	43.0	0.56	5	16.8	0.92
H_s (m)	0.42	13.0	0.19	0.17	7.5	0.93
T_e (s)	1.0	7.5	0.11	0.6	6.8	0.91
ϵ_0 (-)	0.07	9.6	0.21	0.02	7.5	0.64
θ (degrees)	29.3	-3.0	0.09	-11	-3.6	0.79
d_θ (-)	0.11	2.4	0.13	0.01	0.9	0.55

Table C.27. UnSWAN performance metrics for NDBC Station 46022 for 2007.

Parameter	RMSE	PE (%)	SI	Bias	Bias (%)	R
J (kW/m)	18	39.9	0.59	4	12.7	0.93
H_s (m)	0.41	12.1	0.19	0.14	6.1	0.94
T_e (s)	0.9	7.0	0.11	0.6	6.4	0.91
ϵ_0 (-)	0.07	10.8	0.21	0.03	8.6	0.59
θ (degrees)	29.2	-2.8	0.10	-11	-3.6	0.70
d_θ (-)	0.10	3.6	0.12	0.02	2.1	0.59

C.1.5 Station 46026

Table C.28. UnSWAN performance metrics for NDBC Station 46026 for 2010.

Parameter	RMSE	PE (%)	SI	Bias	Bias (%)	R
J (kW/m)	19	69.7	0.81	11	44.8	0.90
H_s (m)	0.44	19.6	0.22	0.29	15.0	0.92
T_e (s)	1.4	12.9	0.15	1.1	11.8	0.88
ϵ_0 (-)	0.06	-0.3	0.16	0.00	-1.4	0.75
θ (degrees)	24.0	-1.1	0.08	-4	-1.4	0.50
d_θ (-)	0.12	8.9	0.17	0.05	7.4	0.58

Table C.29. UnSWAN performance metrics for NDBC Station 46026 for 2009.

Parameter	RMSE	PE (%)	SI	Bias	Bias (%)	R
J (kW/m)	12	51.2	0.58	6	30.2	0.91
H_s (m)	0.34	13.1	0.18	0.17	8.9	0.92
T_e (s)	1.3	11.8	0.15	1.0	10.7	0.89
ϵ_0 (-)	0.06	-4.3	0.17	-0.02	-5.6	0.74
θ (degrees)	15.2	0.5	0.05	1	0.2	0.81
d_θ (-)	0.10	1.3	0.12	0.00	0.2	0.60

Table C.30. UnSWAN performance metrics for NDBC Station 46026 for 2008.

Parameter	RMSE	PE (%)	SI	Bias	Bias (%)	R
J (kW/m)	14	46.8	0.60	6	26.5	0.93
H_s (m)	0.34	12.4	0.17	0.16	8.1	0.94
T_e (s)	1.3	12.0	0.14	1.0	11.0	0.91
ϵ_0 (-)	0.06	-5.1	0.17	-0.02	-6.3	0.73
θ (degrees)	16.0	0.2	0.06	0	0.0	0.77
d_θ (-)	0.08	-2.2	0.10	-0.02	-2.9	0.74

Table C.31. UnSWAN performance metrics for NDBC Station 46026 for 2007.

Parameter	RMSE	PE (%)	SI	Bias	Bias (%)	R
J (kW/m)	10	37.9	0.51	4	18.0	0.92
H_s (m)	0.33	14.3	0.18	0.19	10.4	0.94
T_e (s)	1.2	11.7	0.14	0.9	10.5	0.91
ϵ_0 (-)	0.06	-4.5	0.16	-0.02	-5.4	0.77
θ (degrees)	15.9	1.5	0.06	4	1.3	0.65
d_θ (-)	0.07	-1.0	0.09	-0.01	-1.4	0.77

C.1.6 Station 46015

Table C.32. WWIII performance metrics for NDBC Station 46015 for 2010.

Parameter	RMSE	PE (%)	SI	Bias	Bias (%)	R
J (kW/m)	22	35.1	0.52	6	14.8	0.92
H_s (m)	0.42	6.1	0.16	0.09	3.6	0.94
T_e (s)	1.6	15.2	0.17	1.2	13.3	0.86
ϵ_0 (-)	0.08	8.3	0.23	0.02	6.5	0.61
θ (degrees)	35.8	-3.5	0.12	-13	-4.5	0.57
d_θ (-)	0.12	3.6	0.16	0.02	2.2	0.36

Table C.33. WWIII performance metrics for NDBC Station 46015 for 2009.

Parameter	RMSE	PE (%)	SI	Bias	Bias (%)	R
J (kW/m)	22	35.1	0.52	6	14.8	0.92
H_s (m)	0.42	6.1	0.16	0.09	3.6	0.94
T_e (s)	1.6	15.2	0.17	1.2	13.3	0.86
ϵ_0 (-)	0.08	8.3	0.23	0.02	6.5	0.61
θ (degrees)	35.8	-3.5	0.12	-13	-4.5	0.57
d_θ (-)	0.12	3.6	0.16	0.02	2.2	0.36

Table C.34. WWIII performance metrics for NDBC Station 46015 for 2008.

Parameter	RMSE	PE (%)	SI	Bias	Bias (%)	R
J (kW/m)	20	37.7	0.52	5	12.8	0.92
H_s (m)	0.42	8.5	0.17	0.10	4.2	0.94
T_e (s)	1.3	11.3	0.14	0.9	10.1	0.89
ϵ_0 (-)	0.07	3.2	0.21	0.00	0.9	0.62
θ (degrees)	27.7	-2.5	0.09	-9	-3.2	0.70
d_θ (-)	0.13	5.8	0.16	0.03	3.9	0.37

Table C.35. WWIII performance metrics for NDBC Station 46015 for 2007.

Parameter	RMSE	PE (%)	SI	Bias	Bias (%)	R
J (kW/m)	18	30.7	0.56	3	9.3	0.96
H_s (m)	0.35	6.4	0.16	0.05	2.4	0.96
T_e (s)	1.2	11.2	0.14	0.9	10.3	0.90
ϵ_0 (-)	0.07	8.0	0.22	0.02	5.7	0.57
θ (degrees)	26.5	-3.9	0.09	-13	-4.4	0.74
d_θ (-)	0.12	3.8	0.15	0.02	2.3	0.40

C.1.7 Station 46028

Table C.36. WWIII performance metrics for NDBC Station 46028 for 2010.

Parameter	RMSE	PE (%)	SI	Bias	Bias (%)	R
J (kW/m)	18	31.6	0.53	6	16.4	0.92
H_s (m)	0.41	6.2	0.17	0.09	3.6	0.92
T_e (s)	1.4	12.5	0.15	1.1	11.0	0.88
ϵ_0 (-)	0.06	1.0	0.18	0.00	0.1	0.72
θ (degrees)	37.8	-3.1	0.13	-10	-3.5	0.25
d_θ (-)	0.12	1.6	0.16	0.00	0.5	0.57

Table C.37. WWIII performance metrics for NDBC Station 46028 for 2009.

Parameter	RMSE	PE (%)	SI	Bias	Bias (%)	R
J (kW/m)	12	23.6	0.45	1	5.2	0.90
H_s (m)	0.38	4.2	0.17	-0.01	-0.4	0.92
T_e (s)	1.3	10.2	0.14	0.9	9.0	0.88
ϵ_0 (-)	0.06	0.2	0.18	0.00	-1.2	0.71
θ (degrees)	27.9	-2.8	0.09	-9	-3.2	0.62
d_θ (-)	0.12	7.2	0.16	0.04	5.5	0.61

Table C.38. WWIII performance metrics for NDBC Station 46028 for 2008.

Parameter	RMSE	PE (%)	SI	Bias	Bias (%)	R
J (kW/m)	16	23.7	0.52	2	6.0	0.89
H_s (m)	0.40	3.6	0.17	-0.01	-0.3	0.91
T_e (s)	1.4	11.7	0.15	1.0	10.5	0.88
ϵ_0 (-)	0.06	-1.1	0.17	-0.01	-2.6	0.71
θ (degrees)	34.2	0.6	0.11	-12	-3.9	0.44
d_θ (-)	0.11	3.6	0.15	0.01	1.7	0.65

Table C.39. WWIII performance metrics for NDBC Station 46028 for 2007.

Parameter	RMSE	PE (%)	SI	Bias	Bias (%)	R
J (kW/m)	13	17.8	0.45	1	3.7	0.89
H_s (m)	0.39	-0.2	0.17	-0.08	-3.3	0.91
T_e (s)	1.5	14.8	0.17	1.2	13.5	0.88
ϵ_0 (-)	0.08	-2.9	0.21	-0.02	-4.7	0.58
θ (degrees)	28.2	-3.4	0.09	-12	-3.8	0.35
d_θ (-)	0.11	4.3	0.14	0.03	3.7	0.62

Table C.40. WWIII performance metrics for NDBC Station 46028 for 2006.

Parameter	RMSE	PE (%)	SI	Bias	Bias (%)	R
J (kW/m)	15	17.1	0.48	2	7.6	0.90
H_s (m)	0.39	0.8	0.16	-0.03	-1.3	0.91
T_e (s)	1.4	12.0	0.14	1.0	10.6	0.90
ϵ_0 (-)	0.07	-2.5	0.20	-0.01	-3.8	0.63
θ (degrees)	26.8	-2.8	0.09	-10	-3.2	0.62
d_θ (-)	0.10	2.7	0.13	0.02	2.1	0.68

Table C.41. WWIII performance metrics for NDBC Station 46028 for 2005.

Parameter	RMSE	PE (%)	SI	Bias	Bias (%)	R
J (kW/m)	11	10.6	0.38	0	0.9	0.92
H_s (m)	0.34	-1.3	0.15	-0.08	-3.4	0.93
T_e (s)	1.3	11.5	0.14	1.0	10.0	0.91
ϵ_0 (-)	0.06	-2.8	0.18	-0.01	-4.2	0.74
θ (degrees)	29.2	-3.0	0.10	-10	-3.4	0.54
d_θ (-)	0.10	-1.6	0.12	-0.02	-2.2	0.72

Table C.42. WWIII performance metrics for NDBC Station 46028 for 2004.

Parameter	RMSE	PE (%)	SI	Bias	Bias (%)	R
J (kW/m)	13	1.2	0.45	-2	-8.5	0.90
H_s (m)	0.39	-4.0	0.17	-0.14	-6.4	0.90
T_e (s)	1.1	6.6	0.12	0.5	5.3	0.87
ϵ_0 (-)	0.07	-3.0	0.17	-0.02	-4.0	0.74
θ (degrees)	30.6	-3.1	0.10	-10	-3.4	0.35
d_θ (-)	0.12	1.0	0.15	0.00	0.6	0.61

Table C.43. WWIII performance metrics for NDBC Station 46028 for 2003.

Parameter	RMSE	PE (%)	SI	Bias	Bias (%)	R
J (kW/m)	13	4.3	0.42	-1	-4.6	0.90
H_s (m)	0.39	-1.8	0.17	-0.10	-4.2	0.90
T_e (s)	1.1	5.5	0.11	0.4	4.2	0.90
ϵ_0 (-)	0.07	-5.8	0.18	-0.03	-6.8	0.75
θ (degrees)	33.1	-1.6	0.11	-6	-1.9	0.51
d_θ (-)	0.12	3.2	0.16	0.02	2.1	0.52

Table C.44. WWIII performance metrics for NDBC Station 46028 for 2002.

Parameter	RMSE	PE (%)	SI	Bias	Bias (%)	R
J (kW/m)	32	-4.0	0.64	-7	-13.3	0.92
H_s (m)	0.49	-5.8	0.19	-0.19	-7.2	0.94
T_e (s)	1.1	4.3	0.10	0.3	3.0	0.90
ϵ_0 (-)	0.06	-6.5	0.18	-0.02	-7.3	0.79
θ (degrees)	41.8	1.7	0.14	4	1.2	0.11
d_θ (-)	0.15	6.1	0.18	0.03	4.2	0.37

C.1.8 Station 46025

Table C.45. WWIII performance metrics for NDBC Station 46025 for 2010.

Parameter	RMSE	PE (%)	SI	Bias	Bias (%)	R
J (kW/m)	4	14.6	0.54	0	-0.7	0.90
H_s (m)	0.24	-1.5	0.19	-0.05	-4.0	0.90
T_e (s)	1.7	13.5	0.19	1.1	12.3	0.78
ϵ_0 (-)	0.09	4.4	0.21	0.01	2.3	0.59
θ (degrees)	33.1	-7.4	0.13	-21	-8.2	0.55
d_θ (-)	0.17	18.6	0.23	0.11	15.0	0.27

Table C.46. WWIII performance metrics for NDBC Station 46025 for 2009.

Parameter	RMSE	PE (%)	SI	Bias	Bias (%)	R
J (kW/m)	3	9.7	0.51	0	-6.9	0.86
H_s (m)	0.21	-3.1	0.19	-0.06	-5.9	0.89
T_e (s)	1.7	12.7	0.19	1.0	11.0	0.75
ϵ_0 (-)	0.09	4.9	0.21	0.01	2.5	0.56
θ (degrees)	32.1	-1.9	0.13	-21	-8.1	0.38
d_θ (-)	0.15	16.8	0.22	0.10	13.6	0.30

Table C.47. WWIII performance metrics for NDBC Station 46025 for 2008.

Parameter	RMSE	PE (%)	SI	Bias	Bias (%)	R
J (kW/m)	2	21.3	0.49	0	8.6	0.81
H_s (m)	0.20	1.9	0.19	0.00	-0.1	0.84
T_e (s)	1.7	13.5	0.20	1.0	12.0	0.74
ϵ_0 (-)	0.09	4.6	0.20	0.01	2.6	0.50
θ (degrees)	33.1	-5.2	0.13	-20	-8.2	0.48
d_θ (-)	0.17	19.2	0.25	0.11	15.8	0.01

C.1.9 Station 46042

Table C.48. WWIII performance metrics for NDBC Station 46042 for 2010.

Parameter	RMSE	PE (%)	SI	Bias	Bias (%)	R
J (kW/m)	19	42.6	0.58	7	21.8	0.91
H_s (m)	0.41	10.6	0.18	0.16	6.9	0.93
T_e (s)	1.4	12.2	0.15	1.1	11.1	0.86
ϵ_0 (-)	0.06	-2.0	0.16	-0.01	-3.4	0.76
θ (degrees)	30.2	-1.2	0.10	-5	-1.7	0.53
d_θ (-)	0.12	-5.1	0.14	-0.05	-5.8	0.70

Table C.49. WWIII performance metrics for NDBC Station 46042 for 2009.

Parameter	RMSE	PE (%)	SI	Bias	Bias (%)	R
J (kW/m)	12	29.3	0.48	3	10.8	0.90
H_s (m)	0.34	6.6	0.16	0.07	3.1	0.93
T_e (s)	1.3	10.3	0.13	0.9	9.3	0.89
ϵ_0 (-)	0.06	-3.8	0.17	-0.02	-5.4	0.74
θ (degrees)	22.6	-1.1	0.08	-4	-1.5	0.74
d_θ (-)	0.10	-3.0	0.11	-0.03	-3.8	0.74

Table C.50. WWIII performance metrics for NDBC Station 46042 for 2008.

Parameter	RMSE	PE (%)	SI	Bias	Bias (%)	R
J (kW/m)	14	26.6	0.43	2	7.1	0.94
H_s (m)	0.34	5.9	0.15	0.05	2.1	0.95
T_e (s)	1.2	9.9	0.13	0.9	9.0	0.89
ϵ_0 (-)	0.06	-4.0	0.18	-0.02	-5.7	0.70
θ (degrees)	23.3	-0.3	0.08	-2	-0.6	0.75
d_θ (-)	0.09	-3.0	0.12	-0.03	-3.6	0.76

Table C.51. WWIII performance metrics for NDBC Station 46042 for 2007.

Parameter	RMSE	PE (%)	SI	Bias	Bias (%)	R
J (kW/m)	14	26.6	0.43	2	7.1	0.94
H_s (m)	0.34	5.9	0.15	0.05	2.1	0.95
T_e (s)	1.2	9.9	0.13	0.9	9.0	0.89
ϵ_0 (-)	0.06	-4.0	0.18	-0.02	-5.7	0.70
θ (degrees)	23.3	-0.3	0.08	-2	-0.6	0.75
d_θ (-)	0.09	-3.0	0.12	-0.03	-3.6	0.76

Table C.52. WWIII performance metrics for NDBC Station 46042 for 2006.

Parameter	RMSE	PE (%)	SI	Bias	Bias (%)	R
J (kW/m)	14	26.6	0.43	2	7.1	0.94
H_s (m)	0.34	5.9	0.15	0.05	2.1	0.95
T_e (s)	1.2	9.9	0.13	0.9	9.0	0.89
ϵ_0 (-)	0.06	-4.0	0.18	-0.02	-5.7	0.70
θ (degrees)	23.3	-0.3	0.08	-2	-0.6	0.75
d_θ (-)	0.09	-3.0	0.12	-0.03	-3.6	0.76

Table C.53. WWIII performance metrics for NDBC Station 46042 for 2005.

Parameter	RMSE	PE (%)	SI	Bias	Bias (%)	R
J (kW/m)	12	23.9	0.45	3	11.4	0.91
H_s (m)	0.31	5.5	0.14	0.07	3.2	0.94
T_e (s)	1.2	9.0	0.12	0.8	7.9	0.90
ϵ_0 (-)	0.06	-4.7	0.17	-0.02	-6.2	0.78
θ (degrees)	24.0	0.2	0.08	-1	-0.4	0.62
d_θ (-)	0.09	-4.0	0.11	-0.04	-4.5	0.77

Table C.54. WWIII performance metrics for NDBC Station 46042 for 2004.

Parameter	RMSE	PE (%)	SI	Bias	Bias (%)	R
J (kW/m)	12	28.2	0.49	3	10.9	0.92
H_s (m)	0.32	8.1	0.16	0.10	4.8	0.94
T_e (s)	1.0	6.6	0.10	0.6	6.0	0.89
ϵ_0 (-)	0.06	-8.0	0.16	-0.04	-8.9	0.81
θ (degrees)	24.8	-1.0	0.09	-4	-1.3	0.62
d_θ (-)	0.09	-0.1	0.12	-0.01	-0.8	0.76

Table C.55. WWIII performance metrics for NDBC Station 46042 for 2003.

Parameter	RMSE	PE (%)	SI	Bias	Bias (%)	R
J (kW/m)	12	24.1	0.43	3	10.4	0.91
H_s (m)	0.32	6.0	0.15	0.07	3.3	0.93
T_e (s)	1.0	7.4	0.11	0.7	6.6	0.91
ϵ_0 (-)	0.07	-10.1	0.18	-0.04	-10.9	0.78
θ (degrees)	23.9	-0.8	0.08	-3	-1.1	0.73
d_θ (-)	0.11	4.8	0.14	0.03	3.6	0.64

Table C.56. WWIII performance metrics for NDBC Station 46042 for 2002.

Parameter	RMSE	PE (%)	SI	Bias	Bias (%)	R
J (kW/m)	17	18.8	0.56	2	6.2	0.93
H_s (m)	0.33	4.5	0.15	0.04	2.0	0.95
T_e (s)	0.9	5.9	0.10	0.5	5.3	0.92
ϵ_0 (-)	0.06	-8.3	0.15	-0.03	-8.9	0.84
θ (degrees)	24.6	-2.3	0.08	-8	-2.5	0.44
d_θ (-)	0.10	4.8	0.12	0.03	4.2	0.71

Table C.57. WWIII performance metrics for NDBC Station 46042 for 2001.

Parameter	RMSE	PE (%)	SI	Bias	Bias (%)	R
J (kW/m)	17	18.7	0.48	1	4.0	0.91
H_s (m)	0.36	4.3	0.15	0.03	1.3	0.94
T_e (s)	0.9	6.3	0.09	0.5	5.5	0.93
ϵ_0 (-)	0.06	-8.9	0.15	-0.04	-9.6	0.84
θ (degrees)	23.9	-1.2	0.08	-5	-1.6	0.66
d_θ (-)	0.09	0.6	0.11	0.00	-0.2	0.77

Table C.58. WWIII performance metrics for NDBC Station 46042 for 2000.

Parameter	RMSE	PE (%)	SI	Bias	Bias (%)	R
J (kW/m)	15	21.1	0.46	3	9.6	0.92
H_s (m)	0.34	5.8	0.15	0.08	3.4	0.94
T_e (s)	0.9	5.5	0.09	0.5	4.9	0.91
ϵ_0 (-)	0.06	-9.5	0.16	-0.04	-10.3	0.81
θ (degrees)	37.2	-1.1	0.13	-6	-2.0	0.22
d_θ (-)	0.16	12.4	0.21	0.07	10.1	0.41

Table C.59. WWIII performance metrics for NDBC Station 46042 for 1999.

Parameter	RMSE	PE (%)	SI	Bias	Bias (%)	R
J (kW/m)	17	27.8	0.43	4	9.5	0.92
H_s (m)	0.38	7.6	0.16	0.10	4.0	0.94
T_e (s)	1.1	6.8	0.10	0.7	6.1	0.91
ϵ_0 (-)	0.07	-12.2	0.19	-0.05	-12.8	0.79
θ (degrees)	21.9	0.2	0.08	-1	-0.3	0.57
d_θ (-)	0.08	0.1	0.10	0.00	-0.3	0.81

Table C.60. WWIII performance metrics for NDBC Station 46042 for 1998.

Parameter	RMSE	PE (%)	SI	Bias	Bias (%)	R
J (kW/m)	15	23.1	0.46	3	10.3	0.93
H_s (m)	0.34	6.3	0.15	0.09	3.9	0.94
T_e (s)	1.0	6.8	0.10	0.6	5.8	0.92
ϵ_0 (-)	0.06	-9.3	0.16	-0.04	-10.0	0.84
θ (degrees)	26.6	0.7	0.09	0	0.0	0.43
d_θ (-)	0.09	-3.7	0.11	-0.03	-4.0	0.81

C.1.10 Station 46063

Table C.61. WWIII performance metrics for NDBC Station 46063 for 2009.

Parameter	RMSE	PE (%)	SI	Bias	Bias (%)	R
J (kW/m)	13	27.6	0.42	2	6.8	0.89
H_s (m)	0.38	5.4	0.16	0.03	1.2	0.92
T_e (s)	1.4	11.2	0.14	0.9	9.9	0.88
ϵ_0 (-)	0.06	1.9	0.17	0.00	0.4	0.74
θ (degrees)	14.8	0.5	0.05	1	0.3	0.72
d_θ (-)	0.09	-1.6	0.10	-0.02	-2.2	0.61

Table C.62. WWIII performance metrics for NDBC Station 46063 for 2008.

Parameter	RMSE	PE (%)	SI	Bias	Bias (%)	R
J (kW/m)	13	29.8	0.48	3	10.5	0.91
H_s (m)	0.35	5.7	0.15	0.06	2.5	0.93
T_e (s)	1.4	12.9	0.15	1.0	11.7	0.89
ϵ_0 (-)	0.06	-0.5	0.16	-0.01	-1.9	0.72
θ (degrees)	30.9	-1.2	0.10	-5	-1.8	0.42
d_θ (-)	0.11	-4.9	0.13	-0.04	-5.4	0.73

Table C.63. WWIII performance metrics for NDBC Station 46063 for 2007.

Parameter	RMSE	PE (%)	SI	Bias	Bias (%)	R
J (kW/m)	11	24.3	0.40	3	9.7	0.92
H_s (m)	0.33	4.4	0.14	0.04	1.8	0.93
T_e (s)	1.3	11.1	0.14	0.9	10.4	0.90
ϵ_0 (-)	0.06	0.4	0.18	0.00	-1.2	0.68
θ (degrees)	16.0	-1.0	0.05	-3	-1.1	0.56
d_θ (-)	0.09	-1.9	0.11	-0.02	-2.2	0.69

Table C.64. WWIII performance metrics for NDBC Station 46063 for 2006.

Parameter	RMSE	PE (%)	SI	Bias	Bias (%)	R
J (kW/m)	20	21.6	0.58	0	0.4	0.88
H_s (m)	0.44	2.4	0.19	-0.03	-1.3	0.92
T_e (s)	1.4	10.6	0.14	0.9	9.2	0.87
ϵ_0 (-)	0.06	-2.9	0.18	-0.02	-4.9	0.74
θ (degrees)	21.3	-0.6	0.07	-2	-0.6	0.51
d_θ (-)	0.09	-1.8	0.11	-0.02	-2.4	0.70

C.1.11 Station 46087

Table C.65. UnSWAN performance metrics for NDBC Station 46087 for 2009.

Parameter	RMSE	PE (%)	SI	Bias	Bias (%)	R
J (kW/m)	12	38.8	0.66	3	15.0	0.87
H_s (m)	0.40	9.6	0.23	0.08	4.9	0.89
T_e (s)	1.1	9.0	0.13	0.7	8.2	0.82
ϵ_0 (-)	0.07	3.3	0.22	0.00	0.4	0.58
θ (degrees)	24.6	-1.4	0.09	-7	-2.5	0.58
d_θ (-)	0.14	14.2	0.17	0.10	11.9	0.37

Table C.66. UnSWAN performance metrics for NDBC Station 46087 for 2008.

Parameter	RMSE	PE (%)	SI	Bias	Bias (%)	R
J (kW/m)	17	35.0	0.64	4	15.1	0.85
H_s (m)	0.45	8.8	0.21	0.11	5.2	0.90
T_e (s)	1.1	8.2	0.11	0.7	7.3	0.87
ϵ_0 (-)	0.07	0.8	0.22	-0.01	-1.7	0.55
θ (degrees)	24.4	2.3	0.09	2	0.7	0.55
d_θ (-)	0.13	13.1	0.16	0.09	11.1	0.39

Table C.67. UnSWAN performance metrics for NDBC Station 46087 for 2007.

Parameter	RMSE	PE (%)	SI	Bias	Bias (%)	R
J (kW/m)	17	37.6	0.65	4	14.0	0.88
H_s (m)	0.45	8.9	0.22	0.09	4.4	0.91
T_e (s)	1.1	8.7	0.12	0.7	7.9	0.88
ϵ_0 (-)	0.07	4.7	0.23	0.01	2.3	0.50
θ (degrees)	16.1	0.1	0.06	-1	-0.4	0.66
d_θ (-)	0.10	8.2	0.12	0.06	6.8	0.44

Table C.68. UnSWAN performance metrics for NDBC Station 46087 for 2006.

Parameter	RMSE	PE (%)	SI	Bias	Bias (%)	R
J (kW/m)	38	31.9	0.57	11	16.8	0.88
H_s (m)	0.63	7.5	0.20	0.19	5.9	0.91
T_e (s)	1.4	10.4	0.13	0.9	8.9	0.80
ϵ_0 (-)	0.07	-3.5	0.24	-0.02	-6.3	0.46
θ (degrees)	27.5	5.5	0.11	9	3.6	0.28
d_θ (-)	0.11	8.2	0.13	0.06	6.4	0.21

Table C.69. UnSWAN performance metrics for NDBC Station 46087 for 2005.

Parameter	RMSE	PE (%)	SI	Bias	Bias (%)	R
J (kW/m)	11	19.0	0.56	2	8.8	0.89
H_s (m)	0.37	2.3	0.20	0.00	0.1	0.90
T_e (s)	1.2	9.0	0.13	0.7	8.1	0.87
ϵ_0 (-)	0.07	3.9	0.23	0.00	1.2	0.55
θ (degrees)	18.6	1.5	0.07	1	0.4	0.69
d_θ (-)	0.09	4.9	0.10	0.03	3.6	0.48

Table C.70. UnSWAN performance metrics for NDBC Station 46087 for 2004.

Parameter	RMSE	PE (%)	SI	Bias	Bias (%)	R
J (kW/m)	11	20.7	0.54	0	1.4	0.92
H_s (m)	0.39	2.8	0.21	-0.03	-1.4	0.91
T_e (s)	1.0	8.1	0.11	0.7	7.4	0.88
ϵ_0 (-)	0.06	5.3	0.21	0.01	2.7	0.63
θ (degrees)	17.3	0.7	0.07	0	0.0	0.59
d_θ (-)	0.09	4.4	0.10	0.03	3.1	0.57

C.1.12 Station 46041

Table C.71. WWIII performance metrics for NDBC Station 46041 for 2010.

Parameter	RMSE	PE (%)	SI	Bias	Bias (%)	R
J (kW/m)	27	37.1	0.48	11	19.2	0.93
H_s (m)	0.43	7.6	0.15	0.15	5.3	0.96
T_e (s)	1.3	12.1	0.14	1.0	10.8	0.87
ϵ_0 (-)	0.06	2.3	0.18	0.00	0.7	0.69
θ (degrees)	21.2	1.2	0.08	1	0.3	0.74
d_θ (-)	0.09	3.7	0.11	0.02	2.4	0.60

Table C.72. WWIII performance metrics for NDBC Station 46041 for 2009.

Parameter	RMSE	PE (%)	SI	Bias	Bias (%)	R
J (kW/m)	15	33.8	0.46	2	7.2	0.94
H_s (m)	0.35	6.3	0.16	0.04	1.9	0.96
T_e (s)	1.3	12.0	0.15	1.0	10.8	0.89
ϵ_0 (-)	0.07	3.6	0.20	0.00	1.4	0.66
θ (degrees)	20.7	2.8	0.08	-6	-2.1	0.74
d_θ (-)	0.09	2.2	0.11	0.01	0.9	0.55

Table C.73. WWIII performance metrics for NDBC Station 46041 for 2008.

Parameter	RMSE	PE (%)	SI	Bias	Bias (%)	R
J (kW/m)	18	33.6	0.53	3	7.7	0.92
H_s (m)	0.36	5.8	0.16	0.04	1.7	0.95
T_e (s)	1.3	12.6	0.15	1.0	11.0	0.89
ϵ_0 (-)	0.07	4.1	0.21	0.01	2.0	0.63
θ (degrees)	20.5	-0.7	0.08	-4	-1.6	0.74
d_θ (-)	0.09	0.4	0.11	-0.01	-0.8	0.48

Table C.74. WWIII performance metrics for NDBC Station 46041 for 2007.

Parameter	RMSE	PE (%)	SI	Bias	Bias (%)	R
J (kW/m)	33	22.4	0.45	3	4.0	0.94
H_s (m)	0.48	3.5	0.15	0.01	0.3	0.95
T_e (s)	1.0	7.9	0.10	0.7	7.1	0.88
ϵ_0 (-)	0.05	-1.8	0.16	-0.01	-3.5	0.71
θ (degrees)	16.6	1.6	0.06	2	0.9	0.85
d_θ (-)	0.09	4.5	0.10	0.03	3.1	0.71

Table C.75. WWIII performance metrics for NDBC Station 46041 for 2006.

Parameter	RMSE	PE (%)	SI	Bias	Bias (%)	R
J (kW/m)	10	43.0	0.49	2	9.9	0.96
H_s (m)	0.27	8.7	0.15	0.08	4.0	0.97
T_e (s)	1.4	15.0	0.17	1.1	13.7	0.84
ϵ_0 (-)	0.07	6.6	0.21	0.02	4.3	0.66
θ (degrees)	21.9	-3.8	0.08	-12	-4.3	0.72
d_θ (-)	0.09	-3.8	0.10	-0.04	-4.6	0.56

Table C.76. WWIII performance metrics for NDBC Station 46041 for 2005.

Parameter	RMSE	PE (%)	SI	Bias	Bias (%)	R
J (kW/m)	16	22.8	0.51	3	10.8	0.92
H_s (m)	0.34	4.5	0.15	0.05	2.3	0.95
T_e (s)	1.0	8.6	0.11	0.7	7.8	0.93
ϵ_0 (-)	0.06	-4.1	0.17	-0.02	-4.9	0.71
θ (degrees)	18.8	-0.2	0.07	-2	-0.9	0.77
d_θ (-)	0.09	4.6	0.11	0.03	3.2	0.52

Table C.77. WWIII performance metrics for NDBC Station 46041 for 2004.

Parameter	RMSE	PE (%)	SI	Bias	Bias (%)	R
J (kW/m)	14	24.2	0.45	2	6.3	0.93
H_s (m)	0.33	5.3	0.15	0.04	1.8	0.95
T_e (s)	1.0	8.1	0.11	0.7	7.5	0.89
ϵ_0 (-)	0.05	-4.2	0.15	-0.02	-4.9	0.78
θ (degrees)	19.3	-0.2	0.07	-2	-0.9	0.75
d_θ (-)	0.09	4.9	0.11	0.03	3.6	0.57

Table C.78. WWIII performance metrics for NDBC Station 46041 for 2003.

Parameter	RMSE	PE (%)	SI	Bias	Bias (%)	R
J (kW/m)	17	23.9	0.46	2	5.4	0.95
H_s (m)	0.33	5.3	0.14	0.05	2.1	0.97
T_e (s)	1.0	8.1	0.11	0.7	7.4	0.91
ϵ_0 (-)	0.06	-5.0	0.16	-0.02	-5.8	0.78
θ (degrees)	21.5	-0.9	0.08	-4	-1.5	0.60
d_θ (-)	0.09	4.6	0.11	0.03	3.5	0.58

Table C.79. WWIII performance metrics for NDBC Station 46041 for 2002.

Parameter	RMSE	PE (%)	SI	Bias	Bias (%)	R
J (kW/m)	30	31.2	0.51	10	17.4	0.92
H_s (m)	0.44	8.4	0.15	0.17	5.8	0.96
T_e (s)	1.2	7.9	0.11	0.7	7.2	0.88
ϵ_0 (-)	0.07	-10.1	0.20	-0.04	-11.5	0.62
θ (degrees)	23.0	-1.7	0.09	-6	-2.2	0.39
d_θ (-)	0.20	24.7	0.28	0.15	21.0	-0.05

Table C.80. WWIII performance metrics for NDBC Station 46041 for 2001.

Parameter	RMSE	PE (%)	SI	Bias	Bias (%)	R
J (kW/m)	17	28.3	0.53	2	6.2	0.94
H_s (m)	0.33	6.8	0.15	0.07	3.0	0.96
T_e (s)	1.0	8.2	0.11	0.6	7.3	0.90
ϵ_0 (-)	0.06	-2.5	0.15	-0.01	-3.6	0.78
θ (degrees)	18.6	-2.0	0.07	-7	-2.5	0.77
d_θ (-)	0.09	3.3	0.10	0.02	2.0	0.63

Table C.81. WWIII performance metrics for NDBC Station 46041 for 2000.

Parameter	RMSE	PE (%)	SI	Bias	Bias (%)	R
J (kW/m)	18	27.8	0.50	4	10.1	0.92
H_s (m)	0.35	6.6	0.15	0.08	3.3	0.95
T_e (s)	1.1	8.2	0.11	0.7	7.3	0.92
ϵ_0 (-)	0.06	-5.5	0.16	-0.02	-6.3	0.81
θ (degrees)	23.8	-0.2	0.09	-2	-0.8	0.36
d_θ (-)	0.11	7.3	0.13	0.05	5.9	0.45

Table C.82. WWIII performance metrics for NDBC Station 46041 for 1999.

Parameter	RMSE	PE (%)	SI	Bias	Bias (%)	R
J (kW/m)	14	49.6	0.48	5	16.1	0.95
H_s (m)	0.34	12.9	0.16	0.14	7.0	0.97
T_e (s)	1.2	11.0	0.13	0.9	10.2	0.88
ϵ_0 (-)	0.06	-2.3	0.17	-0.01	-3.5	0.69
θ (degrees)	19.4	-2.9	0.07	-9	-3.3	0.72
d_θ (-)	0.09	0.9	0.10	0.00	-0.1	0.55

Table C.83. WWIII performance metrics for NDBC Station 46041 for 1998.

Parameter	RMSE	PE (%)	SI	Bias	Bias (%)	R
J (kW/m)	25	75.1	1.07	11	46.1	0.95
H_s (m)	0.47	22.4	0.25	0.34	17.9	0.96
T_e (s)	1.2	11.3	0.14	0.9	10.5	0.88
ϵ_0 (-)	0.06	2.8	0.17	0.01	1.4	0.73
θ (degrees)	18.7	-1.3	0.07	-6	-2.3	0.65
d_θ (-)	0.10	0.9	0.12	0.00	-0.6	0.36

C.2 CDIP Tables

C.2.1 Station 46215

Table C.84. UnSWAN performance metrics for CDIP Station 46215 for 2010.

Parameter	RMSE	PE (%)	SI	Bias	Bias (%)	R
J (kW/m)	13	33.5	0.69	5	25.2	0.91
H_s (m)	0.32	7.9	0.19	0.10	6.0	0.91
T_e (s)	1.4	12.3	0.15	1.1	11.7	0.89
ϵ_0 (-)	0.06	-5.2	0.16	-0.02	-5.6	0.78
θ (degrees)	10.8	-0.5	0.04	-2	-0.6	0.68
d_θ (-)	0.05	2.5	0.06	0.02	2.4	0.82

Table C.85. UnSWAN performance metrics for CDIP Station 46215 for 2009.

Parameter	RMSE	PE (%)	SI	Bias	Bias (%)	R
J (kW/m)	7	29.3	0.49	2	15.2	0.88
H_s (m)	0.26	7.8	0.17	0.07	4.4	0.91
T_e (s)	1.3	8.9	0.13	0.8	8.3	0.87
ϵ_0 (-)	0.06	-5.1	0.16	-0.02	-5.5	0.77
θ (degrees)	9.9	0.1	0.04	0	0.0	0.80
d_θ (-)	0.05	2.8	0.06	0.02	2.6	0.80

Table C.86. UnSWAN performance metrics for CDIP Station 46215 for 2008.

Parameter	RMSE	PE (%)	SI	Bias	Bias (%)	R
J (kW/m)	9	27.9	0.57	2	14.0	0.89
H_s (m)	0.27	6.5	0.17	0.05	3.4	0.90
T_e (s)	1.3	10.0	0.14	0.9	9.6	0.88
ϵ_0 (-)	0.06	-5.4	0.16	-0.02	-6.0	0.76
θ (degrees)	10.6	-0.5	0.04	-2	-0.6	0.73
d_θ (-)	0.05	2.3	0.06	0.02	2.2	0.77

Table C.87. UnSWAN performance metrics for CDIP Station 46215 for 2007.

Parameter	RMSE	PE (%)	SI	Bias	Bias (%)	R
J (kW/m)	9	27.4	0.59	2	16.1	0.86
H_s (m)	0.27	6.2	0.17	0.06	3.6	0.89
T_e (s)	1.3	9.9	0.14	0.9	9.5	0.88
ϵ_0 (-)	0.06	-6.3	0.16	-0.03	-7.0	0.76
θ (degrees)	9.2	0.7	0.03	2	0.6	0.70
d_θ (-)	0.05	3.7	0.06	0.03	3.6	0.82

Table C.88. UnSWAN performance metrics for CDIP Station 46215 for 2006.

Parameter	RMSE	PE (%)	SI	Bias	Bias (%)	R
J (kW/m)	9	25.1	0.58	3	17.6	0.90
H_s (m)	0.27	5.8	0.17	0.07	4.1	0.92
T_e (s)	1.2	9.1	0.12	0.8	8.6	0.90
ϵ_0 (-)	0.06	-7.6	0.16	-0.03	-7.9	0.78
θ (degrees)	10.4	0.7	0.04	1	0.6	0.74
d_θ (-)	0.06	3.8	0.07	0.03	3.7	0.80

Table C.89. UnSWAN performance metrics for CDIP Station 46215 for 2005.

Parameter	RMSE	PE (%)	SI	Bias	Bias (%)	R
J (kW/m)	8	21.3	0.52	2	12.9	0.91
H_s (m)	0.26	4.4	0.16	0.04	2.4	0.91
T_e (s)	1.2	8.6	0.13	0.8	8.1	0.89
ϵ_0 (-)	0.06	-7.5	0.16	-0.03	-7.8	0.82
θ (degrees)	11.0	0.4	0.04	1	0.3	0.66
d_θ (-)	0.05	3.1	0.06	0.03	3.0	0.81

Table C.90. UnSWAN performance metrics for CDIP Station 46215 for 2004.

Parameter	RMSE	PE (%)	SI	Bias	Bias (%)	R
J (kW/m)	7	23.3	0.52	2	12.5	0.90
H_s (m)	0.25	5.9	0.16	0.05	3.4	0.90
T_e (s)	1.1	7.2	0.12	0.6	6.6	0.89
ϵ_0 (-)	0.06	-6.2	0.14	-0.03	-6.4	0.82
θ (degrees)	10.0	0.2	0.04	0	0.1	0.68
d_θ (-)	0.05	2.6	0.06	0.02	2.6	0.79

Table C.91. UnSWAN performance metrics for CDIP Station 46215 for 2003.

Parameter	RMSE	PE (%)	SI	Bias	Bias (%)	R
J (kW/m)	7	28.2	0.50	2	16.0	0.90
H_s (m)	0.25	7.8	0.17	0.08	5.1	0.91
T_e (s)	1.1	7.3	0.11	0.6	6.6	0.89
ϵ_0 (-)	0.06	-7.6	0.15	-0.03	-7.9	0.81
θ (degrees)	9.5	0.5	0.04	1	0.4	0.80
d_θ (-)	0.06	3.0	0.07	0.03	3.0	0.76

Table C.92. UnSWAN performance metrics for CDIP Station 46215 for 2002.

Parameter	RMSE	PE (%)	SI	Bias	Bias (%)	R
J (kW/m)	10	24.6	0.62	2	15.5	0.93
H_s (m)	0.26	6.4	0.17	0.07	4.4	0.94
T_e (s)	1.1	7.1	0.11	0.6	6.7	0.92
ϵ_0 (-)	0.06	-7.6	0.15	-0.03	-7.9	0.85
θ (degrees)	9.3	0.3	0.03	1	0.2	0.75
d_θ (-)	0.05	3.5	0.06	0.03	3.4	0.83

Table C.93. UnSWAN performance metrics for CDIP Station 46215 for 2001.

Parameter	RMSE	PE (%)	SI	Bias	Bias (%)	R
J (kW/m)	10	24.3	0.54	2	11.6	0.91
H_s (m)	0.28	6.6	0.17	0.06	3.8	0.93
T_e (s)	1.1	5.9	0.11	0.5	5.3	0.89
ϵ_0 (-)	0.06	-7.3	0.15	-0.03	-7.8	0.82
θ (degrees)	10.1	1.1	0.04	3	1.1	0.70
d_θ (-)	0.05	2.9	0.06	0.02	2.8	0.80

Table C.94. UnSWAN performance metrics for CDIP Station 46215 for 2000.

Parameter	RMSE	PE (%)	SI	Bias	Bias (%)	R
J (kW/m)	9	27.1	0.52	2	12.2	0.92
H_s (m)	0.26	7.9	0.17	0.08	5.0	0.93
T_e (s)	1.1	5.9	0.11	0.5	5.1	0.89
ϵ_0 (-)	0.06	-6.0	0.14	-0.03	-6.4	0.84
θ (degrees)	10.3	1.0	0.04	2	0.9	0.73
d_θ (-)	0.06	4.4	0.07	0.04	4.3	0.82

Table C.95. UnSWAN performance metrics for CDIP Station 46215 for 1999.

Parameter	RMSE	PE (%)	SI	Bias	Bias (%)	R
J (kW/m)	8	28.1	0.44	2	10.0	0.91
H_s (m)	0.27	7.2	0.16	0.06	3.4	0.92
T_e (s)	1.1	8.1	0.11	0.7	7.4	0.91
ϵ_0 (-)	0.06	-7.0	0.15	-0.03	-7.3	0.84
θ (degrees)	10.0	0.7	0.04	2	0.6	0.72
d_θ (-)	0.05	3.2	0.06	0.03	3.2	0.83

Table C.96. UnSWAN performance metrics for CDIP Station 46215 for 1998.

Parameter	RMSE	PE (%)	SI	Bias	Bias (%)	R
J (kW/m)	19	32.7	0.74	6	23.3	0.91
H_s (m)	0.36	9.9	0.19	0.14	7.5	0.94
T_e (s)	1.2	7.3	0.12	0.7	6.8	0.89
ϵ_0 (-)	0.06	-6.9	0.15	-0.03	-7.4	0.82
θ (degrees)	10.7	1.9	0.04	5	1.8	0.74
d_θ (-)	0.06	5.0	0.07	0.04	4.9	0.85

Table C.97. UnSWAN performance metrics for CDIP Station 46215 for 1997.

Parameter	RMSE	PE (%)	SI	Bias	Bias (%)	R
J (kW/m)	10	37.8	0.59	4	21.5	0.85
H_s (m)	0.31	10.2	0.19	0.12	7.1	0.90
T_e (s)	1.5	10.5	0.15	1.0	9.9	0.85
ϵ_0 (-)	0.06	-8.0	0.16	-0.03	-8.5	0.81
θ (degrees)	11.0	1.0	0.04	2	0.9	0.68
d_θ (-)	0.06	5.3	0.08	0.04	5.2	0.79

Table C.98. UnSWAN performance metrics for CDIP Station 46215 for 1996.

Parameter	RMSE	PE (%)	SI	Bias	Bias (%)	R
J (kW/m)	5	25.5	0.41	1	10.8	0.89
H_s (m)	0.22	6.4	0.15	0.05	3.4	0.90
T_e (s)	1.1	7.8	0.12	0.6	7.1	0.86
ϵ_0 (-)	0.06	-7.1	0.15	-0.03	-7.9	0.76
θ (degrees)	10.7	0.3	0.04	0	0.2	0.80
d_θ (-)	0.05	2.1	0.06	0.02	1.9	0.76

C.2.2 Station 46236

Table C.99. UnSWAN performance metrics for CDIP Station 46236 for 2010.

Parameter	RMSE	PE (%)	SI	Bias	Bias (%)	R
J (kW/m)	15	37.8	0.73	5	26.2	0.92
H_s (m)	0.37	13.6	0.21	0.20	11.1	0.93
T_e (s)	1.4	13.3	0.15	1.1	12.3	0.89
ϵ_0 (-)	0.07	-10.7	0.19	-0.04	-11.8	0.81
θ (degrees)	10.2	1.2	0.04	3	1.2	0.67
d_θ (-)	0.04	1.0	0.04	0.01	1.0	0.84

Table C.100. UnSWAN performance metrics for CDIP Station 46236 for 2009.

Parameter	RMSE	PE (%)	SI	Bias	Bias (%)	R
J (kW/m)	8	37.9	0.58	3	20.8	0.87
H_s (m)	0.31	13.0	0.20	0.15	9.6	0.91
T_e (s)	1.4	14.2	0.16	1.2	13.1	0.88
ϵ_0 (-)	0.08	-14.5	0.22	-0.06	-15.6	0.76
θ (degrees)	9.6	1.4	0.03	4	1.3	0.82
d_θ (-)	0.05	2.9	0.05	0.02	2.8	0.81

Table C.101. UnSWAN performance metrics for CDIP Station 46236 for 2008.

Parameter	RMSE	PE (%)	SI	Bias	Bias (%)	R
J (kW/m)	8	33.5	0.56	3	18.6	0.92
H_s (m)	0.30	11.7	0.19	0.14	8.8	0.92
T_e (s)	1.4	14.2	0.16	1.1	13.1	0.88
ϵ_0 (-)	0.09	-14.6	0.23	-0.06	-15.9	0.73
θ (degrees)	8.9	0.8	0.03	2	0.8	0.78
d_θ (-)	0.05	1.9	0.05	0.02	1.8	0.80

Table C.102. UnSWAN performance metrics for CDIP Station 46236 for 2007.

Parameter	RMSE	PE (%)	SI	Bias	Bias (%)	R
J (kW/m)	10	39.6	0.82	3	24.3	0.91
H_s (m)	0.29	14.1	0.20	0.16	11.1	0.92
T_e (s)	1.4	15.2	0.17	1.1	13.5	0.89
ϵ_0 (-)	0.09	-15.3	0.23	-0.06	-16.6	0.77
θ (degrees)	10.2	1.5	0.04	4	1.4	0.56
d_θ (-)	0.05	2.2	0.05	0.02	2.0	0.76

C.2.3 Station 46211

Table C.103. UnSWAN performance metrics for CDIP Station 46211 for 2010.

Parameter	RMSE	PE (%)	SI	Bias	Bias (%)	R
J (kW/m)	21	41.9	0.57	8	22.7	0.94
H_s (m)	0.37	10.0	0.16	0.15	6.6	0.96
T_e (s)	1.3	12.6	0.14	1.0	11.4	0.91
ϵ_0 (-)	0.06	-2.9	0.18	-0.01	-4.0	0.73
θ (degrees)	12.6	-1.0	0.05	-3	-1.3	0.86
d_θ (-)	0.05	1.9	0.05	0.01	1.6	0.67

Table C.104. UnSWAN performance metrics for CDIP Station 46211 for 2009.

Parameter	RMSE	PE (%)	SI	Bias	Bias (%)	R
J (kW/m)	14	37.4	0.55	4	15.3	0.92
H_s (m)	0.34	8.3	0.17	0.08	4.1	0.94
T_e (s)	1.2	11.1	0.14	0.9	10.1	0.90
ϵ_0 (-)	0.07	-6.1	0.20	-0.03	-7.7	0.72
θ (degrees)	12.4	-1.7	0.05	-5	-1.9	0.84
d_θ (-)	0.06	3.2	0.06	0.02	2.8	0.69

Table C.105. UnSWAN performance metrics for CDIP Station 46211 for 2008.

Parameter	RMSE	PE (%)	SI	Bias	Bias (%)	R
J (kW/m)	16	34.2	0.55	4	15.2	0.93
H_s (m)	0.32	7.4	0.16	0.07	3.6	0.95
T_e (s)	1.2	11.3	0.13	0.9	10.2	0.92
ϵ_0 (-)	0.06	-5.8	0.17	-0.03	-7.1	0.78
θ (degrees)	13.5	-1.2	0.05	-4	-1.6	0.80
d_θ (-)	0.05	2.9	0.06	0.02	2.6	0.72

Table C.106. UnSWAN performance metrics for CDIP Station 46211 for 2007.

Parameter	RMSE	PE (%)	SI	Bias	Bias (%)	R
J (kW/m)	18	36.5	0.55	4	14.0	0.95
H_s (m)	0.33	8.5	0.16	0.08	4.0	0.96
T_e (s)	1.2	11.0	0.13	0.9	9.9	0.92
ϵ_0 (-)	0.06	-5.0	0.17	-0.02	-6.2	0.74
θ (degrees)	11.3	-1.1	0.04	-3	-1.3	0.85
d_θ (-)	0.05	2.9	0.05	0.02	2.7	0.71

Table C.107. UnSWAN performance metrics for CDIP Station 46211 for 2006.

Parameter	RMSE	PE (%)	SI	Bias	Bias (%)	R
J (kW/m)	22	26.7	0.65	4	10.3	0.93
H_s (m)	0.34	5.1	0.16	0.04	1.8	0.96
T_e (s)	1.1	10.3	0.13	0.8	9.4	0.92
ϵ_0 (-)	0.06	-4.4	0.16	-0.02	-5.6	0.81
θ (degrees)	12.0	-1.5	0.04	-5	-1.8	0.85
d_θ (-)	0.04	1.7	0.05	0.01	1.5	0.74

Table C.108. UnSWAN performance metrics for CDIP Station 46211 for 2005.

Parameter	RMSE	PE (%)	SI	Bias	Bias (%)	R
J (kW/m)	14	28.5	0.54	4	15.1	0.93
H_s (m)	0.30	5.9	0.15	0.06	2.9	0.95
T_e (s)	1.1	9.7	0.12	0.8	8.8	0.94
ϵ_0 (-)	0.06	-6.2	0.18	-0.03	-7.3	0.74
θ (degrees)	11.0	-1.1	0.04	-4	-1.3	0.86
d_θ (-)	0.05	2.1	0.05	0.02	1.8	0.72

Table C.109. UnSWAN performance metrics for CDIP Station 46211 for 2004.

Parameter	RMSE	PE (%)	SI	Bias	Bias (%)	R
J (kW/m)	11	20.6	0.41	2	6.2	0.94
H_s (m)	0.29	3.1	0.15	0.00	0.0	0.95
T_e (s)	1.1	9.2	0.12	0.8	8.3	0.91
ϵ_0 (-)	0.06	-5.5	0.16	-0.02	-6.7	0.80
θ (degrees)	13.1	-0.9	0.05	-4	-1.3	0.81
d_θ (-)	0.05	3.0	0.06	0.02	2.7	0.72

Table C.110. UnSWAN performance metrics for CDIP Station 46211 for 2003.

Parameter	RMSE	PE (%)	SI	Bias	Bias (%)	R
J (kW/m)	18	25.5	0.57	2	6.4	0.93
H_s (m)	0.34	5.0	0.16	0.03	1.4	0.96
T_e (s)	1.1	9.3	0.12	0.7	8.3	0.92
ϵ_0 (-)	0.06	-6.2	0.17	-0.03	-7.2	0.81
θ (degrees)	11.8	-1.0	0.04	-3	-1.2	0.83
d_θ (-)	0.05	2.9	0.06	0.02	2.6	0.75

Table C.111. UnSWAN performance metrics for CDIP Station 46211 for 2002.

Parameter	RMSE	PE (%)	SI	Bias	Bias (%)	R
J (kW/m)	15	28.4	0.62	4	14.6	0.95
H_s (m)	0.29	6.2	0.15	0.05	2.9	0.96
T_e (s)	1.1	9.8	0.12	0.8	9.0	0.93
ϵ_0 (-)	0.07	-6.4	0.18	-0.03	-7.7	0.80
θ (degrees)	13.2	-1.3	0.05	-5	-1.7	0.84
d_θ (-)	0.05	2.3	0.06	0.02	2.1	0.71

Table C.112. UnSWAN performance metrics for CDIP Station 46211 for 2001.

Parameter	RMSE	PE (%)	SI	Bias	Bias (%)	R
J (kW/m)	32	33.2	1.00	3	7.9	0.73
H_s (m)	0.57	5.2	0.27	0.01	0.7	0.86
T_e (s)	1.3	9.7	0.14	0.7	8.2	0.86
ϵ_0 (-)	0.07	-6.1	0.21	-0.03	-7.8	0.68
θ (degrees)	13.6	-1.0	0.05	-3	-1.3	0.74
d_θ (-)	0.06	2.4	0.06	0.02	2.1	0.62

Table C.113. UnSWAN performance metrics for CDIP Station 46211 for 2000.

Parameter	RMSE	PE (%)	SI	Bias	Bias (%)	R
J (kW/m)	16	37.5	0.60	5	19.4	0.93
H_s (m)	0.33	8.8	0.17	0.10	5.2	0.95
T_e (s)	1.2	10.3	0.13	0.8	9.1	0.93
ϵ_0 (-)	0.07	-7.2	0.17	-0.03	-8.5	0.82
θ (degrees)	13.2	-0.8	0.05	-3	-1.3	0.79
d_θ (-)	0.05	3.4	0.06	0.03	3.0	0.78

Table C.114. UnSWAN performance metrics for CDIP Station 46211 for 1999.

Parameter	RMSE	PE (%)	SI	Bias	Bias (%)	R
J (kW/m)	17	38.6	0.54	5	16.9	0.94
H_s (m)	0.32	8.9	0.15	0.10	4.5	0.96
T_e (s)	1.2	11.6	0.14	1.0	10.7	0.91
ϵ_0 (-)	0.06	-6.2	0.17	-0.03	-7.4	0.77
θ (degrees)	10.7	-1.0	0.04	-3	-1.1	0.83
d_θ (-)	0.05	2.7	0.05	0.02	2.5	0.71

Table C.115. UnSWAN performance metrics for CDIP Station 46211 for 1998.

Parameter	RMSE	PE (%)	SI	Bias	Bias (%)	R
J (kW/m)	28	39.4	0.71	10	26.0	0.92
H_s (m)	0.39	9.7	0.17	0.15	6.6	0.96
T_e (s)	1.2	10.9	0.13	0.9	10.0	0.92
ϵ_0 (-)	0.06	-4.4	0.16	-0.02	-5.5	0.80
θ (degrees)	11.4	-0.7	0.04	-2	-0.9	0.83
d_θ (-)	0.05	2.5	0.05	0.02	2.2	0.75

Table C.116. UnSWAN performance metrics for CDIP Station 46211 for 1997.

Parameter	RMSE	PE (%)	SI	Bias	Bias (%)	R
J (kW/m)	22	43.8	0.64	9	25.7	0.92
H_s (m)	0.41	10.7	0.18	0.16	7.1	0.95
T_e (s)	1.4	11.6	0.15	1.0	11.0	0.90
ϵ_0 (-)	0.06	-3.9	0.16	-0.02	-4.9	0.80
θ (degrees)	11.0	-0.7	0.04	-2	-0.8	0.83
d_θ (-)	0.04	2.2	0.05	0.02	2.0	0.75

Table C.117. UnSWAN performance metrics for CDIP Station 46211 for 1996.

Parameter	RMSE	PE (%)	SI	Bias	Bias (%)	R
J (kW/m)	13	31.7	0.54	3	14.3	0.93
H_s (m)	0.31	8.1	0.16	0.09	4.6	0.95
T_e (s)	1.0	9.1	0.12	0.7	8.2	0.90
ϵ_0 (-)	0.06	-4.3	0.17	-0.02	-5.8	0.79
θ (degrees)	12.5	-0.9	0.05	-3	-1.3	0.84
d_θ (-)	0.05	2.6	0.06	0.02	2.3	0.70

Table C.118. UnSWAN performance metrics for CDIP Station 46211 for 1995.

Parameter	RMSE	PE (%)	SI	Bias	Bias (%)	R
J (kW/m)	19	40.9	0.66	7	24.4	0.90
H_s (m)	0.39	10.3	0.19	0.14	7.0	0.94
T_e (s)	1.2	10.4	0.13	0.9	9.5	0.91
ϵ_0 (-)	0.06	-6.3	0.18	-0.03	-7.6	0.76
θ (degrees)	10.8	-1.1	0.04	-3	-1.2	0.86
d_θ (-)	0.05	2.5	0.06	0.02	2.2	0.72

Table C.119. UnSWAN performance metrics for CDIP Station 46211 for 1994.

Parameter	RMSE	PE (%)	SI	Bias	Bias (%)	R
J (kW/m)	17	39.1	0.55	7	21.9	0.93
H_s (m)	0.34	9.7	0.16	0.13	6.2	0.96
T_e (s)	1.1	10.7	0.13	0.9	9.7	0.92
ϵ_0 (-)	0.06	-7.1	0.17	-0.03	-8.3	0.78
θ (degrees)	11.5	-0.4	0.04	-2	-0.6	0.78
d_θ (-)	0.05	2.6	0.05	0.02	2.4	0.77

Table C.120. UnSWAN performance metrics for CDIP Station 46211 for 1993.

Parameter	RMSE	PE (%)	SI	Bias	Bias (%)	R
J (kW/m)	19	54.0	0.71	8	30.5	0.94
H_s (m)	0.35	13.0	0.19	0.18	9.3	0.96
T_e (s)	1.6	13.5	0.16	1.2	12.0	0.82
ϵ_0 (-)	0.08	-8.2	0.22	-0.04	-10.4	0.69
θ (degrees)	13.3	-2.3	0.05	-7	-2.4	0.69
d_θ (-)	0.05	1.8	0.06	0.01	1.5	0.68

C.2.4 Station 46221

Table C.121. UnSWAN performance metrics for CDIP Station 46221 for 2010.

Parameter	RMSE	PE (%)	SI	Bias	Bias (%)	R
J (kW/m)	5	13.2	0.66	-1	-7.1	0.81
H_s (m)	0.28	-2.5	0.24	-0.07	-5.9	0.83
T_e (s)	2.4	17.7	0.26	1.6	16.8	0.70
ϵ_0 (-)	0.11	0.5	0.25	-0.01	-1.4	0.46
θ (degrees)	22.1	-6.6	0.09	-16	-6.7	0.74
d_θ (-)	0.09	6.3	0.11	0.05	5.7	0.21

Table C.122. UnSWAN performance metrics for CDIP Station 46221 for 2009.

Parameter	RMSE	PE (%)	SI	Bias	Bias (%)	R
J (kW/m)	5	13.2	0.66	-1	-7.1	0.81
H_s (m)	0.28	-2.5	0.24	-0.07	-5.9	0.83
T_e (s)	2.4	17.7	0.26	1.6	16.8	0.70
ϵ_0 (-)	0.11	0.5	0.25	-0.01	-1.4	0.46
θ (degrees)	22.1	-6.6	0.09	-16	-6.7	0.74
d_θ (-)	0.09	6.3	0.11	0.05	5.7	0.21

Table C.123. UnSWAN performance metrics for CDIP Station 46221 for 2008.

Parameter	RMSE	PE (%)	SI	Bias	Bias (%)	R
J (kW/m)	3	10.2	0.63	0	-6.1	0.73
H_s (m)	0.25	-3.1	0.24	-0.06	-5.8	0.78
T_e (s)	2.2	17.5	0.25	1.5	16.5	0.70
ϵ_0 (-)	0.11	-2.7	0.23	-0.02	-4.5	0.42
θ (degrees)	24.4	-6.8	0.10	-18	-7.4	0.61
d_θ (-)	0.10	6.7	0.12	0.05	6.0	0.13

Table C.124. UnSWAN performance metrics for CDIP Station 46221 for 2007.

Parameter	RMSE	PE (%)	SI	Bias	Bias (%)	R
J (kW/m)	4	-0.7	0.70	-1	-16.1	0.74
H_s (m)	0.27	-5.6	0.27	-0.09	-8.6	0.76
T_e (s)	1.9	12.5	0.22	1.0	11.1	0.69
ϵ_0 (-)	0.11	1.0	0.22	0.00	-0.7	0.47
θ (degrees)	22.3	-6.1	0.09	-16	-6.2	0.65
d_θ (-)	0.08	4.6	0.11	0.03	4.0	0.29

Table C.125. UnSWAN performance metrics for CDIP Station 46221 for 2006.

Parameter	RMSE	PE (%)	SI	Bias	Bias (%)	R
J (kW/m)	4	1.7	0.66	-1	-13.5	0.75
H_s (m)	0.25	-6.2	0.25	-0.09	-8.6	0.78
T_e (s)	2.1	14.5	0.23	1.2	13.4	0.68
ϵ_0 (-)	0.11	-2.2	0.22	-0.02	-4.2	0.48
θ (degrees)	24.0	-6.8	0.10	-17	-7.0	0.65
d_θ (-)	0.10	8.3	0.13	0.06	7.5	0.26

Table C.126. UnSWAN performance metrics for CDIP Station 46221 for 2005.

Parameter	RMSE	PE (%)	SI	Bias	Bias (%)	R
J (kW/m)	4	0.9	0.66	-1	-15.0	0.78
H_s (m)	0.25	-5.0	0.25	-0.07	-7.3	0.77
T_e (s)	1.9	11.1	0.21	0.9	9.6	0.67
ϵ_0 (-)	0.11	-1.7	0.24	-0.02	-4.1	0.49
θ (degrees)	21.1	-4.9	0.09	-12	-5.2	0.66
d_θ (-)	0.09	7.2	0.12	0.05	6.4	0.36

Table C.127. UnSWAN performance metrics for CDIP Station 46221 for 2004.

Parameter	RMSE	PE (%)	SI	Bias	Bias (%)	R
J (kW/m)	3	-4.6	0.63	-1	-14.4	0.72
H_s (m)	0.24	-6.4	0.24	-0.08	-8.0	0.78
T_e (s)	1.7	9.2	0.20	0.7	8.1	0.66
ϵ_0 (-)	0.10	0.8	0.21	0.00	-0.9	0.55
θ (degrees)	21.5	-4.4	0.09	-14	-5.7	0.58
d_θ (-)	0.08	5.7	0.10	0.04	5.2	0.40

Table C.128. UnSWAN performance metrics for CDIP Station 46221 for 2003.

Parameter	RMSE	PE (%)	SI	Bias	Bias (%)	R
J (kW/m)	4	-0.3	0.64	-1	-15.0	0.62
H_s (m)	0.26	-4.6	0.25	-0.07	-7.0	0.71
T_e (s)	1.8	8.4	0.20	0.7	7.4	0.64
ϵ_0 (-)	0.11	1.7	0.23	0.00	-0.5	0.43
θ (degrees)	20.2	-5.4	0.08	-13	-5.5	0.71
d_θ (-)	0.08	6.2	0.11	0.05	5.7	0.32

Table C.129. UnSWAN performance metrics for CDIP Station 46221 for 2002.

Parameter	RMSE	PE (%)	SI	Bias	Bias (%)	R
J (kW/m)	3	-12.0	0.59	-1	-21.7	0.87
H_s (m)	0.23	-8.1	0.23	-0.10	-9.9	0.84
T_e (s)	1.6	6.9	0.18	0.5	6.1	0.73
ϵ_0 (-)	0.10	2.6	0.21	0.00	0.9	0.57
θ (degrees)	17.9	-4.3	0.07	-11	-4.4	0.74
d_θ (-)	0.08	5.3	0.10	0.04	4.9	0.41

Table C.130. UnSWAN performance metrics for CDIP Station 46221 for 2001.

Parameter	RMSE	PE (%)	SI	Bias	Bias (%)	R
J (kW/m)	5	-6.3	0.76	-1	-23.6	0.69
H_s (m)	0.29	-7.2	0.27	-0.11	-10.6	0.76
T_e (s)	1.8	8.7	0.19	0.7	7.5	0.71
ϵ_0 (-)	0.11	-0.4	0.22	-0.01	-2.7	0.50
θ (degrees)	18.8	-4.3	0.08	-11	-4.5	0.75
d_θ (-)	0.09	6.8	0.11	0.05	6.1	0.40

Table C.131. UnSWAN performance metrics for CDIP Station 46221 for 2000.

Parameter	RMSE	PE (%)	SI	Bias	Bias (%)	R
J (kW/m)	3	-1.0	0.65	-1	-11.2	0.52
H_s (m)	0.25	-4.9	0.25	-0.06	-6.3	0.67
T_e (s)	1.7	9.1	0.19	0.7	7.7	0.68
ϵ_0 (-)	0.10	0.3	0.21	-0.01	-2.0	0.51
θ (degrees)	19.5	-4.9	0.08	-12	-5.1	0.69
d_θ (-)	0.09	6.7	0.11	0.05	6.1	0.30

C.2.5 Station 46224

Table C.132. UnSWAN performance metrics for CDIP Station 46224 for 2010.

Parameter	RMSE	PE (%)	SI	Bias	Bias (%)	R
J (kW/m)	4	34.1	0.65	1	18.3	0.83
H_s (m)	0.20	7.8	0.20	0.05	5.3	0.88
T_e (s)	2.1	16.4	0.21	1.5	15.5	0.77
ϵ_0 (-)	0.10	-9.0	0.23	-0.04	-10.2	0.57
θ (degrees)	17.2	-4.1	0.07	-10	-4.3	0.83
d_θ (-)	0.08	4.1	0.09	0.03	3.6	0.38

Table C.133. UnSWAN performance metrics for CDIP Station 46224 for 2009.

Parameter	RMSE	PE (%)	SI	Bias	Bias (%)	R
J (kW/m)	3	21.5	0.62	0	6.7	0.77
H_s (m)	0.18	3.3	0.20	0.01	0.7	0.85
T_e (s)	2.0	16.7	0.21	1.5	15.4	0.71
ϵ_0 (-)	0.11	-10.4	0.24	-0.06	-12.1	0.50
θ (degrees)	19.2	-5.1	0.08	-13	-5.4	0.77
d_θ (-)	0.08	4.6	0.10	0.03	4.0	0.30

Table C.134. UnSWAN performance metrics for CDIP Station 46224 for 2008.

Parameter	RMSE	PE (%)	SI	Bias	Bias (%)	R
J (kW/m)	3	26.5	0.55	1	13.1	0.71
H_s (m)	0.19	5.0	0.20	0.02	2.5	0.80
T_e (s)	2.0	16.7	0.21	1.5	15.7	0.78
ϵ_0 (-)	0.10	-8.9	0.22	-0.05	-10.4	0.51
θ (degrees)	19.3	-5.1	0.08	-13	-5.5	0.79
d_θ (-)	0.08	4.4	0.10	0.03	4.0	0.38

Table C.135. UnSWAN performance metrics for CDIP Station 46224 for 2007.

Parameter	RMSE	PE (%)	SI	Bias	Bias (%)	R
J (kW/m)	3	16.5	0.59	0	2.8	0.79
H_s (m)	0.18	1.2	0.20	-0.01	-1.1	0.83
T_e (s)	2.0	16.7	0.22	1.4	15.4	0.73
ϵ_0 (-)	0.11	-7.7	0.23	-0.04	-9.3	0.47
θ (degrees)	20.2	-5.5	0.08	-14	-5.7	0.77
d_θ (-)	0.08	3.5	0.09	0.02	3.0	0.39

Table C.136. UnSWAN performance metrics for CDIP Station 46224 for 2006.

Parameter	RMSE	PE (%)	SI	Bias	Bias (%)	R
J (kW/m)	3	14.7	0.61	0	5.0	0.73
H_s (m)	0.18	1.4	0.20	0.00	-0.3	0.81
T_e (s)	1.8	13.5	0.18	1.2	12.6	0.79
ϵ_0 (-)	0.10	-9.4	0.22	-0.05	-10.6	0.61
θ (degrees)	16.0	-3.8	0.07	-9	-4.0	0.84
d_θ (-)	0.08	5.6	0.10	0.04	5.1	0.35

Table C.137. UnSWAN performance metrics for CDIP Station 46224 for 2005.

Parameter	RMSE	PE (%)	SI	Bias	Bias (%)	R
J (kW/m)	2	11.9	0.50	0	-1.9	0.80
H_s (m)	0.18	1.6	0.20	-0.01	-0.6	0.82
T_e (s)	1.6	10.3	0.16	0.9	9.3	0.77
ϵ_0 (-)	0.09	-7.0	0.21	-0.04	-8.7	0.57
θ (degrees)	16.4	-3.8	0.07	-9	-4.0	0.81
d_θ (-)	0.07	3.6	0.09	0.03	3.2	0.41

Table C.138. UnSWAN performance metrics for CDIP Station 46224 for 2004.

Parameter	RMSE	PE (%)	SI	Bias	Bias (%)	R
J (kW/m)	3	14.8	0.56	0	3.6	0.75
H_s (m)	0.18	2.7	0.20	0.01	1.0	0.83
T_e (s)	1.6	10.7	0.17	0.9	9.5	0.70
ϵ_0 (-)	0.10	-8.2	0.21	-0.04	-9.6	0.56
θ (degrees)	16.9	-3.5	0.07	-9	-3.8	0.81
d_θ (-)	0.07	4.5	0.09	0.03	4.0	0.46

Table C.139. UnSWAN performance metrics for CDIP Station 46224 for 2003.

Parameter	RMSE	PE (%)	SI	Bias	Bias (%)	R
J (kW/m)	3	20.5	0.55	0	7.8	0.67
H_s (m)	0.20	5.8	0.22	0.03	3.6	0.76
T_e (s)	1.5	8.8	0.15	0.8	7.9	0.72
ϵ_0 (-)	0.09	-6.8	0.21	-0.04	-8.2	0.55
θ (degrees)	16.9	-3.0	0.07	-7	-3.1	0.77
d_θ (-)	0.07	4.3	0.09	0.03	4.0	0.50

Table C.140. UnSWAN performance metrics for CDIP Station 46224 for 2002.

Parameter	RMSE	PE (%)	SI	Bias	Bias (%)	R
J (kW/m)	2	10.6	0.50	0	0.1	0.82
H_s (m)	0.16	2.2	0.18	0.00	0.5	0.85
T_e (s)	1.4	9.1	0.15	0.8	8.2	0.78
ϵ_0 (-)	0.09	-7.1	0.20	-0.04	-8.1	0.66
θ (degrees)	15.4	-2.3	0.06	-6	-2.5	0.81
d_θ (-)	0.07	4.0	0.09	0.03	3.6	0.51

Table C.141. UnSWAN performance metrics for CDIP Station 46224 for 2001.

Parameter	RMSE	PE (%)	SI	Bias	Bias (%)	R
J (kW/m)	3	7.8	0.53	0	-5.8	0.71
H_s (m)	0.19	0.2	0.20	-0.02	-2.4	0.80
T_e (s)	1.6	9.2	0.16	0.8	8.0	0.75
ϵ_0 (-)	0.09	-7.2	0.21	-0.04	-8.7	0.59
θ (degrees)	15.9	-2.7	0.07	-7	-2.9	0.82
d_θ (-)	0.07	3.4	0.09	0.02	3.0	0.50

Table C.142. UnSWAN performance metrics for CDIP Station 46224 for 2000.

Parameter	RMSE	PE (%)	SI	Bias	Bias (%)	R
J (kW/m)	2	6.7	0.45	0	-0.5	0.78
H_s (m)	0.17	0.1	0.18	-0.01	-1.1	0.82
T_e (s)	1.5	8.8	0.15	0.8	7.7	0.72
ϵ_0 (-)	0.09	-5.3	0.19	-0.03	-6.9	0.60
θ (degrees)	15.4	-2.9	0.07	-7	-3.1	0.81
d_θ (-)	0.07	4.0	0.09	0.03	3.5	0.36

Table C.143. UnSWAN performance metrics for CDIP Station 46224 for 1999.

Parameter	RMSE	PE (%)	SI	Bias	Bias (%)	R
J (kW/m)	3	14.7	0.55	0	1.1	0.69
H_s (m)	0.20	1.7	0.20	-0.01	-0.9	0.79
T_e (s)	1.6	10.5	0.16	1.0	9.7	0.79
ϵ_0 (-)	0.09	-6.4	0.20	-0.03	-7.6	0.57
θ (degrees)	15.7	-3.5	0.07	-9	-3.7	0.84
d_θ (-)	0.07	3.2	0.09	0.02	2.8	0.36

Table C.144. UnSWAN performance metrics for CDIP Station 46224 for 1998.

Parameter	RMSE	PE (%)	SI	Bias	Bias (%)	R
J (kW/m)	3	9.0	0.49	0	-2.1	0.87
H_s (m)	0.20	0.7	0.18	-0.01	-1.3	0.88
T_e (s)	1.4	9.0	0.15	0.8	8.2	0.80
ϵ_0 (-)	0.08	-4.1	0.17	-0.02	-5.4	0.65
θ (degrees)	13.9	-2.0	0.06	-5	-2.3	0.86
d_θ (-)	0.07	3.6	0.08	0.03	3.2	0.56

Table C.145. UnSWAN performance metrics for CDIP Station 46224 for 1997.

Parameter	RMSE	PE (%)	SI	Bias	Bias (%)	R
J (kW/m)	3	31.5	0.58	1	14.5	0.74
H_s (m)	0.21	8.3	0.22	0.05	5.6	0.80
T_e (s)	1.8	14.0	0.19	1.2	12.9	0.74
ϵ_0 (-)	0.10	-10.8	0.23	-0.06	-12.3	0.55
θ (degrees)	14.3	-2.0	0.06	-5	-2.3	0.81
d_θ (-)	0.08	6.0	0.10	0.04	5.5	0.46

C.2.6 Station 46213

Table C.146. WWIII performance metrics for CDIP Station 46213 for 2010.

Parameter	RMSE	PE (%)	SI	Bias	Bias (%)	R
J (kW/m)	16	22.0	0.39	2	5.5	0.92
H_s (m)	0.39	9.5	0.15	0.17	6.5	0.94
T_e (s)	1.1	9.8	0.12	0.8	9.0	0.89
ϵ_0 (-)	0.05	-1.3	0.14	-0.01	-2.3	0.83
θ (degrees)	32.5	-0.3	0.11	-4	-1.3	0.66
d_θ (-)	0.08	1.8	0.11	0.01	1.2	0.74

Table C.147. WWIII performance metrics for CDIP Station 46213 for 2009.

Parameter	RMSE	PE (%)	SI	Bias	Bias (%)	R
J (kW/m)	14	18.7	0.40	0	0.3	0.92
H_s (m)	0.37	8.3	0.16	0.11	4.5	0.93
T_e (s)	1.0	7.3	0.11	0.6	6.8	0.91
ϵ_0 (-)	0.06	-1.6	0.15	-0.01	-3.0	0.78
θ (degrees)	20.5	-0.7	0.07	-4	-1.3	0.86
d_θ (-)	0.07	1.9	0.09	0.01	1.4	0.79

Table C.148. WWIII performance metrics for CDIP Station 46213 for 2008.

Parameter	RMSE	PE (%)	SI	Bias	Bias (%)	R
J (kW/m)	18	21.4	0.48	0	0.1	0.92
H_s (m)	0.41	9.0	0.17	0.12	4.9	0.93
T_e (s)	1.0	8.2	0.11	0.7	7.5	0.92
ϵ_0 (-)	0.06	-1.5	0.16	-0.01	-3.2	0.78
θ (degrees)	21.3	-0.2	0.07	-3	-1.0	0.81
d_θ (-)	0.07	0.3	0.09	0.00	0.0	0.80

Table C.149. WWIII performance metrics for Station 46213 for 2007.

Parameter	RMSE	PE (%)	SI	Bias	Bias (%)	R
J (kW/m)	18	23.5	0.48	1	2.1	0.90
H_s (m)	0.41	10.4	0.17	0.14	5.7	0.94
T_e (s)	1.0	8.1	0.11	0.7	7.7	0.91
ϵ_0 (-)	0.06	-3.0	0.15	-0.02	-4.4	0.78
θ (degrees)	19.3	-0.8	0.07	-3	-1.1	0.80
d_θ (-)	0.07	1.8	0.09	0.01	1.6	0.80

Table C.150. WWIII performance metrics for Station 46213 for 2006.

Parameter	RMSE	PE (%)	SI	Bias	Bias (%)	R
J (kW/m)	18	23.5	0.48	1	2.1	0.90
H_s (m)	0.41	10.4	0.17	0.14	5.7	0.94
T_e (s)	1.0	8.1	0.11	0.7	7.7	0.91
ϵ_0 (-)	0.06	-3.0	0.15	-0.02	-4.4	0.78
θ (degrees)	19.3	-0.8	0.07	-3	-1.1	0.80
d_θ (-)	0.07	1.8	0.09	0.01	1.6	0.80

Table C.151. WWIII performance metrics for Station 46213 for 2005.

Parameter	RMSE	PE (%)	SI	Bias	Bias (%)	R
J (kW/m)	17	14.6	0.45	1	1.4	0.90
H_s (m)	0.39	7.1	0.16	0.10	4.2	0.93
T_e (s)	0.9	6.4	0.10	0.6	5.9	0.93
ϵ_0 (-)	0.05	-2.2	0.15	-0.01	-3.3	0.80
θ (degrees)	19.4	-0.2	0.07	-2	-0.7	0.84
d_θ (-)	0.06	0.9	0.08	0.01	0.7	0.83

Table C.152. WWIII performance metrics for Station 46213 for 2004.

Parameter	RMSE	PE (%)	SI	Bias	Bias (%)	R
J (kW/m)	16	16.6	0.44	-1	-2.7	0.91
H_s (m)	0.39	8.4	0.17	0.09	3.8	0.93
T_e (s)	0.9	5.7	0.10	0.5	5.5	0.90
ϵ_0 (-)	0.06	-1.9	0.15	-0.01	-3.2	0.80
θ (degrees)	24.0	-0.2	0.08	-2	-0.8	0.75
d_θ (-)	0.08	1.4	0.10	0.01	1.1	0.78

C.2.7 Station 46229

Table C.153. WWIII performance metrics for Station 46229 for 2010.

Parameter	RMSE	PE (%)	SI	Bias	Bias (%)	R
J (kW/m)	20	17.8	0.43	1	3.1	0.94
H_s (m)	0.40	5.6	0.15	0.08	3.1	0.95
T_e (s)	1.3	12.8	0.15	1.0	11.6	0.89
ϵ_0 (-)	0.06	0.5	0.19	0.00	-1.0	0.66
θ (degrees)	20.0	-1.0	0.07	-4	-1.6	0.79
d_θ (-)	0.07	0.4	0.09	0.00	0.1	0.64

Table C.154. WWIII performance metrics for Station 46229 for 2009.

Parameter	RMSE	PE (%)	SI	Bias	Bias (%)	R
J (kW/m)	15	13.1	0.46	-1	-2.1	0.92
H_s (m)	0.35	3.3	0.15	0.01	0.5	0.95
T_e (s)	1.3	12.3	0.15	1.0	11.1	0.91
ϵ_0 (-)	0.07	-5.6	0.19	-0.03	-7.2	0.71
θ (degrees)	18.1	-1.3	0.06	-5	-1.8	0.84
d_θ (-)	0.07	3.3	0.09	0.02	2.7	0.70

Table C.155. WWIII performance metrics for Station 46229 for 2008.

Parameter	RMSE	PE (%)	SI	Bias	Bias (%)	R
J (kW/m)	19	11.8	0.50	-2	-4.1	0.93
H_s (m)	0.37	3.1	0.16	0.00	0.0	0.95
T_e (s)	1.2	11.6	0.14	0.9	10.3	0.91
ϵ_0 (-)	0.07	-3.8	0.19	-0.02	-5.3	0.69
θ (degrees)	16.5	-0.9	0.06	-5	-1.6	0.85
d_θ (-)	0.07	1.1	0.08	0.01	0.8	0.68

Table C.156. WWIII performance metrics for Station 46229 for 2007.

Parameter	RMSE	PE (%)	SI	Bias	Bias (%)	R
J (kW/m)	21	20.4	0.56	2	4.7	0.93
H_s (m)	0.36	6.7	0.16	0.09	3.8	0.96
T_e (s)	1.3	12.5	0.14	1.0	11.3	0.92
ϵ_0 (-)	0.07	-6.4	0.19	-0.03	-7.9	0.69
θ (degrees)	16.9	-1.0	0.06	-4	-1.5	0.83
d_θ (-)	0.07	3.0	0.08	0.02	2.7	0.70

Table C.157. WWIII performance metrics for Station 46229 for 2006.

Parameter	RMSE	PE (%)	SI	Bias	Bias (%)	R
J (kW/m)	23	9.2	0.54	-2	-4.2	0.93
H_s (m)	0.38	2.0	0.16	0.00	0.2	0.96
T_e (s)	1.3	11.8	0.15	0.9	10.7	0.88
ϵ_0 (-)	0.06	-3.1	0.18	-0.02	-4.9	0.77
θ (degrees)	19.0	-2.1	0.07	-7	-2.4	0.79
d_θ (-)	0.06	0.4	0.08	0.00	0.1	0.71

C.2.8 Station 46216

Table C.158. WWIII performance metrics for Station 46216 for 2010.

Parameter	RMSE	PE (%)	SI	Bias	Bias (%)	R
J (kW/m)	6	-37.2	0.73	-3	-39.6	0.90
H_s (m)	0.37	-24.1	0.31	-0.28	-24.1	0.90
T_e (s)	1.6	13.4	0.20	0.9	11.2	0.77
ϵ_0 (-)	0.10	7.0	0.23	0.02	5.6	0.64
θ (degrees)	9.9	1.1	0.04	3	1.0	0.57
d_θ (-)	0.05	2.4	0.06	0.02	2.2	0.73

Table C.159. WWIII performance metrics for Station 46216 for 2009.

Parameter	RMSE	PE (%)	SI	Bias	Bias (%)	R
J (kW/m)	4	-38.9	0.75	-2	-45.2	0.81
H_s (m)	0.35	-25.4	0.34	-0.27	-26.3	0.84
T_e (s)	1.5	12.1	0.20	0.8	10.0	0.76
ϵ_0 (-)	0.10	4.3	0.23	0.01	2.3	0.61
θ (degrees)	9.8	1.5	0.04	4	1.4	0.37
d_θ (-)	0.06	3.8	0.06	0.03	3.5	0.67

Table C.160. WWIII performance metrics for Station 46216 for 2008.

Parameter	RMSE	PE (%)	SI	Bias	Bias (%)	R
J (kW/m)	4	-39.8	0.75	-2	-43.9	0.91
H_s (m)	0.35	-25.2	0.33	-0.28	-25.8	0.85
T_e (s)	1.4	11.3	0.19	0.7	9.7	0.78
ϵ_0 (-)	0.10	5.8	0.22	0.02	4.1	0.55
θ (degrees)	12.5	1.4	0.05	3	1.2	0.51
d_θ (-)	0.06	3.3	0.07	0.03	3.0	0.69

Table C.161. WWIII performance metrics for Station 46216 for 2007.

Parameter	RMSE	PE (%)	SI	Bias	Bias (%)	R
J (kW/m)	5	-40.9	0.82	-3	-44.3	0.85
H_s (m)	0.36	-25.0	0.33	-0.28	-25.5	0.81
T_e (s)	1.2	6.9	0.15	0.5	5.8	0.80
ϵ_0 (-)	0.10	7.6	0.23	0.02	5.4	0.48
θ (degrees)	9.9	1.7	0.04	4	1.6	0.19
d_θ (-)	0.06	2.6	0.06	0.02	2.5	0.48

Table C.162. WWIII performance metrics for Station 46216 for 2006.

Parameter	RMSE	PE (%)	SI	Bias	Bias (%)	R
J (kW/m)	4	-40.1	0.75	-2	-41.7	0.84
H_s (m)	0.35	-25.4	0.33	-0.27	-25.3	0.85
T_e (s)	1.4	10.0	0.17	0.7	8.3	0.78
ϵ_0 (-)	0.10	5.7	0.22	0.02	3.9	0.61
θ (degrees)	11.9	1.8	0.05	4	1.6	0.27
d_θ (-)	0.06	4.5	0.07	0.04	4.2	0.65

Table C.163. WWIII performance metrics for Station 46216 for 2005.

Parameter	RMSE	PE (%)	SI	Bias	Bias (%)	R
J (kW/m)	5	-38.6	0.83	-3	-43.0	0.89
H_s (m)	0.35	-23.8	0.33	-0.26	-24.5	0.86
T_e (s)	1.3	8.1	0.16	0.5	6.3	0.84
ϵ_0 (-)	0.10	5.1	0.23	0.02	3.6	0.63
θ (degrees)	12.6	2.0	0.05	5	1.8	0.46
d_θ (-)	0.06	4.0	0.07	0.03	3.7	0.73

Table C.164. WWIII performance metrics for Station 46216 for 2004.

Parameter	RMSE	PE (%)	SI	Bias	Bias (%)	R
J (kW/m)	4	-34.4	0.74	-2	-38.2	0.87
H_s (m)	0.31	-21.5	0.31	-0.22	-22.0	0.83
T_e (s)	1.2	7.4	0.16	0.5	6.0	0.83
ϵ_0 (-)	0.10	2.7	0.21	0.01	1.5	0.62
θ (degrees)	12.9	2.2	0.05	5	2.1	0.54
d_θ (-)	0.07	4.9	0.08	0.04	4.6	0.70

Table C.165. WWIII performance metrics for Station 46216 for 2003.

Parameter	RMSE	PE (%)	SI	Bias	Bias (%)	R
J (kW/m)	4	-34.3	0.70	-2	-39.1	0.86
H_s (m)	0.32	-21.3	0.30	-0.23	-22.0	0.84
T_e (s)	1.4	10.0	0.18	0.7	8.4	0.81
ϵ_0 (-)	0.10	3.9	0.23	0.01	2.2	0.61
θ (degrees)	13.6	2.5	0.05	6	2.2	0.58
d_θ (-)	0.07	4.7	0.08	0.04	4.2	0.62

Table C.166. WWIII performance metrics for Station 46216 for 2002.

Parameter	RMSE	PE (%)	SI	Bias	Bias (%)	R
J (kW/m)	5	-42.7	0.81	-3	-42.6	0.92
H_s (m)	0.34	-26.6	0.33	-0.27	-26.4	0.90
T_e (s)	1.3	9.1	0.16	0.6	7.5	0.86
ϵ_0 (-)	0.10	9.5	0.24	0.03	8.0	0.68
θ (degrees)	11.6	2.0	0.04	5	1.9	0.36
d_θ (-)	0.06	3.5	0.07	0.03	3.1	0.73

Appendix D – Temporal Averages of Performance Metrics for Simulated IEC Resource Parameters

Table D.1 is the National Data Buoy Center-related table; Table D.2 is the Coastal Data Information Program-related table.

D.1 NDBC Table

Table D.1. WWIII temporal averages of performance metrics at NDBC stations.

Buoy #	Parameter	RMSE	PE (%)	SI	Bias	Bias (%)	R
46029	J (kW/m)	21	31.1	0.53	5	11.7	0.93
	H_s (m)	0.40	6.6	0.16	0.09	3.3	0.96
	T_e (s)	1.2	9.2	0.13	0.8	8.3	0.88
	ϵ_0 (-)	0.06	0.3	0.17	0.00	-0.9	0.72
	θ (degrees)	22.8	-0.1	0.08	-5	-1.6	0.66
	d_θ (-)	0.10	2.5	0.12	0.01	1.2	0.55
46050	J (kW/m)	17	30.7	0.51	4	11.2	0.93
	H_s (m)	0.37	4.8	0.16	0.05	1.9	0.95
	T_e (s)	1.3	12.4	0.15	1.0	11.0	0.88
	ϵ_0 (-)	0.07	7.4	0.23	0.02	5.5	0.58
	θ (degrees)	25.2	0.0	0.09	-8	-2.7	0.70
	d_θ (-)	0.11	5.4	0.14	0.03	3.9	0.36
46027	J (kW/m)	19	20.2	0.53	2	5.2	0.90
	H_s (m)	0.45	1.2	0.19	-0.05	-2.4	0.91
	T_e (s)	1.2	10.4	0.13	0.9	9.7	0.91
	ϵ_0 (-)	0.07	4.2	0.20	0.01	2.7	0.63
	θ (degrees)	14.9	-1.7	0.05	-6	-2.0	0.84
	d_θ (-)	0.08	0.8	0.10	0.00	0.1	0.51
46022	J (kW/m)	24	40.5	0.58	9	19.0	0.91
	H_s (m)	0.48	11.6	0.19	0.19	7.1	0.92
	T_e (s)	1.1	8.1	0.12	0.7	7.5	0.89
	ϵ_0 (-)	0.06	7.2	0.20	0.02	5.4	0.62
	θ (degrees)	28.8	-0.7	0.10	-5	-1.5	0.75
	d_θ (-)	0.10	4.8	0.13	0.03	3.4	0.54
46026	J (kW/m)	14	51.4	0.62	7	29.9	0.91
	H_s (m)	0.36	14.8	0.19	0.20	10.6	0.93
	T_e (s)	1.3	12.1	0.14	1.0	11.0	0.90
	ϵ_0 (-)	0.06	-3.6	0.17	-0.02	-4.7	0.75
	θ (degrees)	17.8	0.3	0.06	0	0.0	0.68
	d_θ (-)	0.09	1.8	0.12	0.01	0.8	0.67
46015	J (kW/m)	20	34.7	0.53	5	12.9	0.93
	H_s (m)	0.40	6.8	0.16	0.09	3.4	0.95
	T_e (s)	1.4	13.2	0.16	1.1	11.7	0.88
	ϵ_0 (-)	0.08	6.9	0.22	0.02	4.9	0.61
	θ (degrees)	31.5	-3.4	0.11	-12	-4.2	0.64
	d_θ (-)	0.12	4.2	0.16	0.02	2.6	0.37
46028	J (kW/m)	16	14.0	0.48	0	1.5	0.91
	H_s (m)	0.40	0.2	0.17	-0.06	-2.5	0.92

Buoy #	Parameter	RMSE	PE (%)	SI	Bias	Bias (%)	R
	T_e (s)	1.3	9.9	0.13	0.8	8.6	0.89
	ϵ_0 (-)	0.07	-2.6	0.18	-0.01	-3.8	0.71
	θ (degrees)	32.2	-1.9	0.11	-8	-2.8	0.42
	d_θ (-)	0.12	3.1	0.15	0.02	2.0	0.59
46025	J (kW/m)	3	15.2	0.51	0	0.3	0.86
	H_s (m)	0.21	-0.9	0.19	-0.04	-3.3	0.88
	T_e (s)	1.7	13.2	0.19	1.0	11.8	0.76
	ϵ_0 (-)	0.09	4.7	0.21	0.01	2.5	0.55
	θ (degrees)	32.7	-4.8	0.13	-21	-8.2	0.47
	d_θ (-)	0.16	18.2	0.23	0.10	14.8	0.19
46063	J (kW/m)	14	25.8	0.47	2	6.8	0.90
	H_s (m)	0.37	4.5	0.16	0.02	1.0	0.92
	T_e (s)	1.3	11.4	0.14	1.0	10.3	0.88
	ϵ_0 (-)	0.06	-0.3	0.17	-0.01	-1.9	0.72
	θ (degrees)	20.8	-0.6	0.07	-2	-0.8	0.55
	d_θ (-)	0.09	-2.5	0.11	-0.03	-3.0	0.68
Buoy #	Parameter	RMSE	PE (%)	SI	Bias	Bias (%)	R
46042	J (kW/m)	15	26.0	0.47	3	9.7	0.92
	H_s (m)	0.35	6.4	0.15	0.07	3.3	0.94
	T_e (s)	1.1	8.2	0.11	0.7	7.4	0.90
	ϵ_0 (-)	0.06	-6.8	0.17	-0.03	-8.0	0.78
	θ (degrees)	25.3	-0.7	0.09	-3	-1.1	0.60
	d_θ (-)	0.10	-0.2	0.13	-0.01	-1.0	0.72
46087	J (kW/m)	18	30.5	0.60	4	11.8	0.88
	H_s (m)	0.45	6.6	0.21	0.07	3.2	0.90
	T_e (s)	1.1	8.9	0.12	0.7	8.0	0.85
	ϵ_0 (-)	0.07	2.4	0.22	0.00	-0.2	0.54
	θ (degrees)	21.4	1.5	0.08	1	0.3	0.56
	d_θ (-)	0.11	8.8	0.13	0.06	7.2	0.41
46041	J (kW/m)	20	34.8	0.53	5	12.8	0.94
	H_s (m)	0.37	8.0	0.16	0.10	4.3	0.96
	T_e (s)	1.2	10.1	0.13	0.8	9.1	0.89
	ϵ_0 (-)	0.06	-1.2	0.18	-0.01	-2.6	0.71
	θ (degrees)	20.3	-0.6	0.08	-4	-1.6	0.68
	d_θ (-)	0.10	4.5	0.12	0.02	3.0	0.50

D.2 CDIP Table

Table D.2. UnSWAN temporal averages of performance metrics at CDIP stations.

Buoy #	Parameter	RMSE	PE (%)	SI	Bias	Bias (%)	R
46215	J (kW/m)	9	27.7	0.56	3	15.6	0.90
	H_s (m)	0.27	7.1	0.17	0.07	4.5	0.91
	T_e (s)	1.2	8.4	0.12	0.8	7.8	0.89
	ϵ_0 (-)	0.06	-6.7	0.15	-0.03	-7.2	0.80
	θ (degrees)	10.2	0.5	0.04	1	0.4	0.73
	d_θ (-)	0.05	3.3	0.06	0.03	3.3	0.80
46236	J (kW/m)	10	37.2	0.67	3	22.5	0.91
	H_s (m)	0.32	13.1	0.20	0.16	10.2	0.92
	T_e (s)	1.4	14.2	0.16	1.1	13.0	0.88
	ϵ_0 (-)	0.08	-13.8	0.21	-0.06	-15.0	0.77
	θ (degrees)	9.7	1.2	0.03	3	1.2	0.71
	d_θ (-)	0.04	2.0	0.05	0.02	1.9	0.80
46211	J (kW/m)	18	35.5	0.61	5	17.0	0.92
	H_s (m)	0.35	8.0	0.17	0.09	4.4	0.95
	T_e (s)	1.2	10.7	0.13	0.9	9.7	0.91
	ϵ_0 (-)	0.06	-5.7	0.18	-0.03	-7.0	0.77
	θ (degrees)	12.2	-1.1	0.05	-4	-1.4	0.82
	d_θ (-)	0.05	2.5	0.06	0.02	2.3	0.72
46221	J (kW/m)	4	1.3	0.66	-1	-13.7	0.73
	H_s (m)	0.26	-5.1	0.25	-0.08	-7.6	0.77
	T_e (s)	1.9	12.1	0.22	1.0	11.0	0.69
	ϵ_0 (-)	0.11	0.0	0.23	-0.01	-2.0	0.49
	θ (degrees)	21.3	-5.6	0.09	-14	-5.9	0.68
	d_θ (-)	0.09	6.4	0.11	0.05	5.8	0.30
46224	J (kW/m)	3	17.2	0.55	0	4.5	0.76
	H_s (m)	0.19	3.0	0.20	0.01	0.8	0.82
	T_e (s)	1.7	12.2	0.18	1.1	11.1	0.75
	ϵ_0 (-)	0.10	-7.7	0.21	-0.04	-9.1	0.57
	θ (degrees)	16.6	-3.5	0.07	-9	-3.7	0.81
	d_θ (-)	0.07	4.2	0.09	0.03	3.7	0.42
46213	J (kW/m)	17	20.1	0.44	1	1.3	0.91
	H_s (m)	0.40	9.0	0.16	0.12	5.0	0.93
	T_e (s)	1.0	7.6	0.11	0.7	7.1	0.91
	ϵ_0 (-)	0.06	-2.1	0.15	-0.01	-3.4	0.79
	θ (degrees)	22.3	-0.5	0.08	-3	-1.0	0.79
	d_θ (-)	0.07	1.4	0.09	0.01	1.1	0.79
46229	J (kW/m)	19	14.5	0.50	0	-0.5	0.93
	H_s (m)	0.37	4.1	0.16	0.04	1.5	0.95

Buoy #	Parameter	RMSE	PE (%)	SI	Bias	Bias (%)	R
	T_e (s)	1.3	12.2	0.14	1.0	11.0	0.90
	ϵ_0 (-)	0.07	-3.7	0.19	-0.02	-5.3	0.70
	θ (degrees)	18.1	-1.3	0.06	-5	-1.8	0.82
	d_θ (-)	0.07	1.6	0.08	0.01	1.3	0.68
46216	J (kW/m)	5	-38.6	0.76	-3	-42.0	0.87
	H_s (m)	0.34	-24.3	0.32	-0.26	-24.7	0.85
	T_e (s)	1.4	9.8	0.17	0.6	8.1	0.80
	ϵ_0 (-)	0.10	5.7	0.23	0.02	4.0	0.60
	θ (degrees)	11.6	1.8	0.04	4	1.6	0.43
	d_θ (-)	0.06	3.7	0.07	0.03	3.4	0.67

Pacific Northwest
NATIONAL LABORATORY

www.pnnl.gov

902 Battelle Boulevard
P.O. Box 999
Richland, WA 99352
1-888-375-PNNL (7665)

U.S. DEPARTMENT OF
ENERGY